4295

CONFIDENTIAL

WADC TECHNICAL REPORT 52-[illegible]

SECURITY INFORMATION

AD001940l

METHODS OF CONTROLLING TEMPERATURE RISE IN AIRBORNE COMPARTMENTS AT SUPERSONIC VELOCITIES WITH AND WITHOUT INTERNAL HEAT GENERATION

EDITED BY
WALTER ROBINSON

THE OHIO STATE UNIVERSITY RESEARCH FOUNDATION

AUGUST 1952

WRIGHT AIR DEVELOPMENT CENTER

DOWNGRADED AT 3 YEAR INTERVALS;
DECLASSIFIED AFTER 12 YEARS.
DOD DIR 5200.10

Statement A
Approved for Public Release

AF-WP-(B)-O-16 SEP 53 100

NOTICES

When Government drawings, specifications, or other data are used for any purpose other than in connection with a definitely related Government procurement operation, the United States Government thereby incurs no responsibility nor any obligation whatsoever; and the fact that the Government may have formulated, furnished, or in any way supplied the said drawings, specifications, or other data, is not to be regarded by implication or otherwise as in any manner licensing the holder or any other person or corporation, or conveying any rights or permission to manufacture, use, or sell any patented invention that may in any way be related thereto.

The information furnished herewith is made available for study upon the understanding that the Government's proprietary interests in and relating thereto shall not be impaired. It is desired that the Judge Advocate (WCJ), Wright Air Development Center, Wright-Patterson Air Force Base, Ohio, be promptly notified of any apparent conflict between the Government's proprietary interests and those of others.

[redacted]

WADC TECHNICAL REPORT 53-114 SECURITY INFORMATION

METHODS OF CONTROLLING TEMPERATURE RISE IN AIRBORNE COMPARTMENTS AT SUPERSONIC VELOCITIES WITH AND WITHOUT INTERNAL HEAT GENERATION

Edited by
Walter Robinson

The Ohio State University Research Foundation

August 1952

CLASSIFICATION CANCELLED
~~(OR CHANGED TO~~ ______________________)
BY AUTHORITY OF DOD Dir 5200.10
(OFFICIAL OR WRITTEN AUTHORITY)
BY ______________ 18 Aug '66
(NAME & GRADE OF INDIVIDUAL MAKING CHANGE) (DATE)

Power Plant Laboratory
Contract No. AF 33(038)-23288
RDO No. 540-42

Wright Air Development Center
Air Research and Development Command
United States Air Force
Wright-Patterson Air Force Base, Ohio

[redacted]

55WCOS-2033

FOREWORD

This report was prepared in the Mechanical Engineering Department of the Ohio State University by S. M. Marco, W. Robinson, M. L. Smith, Y. H. Sun, T. C. Taylor and R. H. Zimmerman. The work was performed under Contract AF33(038)-23288 with The Ohio State University Research Foundation. It was administered under the direction of the Power Plant Laboratory, Directorate of Laboratories, Wright Air Development Center, Mr. D. M. Chisel acting as project engineer. The research covered in this report was started 1 April 1951 and was completed 30 June 1952.

[redacted]

ABSTRACT

Methods of controlling equipment temperature rise in airborne compartments at supersonic flight speed are investigated. Design and performance data for expanded ram air cooling systems and various types of fuel-cooled equipment cases are presented for steady-state thermal operation. Other methods of controlling temperature rise are analyzed for transient thermal performance and design procedures for their applications are developed. Calculation methods are given in detail. Design procedures are illustrated by examples. The performance characteristics of the following methods are investigated (1) insulation of equipment compartment walls without cooling, (2) insulation of individual equipment items, (3) fuel-jacketing of equipment compartments, (4) cooling of the compartment atmosphere by means of a central fuel-cooled heat exchanger, (5) cooling of individual equipment items by installation on a fuel-cooled plate, and (6) cooling of individual equipment items by evaporation of an expendable coolant. Methods of analysis and criteria for the selection of specific means for the control of temperature rise are emphasized. The large number of variables by which each practical situation would be defined does not permit a concise description of the optimum range of conditions for the application of each method.

The security classification of the title of this report is UNCLASSIFIED.

PUBLICATION REVIEW

The publication of this report does not constitute approval by the Air Force of the findings or the conclusions contained therein. It is published only for the exchange and stimulation of ideas.

FOR THE COMMANDER:

NORMAN C. APPOLD
Colonel, USAF
Chief, Power Plant Laboratory

[redacted]

TABLE OF CONTENTS

LIST OF ILLUSTRATIONS

SECTION I

INTRODUCTION

This report is concerned with the presentation of the information developed in an investigation with the general objective of studying methods of cooling airborne equipment, but specifically intended to produce data on methods for controlling the temperature rise of electronic and mechanical control equipment components in ramjet installations. Therefore, only Sections I and II are concerned with analyses assuming steady-state thermal operation, while Sections III through XI and Appendix III on fuel temperature rise in flight are concerned with methods of analysis and results obtained in the study of transient thermal operation. The latter approach has been chosen because when operating under constant environmental conditions conducive to high heat gain, few equipments would reach thermal equilibrium in less than two hours, which has been considered as a reasonably long operating time for the specified applications under consideration. The reductions in size and weight of insulation or cooling apparatus, realized by designing for specified terminal temperatures to be reached in the transient state, rather than to be maintained in the steady state under terminal environmental conditions, are substantial, as indicated repeatedly in this report.

It has been the intention in preparing this report to present in each section a phase of study as a self-contained unit since the variety of aspects covered in the report has not been found to lend itself readily to joint summarization. Therefore, the summary presented in each section after the introductory remarks is intended to provide an indication of the analyses, data, conclusions, design procedures, etc. contained in that particular section. Throughout the report methods of analysis, calculations and design are emphasized since it is intended to provide the necessary information that would enable the reader to cope with specific problems of similar nature in which all variables are defined. Because of the large number of variables and their possible combinations few unconditional recommendations are presented. Instead an attempt is made to develop in each section the necessary criteria for the selection of each means of limiting equipment temperature rise, as summarized in Section XI.

Section I is concerned with the analysis, performance and design of expanded ram air systems for compartment or heat exchanger cooling by means of atmospheric air reduced in temperature by expansion through a turbine operating under load. Off-design performance of such systems is not analyzed but indications of size, weight and most practical ranges of design operating conditions are given on the basis of steady-state performance. Section II deals with the evaluation of various heat exchanger configurations, as applied to equipment cases cooled by fuel flow to the power plant. The performance of the heat exchangers is analyzed in terms of steady-state operation, but can be interpreted on the basis of a constant temperature difference between the fuel coolant and the internal equipment atmosphere which may cause the equipment temperature to vary with the fuel temperature, while the rate of heat generation within the equipment case would remain constant. Sections I and II need not be studied for an understanding of the subsequent sections.

Sections III through XI are interrelated in that they are all concerned with non-steady state analysis and methods of controlling temperature rise, taking into account thermal capacity of equipment and compartment, with and without heat generation. In Section III a general system for transient analysis of installation compartments is developed which takes into consideration most possible variables. Section IV contains a study on skin temperature rise which indicates the basis for simplifying assumptions made in the subsequent sections. Sections IV through X deal with specific characteristics of the various methods suggested as applicable to the control of equipment temperature rise. In these sections, in particular, procedures of analysis, calculation and design should be noted since they are general and can be applied readily to fully defined situations. As mentioned previously, Section XI summarizes the criteria for the selection of methods in specific situations, based on the preceding seven sections, and is intended to outline a design approach.

This report does not present a specific recommendation for every situation that may be encountered when an attempt is made to control the temperature rise of equipment components at high flight speed. However, it is believed to fulfill two functions. First, it demonstrates the feasibility of temperature rise limitation by simple means for relatively long flight times and severe environmental conditions. Second, it provides calculation methods for analysis and design which can be utilized without undue effort to the solution of specific problems.

SECTION I

GENERAL PERFORMANCE AND PHYSICAL CHARACTERISTICS OF EXPANDED RAM AIR SYSTEMS

By M. L. Smith and R. H. Zimmerman

Utilization of atmospheric air as a thermal sink for direct cooling of aircraft auxiliaries, i.e. by air taken aboard an aircraft and passed directly over or through the equipments to be cooled, is limited by flight speed of the aircraft. The temperature of the air once aboard the aircraft is equal to or exceeds the desirable operating temperature level for most aircraft auxiliaries whenever the flight Mach number is in excess of the range 1.0 to 1.5. From a practical viewpoint, this type of direct cooling is limited to aircraft designed for flight in the subsonic range, since for flight in the supersonic range, even when the temperature of the ram cooling air does not exceed the desired temperature level of the equipment, the quantity of cooling air required becomes excessive as a result of the small temperature differential available for transfer of heat from the surfaces being cooled to the air.

Practical utilization of atmospheric air for cooling of auxiliaries in aircraft operating in the supersonic region requires, therefore, some means for reducing the temperature of the air once it is aboard the aircraft. An air cycle refrigeration system capable of accomplishing this purpose, which is mechanically relatively simple and does not require a separate high pressure air source for operation, such as, for example, bleed air from a turbojet engine compressor, is the expanded ram air system. This system depends solely on ram air for its operation and consists of five basic components. They are: 1) ram intake, 2) expander, 3) heat exchanger, 4) compressor and 5) exhaust.

Atmospheric air is taken aboard the aircraft through a ram intake and ducted directly to the expander component of the cycle. The ram intake must also serve as a means for pressure increase of the air, so that it may subsequently be expanded in the cycle. Hence, the intake component must be designed as an efficient diffuser, increasing the total pressure of the air at discharge of the diffuser as nearly as possible to the total pressure of the air in the free stream ahead of the intake. The intake component could be separate from other intakes serving the aircraft, but more logically would be designed as an integral part of any primary intake supplying atmospheric air to a power plant.

The expander component of the system produces the refrigeration effect by expanding the air to permit extraction of mechanical work and, thereby, reduction of the temperature of the air. This component would logically be a steady-flow turbine of the axial or radial type. The temperature drop of the air while passing through the turbine is a function of the air temperature at entrance to the turbine, the pressure drop of the air across the turbine and the efficiency of the turbine. Load for the turbine is provided by the compressor component.

The heat sink for the auxiliaries being cooled is the heat exchanger located between the turbine and compressor. The cooled air leaving the turbine passes directly through a heat exchanger which serves all equipments being cooled. Sometimes, it may be practical to pass the refrigerated air directly over or through one or several equipments within an installation compartment. Then, the heat exchanger component of the system becomes the heat transfer surfaces of the equipment items, and no intermediate heat exchanger would be employed. Otherwise, the heat exchanger in the expanded ram air system provides an intermediate heat transfer process when the refrigerated air would cool a circulating fluid pumped through the exchanger, and the circulating fluid so cooled would be used to cool the various equipments. Evaluation to determine the suitability of the expanded ram air system for cooling equipment items in high-speed aircraft or missiles may be conducted without detailed regard to the heat transfer processes required of the circulating fluid.

The compressor component, which logically would be an axial or radial steady-flow compressor, is directly coupled to the turbine, and serves the dual purpose of providing a load for the turbine and of increasing the pressure of the air before being discharged back to the atmosphere. The air, after being heated in the heat exchanger component, is ducted directly to the intake of the compressor. Upon discharge from the compressor, the air is ducted to the exhaust component of the system. This component would discharge the air from the aircraft parallel to the direction of flight when the drag imposed by the system on the aircraft is to be minimized. Otherwise, it might be discharged through a flush opening in the aircraft's skin normal to the direction of flight or into another compartment of the airframe.

For aircraft designed to operate at supersonic speed, it is entirely possible that a thermal sink is carried by the aircraft which is at a temperature above or nearly equal to the desired operating temperatures of the equipments, but at a temperature lower than that of air taken aboard the aircraft. Thus, the thermal sink would not be available for direct cooling of the equipments. Also, since the thermal sink might be the fuel for the power plants or some other liquid carried specifically for cooling purposes, it may not always be feasible to employ direct, liquid cooling of the equipments even if the liquid temperature level is sufficiently low for direct cooling. The thermal sink would be best utilized, therefore, by precooling the air used by the expanded ram air system before it enters the turbine component of the cycle. A heat exchanger placed in the air duct between the intake and the turbine would be employed for precooling the air. By this addition, the expanded ram air system provides greater refrigeration effect, and would be applicable for cooling of auxiliaries in aircraft operating at much higher flight speeds than for the expanded ram system without a precooler.

This section is concerned with a study of several expanded ram air systems, with and without precooling of the air, to determine the suitability of this type of system for cooling auxiliaries in high-speed aircraft and missiles. Component sizes and weights are evaluated for various cooling capacities and operational conditions of the aircraft. A heat exchanger, rather than an equipment, is used in the study as the component by which the heat is rejected to the cooling air. The average temperature of the heat exchange surfaces

within the exchanger is varied in the range 140 to 440°F. Flight altitude and speed for the study are 40,000 to 80,000 feet and Mach 1.5 to 3.0, respectively.

SUMMARY

General performance and physical characteristics for the expanded ram air system are presented. The heat exchange component is assumed to be a tubular heat exchanger with the refrigerated air flowing through the tubes. Both radial and axial turbines and compressors are considered and external dimensions of the units are presented.

The expanded ram air system appears as a practical means for cooling aircraft equipments when 1) the desired temperature level for the equipments is in the range of 200 to 500°F, 2) a source of air at a pressure above the ram air pressure, such as bleed air from the mechanical compressor of a turbojet engine, is not available, 3) the design flight speed is within the Mach number range 1.0 to 2.5, 4) the design flight altitude is below 80,000 feet, 5) the design flight time is about 1.5 hours or greater, 6) an efficient ram air intake can be provided, 7) the total cooling load is 750 watts or greater and 8) the relative location of the various equipments to be cooled is such that the expanded ram air system can be designed as a central cooling system.

Systems employing radial turbines and axial compressors are superior in overall performance and size to those employing any other combination of axial and radial turbines and compressors. A system having an axial turbine and axial compressor has only slightly less bulk than one with a radial turbine and axial compressor. Any system employing a radial (centrifugal) compressor has considerably more bulk, whether the companion turbine is radial or axial.

The bulk of a heat exchanger, radial turbine and axial compressor combination is on the order of 1/4 cubic foot per kilowatt cooling capacity within the range of operational and flight conditions for which the system is best suited. Similarly, the bulk of a heat exchanger, axial turbine and radial compressor amounts to about 1/3 cubic foot per kilowatt cooling capacity. For the former combination, the bulk would be nearly evenly distributed between the three components. For the average application, the bulk of an entire system would be on the order of 1/2 cubic foot per kilowatt cooling capacity, excluding the bulk of transfer lines and other auxiliary equipment associated with the heat transfer process between the surfaces of the equipments to be cooled and the heat exchanger in the expanded ram air system.

The weight of expanded ram air systems designed to operate within the range of operational and flight conditions for which they are best suited would be on the order of 15 to 25 pounds per kilowatt cooling capacity, depending upon the distance to intake and exhaust from the turbine, heat exchanger and compressor combination.

Use of a precooling heat exchanger ahead of the turbine for reduction of the air temperature before expansion of the air through the turbine is an effective means for extending the operation of the system to high flight speed. The precooler is applicable only when a coolant is available which is not suitable for direct cooling of the equipments and is at a temperature below the temperature of the ram air. Precooling in an expanded ram air system should be considered as an auxiliary or secondary method of providing additional cooling capacity or extending the permissible operational range.

DESCRIPTION OF SYSTEMS AND EVALUATION METHODS

1. System Designs

A variety of designs for an expanded ram air system is possible by employing various types of components. Since, however, details of all possible system designs could not be evaluated, it was necessary to select as a basis for study several designs which are representative and include all basic system components. Two basic system designs selected for study are illustrated schematically in Figures I-1 and I-2. The design shown in Figure I-1 is an expanded ram air system having an axial-flow turbine and a radial-flow compressor. The design shown in Figure I-2 is a expanded ram air system having a precooling heat exchanger, a radial-flow turbine and an axial-flow compressor and turbine and the system with and without precooling are included in the study.

With reference to Figure I-1, station 0-0 defines the state of the atmospheric air ahead of the aircraft where the pressure and temperature are defined by the flight altitude. Station A-A represents the discharge plane of the diffuser where both pressure and temperature of the air are appreciably above those for the ambient atmosphere defined by station 0-0. The state of the air at entrance to the turbine is defined at station B-B. Total temperature at B-B would always be very nearly equal to that at station A-A, but the total pressure at B-B is always less than at A-A because of frictional resistance to flow imposed by the duct length. Conditions at discharge of the turbine are defined by station C-C, where both pressure and temperature are appreciably below those at station B-B. Station C'-C' defines the state of the air in the inlet planes of the tubes within the heat exchanger. The total temperature at C'-C' equals that at discharge of the turbine but the total pressure here has been decreased to a slight extent because of loss in the inlet header of the heat exchangers.

The total temperature of the air during passage through the heat exchanger is increased due to rejection of heat by the coolant flowing in crossflow over the external surfaces of the tubes. The total pressure of the air at discharge of the heat exchanger, station D'-D', is lower than at entrance to the exchanger as the result of frictional and momentum change effects occurring during flow through the tubes. Station D-D defines the state of the air at entrance to the centrifugal compression. The compressor for the system is designed for maximum air capacity in order to minimize its size for any specified cooling capacity of the system. The state of the air at discharge of the compressor is defined by station E-E, at entrance to the

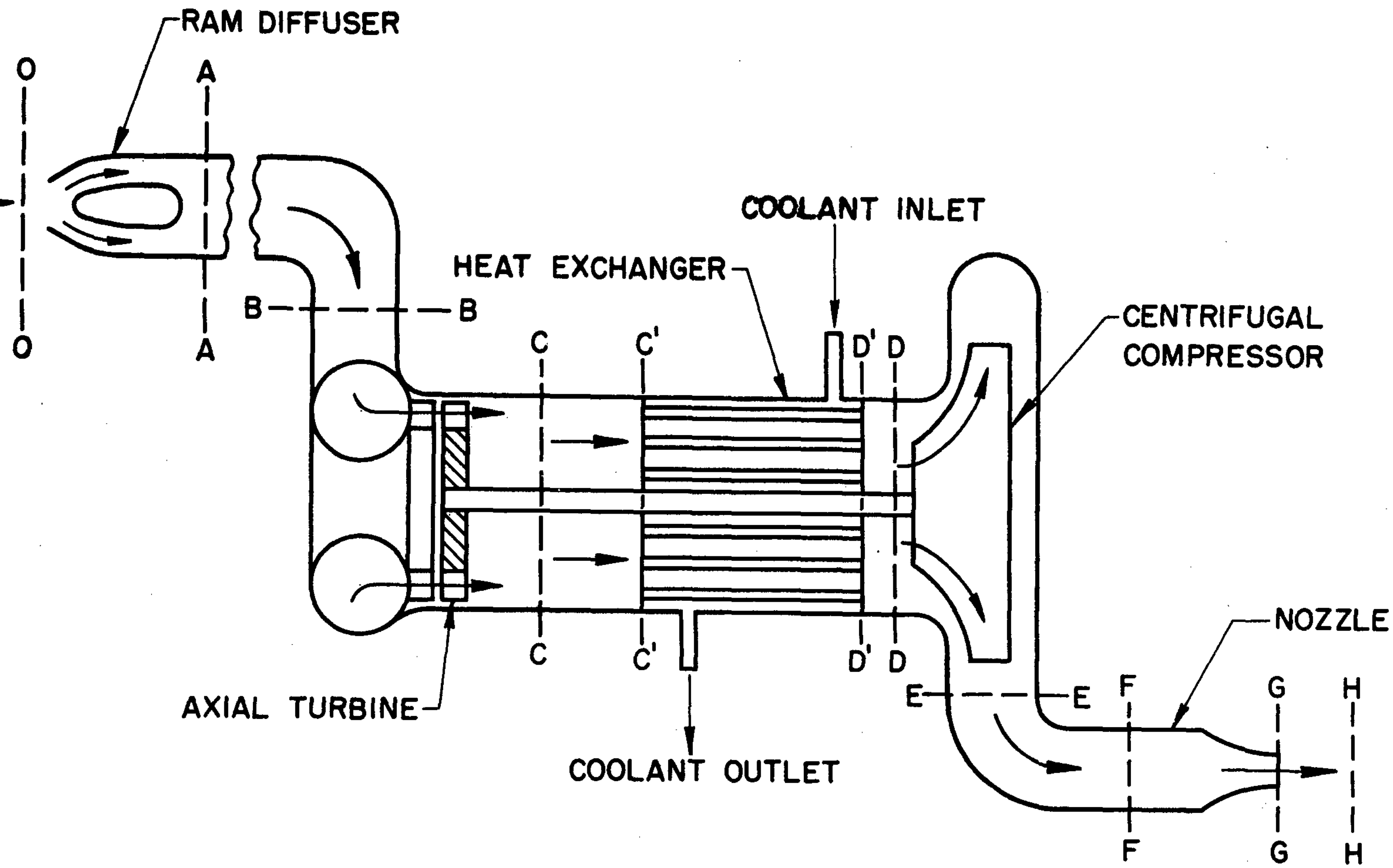

Figure I-1
Schematic of Expanded Ram Air System with Axial
Turbine and Radial Compressor

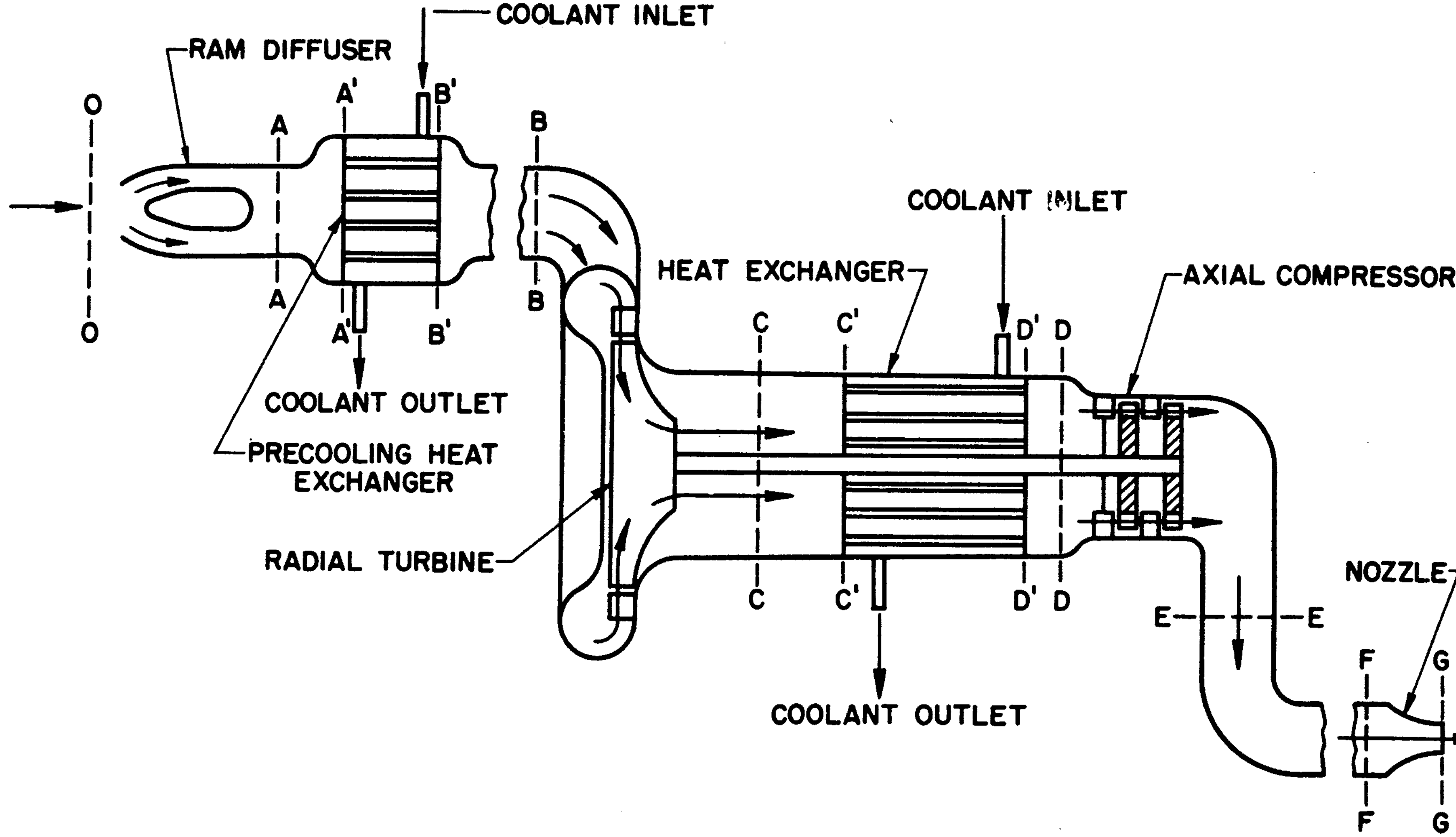

Figure I-2
Schematic of Expanded Ram Air System with Radial Turbine, Axial Compressor, and Precooler

exhaust nozzle F-F, at the exit plane of nozzle G-G and in the final region of discharge by H-H. Only convergent exhaust nozzles are considered. Thus, in some instances the pressure in the exit plane, station G-G, exceeds the back pressure on the nozzle, station H-H. The pressure in the discharge region, station H-H, would be higher than the ambient atmospheric pressure, station O-O in many installations.

Figure I-2 illustrates schematically an expanded ram air system employing a radial-flow turbine and an axial-flow compressor. Also shown in this schematic is the location of the precooling heat exchanger when employed as a part of the system. The various stations located throughout the system define states of the cooling air corresponding to those previously defined for the system shown in Figure I-1, with the exception of stations A'-A' and B'-B' which define the state of the air at inlet and exit of the precooling heat exchanger, respectively.

2. Evaluation Methods

Methods used for analyzing the performance and physical characteristics of expanded ram air systems are presented in the Appendix to this section. The analytical methods are based on conventional one-dimensional theory for steady compressible flow. Losses and inefficiencies for the various components have been included in the analysis by applying correction factors to ideal changes of state. The interrelation of heat transfer and fluid friction for the heat exchanger component is handled in a rational procedure by considering the exchangers of tubular construction and the air used by the expanded ram system as flowing through the tubes. Evaluation of pressure loss due to this component for any specified cooling capacity is based on compressible flow theory. Procedures of evaluation and working charts used to determine results presented in this section are included in the Appendix to this section.

PHYSICAL CHARACTERISTICS AND PERFORMANCE OF SYSTEMS

Numerous expanded ram air systems were designed and evaluated to determine how their physical characteristics and performance would be affected by operational conditions and design requirements. Size of the heat exchanger, turbine and compressor components were determined and are shown in the plots subsequently presented. The weight of the heat exchanger component is also given. Weights of the turbine and compressor components are not presented, but may be defined by comparing the required size of the units with those of existing turbines and compressors.

General results presented for the system with axial turbine shown in Figure I-1 are based on turbine design for 70 per cent peak efficiency, nozzle discharge angle of 20 degrees and a pitch-line velocity of the turbine buckets equal to 45 per cent of the theoretical spouting velocity. The theoretical spouting velocity of the turbine represents a measure of the energy released by the air within the turbine, and a pitch-line velocity of the buckets equal to roughly 45 per cent of the velocity insures designs

operating at or near the peak efficiency. The selection of 70 per cent for the peak efficiency of the turbine is based on a study of peak efficiencies for small radial and axial turbines where it was found that, although higher peak efficiencies are sometimes attained, the value of 70 per cent defines a conservative average value which can be attained for most units without undue design effort and resulting excessive weight or bulk. Somewhat greater refrigeration capacity is obtained with a peak efficiency of 75 per cent, but this increase is found to have only a minor effect upon the required sizes of the system components. The selection of a design nozzle angle for the turbine of 20 degrees represents a compromise between weight and peak efficiency for the unit. Increasing the nozzle angle increases the air handling capacity of the turbine, thereby decreasing the required size for any required air rate, but lowers the peak efficiency. The product of the mechanical efficiencies for the turbine and compressor has been assumed equal to 90 per cent, representing mechanical losses of approximately 5 per cent of the turbine output for both turbine and compressor.

The mechanical efficiencies of the turbine and compressor do not affect overall system performances to any appreciable extent. A low mechanical efficiency reduces the power available for compression of the air, which in turn affects the exhaust velocity and correspondingly the drag, but does not influence the primary components or the cooling capacity of the system. Similarly, high operating efficiency for the compressor would not be considered of principal importance to the system performance, since an increase would be beneficial only from the standpoint of drag imposed on the aircraft by the system. As a matter of fact, reduction in the desired efficiency level of the compressor would permit some reduction in the required size of the unit and may result in a net practical advantage for the application of the system, even though drag is increased. Centrifugal compressors having impellers of 12-inch diameter are assumed to have a peak efficiency of 70 per cent, and 2-inch impellers about 60 per cent. The peak efficiency is arbitrarily assumed to vary linearly with size ofthe impeller within this range.

The efficiency of the diffuser is assumed to vary with the flight Mach number, being 90, 80 and 70 per cent for flight Mach numbers of 1.0, 2.0 and 3.0, respectively. A study of performance of supersonic diffusers is used as the basis for selection of this variation.

Maximum compactness and heat exchange capacity for the primary heat exchanger of the system is obtained by use of tubes having small diameter. A tube diameter of 0.20 inches is selected for use with all systems designed and evaluated. The total pressure loss of the air from discharge of the diffuser to entrance of the turbine is assumed equal to 2 per cent of the total pressure of the air developed by the diffuser, except when a precooling heat exchanger is used. Similarly, the total pressure loss of the air from discharge of the compressor to entrance of the exhaust nozzle is assumed equal to 2 per cent of the total pressure of the air at discharge of the compressor. Discharge pressure at exhaust, station H-H in Figure I-1, is assumed to be equal to the ambient atmospheric pressure, station 0-0.

Radial turbines employed in systems illustrated in Figure I-2 are assumed to have a peak efficiency of 70 per cent for a ratio of the tip speed of the

wheel to the theoretical spouting velocity of 0.60. Axial compressors are designed on the basis of the rotor tip Mach number equal to unity and the relative flow velocity of the air over the tip section of the blades corresponding to a flow Mach number of 0.80. When precooling of the ram air is used, the precooling heat exchanger is assumed to have an effectiveness of 0.80.

1. Nomenclature

Nomenclature used in Figures I-3 through I-22 is summarized below for ready reference and identification of the various variables. A complete list of nomenclature used for analysis and evaluation of this system is given in the Appendix to this section.

A_o flight altitude, ft.

d_{CA} external diameter of axial compressor, psi.

d_{CC} external diameter of centrifugal compressor, in.

d_{TA} external diameter of axial turbine, in.

d_{TR} external diameter of radial turbine, in.

d_x diameter of heat exchanger, in.

M Mach number, dimensionless

q_c cooling capacity of system, watts

T_w average surface temperature of heat exchanger, °R.

ΔT temperature difference of surface of heat exchanger and air at discharge of turbine, °F.

W_x weight of heat exchanger, lb.

x length of heat exchanger, in.

δ ratio of absolute pressure of air to 14.7 psi abs., dimensionless.

η_t adiabatic efficiency of turbine, dimensionless.

σ effectiveness of heat exchanger, dimensionless.

2. Effect of Cooling Capacity on System Requirements

The cooling capacity of an expanded ram air system designed to operate under specified flight and environmental conditions would vary in direct

proportion with the air rate handled by the system. Since the flow cross-sectional areas required to handle the airflow vary in direct proportion to the air rate, other design conditions being equal, it would be expected that diametrical dimensions of the system's components increase very nearly in proportion to the square root of the cooling capacity of the system.

Results of one study to determine the effect of cooling capacity on system size are presented in Figure I-3. The system employs an axial-flow turbine and a centrifugal compressor, and has the general arrangement of that illustrated schematically in Figure I-1. Flight conditions are for an altitude of 80,000 feet and a Mach number of 2.0. The average temperature of the tube surface in the heat exchanger is 240°F, indicating that the various equipment items being cooled would be maintained at surface temperatures in the range of 300 to 450°F. The heat exchanger for the system is designed for an effectiveness of 0.50 and a total pressure loss of 10 per cent of the total pressure at entrance to the exchanger.

Variation of the external diameters of the turbine, heat exchanger and compressor is, for all practical purposes, in proportion to the square root of the cooling capacity. The spatial requirements of the turbine, heat exchanger and compressor amount to roughly 1/3 cubic foot per kilowatt cooling capacity.

An entire expanded ram air system would occupy roughly 1/2 cubic foot per kilowatt cooling, not including the intake and exhaust components. The centrifugal compressor accounts for nearly 35 per cent of the total space required, the axial turbine about 20 per cent, the heat exchanger about 15 per cent, and interconnecting ducts, distribution components and extra required space about 30 per cent. Systems designed to operate at maximum altitudes below 80,000 feet would have considerably reduced spatial requirement. For example, at 40,000 feet altitude the turbine, compressor and heat exchanger diameters would be 40 to 50 per cent of the values shown in Figure I-3. Systems designed for lower maximum flight Mach numbers would not require as much cooling air, but the air density throughout the system would be lower, so that possible reduction in design size with decreased maximum flight speed is not as great as with decrease in design altitude. The heat exchanger configurations for the system designs illustrated in Figure I-3 are "doughnut" shaped, having length-to-diameter ratios ranging from 0.33 to 0.70, thereby permitting compact arrangement of the compressor with the turbine.

The weight of the heat exchanger component for various system designs is shown in Figure I-4.

Weight of the heat exchanger is evaluated on the basis that it would be constructed of aluminum having tubes of 0.2 inch inside diameter and 0.015 inch wall thickness. It is assumed that the cross-sectional area of the exchanger is twice the cross-sectional flow area of the tubes, the outer shell to be of 30 gage aluminum, and that two tube sheets and one tube support, 0.0625 inch in thickness, would be used.

The weight of the heat exchanger is very nearly in direct proportion to the cooling capacity of the system. Minimum weight of the exchanger occurs

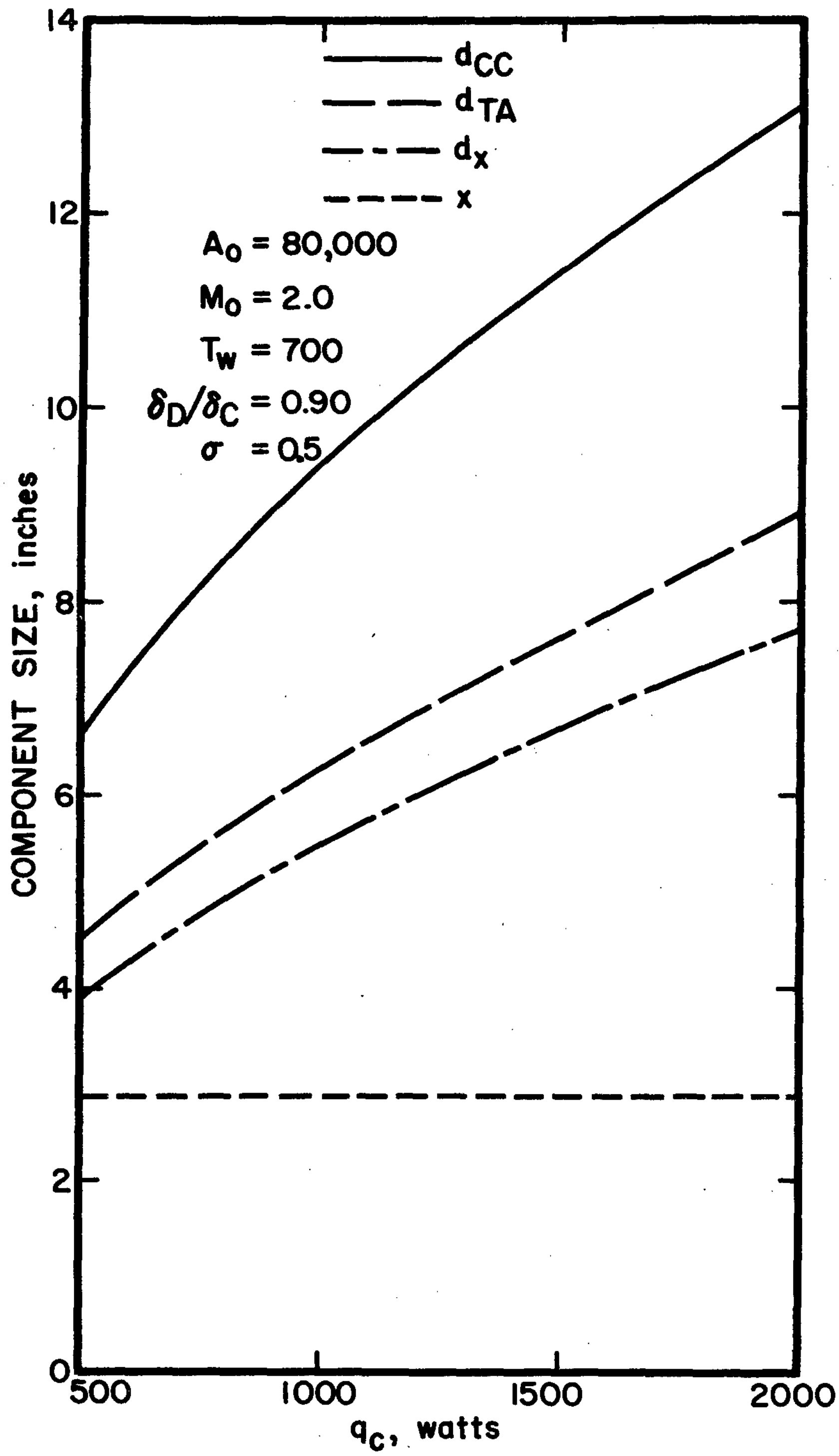

Figure I-3
Effect of Cooling Capacity on Component Size

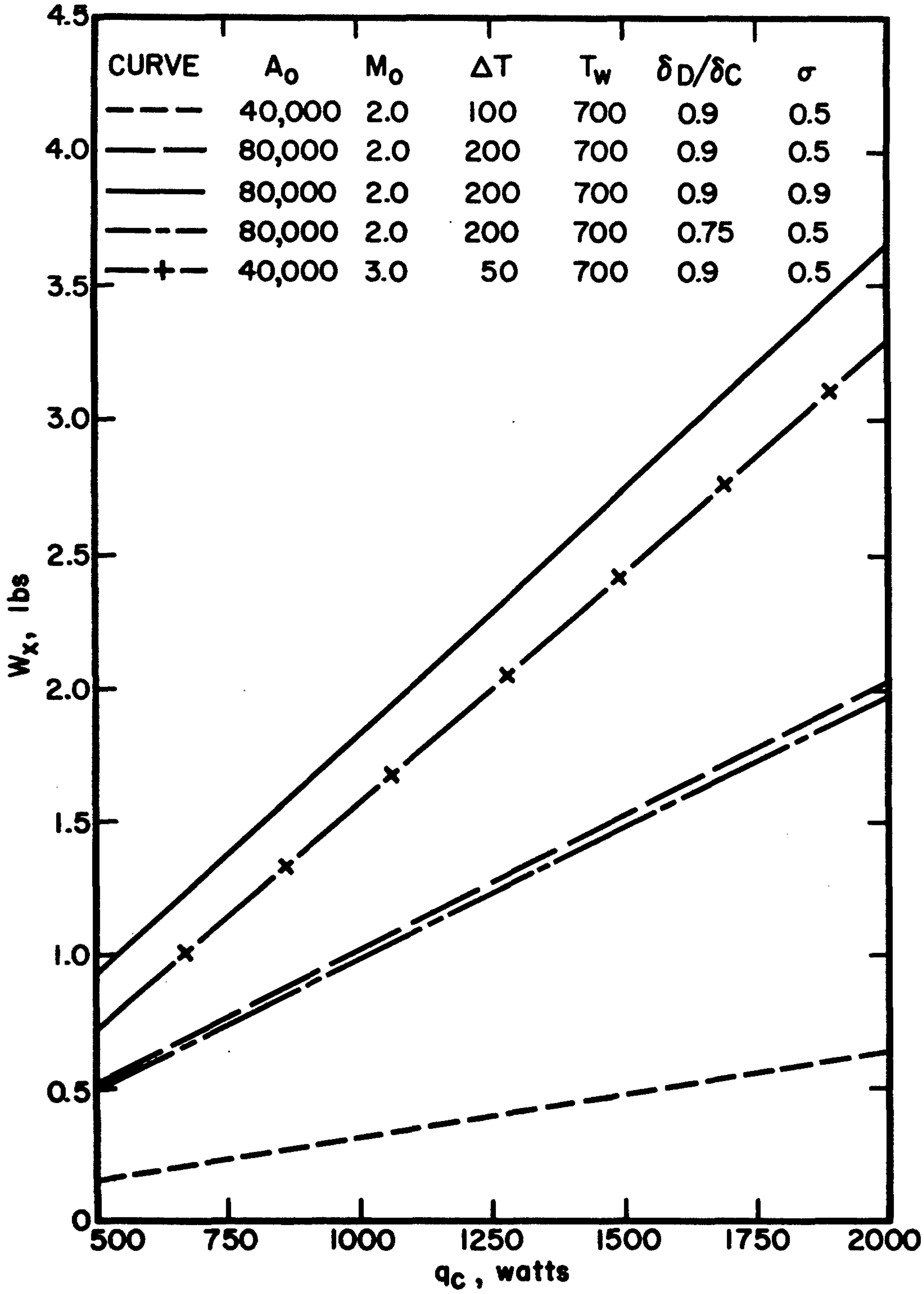

Figure I-4
Effect of Cooling Capacity on Heat Exchanger Weight

for systems designed for low flight altitude and speed and relatively low heat exchange effectiveness. Exchangers designed for high effectiveness have reduced cross-sectional area and greater length, but the required increase in length always creates a weight increase greater than the reduction due to the smaller cross-section. The weight of the heat exchanger is minimized by design for low effectiveness, σ of 0.3 or less. However, design for low effectiveness of the heat exchanger increases the required cooling air rate and, thereby, increases the required size of all other components of the system. Minimum size for the entire system is obtained, therefore, by design of the heat exchanger for high effectiveness which generally would be in the range of 0.80 to 0.95.

The increase in exchanger weight for systems designed to operate at higher flight speeds is due to the increased temperature of the air at entrance to the heat exchanger. Consequently, less heat can be dissipated in the exchanger per pound of air flowing per second and the air rate for the system must be increased. The weight of all components of the system increases with design for higher flight speed. A comparison is shown in Figure I-4 for two systems designed on a comparable basis, except for the pressure loss across the heat exchanger, being 10 per cent or 25 per cent for 80,000 feet altitude. The weight of the heat exchanger is approximately the same for both designs. The greater pressure loss permits design of the heat exchanger for higher flow velocity, but also increases the back pressure on the turbine which increases the air rate required to meet the required cooling capacity.

3. Effect of Heat Exchanger Surface Temperature and Turbine Discharge Temperature on System Requirements

The average surface temperature of the heat exchanger T_w is used as an index to the desired temperature of the equipments to be cooled. The difference of the average temperature T_a and the total temperature of the cooling air at entrance to the heat exchanger T_c is represented by ΔT, a temperature parameter useful for interpretationof the heat exchanger design. Combination of the temperature T_w and the temperature difference ΔT also defines the required temperature of the cooling air at discharge of the turbine. The effect of average surface T_w and the temperature difference ΔT on the diameters of the heat exchanger, turbine and compressor for the system shown in Figure I-1 is given in Figures I-5, I-6 and I-7, respectively. The cooling capacity of the system is 1000 watts and the flight condition is an altitude of 80,000 feet and a Mach number of 2.0. The lines of constant temperature differential ΔT shown in these plots are limited on the right by the condition that the combination of the average surface temperature T_w and the temperature differential ΔT defines a temperature of the air at discharge of the turbine equal to the total temperature of the air ahead of the turbine, i.e. the ram temperature. Thus, at this condition and for higher surface temperatures the turbine component of the system is not required and the simple ram air system is more than adequate for meeting the cooling requirements. The curves of constant temperature differential ΔT are limited on the left in Figures I-5, I-6 and I-7 by the condition when the total pressure at discharge of the turbine equals the atmospheric pressure. This limit is arbitrarily defined, since pressures below atmospheric at exit of the turbine

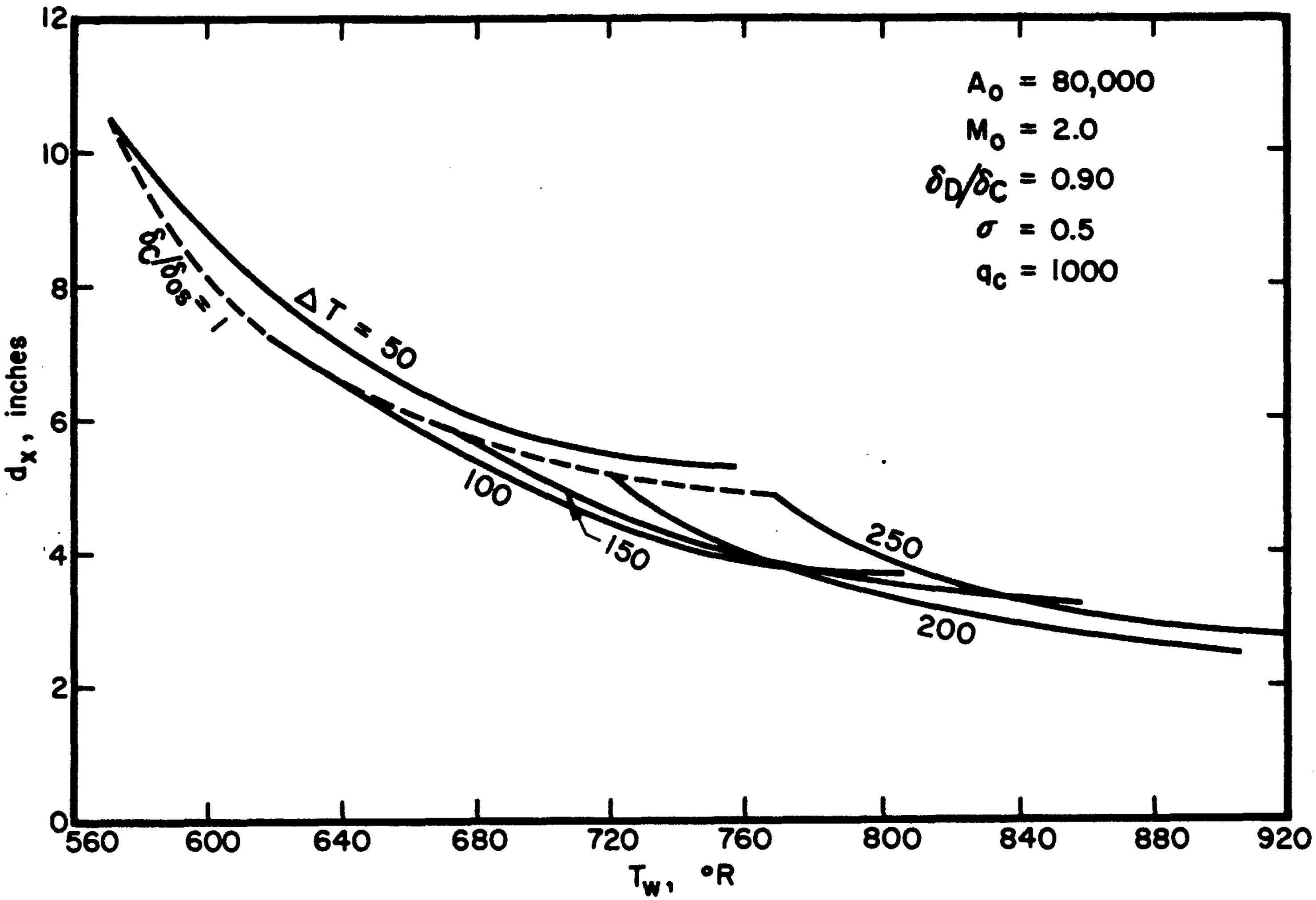

Figure I-5
Effect of Heat Exchanger Surface Temperature and Turbine Discharge Temperature on Heat Exchanger Diameter

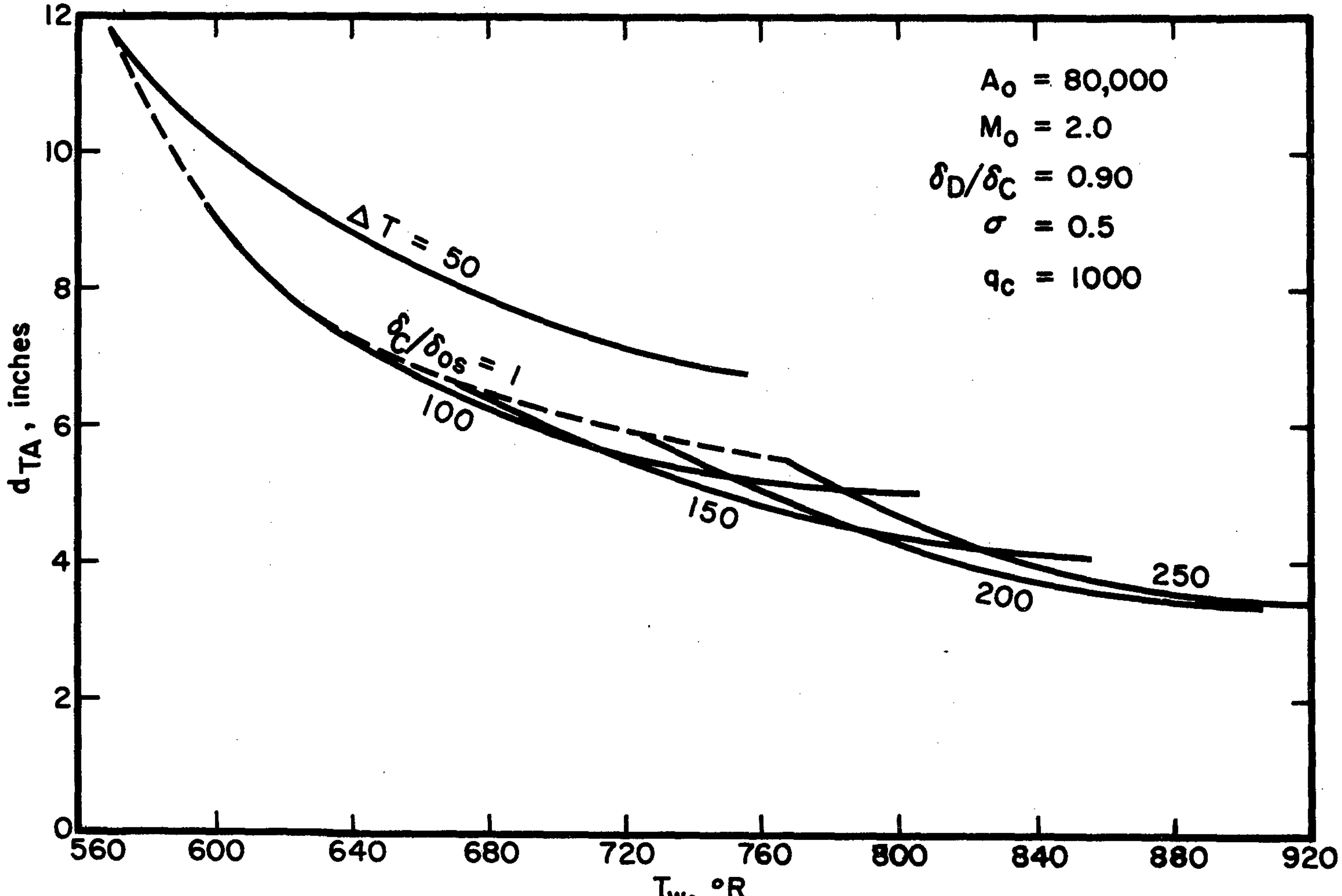

Figure I-6
Effect of Heat Exchanger Surface Temperature and Turbine Discharge Temperature on Turbine Diameter

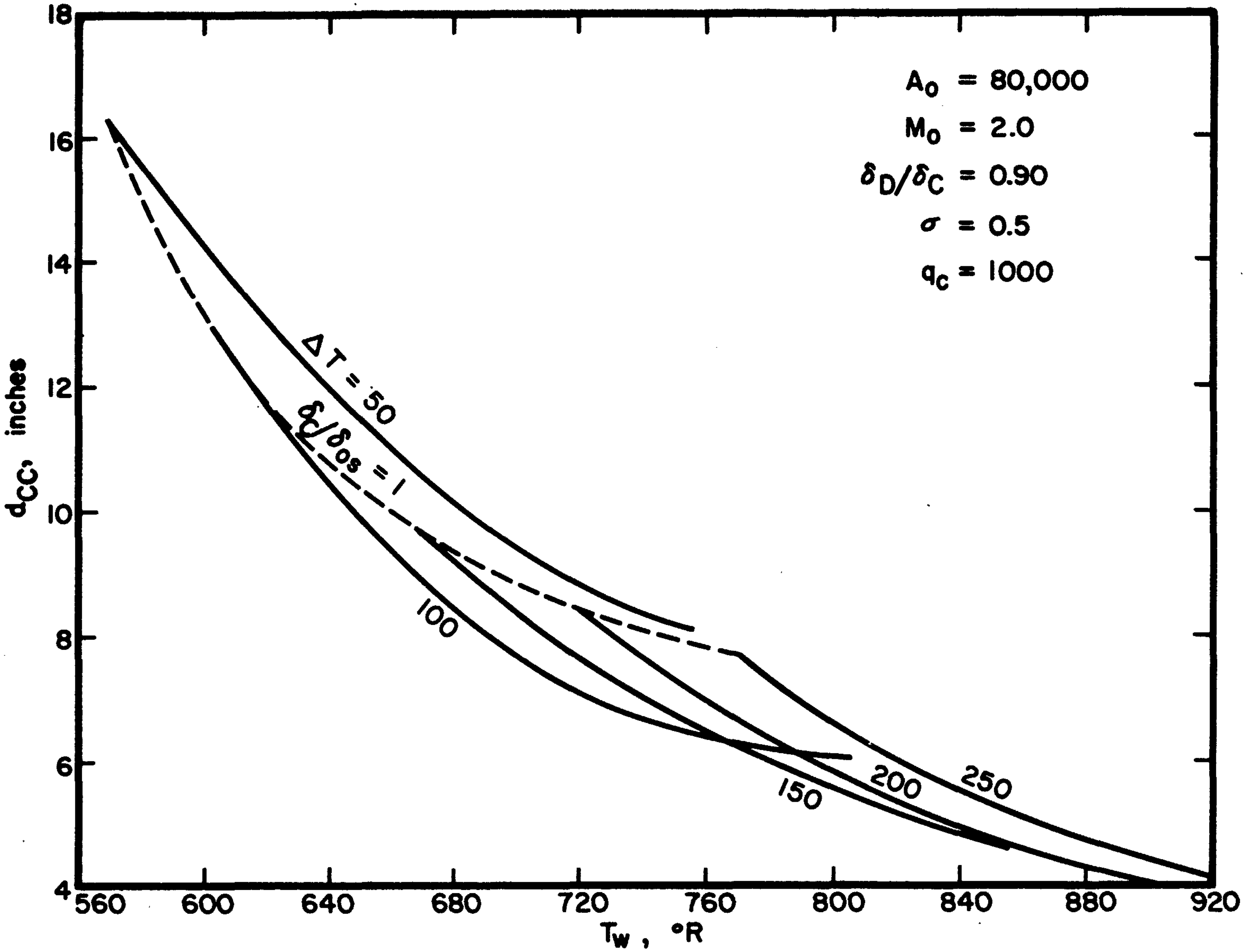

Figure I-7
Effect of Heat Exchanger Surface Temperature and Turbine Discharge Temperature on Compressor Diameter

could be employed with many designs, but the increase in cooling capacity resulting from additional expansion of the air would hardly compensate for the increased component size due to the lowered air density throughout the turbine, heat exchanger, compressor and exhaust components.

The effect of the design temperature differential ΔT on component size is not great. Design for large values of the temperature differential requires greater expansion of the air by the turbine so that the average density level of the cooling air is lowered. This effect in combination with the reduced cooling air rate required with increased temperature differential results in but small change in the component size, except when the temperature differential is quite small. The latter condition is of no appreciable importance to evaluation of the system. When the temperature level of the equipments to be cooled is in the range 400° to 500°F, necessitating an average surface temperature for the heat exchanger of about 350° to 375°F, 810° to 835°R, the optimum temperature differential ΔT is in the range 150° to 200°F; say, for example, 175°F. Thus, the temperature at discharge of the turbine would be about 650°R, and since the ram temperature for the specified flight condition is about 710°R, the required temperature drop of the air across the turbine is about 60°F. The pressure ratio of the cooling air across the turbine would be about 1.6 to 1 while the total pressure ratio developed during diffusion is nearly 5.3. Hence, maximum refrigeration of the air is not always desirable. Equipments requiring temperature levels maintained at about 200°F would necessitate an average surface of the heat exchanger in the range of 100° to 150°F, i.e. T_W from 560 to 610°R. For this temperature range the expanded ram air system should produce as large a refrigeration effect as is practically feasible. The optimum temperature differential is about 75°F, requiring the turbine discharge temperature to be roughly 50°F. The turbine expansion ratio required to produce this refrigeration effect is very nearly equal to that produced by the diffusion process of the intake, as may be noted by the dashed line shown in Figures I-5, I-6, I-7.

Size of the components is principally a function of the desired temperature level, defined by the average surface temperature T_W, the effectiveness of heat exchange and the flight altitude and speed. Two representative values of the average surface temperature T_W required for the usual types of cooling problems are 625°R and 825°R. For the specified flight conditions of 80,000 feet altitude and a Mach number of 2.0, and an effectiveness of 0.5, the required radial dimensions of the heat exchanger, axial turbine and centrifugal compressor would be 7 inches, 8 inches and 12 inches, respectively, for an average surface temperature of 625°R, and 3 inches, 4 inches and 5 inches, respectively, for an average surface temperature of 825°R. If the effectiveness of the heat exchanger would be increased to 0.9, the radial dimensions of the exchanger, axial turbine and centrifugal compressor for an average surface temperature of 825°R would be reduced to roughly 2.5 inches, 3.25 inches and 4 inches, respectively.

The axial length of the heat exchanger required for an effectiveness of 0.50, as affected by the average surface temperature of the heat exchanger and the turbine discharge temperature is illustrated in Figure I-8. The required length is 6 to 6.5 inches for turbulent flow and from about 4 to 6

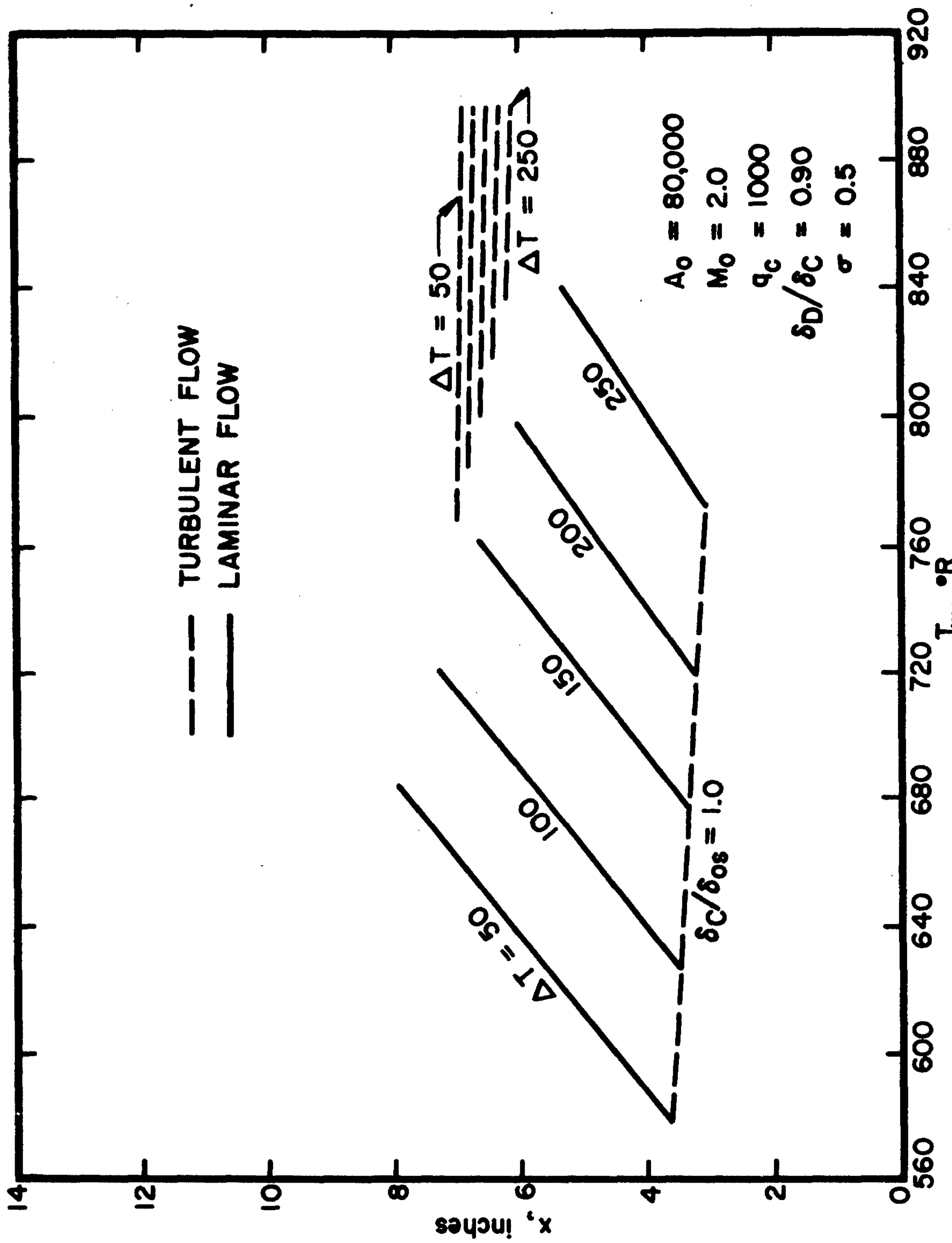

Figure I-8
Effect of Heat Exchanger Surface Temperature and Turbine Discharge Temperature on Heat Exchanger Length

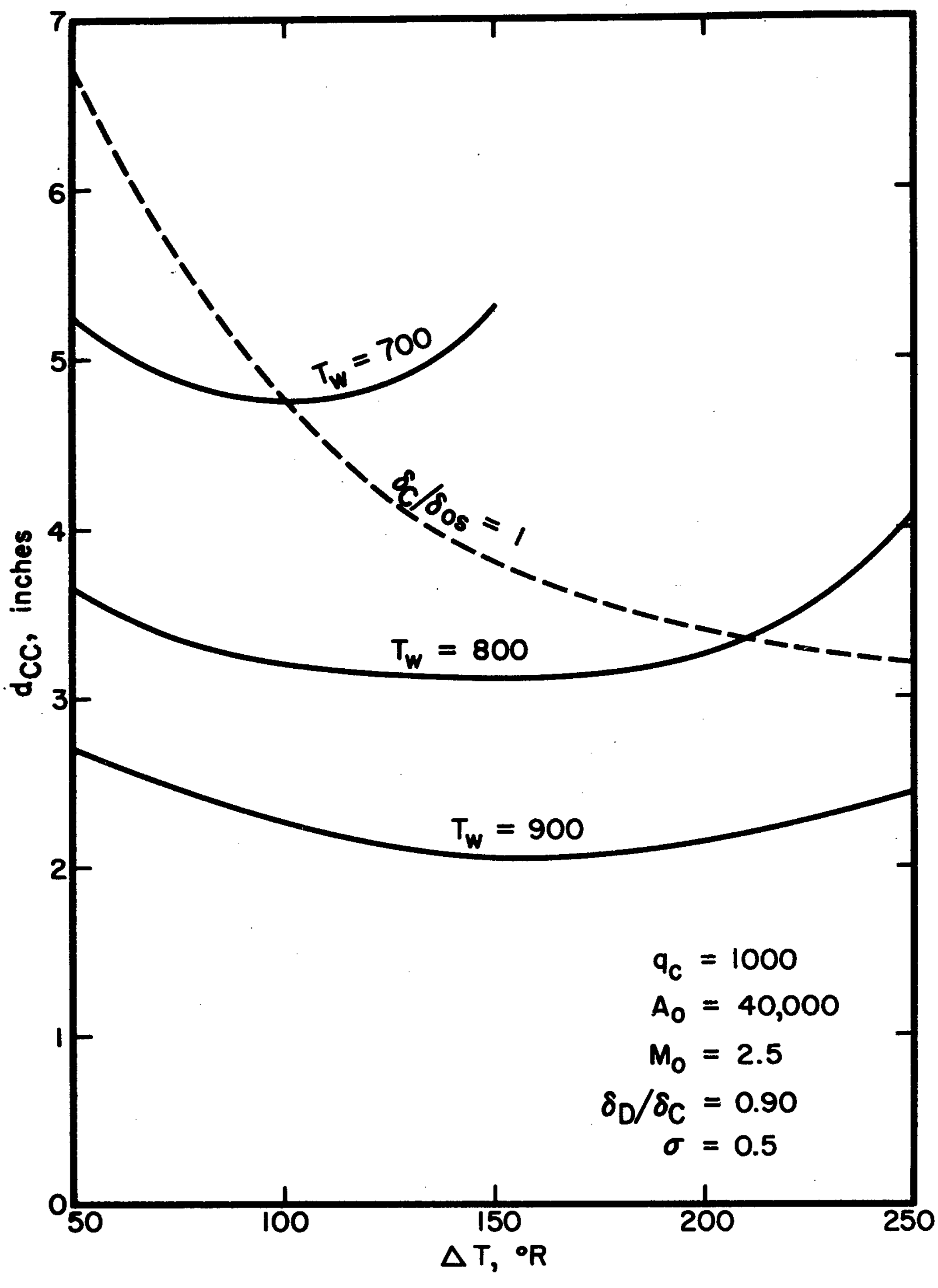

Figure I-9
Effect of Turbine Discharge Temperature at Various Heat Exchanger Surface Temperatures on Compressor Diameter

inches for laminar flow. A crossplot to illustrate the effect of the temperature difference ΔT on the required size of the radial compressor is shown in Figure I-9. The external diameter of the compressor is not greatly affected by the magnitude of the operating temperature differential ΔT.

4. Effect of Design Altitude and Flight Speed on Component Size

The influence of design altitude and flight speed on the size of the heat exchanger, axial turbine and centrifugal compressor components for various average surface temperatures of the heat exchanger is shown in Figures I-10, I-11 and I-12. Design dimensions for altitudes of 40,000 and 80,000 feet and flight Mach numbers of 1.5, 2.0, 2.5 and 3.0 are presented. Component sizes presented in these plots correspond to their minimum values, obtained by taking envelopes of the curves such as shown in Figure I-5, I-6, Radial dimensions of the three components vary about as the square root of the ambient air density. The ratio of air density at 80,000 feet to that at 40,000 feet is about 0.15, so that component sizes for design at 40,000 feet are very nearly 40 per cent of those required for a design altitude of 80,000 feet. The effect of design flight speed on component size is appreciable at flight Mach numbers above about 2.0. The radial dimensions increase roughly 75 per cent for typical designs when the design flight Mach number is increased from 2.5 to 3.0. The components are relatively small in size for design Mach numbers below 2.0 and design altitudes below about 60,000 feet. Increasing the design heat exchanger effectiveness from 0.5 to 0.9 would reduce the radial dimensions for the three components by about 25 per cent. Thus, for an expanded ram air system having an axial turbine, radial compressor and heat exchanger having an effectiveness of 0.90, the radial dimensions of these three components required for a system designed to produce 1000 watts cooling at a flight Mach number of 2.0, an altitude of 80,000 feet and an average surface temperature of the heat exchanger of 700°R would be about 4.3 inches, 5.9 inches and 3.7 inches, respectively. It would appear that weight and spatial requirements of this type system required for a cooling capacity greater than about 1500 watts are excessive when the design operational condition is for flight Mach numbers of 2.5 and higher at altitudes above about 60,000 feet. Required component size appears reasonable for systems applied to aircraft operating at Mach numbers below 2.5 and altitudes in the range from sea level to 60,000 feet.

The influence of design altitude on component sizes for the system shown in Figure I-1 is presented in Figure I-13 for flight Mach numbers of 2.0 and 3.0. Increase in component size required at higher altitude is due entirely to reduced density level of the cooling air. The large component sizes required for high altitude and high flight Mach number are apparent from this plot. Component sizes required for various values of the average surface temperature of the heat exchanger are shown in Figure I-14. The turbine design is controlled to provide a constant discharge temperature of 500°R. Thus with constant turbine discharge temperature, the degree of expansion of the air through the turbine remains constant and the resulting air density at entrance to the heat exchanger is constant. For the specified cooling capacity of 500 watts, as the inlet temperature differential ΔT increases, due to higher surface temperature, a reduced flow rate is required and the radial dimensions required for the various components decrease.

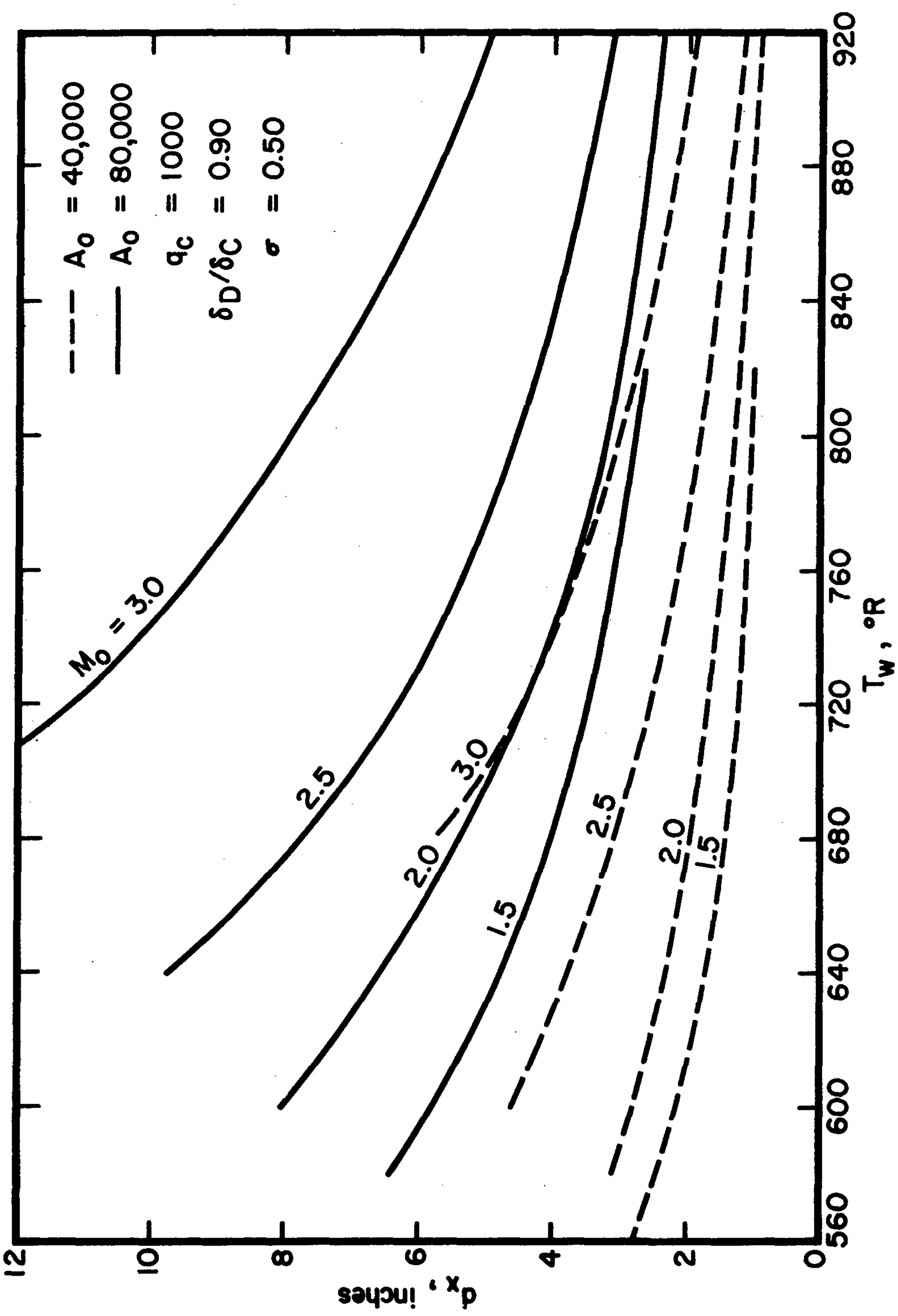

Figure I-10
Effect of Design Altitude and Flight Speed on Heat Exchanger Diameter

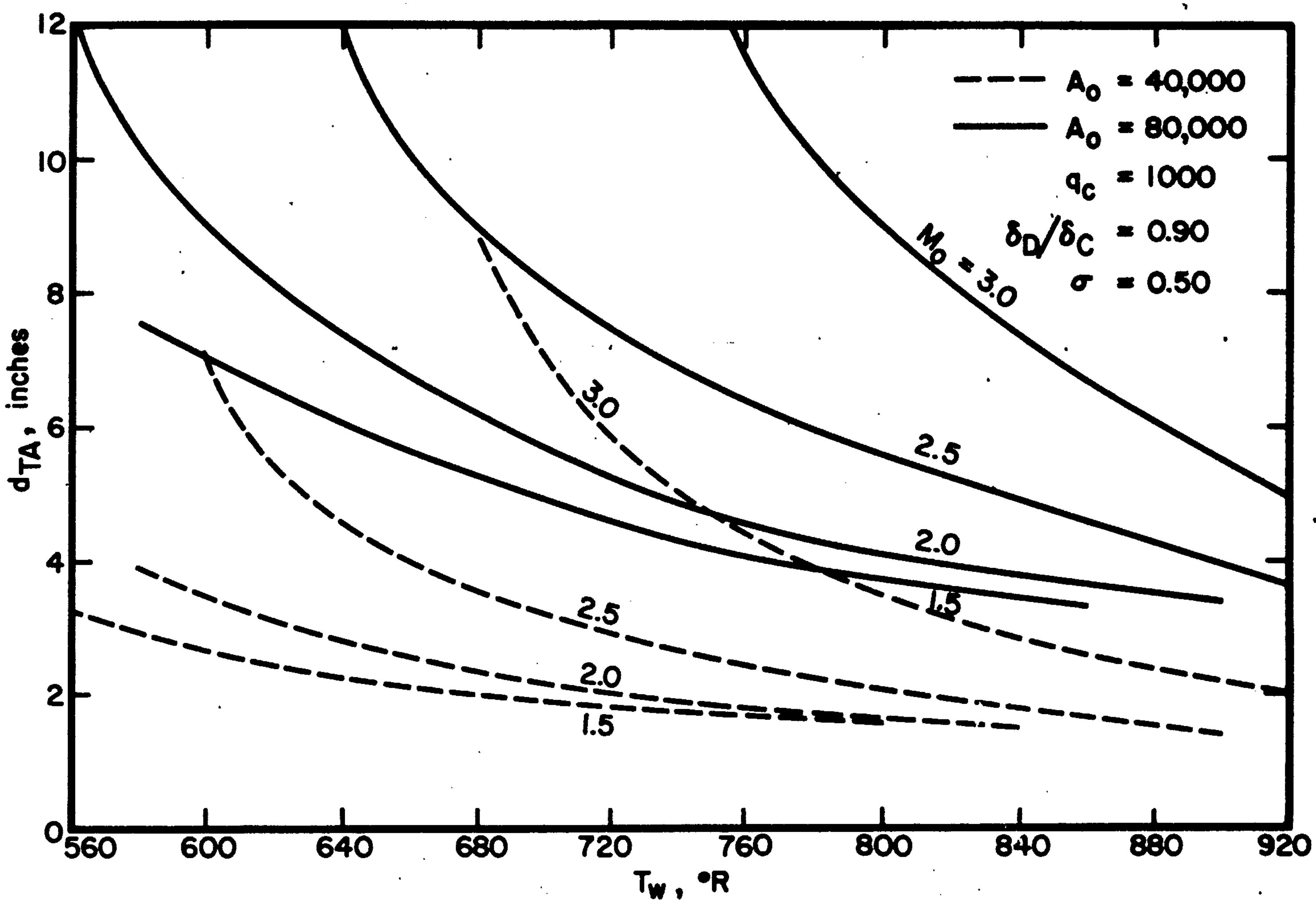

Figure I-11
Effect of Design Altitude and Flight Speed on Turbine Diameter

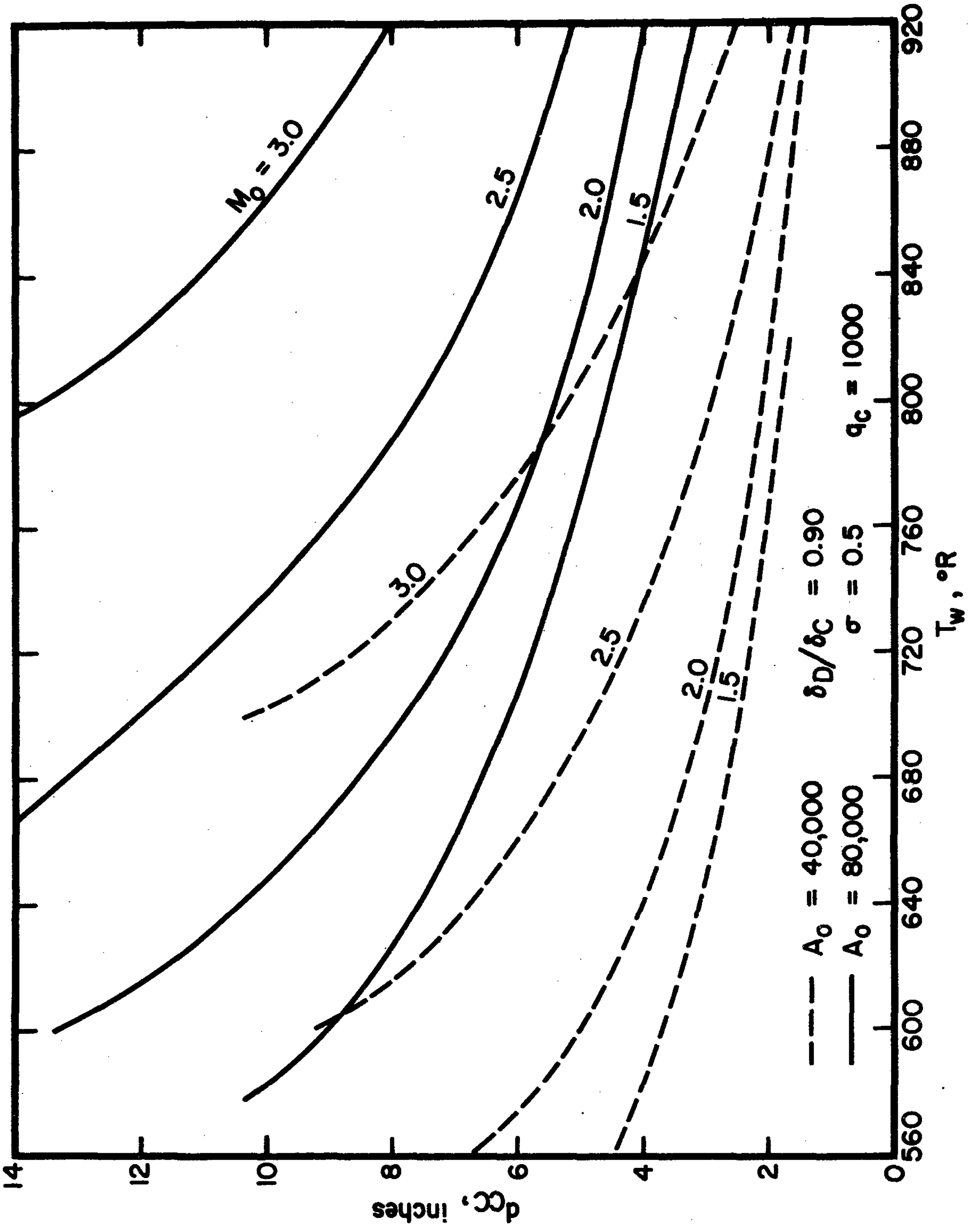

Figure I-12
Effect of Design Altitude and Flight Speed on Compressor Diameter

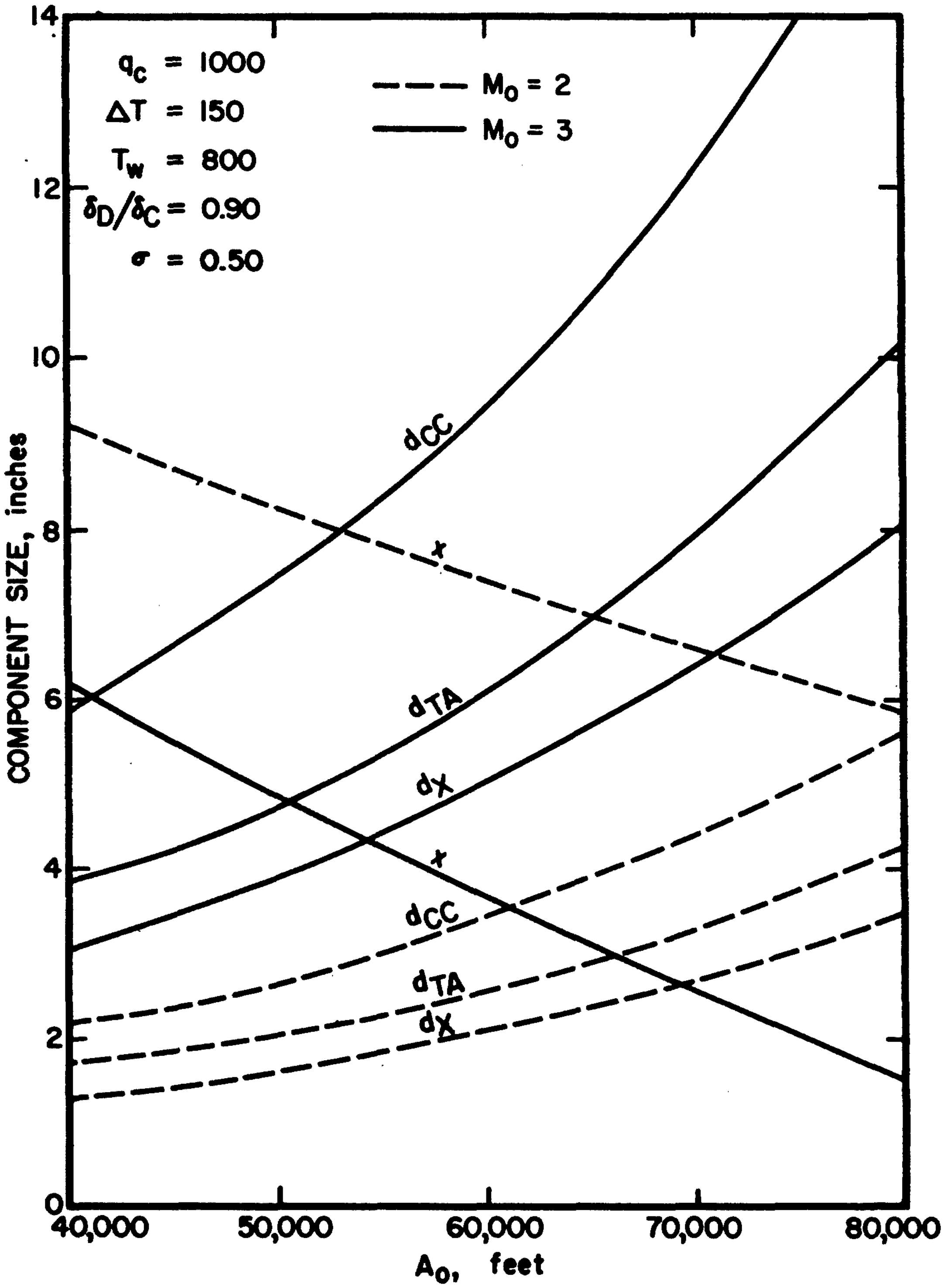

Figure I-13
Effect of Design Altitude on Component Sizes

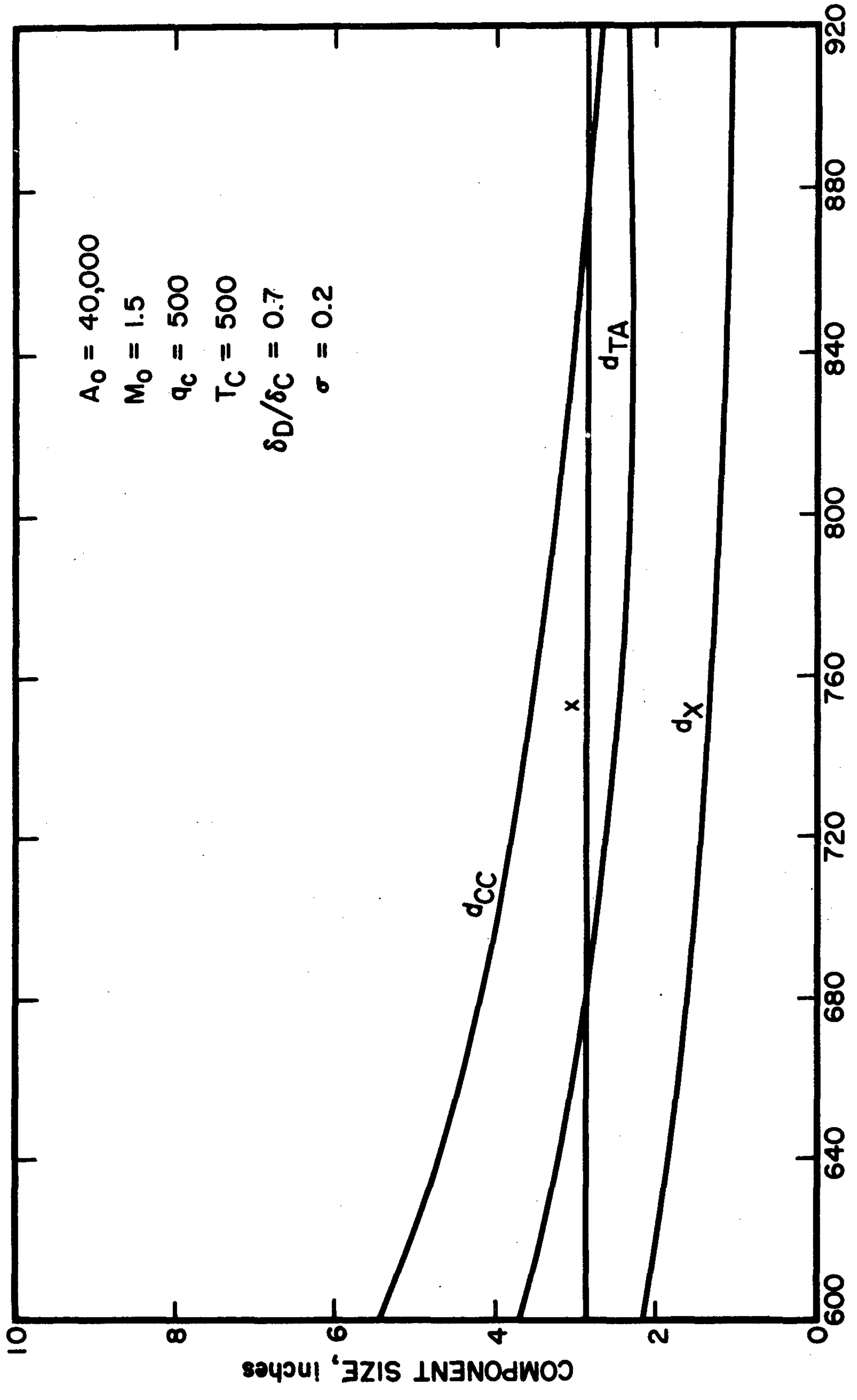

Figure I-14
Effect of Heat Exchanger Surface Temperature on Component Sizes

5. Comparison of Axial and Radial Turbines and Compressors

The expanded ram air system could employ a radial or axial turbine for the expansión component in the cycle and, likewise, could employ a radial or axial compressor for the compression component. Physical characteristics of expanded ram air systems presented throughout the preceding discussion have been for the system shown in Figure I-1, which employs an axial turbine and a radial compressor. This section considers the system shown in Figure I-2, which employs a radial turbine and an axial compressor, as well as the relative merits of axial versus radial units.

For expanded ram air systems, the axial compressor is superior to the radial compressor because of its greater air flow capacity per unit frontal area and higher rotational speeds. These two features permit reduction of not only the weight and space of the compressor component, but also of the turbine component, whether for a radial or axial turbine. Axial compressor design employed for the expanded ram air system favors air flow capacity over efficiency and pressure producing ability. In other words, the axial compressors are not designed to attain maximum efficiency or produce the greatest increase in air pressure, rather the emphasis is placed on design for small size and weight. Design of this type results in an increased drag on the aircraft created by the cooling air, but a reduced drag due to the lowered weight of the cooling system. Depending upon the type of aircraft and its operational conditions, a net reduction in drag would be expected with most systems when the axial compressor is employed.

The differences in performance and physical characteristics for radial and axial turbines are not as pronounced as for the axial and radial compressors. The radial turbine is somewhat larger than an axial unit, when operating with the same type compressor, but has the important advantages of somewhat higher efficiency and better rotor proportions, particularly when the required size is small. From an overall viewpoint, it appears that expanded ram air systems employing radial turbines and axial compressors are superior to those having axial turbines and radial compressors.

A comparison of the external diameters for axial and centrifugal compressors is presented in Figure I-15. The comparison is shown for a range of values for the average surface temperature of the heat exchanger, altitudes of 40,000 and 80,000 feet, and flight Mach numbers of 1.5, 2.0 and 3.0. The centrifugal compressor is driven by an axial turbine, as illustrated in Figure I-1, and the axial compressor by a radial turbine, Figure I-2. For comparable operational conditions of the system, the external diameter of the axial compressor is from 40 to 50 per cent of that required of the centrifugal compressor. The length of an axial compressor for an expanded ram air system would be somewhat greater but comparable to that of a centrifugal compressor. Thus, the spatial requirements are greatly reduced,as would be the weight. Savings in weight, and space of a system employing an axial compressor in favor of the centrifugal unit are greatest at high flight Mach number and low average surface temperature of the heat exchanger.

Relative size of axial and radial turbines are shown in Figure I-16 for various values of the average surface temperature of the heat exchanger, flight

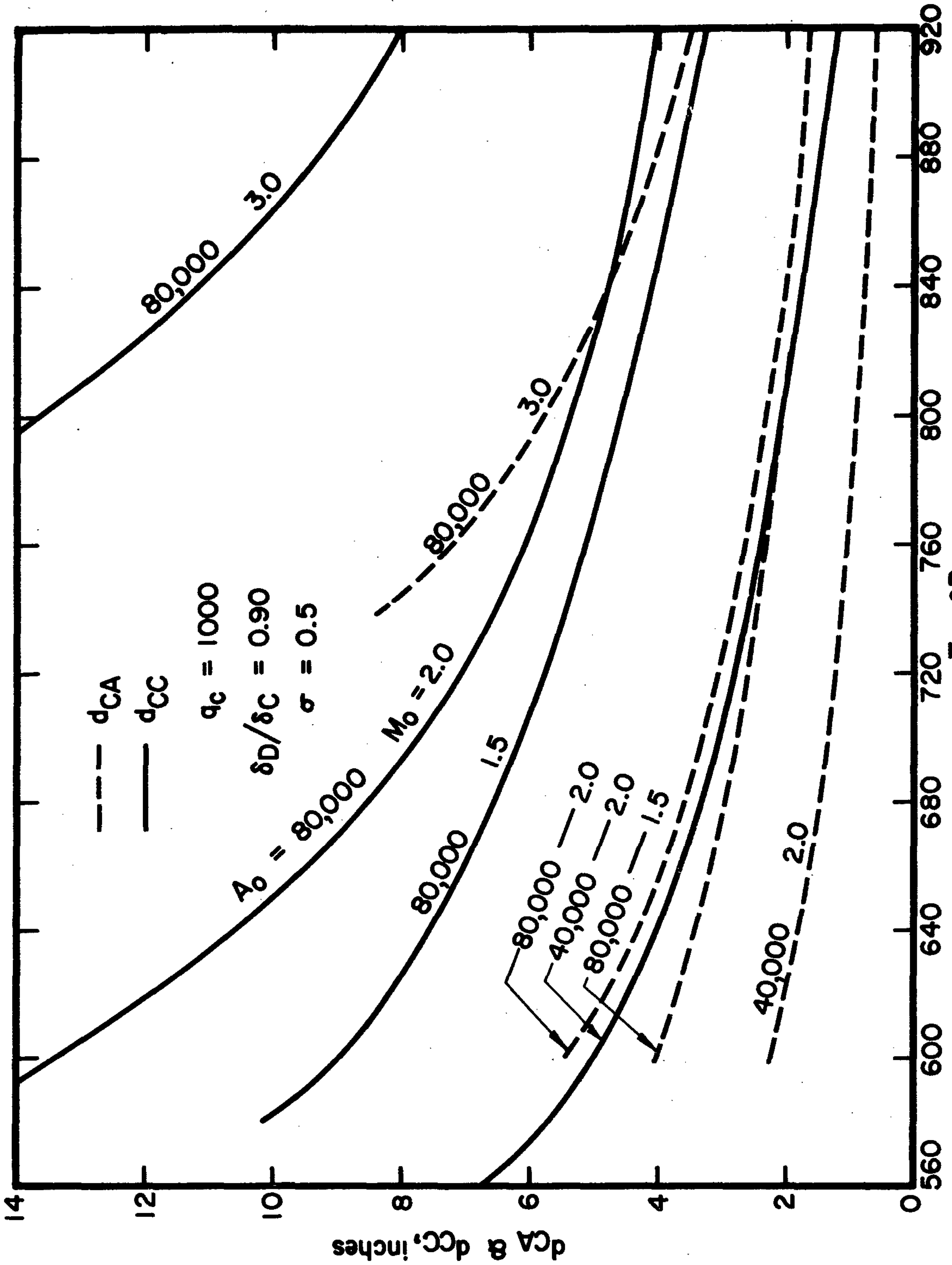

Figure I-15
Comparison of Diameters of Axial and Centrifugal Compressors, Including Effects of Heat Exchanger Surface Temperature, Design Altitude, and Flight Speed

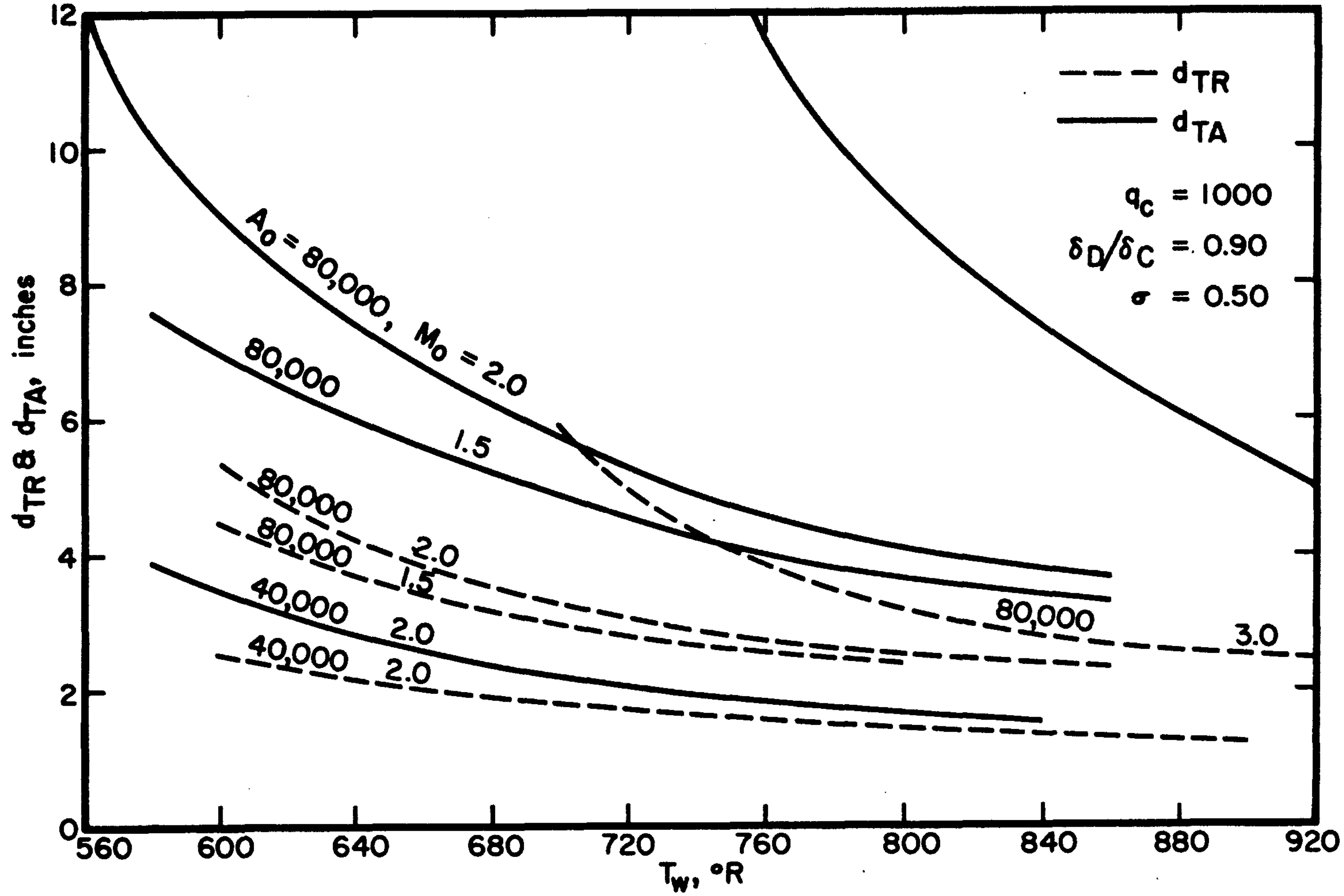

Figure I-16
Comparison of Diameters of Radial and Axial Turbines, Including Effects of Heat Exchanger Surface Temperature, Design Altitude and Flight Speed

Mach number and flight altitude. The radial turbine drives an axial compressor, Figure I-2, and the axial turbine drives a radial compressor, Figure I-1. Differences in size are not great for operational conditions of low altitude, say below 60,000 feet, and flight Mach number below about 2.0. In this range the external diameter for the axial turbine is from 60 to 70 per cent of that required for the radial turbine. Under operational conditions of high altitude and high flight Mach number, above 2.5, the difference in required external diameter becomes appreciable.

The size of either type turbine is greatly affected by the type compressor used for the turbine's load. This is illustrated in Figure I-17, where the required external diameter of an axial turbine is presented as a function of the average surface temperature of the heat exchanger for both centrifugal and axial compressors. The turbine is considerably smaller when driving an axial compressor, chiefly because of the higher rotational speed permitted with this arrangement. For example, at an average surface temperature of 640°R and flight conditions of 80,000 feet and a Mach number of 2.0, the turbine's external diameter when driving an axial compressor is about 50 per cent of that required when driving a centrifugal compressor. The difference is somewhat less for lower flight altitudes and Mach numbers and for high equipment temperatures, but, in general, is sufficiently great to indicate the superiority of the axial-type compressor for the expanded ram air system. The relative size of radial and axial turbines when driving axial compressors may be compared by Figures I-16 and I-17. On the average, the external diameter of the radial turbine is 15 to 30 per cent greater than for the axial turbine. Operational conditions of high equipment temperature and low flight altitude results in very small difference between the diameters required for axial and radial turbines.

For flight conditions corresponding to an altitude of 80,000 feet and a Mach number of 2.0, the spatial requirement of an expanded ram air system having an average heat exchanger surface temperature of about 200°F and a radial turbine and axial compressor is about 1/4 cubic foot per kilowatt cooling capacity, not including intake or exhaust components. This amounts to roughly 75 per cent of the bulk required for systems employing axial turbines and radial compressors. The bulk of a system having a radial turbine and an axial compressor would be fairly evenly distributed between the turbine, heat exchanger and compresser.

6. Influence of Effectiveness and Pressure Loss of Heat Exchanger on Component Size

An increase in the design effectiveness of the heat exchanger reduces in direct proportion the amount of cooling air required for any specified cooling capacity of the system. This reduction in air rate decreases the required size of all system components, except the heat exchanger. Should the weight and bulk of the heat eschanger represent a small percentage of the system weight and bulk, it would be desirable to employ heat exchangers having high effectiveness. Normally this is the situation for the expanded ram air system. Figure I-18 presents for the system described in Figure I-1 the variation of component dimensions and heat exchanger weight as a function of

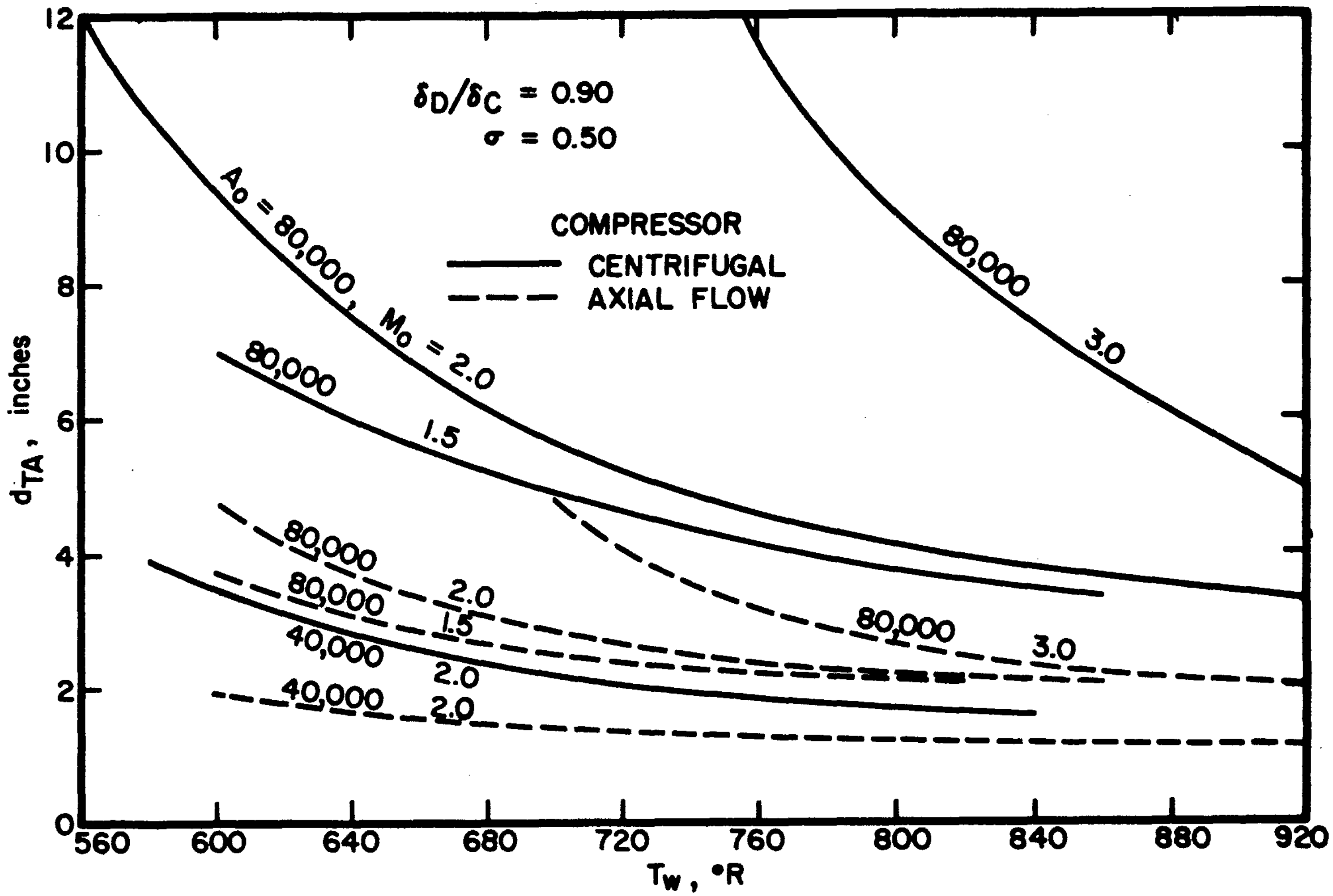

Figure I-17
Effect of Centrifugal or Axial Compressor as Load on Axial Turbine Diameter at Various Heat Exchanger Surface Temperatures, Design Altitudes, and Flight Speeds

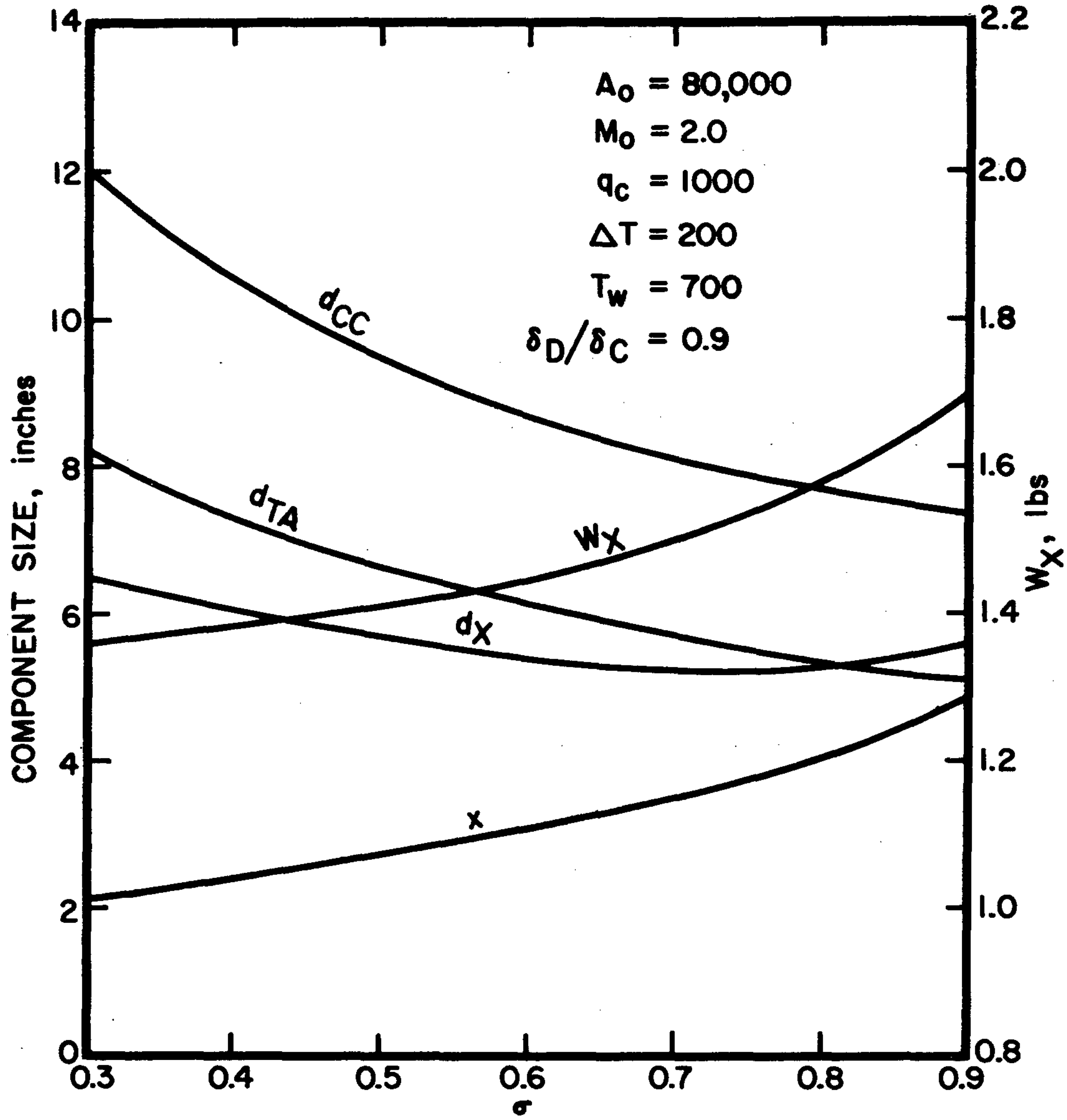

Figure I-18
Effect of Heat Exchanger Design Effectiveness on Component Sizes and Heat Exchanger Weight for Axial Turbine and Centrifugal Compressor

the design effectiveness. The diameters of the turbine and compressor decrease appreciably with increasing effectiveness. For a specified air pressure loss across the heat exchanger, the diameter of the heat exchanger is a minimum at an effectiveness of about 0.70. A minimum value for this dimension is reached since an increase in effectiveness reduces the required air rate but also reduces the permissible flow-Mach number at inlet of the tubes in order that the pressure loss across the heat exchanger remains constant. The volume and weight of the heat exchanger always increase with increasing effectiveness. Detailed study of expanded ram air systems to determine the design effectiveness for the heat exchanger resulting in minimum overall drag imposed on an aircraft has not been conducted. However, on basis of the available data it should be condluded that the optimum effectiveness lies in the range 0.80 to 0.95 for most expanded ram air systems.

For systems employing axial comprssors and radial turbines, as illustrated in Figure I-2, the design effectiveness of the heat exchanger influences the component size in a manner similar to that for systems employing axial turbines and radial compressors, Figure I-1. This is illustrated in Figure I-19 where the external diameters of an axial compressor, radial turbine, axial turbine and the heat exchanger are presented for effectiveness of the heat exchanger from 0.30 to 0.90.

The influence of total pressure loss across the heat exchanger on component size is presented in Figure I-20 for typical operational conditions of an expanded ram air system. An increase in the total pressure loss, i.e. lower values of the pressure ratio δ_D/δ_C as shown in the plot, increases the permissible flow Mach number at the inlet to the heat exchanger and, thereby, reduces the required size and weight of the heat exchanger. External diameters of the compressor and turbine increase with increased pressure loss due to the reduced air density at inlet to the compressor. The compressor size must be increased to accommodate the same air flow, but this results in a lower rotational speed for the compressor and, consequently, larger required size of the turbine. A pressure loss across the heat exchanger of about 10 per cent appears to be a practical design value. When the bulk and weight of the heat exchanger represent an important part of the system bulk and weight, and the drag imposed upon the aircraft is critical, it would be desirable to conduct fairly extensive performance analysis of the system to define an optimum value for the pressure loss of the heat exchanger.

Typical values of the duct diameter required to transport the cooling air from the intake of the system to the turbine are shown in Figure I-21. The duct diameter would vary in proportion to the square root of the cooling capacity of the system, other operational conditions remaining the same. For example, a duct of roughly 1.25-inch diameter would be required for a cooling capacity of 1000 watts and a duct length of five feet at a flight speed of Mach 2.0 and 60,000 feet altitude.

7. Influence of Precooling on System Cooling Capacity

The potential for increasing the cooling capacity of an expanded ram air system by use of a heat exchanger ahead of the turbine is presented in

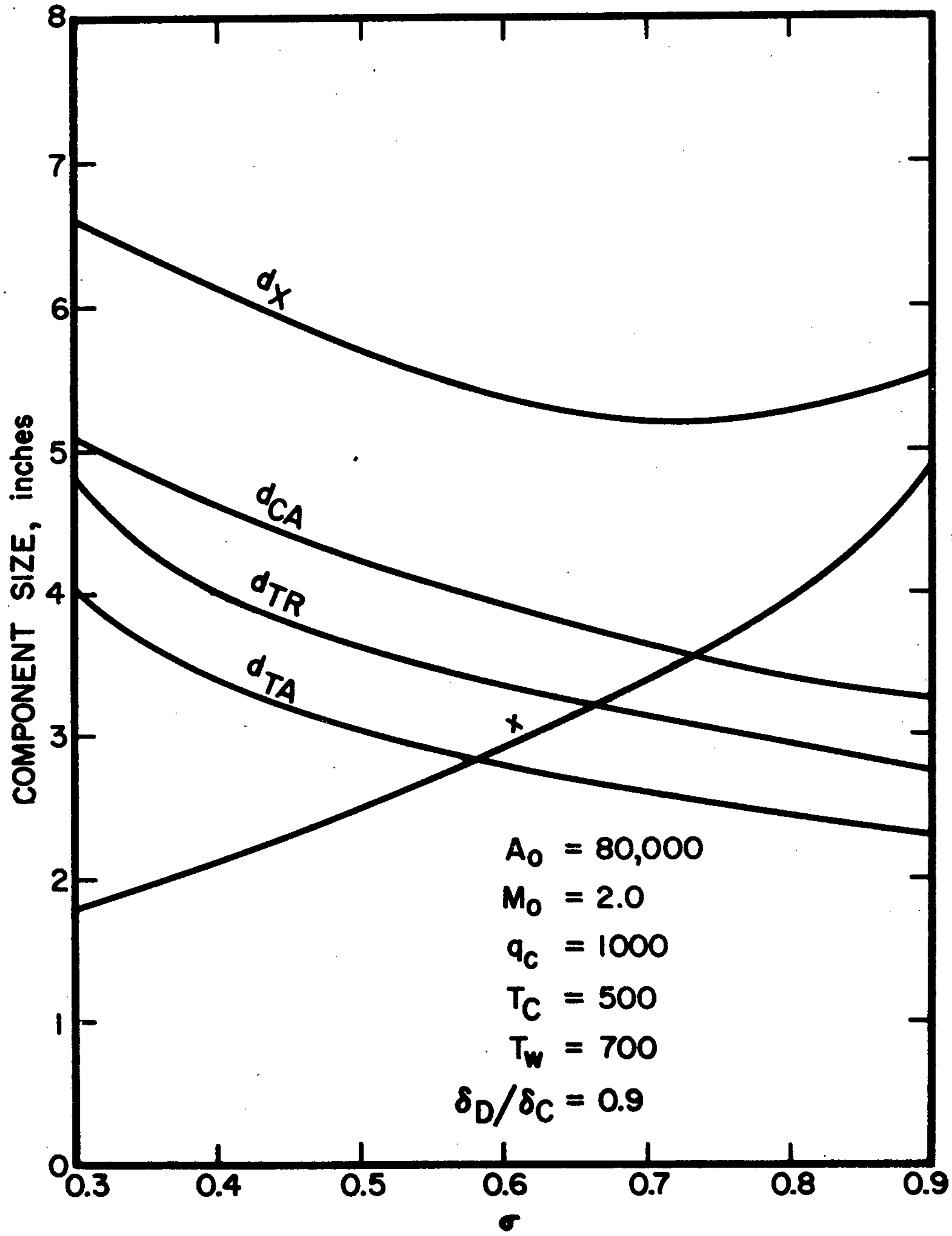

Figure I-19
Effect of Heat Exchanger Design Effectiveness on Component Sizes and Heat Exchanger Weight for Radial Turbine and Axial Compressor

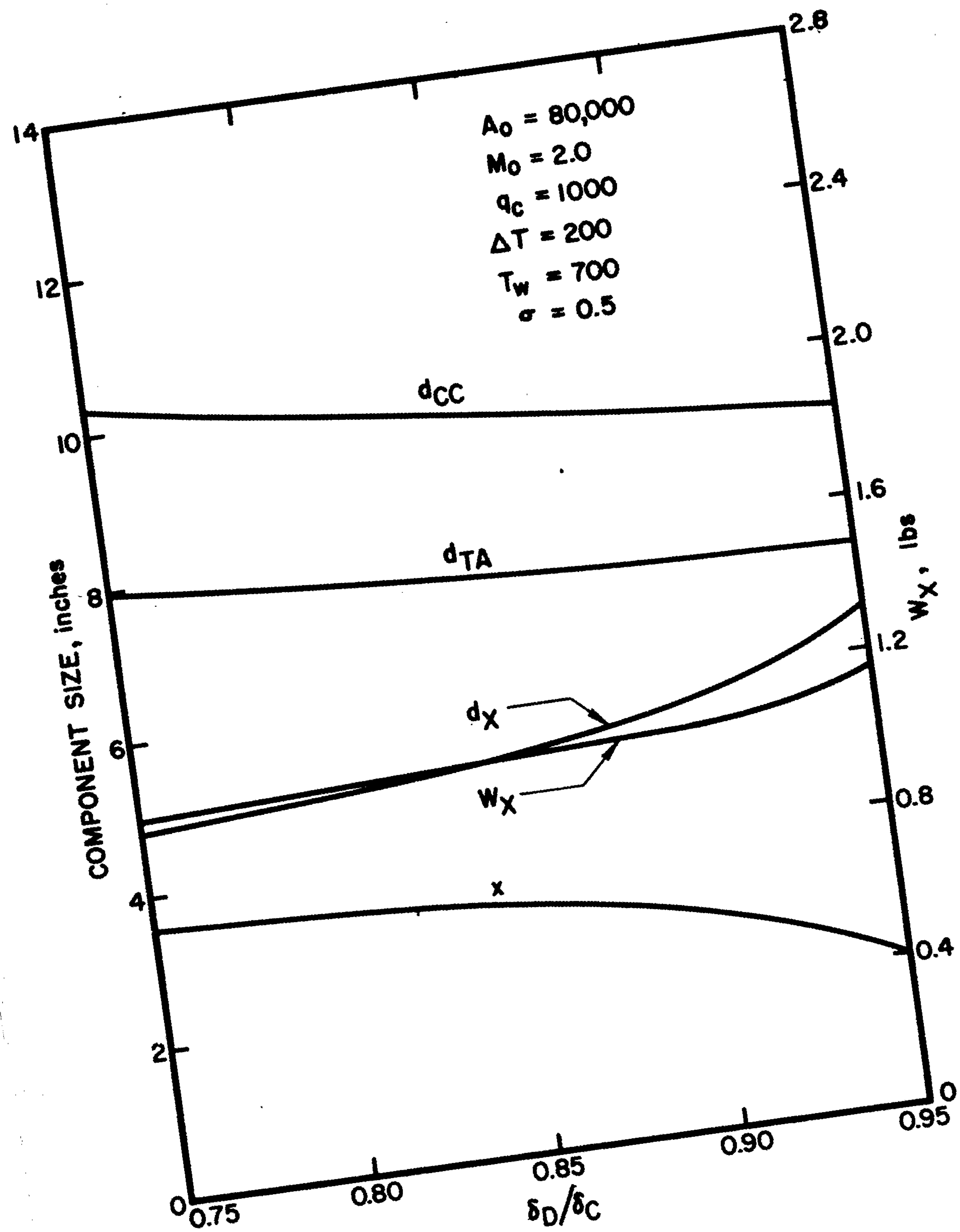

Figure I-20
Effect of Heat Exchanger Pressure Loss on Component Size

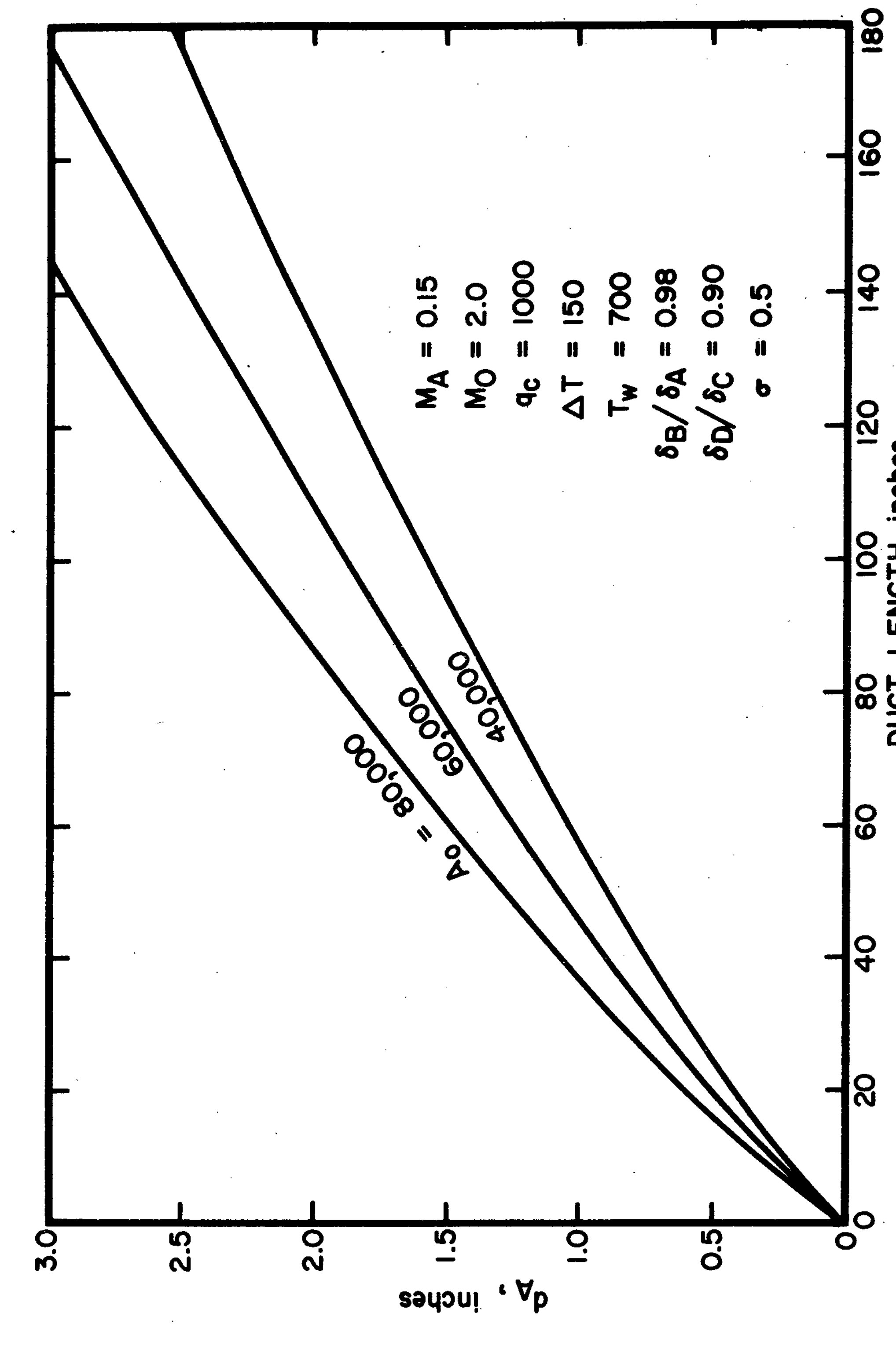

Figure I-21
Inlet Air Duct Diameter and Length for Permissible Pressure Losses

Figure I-22. The graph presents values of the turbine discharge temperature which could be obtained for various amounts of cooling in the precooling heat exchanger. The temperature of the precoolant and the effectiveness of the heat exchanger are assumed to be 600°R and 0.80, respectively. Also, it is assumed that the turbine discharge pressure is atmospheric and the turbine has an efficiency of 70 per cent. The total pressure ratio of the air from discharge of the diffuser to inlet of the turbine is 0.91 accounting for pressure loss of the ducting and the heat exchangers. It is unlikely that precoolant temperatures much less than 600°R would be available since otherwise the precoolant would be used to cool equipments directly.

As shown in Figure I-22, a minimum turbine discharge temperature is reached for each flight Mach number, because the amount of precooling is limited by the precoolant temperature of 600°R and the heat exchanger effectiveness of 0.80. Also, as the turbine inlet temperature is reduced by precooling, equal pressure ratios across the turbine yield lower temperature drops of the cooling air, since the temperature drop across the turbine for any fixed pressure ratio is proportional to the absolute temperature of the air at the turbine inlet. The minimum turbine discharge temperature at a flight Mach number of 3.0 is -6°F, whereas without precooling this temperature would be about 247°F.

Effective operation of the expanded ram air system may be extended to higher flight speed by use of precooling. Without precooling at a flight Mach number of 2.0, the turbine discharge temperature is 60°F, a limiting value for the system when used to cool low-temperature equipments. However, this same temperature is possible at flight Mach numbers of 2.5 and 3.0 by precooling to the extent of 4100 and 9750 Btu per hour, respectively, i.e. precooling of 1200 and 2860 watts. Precooling, like other auxiliary devices used to extend performance of any power plant or cooling system, is basically inefficient in that normally it requires dissipation of more heat in the precooler than it makes possible to dissipate by the cooling system. It is doubtful if precooling would ever be employed unless the precoolant would be fuel and equipment temperatures must be maintained at relatively low values at flight Mach numbers in the range of 2.5 to 3.5.

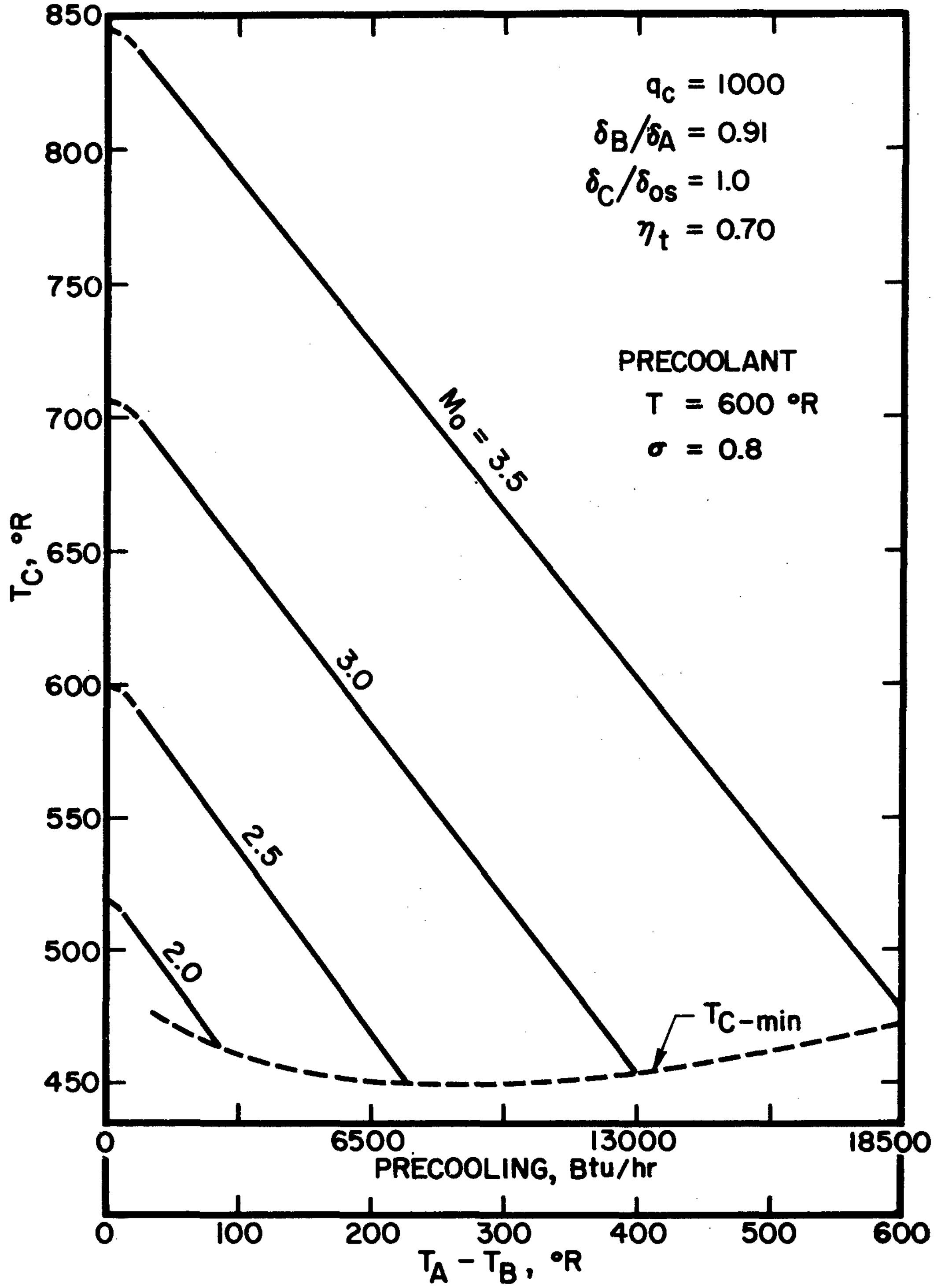

Figure I-22
Effect of Precooling on Turbine Discharge Temperature at Various Flight Speeds

APPENDIX TO SECTION I

ANALYSIS AND EVALUATION PROCEDURES FOR THE DETERMINATION OF PERFORMANCE AND PHYSICAL CHARACTERISTICS OF EXPANDED RAM AIR SYSTEMS

1. Nomenclature

Symbols for general concepts:

A_o	Altitude, ft
a	Cross-sectional area for flow, in.^{2}
C_o	Theoretical spouting velocity of turbine, ft/sec
d	Diameter, in.
f	Darcy friction factor, dimensionless
g	Dimensional constant, 32.2 lb/slug
G	Flow rate, lb/sec
h	Turbine bucket height, in.
k	Ratio of specific heat at constant pressure to specific heat at constant volume, Btu/lb-^{o}F
M	Mach number, dimensionless
N	Rotational speed, rpm
P	Pressure, p.s.i. abs.
q_c	Cooling capacity, watts
R	Gas constant, ft/^{o}R
Re	Reynolds number, dimensionless
s	Stress, p.s.i.
T	Temperature, ^{o}R
ΔT	Difference of surface temperature of heat exchanger T_w and discharge temperature of turbine T_C
u	Flow velocity, ft/sec
W	Weight, lb
x	Length, in.

α	Nozzle angle of turbine, degrees
β	Ratio of total to static temperature, $1+0.2M^2$, dimensionless, (see Table I-1)
γ	Specific weight, lb/ft^3
δ	Ratio of pressure to 14.7 p.s.i. abs., dimensionless
η	Efficiency, dimensionless
θ	Ratio of absolute temperature to $519^{\circ}R$, dimensionless
μ	Absolute viscosity, $lb\text{-}sec/ft^2$
σ	Effectiveness of heat exchanger, dimensionless
ψ	Pressure coefficient, dimensionless

Subscripts:

Note: Pressures and temperatures having the subscript (s) refer to static values; without this subscript all pressures and temperatures refer to the values for total conditions.

Symbol	Refers to
A	Station at exit of intake diffuser
A'	Station at entrance to precooler
av	Average conditions
B	Station at entrance to turbine
B'	Station at discharge of precooler
br	Root section of turbine bucket
C	Station at discharge of turbine
C'	Station at entrance to tubes in heat exchanger
CA	External diameter of axial compressor
CC	External diameter of centrifugal compressor
c	Compressor in general
D	Station at entrance to compressor
D'	Station at exit of tubes in heat exchanger

Symbol	Refers to
E	Station at discharge of compressor
F	Station at entrance to exhaust nozzle
G	Exit plane of exhaust nozzle
H	Station at exit of exhaust nozzle
IA	Impeller of axial compressor
IC	Impeller of centrifugal compressor
i	Inlet or internal
m	Mechanical efficiency of turbine or compressor
N	Exit plane of nozzle
o	Ambient conditions, except for C_o which is theoretical spouting velocity
p	Pitch line of turbine
P	Precoolant
r	Ram
s	Static conditions for pressure and temperature
t	Turbine in general
TA	External diameter of axial turbine
TR	External diameter of radial turbine
w	Average surface or wall temperature of heat exchanger
WA	Wheel diameter of axial turbine
WR	Wheel diameter of radial turbine
x	Heat exchanger
xP	Precooling heat exchanger

2. Analysis for Procedure (1)

Procedure (1) is used to evaluate temperature and pressures existing at key locations throughout the expanded ram air system shown in Figure I-1 for any assigned operational conditions of the aircraft in which the system is installed and any desired thermal conditions of the equipments specified by cooling capacity and average surface temperature of the heat exchanger. The cooling potential and general feasibility of the system for the intended application may be established from this evaluation procedure. The analysis for this procedure is presented in the subsequent paragraphs.

The total temperature at discharge from the intake is evaluated from the flight Mach number and atmospheric temperature by

$$T_A = T_{os}\left[1 + 0.2\ M_o^2\right] = T_{os}\ \beta_o \tag{I-1}$$

or,

$$\theta_B = \theta_{os}\ \beta_o \tag{I-2}$$

Values of β_o are given in Table I-1. The flow process from discharge of the intake to entrance of the turbine is assumed to be adiabatic; hence,

$$T_B = T_A = T_{os}\ \beta_o \tag{I-3}$$

The temperature at discharge of the turbine T_C is specified by the assumed values for the average surface temperature of the heat exchanger T_W and the inlet temperature differential ΔT.

$$T_C = T_W - \Delta T \tag{I-4}$$

The temperature of the air leaving the heat exchanger T_D is defined by

$$T_D = T_C + \sigma\Delta T \tag{I-5}$$

where σ is the effectiveness of the heat exchanger, defined as the ratio of the actual temperature rise of the air T_D-T_C to the maximum theoretical temperature rise ΔT.

The expansion pressure ratio of the turbine required to reduce the temperature of the cooling air from the temperature T_B to the temperature T_C is defined by

$$T_B - T_C = \eta_t\ T_B\left[1 - (P_C/P_B)^{1/3.5}\right]$$

or, by use of equation (I-3)

$$T_C/T_{os} = \beta_o\left\{1 - \eta_t\left[1 - (P_C/P_B)^{1/3.5}\right]\right\} \tag{I-4}$$

The expansion ratio of the air across the turbine P_B/P_C is related to the atmospheric pressure P_{os} by

$$P_B/P_C = (P_A/P_{os})(P_B/P_A)(P_{os}/P_C) \tag{I-5}$$

where P_A/P_{os} represents the pressure ratio developed by the diffuser, P_B/P_A the total pressure ratio of the air from discharge of the intake to entrance of the turbine, and P_C/P_{os} the selected total pressure of the air at entrance to the heat exchanger relative to the atmospheric pressure. The pressure ratio developed by diffusion during intake of the air is evaluated by the equation

$$P_A/P_{os} = \beta_o^{3.5\,r} \quad \text{(I-6)}$$

These values are given in Table I-1. A study of literature data on the efficiency of supersonic diffusers (Ref. I-7 and -8), indicates that equation (I-6) may be used to predict the total pressure at discharge of the intake when the efficiency η_r is evaluated from the flight Mach number by the equation

$$\eta_r = 0.92 - 0.024\, M_o^2 \quad \text{(I-7)}$$

The total pressure P_A defined in this manner agrees quite satisfactorily with experimental data for Mach numbers below 3.5.

Combination of equations (I-4, -5 and -6), and referring all pressures to the standard pressure of 14.7 psia yields

$$T_C/T_{os} = \Theta_C/\Theta_{os} = \beta_o \left\{1 - \eta_t \left[1 - (\delta_C/\delta_{os})^{1/3.5}/\beta_o^{\eta_r}(\delta_B/\delta_A)^{1/3.5}\right]\right\} \quad \text{(I-8)}$$

the equation used to define the pressure at entrance to the heat exchanger relative to the atmospheric pressure δ_C/δ_{os} for any specified flight Mach number and altitude, pressure loss in the duct leading to the turbine and required temperature of the air at entrance to the heat exchanger. The chart presented in Figure I-23 is used for graphical solution of this equation. The chart shown in Figure I-24 would be used for solution of equation (I-8) when the turbine efficiency is assumed equal to 70 per cent the atmospheric temperature is -67^oF, and the total pressure ratio δ_B/δ_C is 0.98, values which are considered to be representative of those which would exist for typical systems.

The power developed by turbine is absorbed by the centrifugal compressor. Thus, since the air flow through the turbine and compressor are equal,

$$\eta_{mt}(T_B - T_C) = (T_E - T_D)/\eta_{mc} \quad \text{(I-9)}$$

or,

$$\eta_{mc}\,\eta_{mt}(T_B - T_C) = (T_D/\eta_c)\left[(P_E/P_D)^{1/3.5} - 1\right] \quad \text{(I-10)}$$

The total pressure ratio developed by the compressor P_E/P_D is defined by the pressure coefficient ψ and the Mach number of the tip of the impeller M_{IC} by the expression

$$P_E/P_D = (1 + 0.4\,\psi M_{IC}^2)^{3.5} \quad \text{(I-11)}$$

where the Mach number M_{IC} is defined as the ratio of the peripheral speed of

the impeller to the velocity of sound based on the total temperature of the air at entrance to the compressor. The pressure coefficient ψ is defined as the ratio of the actual head of air produced to the theoretical head produced by a centrifugal compressor having an infinite number of vanes. The magnitude of the pressure coefficient is assumed to be 90 per cent of the compressor adiabatic efficiency, i.e., the circulatory flow coefficient is assumed equal to 0.90, a value typical of impellers having 12 to 20 radial vanes. Using this relation between pressure coefficient and efficiency and equations (I-10 and -11), the tip Mach number M_{IC} required of the centrifugal compressor is defined by

$$M_{IC} = (2.78\, \eta_{mc}\, \eta_{mt}\, \Delta\theta_t/\theta_D)^{1/2} \qquad \text{(I-12)}$$

where the temperatures have been reduced to values relative to the standard of 519°R. Values of the tip Mach number may be determined from the chart presented in Figure I-25.

The ratio of the total temperature at discharge of the compressor to that at its entrance T_E/T_D is defined by the tip Mach number M_{IC} according to the expression

$$T_E/T_D = \theta_E/\theta_D = 1 + 0.36\, M_{IC}^2 \qquad \text{(I-12)}$$

which is derived from the definition of adiabatic efficiency for the compressor as the ratio of the isentropic to the actual temperature rise of the air. The pressure coefficient ψ is again taken as 90 per cent of the adiabatic efficiency. Equation (I-12) may be solved graphically by the chart in Figure I-26.

The loss in total pressure of the cooling air from inlet to exit of the heat exchanger is defined on the basis of compressible flow theory, taking into account the simultaneous action of friction and heat exchange within the tube section proper, loss at entrance to the tubes due to contraction of the stream and loss at exit of the tubes due to abrupt expansion of the air. Data derived by mechanical integration of basic differential equations, as illustrated in Ref. (I-2 and -3), are presented in Figures I-27 through I-35. The heat transfer coefficient of forced convection between the tube surface and the cooling air is assumed to be constant over the entire tube length and is evaluated by use of the Reynolds' analogy between fluid friction and heat transfer. The effectiveness of heat exchange σ is related to the length-to-internal diameter ratio of the tube and the Darcy friction factor, assuming a Prandtl number of unity, by the equation

$$fx/2d_i = \log_e \left[1/(1-\sigma)\right] \qquad \text{(I-13)}$$

The inlet Mach number shown on the plots in Figures I-27 through I-35 represents the Mach number of flow based on the cross-sectional flow area of the tubes, and is not to be used as the Mach number of flow in the inlet header of the heat exchanger.

The length of the tubes x for the heat exchanger required to develop the design value for the effectiveness σ is determined by use of equation

(I-13), the inside tube diameter d_i of 0.20 inch, used for all designs, and the average value of the Darcy friction factor f over the length of the tube. The friction factor is defined for laminar flow by

$$f = 64/Re \tag{I-14}$$

and for turbulent flow by

$$f = 0.264/Re^{0.23} \tag{I-15}$$

The Reynolds number of the flow Re is defined by

$$Re = \gamma_{C'}\, u_{C'}\, d_i/12\mu_{av}$$

However,

$$\gamma_{C'}\, u_{C'} = (kg/R)^{1/2}(P_{C'}M_{C'})/\beta^3_{C'}(T_{C'})^{1/2}$$

The total pressure at inlet to the tube is assumed to vary with the discharge total pressure of the turbine by

$$P_{C'} = (1 - 0.175\, M^2_{C'})\, P_C$$

to account for the pressure loss of the air in the inlet header of the heat exchanger. The tube diameter d_i is constant and equal to 0.20 inch and the total temperature $T_{C'}$ is equal to the total temperature T_C. Hence, the combination of the previous set of equations yields

$$Re = 1.425\, \delta_C M_{C'}(1-0.175M^2_{C'})/\mu_{av}\beta^3_{C'}(\theta_C)^{1/2} \tag{I-16}$$

Graphical solution to this expression for determination of the Reynolds number of flow may be obtained by use of the chart presented in Figure I-36. Once having defined the friction factor from the Reynolds number and equation (I-14) or (I-15), the effectiveness of heat exchange may be defined by use of the chart presented in Figure I-37, based on equation(I-13).

In defining the required cross-sectional area of the heat exchanger it is assumed that 2 per cent of the cross-section is required as free space for the shaft connecting the turbine and compressor, and that of the remaining cross-section 50 per cent would be available for free-flow area of the tubes. Thus, by continuity, the cross-section of the heat exchanger a_x is defined by

$$a_x = 144G/(0.98x0.50\,\gamma_{C'}u_{C'}) \tag{I-17}$$

However, as determined previously in defining the equation for evaluation of Reynolds number,

$$\gamma_{C'}u_{C'} = 85.5\,\delta_C M_{C'}(1-0.175M^2_{C'})/\beta^3_{C'}(\theta_C)^{1/2}$$

so that

$$a_x/G = 3.44\beta^3_{C'}(\theta_C)^{1/2}/\delta_C M_{C'}(1-0.175M^2_{C'}) \tag{I-18}$$

and

$$d_x = (a_x/0.785)^{1/2} \quad \text{(I-19)}$$

Equation (I-18) may be solved graphically by the chart of Figure I-38.

The required area at inlet to the diffuser for subsonic flight is defined on the basis of a flow Mach number at this section equal to 60 per cent of the flight Mach number and a flow coefficient of 0.95. Thus,

$$T_{ir} = T_{os}\,\beta_o/\beta_{ir} = 519\,\theta_{os}\,\beta_o/\beta_{ir} \quad \text{(I-20)}$$

and

$$P_{irs} = P_{os}\,\beta_o^{3.5}/\beta_{ir}^{3.5} = 14.7\,\delta_{os}\,\beta_o^{3.5}/\beta_{ir}^{3.5} \quad \text{(I-21)}$$

where

$$\beta_{ir} = 1 + 0.2(0.6\,M_o)^2 = 1 + 0.072\,M_o^2 \quad \text{(I-22)}$$

The intake area required by the diffuser is defined by combination of the continuity equation and the above relationships. The expression for subsonic flight is

$$a_{ir}/G = 2.96(\theta_{os})^{1/2}(1+0.072M_o^2)^3/\delta_{os}M_o\beta_o^3 \quad \text{(I-23)}$$

The intake area of the expanded ram air system required for aircraft operating at flight Mach numbers greater than 1.25 is defined by assuming all shocks to exist inside of the intake so that free stream conditions may be assumed to define the state of the air at the inlet plane of the intake. A flow coefficient of 0.95 is employed to account for boundary layer effect. Based on free stream pressure, temperature and Mach number, the equation of continuity yields

$$a_{ir}/G = 1.775(\theta_{os})^{1/2}/M_o\,\delta_{os} \quad \text{(I-24)}$$

Inlet areas of the intake required for design flight Mach numbers in the range 1.0 to 1.25 are obtained by trend curves established on the basis of the subsonic equation (I-23) and the supersonic equation (I-24). The inlet area equations may be solved graphically by use of the chart in Figure I-39.

3. Analysis for Procedure (2)

Evaluation procedure (2) is used to establish the required size of the various components for a expanded ram air system designed to provide the required cooling capacity at the specified flight operational conditions of the aircraft and for the desired thermal conditions of the equipments being cooled. The evaluation procedure is for the type of expanded ram air system illustrated schematically in Figure I-1. Temperatures and pressures of the cooling air corresponding to the various stations throughout the system shown in Figure I-1 are defined by the evaluation procedure (1).

The rate of cooling air flow required for a specified cooling capacity is defined by heat balance. Assuming a constant specific heat c_p for

air eoual to 0.24 Btu per pound-^{o}F, the cooling capacity in watts is defined by

$$q_c = 3600 \times 0.24\, G(T_D - T_C)/3.413$$

or,

$$G = q_c/131,300(\theta_D - \theta_C) \qquad \text{(I-25)}$$

The cross-sectional area and diameter of the heat exchanger are evaluated from equations (I-18 and -19), using the required cooling air rate defined from equation (I-25). Similarly, the required inlet area a_{iE} is defined by equation (I-23 or -24), depending upon whether the flight Mach number is greater than 1.25 or less than unity.

The size of the centrifugal compressor is determined on the basis of design for maximum capacity, rather than maximum efficiency. Results of a study conducted to determine the maximum air flow capacity of centrifugal compressors (Ref. I-4) have shown that the inlet diameter of the impeller should be defined by

$$d_{ic}/d_{IC} = 0.778/M_{IC}$$

This expression is used to define the relation of inlet and tip diameters of the compressor, except when the ratio of diameters exceeds 0.70, whereupon the ratio is limited to a value of 0.70 for practical design reasons. The tip Mach number of the impeller M_{IC} is about 1.11 for the limiting diameter ratio of 0.70. Thus, when

$$M_{IC} > 1.11, \quad d_{ic}/d_{IC} = 0.778/M_{IC} \qquad \text{(I-26)}$$

and when

$$M_{IC} < 1.11, \quad d_{ic}/d_{IC} = 0.70 \qquad \text{(I-27)}$$

The actual Mach number of flow through the inlet for units having pure axial entry has also been defined (Ref. I-4) and is determined to be nearly constant at a value of about 0.43.

The equation of continuity applied to the inlet section of the compressor for an inlet Mach number of 0.30 yields

$$G(\theta_D)^{1/2}/\delta_D = 85.5 \times 0.43\, a_{ic}/144(1+0.2 \times 0.43^2)^3$$

or,

$$G(\theta_D)^{1/2}/\delta_D = 0.229\, a_{ic} \qquad \text{(I-28)}$$

If it is assumed that the hub of the impeller is 0.25 of the impeller tip diameter, then

$$a_{ic} = 0.785\left[d_{ic}^2 - (d_{IC}/4)^2\right] = 0.785 d_{IC}^2\left[(d_{ic}/d_{IC})^2 - 1/16\right]$$

When the impeller tip Mach number exceeds 1.11 equation (I-26) is used and

$$a_{ic} = 0.785\, d_{IC}^2\left[0.778^2/M_{IC}^2 - 1/16\right]$$

so that introduction of this expression into equation (I-28) yields

$$G(\Theta_D)^{1/2}/\delta_D = 0.01124(9.68/M_{IC}^2-1)d_{IC}^2 \tag{I-29}$$

When M_{IC} is less than 1.11, $d_{ic}/d_{IC} = 0.70$. Hence,

$$a_{ic} = 0.785\, d_{IC}^2(0.70^2 - 1/16)$$

and

$$G(\Theta_D)^{1/2}/\delta_D = 0.0768\, d_{IC}^2 \tag{I-30}$$

Equations (I-29 and -30) are used to define the required diameter of the impeller for the centrifugal compressor.

The average external diameter of the centrifugal compressor is assumed to be 80 per cent greater than the impeller diameter. The inlet diameter of the compressor is defined by equation (I-26 or -27). The required rotational speed of the impeller is determined from the impeller diameter and tip speed in the following manner.

$$u_{IC} = M_{IC}\sqrt{kgRT_D}$$

or,

$$u_{IC} = 1117(\Theta_D)^{1/2}M_{IC} \tag{I-31}$$

Also,

$$u_{IC} = \pi\, d_{IC}\, N/720 \tag{I-32}$$

so that

$$N = 256{,}000\, M_{IC}(\Theta_D)^{1/2}/d_{IC} \tag{I-33}$$

The required pitch diameter of the axial turbine for the system shown in Figure I-1 is established from the rotational speed of the turbine, being equal to that defined for the compressor, the theoretical spouting velocity of the turbine and the ratio of the pitch line tangential velocity of the turbine buckets to the theoretical spouting velocity. The latter ratio is used to define the design for heat efficiency. The theoretical spouting velocity is defined by

$$C_o^2 = 2gJc_pT_B\ 1 - (\delta_C/\delta_B)^{1/3.5} \tag{I-34}$$

and

$$u_p = C_o(u_p/C_o) \tag{I-35}$$

where the ratio u_p/C_o would be selected as about 0.45 for design yielding maximum efficiency. The pitch-line velocity is related to the rotational speed by

$$u_p = \pi\, d_p\, N/720 \tag{I-36}$$

so that equations (I-34, -35, and -36) may be combined to give for the pitch diameter

$$d_p = 5.72\text{x}10^5\ \theta_B(u_p/C_o)\sqrt{1-(\delta_C/\delta_B)^{1/3.5}}/N \qquad \text{(I-36)}$$

A chart for graphical solution of this equation is presented in Figure I-40.

The flow capacity of the turbine is primarily a function of the pitch diameter, the nozzle angle and the bucket height. If the nozzle angle of the turbine is assumed to be 20 degrees, it may be shown that for turbines designed on the basis of vortex theory and zero reaction at the root section (Ref. I-1) the flow capacity is defined by

$$G(\theta_B)^{1/2}/\delta_B = 0.306d_p^2(h/d_p)\left[1+0.1765(h/d_p)(2-h/d_p)\right] \qquad \text{(I-37)}$$

Since the area rate G, temperature θ_B, pressure δ_B and pitch diameter d_p are defined by previously given relationships, equation (I-37) would be used to select the required bucket height of the turbine h. This process may be conducted graphically with the chart presented in Figure I-41. The stress level at the root section of the turbine buckets would be evaluated by

$$s_{br} = h\ d_p\ N^2\ \gamma_b/117{,}200 \qquad \text{(I-38)}$$

where γ_b represents the specific weight of the turbine bucket material in pounds per cubic foot. The tip diameter of the turbine wheel is defined by,

$$d_{WA} = d_p + h \qquad \text{(I-39)}$$

and the average external diameter d_{TA} is assumed to be 50 per cent greater than the tip diameter of the wheel.

The discharge velocity of the system, station H, is defined by the pressure drop available across the exhaust nozzle and the temperature of the air at discharge of the compressor. The temperature at discharge of the compressor T_E is defined by equation (I-12). The pressure of the air at discharge of the compressor P_E may be evaluated by equation (I-11), assuming

$$\psi = 0.90\ \eta_c$$

where

$$\eta_c = 0.58 + 0.01\ d_{Ic} \qquad \text{(I-40)}$$

The discharge velocity is defined then by

$$u_H = 2372(\theta_E)^{1/2}\sqrt{1-(\delta_{os}/\delta_F)^{1/3.5}} \qquad \text{(I-41)}$$

for the discharge pressure δ_H equal to the ambient atmospheric pressure $_{os}$. A flow coefficient for the discharge nozzle of 0.95 is assumed. The chart in Figure I-42 may be used to evaluate the discharge velocity.

The drag imposed on the aircraft by the cooling air taken aboard and subsequently discharged is defined by

$$\text{Drag} = G\left[u_H - 1117\ M_o(\theta_{os})^{1/2}\right]/g \qquad \text{(I-42)}$$

The exhaust nozzle is assumed to be convergent only, whether the pressure ratio of the nozzle is greater or less than critical. When the pressure ratio exceeds the critical value of 1.89, it is assumed that the efficiency of free expansion behind the nozzle is equal to that for expansion within the nozzle; an assumption which is valid for over-all pressure ratios up to about 3 or 3.5. The discharge area required of the nozzle is defined from the continuity equation, and is

$$a_N = 0.838G(\theta_E)^{1/2}/\delta_F \left[(\delta_{Hs}/\delta_F)^{1.43}-(\delta_{Hs}/\delta_F)^{1.72}\right]^{1/2} \qquad \text{(I-43)}$$

The chart presented in Figure I-43 may be used to define the required exit area of the nozzle.

4. Analysis for Procedure (3)

Performance and size of the expanded ram air system employing an axial-flow compressor operating in combination with either a radial or axial turbine are determined by evaluation procedure (3). Required size of the axial compressor is determined on the basis that the compressor would be designed for minimum size, such that the efficiency of the unit would be sacrificed to reduce its weight and space requirements. Hence, in a few stages having small diameter an appreciable amount of power may be absorbed. The pressure rise of the air developed by this type axial compressor would be small, and, correspondingly, the drag of the system imposed on the aircraft by the cooling air would be increased. The over-all drag of the system imposed on the aircraft, from cooling air, weight, etc., may be reduced.

The tip Mach number of the compressor blades is assumed equal to 1.0 and the Mach number of flow relative to the tip section of the blades is limited to 0.8. Employing a symmetrical velocity diagram to yield maximum air capacity of the compressor, the tip diameter of the impeller is defined by

$$d_{IA} = 2.62\, G^{1/2}\theta_D^{1/4}/\delta_D^{1/2} \qquad \text{(I-44)}$$

It is assumed that the average external diameter of the axial compressor d_{CA} is 10 per cent greater than the impeller diameter. The required rotational speed of the impeller is defined by equation (I-33) using $M_{IC}=M_{IA}=1$.

Size and speed for a radial turbine are determined on the basis of design for peak efficiency. A ratio of the wheel tip speed to the theoretical spouting velocity of about 0.60 normally results in design for near peak efficiency. The peak efficiency is assumed to be 70 per cent. The theoretical spouting velocity of the turbine is defined by the air temperature drop, and is

$$C_o = \left[2gJc_p(T_B-T_C)/\eta_t\right]^{1/2}$$

Thus,

$$u_{WR} = 0.60\, C_o$$

Also,

$$u_{WR} = \pi \, d_{WR} \, N/720$$

Combination of these equations defines the required diameter of the wheel as

$$d_{WR} = 4.1\times10^5(\theta_B-\theta_C)^{1/2}/N \qquad \text{(I-45)}$$

for the assumed turbine efficiency of 70 per cent. The average external diameter of the radial turbine d_{TR} is assumed to be 80 per cent greater than the wheel diameter d_{WR}. The axial width of the turbine nozzles is evaluated on the basis of a 15 degree nozzle angle, and may be defined by the chart in Figure I-44 for the specified air rate G and diameter of the wheel d_{WR}.

5. Analysis for Procedure (4)

This procedure is arranged to permit rapid calculations of sizes of components using many of the approximations and assumptions enumerated in the previous derivations. It is intended for systems employing axial compressors and radial turbines, and is so prepared that it may be used to analyze cycles employing precooling as well as simple cycles. The pressure loss ratio, δ_B/δ_A, may be stated for the duct alone, or the value may be made large enough to include the duct loss plus a pressure drop through a precooling heat exchanger located in the duct ahead of the turbine. The method is based upon equations presented in the preceding analyses, except for the precooler analysis which must include pressure and temperature change of the air across the precooler. The pressure loss of the precooling heat exchanger is defined by the chart in Figure I-45, which has been prepared from the work of Ref. (I-6). Figure I-46 is a cross-plot of the data of Figure I-45 for a pressure ratio of 0.918.

The chart presented in Figure I-47 is useful for evaluating total pressure loss in ducts of constant cross section, such as the interconnecting ducts between intake and the turbine and the compressor and discharge. It is assumed that this flow process would be adiabatic. Data in this chart are based on Ref. (I-5), p. 157.

6. Evaluation Procedures

a. Procedure (1)

1. Fixed values: d_i ______, u_p/C_o ______, δ_B/δ_A ______, δ_F/δ_E ______, δ_H/δ_{os} ______, η_t ______, $\eta_{mc}\eta_{mt}$ ______, α ______.
2. Given variables: A_o ______, M_o ______, T_C ______, T_W ______, σ ______, δ_D/δ_C ______.
3. Read θ_{os} and δ_{os} from Table AI-1. θ_{os} ______, δ_{os} ______.
4. Read β_o from Table I-1. β_o ______.

5. Calculate $\theta_C = T_C/519$. θ_C ______.

6. Calculate $T_D = T_C + \sigma(T_W - T_C)$. T_D ______, θ_D ______.

7. Calculate θ_C/θ_{os} ______.

8. Read δ_C/δ_{os} from Figure I-23 or I-24. δ_C/δ_{os} ______.

9. Calculate $\Delta\theta_t/\theta_D = \theta_B - \theta_C/\theta_D =$ ______.

10. Read M_{IC} from Figure I-25. M_{IC} ______.

11. Read θ_E/θ_D from Figure I-26. θ_E/θ_D ______.

12. Calculate $\theta_E = \theta_D(\theta_E/\theta_D)$. θ_E ______.

13. Calculate θ_W/θ_C ______. Read $M_{C'}$ from chart corresponding to selected values for σ and δ_D/δ_C, Figures I-27 to I-35. $M_{C'}$ ______.

14. Calculate $\theta_{av} = (\theta_C+\theta_D)/2 =$ ______.

15. Calculate $\delta_C = \delta_{os}(\delta_C/\delta_{os}) =$ ______.

16. Read Re and f from Figure I-36. Re ______, f ______.

17. Read x from Figure I-37. x ______.

18. Read a_x/G from Figure I-38. a_x/G ______.

19. Read a_{ir}/G from Figure I-39. a_{ir}/G ______.

b. Procedure (2)

20. Fixed values: refer to item (1) of Procedure (1).

21. Given variables: $q_c =$ ______ watts.

22. Calculate $G = q_c/131{,}300(\theta_D - \theta_C) =$ ______.

23. Calculate $a_x = G$ (item 18) $=$ ______.

24. Calculate $d_x = 1.128(a_x)^{0.5} =$ ______.

25. Calculate $a_{ir} = G$ (item 19) $=$ ______.

26. Calculate $\delta_D = \delta_C(\delta_D/\delta_C) =$ ______.

27. Calculate d_{IC} by equation (I-29) or (I-30). d_{IC} ______.

28. Calculate d_{ic} by equation (I-26) or (I-27). d_{ic} ______.

29. Calculate N by equation (I-33). N ______.

30. Find δ_A/δ_{os} from Table I-1. δ_A/δ_{os} ______.

31. Evaluate $\delta_B = \delta_{os}(\delta_A/\delta_{os})(\delta_B/\delta_A)$ = ______.

32. Read d_p from Figure I-40. d_p ______.

33. Calculate $G\theta_B^{0.5}/\delta_B$ = ______.

34. Read h from Figure I-41. h ______.

35. Calculate $d_{WA} = d_p + h$ = ______.

36. Calculate $d_{TA} = 1.5\ d_{WA}$ = ______.

37. Calculate $\delta_E/\delta_D = (1 + 0.4\psi M_{IC})^{3.5}$ = ______, where $\psi = 0.9\eta_c$ and η_c is defined by equation I-40.

38. Evaluate $\delta_E/\delta_{os} = (\delta_C/\delta_{os})(\delta_D/\delta_C)(\delta_E/\delta_D)$ = ______.

39. Evaluate $\delta_{os}/\delta_F = (\delta_{os}/\delta_E)(\delta_E/\delta_F)$ = ______.

40. Read u_H from Figure I-42. u_H = ______.

41. Calculate drag by equation (I-42). Drag ______.

42. Evaluate δ_H/δ_F = ______.

43. Read from Figure I-43, a_N = ______.

44. Calculate $d_N = 1.128(a_N)^{0.5}$ = ______.

c. <u>Procedure (3)</u>

45. Fixed values: refer to item (1) of Procedure (1).

46. Given variables: θ_B ______, θ_C ______, θ_D ______, G ______, δ_B ______, δ_D ______.

47. Calculate by equation (I-44), d_{IA} = ______.

48. Calculate $d_{CA} = 1.1\ d_{IA}$ = ______.

49. Calculate $N = 256{,}000(\theta_D)^{0.5}/d_{IA}$ = ______.

50. Calculate by equation (I-45), d_{WR} = ______.

51. Calculate $d_{TR} = 1.8\ d_{WR}$ = ______.

52. Read turbine nozzle width from Figure I-44 ______.

53. Calculate $d_p = 3.09 \times 10^5(\theta_B-\theta_C)^{0.5}/N =$ ______.

54. Read from Figure I-41, h = ______.

55. Calculate $d_{WA} = d_p + h =$ ______.

56. Calculate $d_{TA} = 1.5\ d_{WA} =$ ______.

d. Procedure (4)

57. Fixed values: $\delta_B/\delta_A =$ ______, $\eta_t =$ ______, $d_i =$ ______.

58. Given variables: A_o ______, M_o ______, T_C ______, T_W ______, σ ______, δ_D/δ_C ______, T_B ______ (for precooling).

59. Read θ_{os} and δ_{os} from Table I-1. θ_{os} ______, δ_{os} ______.

60. Read β_o from Table I-1. β_o ______.

61. Calculate, for precooling, $\theta_B = T_B/519 =$ ______, without precooling, $\theta_B = \beta_o\ \theta_{os} =$ ______.

62. Calculate $\theta_C = T_C/519 =$ ______.

63. Calculate $T_D = T_C + \sigma(T_W-T_C) =$ ______, $\theta_D =$ ______.

64. Calculate $\theta_C/\theta_{os} =$ ______.

65. Read δ_C/δ_{os} for no precooling from Figure I-23 or I-24. $\delta_C/\delta_{os} =$ ______. With precooling calculate $\delta_C/\delta_{os} = (\delta_B/\delta_A)(\delta_A/\delta_{os})\left[1 - (\theta_B-\theta_C)/\eta_t\theta_B\right]^{3.5} =$ ______.

66. Read M_C' from chart corresponding to selected values of σ and δ_D/δ_C, Figures I-27 to I-35. $\theta_W/\theta_C =$ ______, $M_C' =$ ______.

67. Calculate $\theta_{av} = 0.5(\theta_C+\theta_D) =$ ______.

68. Calculate $\delta_C = \delta_{os}(\delta_C/\delta_{os}) =$ ______.

69. Read Re and f from Figure I-36. Re = ______, f = ______.

70. Read x from Figure I-37. x = ______.

71. Read a_x/G from Figure I-38. $a_x/G =$ ______.

72. Read a_{ir}/G from Figure I-39. $a_{ir}/G =$ ______.

73. Cooling capacity $q_c =$ ______.

74. Calculate $G = q_c/131{,}300(\theta_D-\theta_C) =$ ______.

75. Calculate $a_x = G$ (item 71) = ______.

76. Calculate $d_x = 1.128(a_x)^{0.5}$ = ______.

77. Calculate $a_{ir} = G$ (item 72) = ______.

78. Calculate $\delta_D = \delta_C(\delta_D/\delta_C)$ = ______.

79. Calculate d_{IA} by equation (I-44). d_{IA} = ______.

80. Calculate $d_{CA} = 1.1\ d_{IA}$ = ______.

81. Calculate $N = 256{,}000(\theta_D)^{0.5}/d_{IA}$ = ______.

82. Calculate d_{WR} by equation (I-45). d_{WR} = ______.

83. Calculate $d_{TR} = 1.8\ d_{WR}$ = ______.

84. Calculate $\delta_B = \delta_{os}(\delta_B/\delta_A)(\beta_o^{3.5}\ r)$ = ______.

85. Calculate $G(\theta_B)^{0.5}/\delta_B$ = ______.

86. Read turbine nozzle width from Figure I-44 ______.

87. Calculate drag by equation (I-42). Drag ______.

88. Calculate $\theta_A = \theta_{os}\beta_o$ = ______.

89. Calculate for precooling heat exchanger, $\theta_{av} = 0.5(\theta_A + \theta_B)$= ______.

90. Calculate $\sigma_x P = (\theta_A - \theta_B)/(\theta_A - \theta_P)$ = ______.

91. Read δ_A/δ_{os} = ______, from Table I-1.

92. Calculate $\delta_A = \delta_{os}(\delta_A/\delta_{os})$ = ______.

93. Read M_A from Figure I-45 or I-46. M_A = ______.

94. Read f from Figure I-36, using state of air at A rather than at C. f ______.

95. Read x_{pC} from Figure I-37. x_{pC} ______.

96. Read a_{pC}/G from Figure I-38, using state of air at A rather than C. a_{pC}/G = ______.

97. Calculate a_{pC} = ______ and $d_{pC} = 1.128(a_{pC})^{0.5}$ = ______.

7. References

(I-1) Arnett, S. E., "A Study of the Theory of Constant Angular Momentum Flow Through Turbine Nozzles and Buckets," Thesis, Department of Mechanical Engineering, The Ohio State University, 1950.

(I-2) Denzer, R. E., "A Study of Total Pressure Loss, Heat Exchange Effectiveness, and Choking Length for the Steady Flow of a Compressible Fluid Through Tubes of Constant Cross-Sectional Area," Thesis, Department of Mechanical Engineering, The Ohio State University, 1951.

(I-3) Edwards, W. E., "A Study of Methods of Evaluating Effects of Friction and Heat Addition on the Steady Flow of a Perfect Gas Through Smooth Tubes of Constant Diameter," Thesis, Department of Mechanical Engineering, The Ohio State University, 1950.

(I-4) Hudelson, G. D., "An Analytical Study to Determine the Optimum Inlet Diameter and Maximum Air Capacity of Centrifugal Compressors," Thesis, Department of Mechanical Engineering, The Ohio State University, 1951.

(I-5) Keenan, J. H. and Kaye, J., Gas Tables, John Wiley and Sons, Inc., New York, 1948.

(I-6) Mok, Ying-Kei, "An Analytical Study of the Effects of Cooling and Friction on a Compressible Fluid Flowing in a Tube of Constant Diameter," Thesis, Department of Mechanical Engineering, The Ohio State University, 1949.

(I-7) Neumann, E. P. and Lustwerk, F., "Supersonic Diffusers for Wind Tunnels," American Society of Mechanical Engineers Paper No. 48-A-14, presented at annual meeting, New York, 1948.

(I-8) Stanitz, J. D., "Note on the Simple Ram-Air Intake Preceded by Normal Shock in Supersonic Flight," Journal of the Aeronautical Sciences, March 1948.

M_o	β_o	$\beta_o^{3.5}$	$\beta_o^{3.5\eta_r}$ $=\delta_A/\delta_{os}$	$\sqrt{\beta_o}$	β_o^3
0.1	1.0020	1.0070	1.007	1.0010	1.006
0.2	1.0080	1.0283	1.026	1.0040	1.024
0.3	1.0180	1.0645	1.059	1.0090	1.053
0.4	1.0320	1.1166	1.107	1.0159	1.099
0.5	1.0500	1.1862	1.169	1.0246	1.158
0.6	1.0720	1.2755	1.248	1.0354	1.232
0.7	1.0980	1.3871	1.346	1.0479	1.324
0.8	1.1280	1.5244	1.464	1.0621	1.435
0.9	1.1620	1.6914	1.605	1.0780	1.569
1.0	1.2000	1.8929	1.771	1.0955	1.728
1.1	1.2420	2.1351	1.966	1.1145	1.916
1.2	1.2880	2.4251	2.190	1.1349	2.137
1.3	1.3380	2.7708	2.450	1.1567	2.395
1.4	1.3920	3.1823	2.746	1.1798	2.697
1.5	1.4500	3.6712	3.084	1.204	3.049
1.6	1.5120	4.2504	3.463	1.229	3.456
1.7	1.5780	4.9361	3.888	1.256	3.929
1.8	1.6480	5.7459	4.361	1.284	4.476
1.9	1.7220	6.7006	4.880	1.312	5.106
2.0	1.8000	7.8244	5.448	1.342	5.832
2.1	1.8820	9.1448	6.060	1.372	6.666
2.2	1.9680	10.693	6.717	1.403	7.622
2.3	2.0580	12.505	7.413	1.435	8.717
2.4	2.1520	14.620	8.141	1.467	9.966
2.5	2.2500	17.086	8.894	1.500	11.39
2.6	2.3520	19.955	9.663	1.533	13.01
2.7	2.4580	23.283	10.44	1.568	14.85
2.8	2.5680	27.139	11.20	1.602	16.93
2.9	2.6820	31.594	11.94	1.638	19.29
3.0	2.8000	36.733	12.64	1.673	21.95
3.1	2.9220	42.646	13.29	1.709	24.95
3.2	3.0480	49.435	13.88	1.746	28.32
3.3	3.1780	57.216	14.37	1.783	32.10
3.4	3.3120	66.116	14.78	1.820	36.33
3.5	3.4500	76.273	15.08	1.857	41.06

Table I-1

Working Functions of Flight Mach Number for Evaluation of Total Temperature and Pressure

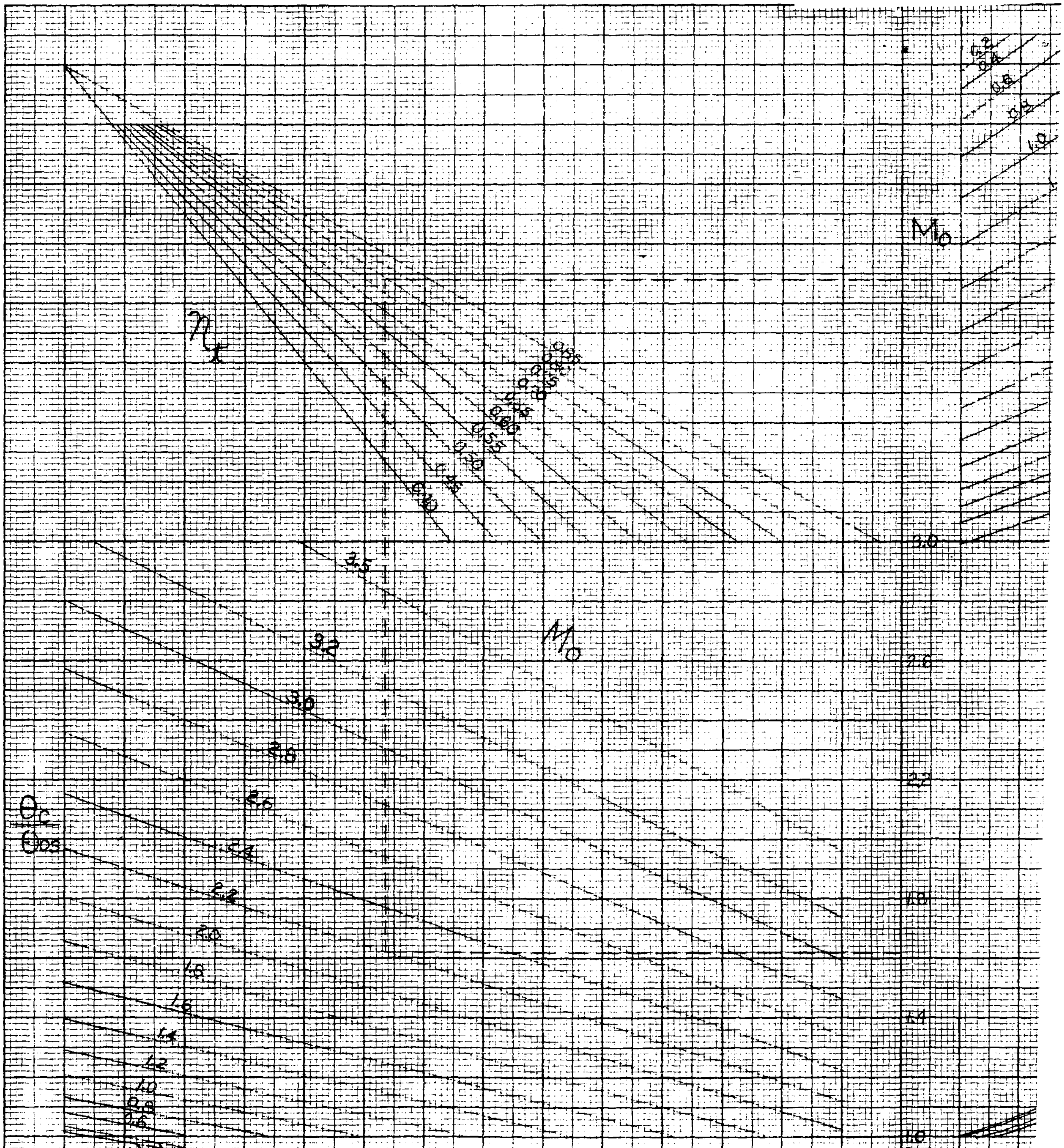

Figure I-23
Working Chart for Determination of Pres
Temperature at Heat Exchanger Entran

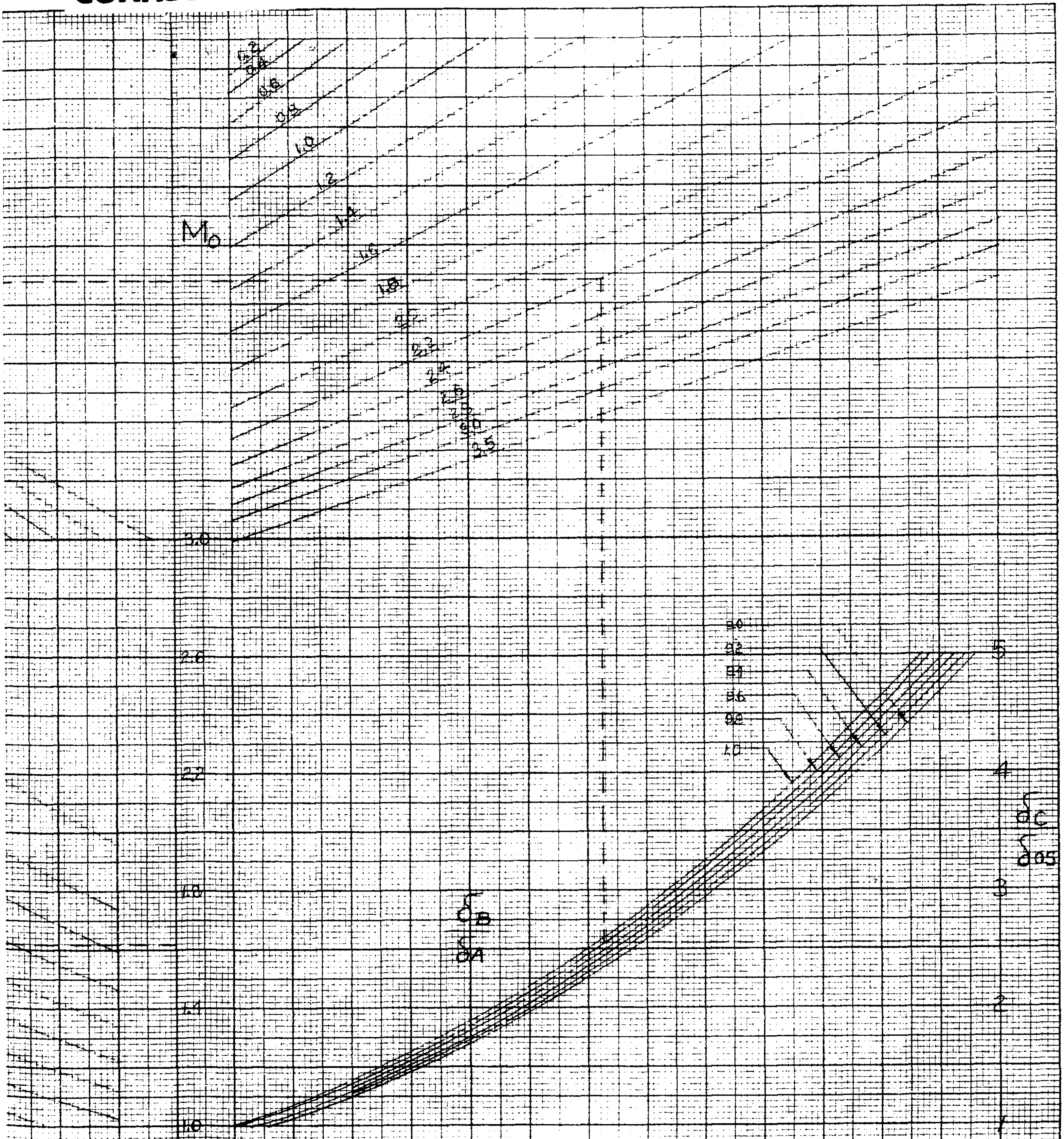

Figure I-23
Chart for Determination of Pressure and
rature at Heat Exchanger Entrance

CONFIDENTIAL

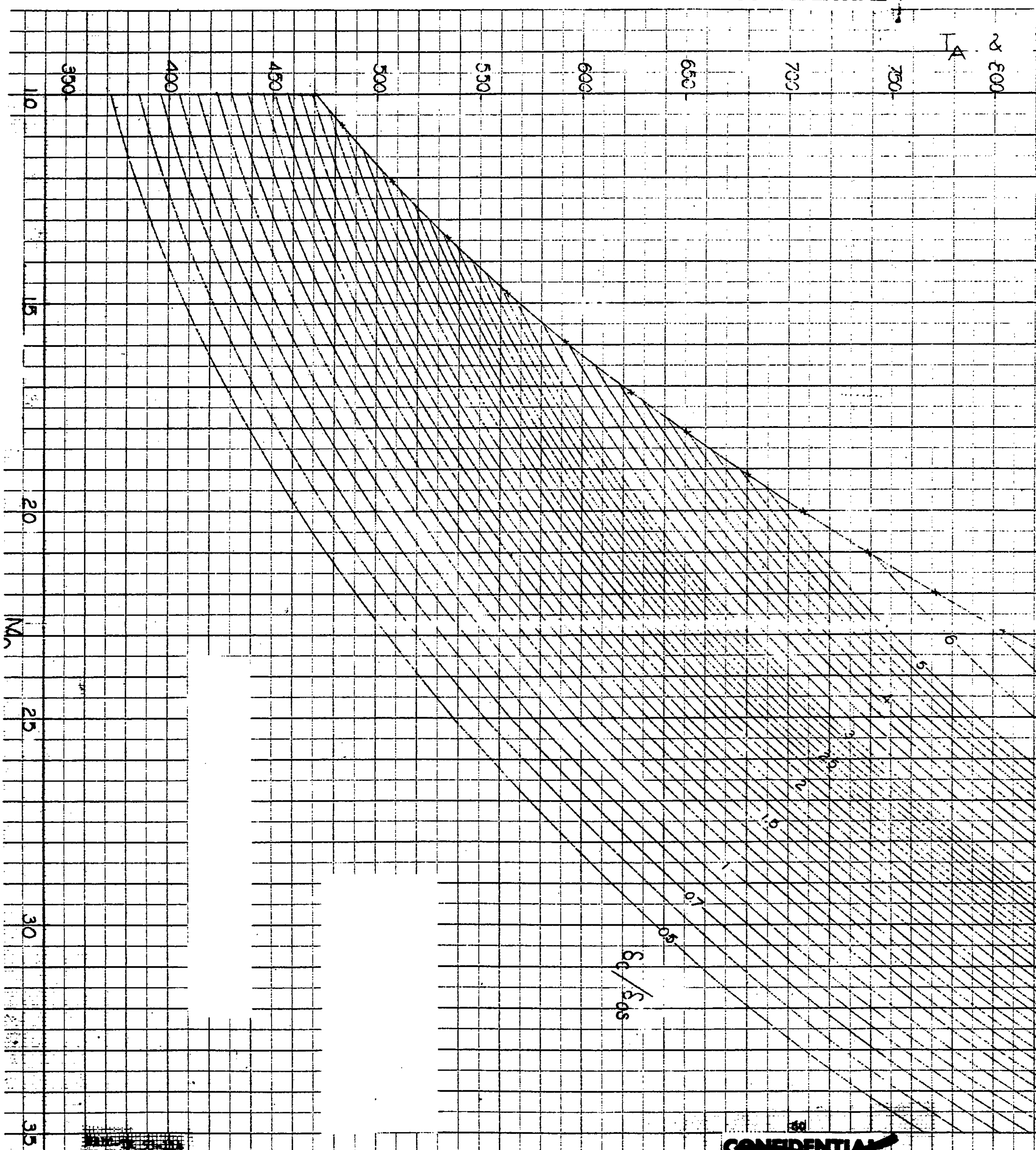

CONFIDENTIAL

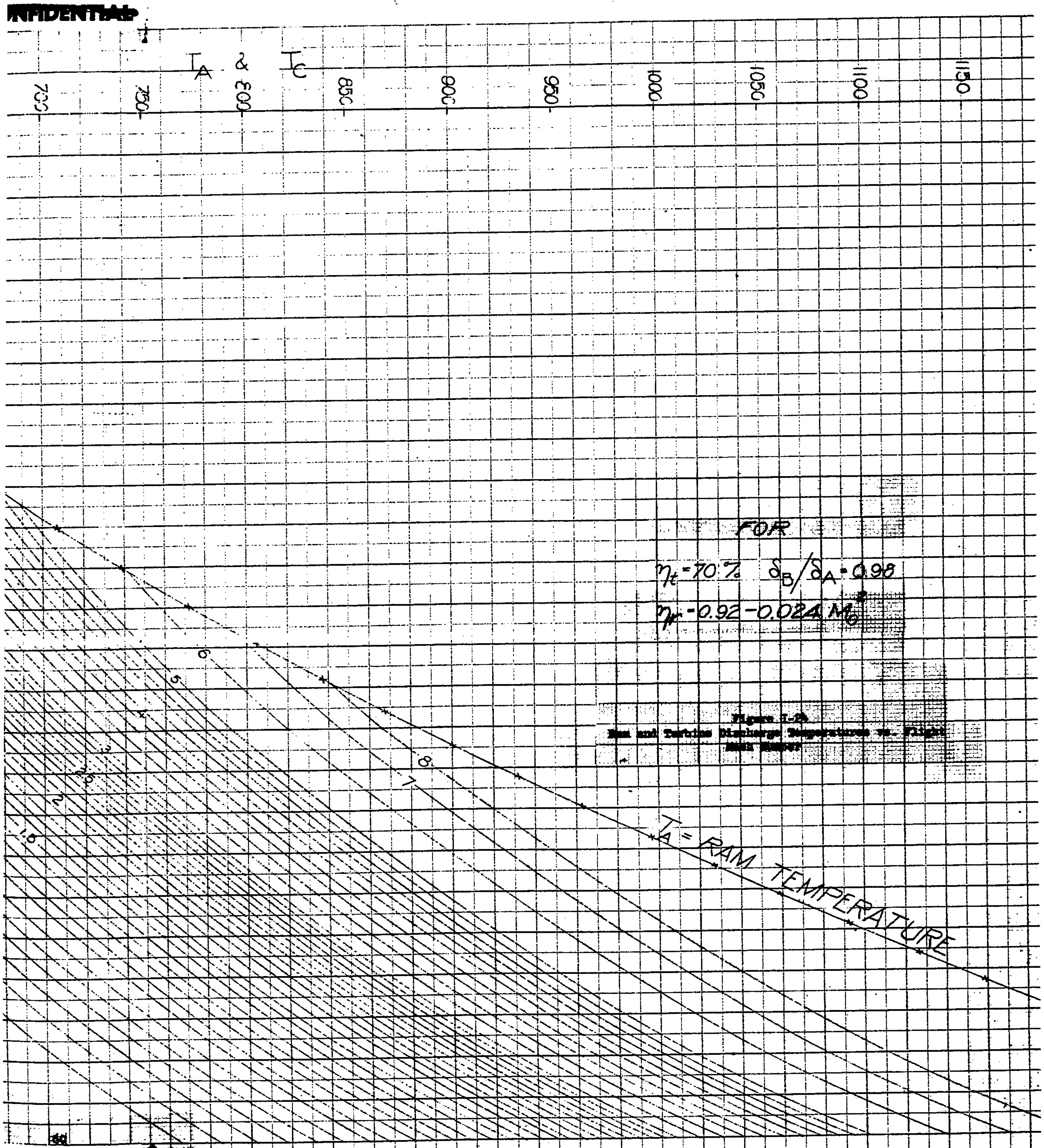

Figure I-2b
Ram and Turbine Discharge Temperatures vs. Flight Mach Number

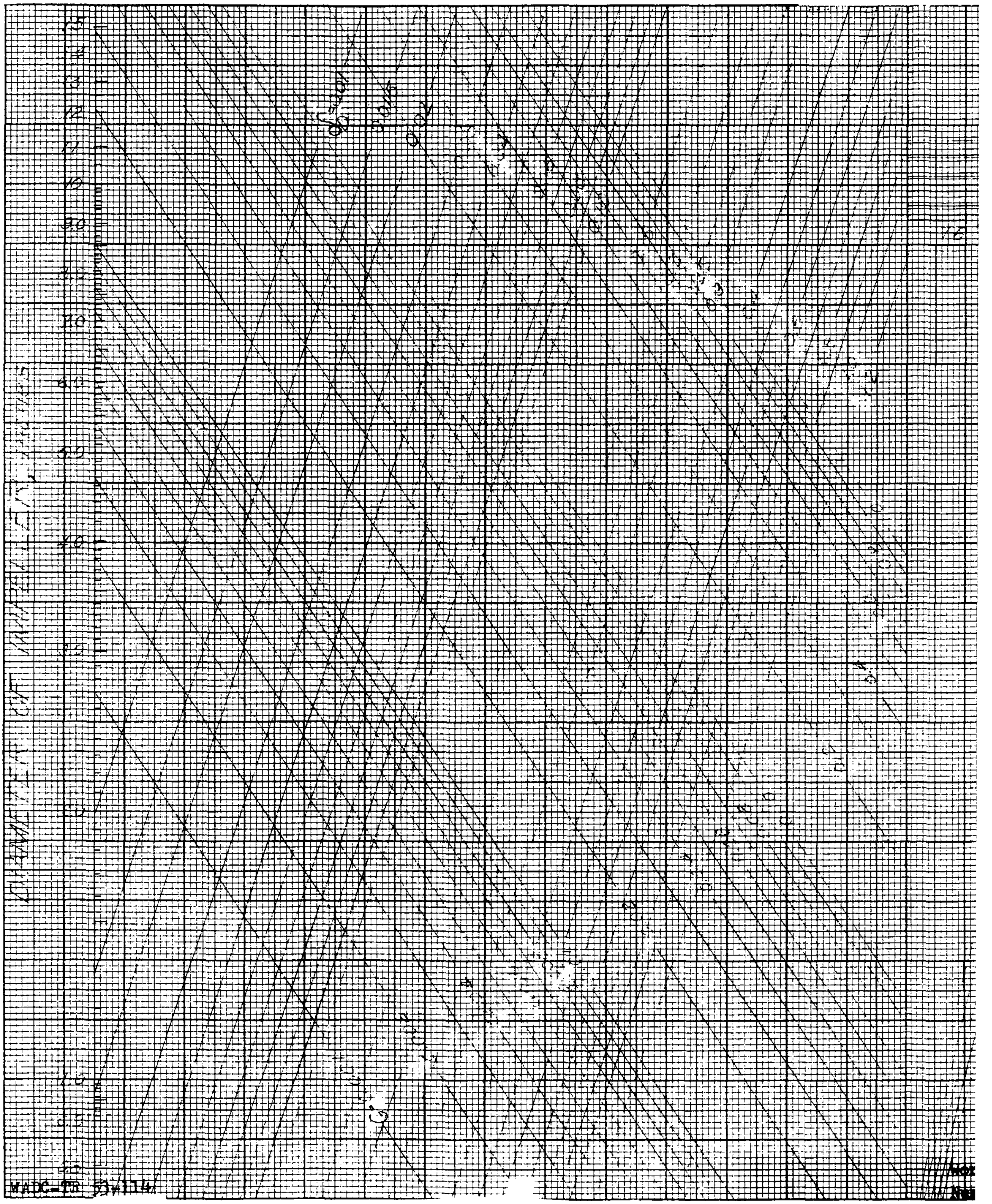

CONFIDENTIAL

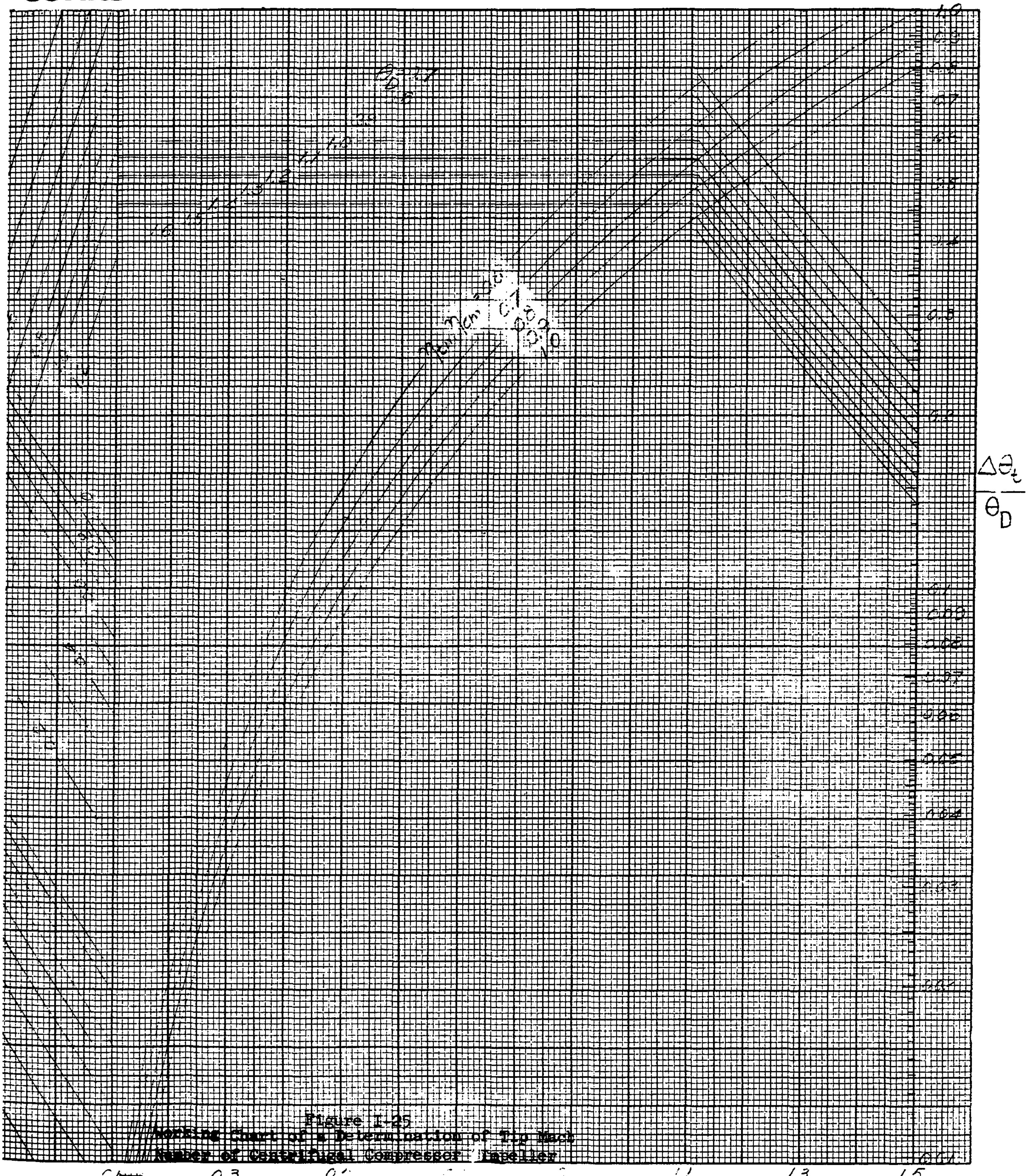

Figure I-25
Working Chart of a Determination of Tip Mach
Number of Centrifugal Compressor Impeller

CONFIDENTIAL

61

(7)

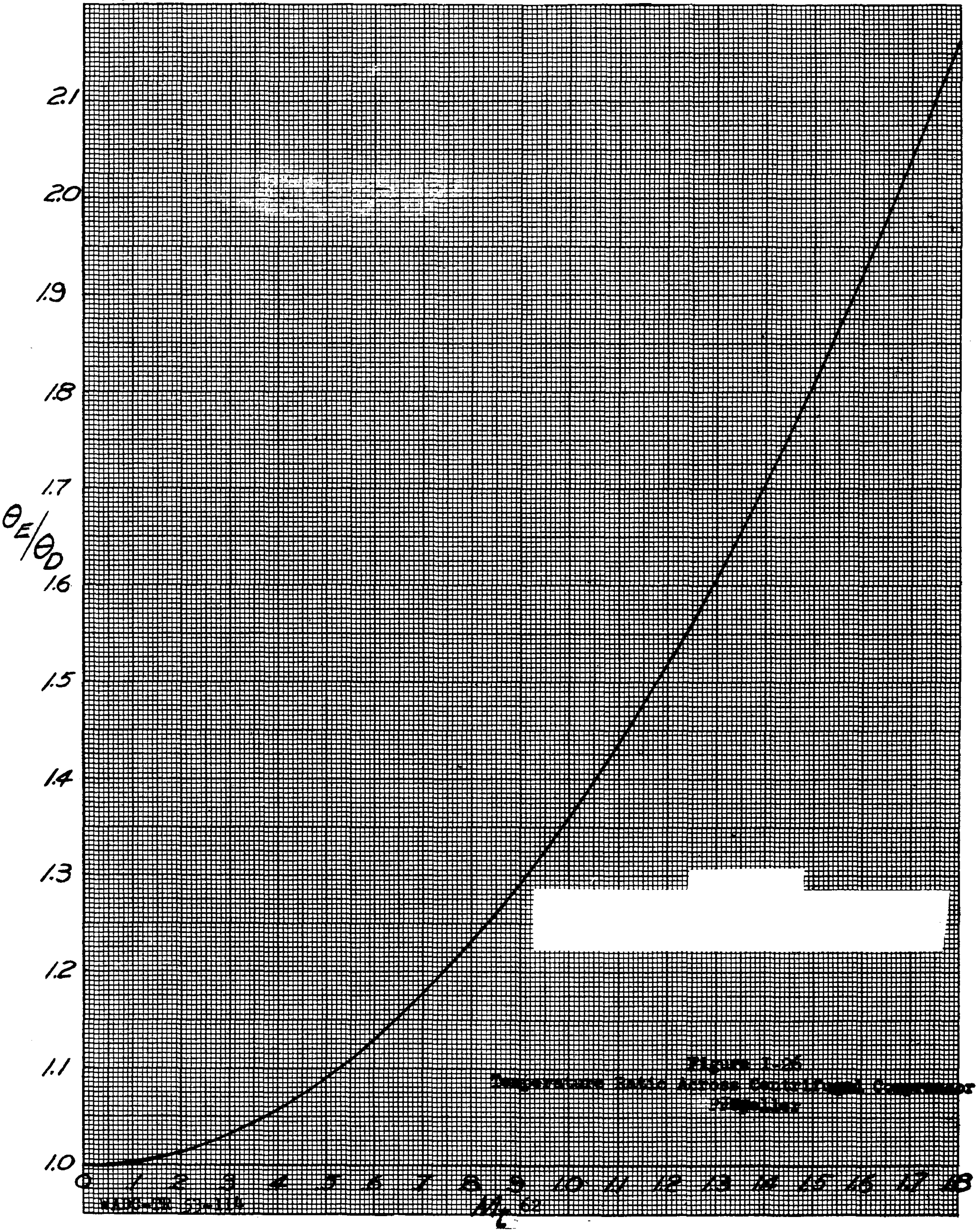

Figure 1-26
Temperature Ratio Across Centrifugal Compressor Impeller

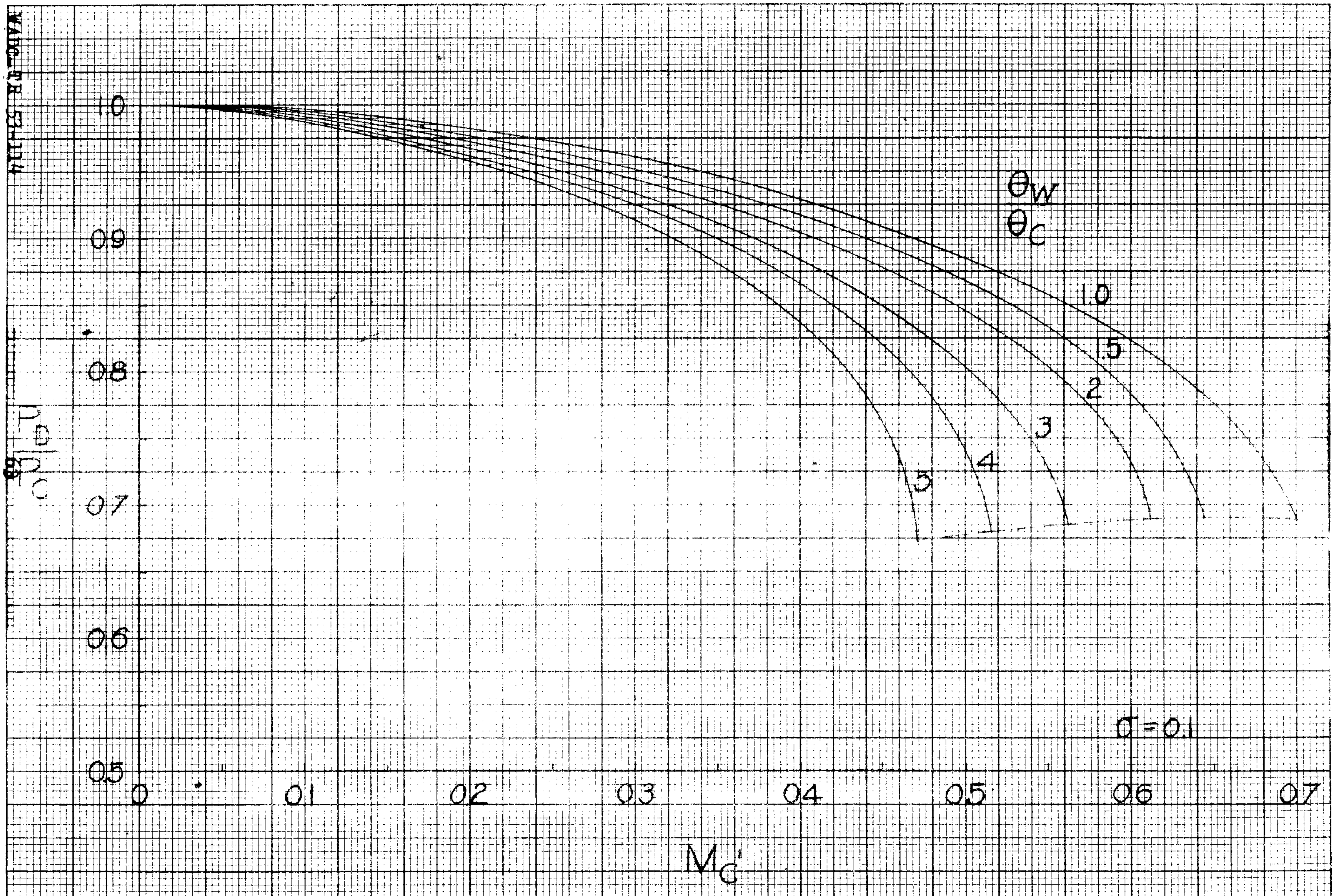

Figure I-27
Pressure Ratio Across Heat Exchanger vs. Tube Inlet Mach Number, σ = 0.1

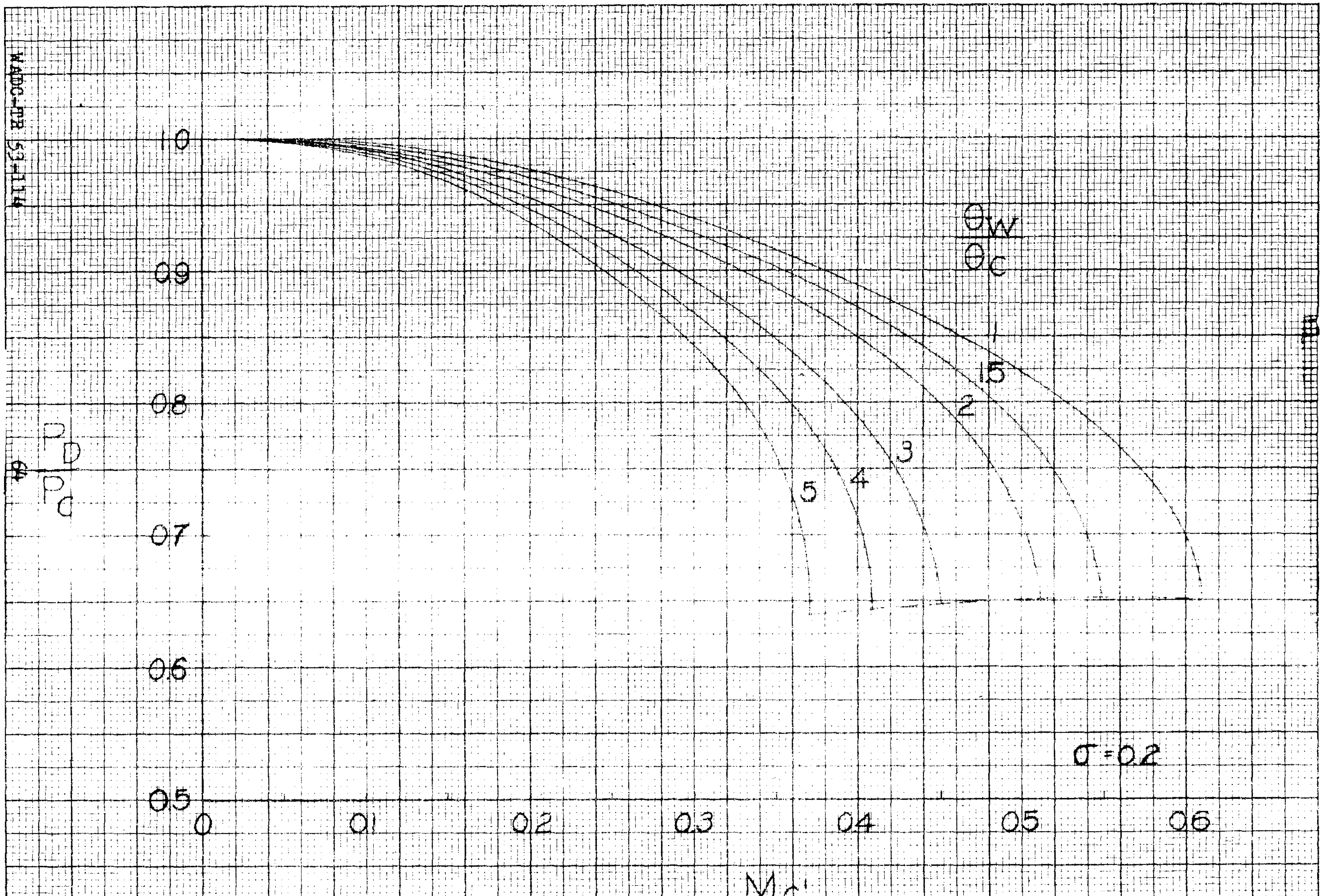

Figure I-28
Pressure Ratio Across Heat Exchanger vs. Tube Inlet Mach Number, $\sigma = 0.2$

CONFIDENTIAL

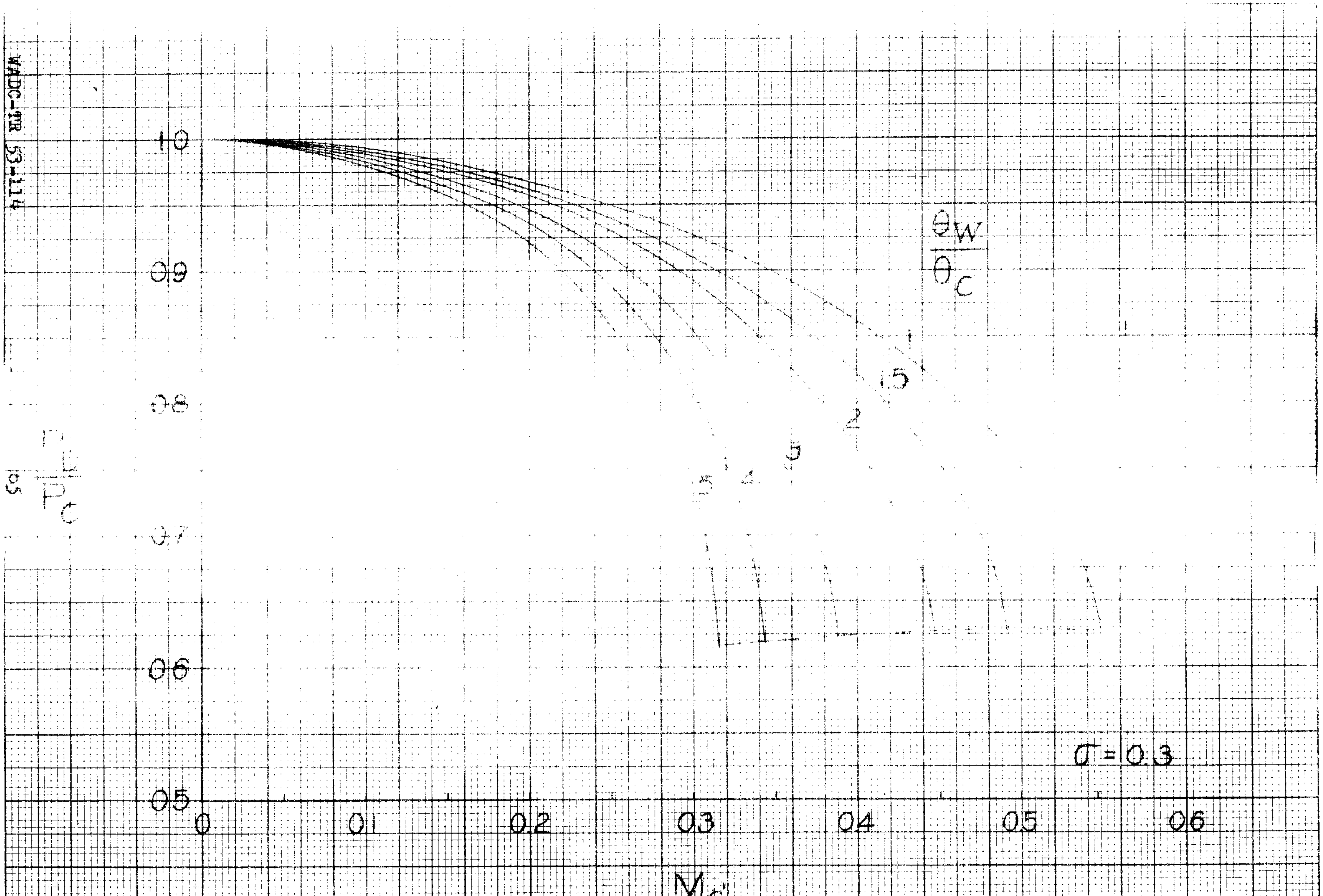

Figure I-29
Pressure Ratio Across Heat Exchanger vs. Tube Inlet Mach Number $\sigma = 0.3$

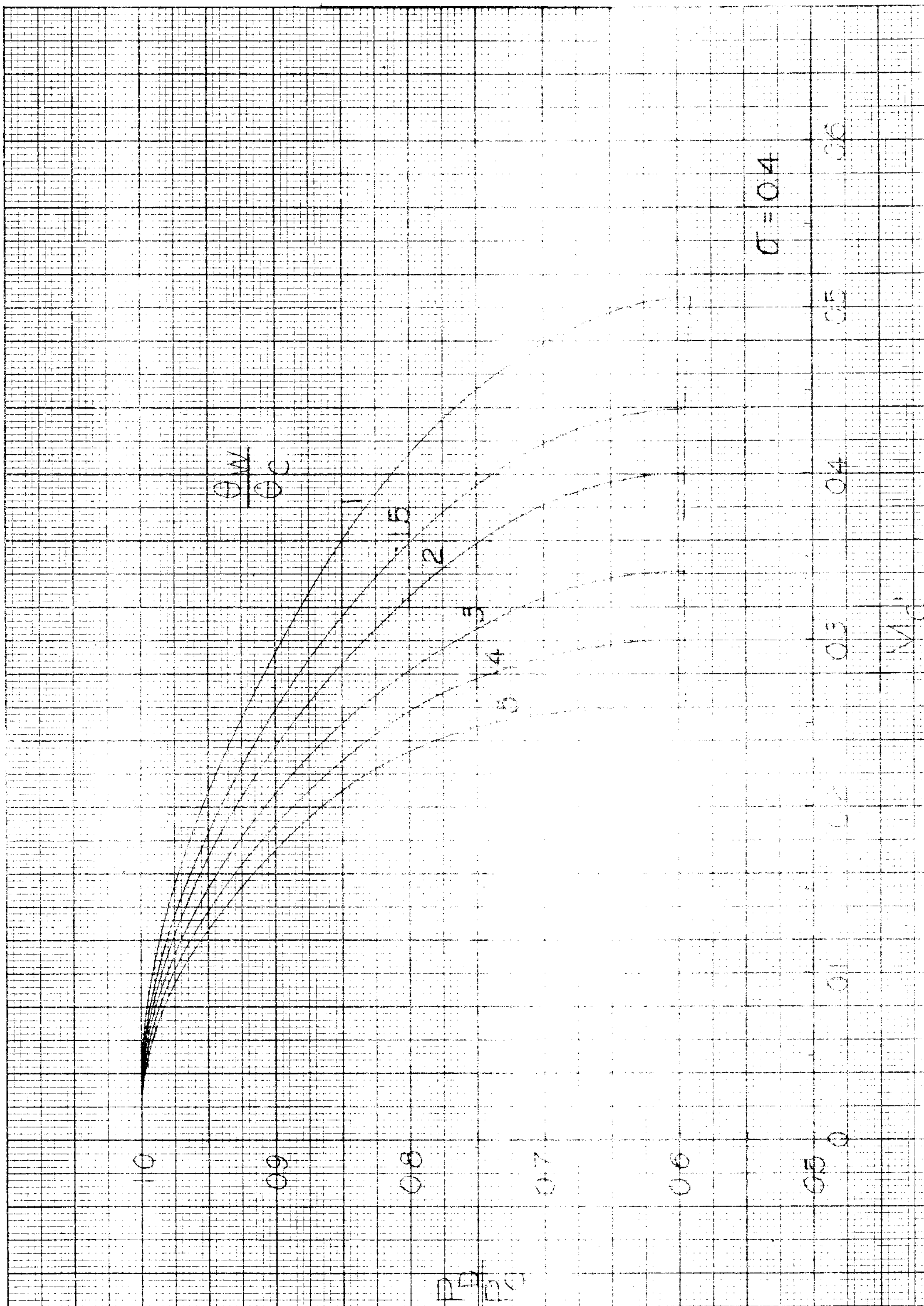

Figure II-30

Pressure Ratio Across Heat Exchanger vs. Tube Inlet Mach Number, σ = 0.4

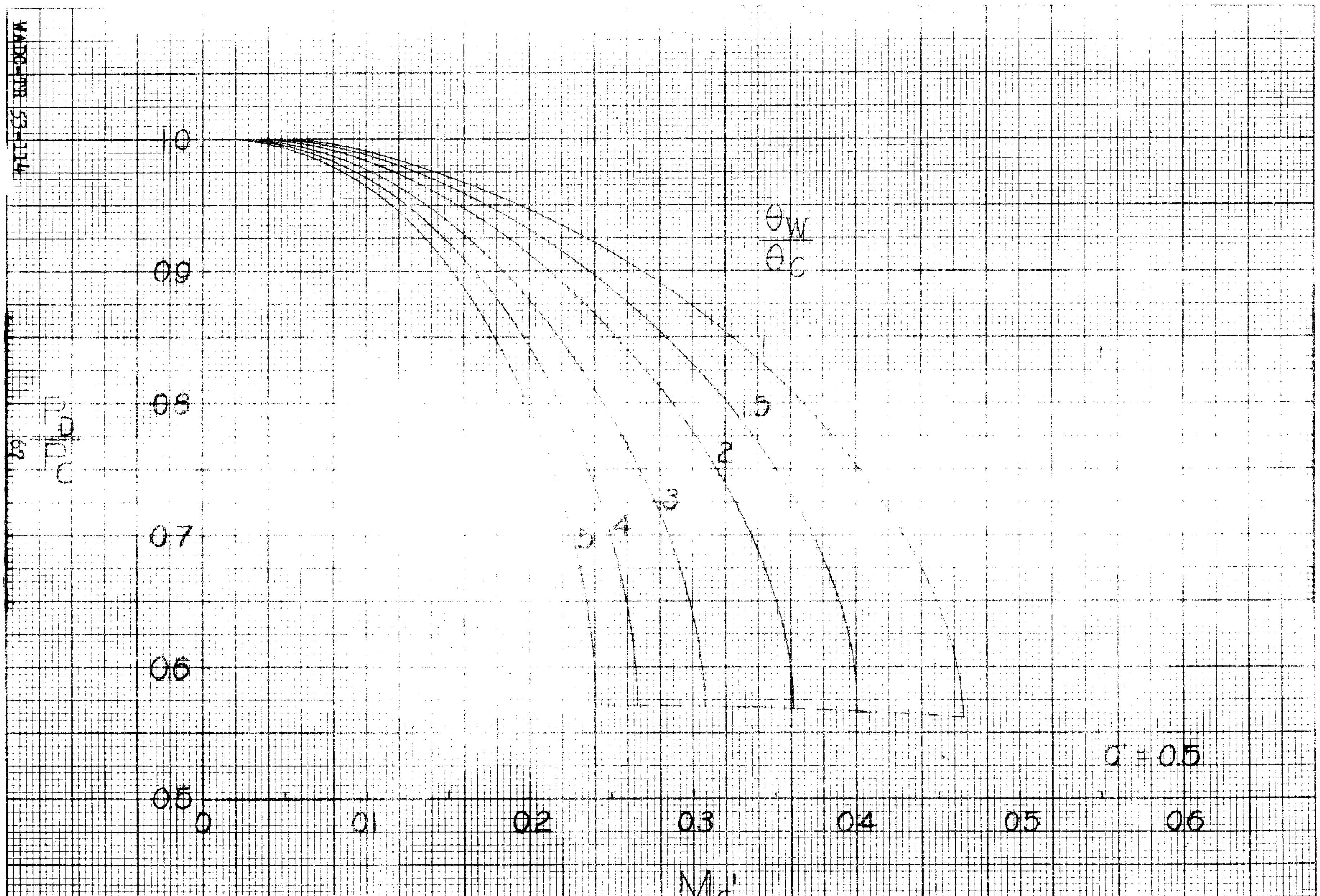

Figure I-31
Pressure Ratio Across Heat Exchanger vs. Tube Outlet Mach Number, σ = 0.5

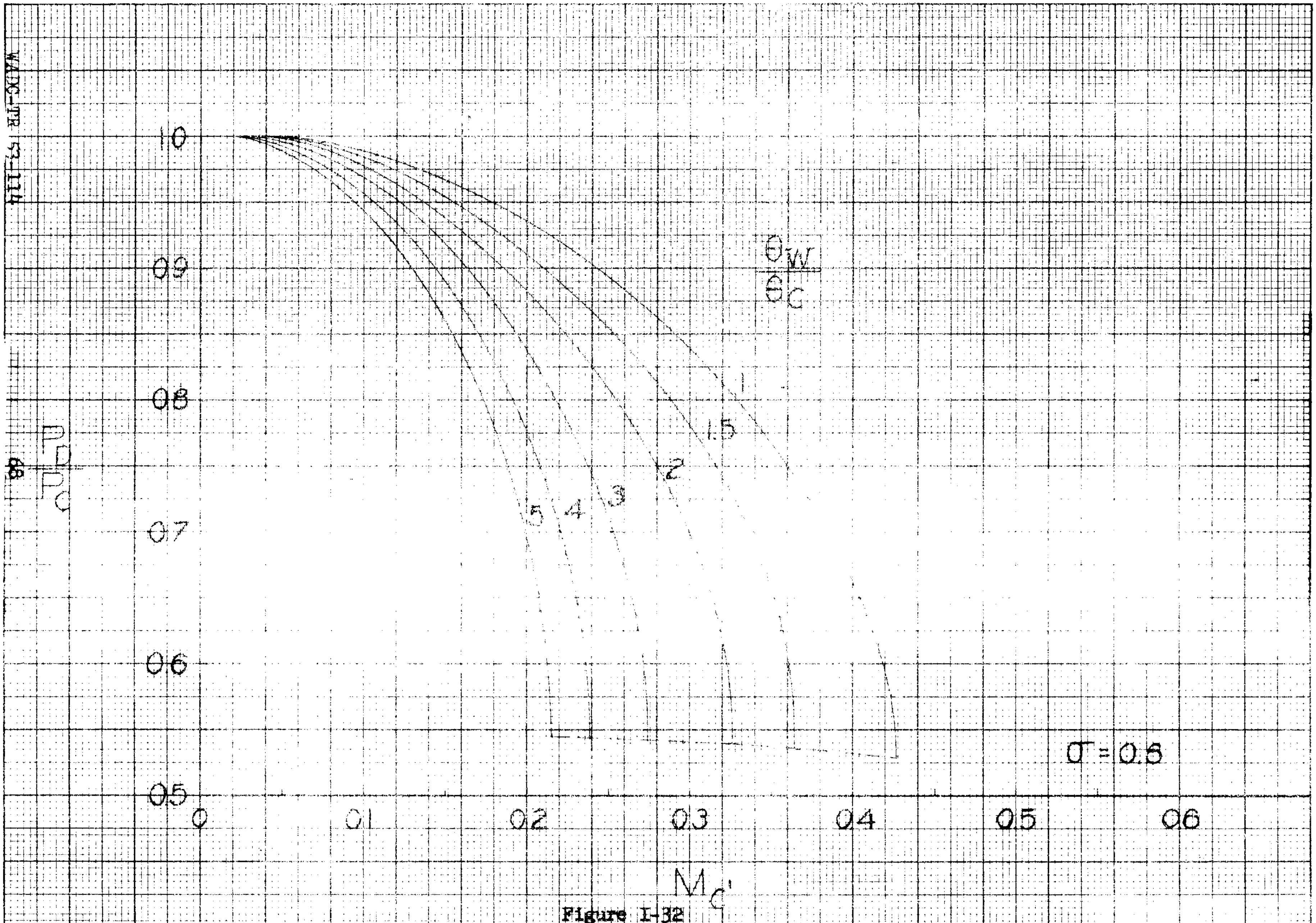

Figure I-32
Pressure Ratio Across Heat Exchanger vs. Tube Inlet Mach Number, $\sigma = 0.6$

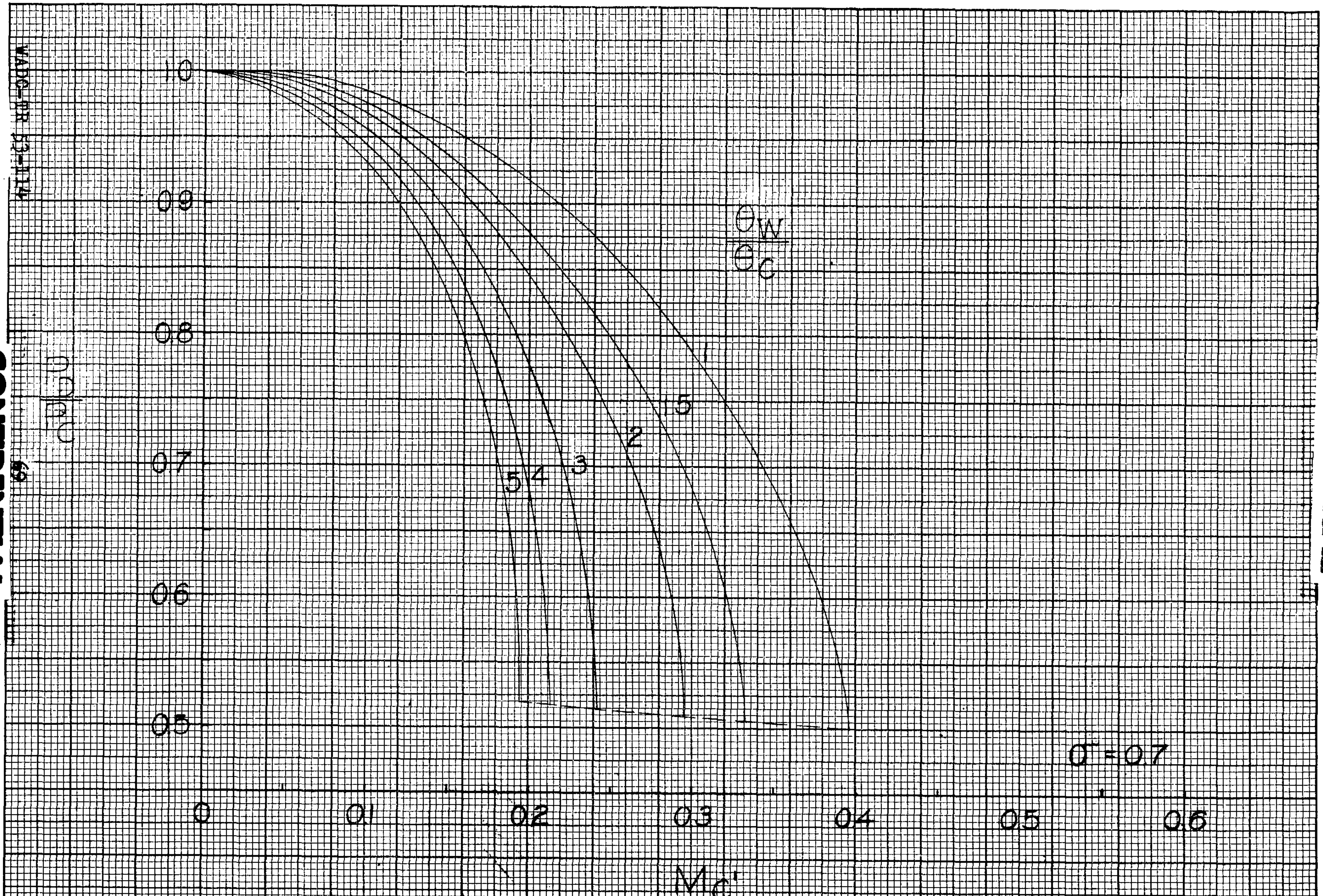

Figure I-33
Pressure Ratio Across Heat Exchanger vs. Tube Inlet Mach Number, $\sigma = 0.7$

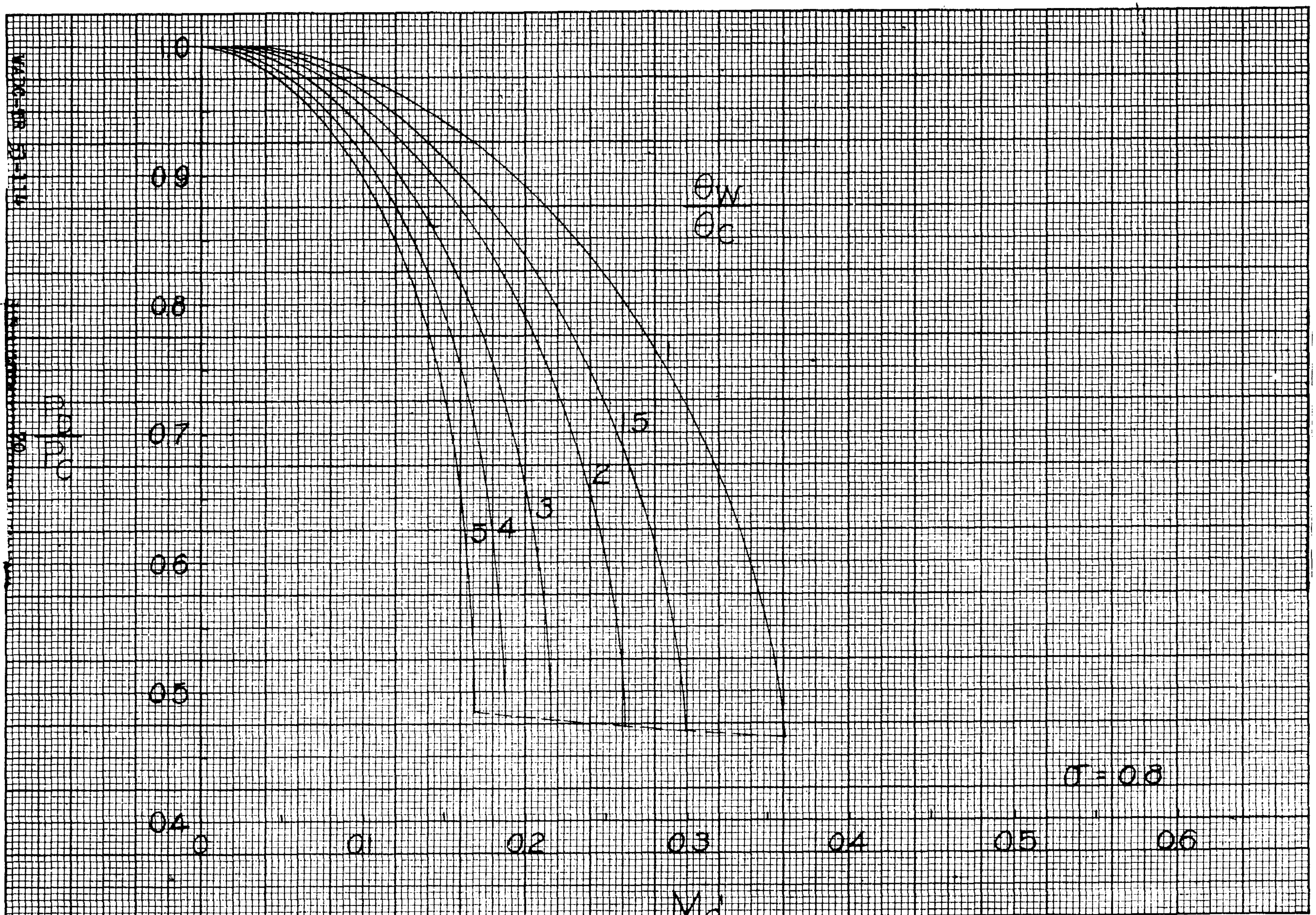

Figure I-34
Pressure Ratio Across Heat Exchanger vs. Tube Inlet Mach Number, $\sigma = 0.8$

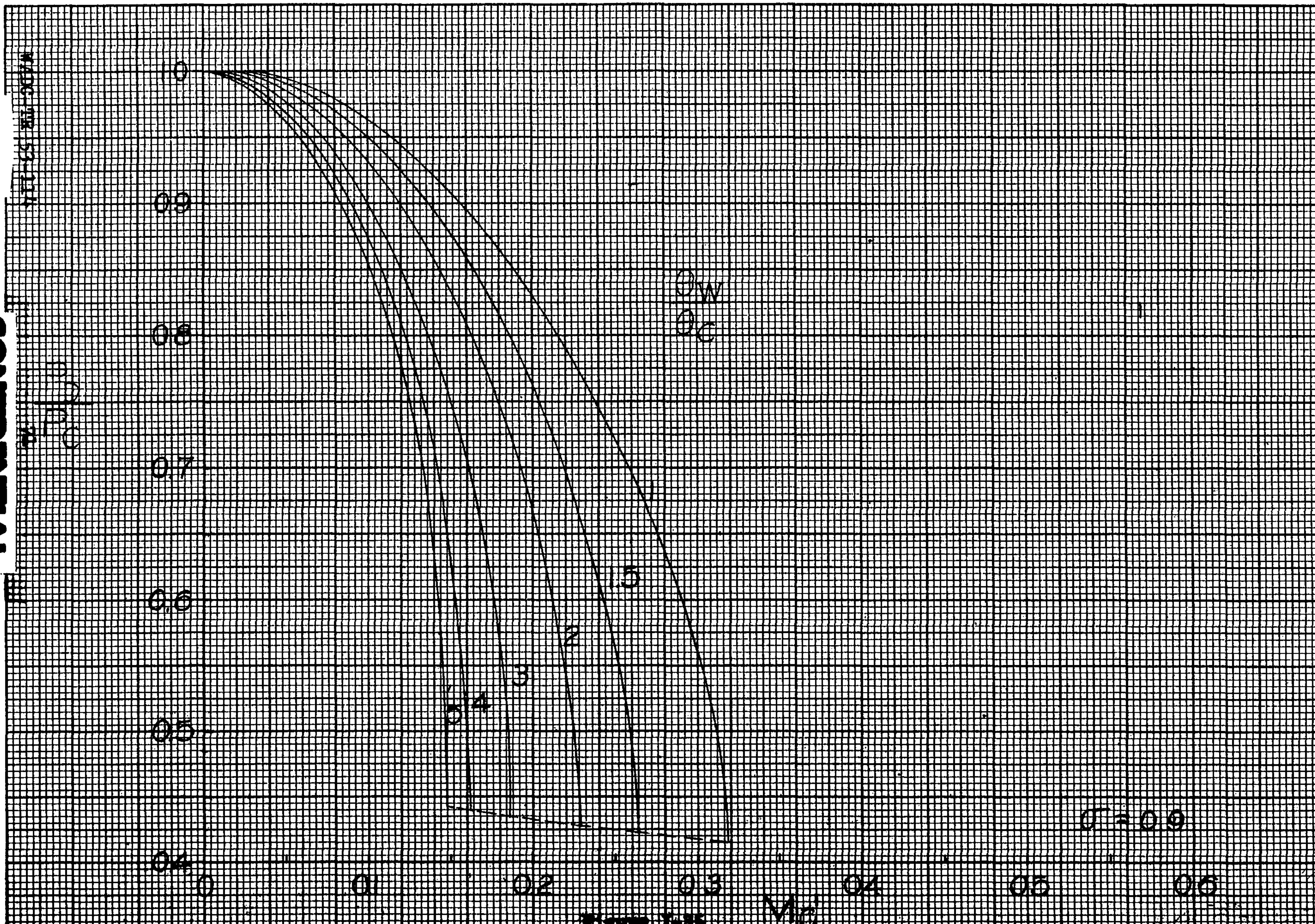

Figure [illegible]
Pressure Ratio Across Heat Exchanger vs. Tube Inlet Mach Number, σ = 0.9

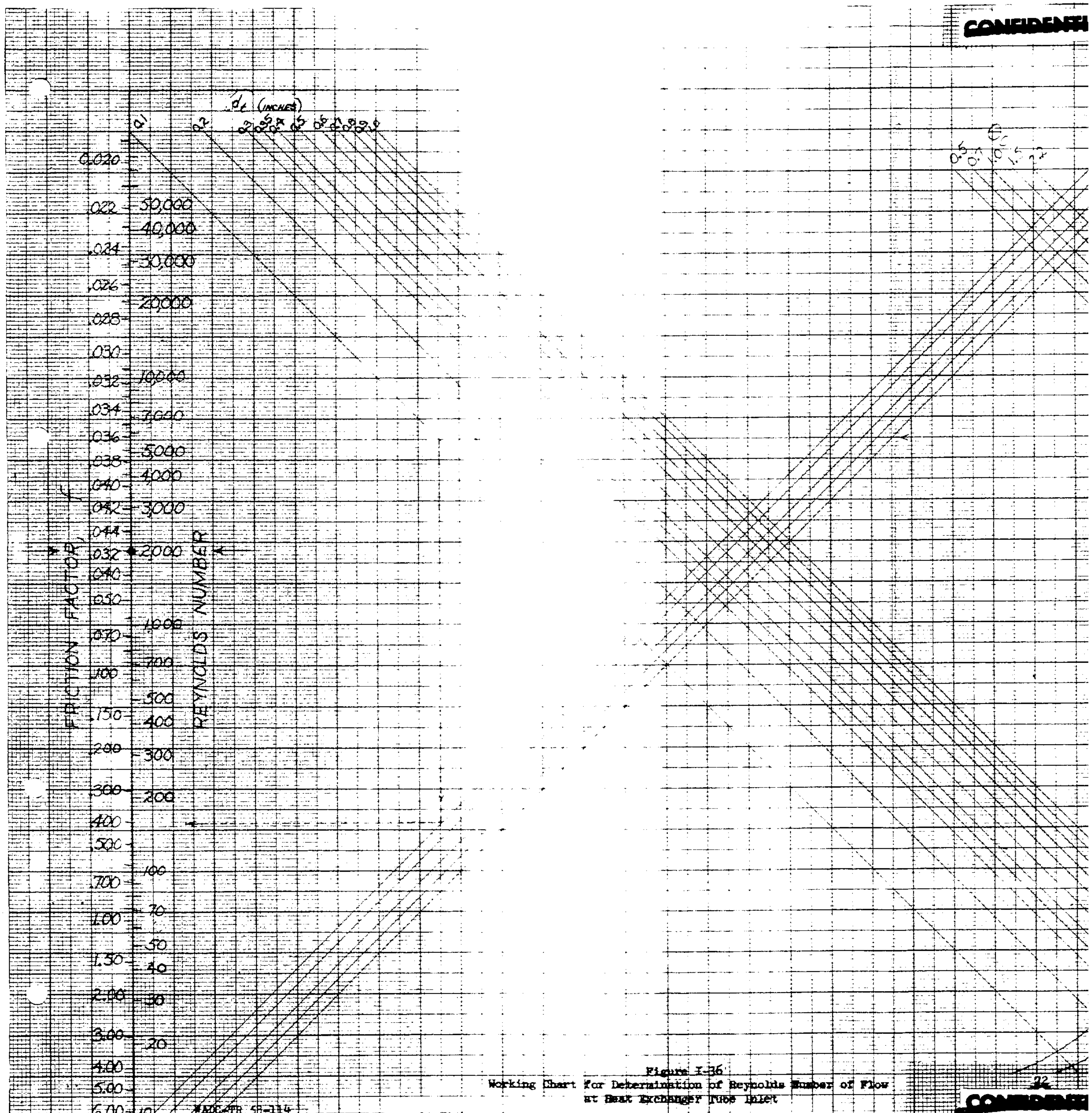

Figure I-36
Working Chart for Determination of Reynolds Number of Flow at Heat Exchanger Tube Inlet

CONFIDENTIAL

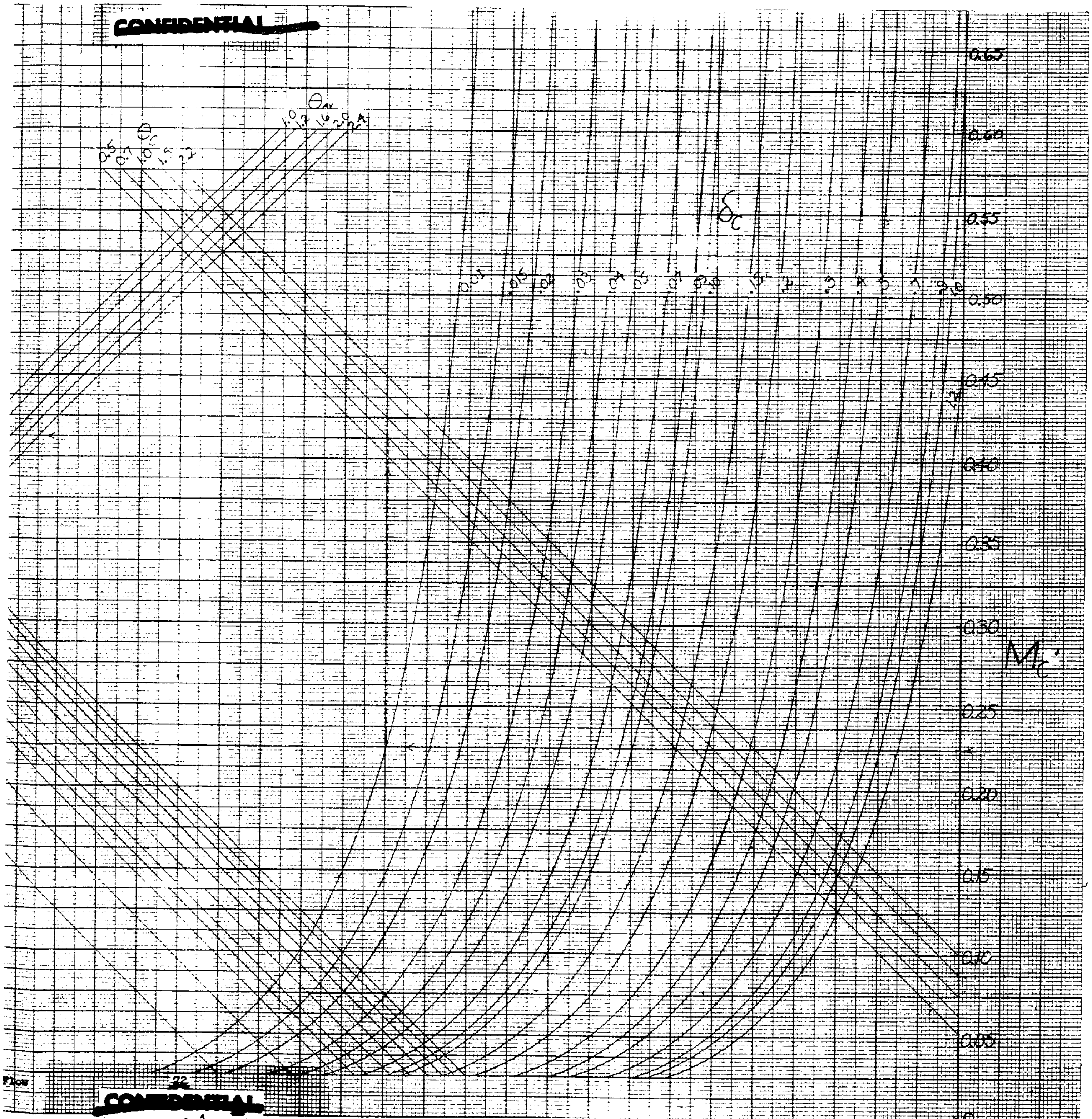

CONFIDENTIAL

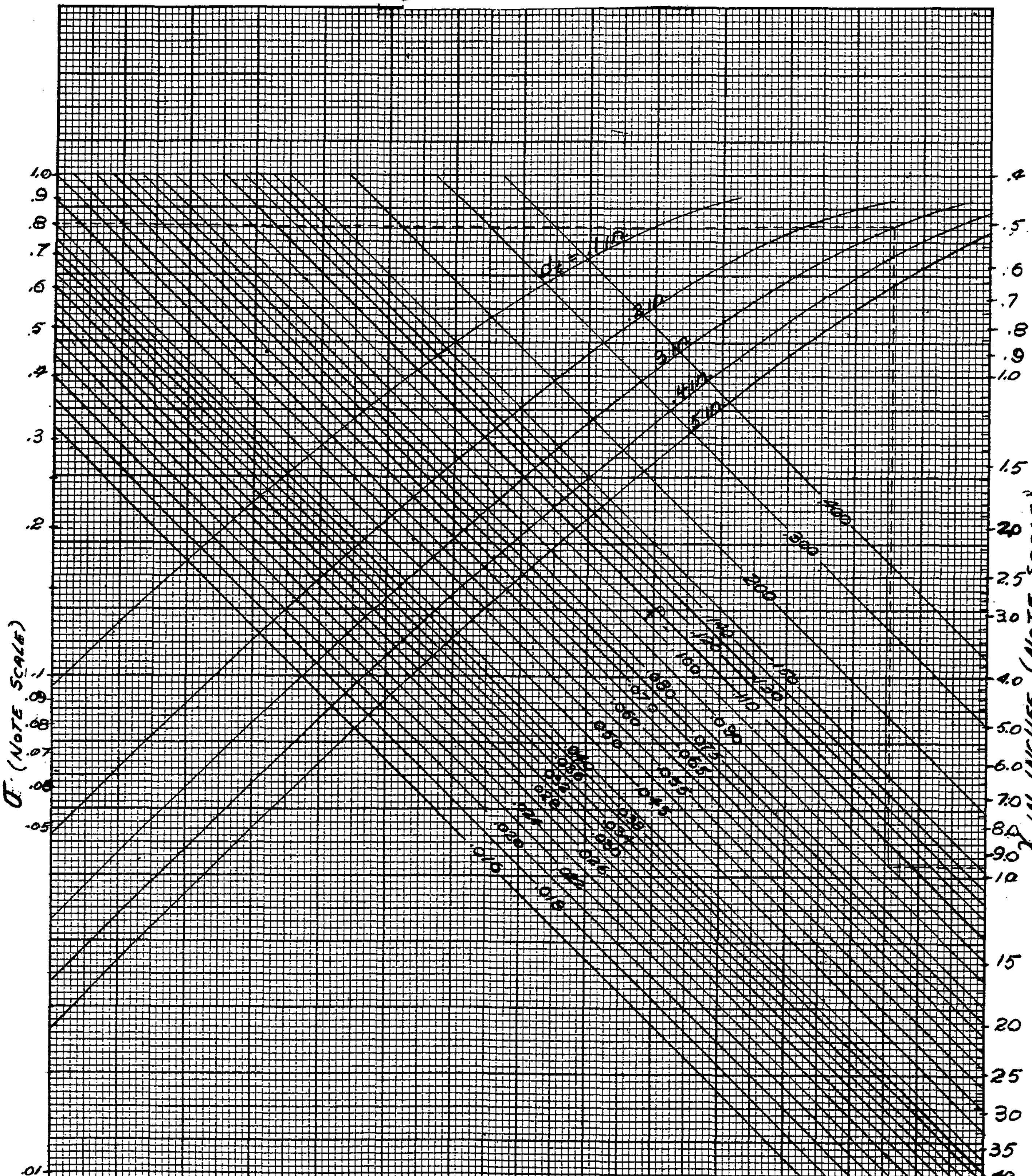

Figure I-37
Working Chart for Determination of Heat Exchanger Effectiveness

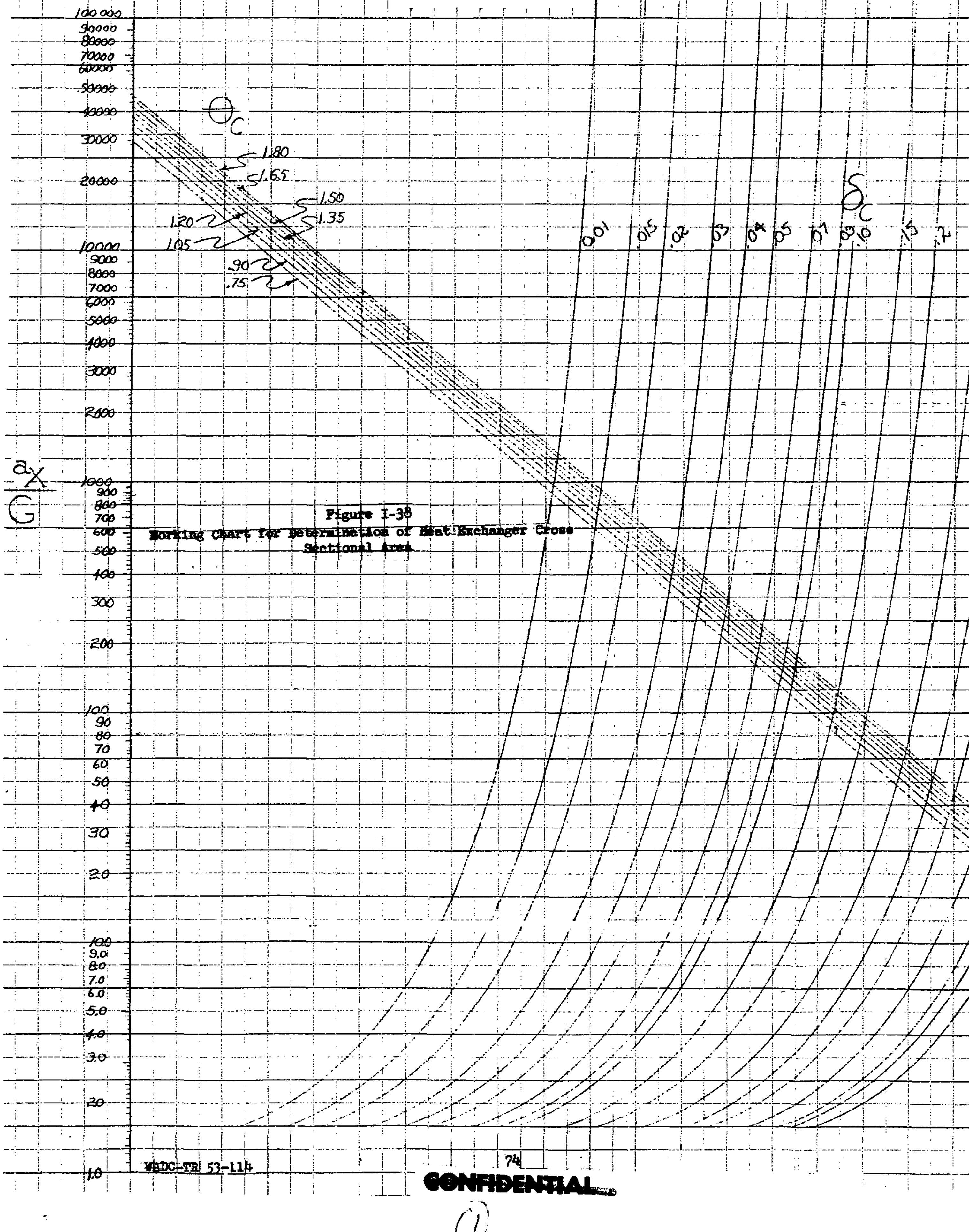

Figure I-38
Working Chart for Determination of Heat Exchanger Cross Sectional Area

(1)

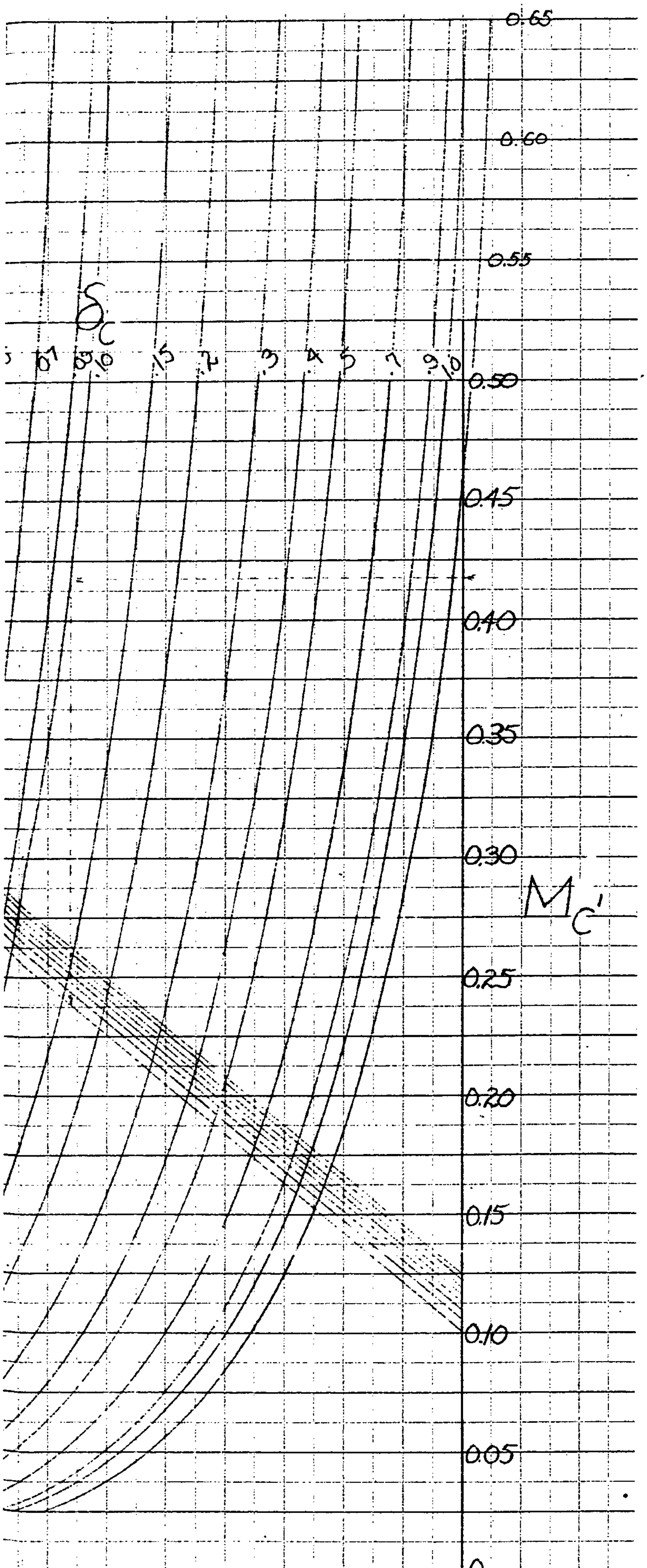

δ_c
.07
.08
.10
.15
.2
.3
.4
.5
.7
.9
1.0
M_c'
0.65
0.60
0.55
0.50
0.45
0.40
0.35
0.30
0.25
0.20
0.15
0.10
0.05
0

(2)

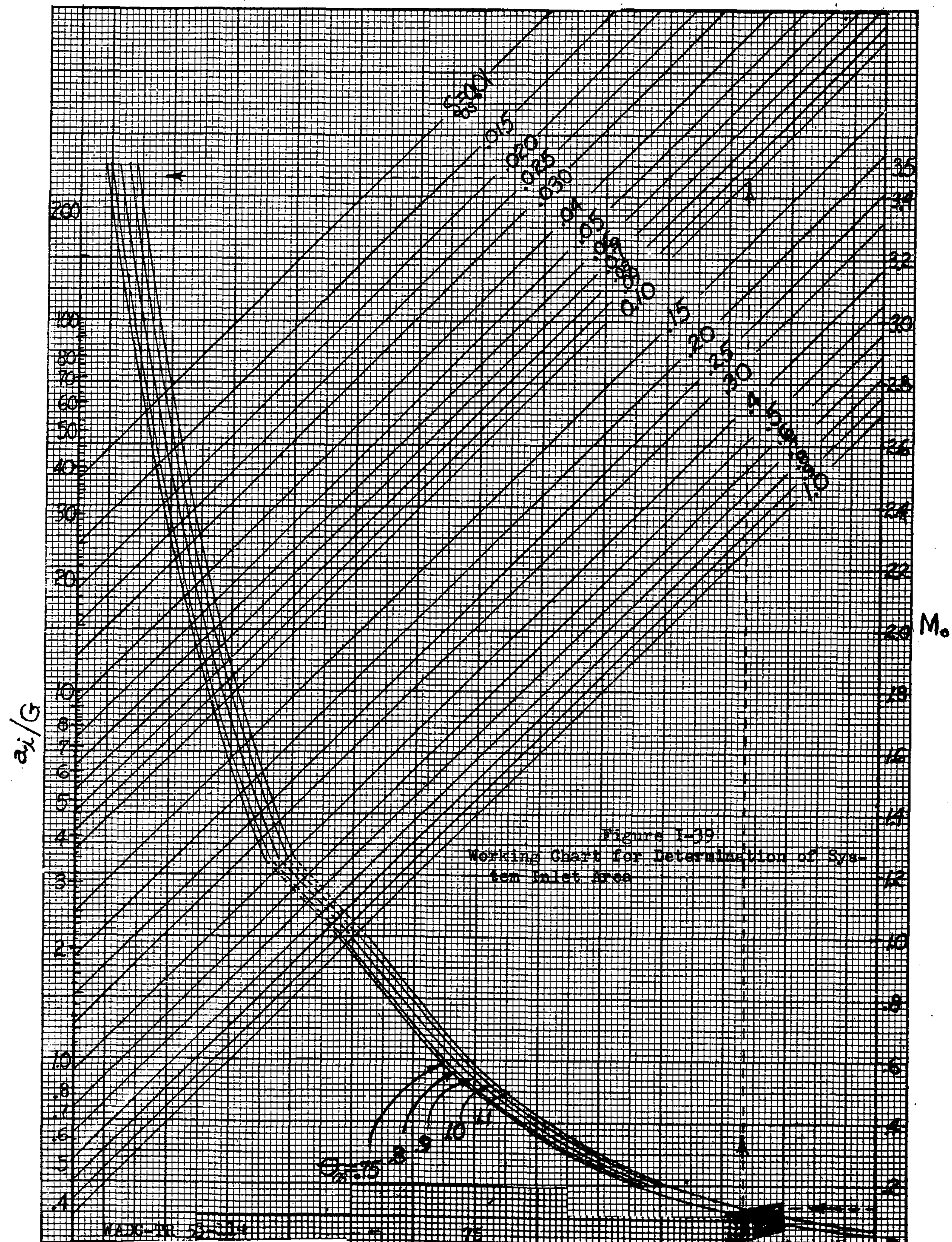

Figure I-39
Working Chart for Determination of System Inlet Area

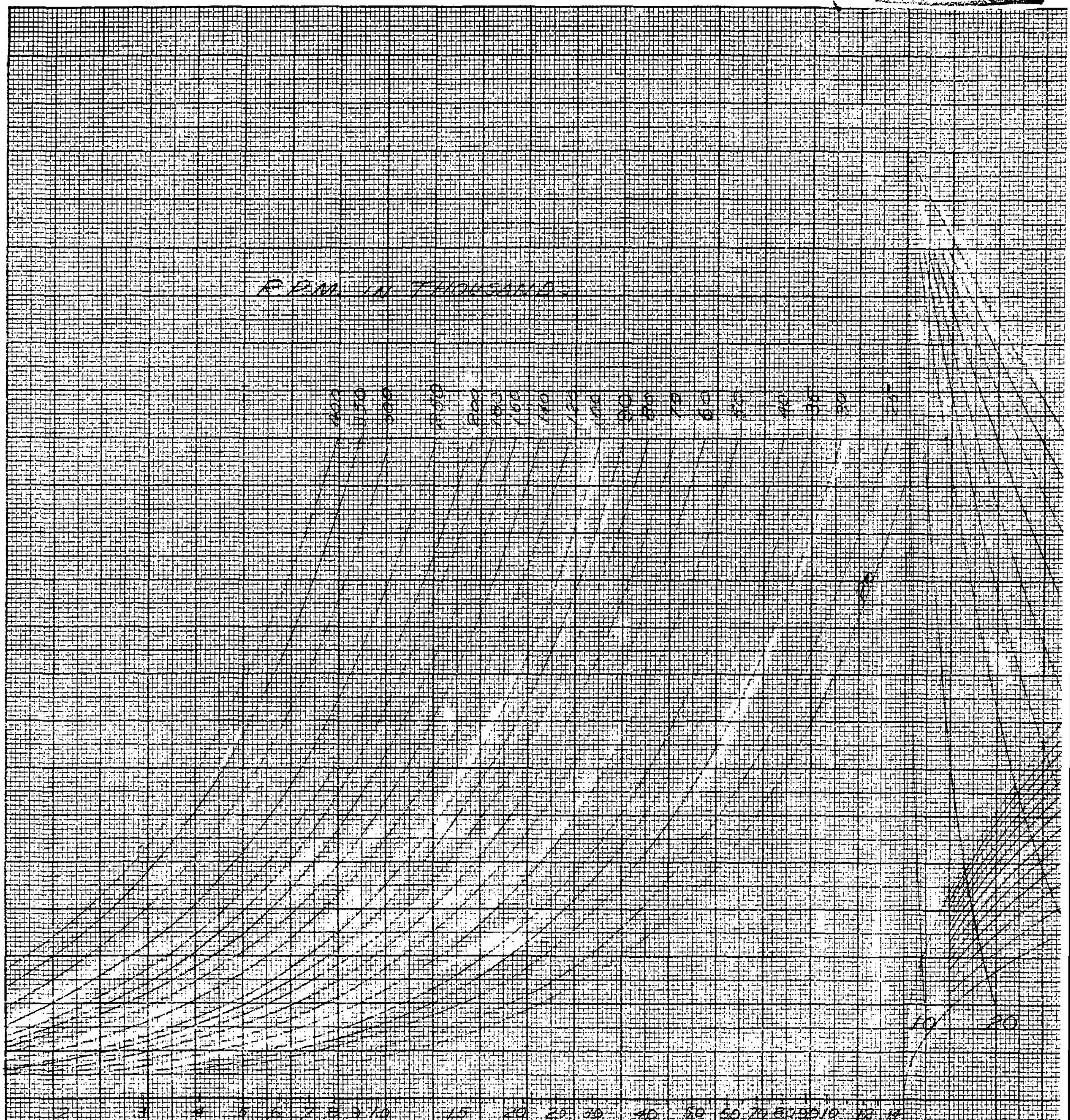

LADC TR 55-110 D_p - INCHES

Figure I-40
Working Chart for Determination of Axial Turbine

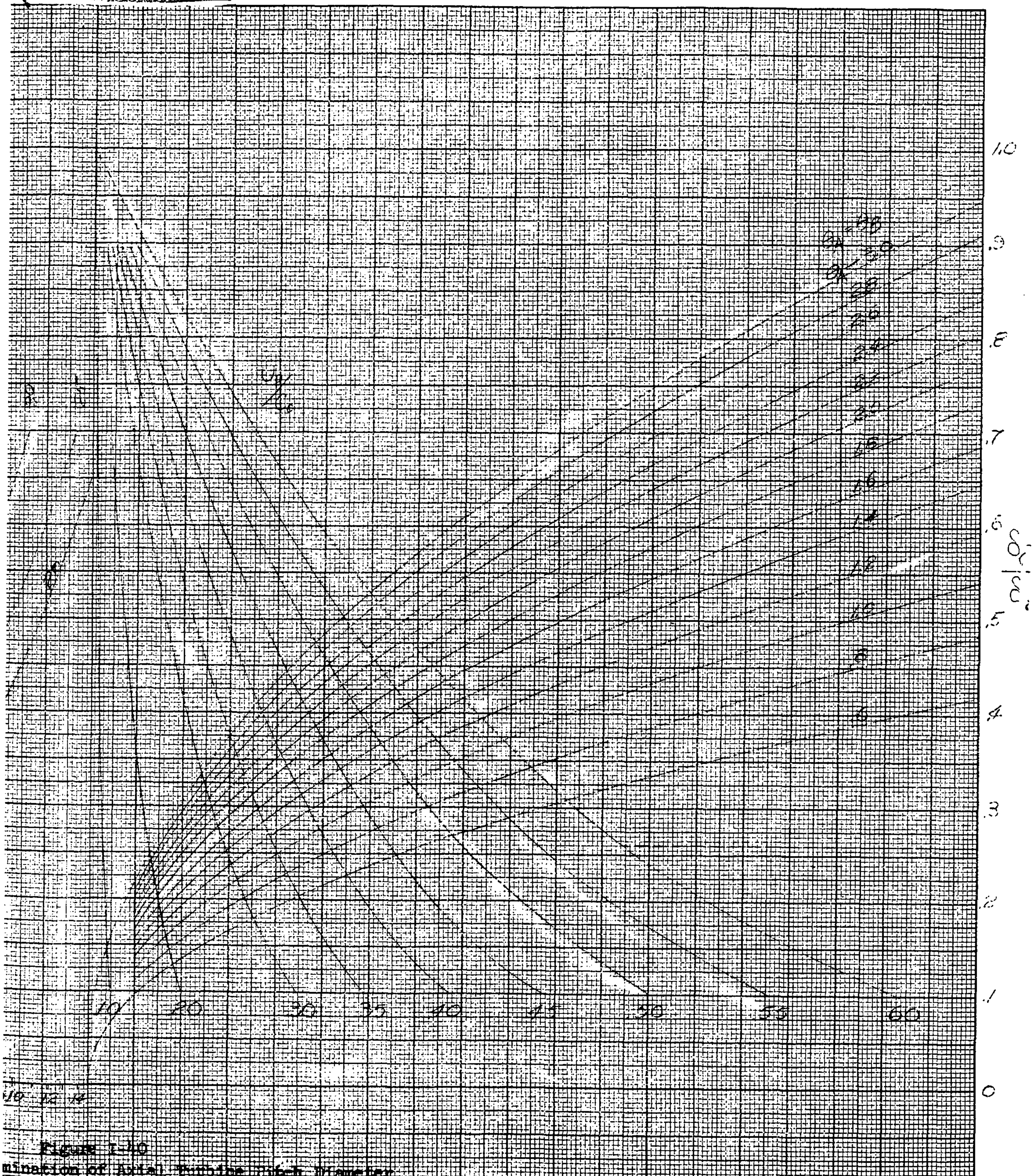

Figure I-40
...mination of Axial Turbine Pitch Diameter

(2)

CONFIDENTIAL

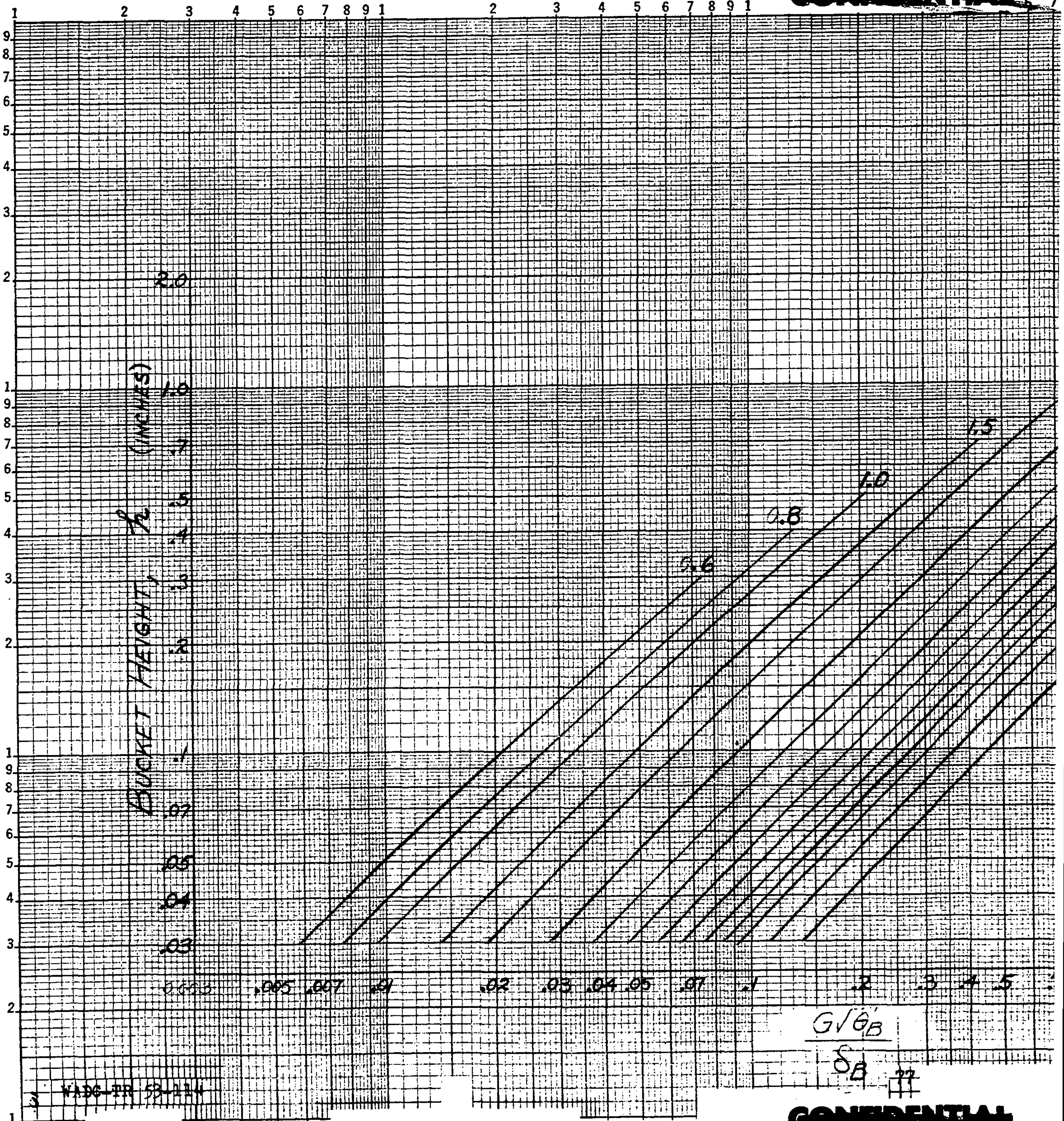

CONFIDENTIAL

1

CONFIDENTIAL

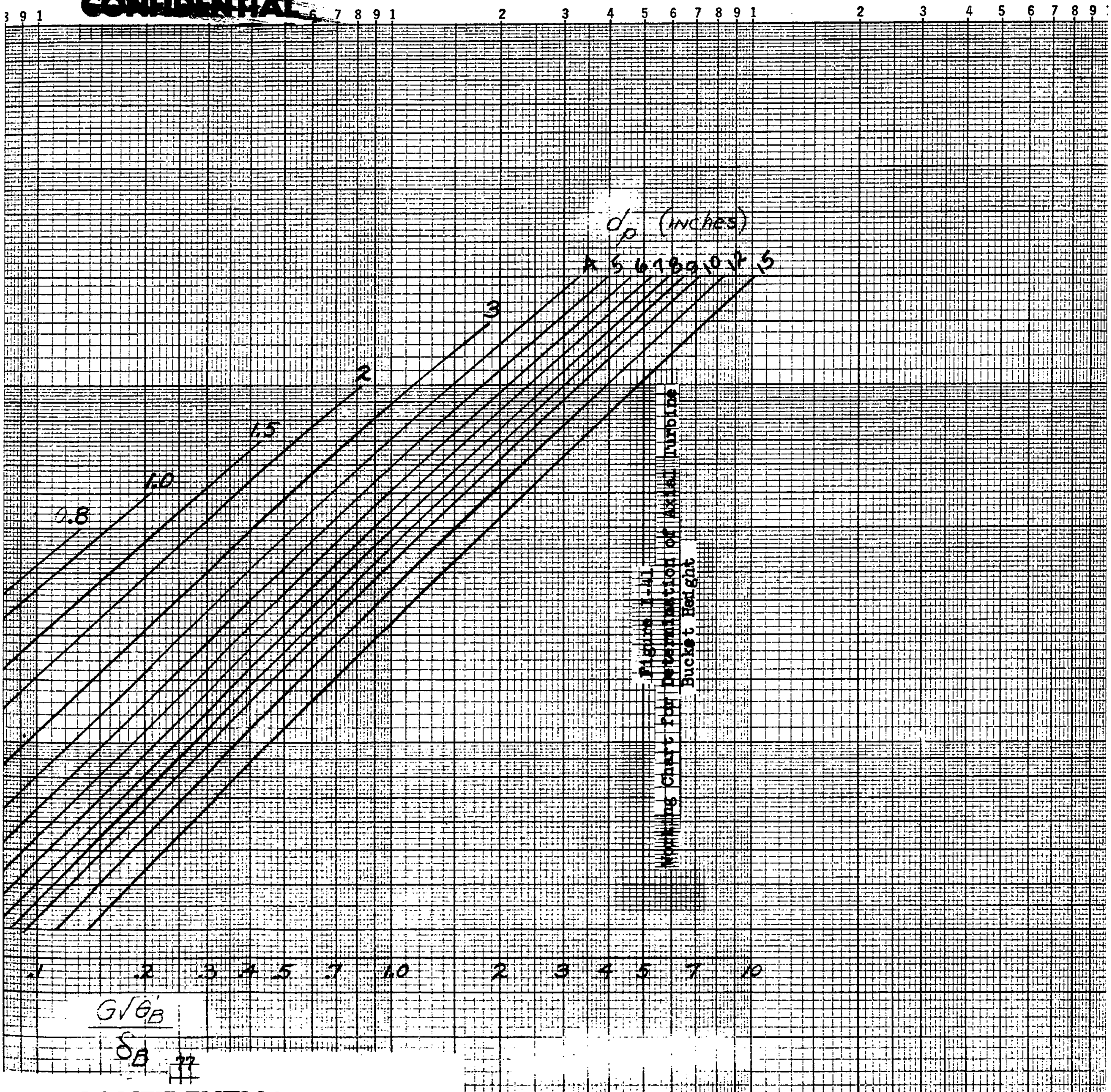

Figure 1-41
Working Chart for Determination of Axial Turbine Bucket Height

CONFIDENTIAL

(2)

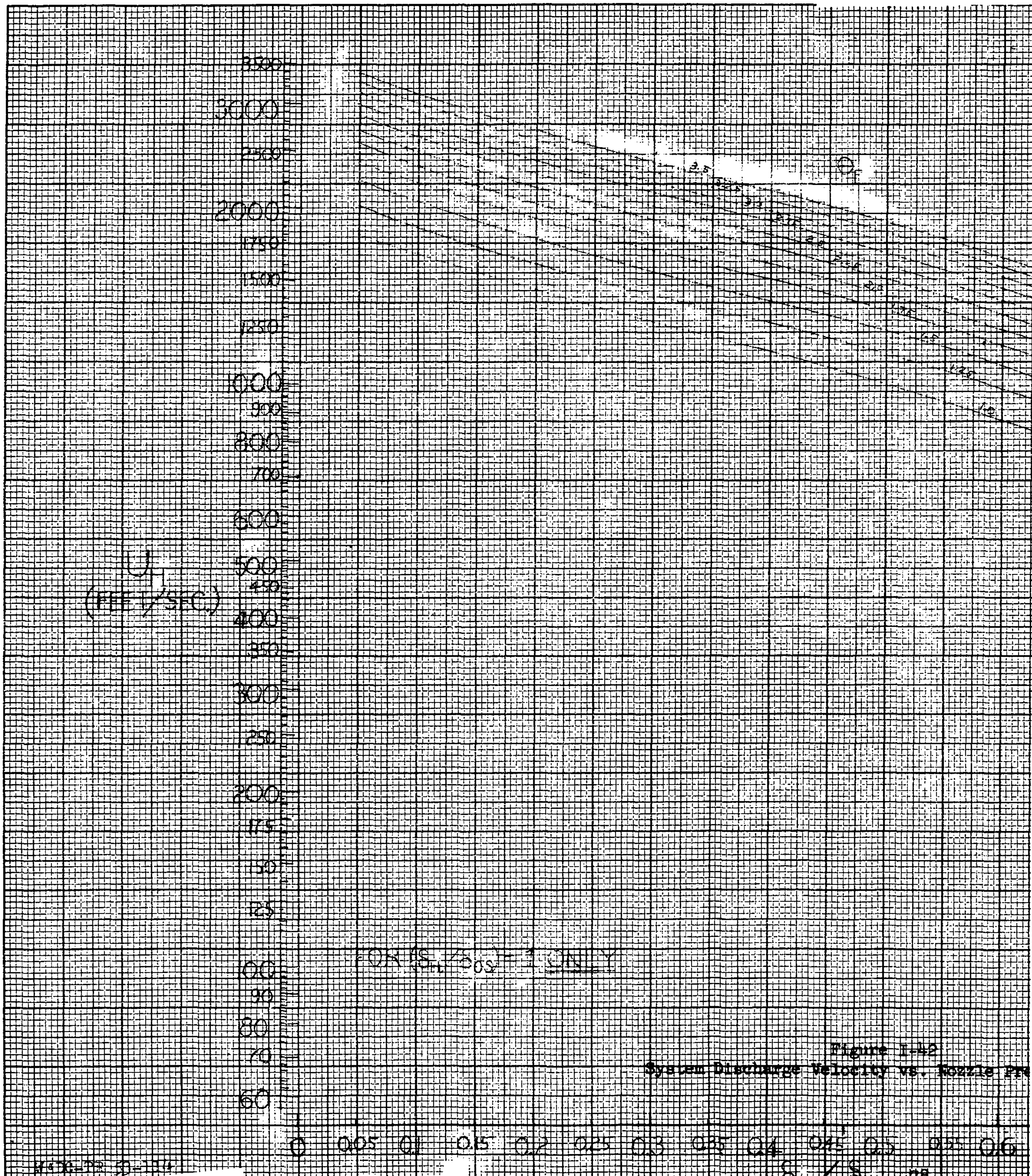

Figure I-42
System Discharge Velocity vs. Nozzle Pre

CONFIDENTIAL

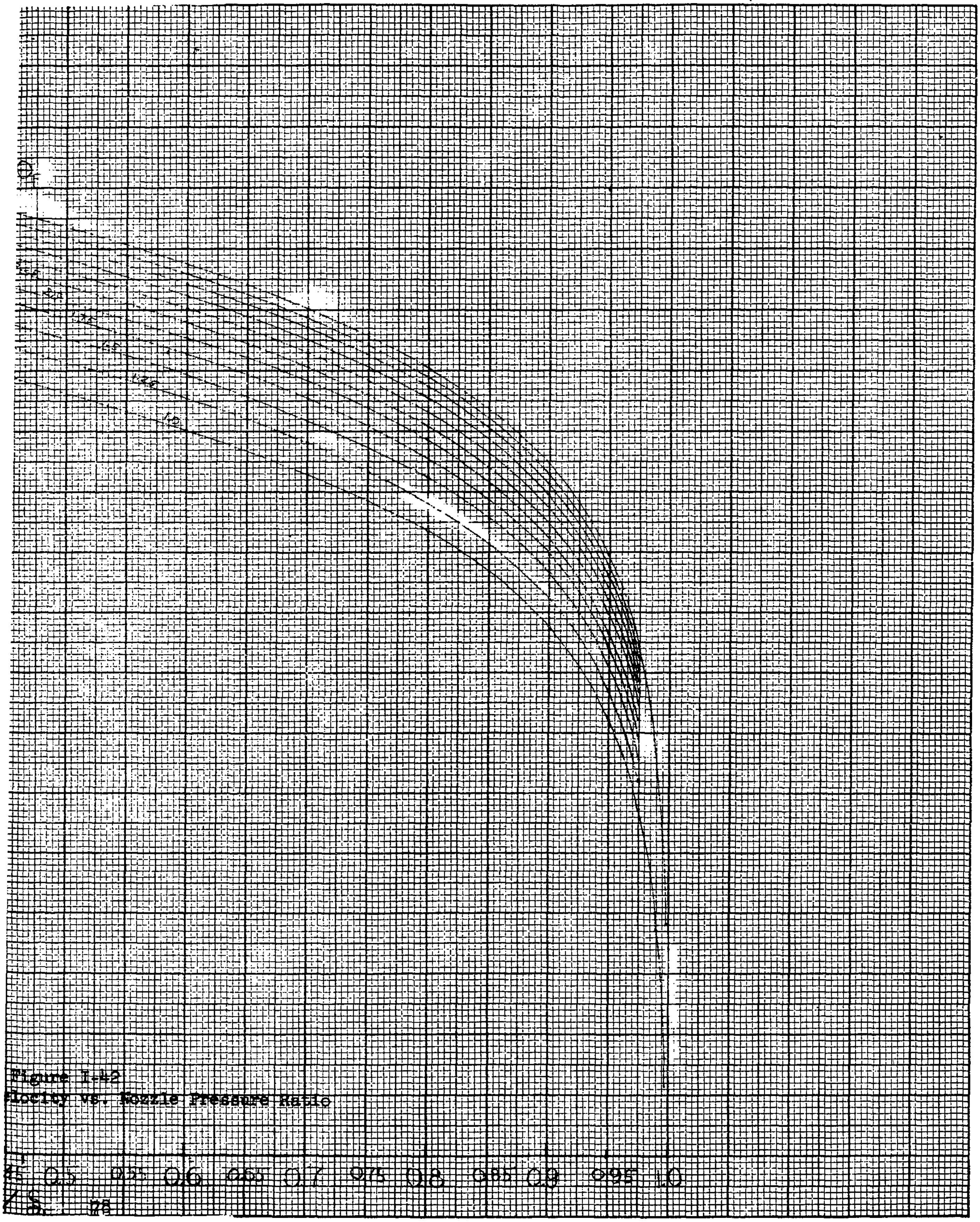

Figure I-42
...locity vs. Nozzle Pressure Ratio

CONFIDENTIAL

78

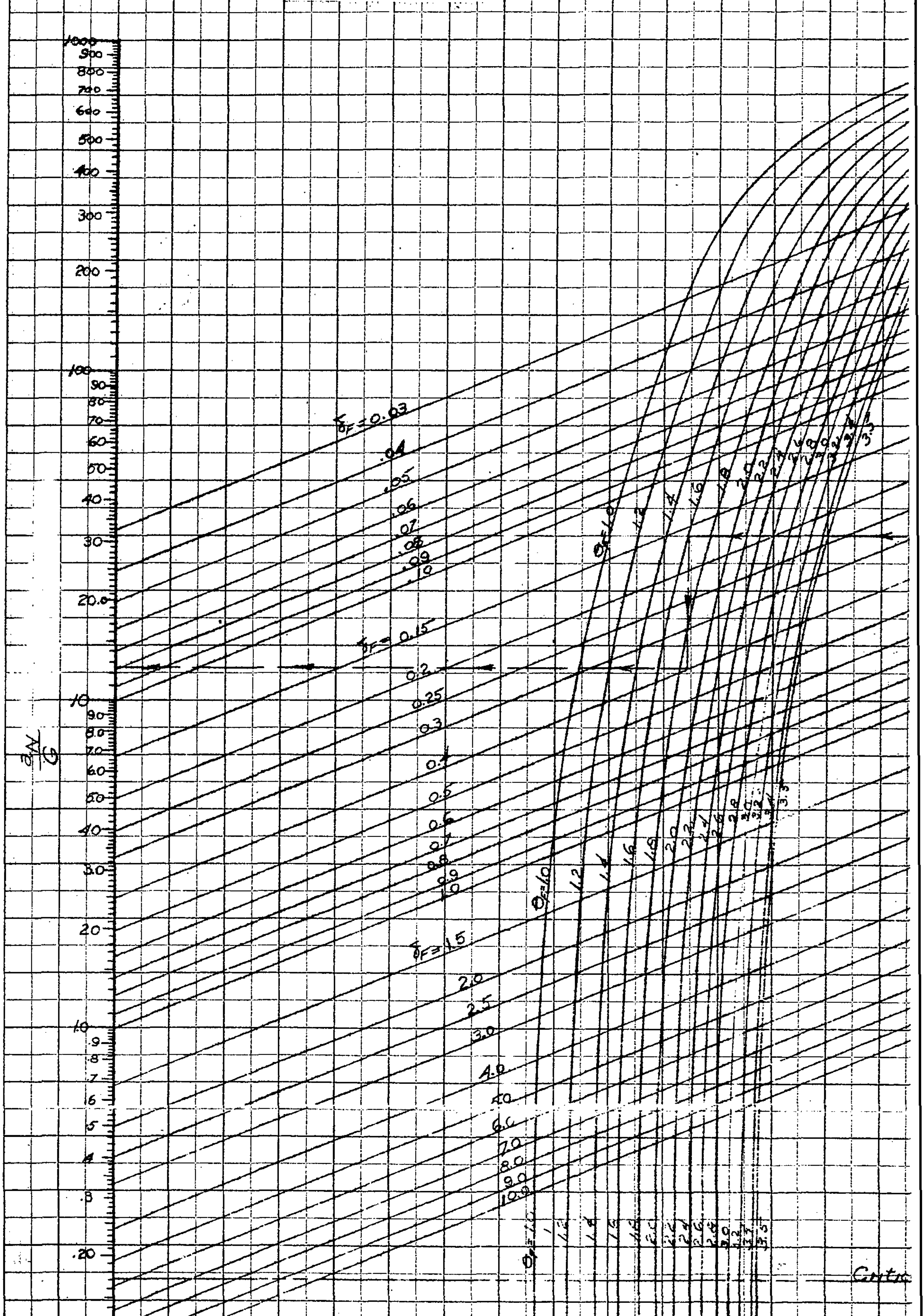

Figure I-43
Working Chart for Determination of Nozzl

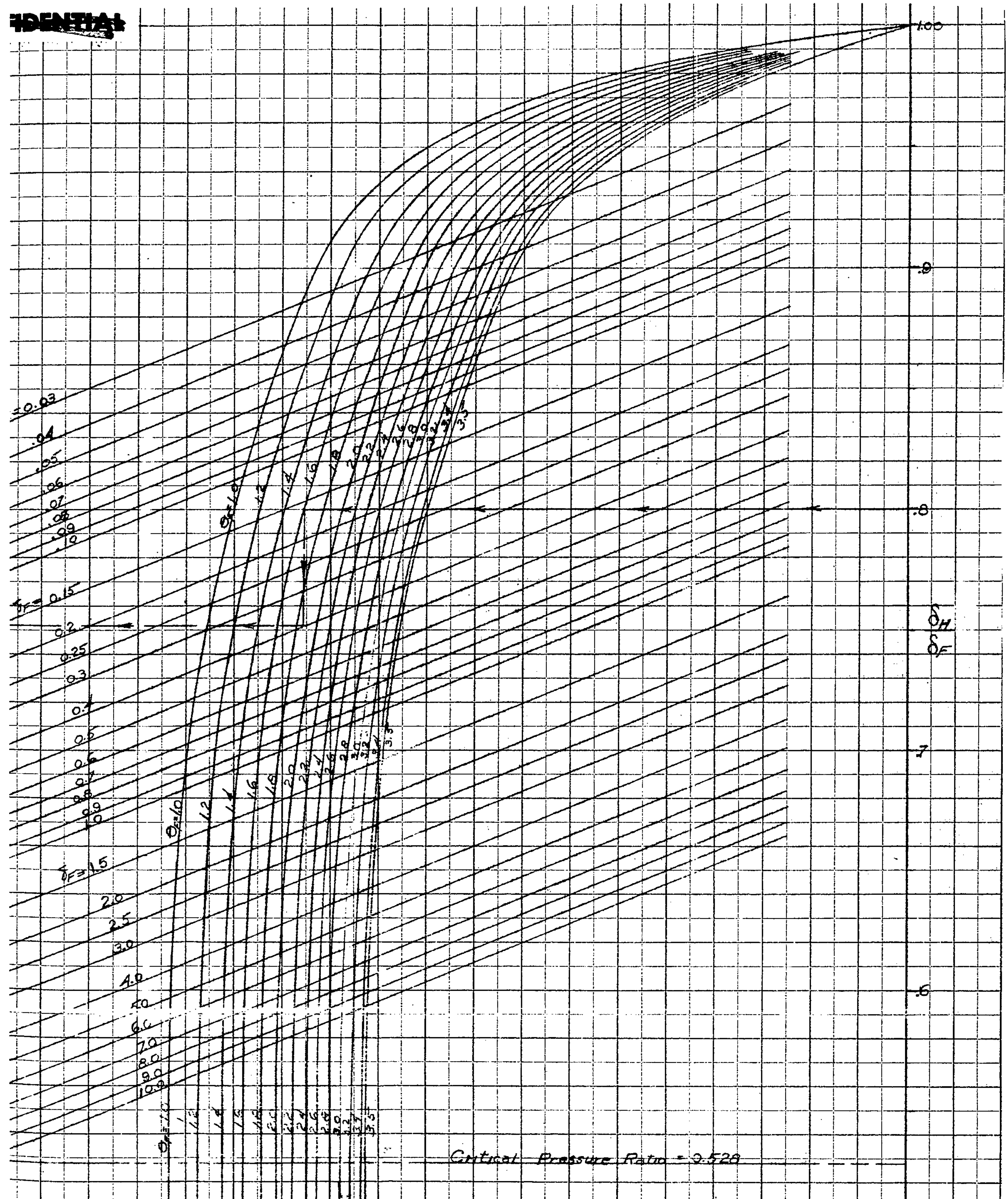

Figure I-43
Working Chart for Determination of Nozzle Exit Area

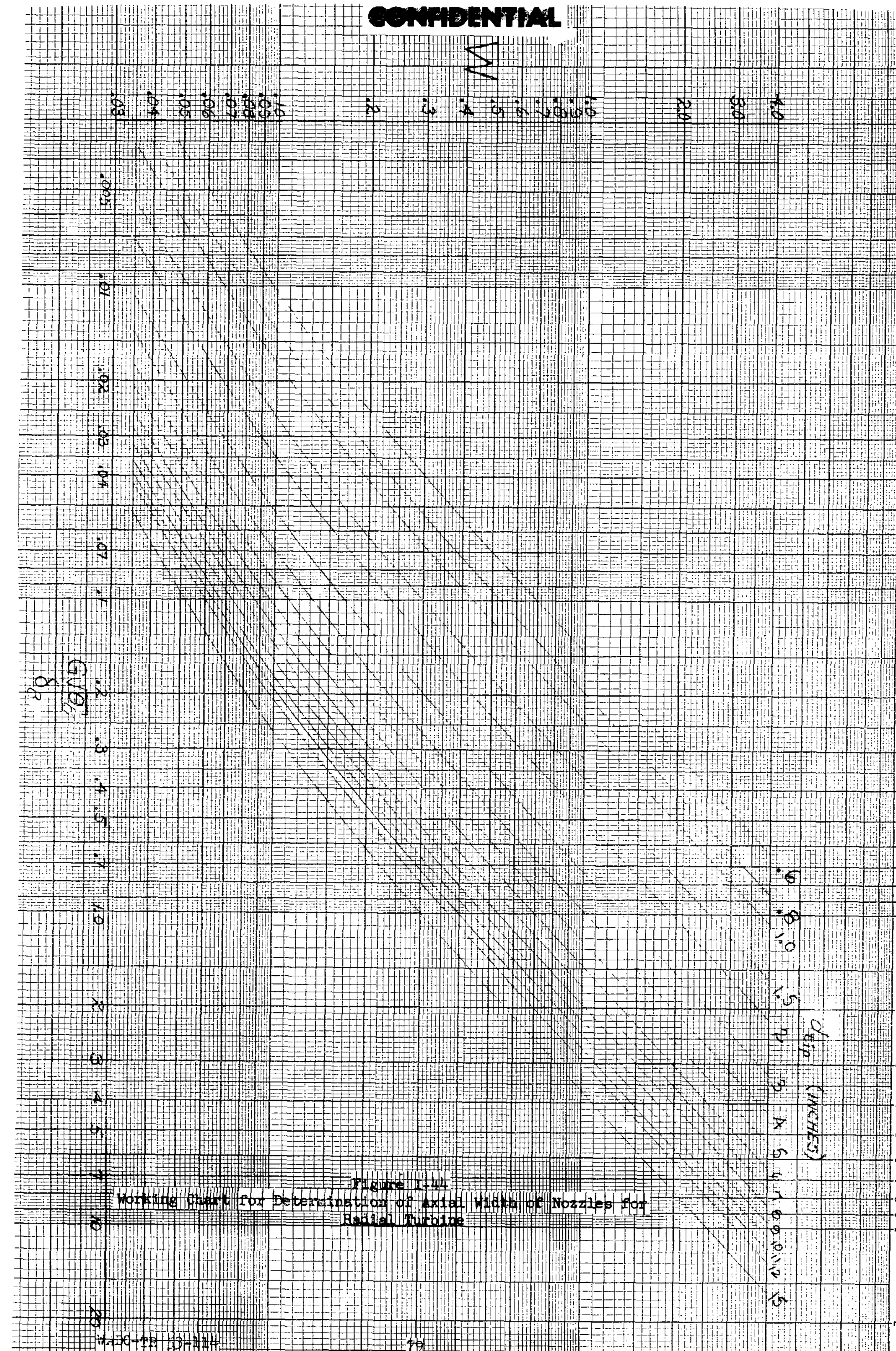

Figure 1-44
Working Chart for Determination of Axial Width of Nozzles for Radial Turbine

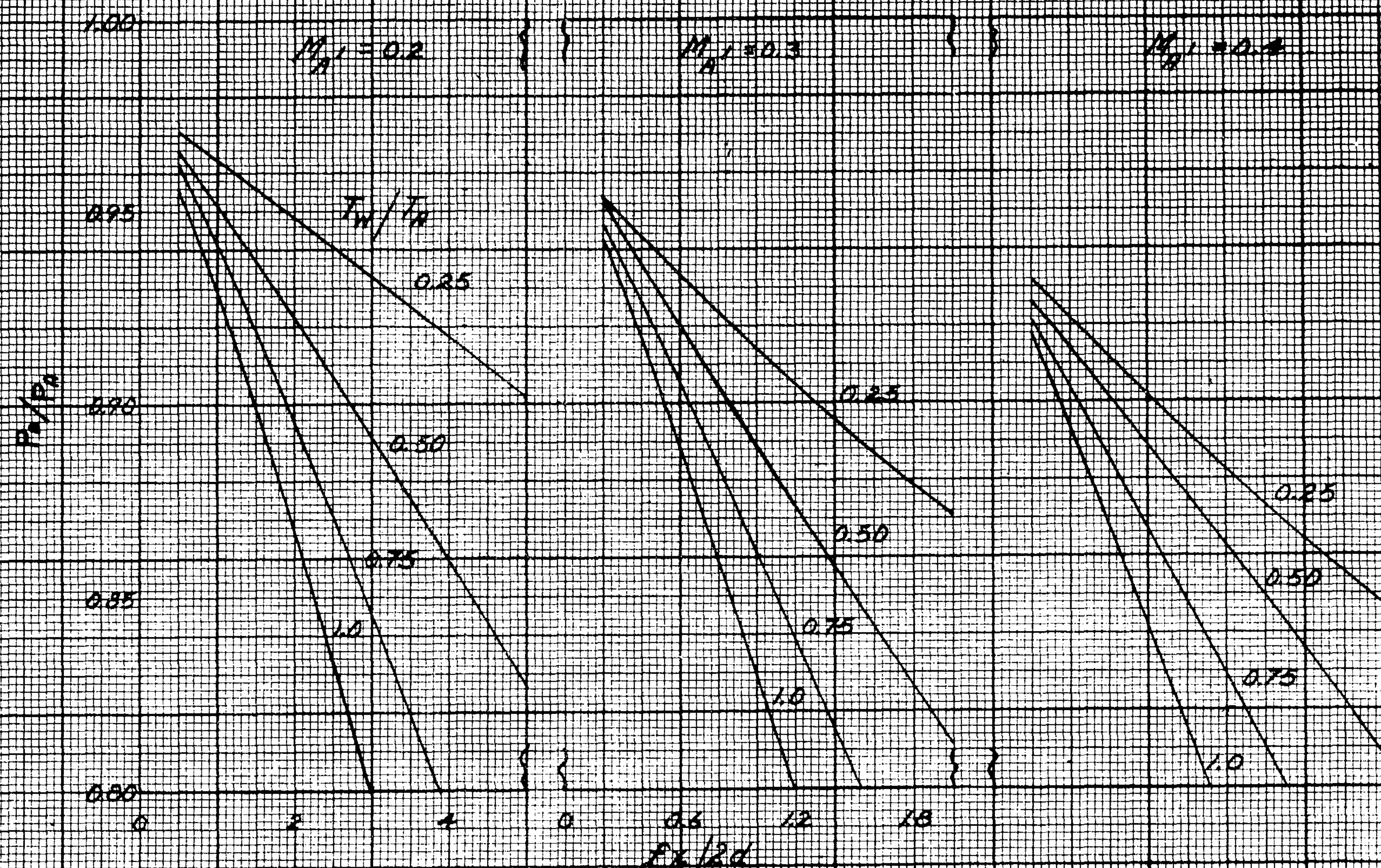

Figure I-45
Pressure Loss Data for Analysis of Air-Side of Precooling Heat Exchanger

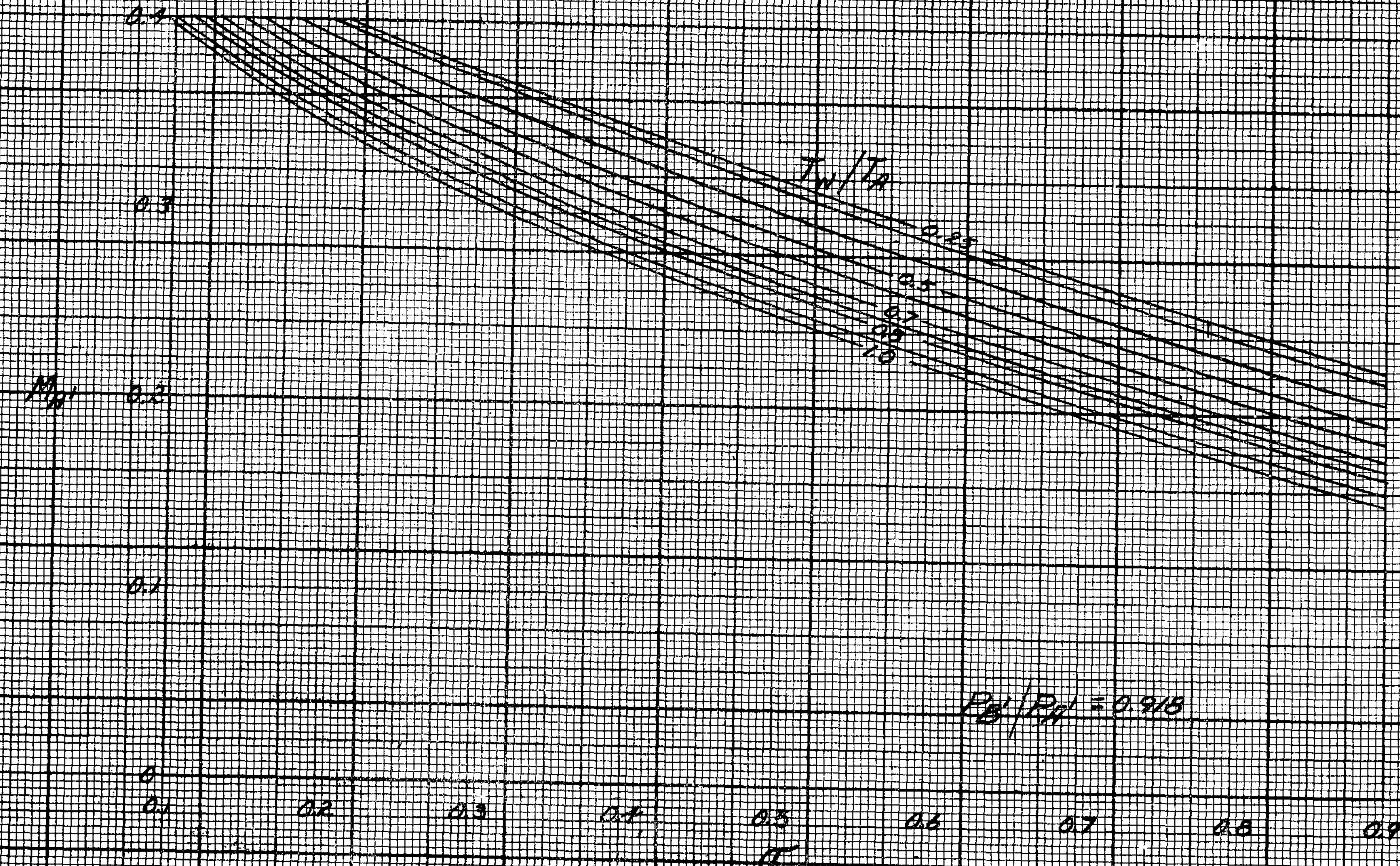

Figure [illegible]
Inlet Mach Number vs. Effectiveness of Precooling Heat Exchanger

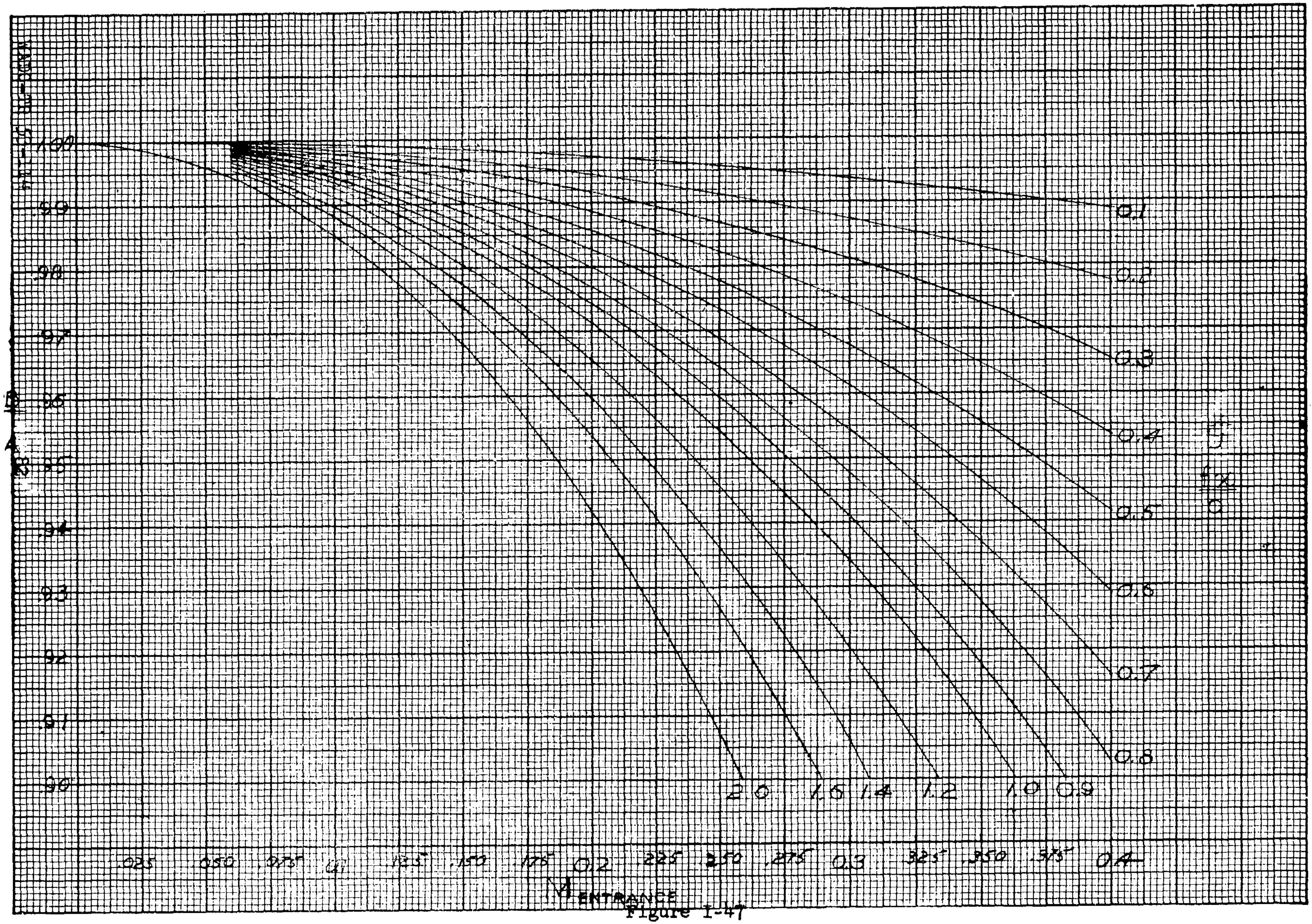

Figure I-47
Pressure Loss Chart for Ducts of Constant Cross Section

SECTION II

FUEL-COOLED EQUIPMENT CASE HEAT EXCHANGERS

By M. L. Smith

One method of keeping equipment temperatures within acceptable limits in high-speed aircraft is to enclose the equipment in a casing which is surrounded by a heat exchanger. The engine fuel might be used as the primary coolant for the heat exchanger, and a forced-air circulating system be used to transfer heat from the equipment to the heat exchanger. This method of protection not only provides cooling for any heat generated by the equipment itself, but also protects the enclosed equipment from external heating effects due to high temperature surroundings. This cooling method is particularly appropriate for electrical components, since they can often operate independently, requiring only simple wiring connections leading from the cooled case. A salient advantage of the system is that it is applicable to many components in their presently used form, and therefore avoids expensive redesign. Although the heat exchanger core could be designed to use other fluids as the primary coolant, the use of fuel is advantageous since the fuel is already present on the aircraft, and special storage and handling problems are therefore avoided. It is assumed, of course, that the fuel is available in sufficient quantity and at a low enough temperature to serve as a satisfactory coolant.

The analysis and results given here are for a fuel-cooled equipment casing which is cylindrical in shape, with the heat exchanger core located in an annular volume around the space for equipment installation. This method of protecting equipment is not limited to this configuration, however, and should certainly be considered where other casing shapes are required.

SUMMARY

The performance of fuel-cooled equipment case heat exchangers is considered. The particular configuration studied in detail consists of a cylindrical shell, having a heat exchanger core installed in an annular volume just inside of the shell. Within this heat exchanger core is another shell, partially enclosing a volume wherein the equipment to be cooled is installed. A motor and fan are provided in the shell at one end, for circulating air in a continuous cycle over the equipment and through the annular heat exchanger core. The same motor which drives the fan is also assumed to drive a fuel pump, which circulates the fuel coolant through the heat exchanger core.

Five types of heat exchanger core are considered. In four of these, the circulated air is passed between the inner and outer shells of the core, while the fuel is passed through tubes in the core. In one of these the tube surface is extended with fins. In the other basic type, fuel is passed

through the space between the inner and outer shells of the core, while the air is passed through tubes. All of the cores are assumed to be used in counterflow heat exchange. Various baffling arrangements are assumed to investigate the heat transfer characteristics of different flow arrangements, both on the fuel and air side of the core.

It is assumed that a fuel-cooled equipment case would be used in a compartment where the surroundings are at a high temperature. Provision is therefore made for including external heat loads to the case heat exchanger in analyzing its performance. In addition to the heat generated by the cooled equipment installed in the case, the power requirements for circulating both the air and the fuel are accounted for in analyzing the performance. It is assumed that operation is in the steady-state insofar as all heat transfer and heat generation rates are concerned. General equations are developed to describe the heat transfer and heat balance relationships of the fuel-cooled equipment case in operation. These equations do not depend on the details of the heat exchanger core design, but only on its basic type, having fuel or air in contact with the outer shell. A summary of heat transfer correlations and pressure drop correlations applying to heat exchanger cores of specific types is given in Appendix B. Examples of using such specific correlations together with the general equations to form a performance calculation procedure are given in Appendices C and D.

The performance of a fuel-cooled equipment case heat exchanger is defined in terms of the net cooling capacity which it provides for the installed equipment, at a given temperature difference between the air and fuel at their respective points of entry to the heat exchanger. The temperature of the equipment is then related to the fuel temperature through performance results in this form, using an expression involving the effectiveness of the equipment as a heat exchange device.

A number of plots showing calculated performance characteristics are given. Based on these results, conclusions on the effects of principal operating variables and comparison of the different heat exchanger cores may be summarized as follows:

1. Plots of net cooling capacity versus the fuel and air entrance temperature difference ($t_{a1}-t_{f1}$) show that for a constant air flow rate, an increase of net cooling capacity requires an increase of ($t_{a1}-t_{f1}$).

2. The temperature difference ($t_{a1}-t_{f1}$) required at a fixed net cooling capacity can be decreased by increasing the air flow rate up to a point. Beyond this point, the increased power requirement for circulating the air causes ($t_{a1}-t_{f1}$) to increase with increasing air flow rate.

3. If a family of cooling performance plots as described in item (1) are constructed for different air flow rates through the same core, an envelope may be drawn tangent to the family of lines. This envelope represents an optimum design condition where ($t_{a1}-t_{f1}$) is at its minimum value for the corresponding net cooling capacity. The

required air flow rate is that which gives a performance plot tangent to the envelope at the design point, and may be found by interpolation.

4. The effect of external heat load on a fuel-cooled equipment case heat exchanger is to reduce the net cooling capacity for a fixed $(t_{a1}-t_{f1})$. This effect is small even for external heat loads which are large compared to the net cooling capacity of the exchanger. The effect is smallest in cores which have the fuel in contact with the outer shell, since the external load enters the fuel directly and is not transferred through the core heat exchanging surface used to cool the equipment. The effect is most severe in designs of high air flow rate, where the temperature difference $(t_{a1}-t_{f1})$ is small compared to the net cooling capacity.

5. The temperature level of operation has only small effect on the cooling performance of a fuel-cooled equipment case heat exchanger. It therefore follows that a unit analyzed for performance at one temperature level can be expected to perform similarly at other temperature levels.

6. The fuel flow rate has very little effect on the temperature difference $(t_{a1}-t_{f1})$ associated with a given heat transfer rate to the fuel unless the flow rate is quite low. For very low fuel flow rates, the high fuel temperature rise and the low fuel film heat transfer coefficients require much larger values of $(t_{a1}-t_{f1})$.

7. By comparing the optimum performance curves for a large number of heat exchanger designs, it is possible to select those designs which offer the best performance for a given size and weight. The plots are altered somewhat from the optimum performance curves described earlier in that the values of net cooling capacity are divided by the heat exchanger volume or weight. A study such as this shows that heat exchangers wherein the fuel contacts the outer shell and the air flows through tubes are generally best from the standpoint of size. They offer the highest net cooling capacity per unit volume at a given $(t_{a1}-t_{f1})$. A comparable performance can be achieved with an exchanger with fuel in tubes if the air-side surface area of the tubes is enlarged with fins, however. Exchangers with fuel inside the outer shell are very inferior in performance on a weight basis to those with fuel in tubes. It is therefore concluded that the best design from the standpoint of both size and weight is that which circulates the fuel through tubes, with fins on the air-side surface of the tubes.

8. Although no data are given to show the effect of air pressure on heat exchanger performance, it is shown to be an important variable. In a fixed system with a constant air circulation rate by volume, it is possible to show the qualitative influences of a change of air pressure. It is not possible in general to determine how the cooling performance varies except by calculation for specific cases. If a fuel-cooled heat exchanger is to be designed, a design

for low air pressure requires a greater power for air circulation than one for higher air pressures. This effect is required to provide identical cooling performance.

DESCRIPTION OF THE SYSTEM AND HEAT EXCHANGER CORES

1. General Configuration

The general configuration assumed for a fuel-cooled equipment case heat exchanger is shown schematically in Figure II-1. The outer casing is cylindrical in shape, and is broken only for fuel lines, pump shaft, and whatever connections are required with the outside by the equipment. An inner casing or shell is also shown, within which the equipment to be cooled is installed. Between the inner and the outer shells is an annular space containing a heat exchanger core. A fan and motor are provided to draw air from the equipment space and force it through the heat exchanger core, where the air is cooled. From the core the cooled air returns to the equipment space, where it is heated by the equipment, thus completing the air flow cycle. The fan and motor are located at the air inlet end of the heat exchanger so that the heat generated by their operation is carried by the air directly to the exchanger. The cooled equipment therefore receives the coolest air in the system, without the air temperature rise caused by operation of the fan and motor. This positioning of the fan has a disadvantage in that the power required to circulate a given weight of air is higher than if the fan were at the cold-air end of the exchanger.

The surfaces of the heat exchanger core are kept cool by fuel which is circulated through the core as the primary coolant. In the example shown, the fuel is passed through the heat exchanger in a direction which gives counterflow heat exchange. This is advantageous in that for fixed fluid temperature conditions and cooling effect, less core surface is required in the counterflow arrangement than if parallel flow were used. In the example shown, the fuel pump is driven by the same motor which drives the fan or air blower. This arrangement is assumed for all cases analyzed here, although in some installations a fuel pump may not be required.

2. Heat Exchanger Cores

Five types of heat exchanger core are considered for application in the fuel-cooled case shown in Figure II-1. The physical arrangements of these cores are described here.

a. Design A

The first core considered is shown at the top of Figure II-2 as Design A. The fuel coolant is pumped through tubes, which encircle the inner shell in helical fashion. The air is blown in crossflow over the outside of the tubes. A small fuel header is located at each end of the core as a common terminal for two or more parallel fuel paths through the tubes. An advantage of this core is that the fuel, which is ordinarily at

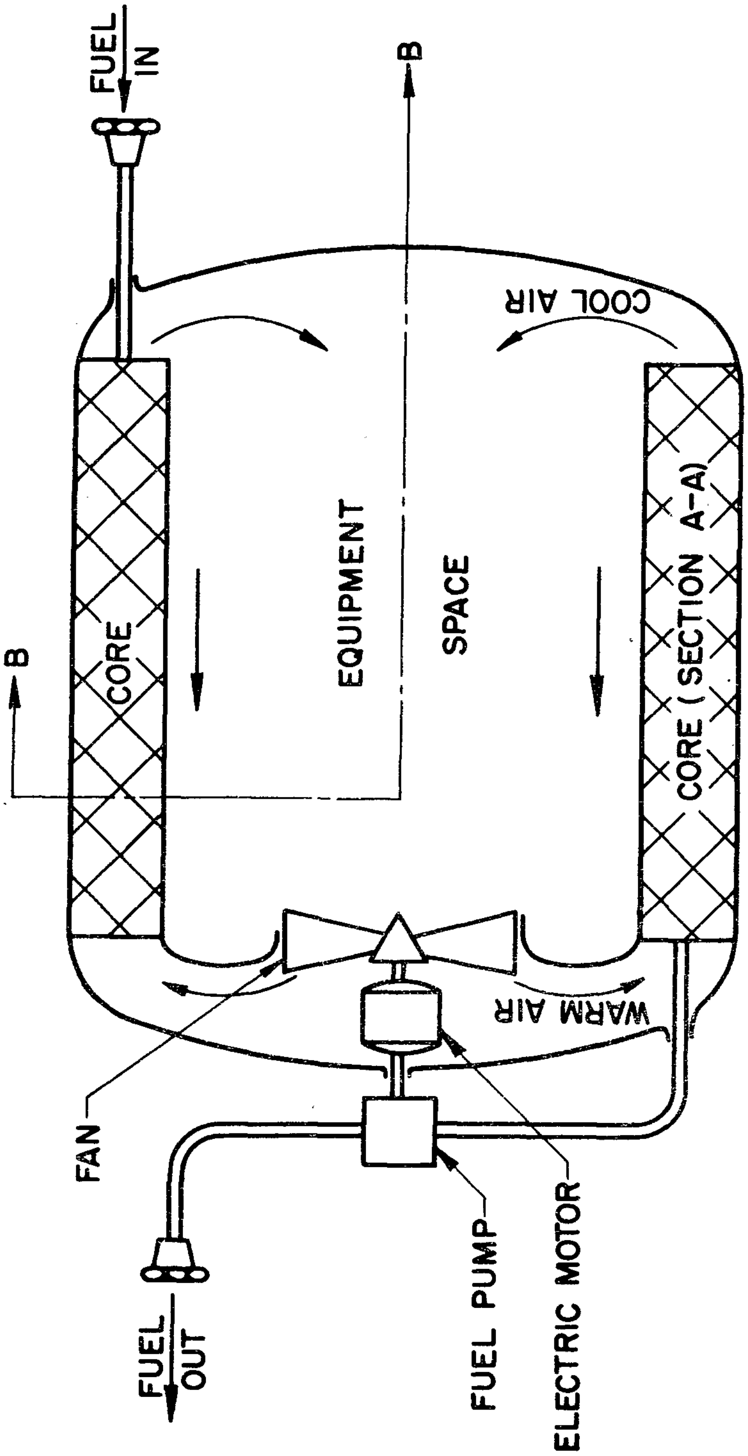

Figure II-1
Schematic of a Fuel-Cooled Equipment Case Heat Exchanger

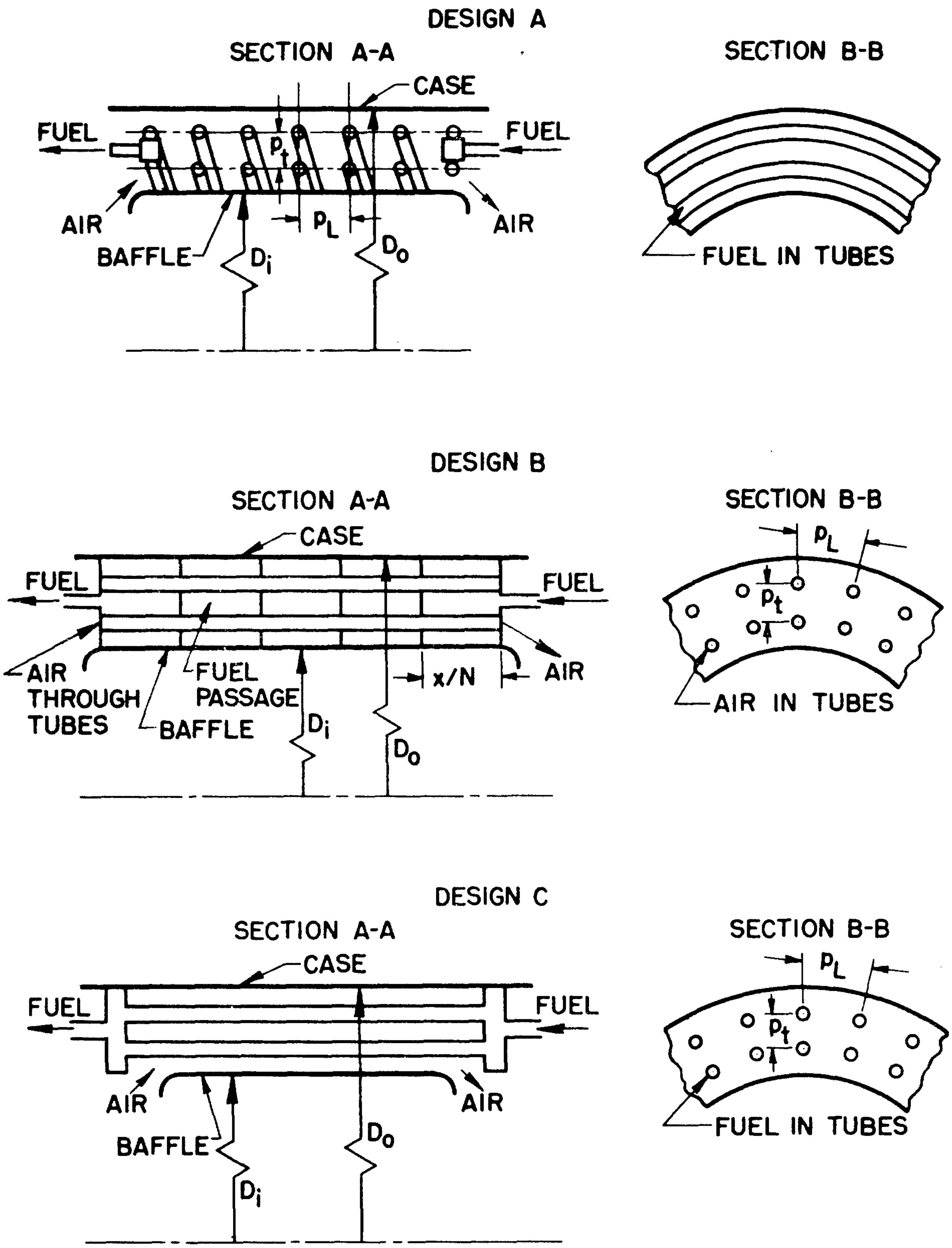

Figure II-2

Schematic of Heat Exchanger Cores, Designs A, B, and C

high pressure, is contained in the small diameter tubes. This results in lightweight construction. In the particular example illustrated, there are two rows of fuel tubes transverse to the axis of the cylindrical case, and the tubes are arranged in-line. Variations on the same basic core design may have more than two or only one row of fuel tubes, and either in-line or staggered tube arrangements.

b. Design B

The core designated as Design B is also shown in Figure II-2. In this case the air is forced through tubes which run parallel to the axis of the cylindrical case, and the fuel is pumped over the air tubes in crossflow. A system of baffles is provided so that the fuel encircles the shell several times in a helical path in traversing from one end to the other of the core. This design has the advantage that heat received through the outer shell from the surroundings passes directly into the fuel coolant, instead of heating the air as in Design A. Another advantage is that Design B cores are thinner for a given cooling capacity than the type shown in Design A, leaving more room in a casing of fixed outer dimensions for equipment installation. A marked disadvantage of Design B is that the inner and outer shells must be thick and suitably ribbed to withstand the high fuel pressures, resulting in heavier and possibly more expensive construction.

c. Design C

The core designated as Design C is also shown in Figure II-2. In this design the fuel flows through straight tubes running parallel to the axis of the casing, with fuel headers provided at each end of the tubes. The air is blown over the tubes in flow parallel to the tube axes. This design can be modified with baffles inside of the fuel headers, so arranged that the fuel passes back and forth through the core several times before being discharged. This situation, however, would not be true counterflow, and therefore requires special analysis. With a given number of tubes it has the advantage of higher fuel velocity and correspondingly high heat transfer coefficients on the fuel side.

d. Design D

Another core design is shown as Design D in Figure II-3. This design is similar to Design A in that the fuel passes through tubes which encircle the case. The tubes are flattened, however, and finned on the external or air side. The air is blown over the tubes in crossflow, and parallel to the fin surfaces. The fins increase the heat transfer area on the air side, and this together with the tube flattening, produces a thinner core section than Design A. The construction cost for a core of Design D would be higher.

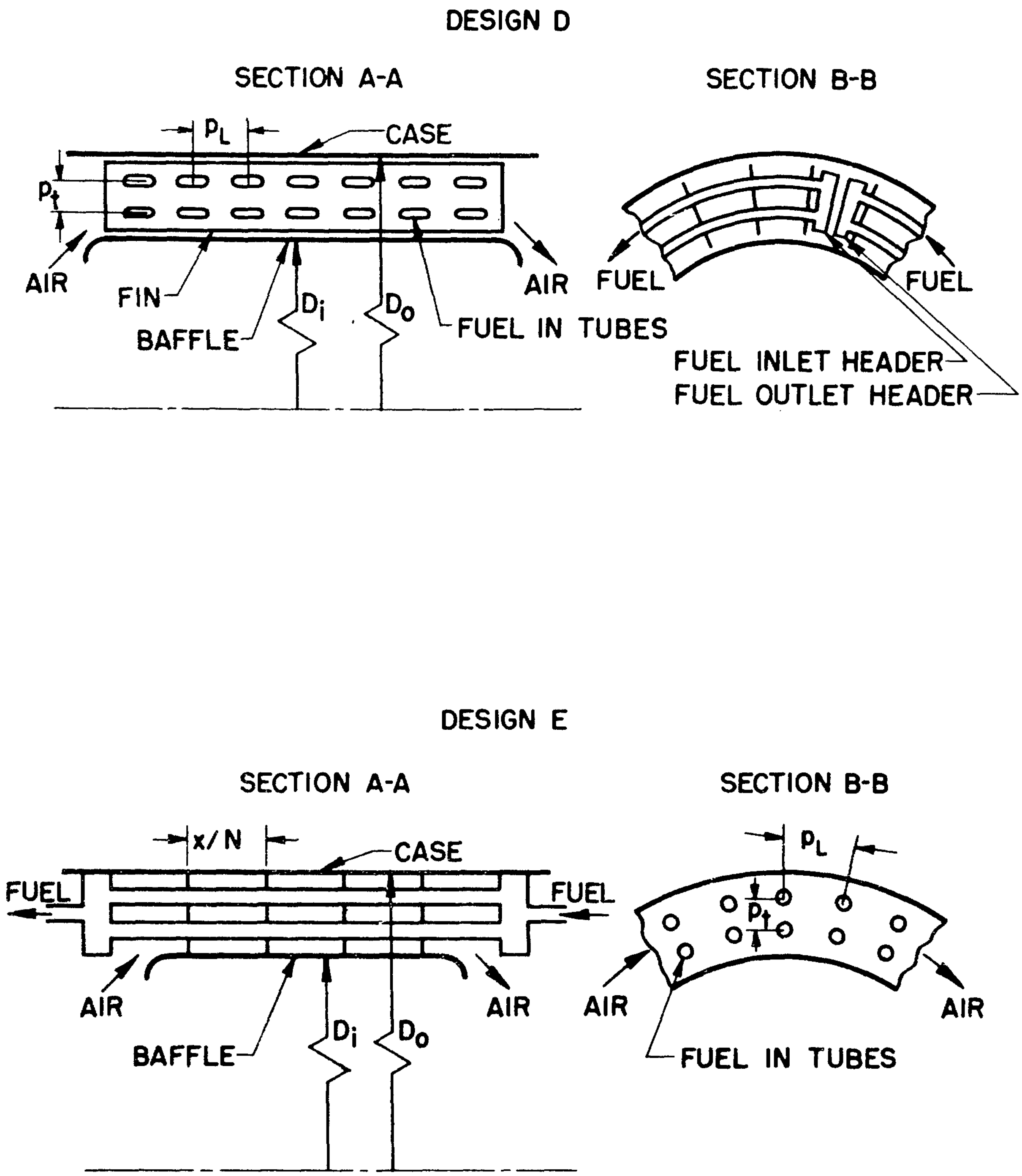

Figure II-3

Schematic of Heat Exchanger Cores, Designs D and E

e. Design E

Design E, shown in Figure II-3, is physically similar to Design B, but the positions of the fluids are reversed. The fuel is inside the tubes, thus requiring fuel headers for the tubes, while the air is baffled to give crossflow over the tubes. Construction of this core would be somewhat lighter and less expensive than that of Design B, since the high pressure fuel is here confined within the small tubes.

GENERAL ANALYSIS

The analysis given here is concerned with establishing the basic equations which describe the performance of a fuel-cooled equipment case as shown in Figure II-1. These performance equations are general, and apply to a large variety of heat exchanger core arrangements. The more detailed equations which describe the heat transfer coefficients and pressure drop of air and fuel are of course dependent on the core used, and are therefore not treated in this general analysis. The detailed relationship for heat transfer coefficients and fluid pressure drop are given for each heat exchanger core in Appendix B to this Section. Examples of using them together with equations from this general analysis to study the performance of a particular fuel-cooled case heat exchanger are given in Appendices C and D to this Section.

1. Assumptions for Analysis

A number of assumptions are made to restrict and describe the system analyzed. They are given in the following paragraphs.

a. External Heat Loads

It is assumed that the fuel-cooled equipment case is located in a compartment exposed to high skin temperatures. As an example, this situation would hold if the case were within the centerbody of a ramjet aircraft flying at supersonic speeds. The skin areas may or may not have insulation to reduce the rate of external heat transfer to the compartment. An example of such an installation is shown schematically in Figure II-4. In addition to the fuel-cooled case, other equipments may be in the compartment. It is assumed here that the external heat load to the cooled equipment case is due only to radiation from nearby high temperature surfaces and free convection of the compartment air. Methods for calculating such heat loads are discussed in Sections V and IX. For purposes of the present study, however, it is sufficient to select some arbitrary external heat load which might vary only insofar as it is affected by the heat exchanger core in the fuel-cooled equipment case. It is therefore assumed that the conditions in the compartment and external to the fuel-cooled case can be described in terms of an average surroundings temperature t_s and an external heat transfer coefficient for the cooled case h_x. Different fuel-cooled cases are compared in their performance for the same assigned values of t_s and h_x.

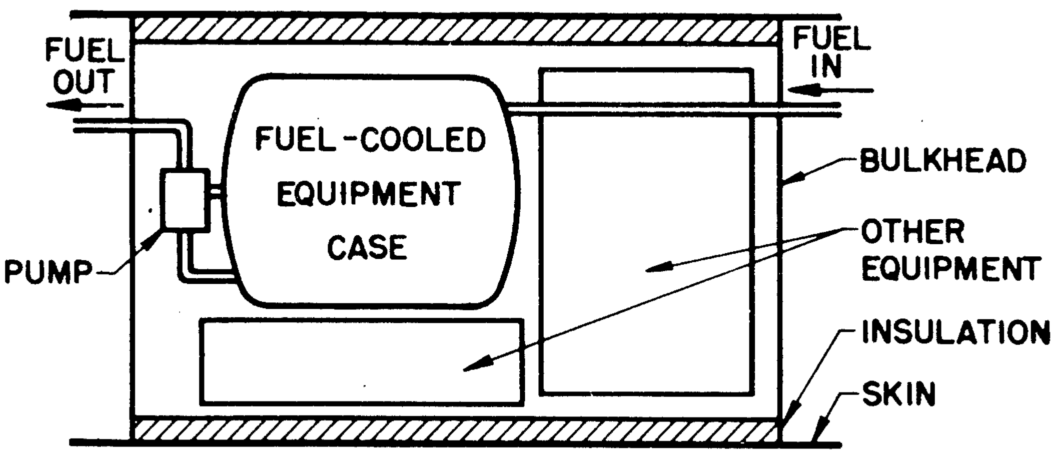

Figure II-4. Schematic of Fuel-Cooled Equipment Case Installed in a Ramjet Centerbody

For simplicity it is also assumed that the major heat transfer to the interior of the fuel-cooled case occurs through the cylindrical surface (see Figure II-1), and the heat transfer through the ends is neglected. This assumption is particularly justified if the ends of the case are insulated.

b. Generated Heat Loads

In addition to the external heat loads to the fuel-cooled case, there are generated heat loads to consider. The equipment installed in the case is assumed to generate heat, since an elaborate protection method such as this would probably not be required for non-heat-generating equipment. As mentioned earlier, there is also a generated heat load due to the operation of the fan or blower, and the motor which drives both this fan and the fuel pump. For small units, it is assumed that the fan, motor, and pump each have an efficiency of about 50 percent. In some installations a fuel pump may not be necessary if there is no objection to imposing the fuel pressure drop in the heat exchanger on the fuel supply line. If so, the pumping power required by the fuel is not included in the heat balance equations.

c. Operating Conditions

It is assumed that the fuel-cooled case operates under steady-state conditions. The air pressure, air circulation rate, external heat load, generated heat load, fuel temperature and fuel supply rate are therefore constant. For this circumstance it is possible to compare the per-

formance of different heat exchanger cores, since the air temperatures in general vary with the core used, other conditions being fixed. A core which can provide a low air temperature at a given cooling capacity is to be preferred from the standpoint of equipment cooling.

2. Heat Balance Relationships

a. External Heat Loads

The external heat load to the fuel-cooled equipment case may be determined from an equation of the form

$$q_e = U_x A_x \theta_x \qquad \text{(II-1)}$$

where q_e is the external heat load, U_x is an over-all heat transfer coefficient between the case surroundings and the fluid in contact with the inner surface of the outer shell, and θ_x is the temperature potential across U_x. For Designs A, C, D, and E this is

$$q_e = U_x A_x (t_s - t_{am}) \qquad \text{(II-2)}$$

where t_{am} is the average air temperature in the heat exchanger. For Design B or any which has the fuel in contact with the outer shell the equation becomes

$$q_e = U_x A_x (t_s - t_{fm}) \qquad \text{(II-3)}$$

where t_{fm} is the average fuel temperature in the heat exchanger.

The coefficient U_x is defined as

$$U_x = \frac{1}{\frac{1}{h_c} + \frac{1}{h_x}} \qquad \text{(II-4)}$$

where h_c is the forced convection heat transfer coefficient for the fluid flowing along the inside of the outer shell, and h_x is an appropriate coefficient for heat transfer from the surroundings to the outer shell. In this study arbitrary values are assigned to h_x and t_s, but the value of h_c is determined for the particular heat exchanger core and its operating conditions. This permits a comparison of the performance of different cores on the basis of an identical environment, but allows for the effect of the core type and the operating condition (such as flow rate and temperature of the fluid) on the external heat load.

An alternative method is to assign arbitrary values of q_e for a performance calculation to compare different heat exchanger cores. This also provides a logical basis of comparison, although different amounts of insulation on the fuel-cooled case would actually be required if the external heat load were to be the same for different heat exchanger cores, even where

internal fluid temperatures are the same.

b. Generated Heat Loads

Under steady-state operation, all of the heat generated by the operation of the fan, motor, and fuel pump is transferred in one way or another to the fuel. Heat generated by the equipment is also transferred to the fuel. The heat balance for the fuel, including the external heat load is therefore given by

$$q_f = q_e + 3.413\,(q_c + q_M) \qquad \text{(II-5)}$$

where q_M is the total motor power input in watts, and q_c is the heat generation rate of the equipment, in watts. q_e and q_f, the total heat load to the fuel, are expressed in Btu/hr.

A more detailed examination of the generated heat loads is required to find the heat transferred to the circulating air. From the configuration shown in Figure II-1, it is clear that if q_{Ma} is the motor input power (expressed in watts) required to circulate the air, all of this is transferred to the air. With q_{Mf}, the motor power required to pump the fuel, this is not the case. That portion of q_{Mf} which goes to supply motor losses is transferred to the air, but that portion which goes to pump losses and to actual pump work in the fuel is transferred directly to the fuel and does not enter the circulating air. The generated heat loads transferred to the air are therefore given by

$$W_a c_p \Delta t_a = 3.413(q_c + q_{Ma} + 1/2\, q_{Mf}) \qquad \text{(II-6)}$$

since a motor efficiency of 50 percent is assumed. The values of fan, motor and pump efficiency are assumed to have been accounted for in finding q_{Ma} and q_{Mf}. In the above equation, W_a is the weight flow rate of air in pounds per hour, and c_p and Δt_a are the specific heat and temperature rise of the air, respectively.

c. Heat Transferred from Air to Fuel

The heat transferred from the air to the fuel is described by different relationships for the two different basic types of heat exchanger core. In the first type, where the air is in contact with the inner surface of the outer shell (Designs A, C, D, E), the relationship is

$$q_f - 3.413(1/2\, q_{Mf}) = U_o A_o \theta_{lm} \qquad \text{(II-7)}$$

since all of the heat received by the fuel, except that due to pumping, is transferred from the air as it passes through the heat exchanger. In the right-hand member of this equation, U_o represents the over-all coefficient of heat transfer between the air and the fuel, based on the outside surface area of the tubes A_o, and θ_{lm} is the logarithmic mean temperature difference

between the air and the fuel.

Where the fuel is in contact with the inner surface of the outer shell, as in Design B, the equation is,

$$q_f - q_e - 3.413(1/2q_{Mf}) = U_o A_o \theta_{lm} \qquad \text{(II-8)}$$

since the external heat load enters the fuel directly through the outer shell, and is not transferred through the surface A_o. For both of these equations the coefficient U_o is defined by

$$U_o = \frac{1}{\frac{1}{h_o} + \frac{d_{to}}{h_i d_{ti}}} \qquad \text{(II-9)}$$

where h_o and h_i are the convection heat transfer coefficients on the outside and inside surface of the tube wall, respectively, and d_{ti} and d_{to} are inner and outer diameters of the tubes.

3. Performance and Temperature Relationships

A convenient measure of the merits of any cooling method is the temperature difference which is required between the cooled component and the coolant for a given heat removal rate, or cooling capacity. In order to determine the temperature difference between the cooled equipment and the coolant, it is necessary to know the effectiveness of the equipment as a heat exchanging device. To avoid this complication and make the evaluation of performance for a particular heat exchanger core of more general value, the difference between the temperatures of the circulating air and the fuel is used as a performance criterion. In the actual system, fuel temperatures and air temperatures vary from one end of their flow path to the other. It is therefore necessary to fix on a particular definition of the difference and use it consistently. The results given later are in terms of the quantity $(t_{a1}-t_{f1})$ or difference between the temperature of the air and the temperature of the fuel at their respective points of entry to the heat exchanger. The calculation procedures of Appendix D to this Section are set up so as to determine this temperature difference. These calculation procedures are based on both the general relationships just given and on the specific equations from Appendix B which apply for the core used. In general, a cooling apparatus which gives a low value of $(t_{a1}-t_{f1})$ for a given cooling capacity q_c is superior to one which requires a high value of the temperature difference.

With results given in terms of $(t_{a1}-t_{f1})$ for a given cooling capacity, the equipment temperature can be found if certain equipment characteristics are known. It is necessary to know the effectiveness of the equipment as a heat exchange device, which is defined as,

$$\sigma_e = \frac{t_{a1}-t_{a2}}{t_e-t_{a2}} \qquad \text{(II-10)}$$

where by current nomenclature, t_{a1} and t_{a2} are the temperatures of the air on entering and leaving the heat exchanger, respectively, equal to those leaving and entering the equipment space, respectively. It is apparent from the definition of equipment heat exchanger effectiveness that it is the ratio of the actual temperature rise of the air in the equipment space to the maximum possible. Although the temperature of various parts of the equipment would actually be different, it is assumed that the equipment can be represented by an average temperature t_e. It should be observed that under the above definition of effectiveness, the motor and fan for circulating the air are grouped together with the installed equipment in the fuel-cooled case. For any given combination and arrangement of equipment, motor, and fan, it is necessary to have experimental data to determine the effectiveness σ_e, for conditions which are appropriate to the contemplated installation.

It is then possible to construct a relationship for the equipment temperature, using equations (II-6 and -10). Combining these equations gives

$$t_e = t_{a1} + \left[\frac{3.413(q_c+q_{Ma}+1/2q_{Mf})}{W_a c_p}\right]\left[\frac{1-\sigma_e}{\sigma_e}\right] \qquad \text{(II-11)}$$

Presumably the coolant temperature is known, so that with a result in the form of $(t_{a1}-t_{f1})$, t_{a1} is known, whereupon t_e can be found from equation (II-11). It should be observed that an equipment of high effectiveness is preferred, since equation (II-11) shows that such an equipment would operate closer to t_{a1} than one of low effectiveness. In general, a high effectiveness for the equipment as a heat exchanging device requires an arrangement which provides for high heat transfer coefficients and/or long lengths for the flow path in which the air contacts the equipment. Both of these requirements lead in turn to high pressure loss and high power requirements for air circulation. The power requirement for air flow over the equipment is neglected in this analysis since it is usually negligible compared to the power required to force air through the heat exchanger.

EFFECTS OF VARIABLES ON THE PERFORMANCE OF FUEL-COOLED EQUIPMENT CASES

Typical performance characteristics of fuel-cooled equipment cases have been calculated for the five heat exchanger cores described earlier. While the range of variables that might be encountered in all types of aircraft application is too broad to permit reaching final conclusions regarding the merits of such equipment, many factors affecting performance are evaluated. It is believed that these results are of value as a guide in designing a fuel-cooled case for a given application.

All results are calculated for equipment cases one foot long and one foot in diameter. The air pressure in each is assumed to be one atmosphere, and aluminum tubes of 3/16 in. outside diameter with 0.007 in. wall thickness are used. Obviously, the smaller the tubes, the more heat transfer area can be enclosed in a given volume of heat exchanger. It is felt that 3/16 in. outside diameter tubes are about as small as would be practical to use in mass production, so no variation of tube size is considered in the following

results. As discussed later, the effect of fuel flow rate on performance is not usually important, so that a value of 500 lb/hr is used unless indicated otherwise in specific cases. The use of JP-3 fuel as the primary coolant is assumed throughout. Unless some other value is specified, the temperature level is established by $t_{a1} = 300^{\circ}F$. In a few special cases the operating temperature level is specified in terms of t_{f1}.

1. General Performance

Figure II-5 shows the performance characteristics calculated for a heat exchanger such as Design B of Figure II-2. Details of the design are given in the figure. The results shown are indicative of the internal heat transfer processes only, since it is assumed that the external heat load q_e is zero. The values for p_L and p_t represent longitudinal and transverse tube pitches, expressed in tube diameters (see Fig. II-2). There is only one row of tubes for air, as represented by $r = 1$. The performance is indicated by plotting the net useful cooling capacity q_c versus the difference in primary and secondary coolant temperatures $(t_{a1}-t_{f1})$. For a given air flow rate W_a the plot shows the steady-state temperature difference between air and fuel at entrance to the heat exchanger for a given cooling capacity. The dashed-lines indicate the total motor power requirement, for both air and fuel, in terms of $(t_{a1}-t_{f1})$.

For a constant W_a it is seen that the cooling capacity and temperature difference have a nearly linear relationship. If the air temperature must be reduced, the cooling capacity available for the equipment must be reduced. From comparison of the plots for different air flow rates, a low air flow rate gives poor performance at high cooling capacities, since it requires a large temperature difference, or a high air temperature in the case. This results from the low heat transfer coefficients on the air side of the heat exchanger at low flow rates. On the other hand, high flow rates are not desirable when only a low capacity is required, because the extra power needed to circulate the air imposes an additional load on the heat exchanger, which tends to increase the temperature difference between the fuel and air. The optimum air flow rate for any combination of net cooling capacity and temperature difference $(t_{a1}-t_{f1})$ can be found. It is necessary to construct an envelope to a series of plots for various air flow rates. The optimum air flow rate can then be found by interpolation, since it is represented by a performance line which is tangent to the envelope at the desired point of q_c and $(t_{a1}-t_{f1})$. A design of this air flow rate represents an optimum in the sense that it gives the smallest value of $(t_{a1}-t_{f1})$ possible for the given heat exchanger core at the desired capacity q_c. If the temperature limitations for the air are not severe, and a large value of $(t_{a1}-t_{f1})$ can be tolerated, lower air flow rates than the optimum should be used. The plots of motor power requirement show clearly that a very great saving in motor power can be effected by using low air flow rates. It is apparent that the power requirement is little affected by change of $(t_{a1}-t_{f1})$ at constant air flow rate.

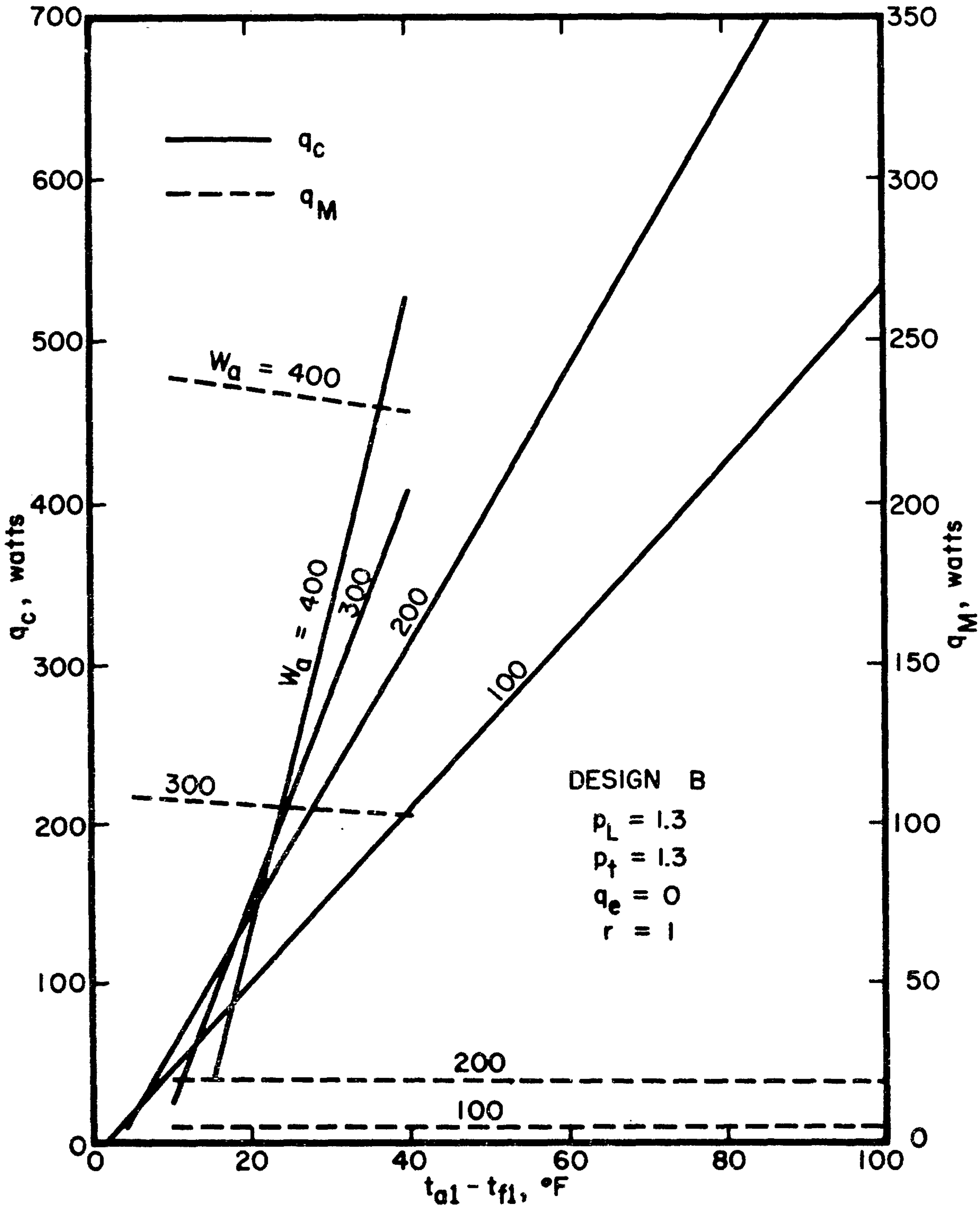

Figure II-5

General Performance Characteristics of a Design B Heat Exchanger

2. External Heat Load

The effects of an external heat load on the performance of the exchanger just discussed appear in Figure II-6. The net cooling capacity in watts q_c (or heat generation allowed for the equipment), and the heat added to the fuel in Btu/hr q_f, are plotted for various arbitrarily assigned external heat loads. Results for four different operating conditions are plotted, including high and low air flow rates and four constant fuel-air temperature differences. The plot shows that a Design B exchanger has a tremendous capacity for absorbing heat from the surroundings without affecting the cooling capacity very greatly. The higher air flow rate shows a more pronounced reduction of cooling capacity with increased external heat load, because of the smaller temperature difference $(t_{a1}-t_{f1})$ in proportion to the net cooling capacity. As the external heat load is increased, the fuel temperature rise increases. This is more serious in its effect where the initial $(t_{a1}-t_{f1})$ is small, since the temperature difference for heat transfer θ_{lm} is reduced by a proportionately greater amount by a given fuel temperature rise.

A comparison of the effects of q_e on the cooling capacity of three types of exchangers, Designs A, B, and C, is shown in Figure II-7. Characteristics of each design are given in the figure. As before, the values of external heat load are arbitrarily assigned in these cases. The external heat load has a greater effect on the cooling capacity in Designs A and C than in Design B, but even with the former, a q_e of as much as 1000 Btu/hr decreases the cooling capacity only a few percent from that when $q_e = 0$. Thus, the use of a little insulation on the outside of the case should suffice to prevent any appreciable reduction of net cooling capacity available to the equipment. The greater importance of external heat load in Designs A and C as compared to Design B is due to the difference in the manner of transferring the external heat loads to the fuel in the two types of design. In Designs A and C, the external heat load is first transferred from the outer shell to the air. It is then transferred through the tube surface to the fuel, thereby increasing the heat flux through the tube surface over that where $q_e = 0$. Clearly then, as q_e increases, for operation at constant air flow rate and constant $(t_{a1}-t_{f1})$, the value of q_c must be reduced noticeably. In an exchanger such as Design B, the external heat load is transferred directly from the outer shell to the fuel. Its only effect on the internal operations in the fuel-cooled equipment case is to increase the temperature rise of the fuel, which also occurs in Designs A and C. Since the heat flux through the tube surface is changed only slightly by the small change of fuel temperature, the cooling capacity at constant $(t_{a1}-t_{f1})$ is changed but little with changing q_e.

Figure II-8 shows the effect of external heat load on the cooling performance of a Design B heat exchanger for two air flow rates. It is clear that a constant cooling capacity can be maintained for large changes of q_e with only small changes of $(t_{a1}-t_{f1})$.

3. Temperature Level

The effect of temperature level on the performance of a fuel-

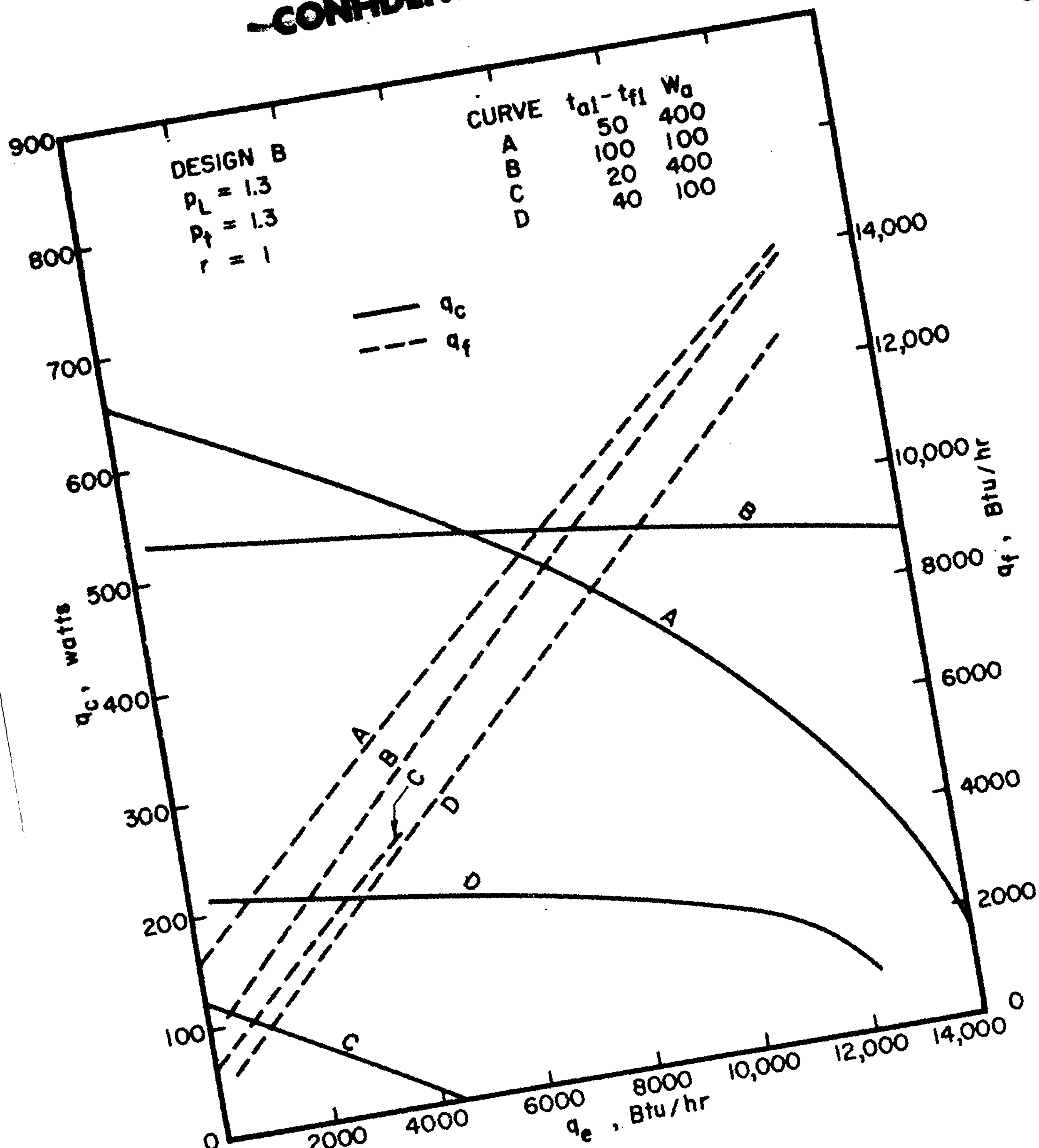

Figure II-6

Effect of External Heat Load on the Performance of a Design B Heat Exchanger

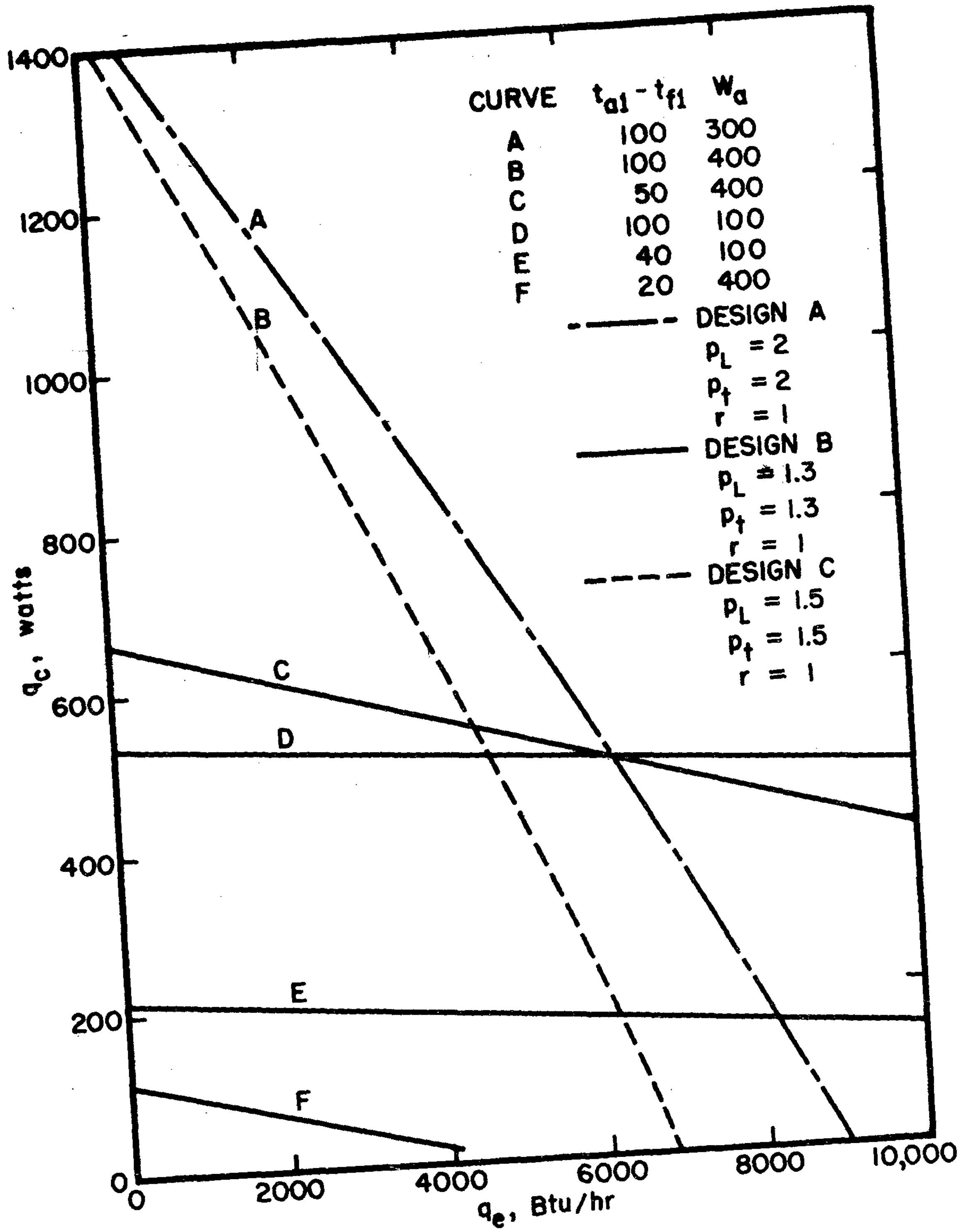

Figure II-7

Effect of External Heat Load on the Performance of Design A, B, and C Heat Exchangers

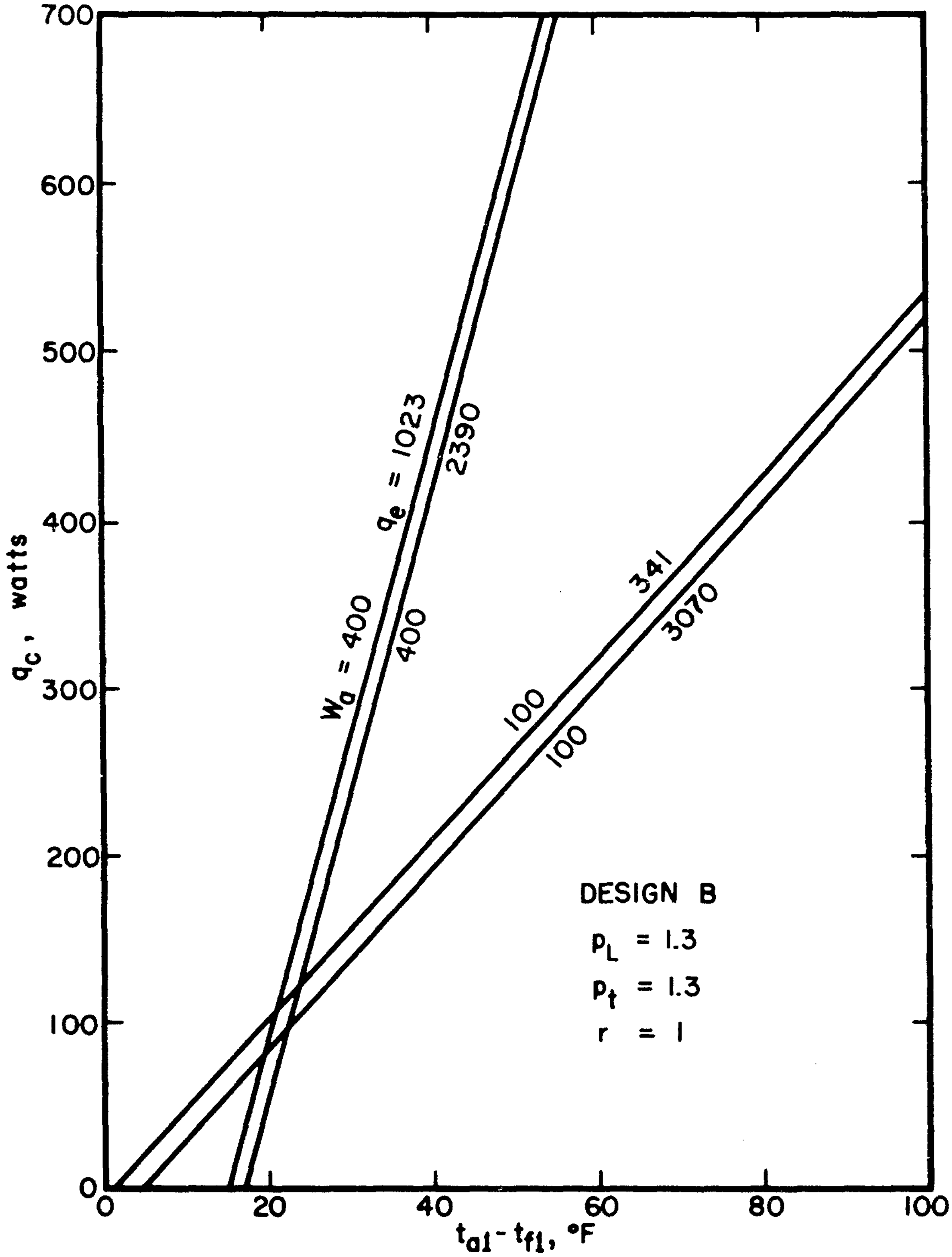

Figure II-8

Effect of External Heat Load on the
Performance of a Design B Heat Exchanger

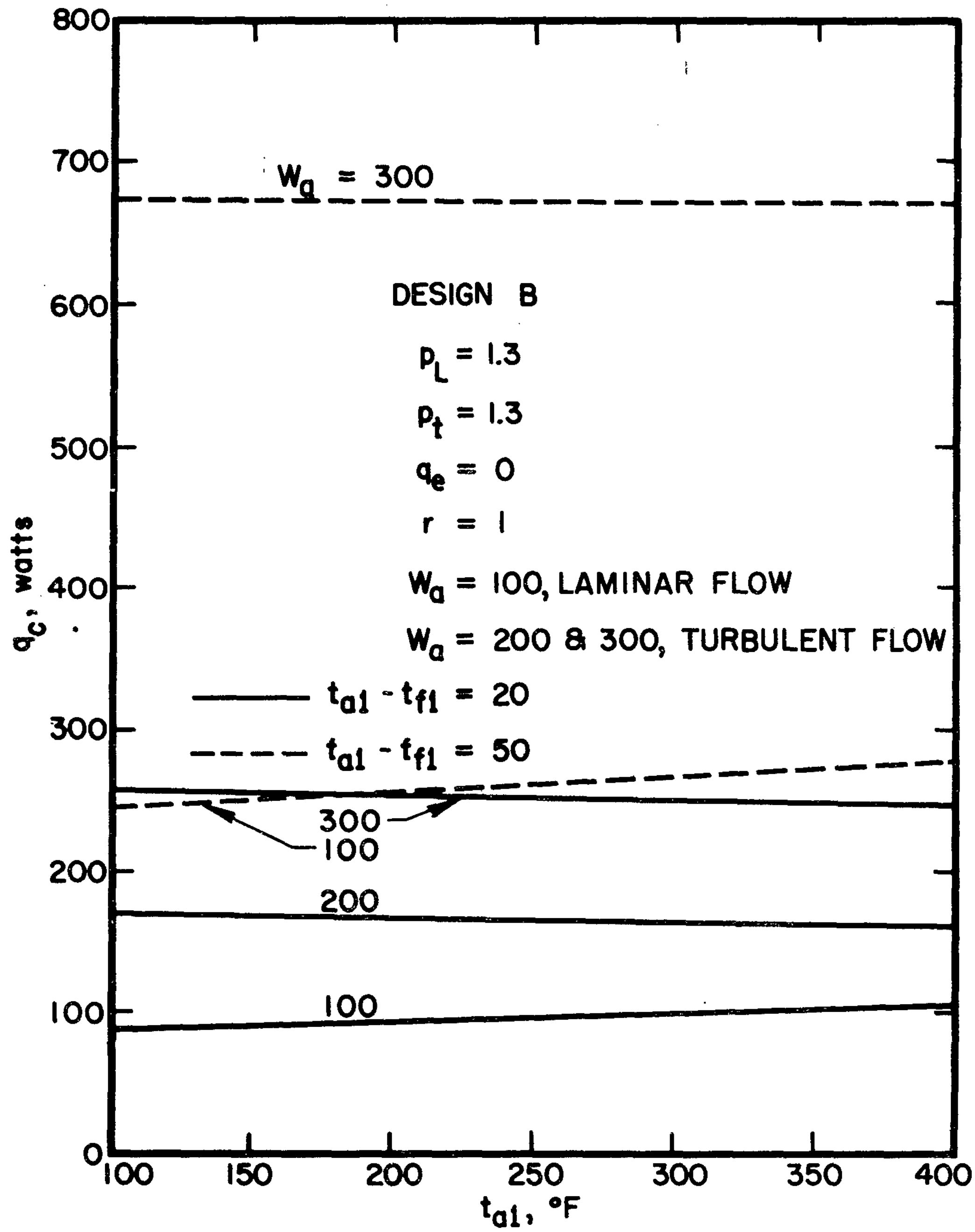

Figure II-9

Effect of Temperature Level on the Performance of a Design B Heat Exchanger

cooled heat exchanger is shown in Figure II-9. The same Design B heat exchanger is used as in Figures II-5, -6, -7, and -8. The plot shows that while cooling capacity varies slightly with temperature level, the variation is only about five percent from the mean in the temperature range shown. The slopes of the lines for $W_a = 100$ are different than for the higher air flow rates, since the former are in the laminar flow region for air in the tubes, while the latter represent turbulent air flow. The slight change in cooling capacity with temperature level is due to changes of physical properties in both the air and the fuel. It is apparent, however, that the air flow rate has much more effect on the cooling capacity than does the temperature level.

Figure II-10 shows the effect on performance of a change in temperature level and the resultant change of external heat load. This plot is for an exchanger of the Design A type, where air is in contact with the outer shell. The external heat load is defined as described in the analysis, in terms of an assigned value of $h_r = 1.5$ Btu/hr-ft^2-^{o}F and $t_s = 500^oF$. As the temperature level is increased, as marked by an increase of the entering fuel temperature, the value of $(t_{a1}-t_{f1})$ required for a given cooling capacity is reduced. This effect is due principally to the change of external heat load with rising temperature level. As the temperature level is raised, the temperature difference between the surroundings and the fuel-cooled case is reduced, giving a smaller external heat load. This tends to give the smaller $(t_{a1}-t_{f1})$ for a given net cooling capacity, as noted.

4. Fuel Flow Rate

The effect of fuel flow rate on heat exchanger performance is shown in Figure II-11. An exchanger core of the Design A type is used, with details indicated in the figure. Both the fuel flow rate W_f and the fuel temperature rise t_f are shown as a function of the temperature difference $(t_{a1}-t_{f1})$. For the conditions of evaluation, the fuel flow rate has almost no effect on the temperature difference $(t_{a1}-t_{f1})$ until a very low flow rate is reached. At low flow rates, there are low heat transfer coefficients on the fuel-side of the exchanger. This requires a large temperature to transfer the $q_f = 700$ Btu/hr to the fuel. It is assumed here that all of the generated and external heat loads are transferred through the tube surface. Thus, the case applies where no fuel pump is used, or where $(1/2q_{Mf})$ is negligibly small (see equation II-7). It is apparent that low fuel flow rates require high temperature rise of the fuel, as indicated by the dashed curve. There are therefore two penalties of operation of a fuel-cooled equipment case at low fuel flow rates. First, the air temperature in the case increases, and hence the equipment temperature must increase (see equation II-11). Second, the fuel temperature rise may become excessive. Good design can be achieved by using a fuel flow rate high enough that $(t_{a1}-t_{f1})$ is relatively unaffected by changes of W_f, and at the same time high enough to give a suitably small value of Δt_f.

The effects of fuel flow rate on performance of a Design E heat exchanger core are shown in Figure II-12. The results are qualitatively the same as those of Figure II-11. Plots are shown for several air flow rates.

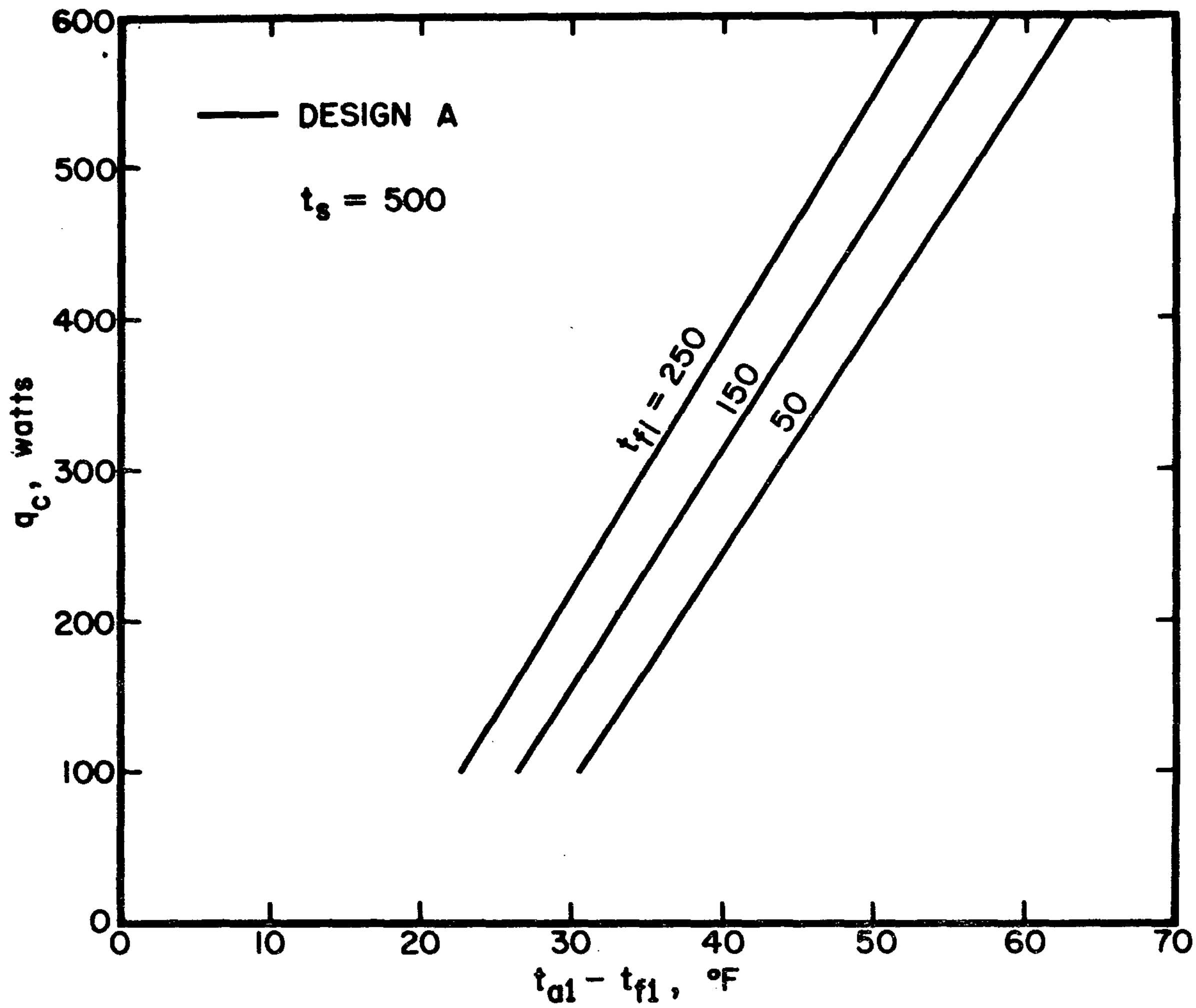

Figure II-10

Effect of Temperature Level on the Performance of a Design A Heat Exchanger

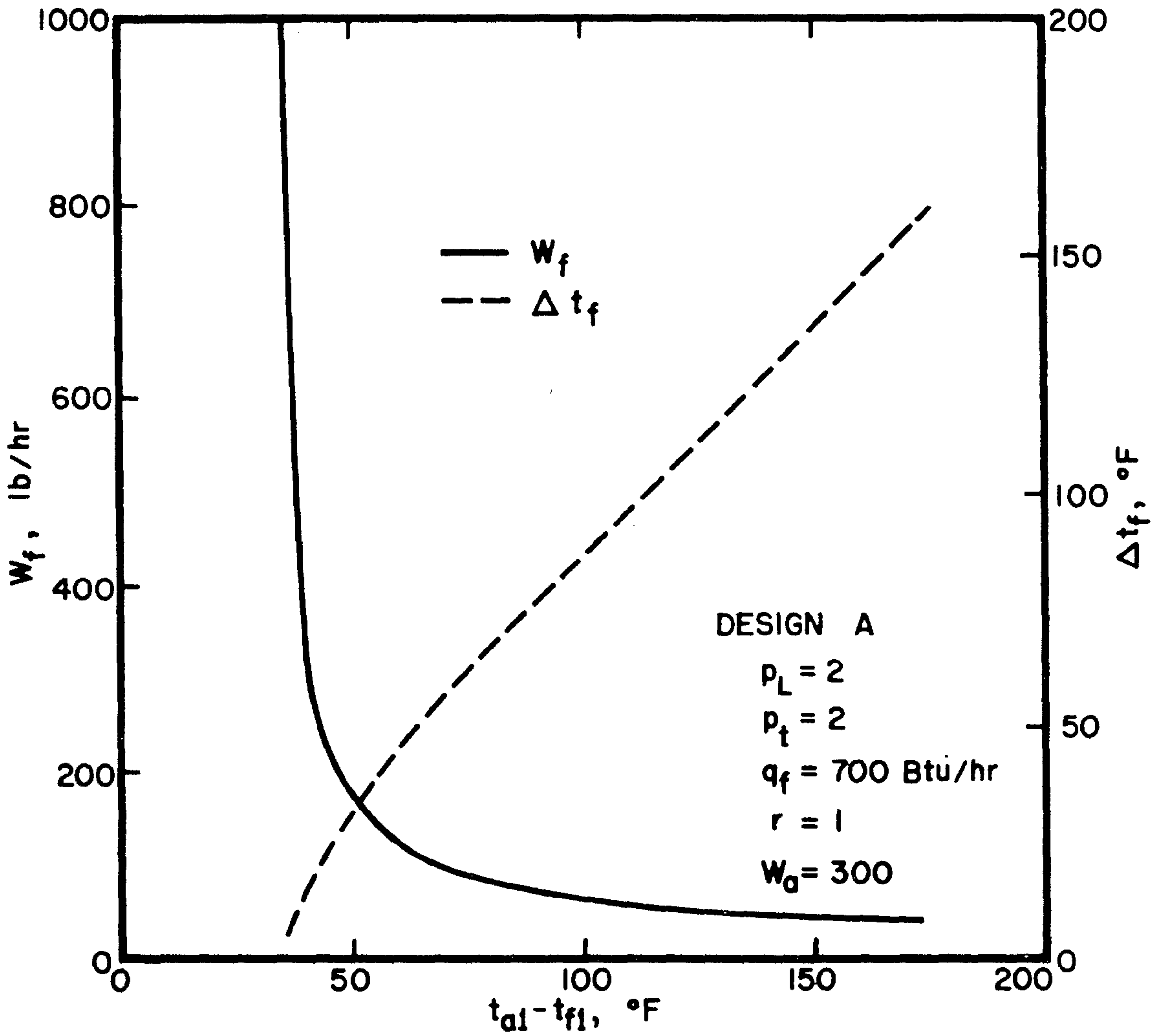

Figure II-11

Effect of Fuel Flow Rate on the Performance of a Design E Heat Exchanger

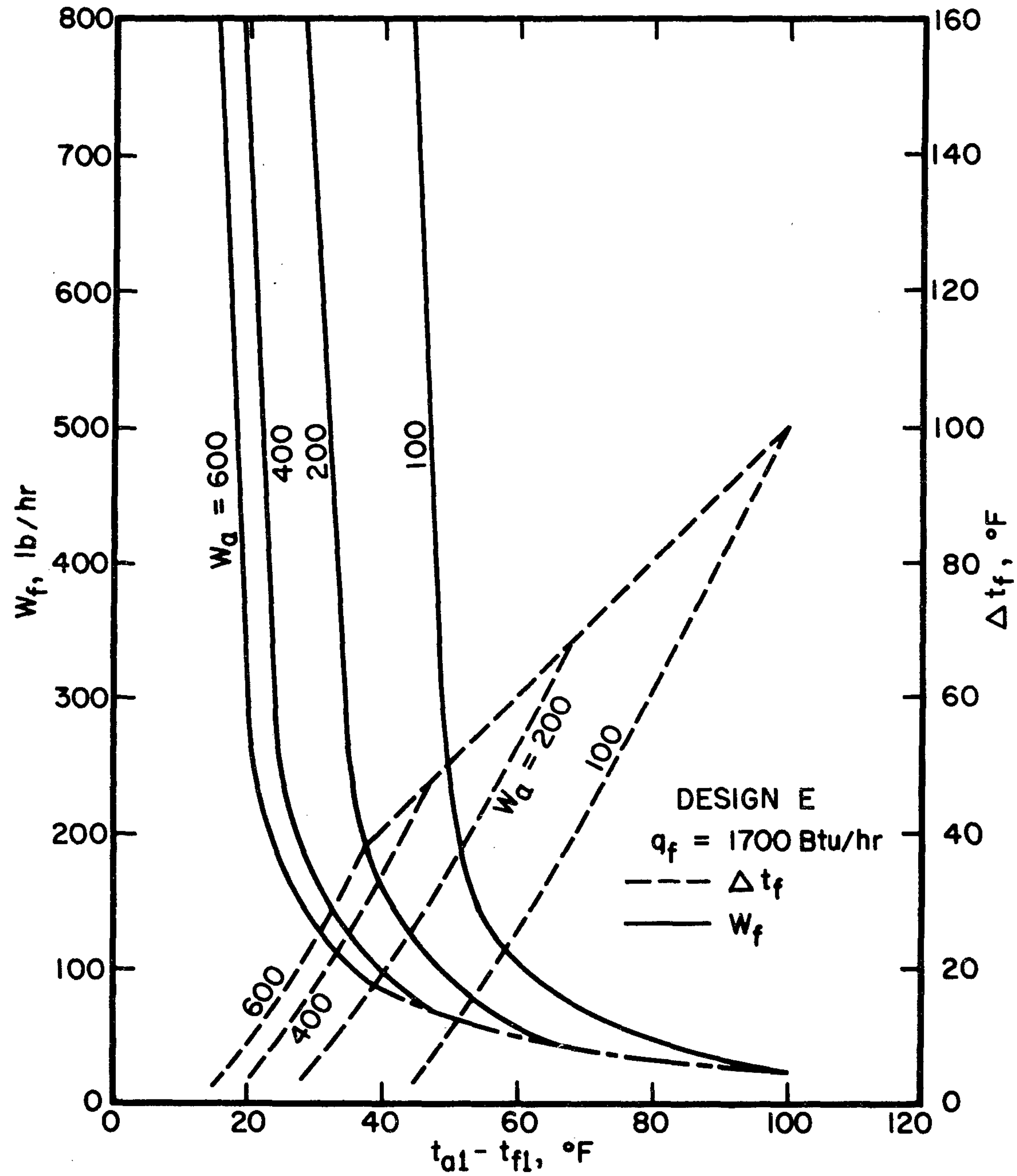

Figure II-12

Effect of Fuel Flow Rate on the Performance of a Design E Heat Exchanger

The plot clearly shows that the air flow rate has more effect on the performance than the fuel flow rate, unless the latter is very low. As expected, a decreased air flow rate requires increased $(t_{a1}-t_{f1})$ for a given heat transfer rate to the fuel.

The design of the fuel side of the exchanger is quite flexible, providing a high flow velocity is maintained to give a high film coefficient. This can always be accomplished by arranging the fuel headers to give a long flow passage of small cross sectional area. The weight of fuel per hour must also be high enough to keep the fuel temperature rise within the limits which might be specified by the fuel-system designer. For the applications considered here, it appears that the fuel temperature rise can always be kept within 5° to $10^{\circ}F$. Separate analyses show that film coefficients of the order of 500 $Btu/hr\text{-}ft^2\text{-}^{\circ}F$ can be developed in all the types of designs given and yet keep the fuel pressure drop under 5 psi. For a proper fuel side design for systems of Design A and B, the fuel flow rate may be varied 100 per cent from the design conditions without changing the fuel-air temperature difference more than 2 percent. Even less change in performance is noted when the exchanger is also operating with a low air flow rate.

5. Comparison of Designs

As mentioned earlier in connection with Figure II-5, the optimum operating condition from the standpoint of minimum $(t_{a1}-t_{f1})$ for a given cooling capacity lies on the envelope to a series of plots for constant air flow rate. It is possible to compare different heat exchanger designs by constructing such an envelope for each. A comparison of this type is given in Figure II-13 for three heat exchanger cores, all Design A, but using different longitudinal pitches for the fuel tubes. It is apparent that for a given cooling capacity the design with the shortest longitudinal pitch gives the best performance, since it can provide the lowest air temperature. This would be expected from the fact that the core with the shortest pitch has more tubes and hence a greater surface area. As described earlier, the air flow rate required for a given combination of q_c and $(t_{a1}-t_{f1})$ is that which gives a performance line (as in Figure II-5) which is tangent to the plot of the envelope curve at the desired point. All of the curves plotted in Figure II-13 represent heat exchanger cores of the same dimensions and over-all volume. The volume is shown as $V_H = 274.5$ in.^{3}

A similar comparison is given in Figure II-14 for heat exchanger cores such as Designs A, B, and C, and for two different heat exchanger volumes in each design type. The volume values are shown simply because they indicate the amount of space used up by each heat exchanger core within the fuel-cooled case. Such space is lost in the sense that it is not available for equipment installation. The Design B exchangers appear on the average to give superior performance, since they do not impose the external heat loads on the tube heat transfer surface, but transfer external heat directly to the fuel. The tube heat transfer surface is therefore used only for the transfer of the internal or generated heat loads. The external heat loads for Figure II-14 were determined by the convention of using $h_x = 1.5$ and $t_s = 500^{\circ}F$.

The effect of the external heat load on optimum performance character-

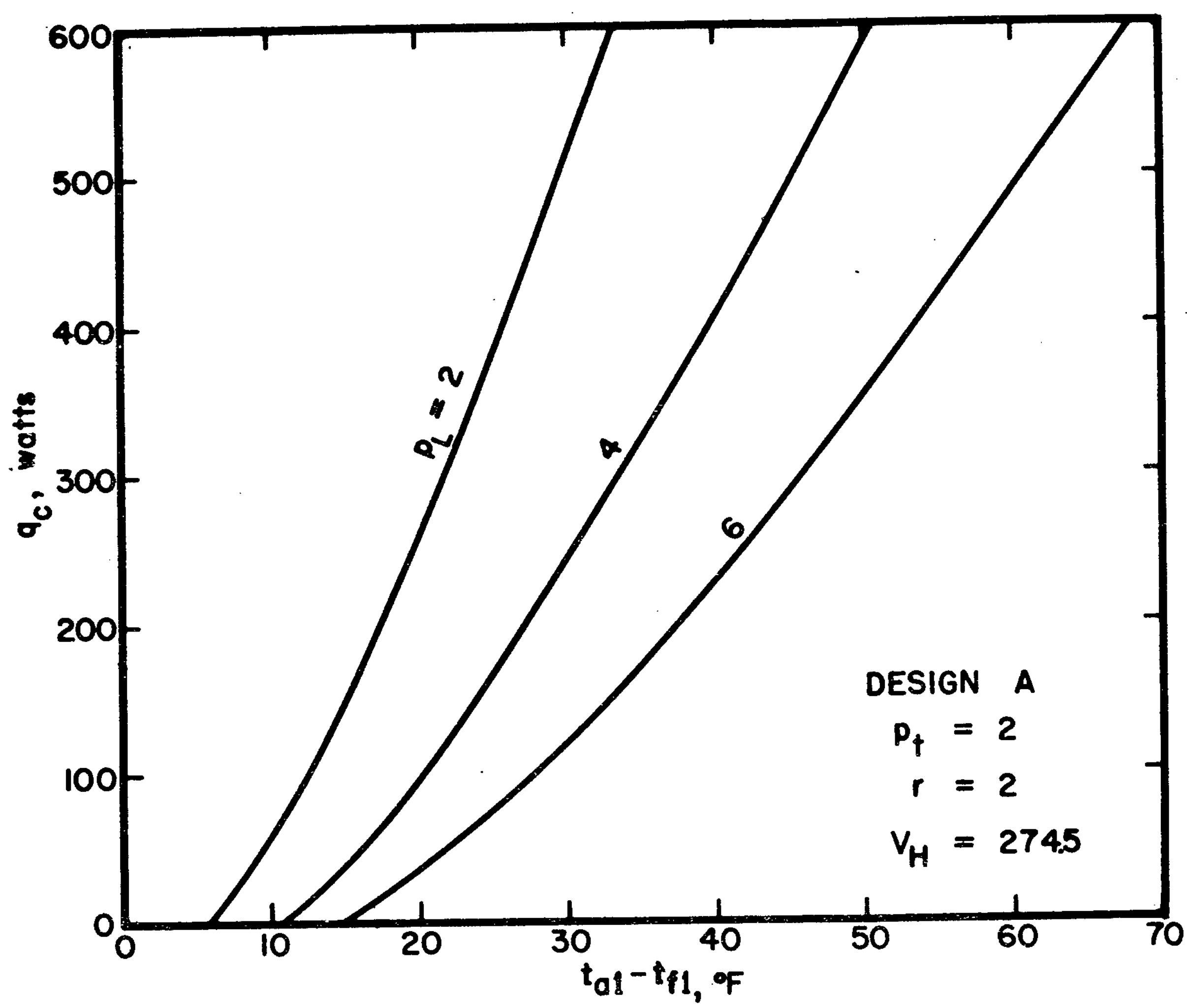

Figure II-13

Comparison of Performance for Design A, B, and C Heat Exchangers

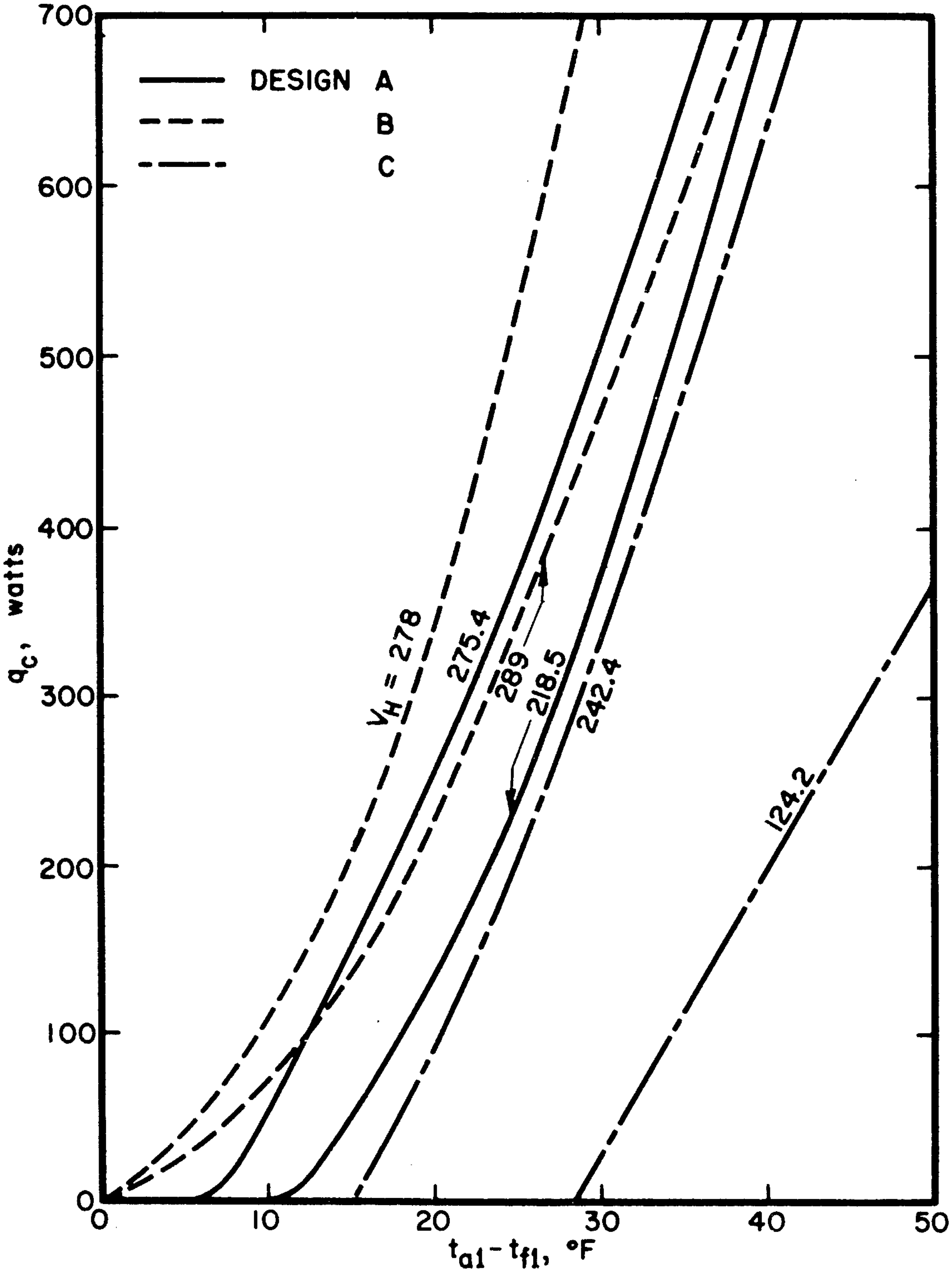

Figure II-14

Comparison of Performance for
Design A, B, and C Heat Exchangers

istics is shown in Figure II-15. Heat exchangers of Design A and B are considered. The external heat loads are defined in terms of two different values of h_x and corresponding values of t_s. This actually does not completely establish the magnitude of the external heat load, since h_c, the heat transfer coefficient on the inside of the outer shell, must still be calculated for each case (see equations II-2, -3, and -4). However, it is obvious in a qualitative sense that the external heat load for $h_x = 3.0$ and $t_s = 660^oF$ must be somewhat larger than when $h_x = 1.5$ and $t_s = 500^oF$. Figure II-15 therefore shows that a Design B exchanger is less sensitive to external heat loads than a Design A exchanger, insofar as optimum performance characteristics are concerned.

Figure II-16 presents a comparison of the performance characteristics for a large number of heat exchangers, expressed in terms of the heat transferred to the fuel per unit volume of heat exchanger core. A similar comparison is given in Figure II-17 expressed in terms of the net cooling capacity available to the installed equipment per unit volume of heat exchanger core. In both figures the data are based on a value of $t_{a1} = 300^oF$ as usual, except for the single plot representing Design D. This is based on $t_{f1} = 200^oF$. Since the air temperature is somewhat above the fuel temperature, the plots for Design D are roughly comparable with the others. Figure II-17 shows the Design B heat exchanger cores to be somewhat better than the others from the standpoint of cooling capacity per unit volume at given temperature conditions. The only other design type which compares favorably with Design B is Design D, which uses fins to extend the surface area on the fuel tubes.

Comparisons of performance based on the weight of the heat exchanger core are given in Figures II-18 and -19 for Designs A and B. The weights of the heat exchangers are calculated for a fuel pressure of 300 lb/in.^{2} At this pressure, using aluminum construction, stresses are held to an acceptable level with 8-gage (0.128 in.) wall thicknesses for the inner and outer shells in Design B. For Design A, shells of 30-gage (0.010 in.) aluminum are used. As described earlier, tubes of 3/16 in. outside diameter and 0.007 in. wall thickness are used for both design types. The weights calculated are for inner and outer shells, tubes, and fuel headers only.

Figure II-19 shows that Design A is considerably superior to Design B on the basis of cooling capacity per unit weight for a given temperature condition. It can therefore be concluded that Design D would be the best from the standpoint of both weight and volume requirements. It was shown in Figure II-17 that Design D is about equal in performance to Design B on a volume basis, and it may be deduced from comparing Figures II-2 and -3 that Designs A and D would have similar weight characteristics. Therefore, although the type core wherein fuel is in contact with the outer shell is superior in performance on a volume or size basis, the difference can be made up for designs with air in contact with the outer shell if extended tube surfaces are used. The latter are therefore to be preferred because of their light weight.

Table II-1 shows the cooling capacity per unit volume and per unit weight that might reasonably be expected for systems of the type presented here. It is emphasized that these values are not necessarily the best possible of attainment, but are representative for their types. In Table II-1,

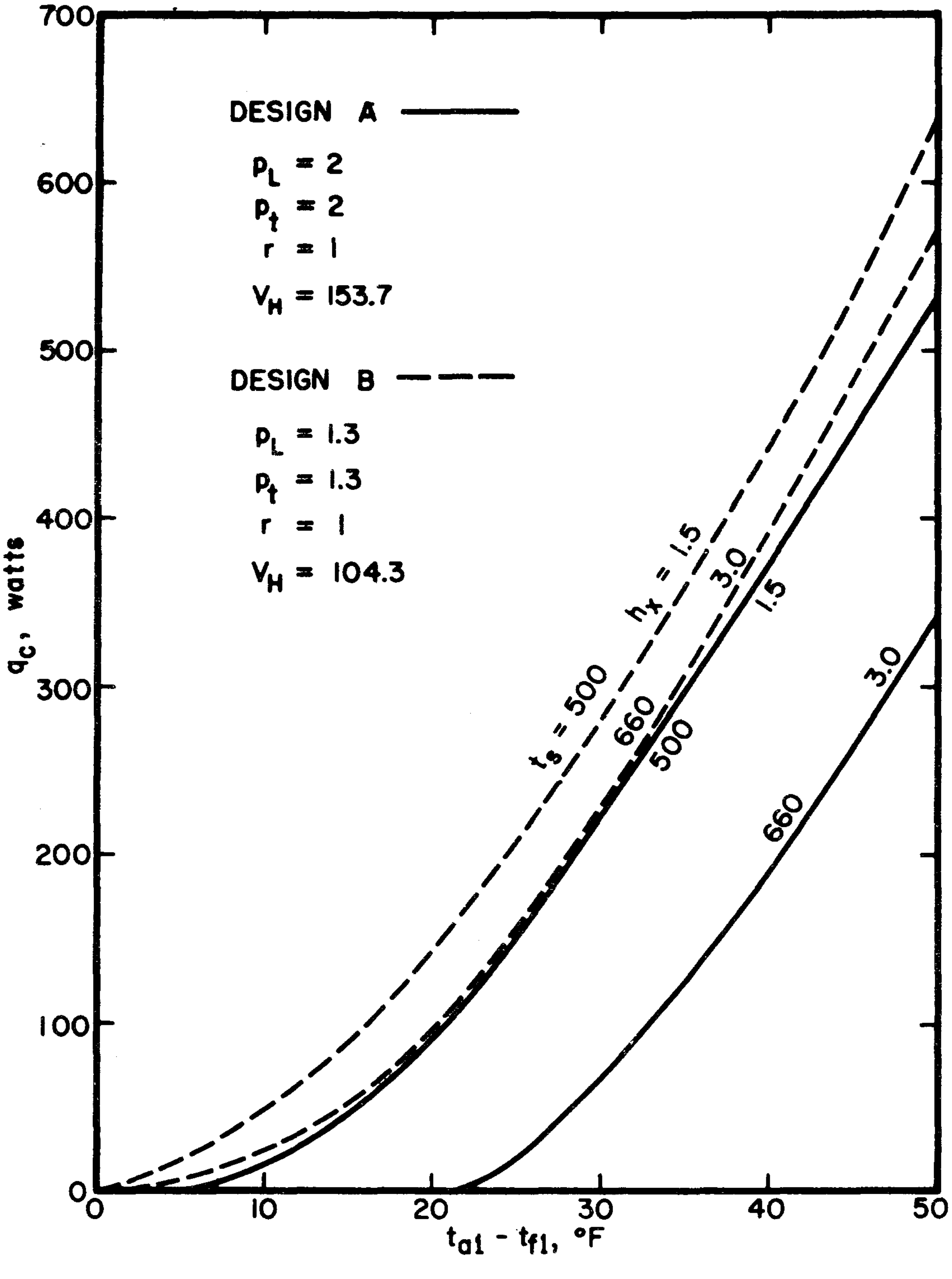

Figure II-15

Comparison of Performance for Design A and B Heat Exchangers, Showing Effects of External Heat Load

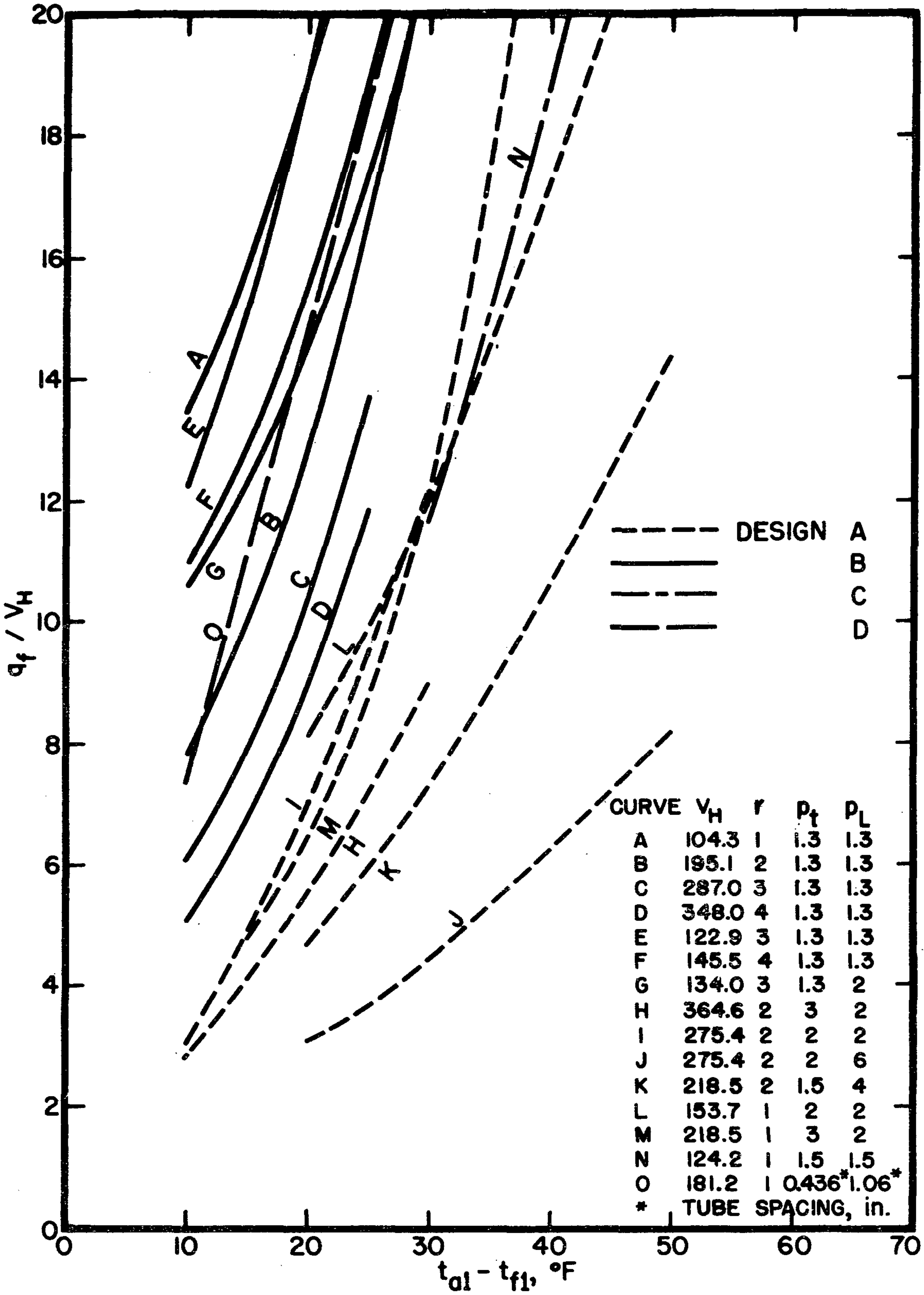

Figure II-16

Comparison of Heat Exchanger Performance
Based on Volume of the Heat Exchanger

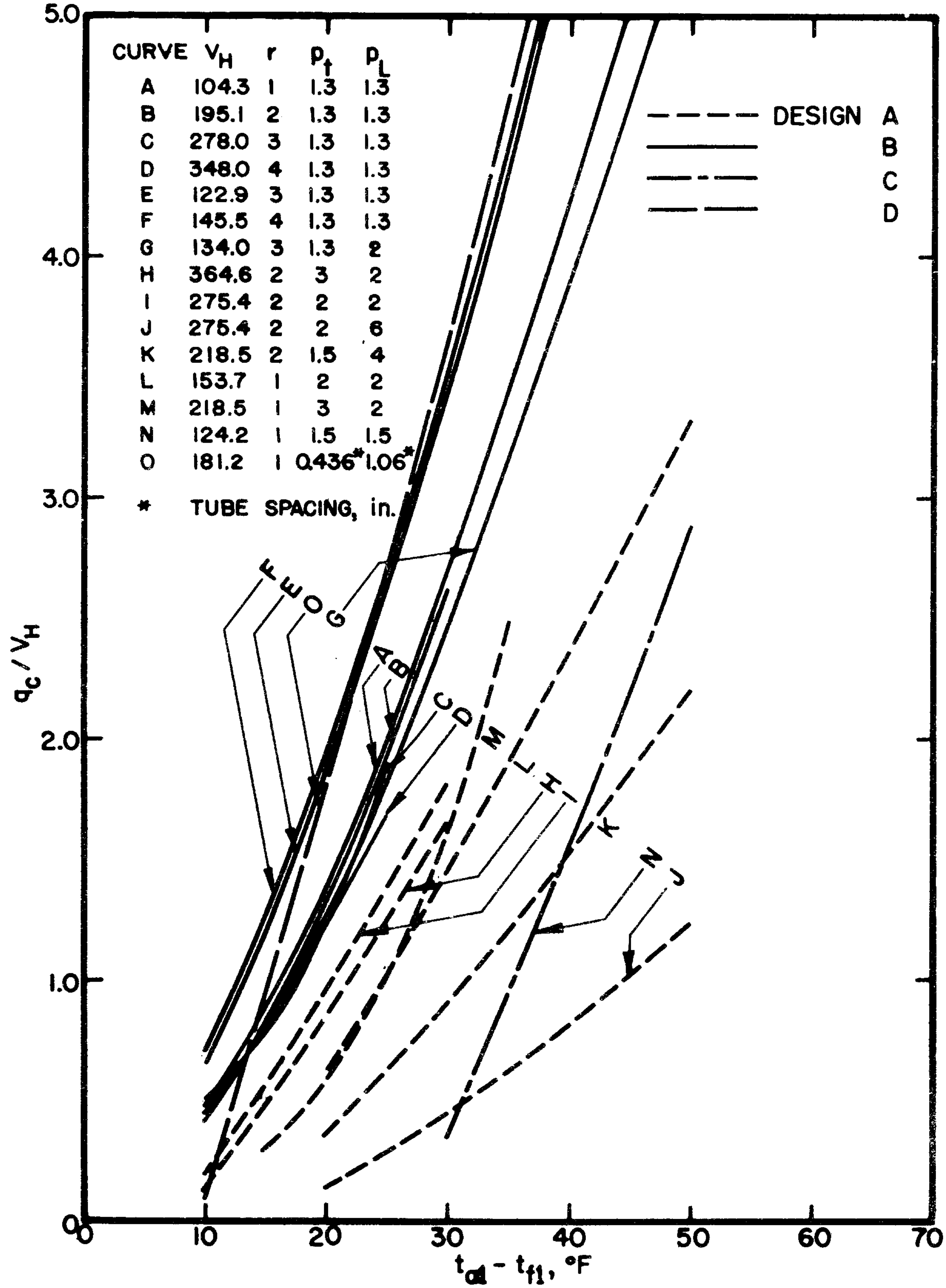

Figure II-17

Comparison of Heat Exchanger Performance
Based on Volume of the Heat Exchanger

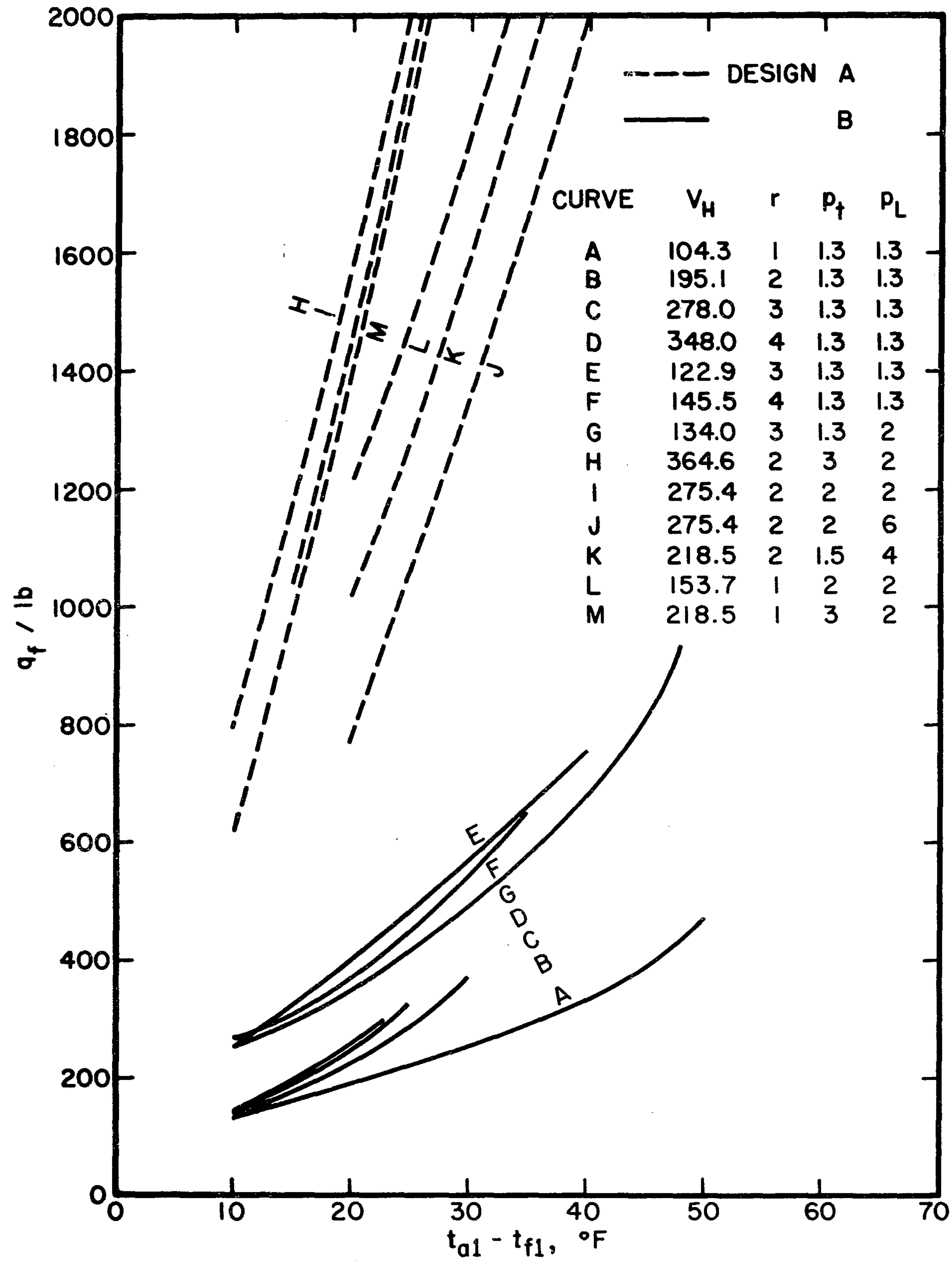

Figure II-18

Comparison of Heat Exchanger Performance
Based on Weight of the Heat Exchanger

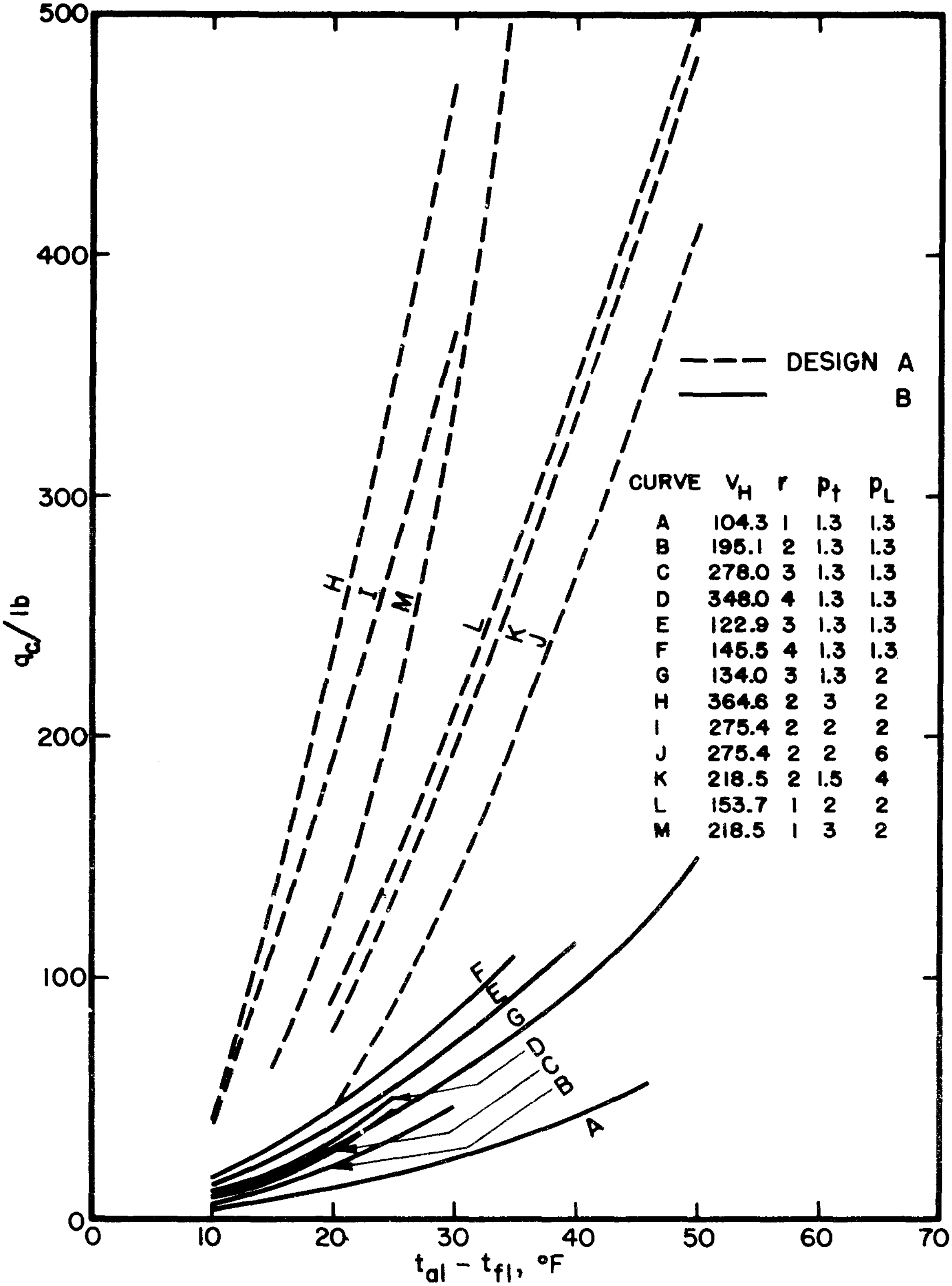

Figure II-19

Comparison of Heat Exchanger Performance
Based on Weight of the Heat Exchanger

Table II-1

Summary of Heat Exchanger Performance Characteristics

	$(q_c/\text{in.}^3)$		$(q_f/\text{in.}^3)$		(q_c/lb)		(q_f/lb)	
$(t_{a1}-t_{f1})$	15	25	15	25	15	25	15	25
Design A	0.5	1.6	5.1	9.6	110	320	1025	1880
Design B	0.8	1.9	15	23.2	15	30	170	307

q_c is expressed in watts, while q_f is expressed in Btu/hr.

Exchangers of Design E, sketched in Figure II-3, appear to have no advantages over the other designs. Such a configuration has the distinct disadvantage that the air is forced to circulate through long tortuous paths around the heat exchanger. Hence, extremely high pumping power is required, or else unusually large cross sections of the heat exchanger are necessary. The latter results in extremely low values of cooling capacity per unit volume. Passing the air parallel to the axis of the case, as in all other designs, gives a much larger air flow area for the same size of exchanger.

6. Air Pressure

The effect of air pressure on the cooling performance of a fuel-cooled case has not been shown in any of the data presented. It is possible, however, to indicate the influence of air pressure on performance without resort to calculation. By the equation of state for perfect gases, the density of air is inversely proportional to the pressure, and it is because of the effects of density that the air pressure is important.

A fixed design of fuel-cooled case is considered first, equipped with a motor and fan operating at constant speed. In such a system, the fan or blower circulates air at a substantially constant volume rate. If the air density changes, and the flow is turbulent, the power requirement for circulating the air varies almost directly as the density of the air. A decrease of density then results in lowered air power requirements, and conversely. However, the weight flow rate also decreases, giving reduced air heat transfer coefficients throughout the system. In general the heat transfer coefficients do not change as rapidly as the density. As the density of air decreases in such a system, the tendency of the reduced power requirement is to reduce the temperature difference required between the equipment and the fuel to dissipate the system heat loads. At the same time, the tendency of the reduced heat transfer coefficients is opposite to this and would predominate in all instances of good design where the air pumping power would represent a small percentage of the net cooling capacity. The effects are reversed for an increase of air density.

In a system where the air flow in the heat exchanger is laminar (as in

a core where the air flows through tubes with Re < 2300), there is theoretically no change of circulating power requirement for changed air density. The heat transfer coefficients are changed, however. As the density decreases, a greater temperature difference is required between the equipment and the fuel for a given cooling capacity, and conversely. The effects of varying air pressure on the performance of a system can be determined quantitatively by calculations of the type given in Appendix D to this Section.

It is next supposed that the system is not already established, and that it is desired to design for a constant net cooling capacity available to the equipment, and a constant temperature difference between the equipment and the fuel. The air heat transfer coefficients remain unchanged so long as the weight rate of air circulation is constant. For turbulent flow with a substantially constant friction factor, a constant weight flow rate is maintained if the volume flow rate is proportioned inversely to the air density. It therefore follows that the power required to circulate the air varies inversely as the square of the air density. Therefore, if the density of the air is reduced, the air flow volume must be increased in a greater than inverse proportion to the density ratio, so as to provide higher heat transfer coefficients to accommodate the increased total of equipment and circulation power heat loads. For laminar flow, the variation required in air flow volume for changing air density is the same as for turbulent flow with a substantially constant friction factor. If the air density is increased, the air flow volume may be reduced in more than inverse proportion to the ratio of densities, since the circulation power requirement is reduced, and smaller heat transfer coefficients are suitable.

From the design standpoint, a system may be operated with low power requirements for a given cooling effect if high air densities are involved. It is therefore more feasible to design a fuel-cooled case for operation in a dense-air environment than in a rarified atmosphere. If the compartment in which the case is located is exposed to low pressures at high altitude, it would be preferred to use a sealed case containing a more dense atmosphere.

APPENDIX A TO SECTION II

Nomenclature

Symbol	Definition	Units
A_a	Net free flow area for air	ft^2
A_f	Net free flow area for fuel	ft^2
A_n	Annular cross-sectional area between inner and outer shells	ft^2
A_o	Heat transfer area based on outside diameter of tubes	ft^2
A_x	Heat transfer area on outside of outer shell of the casing	ft^2

Symbol	Definition	Units
c_f	Specific heat of the fuel	Btu/lb-°F
c_p	Specific heat at constant pressure	Btu/lb-°F
D	Diameter	ft
D_e	Equivalent diameter defined where used	ft
D_i	Diameter of inner shell of the heat exchanger	ft
D_o	Diameter of outer shell of the heat exchanger	ft
d_{eh}	Equivalent diameter for heat transfer on air side (Design C)	in.
d_{ep}	Equivalent diameter for pressure loss on air side (Designs A and C)	in.
d_{efp}	Equivalent diameter for pressure loss on fuel side (Design B)	in.
d_{ti}	Inside diameter of tubes	in.
d_{te}	Outside diameter of tubes	in.
f	Darcy friction factor	dimensionless
G	Weight flow rate of air based on A_a. $G = (W_a/A_a)$	$lb/hr\text{-}ft^2$
g	Gravitational constant = 32.2	ft/sec^2
h_c	Convection heat transfer coefficient on inside of outer shell	$Btu/hr\text{-}ft^2\text{-}^oF$
h_i	Convection heat transfer coefficient on inside of tubes	$Btu/hr\text{-}ft^2\text{-}^oF$
h_o	Convection heat transfer coefficient on outside of tubes	$Btu/hr\text{-}ft^2\text{-}^oF$
h_x	Convection heat transfer coefficient on outside of outer shell	$Btu/hr\text{-}ft^2\text{-}^oF$
j_H	Correlation factor for heat transfer coefficients	dimensionless
k	Thermal conductivity	Btu/hr-ft-°F

Symbol	Definition	Units
L	Length of the fuel-cooled case	ft
L_f	Length of fuel passage (Design B)	ft
n	Number of tubes in the heat exchanger core	dimensionless
n'	Number of parallel paths formed by tubes	dimensionless
N	Number of times the fuel in a single passage traverses the core length (Design C), or number of times it encircles the case (Designs A and B)	dimensionless
P_a	Average air pressure	lb/in.^{2}
ΔP_a	Pressure drop of air through heat exchanger core	in. of water
ΔP_f	Pressure drop of fuel through heat exchanger core	lb/in.^{2}
p_L	Longitudinal pitch of tubes	tube diameters (dimensionless)
p_t	Transverse pitch of tubes	tube diameters (dimensionless)
Pr	Prandtl modulus, air	dimensionless
Pr_f	Prandtl modulus, fuel	dimensionless
q_c	Net cooling capacity required by equipment (heat generated by equipment)	watts
q_e	External heat load to fuel-cooled case	Btu/hr
q_f	Total heat load to fuel	Btu/hr
q_M	Power required to circulate air and fuel through the heat exchanger core	watts
q_{Ma}	Power required for air circulation only	watts
q_{Mf}	Power required for fuel circulation only	watts
Re	Reynolds modulus for air	dimensionless
Re_p	Reynolds modulus for air pressure loss calculations	dimensionless

Symbol	Definition	Units
Re_f	Reynolds number for fuel	dimensionless
Re_{fp}	Reynolds number for fuel pressure loss calculations	dimensionless
r	Number of rows (transverse) of tubes	dimensionless
t_{a1}	Temperature of air entering heat exchanger core	^oF
t_{am}	Arithmetic mean air temperature in heat exchanger core	^oF
t_{f1}	Temperature of fuel entering heat exchanger core	^oF
t_{fm}	Arithmetic mean fuel temperature in heat exchanger core	^oF
Δt_a	Temperature drop of air through the heat exchanger	^oF
Δt_f	Temperature rise of fuel through the heat exchanger	^oF
t_s	Representative temperature for the surroundings of the fuel-cooled case	^oF
t_{shell}	Temperature of the outer shell of the heat exchanger	^oF
U_o	Over-all coefficient of heat transfer between air and fuel, based on outside surface area	Btu/hr-ft^2-^oF
U_x	Over-all coefficient of heat transfer between the surroundings and the fluid inside of the outer shell of the heat exchanger	Btu/hr-ft^2-^oF
u	Velocity of fluid	ft/sec
u_e	Velocity of fluid after exit from a tube	ft/sec
V_H	Volume of a heat exchanger core	in.^{3}
W_a	Air flow rate	lb/hr
W_f	Fuel flow rate	lb/hr
x	Length of the heat exchanger core	in.

Symbol	Definition	Units
x_f	Length of the fuel passage (Design A)	in.
Y	Substitution function	
α	Ratio of cross sectional area filled with tubes to the annular cross sectional area of the heat exchanger	dimensionless
γ_a	Density of air	lb/ft^3
γ_f	Density of fuel	lb/ft^3
θ_a, θ_b	Temperature difference between air and fuel	lb/ft-hr
θ_{lm}	Logarithmic mean temperature difference between fuel and air	^oF
μ	Viscosity of air	lb/ft-hr
μ_f	Viscosity of fuel	lb/ft-hr
μ_w	Viscosity of a fluid at a surface temperature	lb/ft-hr
σ_e	Effectiveness of equipment as a heat-exchange device, defined by equation (II-10)	dimensionless
ϕ	Correlation factor for pressure drop in flow across banks of tubes	dimensionless

APPENDIX B TO SECTION II

Summary of Heat Transfer and Pressure Drop Relationships for Heat Exchanger Cores

The basic equations describing heat transfer coefficients and pressure drop in the various heat exchanger cores are summarized here. References are given to indicate the sources of the data. An example showing the incorporation of these basic equations into a performance evaluation is given for Design A in Appendix C to Section II.

1. Design A. Fuel in Tubes, Air in Crossflow Over Tubes

The heat transfer coefficient for flow of fuel through the tubes is determined from a plot of the factor j_H versus the Reynolds number defined as $Re_f = (d_{ti}W_f/12\mu_f A_f)$ (Ref. II-2). This is based on an original correla-

tion by Seider and Tate (Ref. II-1). The factor is given by

$$j_H = \left(\frac{h_i D}{k}\right)(Pr)^{-1/3}\left(\frac{\mu}{\mu_w}\right)^{-0.14} \tag{II-12}$$

and in the present work the factor $(\mu/\mu_w)^{-0.14}$ is taken as unity. The inside heat transfer coefficient is therefore

$$h_i = j_H \frac{12}{d_{ti}} (k\, Pr^{1/3})_f \tag{II-13}$$

in the form subsequently used for calculation. A plot of the factor j_H is given in Figure II-20, where it is necessary to know the length-to-diameter ratio of the tubes if the fuel flow is in the laminar or transition regions. Values of the combined physical properties $(k\, Pr^{1/3})_f$ are given for a range of temperatures for JP-3 fuel in Figure II-21. They should be evaluated at the mean bulk temperature of the fluid.

The pressure drop for flow of fuel through the tubes is found from equations which allow for the loss at entrance to the tubes, loss in the tubes, and loss at exit from the tubes. For an abrupt tube entrance, the pressure loss is given by (Ref. II-3),

$$\text{entrance loss} = 0.5\left(\frac{\gamma_f}{144}\right)\left(\frac{u^2}{2g}\right) \tag{II-14}$$

The pressure loss through the tubes is given by the Darcy law for pipe friction as (Ref. II-3)

$$\text{tube loss} = \left(\frac{f x_f}{d_{ti}}\right)\left(\frac{\gamma_f}{144}\right)\left(\frac{u^2}{2g}\right) \tag{II-15}$$

The friction factor is a function of the Reynolds number and may be taken from Figure II-22. This is replotted from the Moody chart of friction factors (Ref. II-4), using a relative roughness of 0.0001. The pressure loss at exit of the fuel from the tube is given by

$$\text{exit loss} = \left(\frac{\gamma_f}{144}\right)\frac{(u-u_e)^2}{2g} \tag{II-16}$$

For simplicity, it is assumed that the velocity or exit u_e is about one-half that in the tubes, which gives

$$\text{exit loss} = \left(\frac{\gamma_f}{144}\right)\left(\frac{0.25}{2g}\right) \tag{II-17}$$

The over-all pressure drop is then

$$\Delta P_f = \left(\frac{\gamma_f}{144}\right)\left(\frac{u^2}{2g}\right)\left[\left(\frac{f x_f}{d_{ti}}\right) + 0.75\right] \tag{II-18}$$

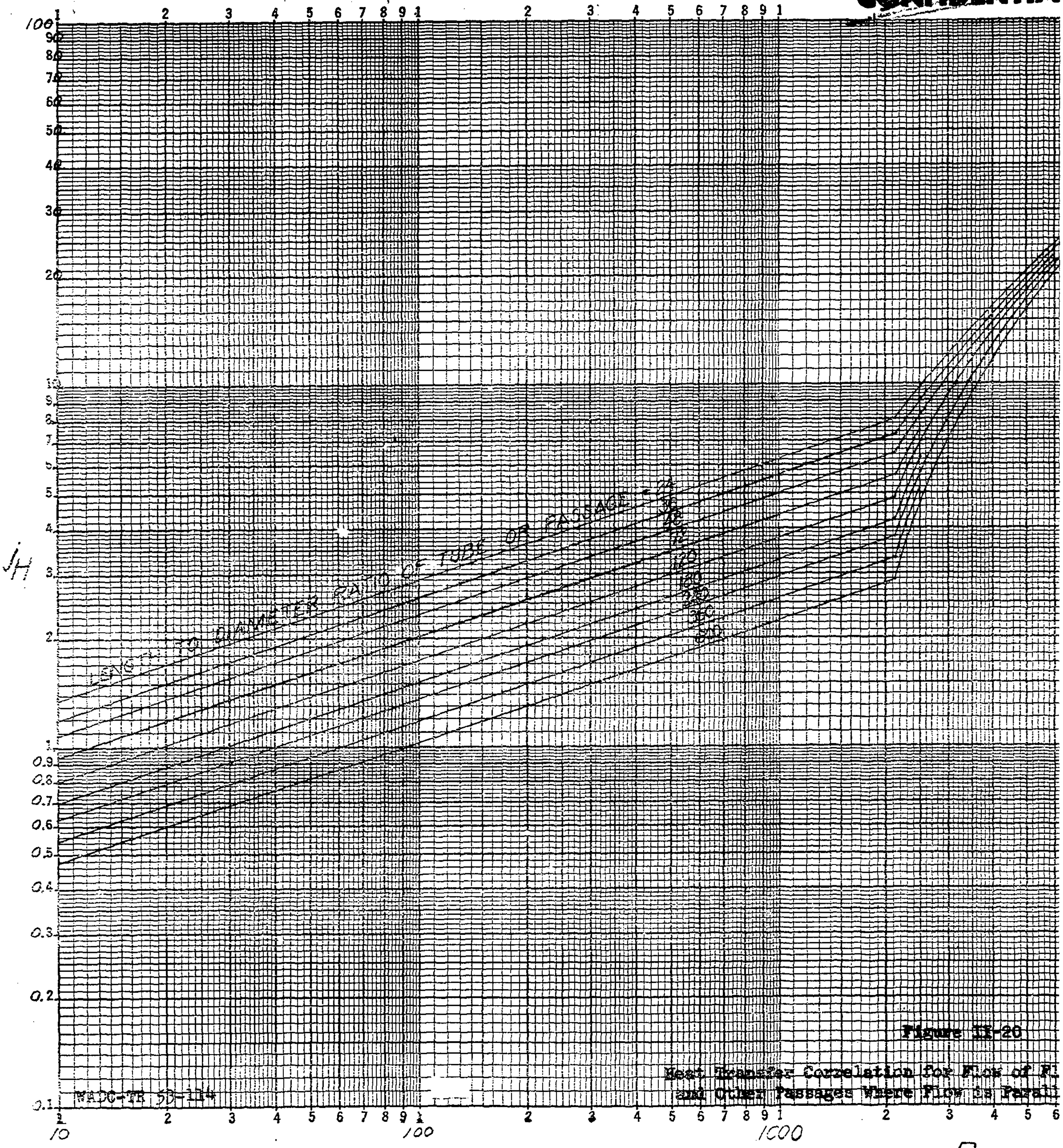

Figure II-26

Heat Transfer Correlation for Flow of Fl
and Other Passages Where Flow is Parall

(i)

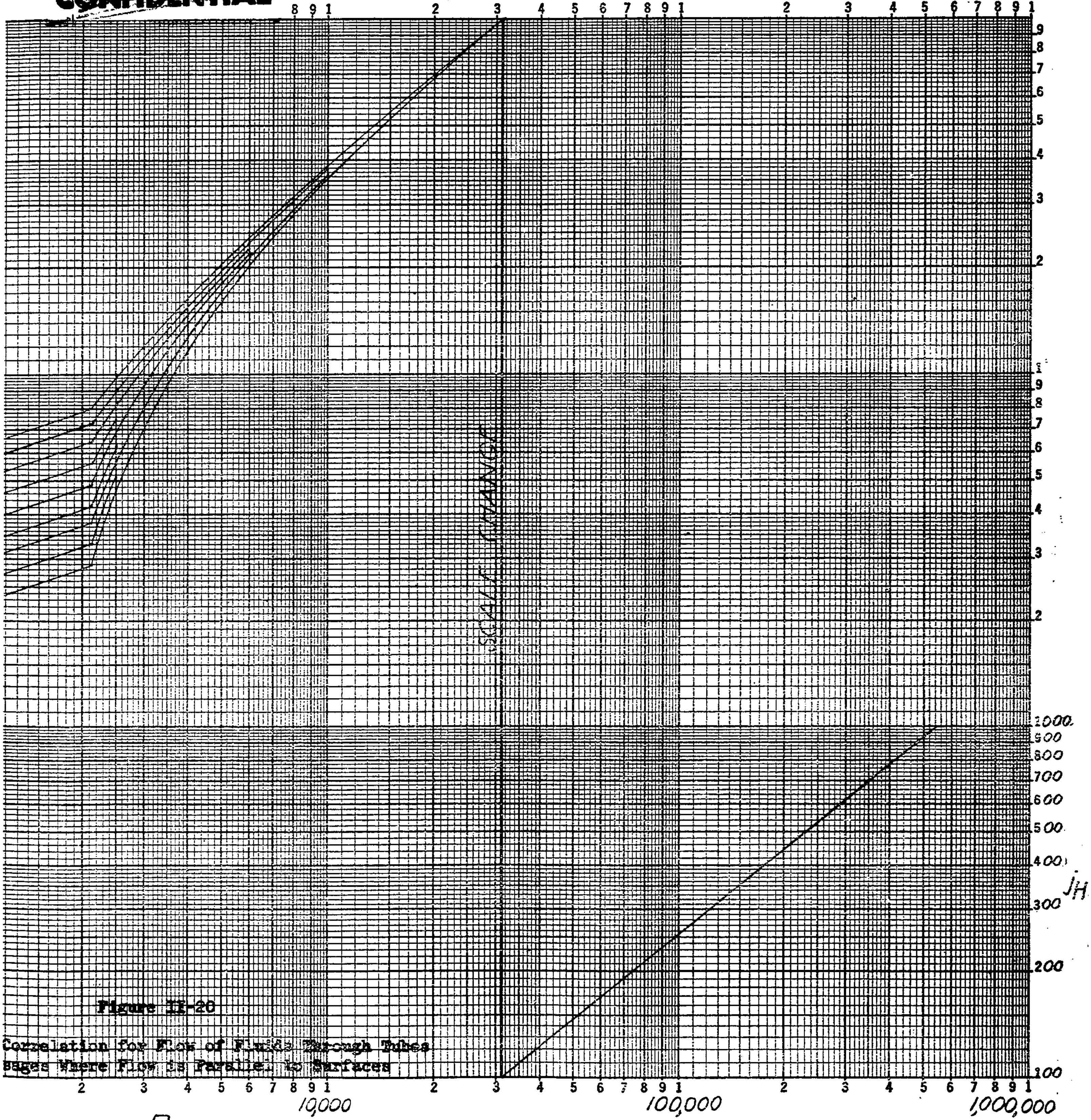

Figure II-20

Correlation for Flow of Fluids Through Tubes
sages Where Flow is Parallel to Surfaces

2

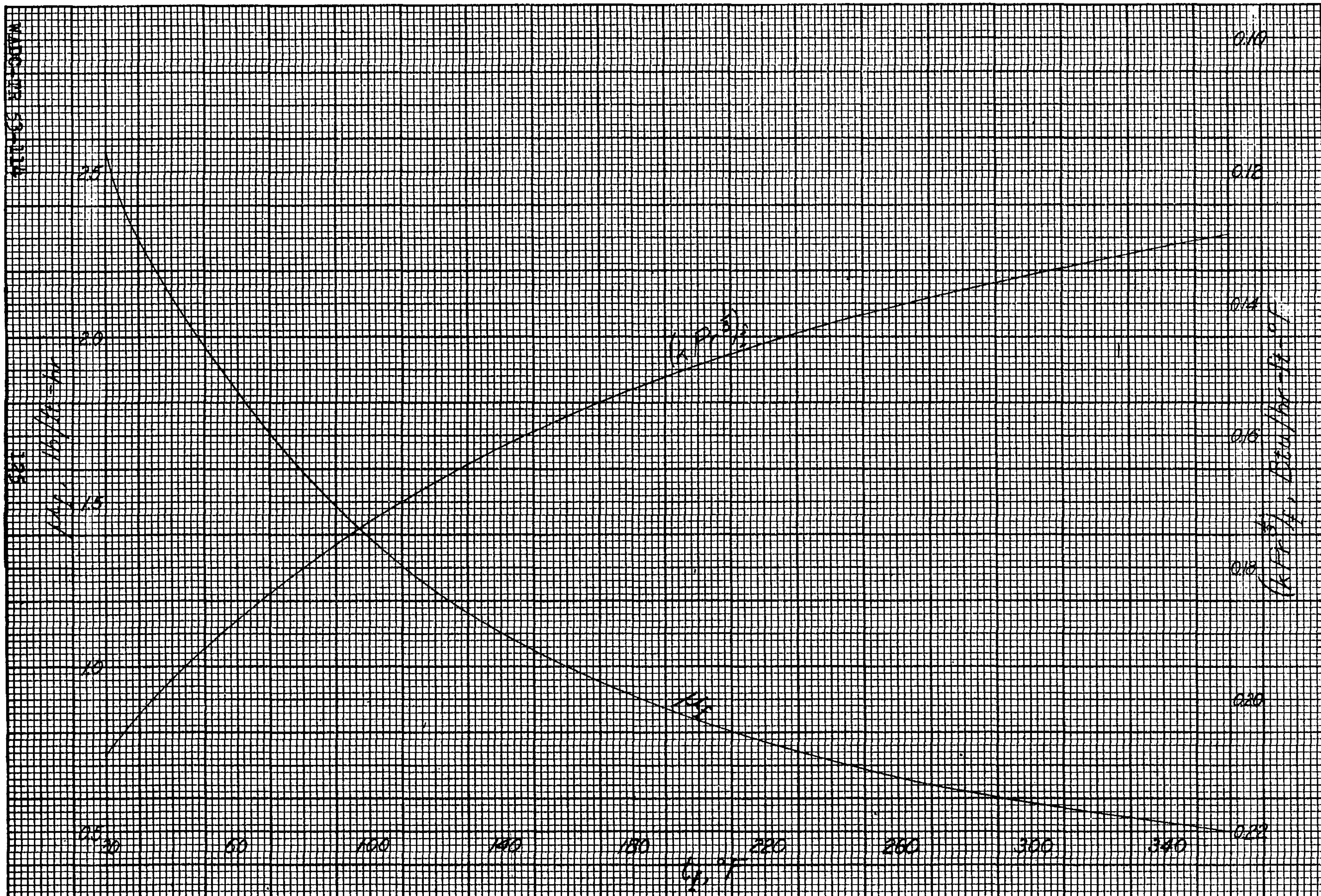

Figure II-21

Physical Properties of JP-3 Fuel

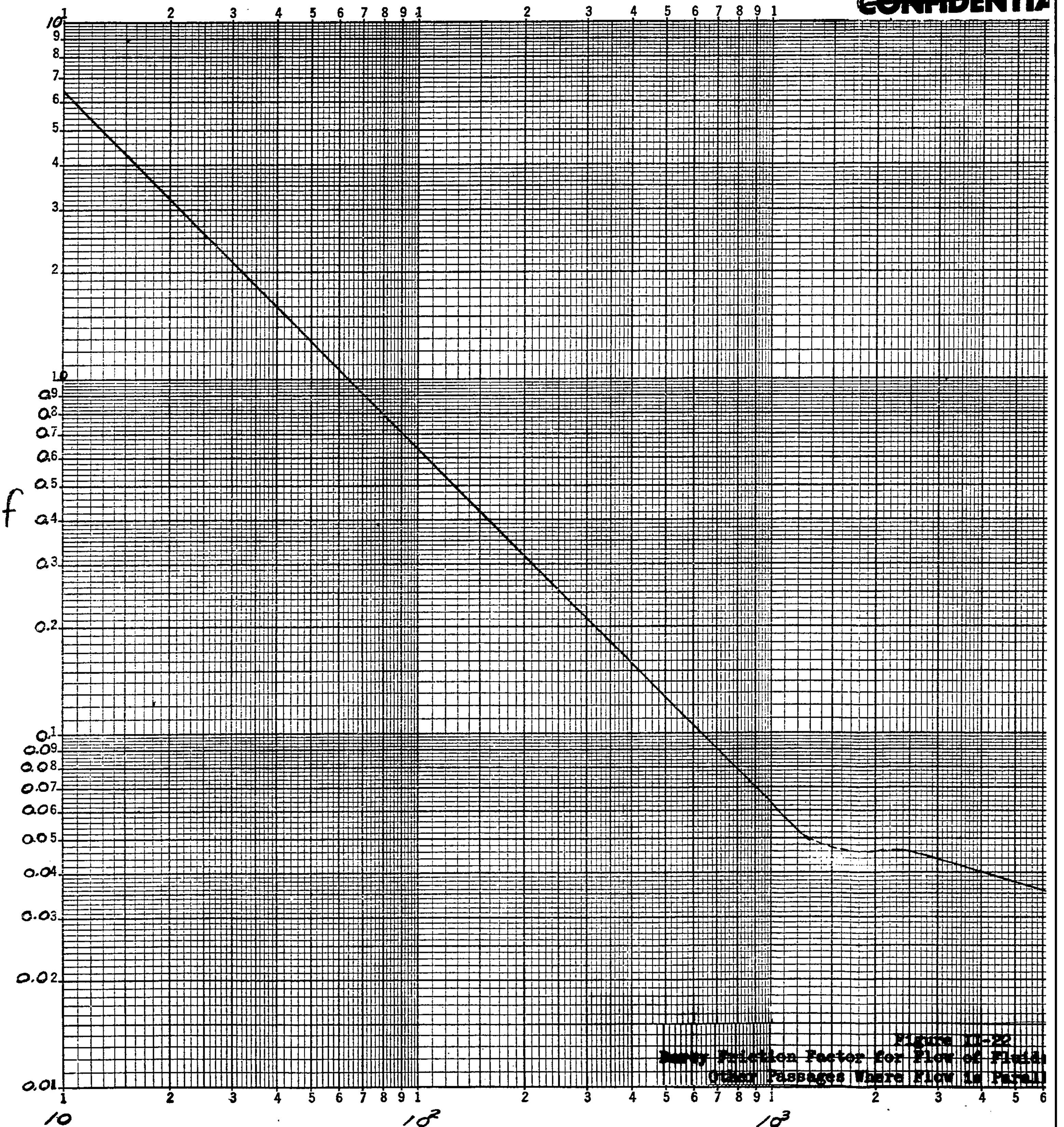

Figure II-22
Darcy Friction Factor for Flow of Fluid
Other Passages Where Flow is Parall

(i)

CONFIDENTIAL

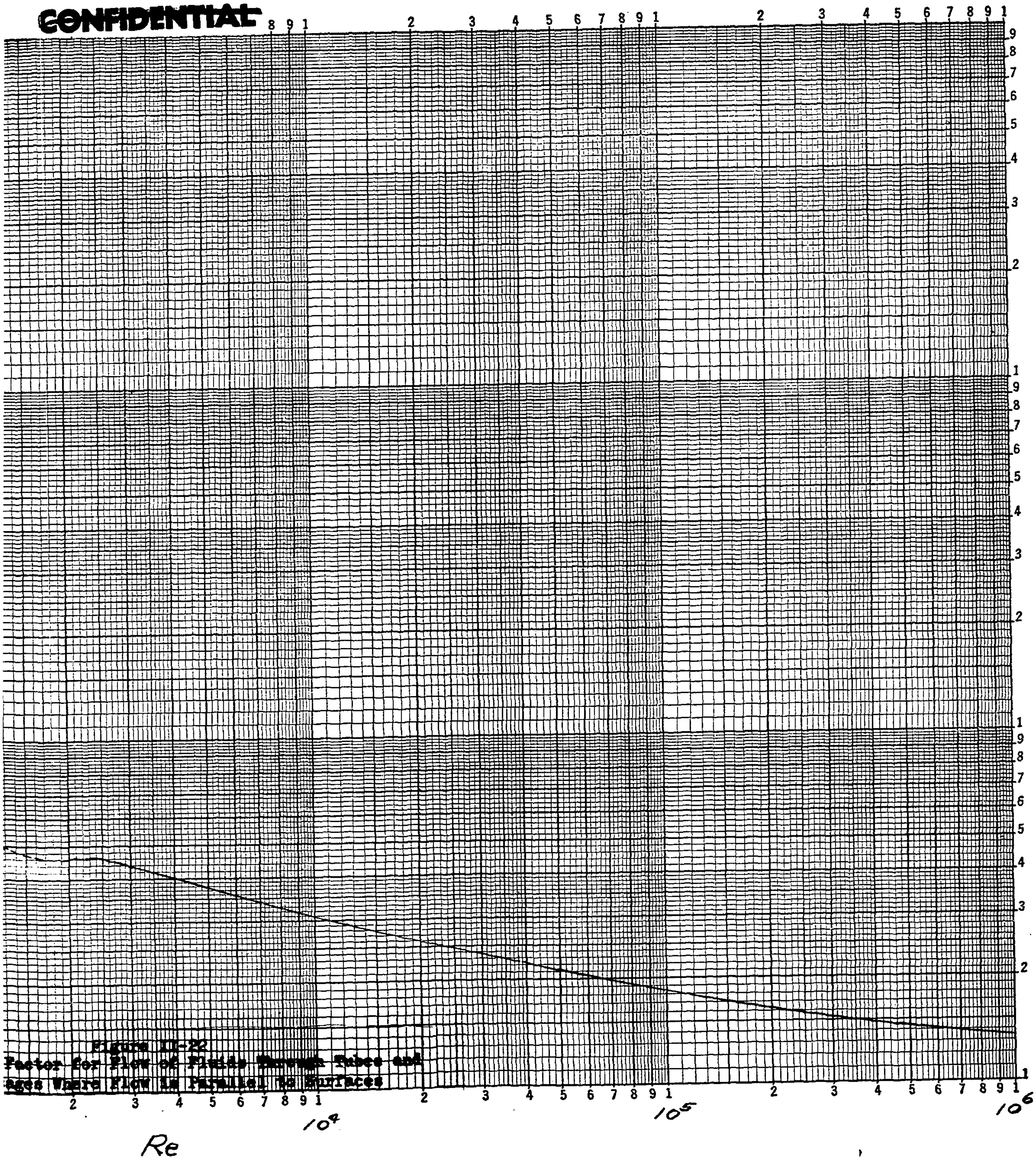

Figure II-22
Factor for Flow of Fluids ... Tubes and
...ages Where Flow is Parallel to Surfaces

CONFIDENTIAL

(2)

This is subsequently simplified further for use in a calculation procedure (see example of Appendix C to Section II).

The heat transfer coefficient for air in crossflow over the tubes is determined using a plot of the j_H factor which applies to such a configuration. A plot of this type is given in Figure II-23, and is taken from Reference (II-5). By this correlation the heat transfer coefficient is given by,

$$h_o = j_H \frac{12}{d_{to}} (k\, Pr^{1/3})_a \qquad \text{(II-19)}$$

where j_H is given as a function of the Reynolds number, defined for this purpose as

$$Re = \frac{d_{to}\, W_a}{12 \mu A_a} \qquad \text{(II-20)}$$

The fluid properties $(k\, Pr^{1/3})$ are given for air in Figure II-24. They are evaluated at the mean bulk temperature of the fluid.

The pressure drop of the air in crossflow over the tubes is calculated using a correlation of Gunter and Shaw (Ref. II-6). Their method employs a friction factor ϕ defined in appropriate units as

$$\phi = 2.17 \times 10^9 \left[\frac{\Delta P_a\, \gamma_a P_t}{x (W_a/A_a)^2} \right] \left(\frac{d_{ep}}{P_L} \right)^{0.6} (d_{to})^{0.4} \qquad \text{(II-21)}$$

where d_{ep} is an equivalent diameter for tube bundles, defined as

$$d_{ep} = \frac{(4 \times \text{net free volume})(\text{in.}^3)}{(\text{friction surface})(\text{in.}^2)} \qquad \text{(II-22)}$$

Values of the factor ϕ are given as a function of the Reynolds number in Figure II-25, where the Reynolds number is defined as

$$Re_p = \frac{d_{ep}\, W_a}{12 \mu A_a} \qquad \text{(II-23)}$$

The equation defining the friction factor ϕ is solved for ΔP_a, the pressure drop.

Another heat transfer coefficient of interest in Design A is that at the inside surface of the outer shell. This is important in determining the external heat transferred into or out of the casing. An equation for the heat transfer coefficient for flow of a fluid past a flat plate is used for this purpose. A suitable equation is (Ref. II-7)

$$h_c = 0.028 \left(\frac{k}{L} \right) \left(\frac{L\, W_a}{\mu A_a} \right)^{0.8} (Pr)^{1/3} \qquad \text{(II-24)}$$

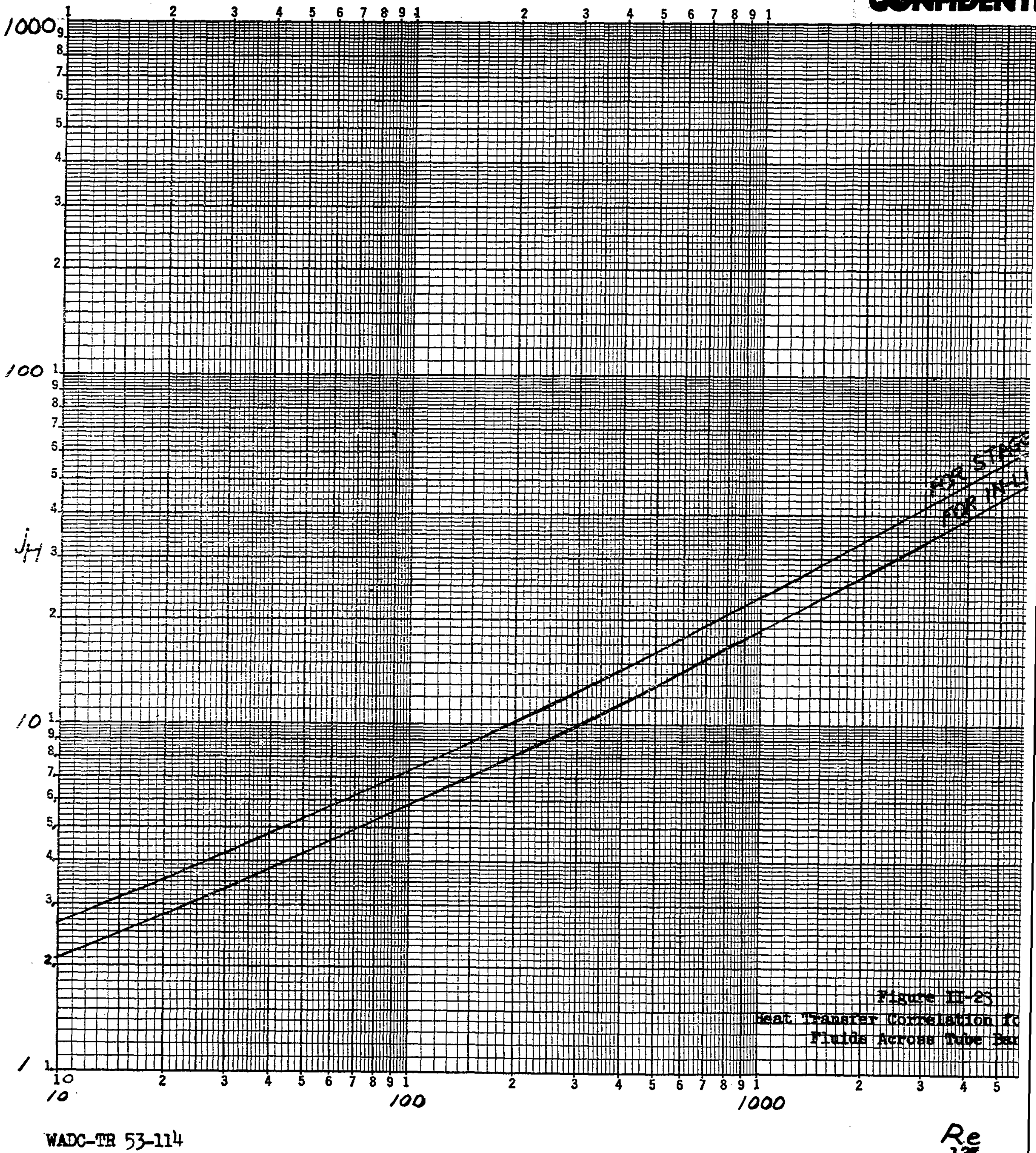

Figure II-23
Heat Transfer Correlation fo
Fluids Across Tube Ba

CONFIDENTIAL

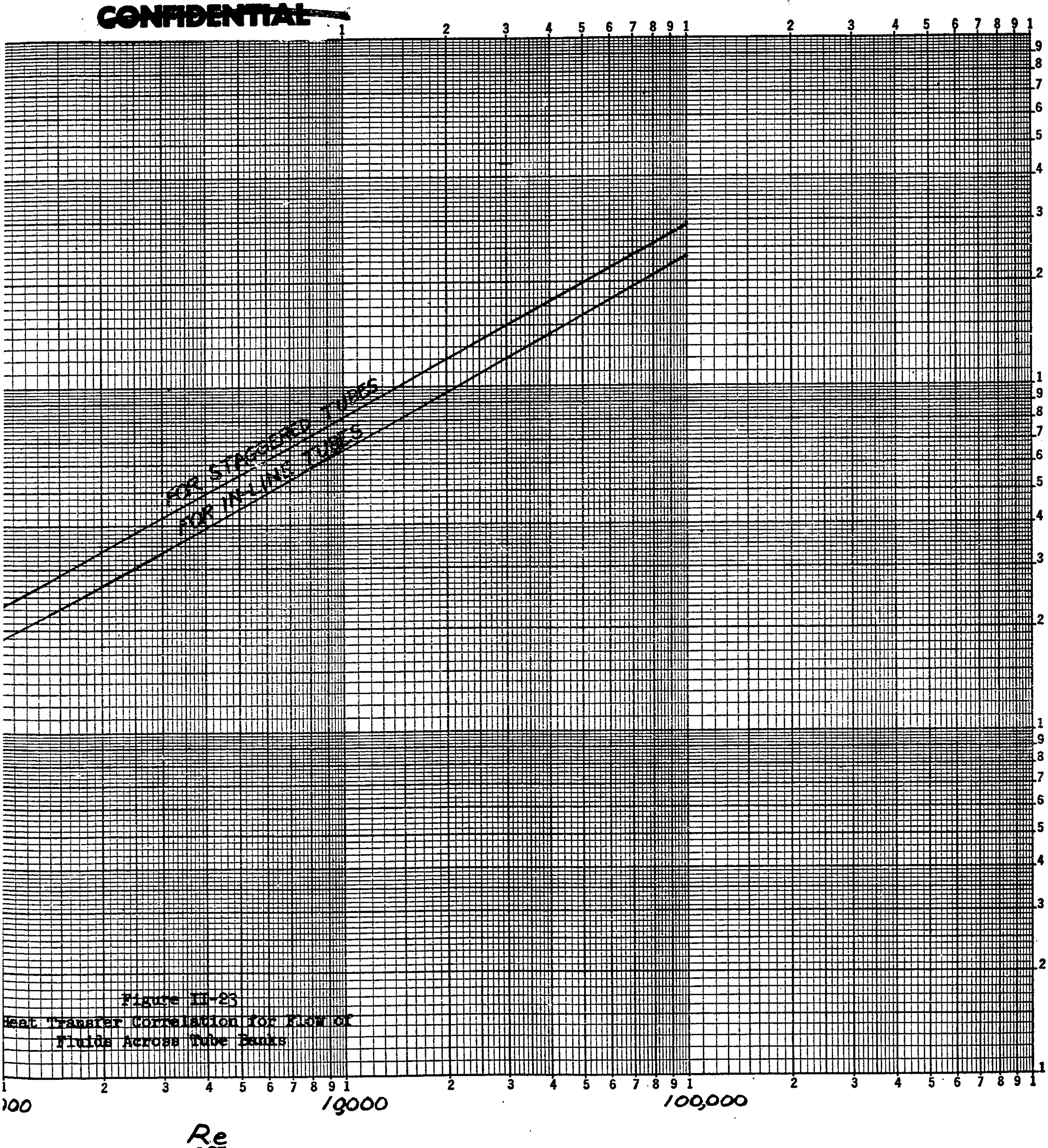

Figure II-23
Heat Transfer Correlation for Flow of Fluids Across Tube Banks

CONFIDENTIAL

2

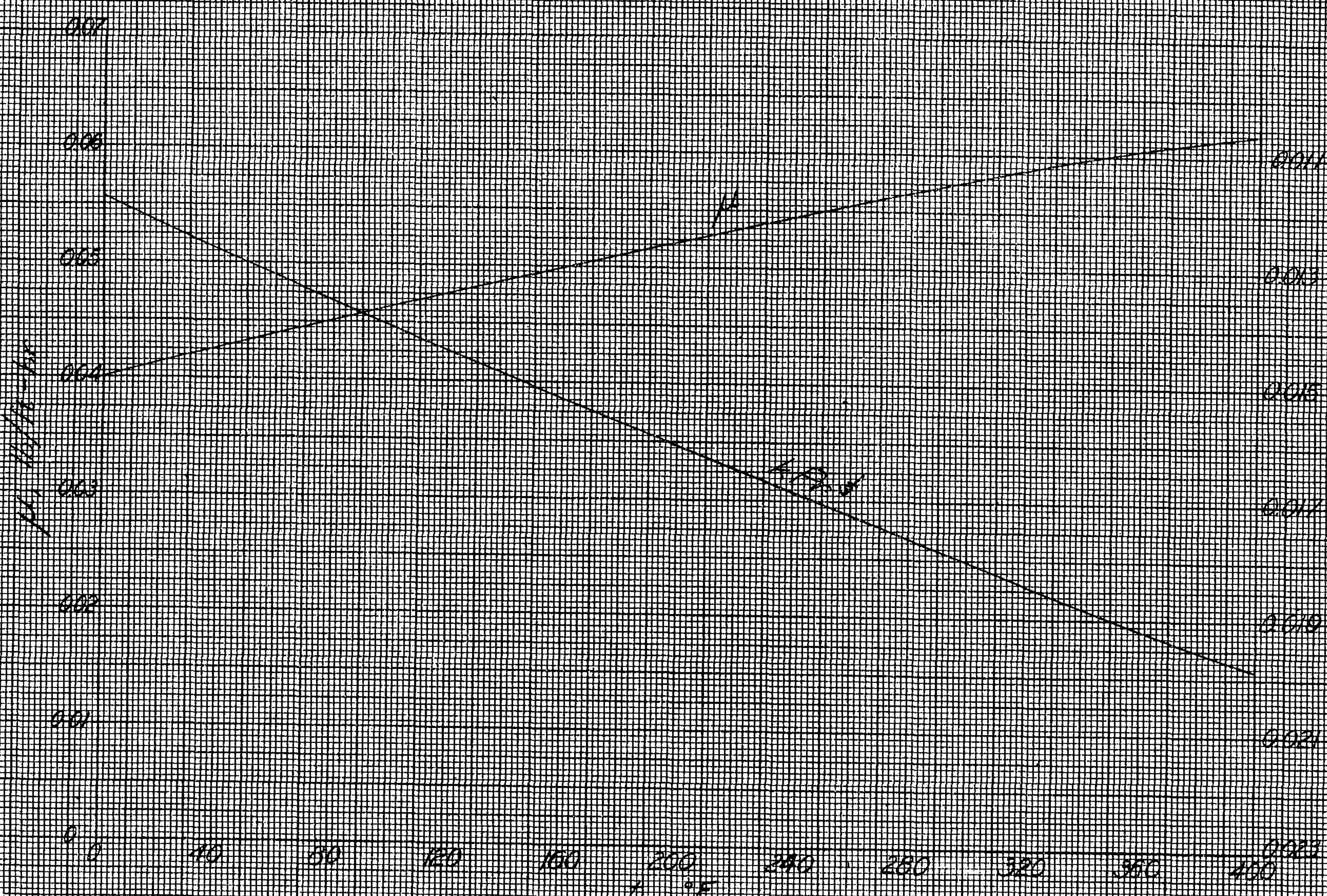

Figure II-24
Physical Properties of Air

CONFIDENTIAL

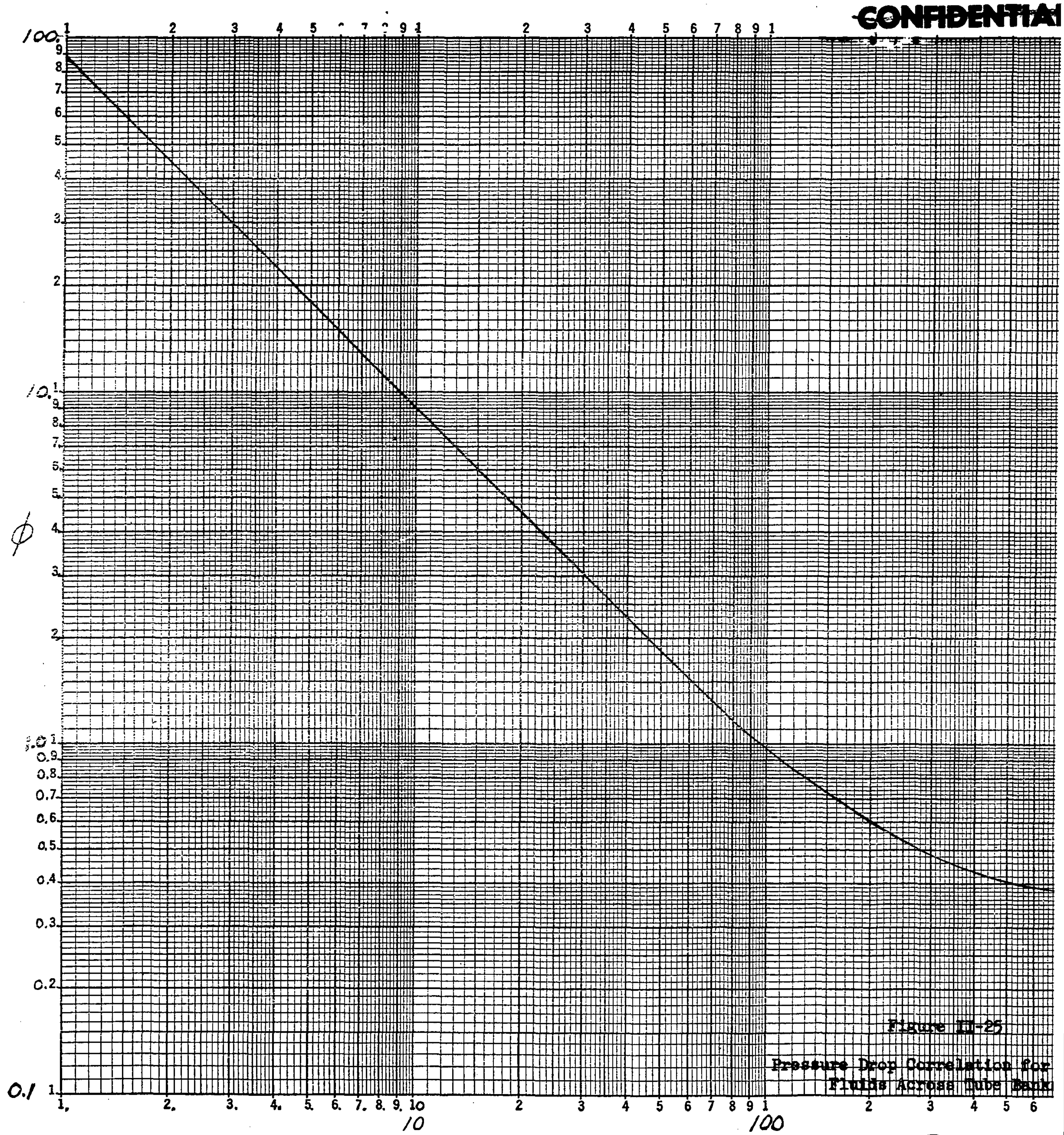

Figure II-25

Pressure Drop Correlation for Fluids Across Tube Bank

1

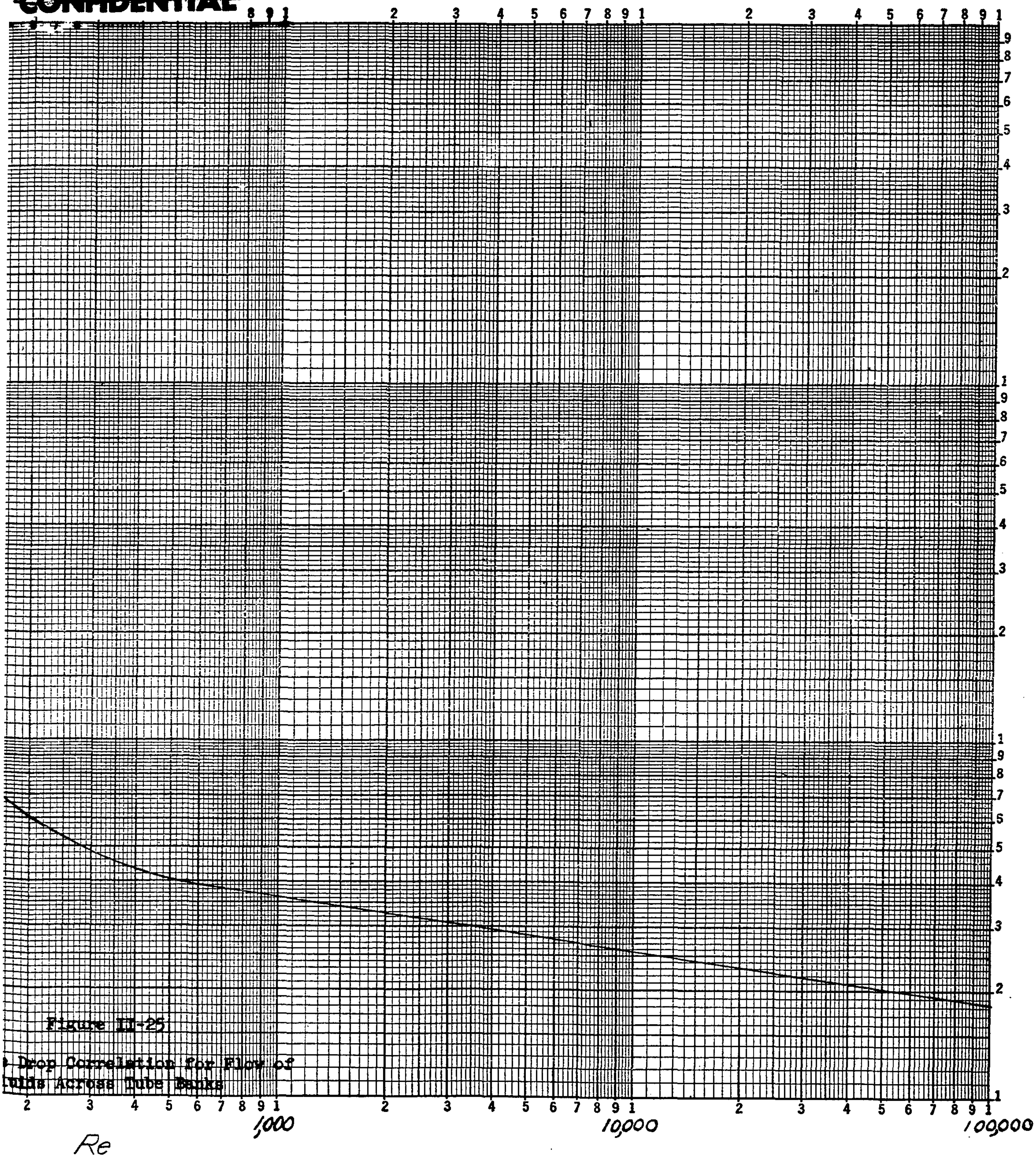

Figure II-25

Drop Correlation for Flow of
luids Across Tube Banks

(2)

Another coefficient of interest is that on the outside of the case. The type of coefficient to use for this application depends on the compartment conditions external to the case. These conditions are not considered in any detail here, so that a value of h_x which is appropriate for free convection and radiation is estimated. An example of this is given in Appendix C to Section II.

2. Design B. Air in Tubes, Fuel in Crossflow Over Tubes

The inside heat transfer coefficient for flow of air through the tubes is determined by equation (II-13). The fluid properties should be those of air rather than fuel. The pressure drop for air flow is found using an equation similar to (II-18).

The heat transfer coefficient on the fuel side can be calculated using the crossflow equation (II-19), except that the fluid is now fuel instead of air. Similarly, equation (II-21) is used to find the pressure drop. All of these correlations for Design B are in a form which permits evaluation of the fluid properties at the mean bulk temperature of the fluid, since the viscosity ratio $(\mu/\mu_w)^{-0.14}$ can be neglected.

The outer casing heat transfer coefficients are found by the same general method as in Design A, equation (II-24), using fuel properties instead of air properties.

3. Design C. Fuel in Tubes, Air in Parallel Flow Over Tubes

For the fuel inside the tubes, the heat transfer coefficient is found by equation (II-13), and the pressure drop by equation (II-18).

For the air flow parallel to the outside of the tubes equation (II-13) is used as before, but it is necessary to replace the tube diameter with an equivalent diameter. The equivalent diameter for this purpose is that which is appropriate to the heat transfer process and is given by

$$d_{eh} = \frac{(4 \text{ x net free cross-section})(\text{in.}^2)}{(\text{wetted perimeter of tubes only})(\text{in.})} \qquad \text{(II-25)}$$

This is used in equation (II-13) in the form

$$h_o = j_H \frac{12}{d_{eh}} (k\, Pr^{1/3})_a \qquad \text{(II-26)}$$

where h_o is the external film coefficient for flow of air parallel to the outside of the tubes.

The pressure drop for air flow parallel to the tubes is found with an equation similar to that given earlier.

$$\Delta P_a = \left(\frac{\gamma_a}{144}\right)\left(\frac{u^2}{2g}\right)\left[\left(\frac{fx_a}{d_{ep}}\right) + 1.5\right] \qquad \text{(II-27)}$$

where x_a is the length of the air flow passage parallel to the tubes. This equivalent diameter for pressure loss is defined as

$$d_{ep} = \frac{4 \times \text{net free cross-section}}{\text{total wetted perimeter}} \qquad \text{(II-28)}$$

where the area and length values must be expressed in in.^{2} and in., respectively. The friction factor is found from a Moody chart, using a Reynolds number based on this same d_{ep}. It is not possible to make as accurate a determination of entrance and exit losses here as in the case of straight tubes. As an estimate 1.5 is used to allow for entrance, exit, and turning effects.

The heat transfer coefficients for the outer casing require no special treatment in Design C, since they may be found by the same method as in Design A.

4. Design D. Fuel in Tubes, Air in Crossflow Over Tubes. Tubes Flattened and Finned on the Air Side

The heat transfer coefficient for fuel flow inside a flattened tube may be approximated with a standard equation of the form (Ref. II-5, p. 165)

$$h_i = 0.023 \frac{k}{D_e} (Re)^{0.8} (Pr)^{1/3} \qquad \text{(II-29)}$$

which is suitable for Re > 10,000. The equivalent diameter is defined as

$$D_e = \frac{(4 \times \text{cross sectional area})(\text{ft}^2)}{(\text{wetted perimeter})(\text{ft})} \qquad \text{(II-30)}$$

where the cross sectional area and perimeter refer to values on the inside of the flattened tube. The Reynolds number should also be based on this equivalent diameter, being defined as

$$Re = \frac{\gamma u D_e}{\mu} \qquad \text{(II-31)}$$

The pressure drop for flow of the fuel may be found as in Design A, by equation (II-18) using the equivalent diameter of the flattened tube in place of the diameter of the round tube, both in the pressure drop equation and in finding the friction factor.

The heat transfer coefficient for the air side may be found from data (Ref. II-8) giving a plot of $(h_o/Gc_p)(Pr)^{2/3}$ versus the Reynolds number based on an equivalent diameter, for crossflow over a finned-tube surface. After determining the Reynolds number and the fluid properties, the heat transfer coefficient is computed directly from the plot. Friction factor data are also available (Ref. II-8) which can be used to calculate the pressure drop for air flow, using the Darcy equation. The data as presented, are actually Fanning friction factors, however, and must be multiplied by four before

using them in the Darcy equation. The entrance and exit losses are neglected for this heat exchanger core, as they would probably not be significant compared to the pressure loss in the core itself.

The heat transfer coefficient for flow of air over the inner surface of the outer casing is taken as equal to that for crossflow over the flattened, finned tubes. The fins are assumed to extend nearly to the outer casing, so that the flow situation is approximately the same in both cases.

5. Design E. Fuel in Tubes, Air in Crossflow Over Tubes

The basic equations describing heat transfer and pressure drop in this case are the same as for Design A. The two designs differ only in details of arrangement which do not affect these basic relationships except in their application. An example of applying the basic relationships is given in Appendix C to Section II.

APPENDIX C TO SECTION II

Evaluation Procedures for Heat Exchanger Cores

In the following, evaluation procedures for Designs A, B, and C are given as examples of calculations necessary to determine the temperature difference $(t_{a1}-t_{f1})$ for a given case of specified cooling capacity.

1. Interpretation of Calculation Items in Procedure for Design A

Certain items given in the following procedure for Design A are here explained for purposes of clarification. Similar considerations are employed in establishing the other calculation procedures given for Designs B and C. The items of corresponding numbers in the procedure for Design A are explained below.

(2) The diameter of the inside shell D_1 is determined by allowing for one-half transverse pitch from each shell (inner and outer) to the centerline of the nearest tube.

(4) The minimum free flow area A_a through the annular space outside of the tubes is the difference between the gross annular area A_n and the projected area of the fuel coils.

(5) The length of the exchanger core x allows for an entrance and exit port at each end of the cylinder, equal in cross-section to the minimum free flow area within the exchanger (A_a).

(7) The number of times N the fuel spirals around the shell before entering the discharge header depends on the number of parallel fuel paths n', the number of rows r and the longitudinal coil spacing $p_L d_{to}$.

(8) The heat transfer area A_o is based on the outside surface area of

the tubes, neglecting the effect of the helical winding on the length of the tubes.

(9) The area for heat transfer to the casing from its surroundings A_x is based on the assumption that no heat is transferred through the ends of the cylinder.

(11) The assumption that t_{fm} is 5^oF greater than t_{a1} is usually satisfactory.

(15) The length-to-diameter ratio of the fuel tubes may be required to find h_i if the flow of fuel is in the laminar or transition regions. It is also required to find the fuel pressure drop.

(16) and (17) The heat transfer coefficient h_i is based on equation (II-13). Figure II-20 is used to obtain j_H, and fluid properties are evaluated at the mean bulk temperature of the fuel from Figure II-21.

(19) The pressure drop of the fuel ΔP_f, is calculated from equation (II-18), transformed by substitution of known variables and combination of constants.

(20) The power q_{Mf} required to pump the fuel is given in watts. The motor and pump efficiencies are 50 percent each, and a standard fuel density of 46.4 lb/ft^3 (about 150^{o}F temperature) is used.

(22) The first assumption of t_{am} may be made by estimating the heat given up by the air as $1.2q_c$, the value of U_o between 10 and 30, and the mean fuel temperature about 5^oF above t_{f1}. Then by approximation, $t_{am} = [(3.413x1.2q_c)/A_oU_o]+t_{f1}+5$.

(26) and (27) The heat transfer coefficient h_o for air in crossflow over the tubes is calculated from equation (II-19).

(28) The over-all heat transfer coefficient U_o from the fuel to the air is calculated from equation (II-9).

(29) and (30) The coefficient for forced convection h_c over the inside surface of the outer shell is computed using equation (II-24), where the group of physical properties of air are given as function of the air temperature in Figure II-24. These properties should actually be taken at the mean film temperature, requiring an estimate of the outer shell temperature. From the environmental conditions it must be estimated whether the shell temperature would be greatly different from t_{am}. The accuracy of the assumption made in item (29) has little bearing on the accuracy of q_e and $(t_{e1}-t_{f1})$ subsequently computed.

(31) The surface coefficient on the outside of the equipment case h_x is taken as the sum of the radiation and convection coefficients at the surface. This is used together with a characteristic temperature for the surroundings to estimate the external heat load to the cooled equipment case. Methods for calculating free convection and radiation heat transfer coefficients are given in Section V. If several cores are to be compared in per-

formance, they can be analyzed on the basis of some reasonable estimated values of t_s and h_x.

(32) The over-all coefficient of heat transfer U_x from the surroundings to the air in the cooled equipment case is calculated from equation (II-4).

(33) The external heat gain, in Btu/hr, is given by equation (II-3).

(34) The equivalent diameter for purposes of calculating the air pressure loss through the row or rows of tubes is calculated from equation (II-22).

(35) The Reynolds number for the air flow is based on the equivalent diameter and equation (II-23).

(36) The weight density γ_a of the air is calculated from the perfect gas law, where the mean bulk temperature and pressure are used, since this density is involved in calculating the pressure loss across the heat exchanger core.

(37) and (38) The pressure drop of the air in crossflow over the tubes is calculated from equation (II-21). The value of ϕ is taken from Figure II-25 and the pressure drop ΔP_a is in inches of water.

(39) The power required for the air circulation q_{Ma} is given in watts. The motor and fan are each assumed to be 50 percent efficient. The power is evaluated at the air density corresponding to t_{a1} (because of the position of the fan). The value of t_{a1} is the last item calculated in the procedure, and must be estimated here. However, a few degrees variation in t_{a1} does not affect q_{Ma} appreciably. The estimate may be based on theassumed value for $t_{am}+ t_a/2$, the latter being approximated by $18q_c/W_a$ (see item 45).

(40) It is assumed that the same motor drives the fan for the air and the fuel pump. Therefore, the total motor power requirement is $q_M = q_{Mf}+q_{Ma}$.

(41) The total heat added to the fuel, in Btu/hr, is given by equation (II-5).

(42) The logarithmic mean temperature difference required to transfer the heat added to the air through the coil surfaces to the fuel is determined from equation (II-7).

(45) The air temperature rise Δt_a through the equipment and fan is found from equation (II-6), using $c_p = 0.24$.

(46) and (47) By definition, the logarithmic mean temperature difference is

$$\theta_{lm} = \frac{(\theta_a - \theta_b)}{\log_e\left(\frac{\theta_a}{\theta_b}\right)}$$

If a counterflow arrangement is used, $\theta_a = (t_{a1}-t_{f2})$ and $\theta_b = (t_{a2}-t_{f1})$

therefore

$$\theta_{lm} = \frac{(t_{a1}-t_{f2}) - (t_{a2}-t_{f1})}{\log_e\left(\frac{(t_{a1}-t_{f2})+t_{f1}-t_{f1}}{(t_{a2}-t_{f1})+t_{a1}-t_{a1}}\right)}$$

or

$$\theta_{lm} = \frac{(\Delta t_a - \Delta t_f)}{\log_e\left(\frac{t_{a1}-t_{f1}-\Delta t_f}{t_{a1}-t_{f1}-\Delta t_a}\right)}$$

letting

$$Y = e^{\left(\frac{\Delta t_a - \Delta t_f}{\theta_{lm}}\right)}$$

$$(t_{a1}-t_{f1}) = \frac{(\Delta t_a)Y - \Delta t_f}{Y - 1}$$

(48) This last item, the arithmetic mean air temperature t_{am} in the heat exchanger, is used to check the accuracy of the assumed value of t_{am} in item (22). The procedure must be repeated from item (22) on until good agreement is achieved, i.e., at least within 30°F of the value for t_{am} assumed in item (22).

2. Procedure for Design A

1. Given data:

Exchanger dimensions				Operating conditions			
D_o	______	d_{ti}	______	q_c	______	t_{f1}	______
L	______	p_L	______	P_a	______	t_s	______
r	______	p_t	______	W_a	______	W_f	______
d_{to}	______	n'	______				

2. Calculate $D_i = D_o - (2r\ p_t\ d_{to})/12$

3. Calculate $A_n = 0.785\ (D_o^2 - D_i^2)$

4. Calculate $A_a = \pi\left(\frac{D_i+D_o}{2}\right)\left(\frac{r\ d_{to}(p_t-1)}{12}\right)$

5. Calculate $x = 12\left(L - \frac{A_a}{1.571\ D_i}\right)$

6. Calculate $V_H = 144\ A_n\ x$

7. Calculate $N = \frac{xr}{d_{to}\ p_L\ n'}$

8. Calculate $A_o = \dfrac{0.411\ xr\ (D_o+D_i)}{P_L}$

9. Calculate $A_x = \pi D_o\ L$

10. Calculate $A_f = \dfrac{0.785(d_{ti})^2 n'}{144}$

11. Assume t_{fm}

12. Find μ_f at assumed t_{fm} from Figure II-21.

13. Find $(k\ Pr^{1/3})_f$ at assumed t_{fm} from Figure II-21.

14. Calculate $Re_f = \dfrac{d_{ti}\ W_f}{12\mu_f\ A_f}$

15. Calculate $\dfrac{x_f}{d_{ti}} = \left(\dfrac{12\pi N}{d_{ti}}\right)\left(\dfrac{D_i+D_o}{2}\right)$

16. Find j_H at Re_f and (x_f/d_{ti}) from Figure II-20.

17. Calculate $h_i = j_H\ (12/d_{ti})(k\ Pr^{1/3})_f$

18. Find f at Re_f from Figure II-22.

19. Calculate $\Delta P_f = 1.80x10^{-13}\ (W_f/A_f)^2 \left[(fx_f/d_{ti})+0.75\right]$

20. Calculate $q_{Mf} = \dfrac{W_f\ \Delta P_f}{214}$

21. Calculate (W_a/A_a).

22. Assume t_{am}.

23. Find μ for assumed t_{am} from Figure II-24.

24. Find $(k\ Pr^{1/3})$ for assumed t_{am} from Figure II-24.

25. Calculate $Re = \dfrac{d_{to}\ W_a}{12\ \ A_a}$

26. Find j_H for in-line tubes at Re from Figure II-23.

27. Calculate $h_o = j_H\ (12/d_{to})(k\ Pr^{1/3})$

28. Calculate $U_o = \dfrac{1}{\dfrac{1}{h_o} + \dfrac{d_{to}}{h_i d_{ti}}}$

29. Find $\dfrac{k\ Pr^{1/3}}{\mu^{0.8}}$ at an assumed $\dfrac{t_{shell} + t_{am}}{2}$ from Figure II-24.

30. Calculate $h_c = \left(\dfrac{0.028}{L^{0.2}}\right)\left(\dfrac{W_a}{A_a}\right)^{0.8}\left(\dfrac{k\ Pr^{1/3}}{\mu^{0.8}}\right)$

31. Calculate or assume h_x.

32. Calculate $U_x = \dfrac{1}{\dfrac{1}{h_c} + \dfrac{1}{h_x}}$

33. Calculate $q_e = U_x A_x (t_s - t_{am})$

34. Calculate $d_{ep} = \dfrac{d_{to}\left[\dfrac{p_L\ p_t}{0.785} - 1\right]}{\left[1 + \dfrac{2p_L}{\pi r}\right]}$

35. Calculate $Re_p = \dfrac{d_{ep}\ W_a}{12 \mu A_a}$

36. Calculate $\gamma_a = \dfrac{P_a\ 144}{53.3(t_{am} + 460)}$

37. Find ϕ at Re_p from Figure II-25.

38. Calculate $\Delta P_a = \dfrac{\phi(P_L)^{0.6}\ x}{2.17x10^9}\left(\dfrac{W_a}{A_a}\right)^2\left(\dfrac{1}{\gamma_a(d_{ep})^{0.6}(p_t)(d_{to})^{0.4}}\right)$

39. Calculate $q_{Ma} = \left(\dfrac{W_a\ \Delta P_a}{344.5}\right)\left(\dfrac{460 + t_{a1}}{P_a}\right)$

40. Calculate $q_M = q_{Ma} + q_{Mf}$

41. Calculate $q_f = q_e + 3.413\ (q_c + q_M)$

42. Calculate $\theta_{1m} = \dfrac{q_f - 3.413\,(1/2 q_{Mf})}{U_o\ A_o}$

43. Calculate $c_f = 0.44 + 0.066\ (t_{fm}/100)$ for JP-3 fuel.

44. Calculate $\Delta t_f = (q_f / c_f \, W_f)$

45. Calculate $\Delta t_a = \dfrac{14.2\,(q_c + q_{Ma} + 1/2 q_{Mf})}{W_a}$

46. Calculate $Y = e^{\left(\frac{\Delta t_a - \Delta t_f}{\Theta_{lm}}\right)}$

47. Calculate $(t_{a1} - t_{f1}) = \dfrac{\Delta t_a\, Y - \Delta t_f}{Y - 1}$

48. Calculate $t_{am} = t_{f1} + (t_{a1} - t_{f1}) - 1/2(\Delta t_a)$

If item (48) is within 30^oF of item (22), $(t_{a1}-t_{f1})$ would change less than one percent by recomputing from item (23) on.

3. Procedure for Design B

1. Given data:

Exchanger dimensions:

D_o	______	d_{ti}	______
L	______	p_L	______
r	______	p_t	______
d_{to}	______	N	______

Operating conditions:

q_c	______	t_{f1}	______
P_a	______	t_s	______
W_a	______	W_f	______

2. Calculate D_i (see Design A)

3. Calculate A_n (see Design A)

4. Calculate $n = \dfrac{18.86\, r\, (D_o + D_i)}{p_L\, d_{to}}$

5. Calculate $A_a = \dfrac{\pi}{4}\,\dfrac{(d_{ti})^2 n}{144}$

6. Calculate $x = 12\left[L - \dfrac{A_a}{0.785\, D_i}\right]$

7. Calculate $V_H = 144\, A_n\, x$

8. Calculate $A_o = \dfrac{\pi\, d_{to}\, nx}{144}$

9. Calculate A_x (see Design A)

10. Calculate $A_f = \dfrac{d_{to}\,(p_t - 1)\, rx}{144\, N}$

11. Assume t_{fm} (see explanation item 11, Design A)

12. Find μ_f at assumed t_{fm} from Figure II-21.

13. Find $(k\ Pr^{1/3})_f$ at assumed t_{fm} from Figure II-21.

14. Calculate $Re_f = \dfrac{d_{to}\ W_f}{12\ \mu_f A_f}$

15. Find j_H at Re_f for in-line tubes from Figure II-23.

16. Calculate $h_o = j_H\ (12/d_{to})(k\ Pr^{1/3})_f$

17. Calculate $d_{efp} = \dfrac{184\ A_n - n(d_{to})^2}{12(D_o+D_i)+n\ d_{to}}$

18. Calculate $Re_{fp} = \dfrac{Re_f\ d_{efp}}{d_{to}}$

19. Find ϕ at Re_{fp} from Figure II-25.

20. Calculate $L_f = (\pi/2)(D_i+D_o)N$

21. Calculate $\Delta P_f = \dfrac{1}{2.33 \times 10^{11}}\ \dfrac{\phi\ L_f(W_f/A_f)^2(p_L)^{0.6}}{(d_{efp})^{0.6}(p_t)(d_{to})^{0.4}}$

22. Calculate $q_{Mf} = \dfrac{W_f\ \Delta P_f}{214}$

23. Calculate (W_a/A_a)

24. Calculate (x/d_{ti})

25. Assume t_{am} (see explanation for item 22, Design A)

26. Find μ at t_{am} from Figure II-24.

27. Find $(k\ Pr^{1/3})$ at t_{am} from Figure II-24.

28. Calculate $Re = \dfrac{d_{ti}\ W_a}{12\ \mu A_a}$

29. Find j_H at Re and (x/d_{ti}) from Figure II-20.

30. Calculate $h_i = j_H(12/d_{ti})(k\ Pr^{1/3})$

31. Calculate U_o (see item 28, Design A)

32. Find $(k\ Pr^{1/3})_f$ and μ_f at an assumed $(t_{shell}+t_{fm})/2$ from

Figure II-21. (See explanation for item 29, Design A.)

33. Calculate $h_c = \frac{0.028}{(L_f)^{0.2}} \left(\frac{W_f}{A_f \mu_f}\right)^{0.8} (k\ Pr^{1/3})_f$

34. Calculate or assume h_x.

35. Calculate U_x (see item 32, Design A)

36. Calculate $q_e = U_x A_x (t_s - t_{fm})$

37. Find f, at Re from item 28, from Figure II-22.

38. Calculate γ_a (see item 36, Design A)

39. Calculate $\Delta P_a = \frac{2.30 \times 10^{-10}}{\gamma_a} \left(\frac{W_a}{A_a}\right)^2 \left(\frac{fx}{d_{ti}} + 1.5\right)$

40. Calculate q_{Ma} (see item 39, Design A)

41. Calculate q_M (see item 40, Design A)

42. Calculate q_f (see item 41, Design A)

43. Calculate $\theta_{1m} = \frac{q_f - q_e - 3.413(1/2 q_{Mf})}{U_o A_o}$

44. Calculate c_f (see item 43, Design A)

45. Calculate Δt_f (see item 44, Design A)

46. Calculate Δt_a (see item 45, Design A)

47. Calculate Y (see item 46, Design A)

48. Calculate $(t_{a1} - t_{f1})$ (see item 47, Design A)

49. Calculate t_{am} (see item 48, Design A)

If item (49) is within 30°F of item (25), $(t_{a1} - t_{f1})$ would change less than one percent by recomputing from item (26) on.

4. Procedure for Design C

1. Given data:

Exchanger dimensions:				Operating conditions:			
D_o	______	d_{ti}	______	q_c	______	t_{fl}	______
L	______	p_L	______	P_a	______	t_s	______
r	______	p_t	______	W_a	______	W_f	______
d_{to}	______	N	______				

2. Calculate D_i (see Design A)
3. Calculate A_n (see Design A)
4. Calculate n (see Design B)
5. Calculate $A_a = A_n - \frac{\pi}{4} \frac{(d_{to})^2 n}{144}$
6. Calculate x (see item 5, Design A)
7. Calculate V_H (see Design B)
8. Calculate A_o (see Design B)
9. Calculate A_x (see Design A)
10. Calculate $A_f = \frac{0.785\ n(d_{ti})^2}{144\ N}$
11. Assume t_{fm} (see explanation item 11, Design A)
12. Find μ_f at assumed t_{fm} from Figure II-21.
13. Find $(k\ Pr^{1/3})_f$ at assumed t_{fm} from Figure II-21.
14. Calculate Re_f (see Design A)
15. Calculate $(12L/d_{ti})$
16. Find j_H for Re_f from Figure II-20.
17. Calculate h_i (see Design A)
18. Find f at Re_f from Figure II-22.
19. Calculate ΔP_f (see Design A)
20. Calculate q_{Mf} (see Design A)
21. Calculate (W_a/A_a)

22. Calculate $d_{eh} = \dfrac{184\ A_a}{n\ d_{to}}$

23. Assume t_{am} (see explanation item 22, Design A)

24. Find μ for assumed t_{am} from Figure II-24.

25. Find $(k\ Pr^{1/3})$ for assumed t_{am} from Figure II-24.

26. Calculate (x/d_{eh})

27. Calculate $Re = \dfrac{d_{eh}\ W_a}{12\mu A_a}$

28. Find j_H at Re from Figure II-20.

29. Calculate $h_o = j_H\ (12/d_{eh})(k\ Pr^{1/3})$

30. Calculate U_o (see item 28, Design A)

31. Find $(k\ Pr^{1/3})/\mu^{0.8}$ at an assumed $(t_{shell}+t_{am})/2$ from Figure II-24. (See explanation for item 29, Design A)

32. Calculate h_c (see item 30, Design A)

33. Calculate or assume h_x.

34. Calculate U_x (see item 32, Design A)

35. Calculate q_e (see item 33, Design A)

36. Calculate $d_{ep} = \dfrac{184\ A_a}{12(D_o+D_i)+nd_{to}}$

37. Calculate $Re_p = \dfrac{(Re)d_{ep}}{d_{eh}}$

38. Find f at Re_p from Figure II-22.

39. Calculate γ_a (see item 36, Design A)

40. Calculate ΔP_a (see item 39, Design B)

41. Calculate q_{Ma} (see item 39, Design A)

42. Calculate q_M (see item 40, Design A)

43. Calculate q_f (see item 41, Design A)

44. Calculate θ_{lm} (see item 42, Design A)

45. Calculate Δt_a (see Design A)

46. Calculate c_f (see item 43, Design A)

47. Calculate Δt_f (see item 44, Design A)

48. Calculate Y (see item 46, Design A)

49. Calculate $(t_{a1}-t_{f1})$ (see item 47, Design A)

50. Calculate t_{am} (see item 48, Design A)

If item (50) is within 30°F of item (23), $(t_{a1}-t_{f1})$ would change less than one percent by recomputing from item (24) on.

APPENDIX D TO SECTION II

References

(II-1) Seider, E. N. and Tate, G. E. Heat Transfer and Pressure Drop of Liquids in Tubes. Industrial and Engineering Chemistry, Volume 28, 1936, p. 1429.

(II-2) Kern, D. Q. Process Heat Transfer. McGraw-Hill Book Company, Inc., New York, 1950, p. 834.

(II-3) Vennard, J. K. Elementary Fluid Mechanics. Second Edition, John Wiley and Sons, Inc., New York, 1947, pp. 157, 173-180.

(II-4) Moody, L. F. Friction Factors for Pipe Flow. Transactions of the American Society of Mechanical Engineers, Volume 66, November 1944, p. 671.

(II-5) McAdams, W. H. Heat Transmission. Second Edition, McGraw-Hill Book Company, Inc., New York, 1942, p. 230.

(II-6) Gunter, A. Y. and Shaw, W. A. A General Correlation of Friction Factors for Various Types of Surfaces in Crossflow. Transactions of the American Society of Mechanical Engineers, Volume 67, 1945, p. 643.

(II-7) Fischer, W. W. and Norris, R. H. Supersonic Convective Heat Transfer Correlation from Skin Temperature Measurements on a V-2 Rocket in Flight. Transactions of the American Society of Mechanical Engineers, Volume 71, 1949, p. 458.

(II-8) Kays, W. M., London, A. L., and Johnson, D. W. Gas Turbine Plant Heat Exchangers. American Society of Mechanical Engineers, New York, April 1951.

SECTION III

A GENERAL SYSTEM FOR THE DETERMINATION OF TEMPERATURE-TIME DISTRIBUTIONS IN AN AIRBORNE EQUIPMENT COMPARTMENT AT HIGH FLIGHT SPEED

By S. M. Marco

The determination of the temperature of the components within an airborne equipment compartment at any time during a flight is of importance if the necessity for and effectiveness of cooling means is to be evaluated. A general method for the determination of the temperature-time curves for such equipment would also be useful in establishing the effectiveness of insulation or other heat barriers located at various places within the compartment.

The primary purpose of this Section is to describe a general method for the determination of the temperature-time curves for the various pieces of equipment in an aircraft compartment, taking into account in detail the characteristics of the compartment. The method is intended to be applicable mainly to the determination of the temperature rise of one critical equipment box in the compartment containing components which may or may not generate heat and which may be sensitive to temperature rise.

For the purpose of this analysis the general heat transfer system being considered may be assumed to consist of an aircraft compartment containing the critical equipment box along with other non-critical components. It may be assumed that at the beginning of the flight the temperatures of all the parts of the system are known. As the flight is started and the aircraft is accelerated to reach supersonic velocity, the compartment wall is heated aerodynamically. At the same time the equipment box may be generating heat. For a time, heat may be flowing into the system from both of these sources. The heat generated within the equipment box may be considered constant for the entire flight or variable according to some predetermined schedule depending upon the function of the equipment and the method of its operation. The heat flow from the skin into the compartment will, of course, depend upon the magnitude of the flight speed, the altitude and existing thermal barriers. If no cooling means are employed, the temperatures of the various parts of the heat transfer system will eventually approach equilibrium, provided the flight pattern is stabilized at a fixed speed and altitude. The rate of temperature rise of any individual member of the heat transfer system at any time will depend upon its thermal capacity,* the conductance** between it and its immediate surroundings and

*Thermal capacity of a body is the amount of heat required to raise its temperature one degree.

**The conductance between two bodies is the amount of heat that will be transferred between them per unit of time and for unit temperature difference between them.

the temperature difference between it and its immediate surroundings. The use of insulation on any part of the system or the use of cooling means will affect both the time rate of temperature rise at any time and the equilibrium temperature.

SUMMARY

A heat transfer system corresponding to an idealized arrangement of an airborne equipment compartment is defined. Features of thermal insulation and cooling effects are included. The equations describing the thermal processes of the system are set up in difference form to describe temperature changes with time in the non-steady thermal state. The criteria for the selection of time intervals of proper length are developed. Computation methods are presented for calculating machine or slide rule work. Equations for the determination of thermal capacities of composite bodies and of thermal conductances in the three basic modes of heat transfer are presented for a variety of possible cases and with particular reference to the previously defined regions of the thermal system. The computation methods and the application of the developed relationships are illustrated by means of an example in which the temperature-time variations of the thermal regions in a high speed aircraft compartment are calculated.

ANALYSIS

1. Choice of Method

A rigid mathematical description of the temperature-time relationships involved in even a simple unsteady-state heat transfer system would be extremely complex and would result in a set of simultaneous partial differential equations with variable coefficients. To solve such a set of equations would require the use of costly, specially designed computing machines. Thus it would be of little advantage to attempt a rigid mathematical analysis unless such equipment were available. The use of such equipment would be desirable principally when a given system is to be analyzed for a considerable range of each variable defining its operating conditions. A simplification of the analysis by using only certain characteristic temperatures rather than actual point temperatures to describe the system would still result in a set of ordinary differential equations with variable coefficients. These equations could be reduced to a single differential equation of a high order and with variable coefficients. The solution of such an equation would require special techniques which would not be readily available.

Since a simplification of the method is necessary if ordinary computation methods are to be used, it is believed that the use of difference equations along with a tabular computation method (Ref. III-2) would best suit the purposes of this problem. This method is based upon the fundamental premise that for a specified short time interval the transient system may be treated as a steady-state system. Thus the temperature rise of a given member during the specified time interval may be computed in the same

way that any steady flow system is computed. The temperatures at the end of that time interval can then be used as the initial temperatures for the next time interval.

In applying numerical analysis to heat transfer problems, the first step is to subdivide the physical system into a number of regions, for each of which a representative temperature may be used to describe the thermal situation. This process calls for some judgement. If the subdivisions are too crude the accuracy may be low. On the other hand, if the subdivisions are too numerous, time will be wasted in obtaining a degree of accuracy not warranted by the data or by the practical application of the solution.

2. Description of Heat Transfer System

The subdivisions of the heat transfer system to which the computation method is to be applied are shown diagrammatically in Figure III-1. The physical system consists of an aircraft compartment which may or may not be ventilated. Within this compartment is located an equipment box for which the temperature-time curve is desired. Also within the compartment are other bodies separate from the equipment box.

In subdividing this heat-transfer system it may be seen from Figure III-1 that the regions for which representative temperatures are used to describe the thermal situation are as follows:

(A) The equipment box in which heat may be generated, heat may be stored and heat may be given off to a cooling system. In addition heat may be transferred between the equipment box and insulation on its surface. It is assumed that the thermal condition of the equipment box can be described in terms of the variation of a single representative temperature.

(B) An insulation or heat barrier surrounding the equipment box which may store heat, have heat transferred between itself and the equipment box, have heat transferred between itself and its surroundings and may have heat removed from it by an integral cooling system. The thermal condition of this insulation or heat barrier is described in terms of the variation of a single representative temperature.

(C) The bodies or masses within the compartment other than the critical component box. For this description it is assumed that all such masses may be lumped together and described in terms of the variation of a single representative temperature. In some situations, where the thermal properties of the various masses are very widely different it may be necessary to use several such regions, each with its own representative temperature. Assuming that only one such region is used, it may be seen that heat may be stored in it and heat may be transferred between it and its surroundings.

(D) The air within the compartment which may receive heat or give off heat to the surfaces of the members within the compartment and which may be cooled by some cooling means. It is assumed that the air cannot store heat since its thermal capacity is small compared to the other regions in the

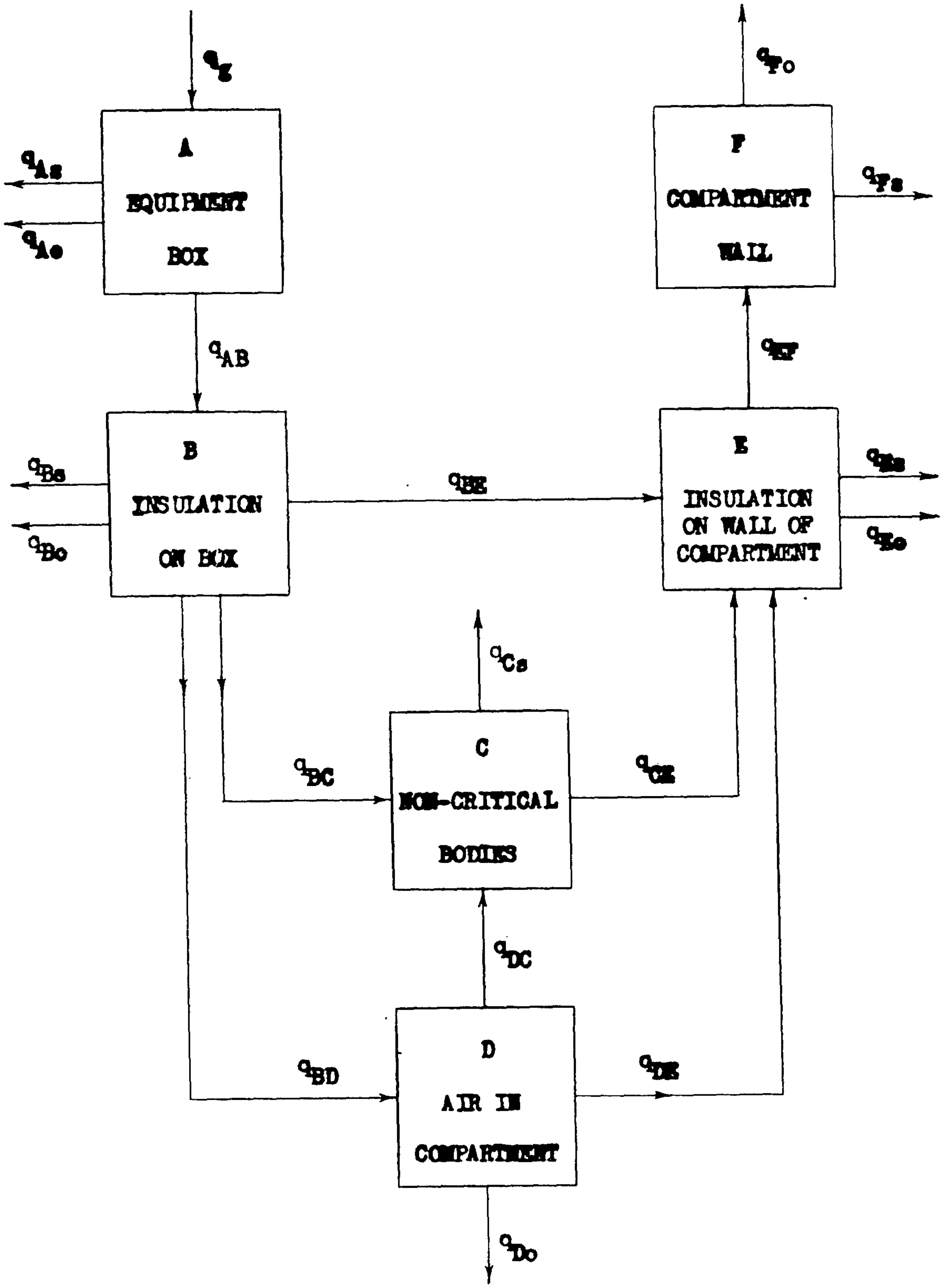

Figure III-1

Schematic Diagram of Heat
Transfer System

system.

(E) Insulation or a heat barrier adjacent to the compartment wall which may store heat, have heat transferred between itself and the compartment wall, have heat transferred between itself and the contents of the compartment and may be cooled by an integral cooling system. The thermal condition of this region is described in terms of a single representative temperature.

(F) The compartment wall which may give off heat or receive heat from the insulation or heat barrier adjacent to it, may store heat, and may have heat exchange with the air flowing over its outer surface. The thermal condition here is described in terms of a single representative temperature.

3. Assumptions

For the development of a calculation method, the following basic assumptions are made.

(a) The characteristic temperature of the components within the equipment box A is described in terms of a single temperature T_A which is assumed to be the temperature at all parts of the surface of the box. Thus it is assumed that the rate of heat storage in the component box can be expressed in terms of the time rate of change of T_A. Also the rate of heat transfer from the equipment box to a cooling system and to the insulation or heat barrier on the box may be expressed in terms of T_A.

(b) The insulation B is assumed to surround the equipment box and the rate of heat storage and the rates of heat transfer from it may be expressed in terms of its outer surface temperature T_B.

(c) The non-critical bodies C within the compartment are assumed to be represented by a single mass, the thermal characteristics of which may be described in terms of a temperature T_C, which is the average surface temperature of all such bodies.

(d) The air D within the compartment is given a separate identity here although it is assumed to have no heat storage capacity. Thus the heat transferred to and from the air may be expressed in terms of a single average temperature T_D. The air is assumed to be always in thermal equilibrium with the other regions in contact with it.

(e) The insulation E is assumed to be on the inner surface of the compartment wall. Its thermal condition is described in terms of a single temperature T_E which is the temperature on the compartment-side surface of the insulation.

(f) The compartment wall F is assumed to have a single temperature T_F at all points. The heat stored in it and transferred to and from it is expressed in terms of this temperature.

4. Nomenclature

A	Surface area. ft^2
a	Free convection modulus, $(N_{Gr}N_{Pr})/(x^3 \Delta t)$
a'	Free convection parameter, $0.12ka^{1/3}\delta^{2/3}$
B	Radiation temperature function, $[(T_a/100)^4-(T_b/100)^4]/(T_a-T_b)$
C	Thermal capacity, Btu/°F
c	Specific heat, Btu/lb-°F
d	Tube diameter, ft
F	Computation factor
F_A	Shape factor in radiation heat transfer
F_e	Emissivity factor in radiation heat transfer
f	Fraction
G	Weight rate of flow per unit area, lb/hr-ft^2
h	Convection heat transfer coefficient, Btu/hr-ft^2-°F
K	Conductance, Btu/hr-°F
k	Thermal conductivity, Btu/hr-ft^2-(°F/ft)
L	Thickness or length of conduction path, ft
N_{Gr}	Grashof number, $56.2(p/\mu)^2(x/T)^3\Delta t$ for air
N_{Pr}	Prandtl number, $c\mu/k$
p	Pressure, in. Hg
q	Heat transfer rate, Btu/hr
T	Absolute temperature, °R
t	Temperature, °F
V	Velocity, ft/hr
v	Volume, ft^3
w	Specific weight, lb/ft^3

x	Distance from leading edge, or length of heat transfer surface, ft
α	Area ratio
Δt	Temperature difference, $^{\circ}F$
$\Delta \tau$	Time interval, hr
δ	Pressure ratio, p/29.92
ϵ	Radiation emissivity
μ	Absolute viscosity, lb/ft-hr
ν	Kinematic viscosity, ft^2/hr
Σ	Sum of
τ	Time, hr

Subscripts

A	Refers to equipment box
av	Refers to average value during time interval
B	Refers to insulation on equipment box
C	Refers to non-critical bodies
cd	Indicates conduction
cv	Indicates convection
D	Refers to air in compartment
E	Refers to insulation on compartment wall
F	Refers to compartment wall
g	Refers to heat generated
m	Refers to mean value, or a general region in the heat transfer system
n	Refers to another general region in the heat transfer system
o	Refers to heat conveyed to cooling system or atmosphere
rd	Indicates radiation

s Refers to heat stored

t Indicates total temperature of air stream

1 Indicates beginning of time interval

2 Indicates end of time interval

5. Derivation of Equations

a. Heat Balance

Based on the system depicted by Figure III-1 and described in part (2), the assumptions stated in part (3), and using the nomenclature given in part (4), a set of heat balance equations may be written for each member of the system. These are

$$q_g + q_{AB} - q_{Ao} - q_{As} = 0 \qquad \text{(III-1a)}$$

$$q_{AB} - q_{BC} - q_{BD} - q_{BE} - q_{Bo} - q_{Bs} = 0 \qquad \text{(III-1b)}$$

$$q_{BC} + q_{DC} - q_{CE} - q_{Cs} = 0 \qquad \text{(III-1c)}$$

$$q_{BE} + q_{CE} + q_{DE} - q_{EF} - q_{Eo} - q_{Es} = 0 \qquad \text{(III-1d)}$$

$$q_{EF} - q_{Fo} - q_{Fs} = 0 \qquad \text{(III-1e)}$$

$$q_{BD} - q_{DC} - q_{DE} - q_{Eo} = 0 \qquad \text{(III-1f)}$$

where q_g is the rate of heat generation in the equipment box A, where all heat storage rates are indicated by the second subscript (s), such as q_{As} signifying the heat storage rate in the equipment box, and where all rates of heat transfer to the external compartment environment or to an internal cooling system are indicated by the second subscript (o), such as q_{Fo} signifying the heat transfer rate from the compartment wall to the atmosphere.

b. Differential Equations and Difference Equations

These heat balance equations may be expressed in differential form in terms of the temperatures, thermal capacities, conductances and time. For example, the differential form of equation (III-1a) is,

$$q_g - K_{AB}(T_A - T_B) - q_{Ao} - C_A \frac{dT_A}{d\tau} = 0, \qquad \text{(III-2)}$$

where the heat transfer term q_{AB} has been replaced by the product of the conductance K_{AB} between the two regions A and B and the temperature differ-

ence $(T_A - T_B)$; while the heat storage term has been replaced by the thermal capacity of body A, C_A, multiplied by the time rate of change of its temperature, $dT_A/d\tau$. The terms q_g and q_{Ao} have been left unaltered since their magnitudes are dependent upon the rate of heat generation and the rate of heat removal by a cooling system, respectively.

In general the conductance K between any two regions is a function of the temperatures of those regions and the time. Thus, equation (III-2) is seen to be a differential equation with variable coefficients. To change equation (III-2) to a difference equation it is necessary to replace dT_A by the difference $(T_{A2} - T_{A1})$ and $d\tau$ by the difference $\Delta\tau$, where T_{A1} is the temperature of region A at the beginning of the time interval $\Delta\tau$ and T_{A2} is its temperature at the end of the time interval. The instantaneous temperature difference $(T_A - T_B)$ is to be replaced by the temperature difference at the beginning of the time interval $(T_{A1} - T_{B1})$. If these substitutions are made in equation (III-2) and the resulting equation is solved for the temperature change $(T_{A2} - T_{A1})$ of region A, equation (III-2) becomes,

$$T_{A2} - T_{A1} = q_g \frac{\Delta\tau}{C_A} - K_{AB}(T_{A1} - T_{B1}) - q_{Ao} \frac{\Delta\tau}{C_A} \qquad \text{(III-3)}$$

If equation (III-3) is solved for T_{A2}, the temperature of region A at the end of the time interval, it becomes,

$$T_{A2} = q_g \frac{\Delta\tau}{C_A} - q_{Ao} \frac{\Delta\tau}{C_A} + K_{AB} \frac{\Delta\tau}{C_A} T_{B1} + (1 - K_{AB} \frac{\Delta\tau}{C_A}) T_{A1} \qquad \text{(III-4)}$$

The factors $K_{AB}(\Delta\tau/C_A)$ and $1-K_{AB}(\Delta\tau/C_A)$ multiply the temperatures of the two regions T_{B1} and T_{A1} respectively. For convenience such factors are designated by the letter F. Thus $K_{AB}(\Delta\tau/C_A)$ is replaced by the symbol F_{AB} and $1-K_{AB}(\Delta\tau/C_A)$ is replaced by the symbol F_{AA}. It may be seen that the factor F_{AA} is the multiplier of the temperature T_{A1} which is the initial temperature of the region A for which the final temperature T_{A2} is being computed, whereas the factor F_{AB} is the multiplier of the temperature T_{B1} which is the initial temperature of the region B which transfers heat with region A. Using these factors, equation (III-4) may be written

$$T_{A2} = q_g \frac{\Delta\tau}{C_A} - q_{Ao} \frac{\Delta\tau}{C_A} + F_{AB}T_{B1} + F_{AA}T_{A1} \qquad \text{(III-5)}$$

The heat balance equations (III-1a through -1e) may be transformed to equations of the form of equation (III-3) to make possible the computation of the temperature rise of each region during the time interval. For computation of the temperature at the end of the time interval the heat balance equations (III-1a through -1e) may be transformed to equations of the form of equation (III-5). The heat balance equation for region D does not directly involve the time τ, since it is assumed that the air (region D) has no thermal capacity. For this reason, equation (III-1f) is treated as a steady state equation and is discussed separately from equations (III-1a through -1e).

When these equations are transformed to the form of equation (III-3), they become,

$$T_{A2}-T_{A1} = q_g \frac{\Delta\tau}{C_A} - K_{AB}\frac{\Delta\tau}{C_A}(T_{A1}-T_{B1}) - q_{Ao}\frac{\Delta\tau}{C_A} \qquad \text{(III-6a)}$$

$$T_{B2}-T_{B1} = K_{AB}\frac{\Delta\tau}{C_B}(T_{A1}-T_{B1}) - K_{BC}\frac{\Delta\tau}{C_B}(T_{B1}-T_{C1}) - K_{BD}\frac{\Delta\tau}{C_B}(T_{B1}-T_{D1}) -$$

$$- K_{BE}\frac{\Delta\tau}{C_B}(T_{B1}-T_{E1}) - q_{Bo}\frac{\Delta\tau}{C_B} \qquad \text{(III-6b)}$$

$$T_{C2}-T_{C1} = K_{BC}\frac{\Delta\tau}{C_C}(T_{B1}-T_{C1}) + K_{DC}\frac{\Delta\tau}{C_C}(T_{D1}-T_{C1}) - K_{CE}\frac{\Delta\tau}{C_C}(T_{C1}-T_{E1}) \qquad \text{(III-6c)}$$

$$T_{E2}-T_{E1} = K_{BE}\frac{\Delta\tau}{C_E}(T_{B1}-T_{E1}) + K_{CE}\frac{\Delta\tau}{C_E}(T_{C1}-T_{E1}) + K_{DE}\frac{\Delta\tau}{C_E}(T_{D1}-T_{E1}) -$$

$$- K_{EF}\frac{\Delta\tau}{C_E}(T_{E1}-T_{F1}) - q_{Eo}\frac{\Delta\tau}{C_E} \qquad \text{(III-6d)}$$

$$T_{F2}-T_{F1} = K_{EF}\frac{\Delta\tau}{C_F}(T_{E1}-T_{F1}) - K_{Fo}(T_{F1}-T_{ot1}) \qquad \text{(III-6e)}$$

The atmospheric temperature T_{ot1} in equation (III-6e) is the total temperature of the air flow enveloping the compartment.

The heat balance equation (III-1f) for the air of region D may be expressed in terms of the temperatures at the end of the time interval $\Delta\tau$ or in terms of the temperature at the beginning of the time interval. This is possible since it is assumed that the air of region D is always in thermal equilibrium with its surroundings. Thus equation (III-1f) may be written

$$K_{BD}(T_{B2}-T_{D2}) - K_{DC}(T_{D2}-T_{C2}) - K_{DE}(T_{D2}-T_{E2}) - q_{De2} = 0$$

or

$$K_{BD}(T_{B1}-T_{D1}) - K_{DC}(T_{D1}-T_{C1}) - K_{DE}(T_{D1}-T_{E1}) - q_{Do1} = 0$$

If the second of these equations is subtracted from the first and the result solved for the temperature difference $T_{D2}-T_{D1}$, the resulting equation is

$$T_{D2}-T_{D1} = \frac{K_{BD}(T_{B2}-T_{B1})}{K_{BD}+K_{DC}+K_{DE}} + \frac{K_{DC}(T_{C2}-T_{C1})}{K_{BD}+K_{DC}+K_{DE}} + \frac{K_{DE}(T_{E2}-T_{E1})}{K_{BD}+K_{DC}+K_{DE}} - \frac{(q_{Do2}-q_{Do1})}{K_{BD}+K_{DC}+K_{DE}}$$

(III-6f)

c. Temperatures at End of Time Interval

When equations (III-6e through -6f) are solved for the temperatures at the end of the time interval, there results a set of equations similar to equation (III-5). These are,

$$T_{A2} = q_g \frac{\Delta\tau}{C_A} - q_{Ao} \frac{\Delta\tau}{C_A} + F_{AB}T_{B1} + F_{AA}T_{A1} \qquad \text{(III-7a)}$$

$$T_{B2} = F_{BA}T_{A1} + F_{BC}T_{C1} + F_{BD}T_{D1} + F_{BE}T_{E1} + F_{BB}T_{B1} - q_{Bo} \frac{\Delta\tau}{C_B} \qquad \text{(III-7b)}$$

$$T_{C2} = F_{CB}T_{B1} + F_{CD}T_{D1} + F_{CE}T_{E1} + F_{CC}T_{C1} \qquad \text{(III-7c)}$$

$$T_{E2} = F_{EB}T_{B1} + F_{EC}T_{C1} + F_{ED}T_{D1} + F_{EF}T_{F1} + F_{EE}T_{E1} - q_{Eo} \frac{\Delta\tau}{C_E} \qquad \text{(III-7d)}$$

$$T_{F2} = F_{FE}T_{E1} + F_{Fo}T_{o1} + F_{FF}T_{F1} \qquad \text{(III-7e)}$$

$$T_{D2} = F_{DB}T_{B2} + F_{DC}T_{C2} + F_{DE}T_{E2} - \frac{q_{Do2}}{K_{BD}+K_{DC}+K_{DE}} \qquad \text{(III-7f)}$$

d. Temperature Change in Time Interval

The equations for the temperature change (III-6a through -6f) may also be written in terms of the F factors. They become

$$T_{A2}-T_{A1} = q_g \frac{\Delta\tau}{C_A} - q_{Ao} \frac{\Delta\tau}{C_A} - F_{AB}(T_{A1}-T_{B1}) \qquad \text{(III-8a)}$$

$$T_{B2}-T_{B1} = F_{BA}(T_{A1}-T_{B1})-F_{BC}(T_{B1}-T_{C1})-F_{BD}(T_{B1}-T_{D1})-F_{BE}(T_{B1}-T_{E1})-q_{Bo} \frac{\Delta\tau}{C_B} \qquad \text{(III-8b)}$$

$$T_{C2}-T_{C1} = F_{CB}(T_{B1}-T_{C1})+F_{CD}(T_{D1}-T_{C1})-F_{CE}(T_{C1}-T_{E1}) \qquad \text{(III-8c)}$$

$$T_{E2}-T_{E1} = F_{EB}(T_{B1}-T_{E1})+F_{EC}(T_{C1}-T_{E1})+F_{ED}(T_{D1}-T_{E1})-F_{EF}(T_{E1}-T_{F1})-q_{Eo} \frac{\Delta\tau}{C_E} \qquad \text{(III-8d)}$$

$$T_{F2}-T_{F1} = F_{FE}(T_{E1}-T_{F1})-F_{Fo}(T_{F1}-T_{ot1}) \qquad \text{(III-8e)}$$

$$T_{D2}-T_{D1} = F_{DB}(T_{B2}-T_{B1})+F_{DC}(T_{C2}-T_{C1})+F_{DE}(T_{E2}-T_{E1})- \frac{(q_{Do2}-q_{Do1})}{K_{BD}+K_{DC}+K_{DE}} \qquad \text{(III-8f)}$$

f. F Factors

The F factors in equations (III-7a through -7f) and equations (III-8a through -8f) have the following definitions,

$$F_{AB} = K_{AB} \ \Delta\tau/C_A \qquad \text{(III-9a)}$$

$$F_{AA} = 1 - F_{AB} \qquad \text{(III-9b)}$$

$$F_{BA} = K_{AB} \ \Delta\tau/C_B \qquad \text{(III-9c)}$$

$$F_{BC} = K_{BC} \ \Delta\tau/C_B \qquad \text{(III-9d)}$$

$$F_{BD} = K_{BD} \ \Delta\tau/C_B \qquad \text{(III-9e)}$$

$$F_{BE} = K_{BE} \ \Delta\tau/C_B \qquad \text{(III-9f)}$$

$$F_{BB} = 1 - (F_{BA}+F_{BC}+F_{BD}+F_{BE}) \qquad \text{(III-9g)}$$

$$F_{CB} = K_{CB} \ \Delta\tau/C_C \qquad \text{(III-9h)}$$

$$F_{CD} = K_{DC} \ \Delta\tau/C_C \qquad \text{(III-9i)}$$

$$F_{CE} = K_{CE} \ \Delta\tau/C_C \qquad \text{(III-9j)}$$

$$F_{CC} = 1 - (F_{CB}+F_{CD}+F_{CE}) \qquad \text{(III-9k)}$$

$$F_{EB} = K_{BE} \ \Delta\tau/C_E \qquad \text{(III-9l)}$$

$$F_{EC} = K_{CE} \ \Delta\tau/C_E \qquad \text{(III-9m)}$$

$$F_{ED} = K_{DE} \ \Delta\tau/C_E \qquad \text{(III-9n)}$$

$$F_{EF} = K_{EF} \ \Delta\tau/C_E \qquad \text{(III-9o)}$$

$$F_{EE} = 1 - (F_{EB}+F_{EC}+F_{ED}+F_{EF}) \qquad \text{(III-9p)}$$

$$F_{FE} = K_{EF} \ \Delta\tau/C_F \qquad \text{(III-9q)}$$

$$F_{Fo} = K_{Fo} \ \Delta\tau/C_F \qquad \text{(III-9r)}$$

$$F_{FF} = 1 - (F_{FE}+F_{Fo}) \qquad \text{(III-9s)}$$

$$F_{DB} = \frac{K_{BD}}{K_{BD}+K_{DC}+K_{DE}} \qquad \text{(III-9t)}$$

$$F_{DC} = \frac{K_{DC}}{K_{DB}+K_{DC}+K_{DE}} \qquad \text{(III-9u)}$$

$$F_{DE} = \frac{K_{DE}}{K_{DB}+K_{DC}+K_{DE}} \qquad \text{(III-9v)}$$

g. Determination of Time Intervals $\Delta\tau$ to be Used

The value of the time interval $\Delta\tau$ which should be used in each step of these computations is the one which will produce the desired accuracy with the least number of computations for the total time for which the temperature-time curve is sought. It may be seen that if $\Delta\tau$ is chosen too small a large number of computations will be required to cover the total time. On the other hand if $\Delta\tau$ is chosen too large serious inaccuracies may result. These inaccuracies may be particularly serious at the start of the temperature-time curve.

By examining any of the sets of equations (III-7) and (III-9), it will be seen that

$$\Sigma F_m = 1 \qquad \text{(III-10)}$$

where ΣF_m is the sum of all the F factors having a first subscript m, e.g. equation (III-9g) shows that

$$F_{BA} + F_{BB} + F_{BC} + F_{BD} + F_{BE} = 1.$$

From the set of equations (III-9) it may be seen that

$$F_{mn} > 0 \qquad \text{(III-11)}$$

for $m \neq n$. This simply states that all conductances, thermal capacities and time intervals are positive. A careful examination of any of the set of equations (III-7) will also lead to the conclusion that

$$F_{mm} \nless 0 \qquad \text{(III-12)}$$

For example, in equation (III-7c) if F_{CC} is negative the product $F_{CC}T_{C1}$ would be negative. This would say that the temperature of the region C at the beginning of the time interval has a negative effect on its own temperature at the end of the time interval. In other words, the higher T_{C1} is the lower will T_{C2} be if F_{CC} is negative. This would not be consistent with the second law of thermodynamics.

It is possible however that regions transferring heat to or receiving heat from a region m may have so large an influence on the temperature of m that the temperature of m at the start of the time interval may have little effect upon its temperature at the end of the time interval. This may be stated by the equation

$$F_{mm} = 0 \qquad \text{(III-13)}$$

Thus, equations (III-12 and -13) may be combined to read

$$F_{mm} \geqq 0 \qquad \text{(III-14)}$$

From the set of equations (III-9) it is seen that

$$F_{mm} = 1 - \frac{\Delta\tau}{C_m} \Sigma K_m \qquad \text{(III-15)}$$

Equations (III-14 and -15) may be combined to give the result

$$\Delta\tau \leq \frac{C_m}{\Sigma K_m} \qquad \text{(III-16)}$$

This leads to the conclusion that the maximum $\Delta\tau$ consistent with the second law of thermodynamics is,

$$\Delta\tau = \frac{C_m}{\Sigma K_m} \qquad \text{(III-17)}$$

Thus, for any heat transfer system such as the one shown in Figure III-1 it is necessary to compute the $\Delta\tau$ according to equation (III-17) for each region and select the smallest. As a rule, it would not be necessary to calculate the $\Delta\tau$ for each region because most conductances vary little with time, except radiation conductances which increase appreciably with the temperature level. It is, therefore, possible to ascertain the critical regions after the first few calculations and to omit thereafter calculations for the other regions.

A careful examination of equations (III-7) will show that values of $\Delta\tau$ that are too large will result in oscillating values of the temperature with time. This oscillation may be serious at small values of τ, i.e., at the start, but will be less serious as steady state temperatures are approached, i.e., after a long time has elapsed. With experience it is possible sometimes to select the value of $\Delta\tau$ which may be too large to give accuracy during the initial part of the temperature curves but which will produce satisfactory results at later times when the temperatures approach their steady state values. This may be necessary in many instances where the thermal capacity is small and the conductances are large, and thus very small values of $\Delta\tau$ would be required according to equation (III-17). This may result in very many calculations to cover even a relatively short total time. For this reason, it is often better to sacrifice some accuracy in determining the initial shape of the temperature-time curves in the interest of speed with fair accuracy in finding the curves for the later stages of the heat transfer process.

COMPUTATION METHODS

1. Basic Methods Based on Conditions at Beginning of Time Interval

Tabular computations forms may be arranged for either the set of equations (III-7a through -7f) or the set (III-8a through -8f). The expressions for the temperatures at the end of the time interval as given in equations (III-7) are most easily adapted to a tabular computation form

since only the sums of products of F's and T's are involved. Computations from this form of the equations, however, may be rather inaccurate unless a calculating machine is used. This occurs because in most cases the value of F_{mn} is only slightly larger than zero whereas the value of F_{mm} is only slightly smaller than unity. In equation (III-7a), for example, F_{AB} might be of the order of magnitude of 1×10^{-3} in which case F_{AA} would be 0.999 (see equation (III-9b)). It would not be possible to distinguish the small difference between T_{A1} and $0.999T_{A1}$ if a slide-rule were used, whereas this difference could be determined readily from the results of a calculating machine. As a general rule, therefore, it is better to use equations (III-7) for the final temperatures when calculations are performed by machine. Equations (III-8) for the temperature changes do not contain the F_{mm} terms and therefore multiplying factors close to unity are not encountered. For this reason it is better to use them in slide-rule computations. These computations are somewhat more cumbersome than those by equations (III-7) but do not present a serious handicap.

a. Calculating Machine Procedure

A convenient tabular form for equations (III-7) is shown in Table III-1.

Table III-1
Computation Table for Equations (III-7a through -7f)

		A	B	C	D*	E	F
(1)	T_{A1}	F_{AA}	F_{BA}				
(2)	T_{B1}	F_{AB}	F_{BB}	F_{CB}	$F_{DB}{}^*$	F_{EB}	
(3)	T_{C1}		F_{BC}	F_{CC}	$F_{DC}{}^*$	F_{EC}	
(4)	T_{D1}		F_{BD}	F_{CD}		F_{ED}	
(5)	T_{E1}		F_{BE}	F_{CE}	$F_{DE}{}^*$	F_{EE}	F_{FE}
(6)	T_{F1}					F_{EF}	F_{FF}
(7)	T_{o1}						F_{Fo}
(8)	q_g	$\Delta\tau/C_A$					
(9)	q_{Ao}	$-\Delta\tau/C_A$					
(10)	q_{Bo}		$-\Delta\tau/C_B$				
(11)	q_{Do}				$-1/(K_{BD}+K_{DC}+K_{DE})$		
(12)	q_{Eo}					$-\Delta\tau/C_E$	
(13)		$T_{A2}=$	$T_{B2}=$	$T_{C2}=$	$T_{D2}=$	$T_{E2}=$	$T_{F2}=$

The following steps are recommended in the use of Table III-1:

1. Determine initial values of T's, C's, K's and q's.

2. Compute value of $\Delta\tau$ from equation (III-17).
3. Compute values of F's and other factors shown in the body of the table.
4. Enter initial values of T's and q's in left-hand column.
5. Multiply initial values in left-hand column by proper F values shown in the table. Enter these products where the F's are shown. For example, T_{A1} is to be multiplied by F_{AA} and F_{BA} with the first product entered where F_{AA} is shown and the second product entered where F_{BA} is shown. This procedure is to be carried out for all columns except D^*. This is starred to indicate that the F-factors in this column are to be multiplied by final temperatures rather than initial temperatures.
6. Sum up all the products in each of the columns A, B, C, E and F and write the final temperatures at the bottom.
7. Form the products in column D^* by multiplying the F-factors indicated by the final temperatures taken from the last line, i.e., F_{DB} is to be multiplied by T_{B2}, etc. Enter these products in column D and take the sum to get T_{D2}.
8. Using the values of the final temperatures in the last line, as the initial temperatures for the next time interval repeat steps (1) to (7).

For accuracy the K's and consequently the F's, which change with temperature, should be computed for each time interval. For approximations and for purpose of simplification, it is possible in some instances to select average values for the K's which would result in F-values constant with time. This greatly reduces the computational effort required to evaluate a set of temperature-time curves.

As a rule it is possible to predetermine the variation of all conductances with temperature and the variation of those conductances which depend on the atmospheric environment with flight time. It is convenient to prepare these variations in graphical form and to utilize the curves to determine instantaneous values corresponding to initial interval temperatures. Conductances whose variations with time are known are best used, for improved accuracy, not as determined at the beginning of the time interval but at its midpoint.

The computation of $\Delta\tau$ from equation (III-17) is also likely to be found laborious. If care is exercised to prevent excessive oscillations in the calculated temperature-time curves, values of $\Delta\tau$ appreciably greater than found by equation (III-17) may be used.

b. Slide Rule Procedure

A tabular form recommended for use in slide rule computations is shown in Table III-2. The procedure in using Table III-2 is similar to that for Table III-1. From the initial temperatures and flight conditions all the values in the left-hand column are determined, except those which are starred. Also for the initial conditions the values of the K's and of the coefficients in the table are determined. The starred values in the

Table III-2

Computation Form for Equations (III-8a through -8f)

		A	B	C	D	E	F
(1)		$T_{A1}=$	$T_{B1}=$	$T_{C1}=$	$T_{D1}=$	$T_{E1}=$	$T_{F1}=$
(2)	$T_{A1}-T_{B1}$	$-F_{AB}$	$+F_{BA}$				
(3)	$T_{B1}-T_{C1}$		$-F_{BC}$	$+F_{CB}$			
(4)	$T_{B1}-T_{D1}$		$-F_{BD}$				
(5)	$T_{B1}-T_{E1}$		$-F_{BE}$			$+F_{EB}$	
(6)	$T_{C1}-T_{E1}$			$-F_{CE}$		$+F_{EC}$	
(7)	$T_{D1}-T_{C1}$			$+F_{CD}$			
(8)	$T_{D1}-T_{E1}$					$+F_{ED}$	
(9)	$T_{E1}-T_{F1}$					$-F_{EF}$	$+F_{FE}$
(10)	$T_{F1}-T_{ot1}$						$-F_{Fo}$
(11)	$T_{B2}-T_{B1}$*				$+F_{DB}$		
(12)	$T_{C2}-T_{C1}$*				$+F_{DC}$		
(13)	$T_{E2}-T_{E1}$*				$+F_{DE}$		
(14)	q_g	$+\Delta\tau/C_A$					
(15)	q_{Ao}	$-\Delta\tau/C_A$					
(16)	q_{Bo}		$-\Delta\tau/C_B$				
(17)	$q_{Do2}-q_{Do1}$*				$-\dfrac{1}{K_{BD}+K_{DC}+K_{DE}}$		
(18)	q_{Eo}					$-\Delta\tau/C_E$	
(19)		$T_{A2}-T_{A1}=$	$T_{B2}-T_{B1}=$	$T_{C2}-T_{C1}=$	$T_{D2}-T_{D1}=$	$T_{E2}-T_{E1}=$	$T_{F2}-T_{F1}=$
(20)		$T_{A2}=$	$T_{B2}=$	$T_{C2}=$	$T_{D2}=$	$T_{E2}=$	$T_{F2}=$

left-hand column can be determined after T_{B2}, T_{C2} and T_{E2} have been determined for the chosen time interval $\Delta\tau$.

The same criteria as those applicable for the determination of conductances K and time intervals $\Delta\tau$ as pointed out for the calculating machine procedure may also be applied in the slide rule procedure.

2. <u>Alternate Computation Method for Simplified System Based on Average Conditions During Time Interval</u>

If the heat transfer system being considered is simpler than that shown in Figure III-1 such as the system shown in Figure III-2, for example, it is possible to modify the computation procedure for greater accuracy than that obtained by the methods already described. This greater accuracy can

be obtained by using average temperatures during the time interval in computing the heat transfer.

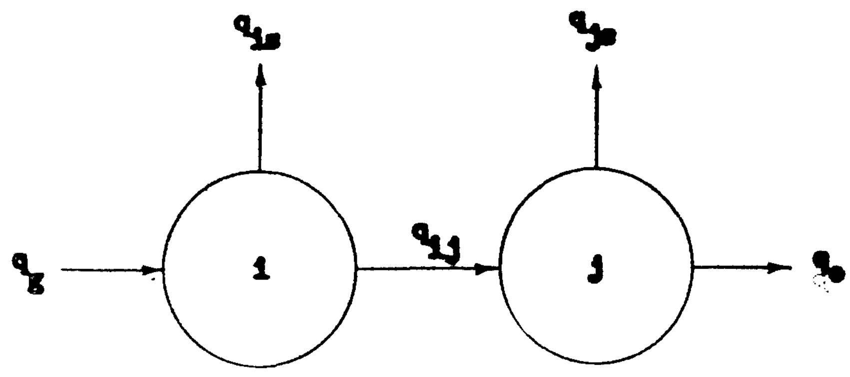

Figure III-2. Two-Body Heat Transfer System

For example for the system in Figure III-2 the difference equation for body (i) may be written,

$$\frac{C_i}{\Delta\tau}(T_{i2}-T_{i1}) = q_g - K_{ij}(T_{i\text{-}av}-T_{j\text{-}av})$$

where,

$$T_{i\text{-}av} = \frac{T_{i1}+T_{i2}}{2}$$

$$T_{j\text{-}av} = \frac{T_{j1}+T_{j2}}{2}$$

Of course it is necessary first to estimate the values of T_{i2} and T_{j2} and then to compute by the tabular methods what those values should be. This results in a trial-and-error process which would be prohibitive if there were very many bodies in the heat transfer system. However, the procedure would not be burdensome for a system containing a small number of bodies. It is usually feasible to make good estimates by extrapolation of the temperature-time curves plotted concurrently with the computations.

THERMAL CAPACITIES AND CONDUCTANCES

1. Thermal Capacities of Composite Bodies

The thermal capacity C of any body is defined as the heat required to raise the temperature of that body one degree. The value of C for any solid or liquid body made up of several components may be found by taking the sum of the products of the weights and specific heats of each component. Thus if an equipment item, such as A in Figure III-1, is made up of materials having volumes v_a, v_b, v_c, etc., specific weights w_a, w_b, w_c, etc., and specific heats, c_a, c_b, c_c, etc., respectively, its thermal capacity would be

$$C_A = v_a w_a c_a + v_b w_b c_b + v_c w_c c_c + \text{etc.} \qquad \text{(III-18)}$$

The specific heats and specific weights of various materials may be found in several handbooks (Ref. III-4, -5, and -7). As an approximate guide, the range of thermal capacities of one cubic foot of various classes of materials are given in Table III-3. The thermal capacities of gases are so small that as a general rule they may be neglected in computations such as those described here.

Table III-3

Ranges of Volumetric Thermal Capacities and Specific Heats of Various Classes of Materials

Material	Btu/ft^3-$^\circ$F	Btu/lb-$^\circ$F
Metals (solid)		
light (less than 300 lb/ft^3)	27 - 40	.14 - .25
medium (less than 600 lb/ft^3)	41 - 60	.09 - .12
heavy (more than 600 lb/ft^3)	18 - 42	.03 - .06
Liquids	15 - 65	.4 - 1
Non-metals (e.g. glass, rubber, plastics, wood, etc.)	10 - 35	.15 - .55
Insulating materials (loose, e.g. rock wool, asbestos, etc.)	1 - 7	.15 - .3

2. Conductances of Heat Transfer Modes

The thermal conductance K is defined as the time rate of heat transfer per degree of temperature difference and is designated. The value of K for heat transferred from one body to another, or from one part of a body to some other part of the body, depends upon the modes of heat transfer involved. Heat may be transferred by conduction, convection, radiation or by some combination of them.

The heat transferred entirely within the boundaries of solid bodies or across the interfaces of adjoining solid bodies, is assumed to be transferred by conduction. Heat transferred from the surface of a solid body to a fluid in contact with it is said to be transferred by convection. When heat is transferred from one surface to other surfaces in a vacuum and without contact, it is transferred by radiation only. Heat may also be transferred by radiation between two surfaces if the intervening medium transmits radiant energy.

Since the thermal conductances for each of these modes of heat transfer are computed by different methods, they are discussed separately in the following.

a. Conduction Heat Transfer

Since the heat transfer computations being described here are

such that differential equations are replaced by difference equations it is possible to consider the heat transfer process in any time interval to be in the steady state.

The basic equation for steady state conductive heat transfer is

$$q = -\int kA \, dt/dL \tag{III-19}$$

For plane solids with heat flow perpendicular to the surface, equation (III-19) integrates to

$$q = \frac{k_m A \Delta t}{L} \tag{III-20}$$

where k_m is the mean thermal conductivity of the material. Equation (III-20) may be written

$$q = K_{Cd} \Delta t \tag{III-21}$$

where K_{Cd} is the thermal conductance for conduction heat transfer and is defined by

$$K_{cd} = \frac{k_m A}{L} \tag{III-22}$$

In many cases the flow of heat occurs through solids in which the area normal to the path of heat flow varies as a function of the distance along the path. In such cases the area to be used in equation (III-22) is the mean value of the area A_m. Thus,

$$K_{cd} = \frac{k_m A_m}{L} \tag{III-23}$$

Values of thermal conductivity k of various materials are given in handbooks and texts on heat transfer (Ref. III-1 to -8).

b. Convection Heat Transfer

The basic equation for the rate of heat transfer by convection from a surface to a fluid in contact with that fluid is,

$$q = hA \Delta t \tag{III-24}$$

The thermal conductance for this mode may therefore be written as

$$K_{cv} = hA \tag{III-25}$$

The value of the heat transfer coefficient h depends upon the type of convection, (free or forced), the geometry, the hydrodynamical characteristics, and the heat transfer characteristics of the system. Equations for

the computation of h in a variety of special cases may be found in any heat transfer text (Ref. III-1, -6, and -8).

c. Radiation Heat Transfer

Heat transfer rates by radiation between two surfaces (a) and (b) may be computed by the approximation

$$q = 0.172 F_A F_e A \left[(T_a/100)^4 - (T_b/100)^4\right] \tag{III-26}$$

where the emissivity factor F_e, the shape factor F_A and the surface area A on which the computation is to be based depend on the configuration of the surfaces and their individual emissivities (see p. 61, Ref. III-1). Equation (III-26) may be written,

$$q = K_{rd}(T_a - T_b) \tag{III-27}$$

where the thermal conductance K_{rd} is defined by

$$K_{rd} = \frac{0.172 F_e F_A A \left[(T_a/100)^4 - (T_b/100)^4\right]}{T_a - T_b} \tag{III-28}$$

3. Combined Conductances

a. Parallel Heat Transfer Paths

In many actual situations it is the usual practice to compute separately the heat transfer between two bodies by each mode. In other instances, however, it may be expedient to compute a combined conductance for the heat transfer from one body to another by more than one mode or through intervening bodies.

If heat is transferred from body (a) at temperature T_a to body (b) at temperature T_b along parallel paths that have conductances K_1, K_2, K_3, . . K_n, then the combined conductance is

$$K = K_1 + K_2 + K_3 + \ldots + K_n \tag{III-29}$$

and the heat transfer rate is $q = K(T_a - T_b)$.

Typical examples of this are found when one body is connected to a second body by two or more conductive paths or when heat is transferred from one body to another by more than one mode. For example, if heat is transferred from one body to another by convection and radiation the combined conductance is

$$K = K_{cv} + K_{rd} \tag{III-30}$$

where K_{cv} and K_{rd} are defined by equations (III-25 and -28), respectively.

b. Series Heat Transfer Paths

In some cases the heat may be transferred from one body or surface to a second body or surface through one or more intervening bodies in series. If it is desired to express this heat transfer rate in terms of a combined conductance and the temperatures of the two bodies, it is necessary to compute the combined conductance as the reciprocal of the sum of the reciprocals of the separate conductances. For example, if heat is transferred from surface (a) at temperature T_a, to surface (b) at temperature T_b, through a fluid medium between them, the combined conductance is,

$$K = \frac{1}{\frac{1}{K_{cv-a}} + \frac{1}{K_{cv-b}}} \qquad \text{(III-31)}$$

and the heat transfer rate is $q = K(T_a - T_b)$, when K_{cv-a} is the conductance due to convective heat transfer from surface (a) to the fluid, and K_{cv-b} is the conductance due to convective heat transfer from the fluid to surface (b), both determined by equation (III-25). Similarly, if surface (a) is separated from surface (b) by several layers of solid bodies in series having conductances, K'_{cd-1}, K'_{cd-2}, K'_{cd-3}, . . . K'_{cd-n}, the combined conductance is,

$$K = \frac{1}{\frac{1}{K'_{cd-1}} + \frac{1}{K'_{cd-2}} + \frac{1}{K'_{cd-3}} + \cdot \cdot \cdot + \frac{1}{K'_{cd-n}}} \qquad \text{(III-32)}$$

c. Series-Parallel Heat Transfer Paths

For the case where heat is transferred from surface (a) to surface (b) through a transparent gas the combined conductance for the heat transferred from surface (a) to surface (b) is,

$$K = K_{rd} + \frac{1}{\frac{1}{K_{cv-a}} + \frac{1}{K_{cv-b}}} \qquad \text{(III-33)}$$

4. Conductances for Specific Cases

To illustrate the methods of determining the conductances for a variety of specific cases, the values of the conductances involved in the heat transfer system of Figure III-1 and expressed in equations (III-6a through -6f) will be developed here.

a. K_{AB} - Conductance between the surface of the equipment box A and the outer surface of the insulation B. Since this process involves only

conduction heat transfer, the conductance is by equation (III-23)

$$K_{AB} = \frac{k_B(A_A+A_B)}{2L_B} \tag{III-34}$$

For most insulating materials used in aircraft the value of k_B is in the range from 0.02 to 0.15 Btu/hr-sq ft- (^oF/ft). (See Appendix II.)

If it is desired to express all conductances in terms of the area of the compartment wall, A_F, then equation (III-34) may be written

$$K_{AB} = \frac{k_B\alpha_{AF}A_F(1+\alpha_{BA})}{2L_B} \tag{III-35}$$

where

$$\alpha_{AF} = A_A/A_F \quad \text{and} \quad \alpha_{BA} = A_B/A_A \tag{III-36}$$

b. K_{BC} - Conductance between the outer surface of the insulation B and the non-heat generating bodies C. Heat may be transferred between the insulation B and the non-heat generating components C by conduction, radiation and convection. Since the portion of the heat transferred by convection must first be transferred between B and the air D in the compartment and between the air D and the non-heat generating bodies C, it is best to separate the conductance due to convection from the conductance due to radiation and conduction.

Since K_{BC} is a combined conductance for two parallel paths of heat transfer (conduction and radiation) the conductance by equations (III-23, -28 and -30) is

$$K_{BC} = \frac{k_{BC}A_{BC}}{L_{BC}} + \frac{0.172F_eF_AA_B\left[(T_B/100)^4-(T_C/100)^4\right]}{(T_B - T_C)} \tag{III-37}$$

where k_{BC}, A_{BC} and L_{BC} are mean values of thermal conductivity, cross sectional area and length of the conduction path connecting B and C.

In many cases, unless metal conduction paths are purposely provided, the term $k_{BC}A_{BC}/L_{BC}$ is so small that it may be neglected. This is the usual situation since equipment component boxes are usually mounted on vibration and shock mounts which are relatively poor heat conductors.

Where the geometry of the system is simple it is possible to compute the values of F_e and F_A from theoretical considerations. However in the usual aircraft equipment compartment being considered, the disposition of the surfaces of body C which may consist of several bodies, lumped together for convenience of calculation, with respect to body B may be very complex. In this case it is suggested that the product F_eF_A be replaced by the product of the emissivity of body B and the estimated fraction of the surface of body B which is "seen" by body C. It is further suggested that the area A_B be expressed in terms of the area of the compartment wall, A_F.

Thus, for the case where no metallic conductive paths are provided and where it is not possible to determine F_e and F_A with any accuracy, equation (III-37) becomes

$$K_{BC} = \frac{0.172\,\epsilon_B f_{BC}(\alpha_{BA}\alpha_{AF}A_F)\left[(T_B/100)-(T_C/100)\right]}{T_B - T_C} \qquad \text{(III-38)}$$

where f_{BC} is the estimated fraction of body B "seen" by body C.

c. K_{BD} - Conductance between the outer surface of the insulation B and the air in the compartment D. This conductance is due to convection alone and is defined by equation (III-25). If the air in the compartment is circulating by virtue of free convection alone the convection coefficient h, may be found by one of the exact equations given in the heat transfer literature. For purposes of estimation the following equation for free convection may be used,

$$K_{BD} = a'(T_B - T_D)^{1/3} A_B \qquad \text{(III-39)}$$

where

$$a' = 0.12 k_D\, a^{1/3} \delta_D^{2/3},$$

the thermal conductivity of the air k_D and the free convection modulus a (see p. 244, Ref. III-1) being both determined at temperature $(T_B+T_D)/2$.

If the air in the compartment is circulating by virtue of forced convection produced by a blower or other means, the convection coefficient will depend upon the shape of the passages through which the air passes and the type of flow involved.

If the flow is streamlined the following approximate equations in which an average N_{Pr} of 0.7 is substituted may be used to determine h.

(a) In circular tube $h = 3.65\, k/d$ (III-40)
(see p. 100, Ref. III-3)

(b) Over flat plate $h = 0.6k(V/x\nu)^{1/2}$ (III-41)
(see p. 93, Ref. III-3)

If the flow is turbulent the following approximate equations in which an average N_{Pr} of 0.7 is substituted may be used:

(a) In circular tube $h = 0.021(k/d^{0.2})(V/\nu)^{0.8}$ (III-42)
(see p. 113, Ref. III-1)

(b) Over flat plate $h = 0.055\,(k/x^{0.25})(V/\nu)^{0.75}$ (III-43)
(see p. 126, Ref. III-1)

(c) Across tubes $h = 0.0032(T)^{0.3}(G^{2/3}/d^{1/3})$ (III-44)
(see p. 125, Ref. III-1)

where x is the length of the plate, V the air velocity and G the weight flow rate of air per unit minimum free flow area.

For the case of forced convection then,

$$K_{BD} = h_{BD} A_B \qquad \text{(III-45)}$$

where h_{BD}, the forced convection coefficient is determined from one of the equations (III-40 to -44) and A_B the area of body B in contact with the air D may be expressed in terms of A_F the area of the compartment wall.

d. K_{BE} - Conductance due to radiation between insulation surfaces B and E. (See K_{BC}.)

$$K_{BE} = \frac{0.172\ \epsilon_B f_{BE}(\alpha_{BA}\alpha_{AF}A_F)\ \left[(T_B/100)^4-(T_E/100)^4\right]}{T_B - T_E} \qquad \text{(III-46)}$$

where f_{BE} is the estimated fraction of body B "seen" by body E.

e. K_{CE} - Conductance due to radiation between non-critical bodies C and insulation E. (See K_{BC}.)

$$K_{CE} = \frac{0.172\ \epsilon_C f_{CE}(\alpha_{CF}A_F)\ \left[(T_C/100)^4-(T_E/100)^4\right]}{T_C - T_E} \qquad \text{(III-47)}$$

where f_{CE} is the estimated fraction of surface of body C "seen" by body E and $\alpha_{CE} = A_C/A_F$.

f. K_{DE} - Conductance due to convection between the air D and the insulation E on the compartment wall. The discussion applying to the conductance K_{BD} applies equally well to conductance K_{DE}.

If the air circulation is entirely by free convection,

$$K_{DE} = a'(T_D-T_E)^{1/3}\ \alpha_{EF}A_F \qquad \text{(III-48)}$$

where a' is defined as for equation (III-38) and $\alpha_{EF} = A_E/A_F$.

If the air circulation is by forced convection,

$$K_{DE} = h_{DE} A_E \qquad \text{(III-49)}$$

where h_{DE}, the forced convection coefficient, is determined from one of the equations (III-40 to -44) and A_E is the area of body E which is in contact with the air.

K_{DC}, the conductance between the air and the non-critical components is determined in the same manner as K_{DE}, using appropriate values corresponding to C rather than E in equations (III-48 or -49).

g. K_{EF} - Conductance between the compartment-side surface of the insulation on the compartment wall E and the compartment wall F. This conductance is similar to conductance K_{AB} and may be expressed by the equation

$$K_{EF} = k_E \frac{\alpha_{EF} A_F}{L_E} \qquad \text{(III-50)}$$

where L_E is the insulation thickness and k_E, its thermal conductivity at its average temperature. The term α_{EF} is defined by A_{Em}/A_F, where $A_{Em} = (A_E+A_F)/2$ and is practically equal to A_F.

h. K_{Fo} - Conductance due to forced convection heat transfer between the compartment wall F and the air flow over it. If it is assumed that the compartment wall is the surface of the aircraft or missile over which air is flowing, that the compartment is short in the direction of air flow, and that it is located on the average, some distance x aft of the most forward point of the surface, then

$$K_{Fo} = \frac{0.028}{x^{0.2}} k_o \left(\frac{V}{\nu}\right)^{0.8} (N_{Pr})^{1/3} A_F, \qquad \text{(III-51)}$$

In equation (III-51) (Ref. III-5), the thermal conductivity k_o, the kinematic viscosity ν, and the Prandtl number N_{Pr} of the air are determined at the mean of the wall surface temperature and the total air temperature, $(T_F+T_{ot})/2$. If the air velocity V over the wall is not defined and the wall forms the boundary of a duct, equation (III-51) may also be written as

$$K_{Fo} = \frac{0.028}{x^{0.2}} \frac{k_o (N_{Pr})^{1/3}}{\mu^{0.8}} G^{0.8} A_F \qquad \text{(III-52)}$$

where G is the weight rate of air flow per unit duct area and the absolute viscosity μ is determined at $(T_F+T_{ot})/2$.

Equations (III-51 and -52) are actually based on the local heat transfer coefficient, as determined by the location x relative to the leading edge of the surface. It can be applied to a short compartment, one to two feet long, by using for x the distance to the midpoint. However, if the compartment extends to the most forward point of the wall surface, or very near to it and is of appreciable length, K_{Fo} should be based on the average heat transfer coefficient. When x is redefined as the over-all length of the wall surface from the leading edge to the aft end of the compartment wall, the constant in equations (III-51 and -52) is changed from 0.028 to 0.036 to give the average value of K_{Fo} for the entire surface.

CALCULATION EXAMPLE

The following is presented as an abbreviated numerical revue of the calculation methods and application of heat transfer equations given in the preceding parts of this Section.

The temperature-time histories of the various idealized parts constituting a small compartment in a ramjet center body are to be investigated for a given flight plan. The compartment is a short cylinder located on the average 3.3 feet from the forward tip of the center body. The compartment end walls are insulated so that heat flow through these surfaces can be neglected. The stainless steel skin has a moderate insulation thickness within the compartment. The compartment contains two types of equipment items. Mechanical components of high bulk density and large thermal capacity which are relatively insensitive to high temperature, and electronic components of low bulk density and smaller thermal capacity which are sensitive to high temperature. Since the flight plan is such that heat flow into the compartment is to be expected, the electronic components are insulated. There is no heat transfer by conduction between the components and the skin. The compartment is pressurized by ram. Free convective conditions are assumed to exist.

1. Characteristics of Thermal Regions (Figure III-1)

A. Electronic components (represented by one box)
Heat generation rate, $q_g = 670$ Btu/hr
Surface area, $A_A = 5.11$ ft^3
Thermal capacity, $C_A = 8.88$ Btu/^oF
(71 lb at mean specific heat of 0.125 Btu/lb-^oF)

B. Insulation on component box
Inner surface area, $A_A = 5.11$ ft^2
Outer surface area, $A_B = 5.76$ ft^2
Thickness, $L_B = 0.029$ ft
Thermal capacity, $C_B = 0.47$ Btu/^oF
(2.35 lb at specific heat of 0.2 Btu/lb-^oF)
Radiation characteristics
to skin insulation, $\epsilon_B f_{BE} = 0.25$
to other components, $\epsilon_B f_{BC} = 0.25$
(based on assumed mean emissivity of 0.5 and fraction of radiation-exchanging surface area also of 0.50)

C. Mechanical components (non-critical, represented by one unit)
Surface area, $A_C = 5.11$ ft^2
Thermal capacity, $C_C = 33.4$ Btu/^oF
(150 lb at mean specific heat of 0.223 Btu/lb-^oF)
Radiation characteristics
to skin insulation, $\epsilon_C f_{CE} = 0.25$

E. Insulation of skin
Inner surface area, $A_E = 5.95\ ft^2$
Outer surface area, $A_F = 6.28\ ft^2$
Thickness, $L_E = 0.048\ ft$
Thermal capacity, $C_E = 0.94\ Btu/^oF$
(4.7 lb at specific heat of 0.2 Btu/lb-^oF)

F. Compartment skin
Surface area, $A_F = 6.28\ ft^2$
Thermal capacity, $C_F = 4.23\ Btu/^oF$
(38.5 lb stainless steel at specific heat of 0.11 Btu/lb-^oF)

2. Conductances

a. K_{AB} (equation III-34)

$k_B = 0.03\ Btu/hr\text{-}ft^2\text{-}(^oF/ft)$, (assumed constant with temperature change)

$$K_{AB} = \frac{0.03(5.11+5.76)}{2x0.029} = 5.63\ Btu/hr\text{-}^oF$$

b. K_{BC} (equation III-38)

$$K_{BC} = 0.172x0.25x5.76xB_{BC} = 0.0025\ B_{BC}$$

where $B_{BC} = \left[(T_B/100)^4-(T_C/100)^4\right]/(T_B-T_C)$

c. K_{BD} (equation III-39)

$$K_{BD} = 5.76\ a'(T_B-T_D)^{1/3}$$

d. K_{BE} (equation III-46)

$$K_{BE} = 0.172x0.25x5.76xB_{BE} = 0.0025\ B_{BE}$$

e. K_{CE} (equation III-47)

$$K_{CE} = 0.172x0.25x5.11xB_{CE} = 0.00221\ B_{CE}$$

f. K_{CD} (equation III-48)

$$K_{CD} = 5.11\ a'(T_C-T_D)^{1/3}$$

g. K_{DE} (equation III-48)

$$K_{DE} = 5.95\ a'(T_D-T_E)^{1/3}$$

h. K_{EF} (equation III-50)

$$k_E = 0.03 \text{ Btu/hr-ft}^2\text{-}(^\circ F/\text{lb}), \text{ assumed constant}$$

$$K_{EF} = \frac{0.03(6.28+5.95)}{2 \times 0.048} = 3.85 \text{ Btu/hr-}^\circ F$$

i. K_{Fo} (equation III-52)

Since the compartment is short axially, and is located some distance from the forward tip of the center body, it is satisfactory to use equation (III-52) for local values of K_{Fo}, as applied approximately to the axial midpoint of the compartment surface. Also, any conduction along the skin surface is neglected. Thus,

$$K_{Fo} = \frac{0.028}{3.3^{0.2}} \times 6.28 \times \frac{k(N_{Pr})^{1/3}}{\mu^{0.8}} G^{0.8}$$

$$= 0.1387 \frac{k(N_{Pr})^{1/3}}{\mu^{0.8}} G^{0.8}$$

This conductance K_{Fo} determines q_{Fo} when multiplied with the available temperature potential which is the difference between the skin temperature T_F and the total temperature of the enveloping air flow T_{ot}. Actually, the latter should be the adiabatic wall temperature which is lower than T_{ot} and depends on a recovery factor which is determined by the surface configuration and the air temperature conditions surrounding the compartment surface. In this example, these conditions are not well defined. Therefore, equation (III-52) is used since at supersonic flight speed the mass velocity G and the total temperature may be defined directly by the flight Mach number and the atmospheric pressure and temperature conditions, providing the total flow entering the diffuser passes over the center body surface and no prior heat addition takes place.

3. <u>Initial Conditions and Flight Plan</u>

During the brief operation prior to flight, the following temperatures are attained:

$$T_A = 572^\circ R \qquad T_B = 564^\circ R \qquad T_C = 560^\circ R$$

$$T_D = 562^\circ R \qquad T_E = 560^\circ R \qquad T_F = 560^\circ R$$

Conditions during the flight plan are pre-defined in terms of flight speed and altitude. This determines the variation of T_{ot} based on total conditions and of G. Based on knowledge of the extent to which the center body is pressurized in relation to the ram pressure rise (here 50 per cent) the variation of the relative pressure δ with time is found. $G^{0.8}$ and $\delta^{2/3}$, as used in various equations for conductances, and T_{ot} are plotted

versus flight time in Figure III-3, and describe the flight conditions fully for purposes of calculation.

It is also convenient to use plots of other variables as calculation aids such as $a'/\delta^{2/3}$ (Figure AIV-2) and $(k(N_{Pr})^{1/3})/\mu^{0.8}$ (Figure III-4) versus temperature in ^{o}R and the radiation temperature factor B versus $(T_a+T_b)/100$ (Figure AIV-1).

4. Calculation Procedure

The application of the calculation methods previously discussed is illustrated in the following for a time interval beginning at $\tau = 0.3$ hour after initiation of flight conditions. The initial temperature conditions at $\tau = 0.3$ are

$T_A = 607^oR$ $\quad T_B = 674^oR$ $\quad T_C = 567^oR$

$T_D = 693^oR$ $\quad T_E = 824^oR$ $\quad T_F = 1343^oR$

$T_{ot} = 1353^oR$

a. Time Interval Duration

From equation (III-17),

$$\Delta\tau = \frac{C_m}{\Sigma K_m}$$

and is determined from one of bodies A through F which gives the smallest $\Delta\tau$. Thus,

For A, $\Delta\tau = C_A/K_{AB} = 8.88/5.63 = 1.578$

For B, $\Delta\tau = C_B/(K_{AB}+K_{BC}+K_{BD}+K_{BE})$

$K_{BC} = 0.0025B_{BC} = 0.0025x965 = 2.41$

$K_{BD} = 5.76x0.178x0.582x2.67 = 1.58$

where $a'/\delta^{2/3} = 0.178$ (from Fig. AIV-2 at 683.5^oR), $\delta^{2/3} = 0.582$ (from Fig. III-3), and $(T_D-T_B)^{1/3} = (693-674)^{1/3} = 2.67$.

$K_{BE} = 0.0025B_{BE} = 0.0025x1710 = 4.27$

$\Delta\tau = 0.47(5.63+2.41+1.58+4.27) = 0.47/13.89 = 0.0338$

For C, $\Delta\tau = C_C/(K_{CB}+K_{CD}+K_{CE})$

$K_{CD} = 5.11x0.188x0.582x5.01 = 2.80$

where $a'/\delta^{2/3} = 0.188$ (from Fig. AIV-2 at 630^oR), and $(T_D-T_C)^{1/3} =$

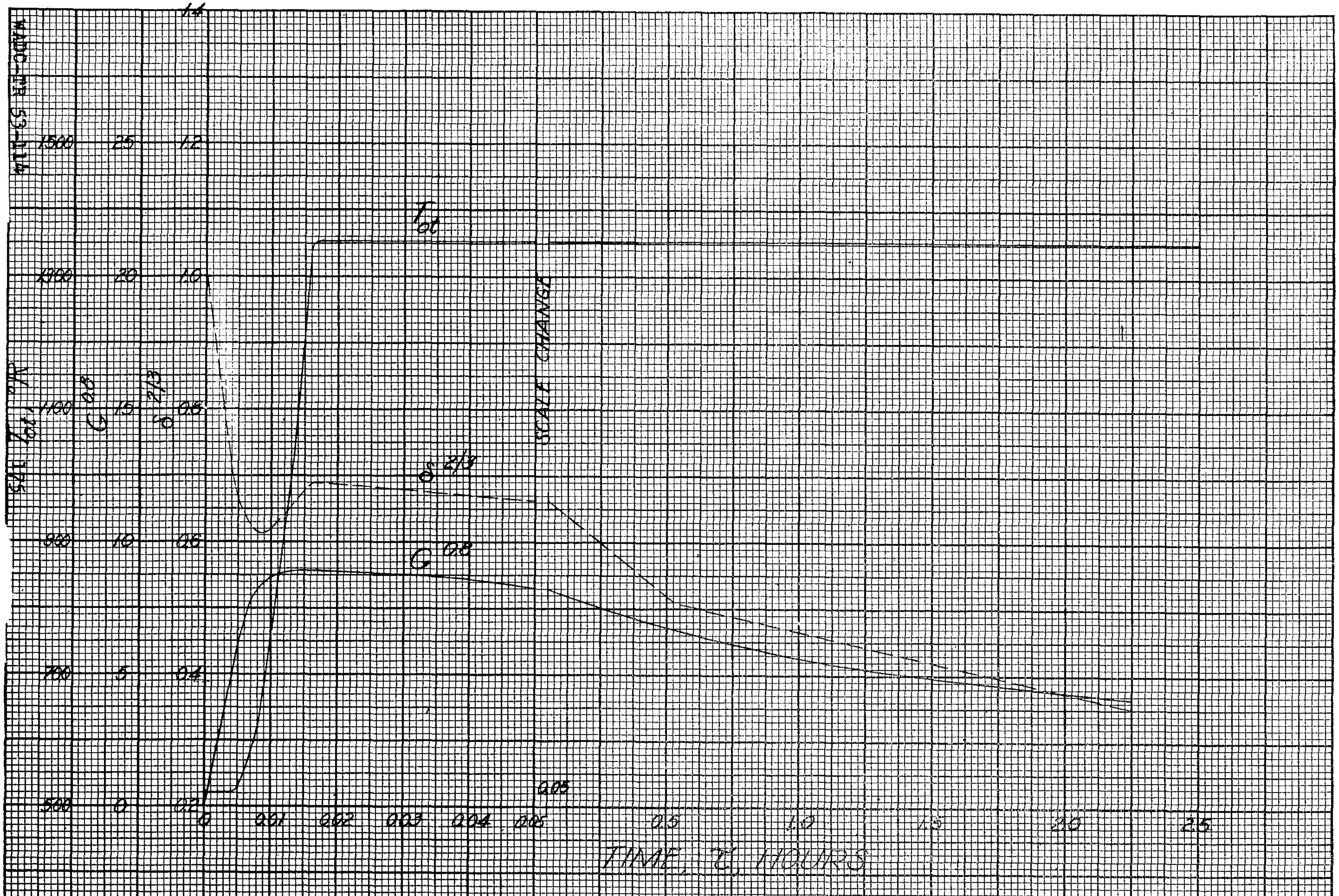

Figure III-3

Definition of Flight Plan

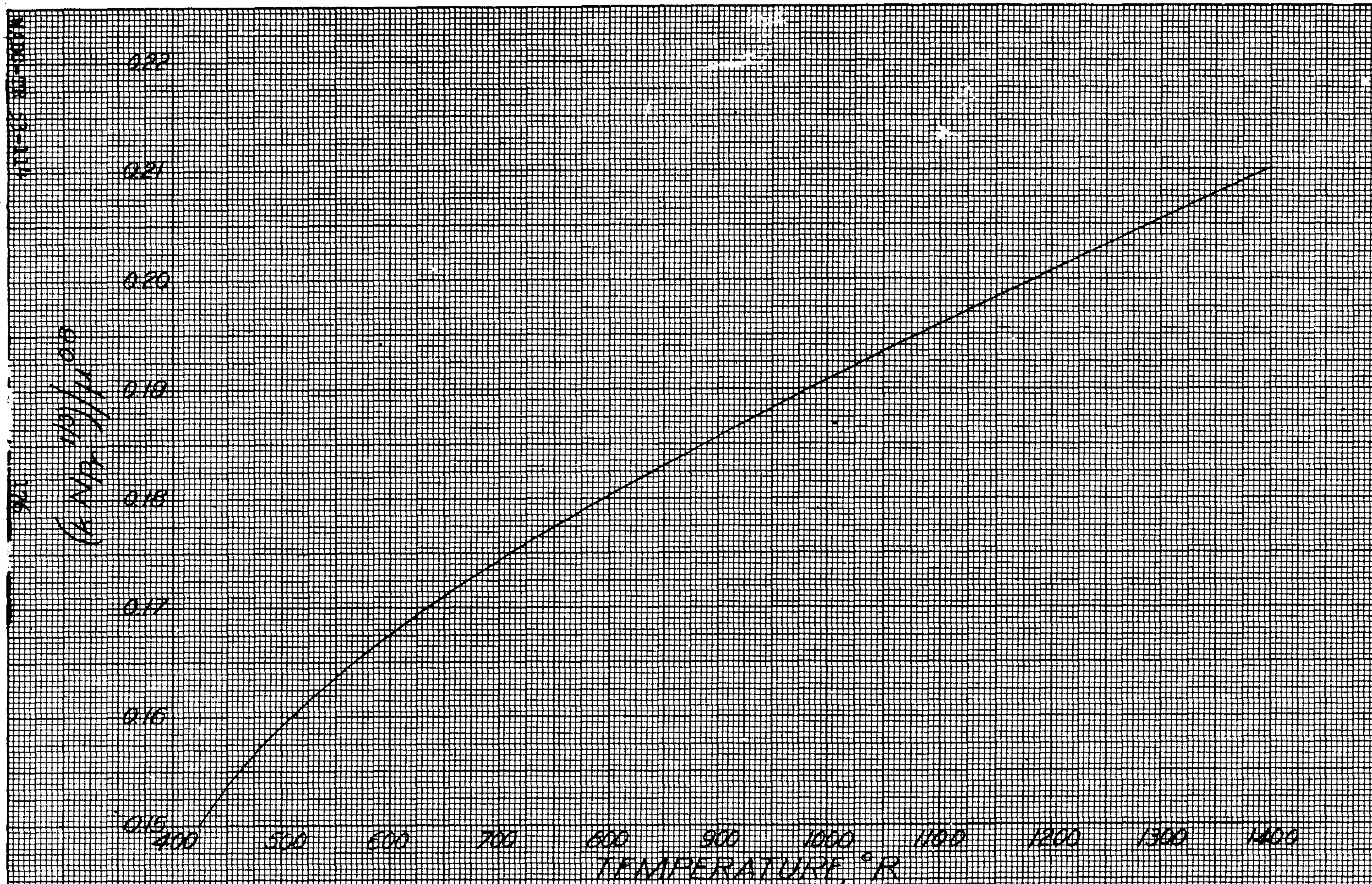

Figure III-4

Plot of $(kN_{Pr}^{1/3})/\mu^{0.8}$ for Air

$(693-567)^{1/3} = 5.01.$

$$K_{CE} = 0.00221B_{CE} = 0.0022x1610 = 3.56$$

$$\Delta\tau = 33.4/(2.41+2.80+3.56) = 3.81$$

Since the thermal capacity of the air D is neglected, the air does not influence the choice of $\Delta\tau$.

$$\text{For E,}\ \Delta\tau = C_E/(K_{EB}+K_{EC}+K_{ED}+K_{EF})$$

$$K_{ED} = 5.95x0.166x0.582x5.06 = 2.90$$

where $a'/\delta^{2/3} = 0.167$ (from Fig. AIV-2 at 758.5°R), and $(T_E-T_D)^{1/3} = (824-693)^{1/3} = 5.06$.

$$\Delta\tau = 0.94/(4.27+3.56+2.90+3.85) = 0.94/14.58 = 0.0645$$

$$\text{For F,}\ \Delta\tau = C_F/(K_{FE}+K_{Fo})$$

$$K_{Fo} = 0.1387x0.2078x7400 = 213$$

where $k(N_{Pr})^{1/3}/\mu^{0.8} = 0.2078$ from Fig. III-4, at $(T_F+T_{ot})/2 = (1343+1353)/2 = 1348°R$, and $G^{0.8} = 7400$ (from Fig. III-3 at $\tau = 0.3$).

$$\Delta\tau = 4.23/(3.85+213) = 0.0196$$

The time interval calculated for F is the shortest and should be used for calculation. This could have been predicted from previous calculations because the ratio of C_F/K_{Fo} would be significantly small throughout the flight plan. The calculated value for $\Delta\tau$ is rounded up to 0.02 for the purpose of determining the resulting changes of temperature.

b. F-Factors

From the conductances determined above, the chosen time interval $\Delta\tau = 0.02$ hr, and the known thermal capacities the F-factors are determined next, as follows.

F_{AB}	= 5.63x0.02/8.88	= 0.0127	(III-9a)
F_{BA}	= 5.63x0.02/0.47	= 0.24	(III-9c)
F_{BC}	= 2.41x0.02/0.47	= 0.1023	(III-9b)
F_{BD}	= 1.58x0.02/0.47	= 0.0672	(III-9e)
F_{BE}	= 4.27x0.02/0.47	= 0.1815	(III-9f)
F_{CB}	= 2.41x0.02/33.4	= 0.001443	(III-9h)
F_{CD}	= 2.80x0.02/33.4	= 0.001678	(III-9i)
F_{CE}	= 3.56x0.02/33.4	= 0.002132	(III-9j)
F_{EB}	= 4.27x0.02/0.94	= 0.0908	(III-9l)

$$F_{EC} = 3.56 \times 0.02/0.94 = 0.0758 \qquad \text{(III-9m)}$$
$$F_{ED} = 2.90 \times 0.02/0.94 = 0.0617 \qquad \text{(III-9n)}$$
$$F_{EF} = 3.85 \times 0.02/0.94 = 0.0820 \qquad \text{(III-9o)}$$
$$F_{FE} = 3.85 \times 0.02/4.23 = 0.0182 \qquad \text{(III-9q)}$$
$$F_{Fo} = 2.13 \times 0.02/4.23 = 1.007 \qquad \text{(III-9r)}$$
$$F_{DB} = 1.58/(1.58+2.80+2.90) = 1.58/7.28 = 0.217 \qquad \text{(III-9t)}$$
$$F_{DC} = 2.80/7.28 = 0.384 \qquad \text{(III-9u)}$$
$$F_{DE} = 2.90/7.28 = 0.398 \qquad \text{(III-9v)}$$

c. Temperatures at End of Interval

Using slide rule computations, the temperatures at the end of $\Delta\tau = 0.02$, $\tau = 0.32$, are determined from Table III-2, omitting items (15) through (18) since q_{Ao}, q_{Bo}, q_{Do} and q_{Eo} are all zero. The numerical values for this time interval are listed as follows.

		A	B	C	D	E	F
(1)	T_{m-1}	607	674	567	693	824	1343
(2)	-67	0.85	-16.08				
(3)	107		-10.96	0.15			
(4)	-19		1.28				
(5)	-150		27.20			-13.64	
(6)	-257			0.55		-19.49	
(7)	126			0.21			
(8)	-131					-8.08	
(9)	-519					42.56	-9.45
(10)	-10						10.07
(11)	1.44				0.31		
(12)	0.91				0.35		
(13)	1.29				0.51		
(14)	670	1.51					
(19)		2.36	1.44	0.91	1.17	1.35	0.62
(20)	T_{m-2}	609.4	675.4	567.9	694.2	825.4	1343.6

5. Results

Figure III-5 contains plots of all temperature variations with time, obtained by interval calculations made by the methods illustrated in the preceding sub-section (4). It is apparent that the choice of the time

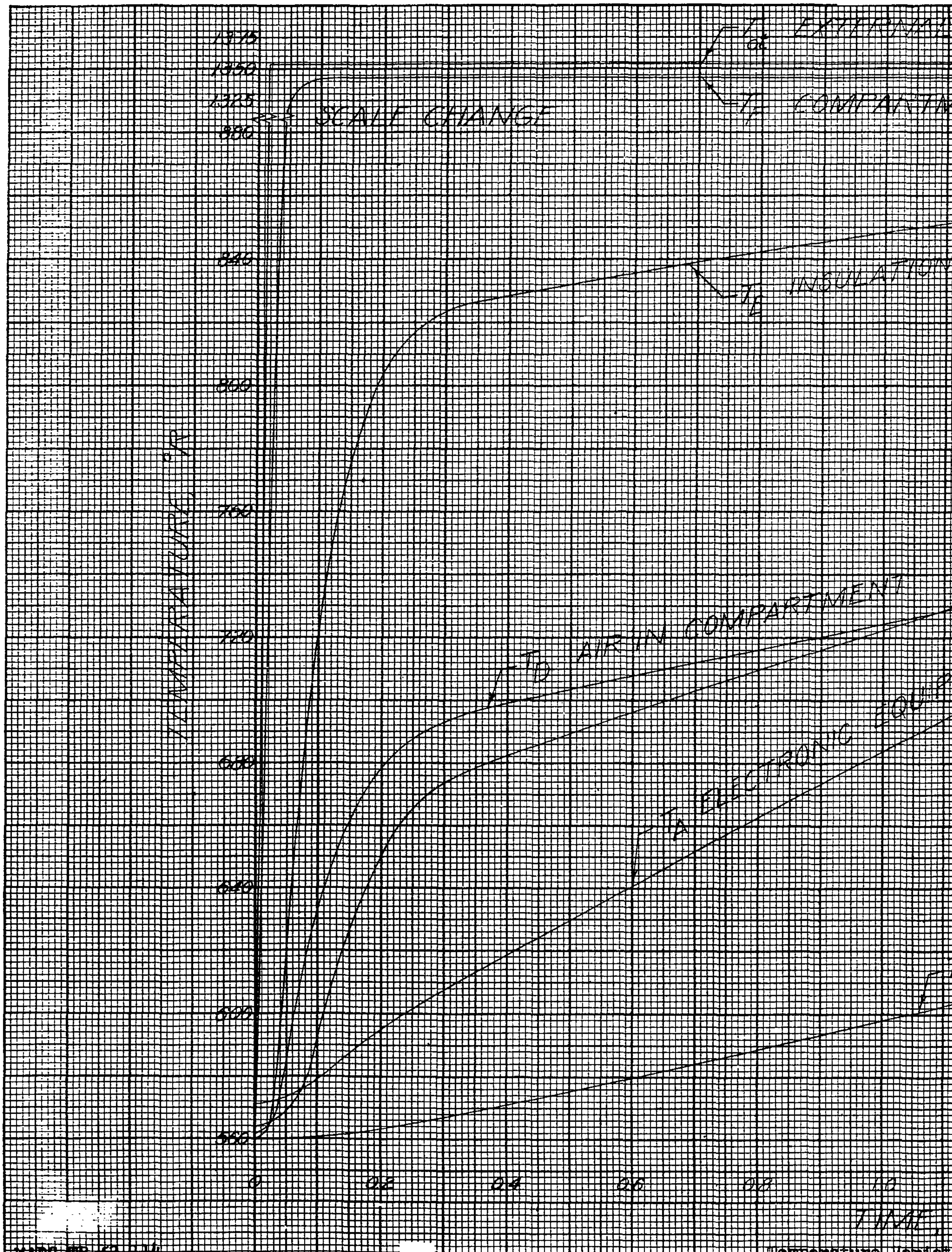

Temperature Variat

Figure 1

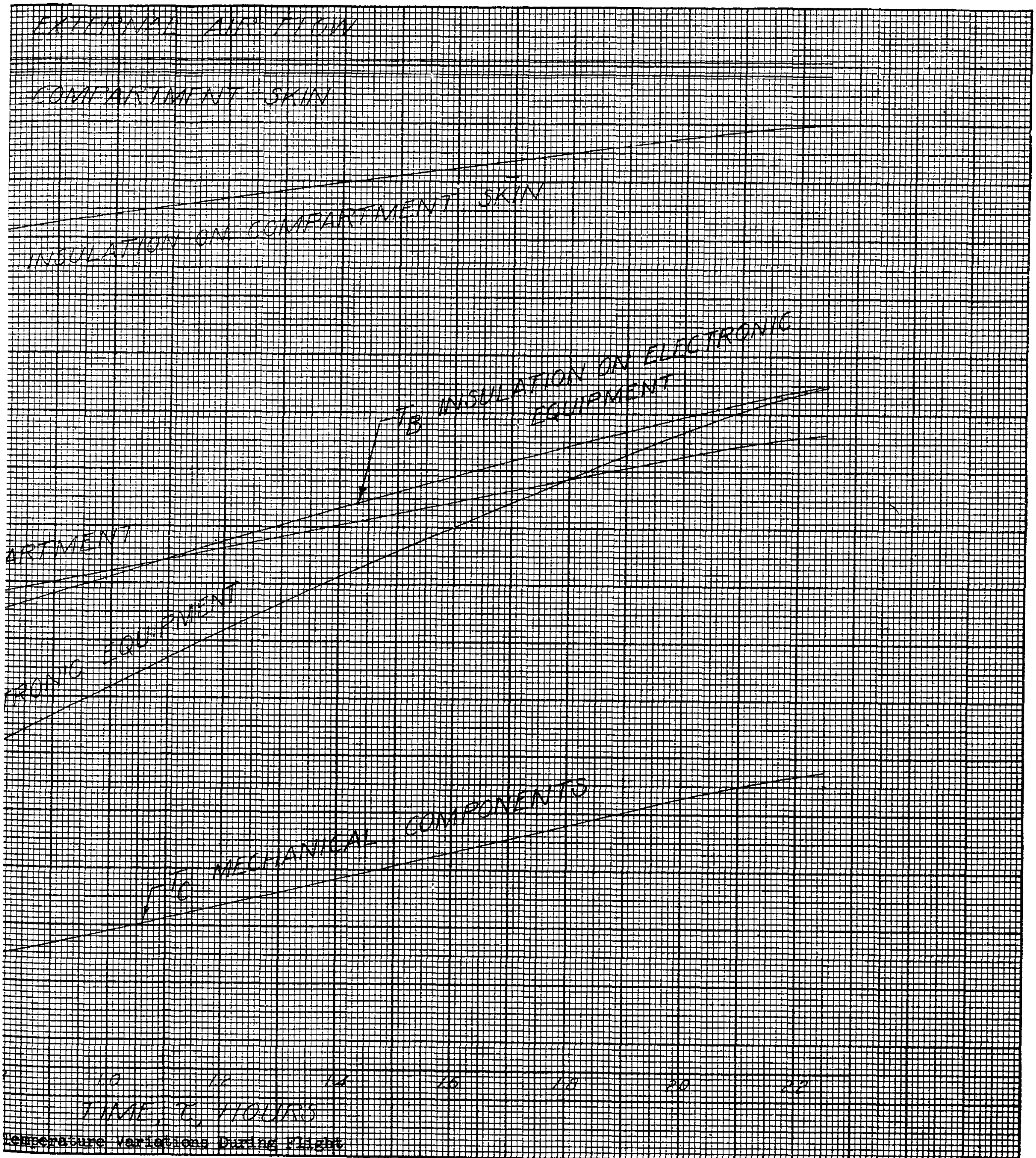

Temperature Variations During Flight

Figure III-5

interval made in (4a) was satisfactory because the end temperatures determined in (4c) are seen to fall on the various curves. Only T_F appears to oscillate slightly about its mean value which remains practically constant at 1343°R after 0.1 hour flight time. The choice of a larger time interval in (4a) would have effected a greater rise of T_F which would have been compensated by a drop in T_F during the next time interval. In the later stages of the analysis, the time interval may be increased, since the time interval is determined by $C_F/(K_{FE}+K_{Fo})$ and $G^{0.8}$ and with it, K_{Fo} decreases with time. Comparing T_F and T_{ot} in Figure III-5, it is apparent that the time lag in heating up the skin is relatively small because of the small magnitude of C_F/K_{Fo}. Thus, subsequent variations in K_{Fo} because of reduced weight flow of atmospheric air over the skin surface have almost no effect on the skin temperature. The temperature of the electronic equipment T_A remains relatively unaffected by the initial skin temperature variation because of intervening thermal barriers and capacities. In this example, assumption of a constant skin temperature of 1353°R, from the time at which the flight is initiated, would have negligible effect on the variation of equipment temperature, but would simplify the calculations.

REFERENCES

III-1 Brown, A. I. and Marco, S. M. Introduction to Heat Transfer, Second Edition, McGraw-Hill Book Co., Inc., New York, 1951.

III-2 Dusinberre, G. M. Numerical Analysis of Heat Flow, First Edition, McGraw-Hill Book Co., Inc., New York, 1949.

III-3 Eckert, E. R. G. Introduction to the Transfer of Heat and Mass, McGraw-Hill Book Co., Inc., New York, 1951.

III-4 Eshbach, O. W. Handbook of Engineering Fundamentals, John Wiley and Sons, Inc., New York, 1952.

III-5 Hodgman, C. D. Handbook of Chemistry and Physics, Chemical Rubber Publishing Co., Cleveland, Ohio, 1952.

III-6 Jacob, M. Heat Transfer, Vol. 1, John Wiley and Sons, Inc., New York, 1949.

III-7 Marks, L. S. Mechanical Engineers' Handbook, Fifth Edition, McGraw-Hill Book Co., Inc., New York, 1951.

III-8 McAdams, W. H. Heat Transmission, Second Edition, McGraw-Hill Book Co., Inc., New York, 1942.

SECTION IV

TEMPERATURE RISE OF AN AIRCRAFT SKIN IN SUPERSONIC FLIGHT

By T. C. Taylor and Y. H. Sun

Heat transferred between the atmosphere and equipment within an aircraft compartment must pass through the aircraft skin and the air film adhering to the outside of the skin. Therefore, the thermal capacity of the skin and the external film heat transfer coefficient are factors to consider in the analysis of aircraft equipment heat transfer processes. The film coefficient is involved in both steady-state and transient heat transfer processes, while the thermal capacity is involved in transient processes only. An analysis is made here to study the importance of these two factors in transient skin heating problems. The analysis is pertinent to the skin heating effects that occur when an aircraft, whose skin is initially at low or moderate temperatures, is suddenly launched or accelerated into supersonic flight at constant flight speed and altitude. The analysis is made with a view towards possible simplification of computational procedures in the study of transient equipment temperatures.

SUMMARY

Heat transfer by convection to an aircraft skin in supersonic flight is analyzed. A thin metallic skin is assumed, and the temperature gradient through the skin is neglected. Equations are developed which describe the effects of heat flux, flight altitude, flight speed, and skin thermal capacity on the skin temperature rise characteristics at constant flight speed and altitude. The basic heat balance equation developed is a first order differential equation and is formally integrated to give an explicit solution for the time required for a given skin temperature rise, corresponding to a set of assigned physical and flight conditions. Calculation procedures are developed for applying the solution to the case of an aircraft skin which is initially at low temperature and suddenly accelerated to high speed flight. The solution and calculation procedures are based on turbulent flow conditions over the skin.

Calculated results are given for a number of conditions to show the qualitative effects of heat flux, flight altitude, flight speed, and skin thermal capacity on skin temperature rise characteristics. The effects and their significance can be summarized as follows:

a. A skin in supersonic flight at constant speed and altitude tends to approach a limiting temperature in a short time. If there is no heat

flow through the skin, the limiting temperature is the adiabatic wall temperature. With heat flow, the skin approaches a temperature sufficiently below adiabatic wall temperature to provide the necessary temperature potential across the external air film. The difference in limiting skin temperatures is small for heat flux rates of zero and 800 Btu/hr-ft^2 at Mach 3.5 and altitude 60,000 feet. This suggests that the assumption of a constant skin temperature in analyzing heat transfer processes between the skin and equipment would introduce small error, although heat flux between the skin and the equipment would vary somewhat with time. The use of this simplifying assumption is justified particularly for cases where the flight time is long compared to the initial period of skin temperature rise. For a flight time of ten times the initial period of skin temperature rise, the assumption is quite accurate.

b. Flight altitude affects skin temperature rise characteristics appreciably due to variation of air pressure with altitude. At high altitudes the lowered air pressure causes reduced external convection heat transfer coefficients, resulting in slower heating of the skin. For a Mach number of 3.5 and a 0.064-inch thick stainless steel skin, the time required for the skin to undergo a given temperature rise is increased about ten-fold by going from 40,000 to 100,000 feet. Therefore, the assumption of a constant skin temperature for flights of short duration is relatively more valid at low altitude than at high altitude.

c. The principal effect of flight speed on temperature rise characteristics of a skin is the dependence of adiabatic wall temperature on flight speed. The time required for a skin to heat within a few degrees of its limiting temperature decreases a little with increased flight speed, but this time is principally determined by other factors unrelated to speed.

d. The time required for a given temperature rise of a skin is nearly proportional to the skin thermal capacity, or skin thickness. Therefore the assumption of constant skin temperature

for internal heat transfer analyses is restricted to long flight durations in the case of thick-skinned aircraft compartments.

ANALYSIS

1. Assumptions for Analysis

A section of an aircraft skin is shown schematically in Figure IV-1. The outer face of the skin is exposed to air flow at supersonic speed, giving rise to aerodynamic heating effects.

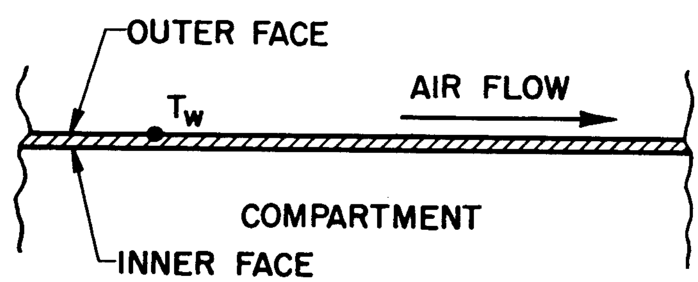

Figure IV-1 Schematic of Aircraft Skin

It is assumed that heat flow takes place through the wall and into the compartment. A thin metallic skin, such as stainless steel is assumed. This permits assigning a uniform temperature T_W to the skin, since the temperature drop between the parallel surfaces of the skin is very small and negligible, compared to other factors in the analysis. In any practical case, the heat flow away from the inner face of the skin would vary as it is dependent both on skin temperature and on thermal and physical conditions in the compartment. However, in this analysis the heat flux will be taken as constant since it is desired only to show the effects of magnitude of the heat flux on skin heating characteristics. It is also assumed that the thermal capacity of a unit skin area is constant, implying a constant specific heat for the skin material.

2. Nomenclature

Symbol	Definition	Units
A,B,	Constants of integration	
Alt.	Altitude	ft.
a,b,c,d	Substitution constants	
c_p	specific heat at constant pressure	Btu/lb-°R
c_v	Specific heat at constant volume	Btu/lb-°R
g	Gravitational constant = 4.17×10^8	ft/hr^2
h	Coefficient for forced convection heat transfer	Btu/hr-ft^2-°R
J	Mechanical equivalent of heat = 778	ft-lb/Btu
k	Thermal conductivity	Btu/hr-ft-°R
M	Flight Mach number	dimensionless
m	weight of skin per unit area	lb/ft^2
Pr	Prandtl modulus $\frac{c_p \mu}{k}$	dimensionless
P	Pressure	lb/ft^2
q	Heat flow or storage rate per unit skin area	Btu/hr-ft^2
R	Gas constant for air = 53.3	ft-lb/lb-°R
Re	Reynolds modulus $\frac{\gamma u x}{\mu}$	dimensionless
r	Recovery factor	dimensionless
T	Absolute temperature	°R
u	Flight speed	ft/hr
v	Substitution variable	
w	Skin thickness	in.
x	Characteristic length	ft.
γ	Weight density	lb/ft3
δ_o	Ratio of pressure to sea level standard conditions	atmospheres
θ_o	Ratio of temperature to sea level standard conditions	dimensionless
μ	Viscosity	lb/ft-hr
τ	Time	hr
τ'	Time	min

Subscripts

1	Denotes initial value
ad	Denotes adiabatic wall temperature
c	Refers to compartment
lim	Denotes limiting temperature
o	Denotes external or outside value
os	Denotes local static temperature
s	Refers to stored quantity
w	Refers to skin

3. Derivation of Equations

The heating or temperature rise characteristics of the skin shown in Figure IV-1 can be described by writing a heat balance equation for the skin. If heat is transferred to the skin from the external air at the rate q_o, stored in the skin at the rate q_c and transferred from skin to the compartment at the rate q_c, the heat balance is,

$$q_o = q_s + q_c \tag{IV-1}$$

The heat transfer rate to the skin, q_o, is given by the equation (Ref. (IV-1)),

$$q_o = h_o(T_{ed}-T_w), \tag{IV-2}$$

where h_o is the external film heat transfer coefficient, which must be selected consistent with the external air flow conditions and the skin temperature. Reference (IV-1) gives point heat transfer coefficients for supersonic air flow over a flat plate. If flow over the skin is laminar,

$$h_o = 0.0077\left(\frac{uP}{x}\right)^{0.5} \tag{IV-3}$$

If flow over the skin is turbulent,

$$h_o = 0.0212\ \frac{(uP)^{0.8}}{(x)^{0.2}}\ (T_w)^{-0.5} \tag{IV-4}$$

For values of the Reynolds number, ($\gamma ux/\mu$), greater than 5×10^5 the flow is turbulent, while for Reynolds numbers less than 8.4×10^4, the flow is laminar. For values between 8.4×10^4 and 5×10^5 either type of flow is possible. The Reynolds number is evaluated at skin temperature. It will be shown later that, for the cases of interest here, the flow is turbulent, so that equation (IV-4) is used to define h_o. The adiabatic wall temperature, T_{ad}, of equation (IV-2) depends on the local static temperature of the atmosphere, the flight speed, and the recovery factor, as defined by the relationship (Ref. IV-1):

$$T_{ad} = T_{os} + r\left(\frac{u^2}{2gJc_p}\right) \tag{IV-5}$$

where c_p is evaluated at T_{os}. If the recovery factor $r = 1$, equation (IV-5), gives the total or stagnation temperature. The recovery factor can be taken as (Ref. (IV-1))

$$r = \sqrt{Pr}\ \text{(laminar flow)} \tag{IV-6}$$
$$r = \sqrt[3]{Pr}\ \text{(turbulent flow)} \tag{IV-7}$$

The recovery factor should be evaluated at skin temperature. For practical purposes, however, it is sufficiently accurate to evalueat r at T_{ad}, since Pr varies only from 0.904 at -100°F to 0.863 at 1600°F, so that the recovery factor is substantially constant even for large changes in skin temperature. For cases of constant flight speed and altitude, T_{os} and u are also constant, giving a constant value of T_{ad}.

The heat storage rate of the skin q_s is given by the equation

$$q_s = m_w c_w \frac{dT_w}{d\tau} \qquad \text{(IV-8)}$$

where the thermal capacity product $m_w c_w$ refers to a unit skin area, and is determined by

$$m_w c_w = \frac{\gamma_w c_w w}{12} \qquad \text{(IV-9)}$$

for the skin thickness w in inches.

Equations (IV-1,-2,-4,-8) are combined and rearranged to give,

$$\left[\left(\frac{0.0212}{m_w c_w}\right)\frac{(uP)^{0.8}}{(x)^{0.2}}\right](T_{ad}-T_w) = (T_w)^{0.5}\frac{dT_w}{d\tau}+\left(\frac{q_c}{m_w c_w}\right)(T_w)^{0.5} \qquad \text{(IV-10)}$$

This is simplified in form by making the substitutions,

$$a = \left[\left(\frac{0.212}{2m_w c_w}\right)\frac{(uP)^{0.8}}{x^{0.2}}\right](T_{ad}),$$

$$b = \frac{-q_c}{2m_w c_w}$$

$$c = -\frac{a}{T_{ad}},$$

$$v^2 = T_w,$$

giving

$$\frac{v^2\,dv}{a + bv + cv^2} = d\tau\,. \qquad \text{(IV-11)}$$

For constant flight speed and altitude a, b, and c are constants. Therefore, equation (IV-11) may be integrated to give,

$$\tau = \frac{v}{c} - \frac{b}{2c^2}\log_e(a + bv + cv^2) + \frac{b^2-2ac}{2c^2}\left(\frac{-2}{\sqrt{-d}}\tanh^{-1}\frac{2cv + b}{\sqrt{-d}}\right) + A \qquad \text{(IV-12)}$$

where $d = 4ac-b^2$, and A is the arbitrary constant of integration, which must be established by assigning a particular value to T_w corresponding to $\tau = 0$.

If the inner face of the skin in Figure IV-1 is perfectly insulated, so that there is no heat flow through the plate, the value of q_c in equation (IV-1) is zero. For this case, equation (IV-12) reduces to

$$\tau = \frac{T_{ad}}{-2c} \log_e \frac{\sqrt{T_{ad}} + v}{\sqrt{T_{ad}} - v} + \frac{v}{c} + B, \qquad \text{(IV-13)}$$

where B is the arbitrary constant of integration, which must be established by assigning a particular value to T_w corresponding to $\tau = 0$.

Equations (IV-12) and (IV-13) are derived for turbulent flow, and therefore should not be used if the Reynolds number is in the laminar flow region. If the flow is laminar, equations (IV-1,-2,-3,-8) are used to derive an equation for the skin temperature rise with time. The equation for laminar flow is easily derived and is simpler in form than equation (IV-12).

4. Procedure for Calculating Skin Temperature Rise

A method for calculating skin temperature rise using equation (IV-12) or (IV-13) is described here. Detailed calculation procedures and sample calculations are appended to this section.

Since equations (IV-12) and (IV-13) are derived for turbulent flow, the Reynolds number must be calculated first to determine if the air flow over the skin is laminar or turbulent. Fluid properties of the Reynolds number are evaluated at skin temperature. The lowest Reynolds number occurs at the highest skin temperature, since the air density is at its lowest value, while viscosity is at its highest value. Therefore, if the flow at a skin temperature equal to the adiabatic wall temperature is turbulent, the flow conditions would have to be turbulent for any skin temperature lower than this limiting value.

The adiabatic wall temperature, T_{ad}, is calculated using equations (IV-5) and (IV-7). The value of T_{os} is determined directly from the NACA standard Atmosphere given in Table AT-1. The table gives values of θ_o corresponding to altitude, where $T_{os} = 519\theta_o$. It is then necessary to assume a value of T_{ad} to evaluate r with equation (IV-7). This value of r is then used in equation (IV-5) to calculate T_{ad}. If the calculated result agrees with that assumed for equation (IV-7), the value of T_{ad} is accurate. Otherwise the calculated value is used to repeat the evaluation of r, and the trial and error process is repeated until agreement between assumed and calculated values of T_{ad} is achieved. Because of the small variation of Pr with temperature, agreement between calculated and assumed values of T_{ad} within 10°R is sufficient.

Values of the Prandtl modulus are given in Figure AI-1.

The characteristic length x of the Reynolds member is assigned a value appropriate to the skin section being analyzed. For flow past a flat plate, x is the distance from the leading edge of the plate to the point of interest. For an application such as a ram-jet centerbody, x can be taken as the distance from the nose of the centerbody to a point about midway in the centerbody skin area being analyzed.

The flight speed u must be known for use of equation (IV-5), equation (IV-12), or for calculating Reynolds number. If the flight speed is given in terms of the flight Mach number, u can be calculated by

$$u = M\sqrt{\left(\frac{c_p}{c_v}\right) g\, RT_{os}} \qquad \text{(IV-14)}$$

The air density γ for the Reynolds number is determined from the perfect gas law

$$\gamma = \frac{P}{R\, T_{ad}} \qquad \text{(IV-15)}$$

for evaluation of the Reynolds number at minimum value conditions. The pressure P is obtained from the NACA Standard Atmosphere of Table AI-1. This table gives values of δ_o corresponding to altitude, where $P = 2118\delta_o$. The use of ambient pressure is strictly correct only for a flat plate skin on the outer surface of the aircraft. For an application, such as a ram-jet centerbody, the local static pressure should be used to evaluate γ. Therefore the use of $P = 2118\delta_o$ gives values of Reynolds number and heat transfer coefficients, by equations (IV-3) and (IV-4), which are applicable to an external aircraft skin but somewhat low for a ram-jet centerbody skin.

With the flight speed, the characteristic length, the air density, and the air viscosity evaluated at T_{ad} (Figure AI-1), the Reynolds number is calculated from

$$Re = (\gamma u x)/\mu$$

With the quantities previously determined, the substitution constants a, b, and c are also calculated. Equation (IV-12) is next used with an assigned value of the substitution variable, $v = \sqrt{T_w}$, corresponding to $\tau = 0$, and solved for the constant of integration, A. It is then possible to solve equation (IV-12) for any value of τ corresponding to any value of T_w in the range from the initial value assigned to determine A to the limiting value of $T_w = T_{ad}$, where $\tau = \infty$.

Equation (IV-13) for the case of no heat flow through the skin is solved in similar fashion.

EFFECTS OF PRINCIPAL VARIABLES ON SKIN TEMPERATURE RISE

1. Heat Flux Through the Skin

The effect of heat flux on the temperature rise of a skin in supersonic flight is shown in Figure IV-2. For the cases shown, it is assumed that the skin is initially at 392°R, the ambient temperature in the isothermal layer, and that the aircraft is suddenly accelerated into flight at Mach number 3.5, altitude 60,000 ft. The upper curve represents the case of no heat flux through the skin and the lower curve represents the case of q_c = 800 Btu/hr-ft^2. The characteristic length for the Reynolds number evaluation and heat transfer coefficient evaluation is 3 feet, which gives a minimum Reynolds number evaluated at adiabatic wall temperature of 1.05×10^6. This is well within the turbulent flow region.

When there is no heat flux, the skin temperature approaches the adiabatic wall temperature (1230°R) as a limit. With heat flux, the skin approaches some temperature sufficiently below the adiabatic wall temperature to provide temperature potential for the heat flux through the air film. In either case it is apparent that the skin achieves substantially its limiting temperature within four minutes flight time. The tick marks at the beginning of the horizontal portion of the curves indicate the time at which the skin temperature is only 2°R below its limiting value. This same indication is used in succeeding plots.

The small difference in limiting temperatures between $q_c = 0$ and q_c = 800 Btu/hr-ft^2 indicates that considerable variation in heat flux could occur during a flight without having appreciable effect on the skin temperature. This suggests the possibility of analyzing heat transfer processes between the skin of a compartment and any equipment within by using a constant skin temperature, since variations of heat flux between the skin and equipment would not have sufficient effect to change the skin temperature appreciably. Figure IV-2 indicates that the skin temperature selected for such an analysis should be selected appropriate to the order of magnitude of the estimated heat flux. If the heat flux is small, the adiabatic wall temperature is used. If the heat flux is large, the external film heat transfer coefficient should be evaluated using equation (IV-3) or (IV-4) and the appropriate skin temperature determined from equation (IV-2). By means of such a preliminary calculation, the evaluation of external film heat transfer coefficients is eliminated from the calculation of heat transfer between the external air and equipment within the aircraft thus reducing labor in making calculations. It is obvious from the results shown that a constant skin temperature could not be assumed for a very short flight. The use of this simplification is restricted to flight durations that are long

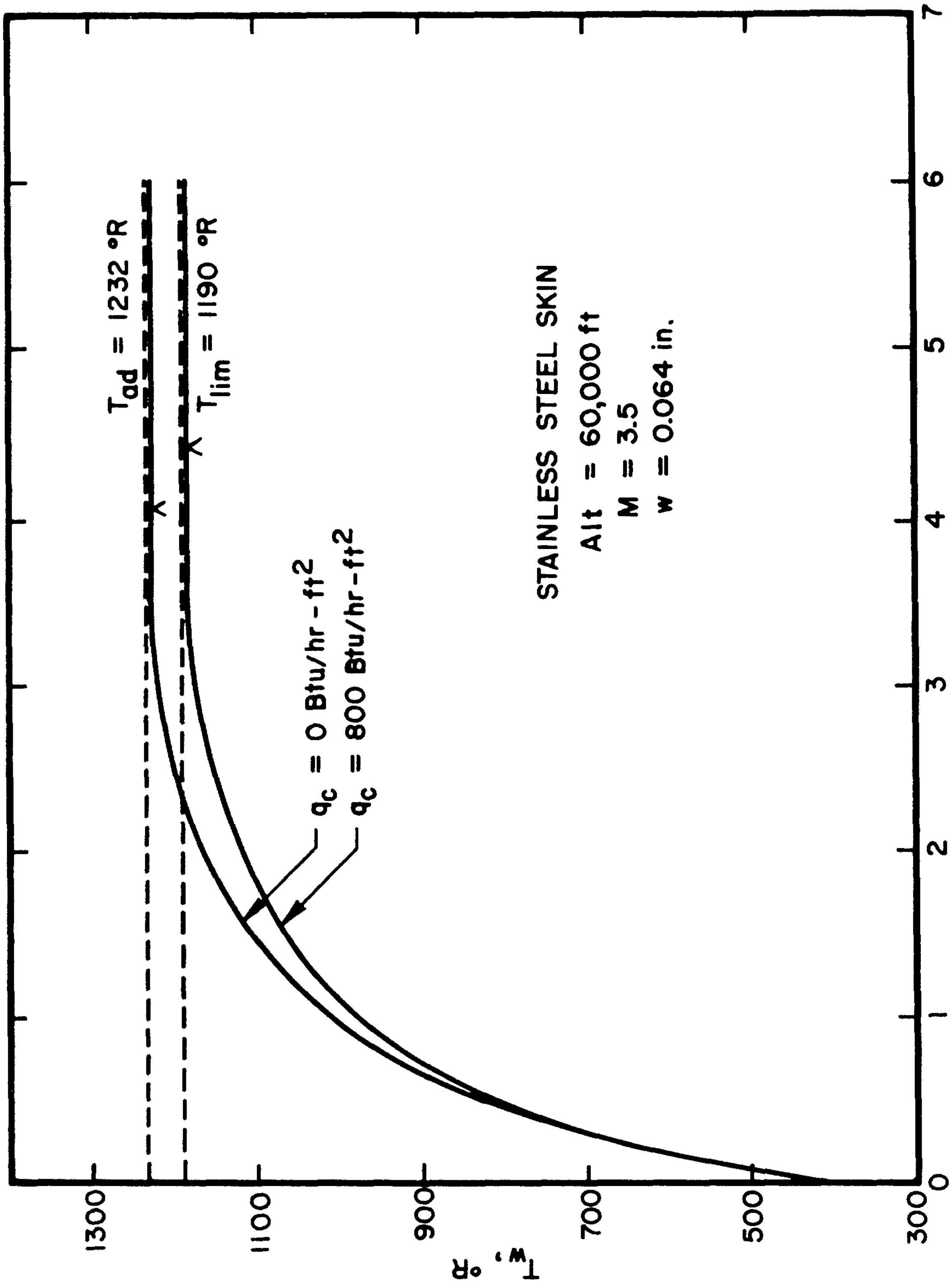

Figure IV-2

Effect of Heat Flux on Skin Temperature Rise

compared to the initial skin heating period. The heat flux is seen to have little effect on the duration of this initial heating period.

2. Flight Altitude

The effects of flight altitude on temperature rise on a skin are shown in Figure IV-3. The cases shown are for no heat flow, Mach number 3.5, and initial skin temperature of 392°R. The minimum Reynolds numbers as evaluated at adiabatic wall temperature and for a characteristic length of 3 feet are as follows:

Altitude	Re
40,000 ft.	2.72×10^6
60,000 ft.	1.05×10^6
80,000 ft.	4.03×10^5
100,000 ft.	1.56×10^5

The values of Re for the two highest altitudes are below the critical turbulent value of Re = 5×10^5 for a flat plate. However, since they are well above the minimum value of Re = 8.4×10^4 for transition flow, turbulent flow heat transfer coefficients are used.

The plots of skin temperature versus time in Figure IV-3 show reduced rates of heating of the skin with increased altitude. Since all cases shown are for the same flight speed and for the ambient temperature of the isothermal layer, the difference in performance is due to the variation of air pressure with altitude only. From equation (IV-4) it is apparent that the film heat transfer coefficient is proportional to $(P)^{0.8}$, so that the lower pressure at higher altitude reduces the heat transfer coefficient. This effect is important in its relation to the assumption of a constant skin temperature for analyzing heat transfer between the skin and equipment. The assumption is not valid for flights at very high altitude, unless the flight time is in the order of about 100 minutes.

3. Flight Speed

The effects of flight speed on temperature rise of a skin are shown in Figure IV-4. The cases shown are for no heat flux, altitude 60,000 feet, and initial skin temperature 392°R. The minimum Reynolds numbers as evaluated at adiabatic wall temperature and for a characteristic length of 3 feet are as follows:

Mach Number	Re
1.5	1.79×10^6
2.5	1.49×10^6
3.5	1.05×10^6

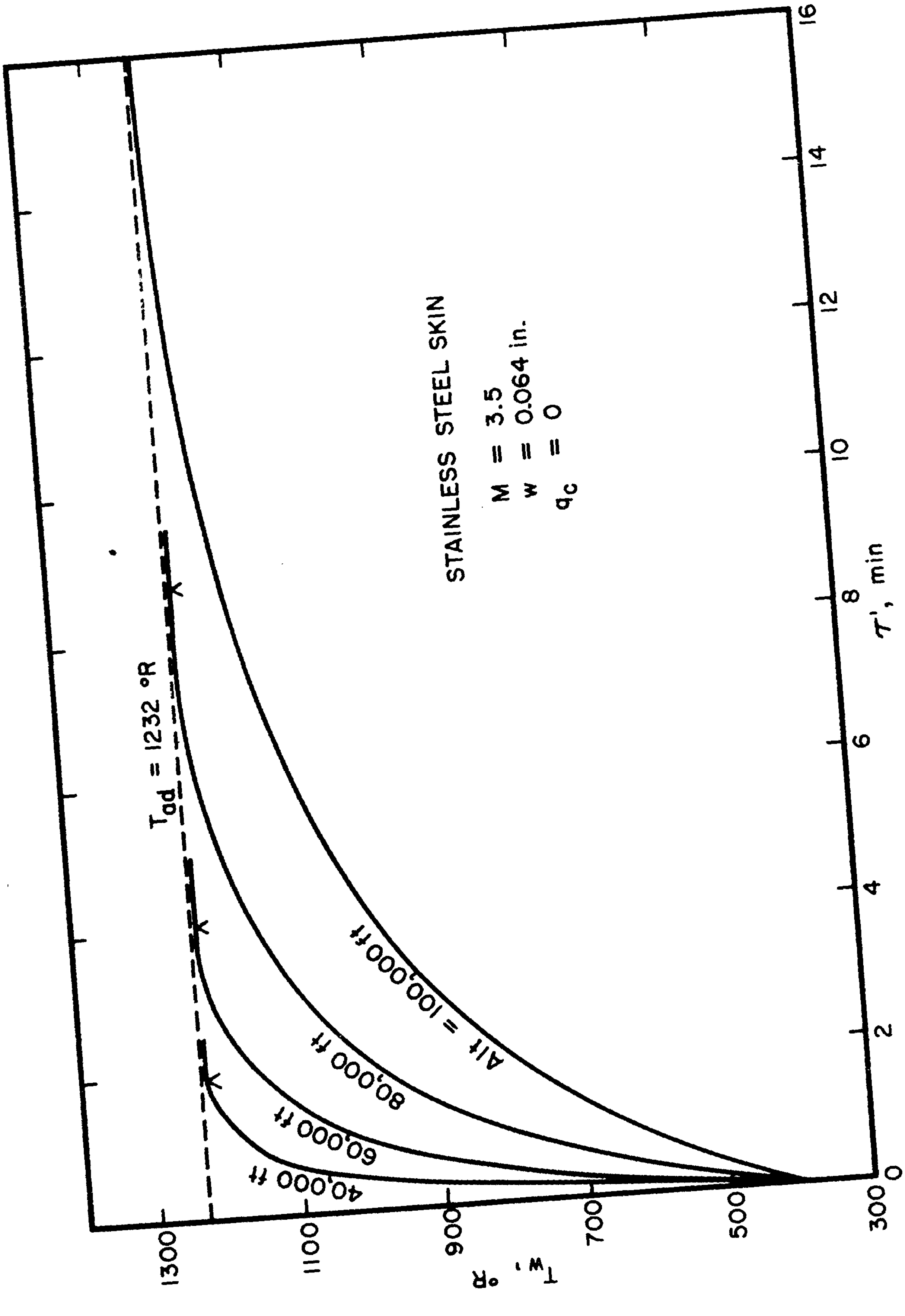

Figure IV-3

Effects of Altitude on Skin Temperature Rise

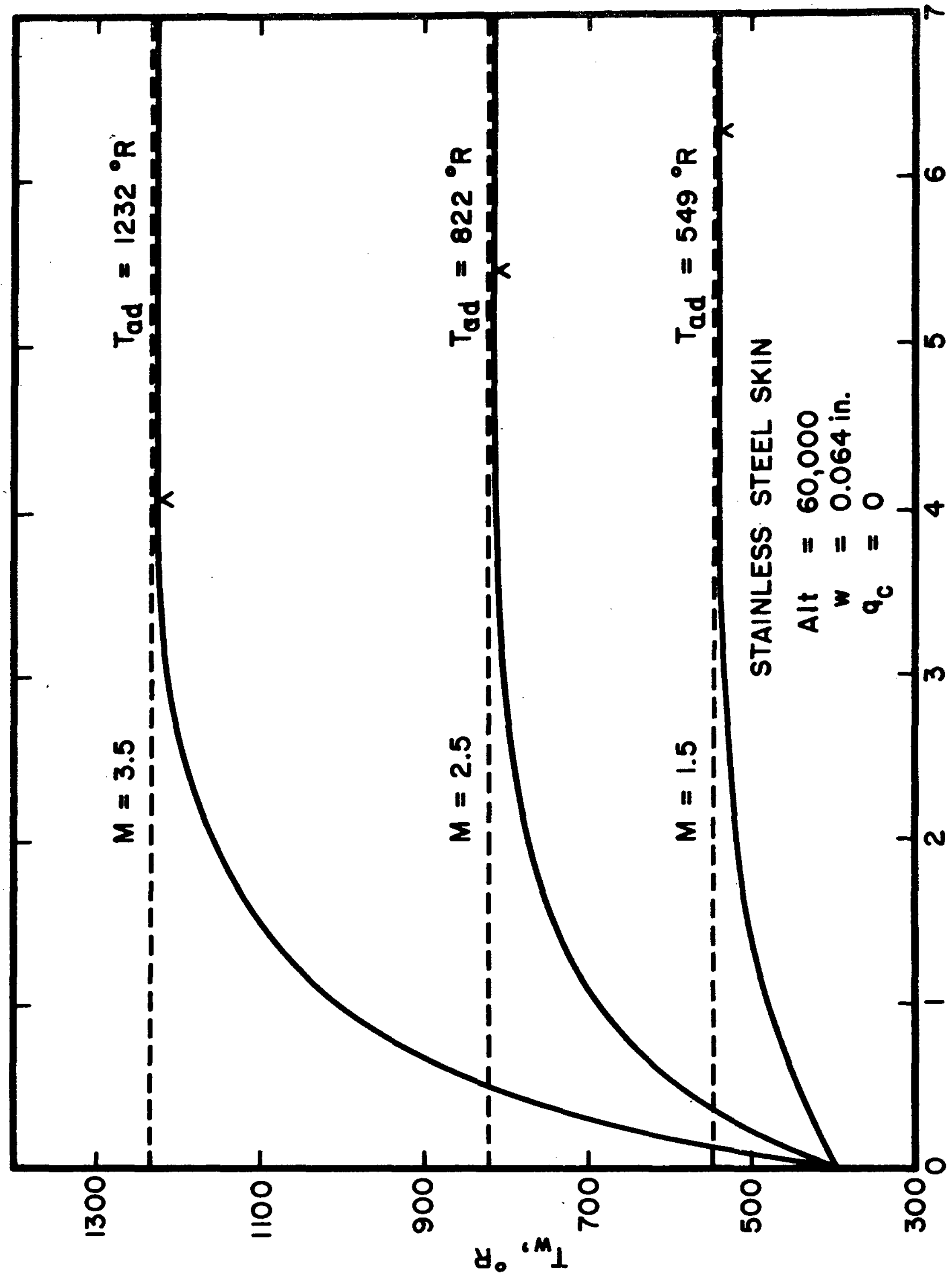

Figure IV-4

Effects of Flight Speed on
Skin Temperature Rise

The Reynolds numbers decrease with increasing flight speed because of the change in adiabatic wall temperature. As flight speed increase, adiabatic wall temperature increases, giving reduced air density and increased viscosity. Both of these effects tend to reduce the Reynolds number, and their combined effect is greater than that of flight speed, which tends to increase the Reynolds number. All of the Reynolds numbers indicate turbulent flow.

The plots of skin temperature versus time given in Figure (IV-4) indicate that the time required for the skin to approach very close to adiabatic wall temperature is decreased slightly for increase of flight speed from Mach = 1.5 to Mach = 3.5. The more rapid heating, in the case of the higher flight speed, results from the higher heat transfer coefficients at higher flight speeds, since h_o is proportional to $(u)^{0.8}$ and the greater average temperature potential, $(T_{ad}-T_W)$. The higher temperature level tends to decrease heat transfer coefficients at higher flight speeds since h_o is proportional to $1/(T_W)^{0.5}$, but this effect is dominated by the other two. It is therefore concluded that the validity of assuming a constant skin temperature for analysis of internal equipment heat transfer processes is nearly independent of flight speed in the supersonic range.

4. Thermal Capacity

The effects of skin thermal capacity on the temperature rise of a skin in supersonic flight are shown in Figure IV-5. The cases shown are for no heat flux, altitude 60,000 feet, and flight Mach number 3.5. As for the earlier cases under these conditions, the minimum Reynolds number is 1.05×10^6, indicating turbulent flow at a characteristic length of 3 feet. The skin thermal capacity is displayed in terms of skin thickness, since, by equation (IV-9), thermal capacity is directly proportional to skin thickness.

The plots of skin temperature versus time show that the time required for a given temperature rise is almost directly proportional to the thermal capacity of the skin. Therefore, if the skin thickness is doubled, the time required for it to rise to nearly its maximum temperature will be approximately doubled. The skin thermal capacity is therefore important in determining the validity of the constant skin temperature assumption for interior heat transfer processes. A thick-skinned missile could not achieve substantially constant skin temperature on a flight of short duration. Therefore the effects of skin thermal capacity and outside film heat transfer coefficient would have to be included in the analysis of heat transfer between the air and the equipment of such a missile.

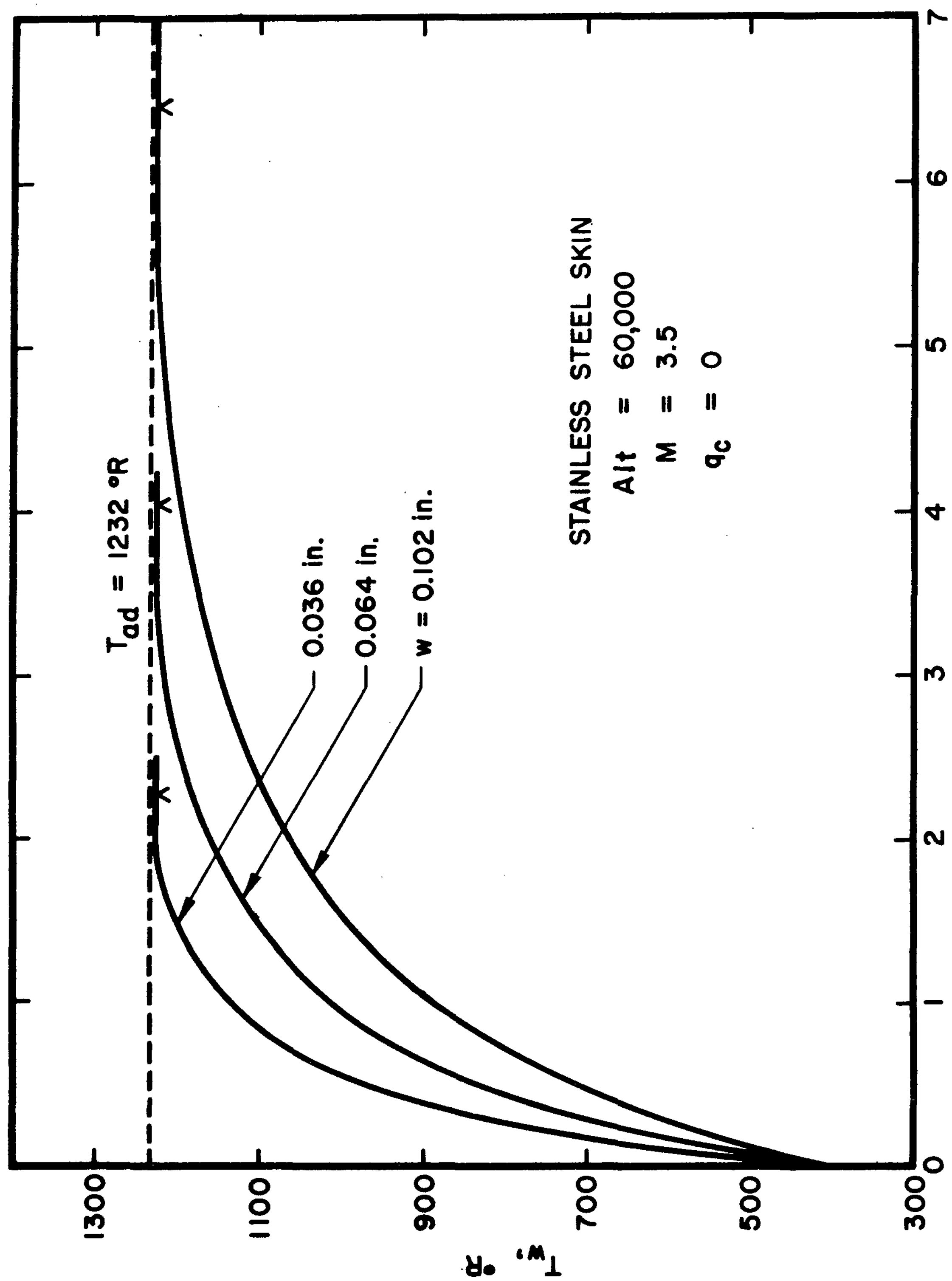

Figure IV-5

Effects of Skin Thickness on Skin Temperature Rise

APPENDIX TO SECTION IV

1. Calculation Procedures and Sample Calculations

Detailed calculation procedures are given here, together with sample calculations, to illustrate the use of equations (IV-12) and (IV-13) for evaluation of skin temperature rise in supersonic flight. There procedures are based on turbulent flow conditions.

Procedure A. Temperature rise of an aircraft skin in supersonic flight with heat flux through the skin.

Given Data:

Altitude = 60,000 ft.
Mach number, $M = 3.5$
Initial skin temperature, $T_{w1} = 392°R$
Stainless steel skin, $w = 0.064$ in.
$c_w = 0.11$ Btu/lb-°R
$\gamma'_w = 490$ lb/ft^3
Characteristic length, $x = 3$ ft.
Heat flux, $q_c = 800$ Btu/hr-ft^2

Calculate time when $T_w = 900°R$

1. Get T_{os} from NACA Standard Atmosphere in Table AI-1,
$T_{os} = 519\theta_o \quad \theta_o = 0.7561 \quad T_{os} = 519 \times 0.07561 = 392°R$

2. Calculate

$$u = M\sqrt{\left(\frac{c_p}{c_v}\right) g\, RT_{os}}$$

$$u = 3.5\sqrt{1.4 \times 4.17 \times 10^8 \times 53.3 \times 392} = 1225 \times 10^4 \text{ft/hr}$$

3. Assume T_{ad} $\quad T_{ad} = 1230°R$

4. Evaluate $r = \sqrt[3]{Pr}$ at T_{ad}, using physical properties of of air from Figure AI-1 at T_{ad}

$$r = \sqrt[3]{.663} = 0.871$$

5. Calculate $T_{ad} = T_{os} + r\left(\frac{u^2}{2gJ\bar{c}_p}\right)$

$$T_{ad} = 392 + \frac{(1225 \times 10^4)^2 \times 0.871}{2 \times 4.17 \times 10^8 \times 778 \times 0.24} = 1232°R$$

(for c_p evaluated at 392°R)

If the calculated value of step 5 agrees within 10°R with the assumed value of step 3, take the calculated value as correct. Otherwise use the calculated result as the assumed value for the next trial, and repeat for agreement within 10°R.

6. Get P from NACA Standard Atmosphere of Table AI-1.
   $P = 2118\delta_o \quad \delta_o = 0.0713 \quad P = 2118 \times 0.0713$
   $= 150.9 \text{lb/ft}^2$

7. Calculate

$$\gamma = \frac{P}{RT_{ad}}$$

$$\gamma = \frac{150.9}{53.3 \times 1232} = 0.0023 \text{ lb/ft}^3$$

8. Get μ at T_{ad} from physical properties of air, Figure AI-1 $\quad \mu = 0.08$ lb/ft-hr

9. Calculate

$$Re = \frac{\gamma ux}{\mu}$$

$$Re = \frac{0.0023 \times 1225 \times 10^4 \times 3}{0.08} = 1,056,000$$

(this value indicates turbulent flow, therefore the remainder of the procedure, based on equation (12), is applicable).

10. Calculate

$$m_w c_w = \frac{\gamma_w c_w W}{12}$$

$$m_w c_w = \frac{470 \times 0.11 \times 0.064}{12} = 0.288 \text{ Btu/°R}$$

11. Calculate

$$a = \left(\frac{0.212}{2m_w c_w}\right)\left[\frac{(uP)^{0.8}}{(x)^{0.2}}\right](T_{ad})$$

$$a = 1.358 \times 10^6$$

12. Calculate

$$b = -\frac{q_c}{2m_w c_w}$$

$$b = -1391$$

13. Calculate

$$c = -\left(\frac{a}{T_{ad}}\right)$$

$$c = -1100$$

14. Calculate

$$v_1 = \sqrt{T_{w1}}$$

$$v_1 = 19.8°R$$

15. Calculate

$$A = -\left(\frac{v_1}{c}\right)+\left(\frac{b}{2c^2}\right)\log_e(a+bv_1+cv_1^2) - \left(\frac{b^2-2ac}{2c^2}\right)\left[\left(\frac{-2}{\sqrt{-d}}\right)\tanh^{-1}\frac{2cv_1+b}{\sqrt{-d}}\right]$$

$$A = -1.108 \times 10^{-2}$$

16. Calculate

$$v = \sqrt{T_w} = \sqrt{1000}$$

$$v = 31.62$$

17. Calculate

$$= \left(\frac{v}{c}\right) - \left(\frac{b}{2c^2}\right)\log_e(a+bv+cv^2) + \left(\frac{b^2-2ac}{2c^2}\right)\frac{-2}{\sqrt{-d}}\tanh^{-1}\left(\frac{2cv+b}{\sqrt{-d}}\right) + A$$

$$\tau = 0.01779 \text{ hr}$$

$$\text{or } \tau' = 1.068 \text{ min}$$

Procedure B. Temperature rise of an aircraft skin in supersonic flight without heat flux throughtthe skin,

Given Data:

Same as example of Procedure A, except q_c = 0 Btu/hr-ft^2

Steps 1 through 13 of Procedure 1 are followed to evaluate the Reynolds number and determine the substitution constant, c.

14. Calculate

$$v_1 = \sqrt{T_{w1}} = \sqrt{392°R}$$

$$v_1 = 19.8$$

15. Calculate

$$B = -\left(\frac{v_1}{c}\right) + \frac{\sqrt{T_{ad}}}{2c}\log_e\left(\frac{\sqrt{T_{ad}}+v_1}{\sqrt{T_{ad}}-v_1}\right)$$

$$B = -0.00232$$

16. Calculate

$$v = \sqrt{T_w} = \sqrt{1000}$$
$$v = 31.62$$

17. Calculate

$$= -\frac{\sqrt{T_{ad}}}{2c} \log_e\left(\frac{\sqrt{T_{ad}}+v}{\sqrt{T_{ad}}-v}\right) + \left(\frac{v}{c}\right) + B$$

$$\tau = 0.01582 \text{ hr}$$
$$\text{or } \tau' = 0.95 \text{ min}$$

2. Reference

(IV-1) Johnson, H.A. etal <u>A Design Manual for Determining the Thermal Characteristics of High Speed Aircraft</u> Army Air Forces Technical Report No. 5632, 10 September 1947, Wright Field, Dayton, Ohio

SECTION V

TEMPERATURE RISE OF EQUIPMENT IN AN UNCOOLED COMPARTMENT DURING SUPERSONIC FLIGHT

By T. C. Taylor, Y. H. Sun, and M. L. Smith

Aircraft equipment will not always require cooling in supersonic flight, even though the flight speed may be great enough to give a skin temperature considerably above the maximum allowable equipment temperature. If at the beginning of flight the equipment is below its maximum allowable temperature, it can absorb heat because of its thermal capacity. The quantity of heat that can be absorbed in this way is proportional to both the thermal capacity and the equipment temperature rise that can be allowed during flight time. Where the combined effect of these factors is great enough, operation of the equipment within the proper temperature range is possible without cooling for flight durations of practical interest. Heat absorbed by uncooled equipment consists of heat which comes into the equipment compartment through the aircraft skin and heat which is generated in the compartment itself. The first of these two heat loads can be reduced by insulation effects and radiation shielding. The generated heat load usually cannot be reduced in an uncooled compartment but its temperature-raising effects can be minimized by increased thermal capacity within the compartment.

The uncooled equipment compartment has the merits of physical simplicity and reliability of performance. Therefore it deserves first consideration in seeking a system to meet desired performance characteristics.

SUMMARY

The temperature rise of equipment due to external and generated heat loads in an uncooled compartment is considered. The external heat load is assumed to consist entirely of free convection and radiation heat transfer from the portion of the aircraft skin or the skin insulation associated with the compartment. The air pressure in the compartment is assumed to be constant and free convection heat transfer is described by using coefficients which are the average of those for a number of regular geometrical shapes. Thermal capacities of skin insulation and air in the compartment are neglected.

Equations are developed, based on a unit skin area, to describe radiation and free convection heat transfer. Calculation procedures based on these equations are given in a general form. The variables describing equipment and compartment characteristics are expressed on a unit skin area basis, permitting wide application of the method to the

study of factors significant to the time-temperature performance of equipment in an uncooled compartment. The significant variables studied are equipment thermal capacity, skin insulation thickness, equipment heat generation rate, ratio of free convection to radiation heat transfer area, compartment air pressure, free convection modulus, and skin temperature. The time-temperature performance evaluations are all made for constant skin temperature, a condition approximated by high flight speeds at constant Mach numbers and constant altitude.

Results of calculations made with the general procedure are used to develop a simplified analysis, based on the nearly linear variation of external heat load with equipment temperature. A design procedure is based on the simplified analysis, and permits determination of the insulation thickness required to limit equipment temperature rise to a desired value. An example design is included with the procedure. The results of a large number of calculations made with the analytical procedures are given. Based on these results, the effects of significant equipment and compartment characteristics can be summarized as follows:

1. Thermal capacity of equipment has a strong delaying effect on equipment temperature rise in an uncooled compartment. The time rate of temperature rise is directly proportional to the sum of external and generated heat loads, and inversely proportional to the thermal capacity of the equipment. Therefore if the thermal capacity of the equipment is doubled, the time required for a given temperature rise is doubled under the same conditions of external and generated heat load. Thermal capacity is the only influence in an uncooled compartment which tends to offset the temperature rise created by both external and generated heat loads. Therefore where space and weight requirements permit, thermal capacity should be added deliberately to a compartment to delay temperature rise.

2. Skin insulation can be used to reduce the external heat load on compartment. In the case of non-heat-generating equipment, insulation is therefore an effective means of delaying equipment temperature rise. In the case of heat generating equipment, insulation is less effective in delaying equipment temperature rise, since it has no effect on the generated heat load. For example, an increase of insulating effect from U_i = 1.0 Btu/hr-ft^2-°R to U_i = 0.20 Btu/hr-ft^2-°R increase the time required for equipment of certain characteristics to heat from 460°R to 860°R from 111 minutes to 385 minutes flight time with a constant skin temperature of 1355°R. For equipment of the same characteristics, but generating 150 watts per square foot of skin area associated with the compartment, the same increase of insulating effect increases flight time only from 50.5 minutes to 75 minutes. Under unfavorable combinations of high generated heat load and low thermal capacity, the space requirements of insulation are likely to be objectionable, particularly in small compartments.

3. The equipment's ratio of free convection surface area to radiation surface area is important in determining the relative magnitude of the equipment's heat gain by free convection. Where possible, equipments should be grouped in a manner which reduces the area available to free convection, such as by butting surfaces against one another, or providing spacings of 3/8-inch and less between equipment surfaces. The same results could sometimes be achieved by encasing a large number of small equipment components together in a single case. The effects of the ratio of convection to radiation surface area are important only where free convection heat load is important compared to generated heat load, radiation heat load, and thermal capacity.

4. Compartment air pressure has great influence on the rate of heat transfer by free convection, and therefore is significant to the rate of equipment temperature rise with time. Heat transfer rate by free convection is proportional to $\delta^{1/2}$ or $\delta^{2/3}$, depending on physical and temperature gradient conditions, where δ is the compartment air pressure, expressed in standard atmospheres. Therefore, the free convection heat load to the equipment can be reduced greatly by maintaining low air pressure in the compartment. If this does not jeopardize equipment operation, it is a good means for obtaining insulating effect against the free convection portion of external heat load, without the spare and weight penalties of insulating materials. As an example, for non-heat-generating equipment in an uninsulated compartment with a skin temperature of 1355°R, a reduction of compartment pressure from $\delta = 1.0$ to $\delta = 0.10$ reduces the average rate of equipment temperature rise by almost 80 percent. This percentage is based on a temperature rise from 460°R to 960°R in both cases. For heat generating equipment, the effect is qualitatively the same, but less pronounced.

5. Surface emissivities of equipment bodies and of the aircraft skin or its insulation are important to heat transferred by radiation. Low emissivities reduce radiation heat transfer. Reflective surfaces should therefore be used to protect equipment from excessive external heat load due to radiation.

ANALYSIS

1. Assumptions for Analysis

Since an uncooled equipment compartment is considered, it is assumed that there is no flow of air into or out of the compartment except as required to maintain constant pressure. It is also assumed that the heat transfer process between the skin and the equipment takes place only through those faces of the equipment compartment which are contiguous with the skin or its insulations, and that no other heat transfer is involved. As an example, Figure V-1 shows a cylindrical compartment containing equipment, and assumed to form part of a ramjet engine centerbody.

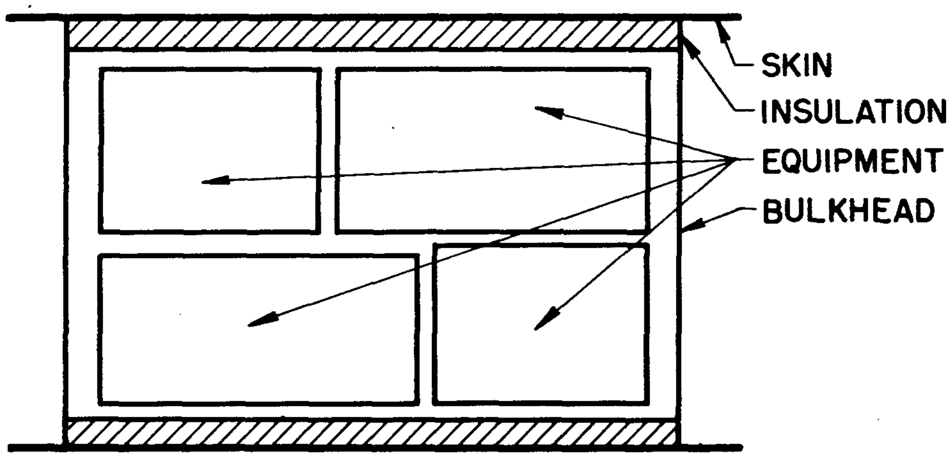

Figure V-1. Schematic of Compartment in a Ramjet Centerbody

Under the assumptions made, heat flows from the centerbody skin into the compartment through the insulated wall only, and no heat is transferred through the interior walls. It is also assumed that no heat is transferred between skin and equipment by solid conduction, which requires that the equipment shock mounts do not attach to the skin or its insulation, or that whatever they do attach to is well insulated and substantially at equipment temperatures. Transfer of heat between the skin and equipment occurs, therefore, by conduction through the skin insulation and by free convection and radiation within the compartment.

It is assumed that efficient use will be made of the compartment space, so that the total of all equipment placed inside will nearly fill the compartment. This permits simple analytical treatment of radiation heat transfer as the case of a totally enclosed body, large compared to its enclosure. Since it is desired to hold radiation heat transfer to a minimum, it is assumed that the skin insulation, where used, is faced on the inner face with a reflective material, such as aluminum foil. It is also assumed that the equipment is cased with a reflective outer surface, although the analysis is general and permits evaluation of instances where reflective protection is not used on either skin insulation or equipment. In addition to the physical configuration and the surface emissivities, radiation heat transfer is also a function of the inner face temperature on the skin or insulation, and of the equipment temperature. For calculation of radiation and free convection heat transfer, it is assumed that all parts of the equipment surface are at the same temperature. This would not actually be true because of variations in surface area, surface emissivity, location, thermal capacity, and heat generation rate of different equipment bodies. The single temperature, however, can be interpreted as a value which appropriately describes an average condition

for the entire equipment surface.

Ordinarily, the equipment installed in an aircraft compartment would be of a variety of shapes and sizes. Fortunately, however, the free convection heat transfer coefficients for vertical plates, horizontal plates facing upward or downward, horizontal and vertical cylinders, and spheres do not vary greatly, so that an average coefficient can be used, eliminating detailed consideration of each equipment surface. This same average value of free convection coefficient applies to the inner surface of the aircraft skin or its insulation, if any. In the use of these coefficients it is assumed that the free convection heat transfer is the same for heating or cooling of a surface. Present knowledge does not warrant making a finer distinction. The surface area of the equipment which is significant to free convection heat transfer is greater than that involved in radiation heat transfer, as there will usually be surfaces accessible to air circulation which are not "seen" by the aircraft skin. This is accounted for in the analysis by introducing the ratio of convective to radiant heat transfer area.

In the derivations to follow, the thermal capacities of the air in the compartment and the skin insulation have been neglected, since they would not be large enough ordinarily to be important. The omission of these two thermal capacity effects has a slightly conservative influence on the calculated equipment temperature rise, since the calculated rise is slightly greater than the actual rise would be.

The heat transfer processes analyzed here are confined to those taking place inside of the aircraft skin, and the equations are put in a form suitable for the case of constant skin temperature during the flight. The assumption of constant skin temperature gives conservative results for equipment temperature rise if the proper interpretation of the skin temperature is observed. For instance, if the skin temperature used is the adiabatic wall temperature corresponding to flight speed and altitude of the aircraft, the calculated equipment temperature rise is greater than would actually occur. The true skin temperature will be less than adiabatic wall temperature by an amount depending on the convection heat transfer coefficient on the outside of the skin and the heat flux through the skin. Therefore, the use of adiabatic wall temperature in place of true skin temperature assumes a greater temperature potential for the transfer of heat from the skin to the equipment than would exist, actually giving conservative results for temperature rise. If the recovery factor for the outside surface of the skin is neglected, and the skin temperature is taken as total temperature for the flight speed and altitude, the results are even more conservative.

2. Nomenclature

Symbol	Definition	Units
A	Surface area	ft^2
a	Empirical constant for external heat load	$Btu/hr\text{-}ft^2$
a'	A convection group, defined in equation (V-7)	
a''	A convection group, defined in equation (V-9)	
B	Temperature function for radiation heat transfer	$°R^3$
b	Empirical constant for external heat load	$Btu/hr\text{-}ft^2\text{-}°R$
C	Empirical coefficient for free convection	dimensionless
c	Specific heat	Btu/lb-°R
c_p	Specific heat at constant pressure	Btu/lb-°R
d	Empirical exponent for free convection	dimensionless
Gr	Grashof modulus = $\frac{gB\theta L^3\gamma^2}{\mu^2}$	dimensionless
g	Gravitational constant = 4.17×10^8	ft/hr^2
h	Heat transfer coefficient	$Btu/hr\text{-}ft^2\text{-}°R$
k	Thermal conductivity	$Btu/hr\text{-}ft^2\text{-}°R$
L	Characteristic length for free convection	ft
M	Weight	lb
m	Weight based on unit skin area	lb/ft^2
P_r	Prandtl modulus $\frac{c_p\mu}{k}$	dimensionless
Q	Heat load	Btu/hr
q	Heat load based on unit skin area	$Btu/hr\text{-}ft^2$
R	Ratio of free convection heat transfer area to radiation heat transfer area	dimensionless
T	Absolute temperature	°R
U	Thermal conductance	$Btu/hr\text{-}ft^2\text{-}°R$
β	Volume coefficient of thermal expansion for air	1/°R
γ	Weight density	lb/ft^3
δ	Pressure	atmospheres
ϵ	Emissivity for radiation heat transfer	dimensionless
ϵ'	Emissivity function	dimensionless
θ	Temperature potential across free convection film	°R

Symbol	Definition	Units
θ_e	Temperature rise	°R
μ	Viscosity	lb/ft-hr
τ	Time	hr
τ'	Time	min

Subscripts

a	Refers to air
c	Denotes free convection value
e	Refers to equipment
g	Denotes generated value
i	Refers to insulation
m	Denotes value at middle of time interval
o	Denotes external value or standard value
r	Denotes radiation value
w	Refers to skin
1	Denotes value at start of a time interval when used with temperature
2	Denotes value at end of a time interval when used with temperature
1,2,..,n	Refers to a series of materials

3. Derivation of Equations

a. Heat Transfer by Conduction Through Skin Insulation

The equation used to describe heat conduction rate from the skin to the inner face of the skin insulation per unit skin area is,

$$q_o = \frac{k_i}{x_i}(T_w - T_i), \tag{V-1}$$

where k_i is the thermal conductivity of the insulating material at the average of the face temperatures, $(T_w+T_i)/2$. This is the equation for a plane wall of insulation (Ref. V-1), since it is assumed that the two face areas of the insulation are substantially the same. During a transient heating problem the average of face temperatures varies with time, making it necessary to account for the variation of insulation thermal conductivity with temperature. For a given thickness of insulation, x_i, the quotient (k_i/x_i) is denoted by U_i, and called the insulation conductance. The variation in value of U_i with temperature can be accounted for in a stepwise calculation of heat conduction by using a plot of values of U_i versus temperature, and using a value for each step of the calculation which is appropriate to the temperature of the insulation during that step. The characteristic of such a plot is different for different insulating materials. Appendix II contains information on the thermal

conductivities of various insulating materials appropriate to this study, and presents graphical aids for computational use.

b. Heat Transfer by Radiation

Heat transferred by radiation from the inner face of the skin or skin insulation to the equipment can be described by the equation,

$$q_r = 0.174 \times 10^{-8}\left(\frac{1}{\frac{1}{\epsilon} + \frac{1}{\epsilon} - 1}\right)(T_i^{\,4} - T_e^{\,4}) \qquad \text{(V-2)}$$

as presented in standard heat transfer texts (Ref. V-1). This equation is more conveniently handled in the form,

$$q_r = h_r\ (T_i - T_e) \qquad \text{(V-3)}$$

where it is apparent that,

$$h_r = 0.174 \times 10^{-8}\ \frac{\left(\frac{1}{\frac{1}{\epsilon_i} + \frac{1}{\epsilon_e} - 1}\right)(T_i^{\,4} - T_e^{\,4})}{(T_i - T_e)}$$

For calculation purposes, this is put in the form

$$h_r = 17.4 \times 10^{-4}\ \frac{1}{\frac{1}{\epsilon_i}+\frac{1}{\epsilon_e} - 1}\left[\frac{\left(\frac{T_i}{100}\right)^4 - \left(\frac{T_e}{100}\right)^4}{\left(\frac{T_i}{100}\right) - \left(\frac{T_e}{100}\right)}\right] \qquad \text{(V-4)}$$

In the evaluation of any particular compartment, the emissivity values for surfaces are taken as constant, so that equation (V-4) can be reduced to a constant times a function of the temperatures, T_i and T_e. Figure AIV-1 gives a chart of this temperature function versus T_i and T_e, which can be used for radiation heat transfer calculations. The individual values of emissivity, ϵ_1 and ϵ_2 are chosen for the material and condition of the radiating and receiving surfaces. The possible range of values is from $\epsilon \approx 0.02$ for highly polished copper to $\epsilon \approx 0.98$, for rough steel plate or certain painted surfaces. In most of the evaluation cases it may be assumed that $\epsilon_i = 0.10$ and $\epsilon_e = 0.20$; values which represent aluminum or aluminum-treated surfaces that are somewhat oxidized from high temperature exposure.

c. Free Convection Heat Transfer Coefficients

An equation to describe free convection heat transfer coefficients is taken from Reference (V-1),

$$h_c = C \frac{k}{L} \left(\frac{g\beta\theta L^3 \gamma^2 c_p}{\mu k} \right)^d \qquad \text{(V-5)}$$

where the exponent, d, assumes values in accordance with the schedule,

$(Gr \times Pr) = \dfrac{\beta\theta L^3 \gamma^2 c_p}{\mu k}$	d	C
10^3-10^9	1/4	0.532
$> 10^9$	1/3	0.120

The value of C to use in equation (V-5) is also dependent upon the value of the modulus (Gr x Pr), but in addition, is dependent on the shape and position of the surface. As discussed earlier, it is convenient to use a value of C which represents a good average for a variety of surface configurations, and those values shown in the schedule are such average values. In particular, it is noted that the free convection coefficient is somewhat simplified when $(Gr \times Pr) > 10^9$, as it becomes,

$$h_c = 0.12k \left(\frac{g\beta\theta \gamma^2 c_p}{\mu\ k} \right)^{1/3} \qquad \text{(V-6)}$$

where the characteristic length L is no longer involved. All of the physical properties of air in equation (V-6) are functions of temperature, except γ which is a function of temperature and pressure. Since γ is directly proportional to pressure, it can be written $\gamma = \delta \gamma_o$ where γ_o is the air density at one standard atmosphere, and δ is the compartment air pressure in atmospheres. Substituting this, and rearranging, equation (V-6) can be written

$$h_c = \left(\frac{a'}{\delta^{2/3}} \right) (\delta^{2/3}) \quad (\theta)^{1/3} \qquad \text{(V-7)}$$

where

$$\left(\frac{a'}{\delta^{2/3}} \right) = 0.12k \left(\frac{g\beta \gamma_o^2 c_p}{\mu k} \right)^{1/3}$$

A plot of the quantity $(a'/\delta^{2/3})$ as a function of temperature may be used in evaluating equation (V-7). When $(Gr \times Pr) = 10^3$-10^9, equation (V-5) becomes,

$$h_c = 0.532 \frac{k}{L} \left(\frac{g\beta\theta L^3 \gamma^2 c_p}{\mu k} \right)^{1/4} \qquad \text{(V-8)}$$

where the characteristic length L remains in the equation, and must be defined before the equation can be used. Applying a similar line of reasoning to that used in deriving equation (V-7), equation (V-8) can be put in the form,

$$h_c = \left(\frac{a'' L^{1/4}}{\delta^{1/2}}\right)\left(\frac{\delta^{1/2}}{L^{1/4}}\right)(\theta)^{1/4} \tag{V-9}$$

where

$$\left(\frac{a'' L^{1/4}}{\delta^{1/2}}\right) = 0.532\ k \left(\frac{g\beta \gamma_o^2 c_p}{\mu k}\right)^{1/4}$$

The problem of assigning an appropriate value to L in equation (V-9) is not clear cut. Reference (V-1) discusses methods for selecting L for single bodies of various configurations. In the case of a number of pieces of equipment installed in a compartment, however, the characteristic length should be properly interpreted. If the separate bodies are freely spaced, individual values of L for the separate bodies might reasonably be averaged for an overall value. If several bodies are closely packed so as not to allow free circulation of air between them, the overall external dimensions of the group could reasonably be used as characteristic dimensions for that group. Fortunately the value used for L does not influence the value of h_c in equation (V-9) heavily, so that approximate values of L can be expected to give good results.

The transient equipment heating problem at hand is one in which both the temperature level and the temperature difference θ vary. It is therefore not immediately clear which of the equations (V-7) or (V-9) to use in a given case of which all initial conditions might be known. It will be shown later that for values of L of approximately one foot, equations (V-7) and (V-9) yield very nearly the same result, making it possible to obtain good results for many problems using either equation.

d. Heat Transfer by Free Convection

It is necessary to develop an equation which makes proper use of the free convection heat transfer coefficients in describing heat transfer between the interior skin or insulation temperature T_i and the equipment temperature T_e. Heat coming in from the skin and through the skin insulation must next pass by free convection to the air in the compartment or by radiation directly to the equipment. That portion of the heat which enters the air by free convection is described by the equation,

$$q_c = h_{ci}\ (T_i - T_a) \tag{V-10}$$

where $(T_i - T_a)$ is the value of θ to use in determining h_{ci} from equation (V-7) or (V-9), and where q_c is the time heat transfer rate by free convection, for a unit skin surface area. The group $(a'/\delta^{2/3})$ of equation

(V-7) or ($a''L^{1/4}/\delta^{1/2}$)of equation (V-9) is evaluated at the temperature $(T_i + T_a)/2$. This same rate of heat transfer must pass by free convection from the air to the equipment, as described by the equation,

$$q_c = Rh_{ce}\,(T_a - T_e) \tag{V-11}$$

where $(T_a - T_e)$ is the value of θ to use in determining h_{ce} from equation (V-7) or (V-9) and R is the ratio of total free convection surface area of equipment to total aircraft skin area associated with the compartment. The group containing physical properties of air for equation (V-7) or (V-9) is evaluated at the temperature $(T_a + T_e)/2$. These two equations are then rearranged and added to give

$$\frac{q_c}{h_{ci}} + \frac{q_c}{Rh_{ce}} = (T_i - T_a) + (T_a - T_e)$$

Then

$$q_c = \frac{1}{\dfrac{1}{h_{ci}} + \dfrac{1}{Rh_{ce}}}\,(T_i - T_e) = h_c\,(T_i - T_e) \tag{V-12}$$

e. Combined Heat Transfer by Conduction, Radiation and Free Convection

As discussed above, equations are available to describe completely the details of the heat transfer processes between the aircraft skin and the equipment. Equation (V-1) is used to describe heat conduction from the skin to the inner face of the insulation, equation (V-3) is used to describe heat radiation from the inner face of the insulation to the equipment, and equation (V-12) is used to describe heat transfer by free convection from the inner face of the insulation to the equipment. Writing a heat balance for the combined effect of all these processes gives the equation,

$$q_o = q_r + q_c$$

Then, by substituting, and denoting the overall free convection coefficient of equation (V-12) by h_c,

$$q_o = U_i(T_w - T_i) = (h_r + h_c)\,(T_i - T_e)$$

Then,

$$\frac{q_o}{U_i} + \frac{q_o}{h_r + h_c} = (T_w - T_i) + (T_i - T_e)$$

or,

$$q_o = \frac{1}{\frac{1}{U_i} + \frac{1}{h_r + h_c}} (T_w - T_e) \qquad \text{(V-13)}$$

where the heat transfer rate per unit skin area is shown as a function of the insulation conductance, the radiation coefficient, the overall free convection coefficient, and the temperature difference between the skin and the equipment. Since all of the heat transferred is stored in the thermal capacity of the equipment, another heat balance equation may be written, for the case where there is no heat generation in the compartment,

$$q_o = m_e c_e \frac{\Delta T_e}{\Delta \tau} \qquad \text{(V-14)}$$

In equation (V-14) the thermal capacity product $m_e c_e$ is based on m_e as the average weight of equipment per unit skin area associated with the compartment, and c_e is a weight-average specific heat for all equipment material. A method for determining the thermal capacity product on a unit skin area basis is given later with the calculation procedure.

If there is heat generation in the compartment, equation (V-14) is modified to

$$q_o + q_g = m_e c_e \frac{\Delta T_e}{\Delta \tau} \qquad \text{(V-15)}$$

where q_g is the heat generation rate of the equipment, based on a unit skin area.

4. Procedure for Calculation of Equipment Temperature Rise with Time

a. General Method

Although the equations developed are sufficient to describe heat transfer from the skin to equipment, they cannot be combined to yield a direct solution for temperature rise of equipment with time. This results from the complicated functions which must be used to describe radiation and free convection heat transfer coefficients. Coefficients of both types are involved in the term q_o of equation (V-15), and are functions of T_i, T_a, and T_e. For any instant of time, the temperatures T_i, T_a, and T_e are in turn functions of q_o itself, indicating the complexity of the problem. It is therefore necessary to use a stepwise calculation process, applying the equations to short, finite intervals of time for which the heat transfer coefficients are substantially constant. Two such stepwise procedures are conveniently applicable to this problem. In one, the values of all coefficients are based on temperatures at the beginning of

an interval. The coefficients are then used to calculate heat transfer rates, and to calculate the temperatures at the end of an interval. This method permits direct calculation for each interval. In the second method, values of the heat transfer coefficients are based on average temperatures within an interval. Since these temperatures are unknown at the beginning of an interval calculation, it is necessary to assume them and then check them later, which is a trial and error process. This method involves more calculation labor and requires more skill than the first one described, but for equally sized intervals it is more accurate. The trial and error method is described here, since it is more generally valid. A detailed calculation procedure, together with a sample calculation, is given in the Appendix to this Section.

The calculation is more conveniently carried out on the basis of heat transfer per unit area of the skin. This requires that the total surface area of the equipment for purposes of free convection heat transfer be determined, and divided by A_w, the total skin area associated with the compartment, to give R_o. The total surface of equipment which is accessible to free convection can only be estimated. In general, it is the entire external surface area, minus those areas which face narrow gaps (3/8-inch and less), or which are located so as to be inaccessible to free circulation of air. The thermal capacity of equipment is also expressed on a unit area basis. Thus, if A_w denotes the skin area and M_e denotes the total weight of equipment in the compartment,

$$m_e = \frac{M_e}{A_w}$$

and if there are M_1 pounds of material having specific heat c_1 in the compartment, M_2 pounds of material having specific heat c_2 in the compartment, and so on,

$$c_e = \frac{M_1c_1 + M_2c_2 + \cdots + M_nc_n}{M_e}$$

Heat generation by the equipment is also expressed on a unit skin area basis. If Q_g is the total heat generation rate for the compartment,

$$q_g = \frac{Q_g}{A_w}$$

The procedure described here is for the case of constant aircraft skin temperature, as approximated by constant flight speed and altitude. Modifications required to account for varying skin temperature will be indicated later. Equation (V-7) is used to describe free convection heat transfer. The corresponding procedure for use of equation (V-9) requires no special attention other than defining a value of L.

b. Calculation of Initial Temperatures

Calculation begins with the value of T_w assigned and the initial value of T_e assigned as T_{e1}. It is then necessary to assume initial values of T_{i1} and T_{a1}, and evaluate h_r using equation (V-4), h_{ci} using equation (V-7), and h_{ce} using equation (V-7). Experience in performing calculation of this type will aid in selecting values of T_{i1} and T_{a1} for the first trial. In the absence of such experience it can only be pointed out that both T_{i1} and T_{a1} lie between T_w and T_{e1} with $T_{i1} > T_{a1}$ for $T_w > T_{e1}$. After determining h_r, h_{ci}, and h_{ce}, equations (V-1) and (V-13) are combined and solved for T_{i1}, and equations (V-10) and (V-12) are combined and solved for T_{a1}. If the values of T_{i1} and T_{a1} resulting from this calculation agree with those assumed, they are correct. If not, new values of T_{i1} and T_{a1} must be assumed and the calculations repeated until agreement of assumed and calculated values is obtained. It has been found from experience that the calculated results are closer to the true values of T_{i1} and T_{a1} than the assumed values, so that in a series of trials, the results of one calculation can be used as assumed values for the next calculation. Thus far the work indicated has determined only the initial values of T_{i1} and T_{a1} corresponding to the assigned values of T_w and initial T_{e1}.

c. Calculation of Transient Temperature Rise

The analysis of transient performance begins with an assumed time interval, $\Delta\tau$, during which all temperatures rise from their initial value, indicated by subscript 1, to their final value for this time interval, indicated by subscript 2. The proper size of time interval to use is dependent on the accuracy required in the transient calculation. The variation of temperature T_i, T_a, and T_e with time is in general not linear, although a time interval calculation process of the type to be described assumes that the variation can be considered linear for short, finite intervals of time. The surest way to determine whether the intervals selected are short enough is to experiment with time intervals of various lengths to find the largest which may be used without detriment to accurate results. The reader is referred to paragraph (d) of this section for a discussion of the size of time interval to use and the agreement which is required between assumed and calculated temperature values.

For any time interval selected, it is necessary to assume values of T_{i2}, T_{a2}, and T_{e2}. Then h_r is determined based on T_{im} and T_{em}, where T_{im} is equal to $(T_{i1} + T_{i2})/2$, and so on for the other temperatures. h_{ci} is found for T_{im} and T_{am}, and h_{ce} is found for T_{am} and T_{em}. Equation (V-13) is then used to determine q_o using the mean temperatures (subscript m), after which equation (V-15) can be solved for ΔT_e. The calculated value of T_{e2} is then found from T_{e1} and ΔT_e. Equations (V-1) and (V-13) are then used as before to check the value of T_{i2}, and equations (V-10) and (V-11) are used to check the value of T_{a2}. If the calculated results of T_{e2}, T_{a2}, and T_{i2}, do not agree with assumed values for the interval $\Delta\tau$, the

calculation is repeated, taking the calculated results of the first trial as the assumed values of the second trial. On successful completion of an interval, the results T_{i2}, T_{a2}, and T_{e2} are used as initial values T_{i1}, T_{a1}, and T_{e1} for the next interval, and the entire trial and error process is repeated until the time span or temperature span of interest for the equipment has been covered.

The calculation procedure described above is given in greater detail in the Appendix to this Section. Although the detailed procedure in analytically the same as described, in certain cases algebraic modifications are made to make the procedure amenable to slide rule calculations. The procedure is somewhat simplified in cases where there is no skin insulation, since T_i then becomes T_w, and the number of assumed values required for calculating an interval is reduced from three to two. This simpler procedure for an uninsulated compartment is also given in the Appendix to this Section.

d. Characteristics of the Calculation Procedure

The trial and error calculation procedures are somewhat lengthy, and require some practice before a computor can advance from one interval to the next with only one or two trials. Fortunately, however, a rather wide discrepancy can exist between the assumed temperature values and the calculated temperature values without affecting the accuracy of the latter appreciably. A careful analysis has shown that the most serious error in equipment temperature rise calculated for an interval occurs when there is no skin insulation, and no heat generation by the equipment. Under these circumstances it was found that if the calculated equipment temperature is within 7°R of the assumed value, the calculated value of equipment temperature rise for the interval is accurate within one per cent. For cases with insulation and/or heat generation, the discrepancy allowable between assumed and calculated values is greater. Actually the discrepancy of 7°R is most ample, since a computor can easily assume values within 3 or 4°R of the calculated results, which is the standard of accuracy maintained in all of the calculations reported in this Section.

The analysis of the effect of interval size on the accuracy of calculated equipment temperature rise has shown that initial intervals of $\Delta \tau' = 15$ minutes are sufficiently small to give at least one per cent accuracy of the calculated temperature rise. This applies only to the calculations made for this Section, however, and in general it is necessary to experiment with differently sized intervals to determine the largest that can be used. For example, a calculation may be started using a single ten-minute interval, and then reworked using two five-minute intervals. If the results at ten minutes are in substantial agreement, the ten-minute interval can be used with confidence. If not, further reduction of the interval size should be tried until the largest accurate time interval allowed is found. It should also be noted that an interval which is appropriately sized for the initial part of a calculation may be too large or unnecessarily small for later intervals in the calculation.

Therefore a few spot checks should be made during a calculation to see that the proper size of time interval is being maintained.

e. Extension of the Procedure Required in the Case of Variable Skin Temperature

Although the procedure described is for the case where the skin temperature can be considered constant, it is also possible to evaluate a case in which the skin temperature varies. This would occur for varying flight speed, or where the heat flow through the skin is large and varying, while the outside convection coefficient on the skin is small. To evaluate such a case, the outside convection coefficient must be evaluated for each time interval, using the relationships given in Section IV. This requires the introduction of another assumed value, T_w, into the procedure for calculating each time interval. In most cases the skin thermal capacity can be neglected, as found in Section IV.

EFFECTS OF EQUIPMENT AND COMPARTMENT CHARACTERISTICS

1. Thermal Capacity

The effects of thermal capacity of equipment on the temperature rise of equipment with time are shown in Figure V-2. The cases shown are for non-heat-generating equipment in a compartment without insulation. The initial equipment temperature is 460°R, and the constant skin temperature is 1355°R (the total temperature corresponding to to a flight Mach number of 3.5 in the isothermal layer). Equation (V-7) is used to describe the face convection relationships for this figure. To illustrate the significance of the thermal capacity values shown, consider a compartment having an associated skin area of 18 square feet, and containing 200 pounds of equipment. If the equipment consists of aluminum, iron, and ceramic parts, the entire mass of equipment might have an average specific heat of the order of 0.18 Btu/lb-°R, so that the thermal capacity on a unit area basis would be (200 x 0.18)/18 = 2, which is one of the cases shown.

It is readily seen from the cases shown in Figure V-2 that the time required for equipment to heat to any given temperature is about proportional to the thermal capacity of the non-heat-generating equipment. Equation (V-15) can be rearranged to the form,

$$\Delta\tau = m_e c_e \frac{\Delta T_e}{(q_o + q_g)} \qquad \text{(V-16)}$$

This shows the analytical basis for the effect of thermal capacity as shown by the cases of Figure V-2, and indicates that a similar result can be expected for heat generating equipment. To consider this from

another standpoint, equation (V-16) can be rearranged to,

$$\frac{\Delta T_e}{\Delta \tau} = \frac{q_o + q_g}{m_e c_e}$$

This indicates that the slope of the curves, or time rate of temperature rise, is directly proportional to the instantaneous heat load, and inversely proportional to the thermal capacity. All of the cases shown in Figure V-2 have the same instantaneous heat load at their starting point, 460°R, so that their initial rates of temperature rise are inversely proportional to thermal capacity. Similarly, the temperature curves shown intersect any horizontal line of constant temperature at a slope which is inversely proportional to their respective thermal capacities and directly proportional to the external heat load corresponding to that temperature.

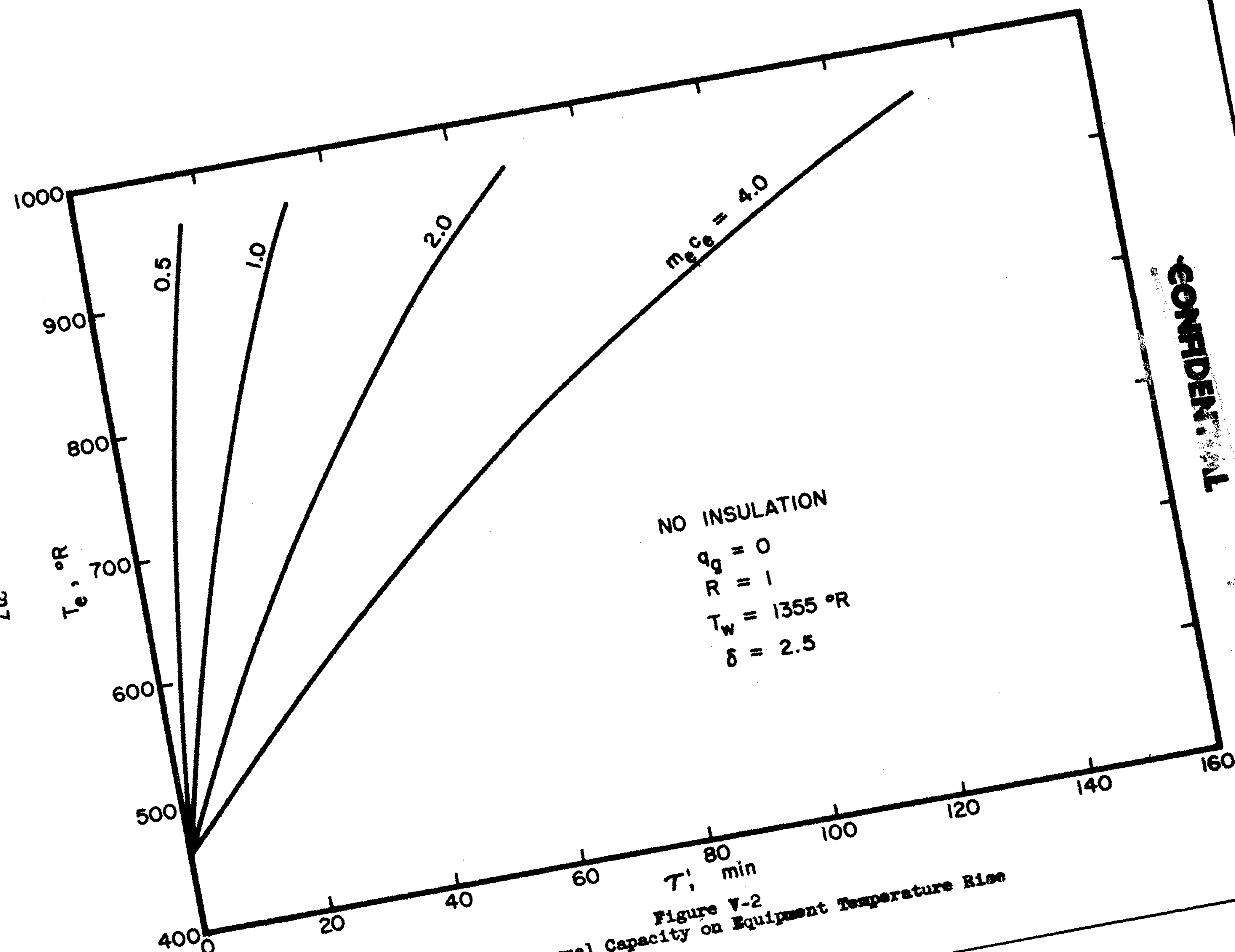

Figure V-2
Effect of Thermal Capacity on Equipment Temperature Rise

It should be noted from equation (V-16) that the temperature rise delaying action of thermal capacity tends to offset the sum of both external and generated heat loads. Thermal capacity is thus more effective in delaying temperature rise of heat generating equipment then insulating effects, since the latter affect only the external heat load. The strong temperature rise delaying effect of thermal capacity suggests that in cases where space and weight requirements permit, thermal capacity could be added deliberately to prevent equipment overheating. For example, cans of water have a high ratio of thermal capacity to weight and could be used for this purpose. As an illustration, it is interesting to consider the compartment described earlier containing 200 pounds of equipment. If 36 pounds of water were added to this compartment, the thermal capacity based on a unit of skin area would be increased to (200

$$(200x.18+36x1)/18 = 4$$

thereby reducing the time rate of temperature rise to one-half its former value. This assumes no essential change in the other configuration features of the compartment or equipment.

The results shown in Figure V-2 can be applied to initial equipment temperatures other than 460°R; provided the skin temperature remains the same. To do this, it is only necessary to shift the time axis so that its zero point ($\tau = 0$) lies directly beneath the new initial temperature on the curve representing the $m_e c_e$ value considered. As an example, for a compartment having $R = 1$, $M_e c_e = 4$, $\delta = 2.5$, $T_w = 1355°R$, $T_{e_1} = 600°R$, the time axis is shifted to the right so that the $\tau = 0$ point lies at the 27 minute point as plotted in Figure V-2.

2. Insulation

The effects of skin insulation of the temperature rise of equipment with time are shown in Figure V-3. The cases shown are for non-heat-generating equipment, initially at 460°R, and a compartment skin temperature of 1355°R. The insulation thickness is defined in terms of the insulation conductance, $U_i = (k_i/x_i.)$ Thus, the case of $U_i = \infty$ represents no insulation, while $U_i = 0.20$ represents the greatest insulation thickness shown. The value of k_i, insulation thermal conductivity, varies with temperature in a manner dependent on the type of insulation material used (see Appendix II). All of the cases of Figure V-3 are for a temperature variation of thermal conductivity representative of rock wool insulation. It is emphasized that although insulation thermal conductivity should be based on average insulation temperature, the insulation used must be able to withstand the skin temperature without physical deterioration. The skin temperature of the cases shown in Figure V-3 and elsewhere is above the maximum value generally quoted for rock wool, which is 600°F or 1060°R. The rock wool designation was selected solely to represent a type variation of thermal conductivity with temperature, which seems to be representative also of other insulating materials (Appendix II).

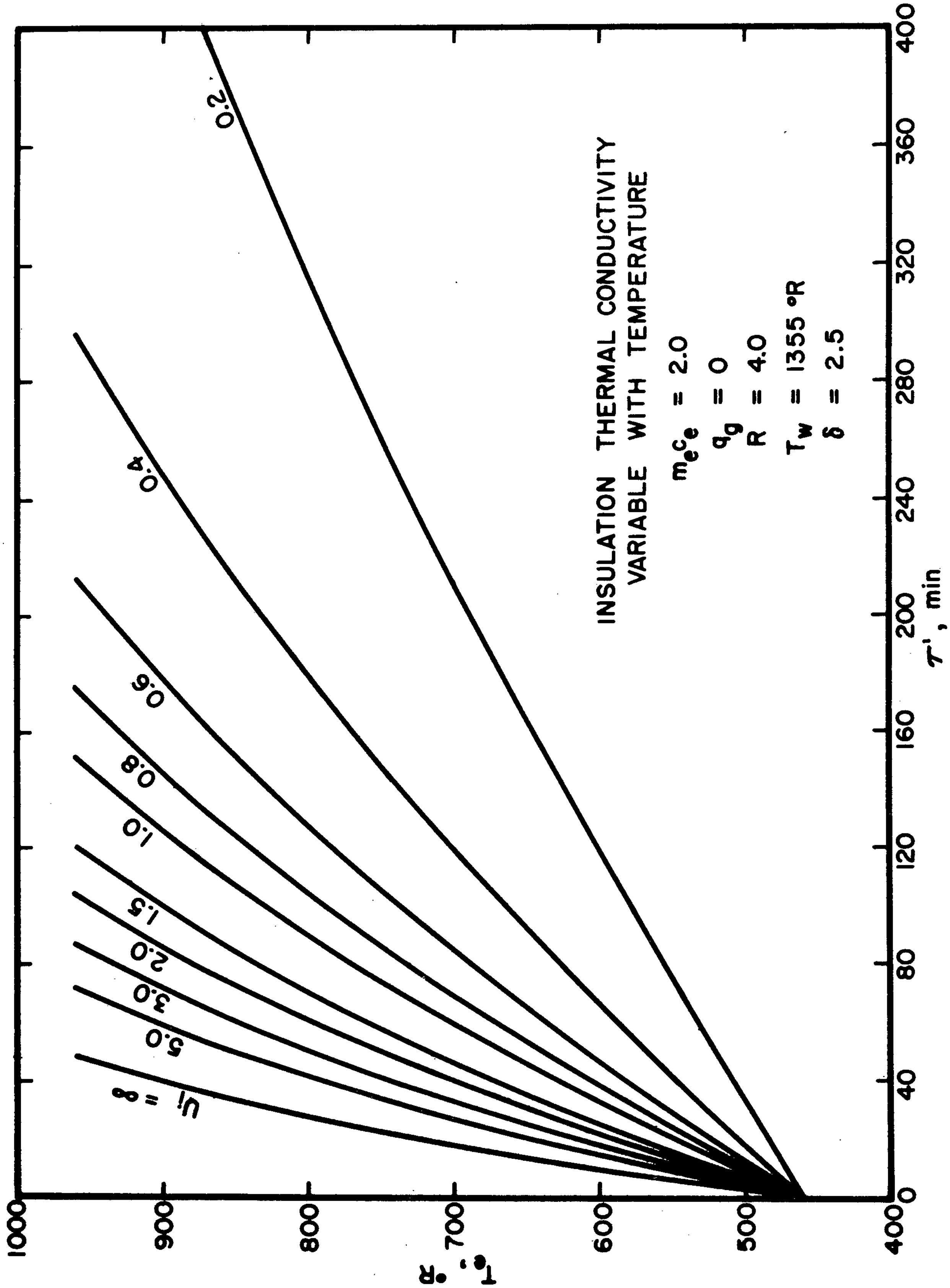

Figure V-3
Effect of Insulation Conductance on Equipment Temperature Rise

The value of U_i shown for each case is that which applies to the mean temperature of insulation at the start of transient heating, when $T_e = 460°R$. This same method of defining U_i is used wherever insulated compartments are considered.

From Figure V-3 it is apparent that insulation has a strong effect in delaying equipment temperature rise for non-heat-generating equipment. The rearrangement of equation (V-16), taking $q_g = 0$, shows that the time rate of equipment temperature rise in proportional to the external heat load. The effect of increased insulation thickness is to reduce this heat load, explaining the results shown. The external heat load is a function of other factors besides insulation, however, so that its effects cannot be determined quantitatively except in terms of specific examples, such as given in Figure V-3.

The effect of using different insulating materials to achieve the same initial insulation effect is shown in Figure V-4 for two values of initial conductance, U_i. The curves shown for constant conductance are given as standards of comparison only, since there are no actual insulating materials whose thermal conductivity does not vary with temperature. The curves shown for rock wool and Refrasil show more rapid heating of the equipment than for constant thermal conductivity insulation. This is due to the increase of thermal conductivity with increase of temperature.

Some representative cases with heat generating equipment in an uninsulated compartment are shown in Figure V-5. Although the effect of insulation is qualitatively the same as when used with non-heat-generating equipment as in Figure V-3, it is seen that for a change from $U_i = 1.0$ to $U_i = 0.2$ the change in time to heat to a given temperature is relatively smaller for the case with heat generation. This could be expected from equation (V-16), since the insulation affects only external heat load, and in Figure V-5 the equipment is subject to generated heat load in addition to the external heat load. Rock wool type insulation is used for the cases of Figure V-5, and equation (V-7) is used to describe free convection for all of the cases in Figures V-3,-4, and 5.

It is convenient to consider an example to illustrate the value and limitations of using insulation to limit rate of equipment temperature rise. Suppose it is desired to extend the temperature rise of non-heat-generating equipment from 460°R to 900°R to a time in excess of 80 minutes, where $R = 4$, $\delta = 2.5$, $M_e c_e = 2.0$, $T_w = 1355°R$. Figure V-3 shows that this condition will be met by an insulating effect of $U_i = 2.0$. If the equipment has a heat generation rate of $q_g = 150$ watts/ft^2, however, Figure V-5 shows that $U_i = 0.20$ would be required, or ten-times the insulation thickness of the non-heat-generating case. For an insulation having $k_i = 0.05$ Btu/hr-ft-°R $U_i = 2.0$ would represent only 0.3 inch insulation, while for $U_i = 0.2$, 3 inches of insulation are required. In the case of a medium or small compartment 3 inch insulation might

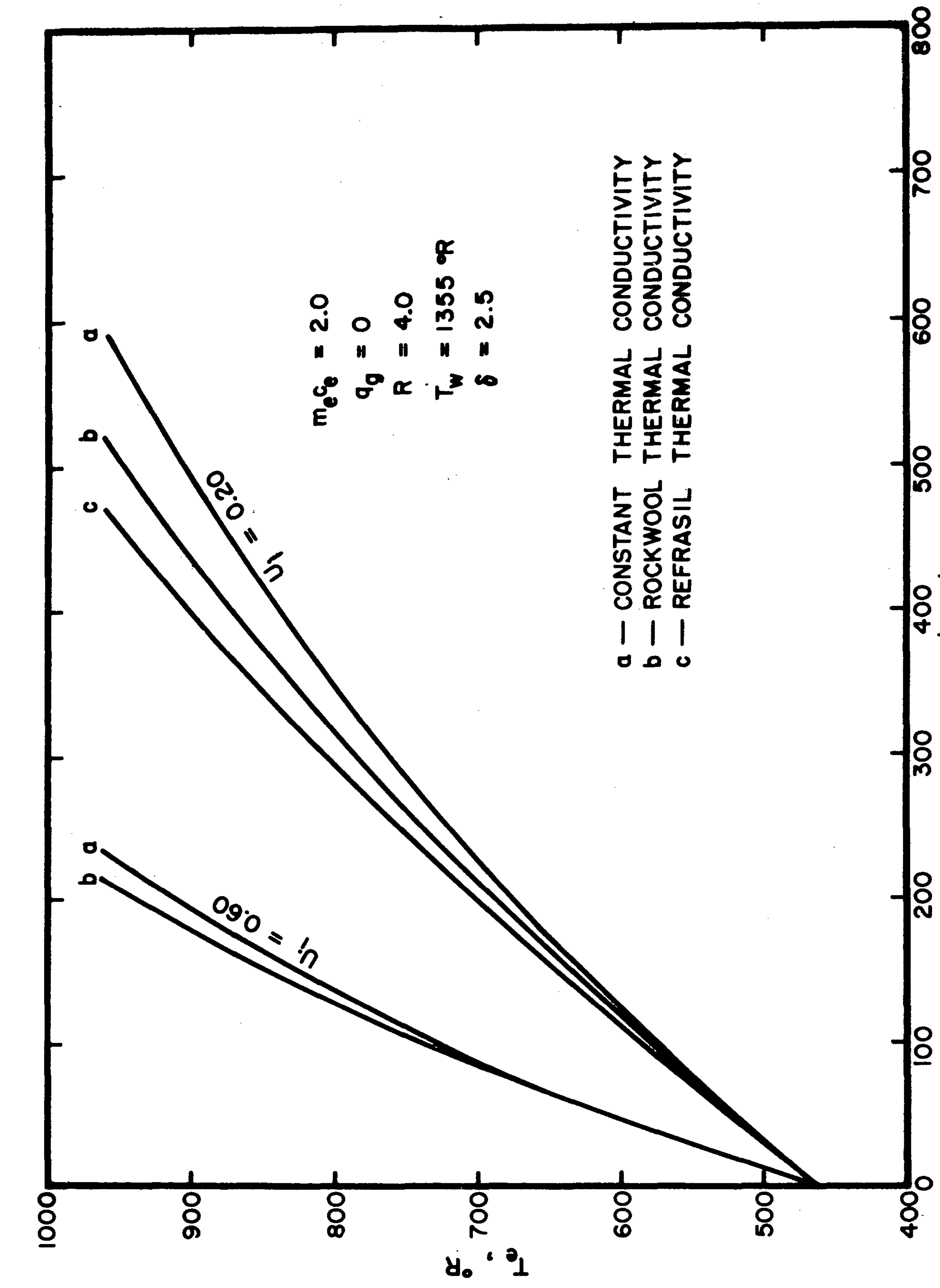

Figure V-4
Effect of Insulation Thermal Conductivity Characteristics on Equipment Temperature Rise

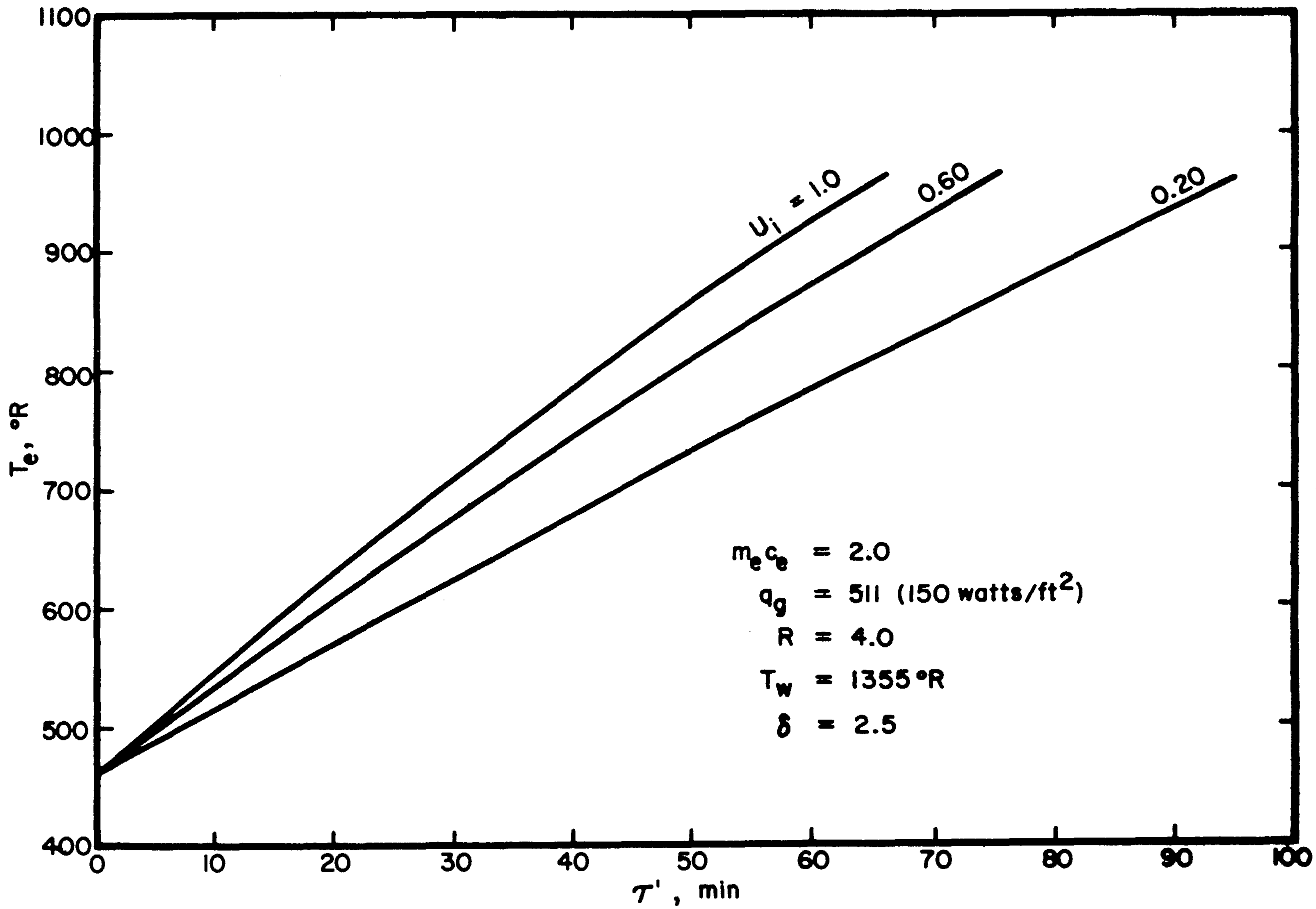

Figure V-5
Effect of Insulation Conductance on Equipment Temperature Rise

seriously limit space in the compartment. The example serves to point up the smaller effectiveness, or higher cost in terms of space, that insulation has with heat generating equipment. The insulation limitation derives from the fact that it has no effect on generated heat load, so that if insulation alone must delay temperature rise, extreme reduction of the external heat load may be required. There are cases, of course, where no amount of insulation could delay temperature rise enough, if the heat generation rate is great enough. Such a case would require the use of added thermal capacity or some cooling method.

The results shown in Figures V-3, -4, and -5 are not restricted to an initial equipment temperature of 460°R. If the initial temperature of equipment is any value above 460°R, it is only necessary to shift the time axis horizontally so that the zero point ($\tau = 0$) lies directly below the new initial T_e on the curve for the insulating effect of interest. The curve from this point to the right will then represent the temperature rise of equipment which starts at the new initial temperature, and has the same insulation thickness as would give U_i the assigned value when $T_e = 460$°R. Thus the plotted cases can be used for any initial equipment temperature of 460°R or greater, and for a constant thickness of insulation, although the insulating effect, U_i, is defined in terms of $T_e = 460$°R.

3. Heat Generation

The effect of heat generation on the equipment temperature rise is shown in Figure V-6. The cases shown are for a skin temperature of 1355°R, initial equipment temperature of 460°R, and insulating effect of $T_i = 0.60$ using rock wool. Equation (V-7) is used for free convection coefficients. It is apparent that the time rate of temperature rise increases with increased heat generation rate, as indicated by equation (V-16). It is of interest to note that with increased heat generation rate, the time temperature plots approach straight lines, indicating that the constant heat generation rate is becoming the dominant factor in determining $(\Delta T_e/\Delta \tau)$. This serves to emphasize that temperature rise rate is relatively independent of external heat load at high heat generation rates, and indicates that the use of insulation alone cannot effectively limit temperature rise in many cases.

The plots of Figure V-6 can be used to represent cases with an initial equipment temperature above 460°R in the manner described under the subject heading of insulation.

4. Ratio of Free Convection to Radiation Heat Transfer Area

The effect of the ratio of free convection to radiation heat transfer area on the temperature rise of equipment with time is shown in Figure V-7 for non-heat-generating equipment in an uninsulated compartment. The case of $R = 1$ corresponds to parallel planes, or the case of equipment and compartment both cylindrical in shape, and nearly the same size. The case of $R = 8$ represents a compartment containing many small equipment

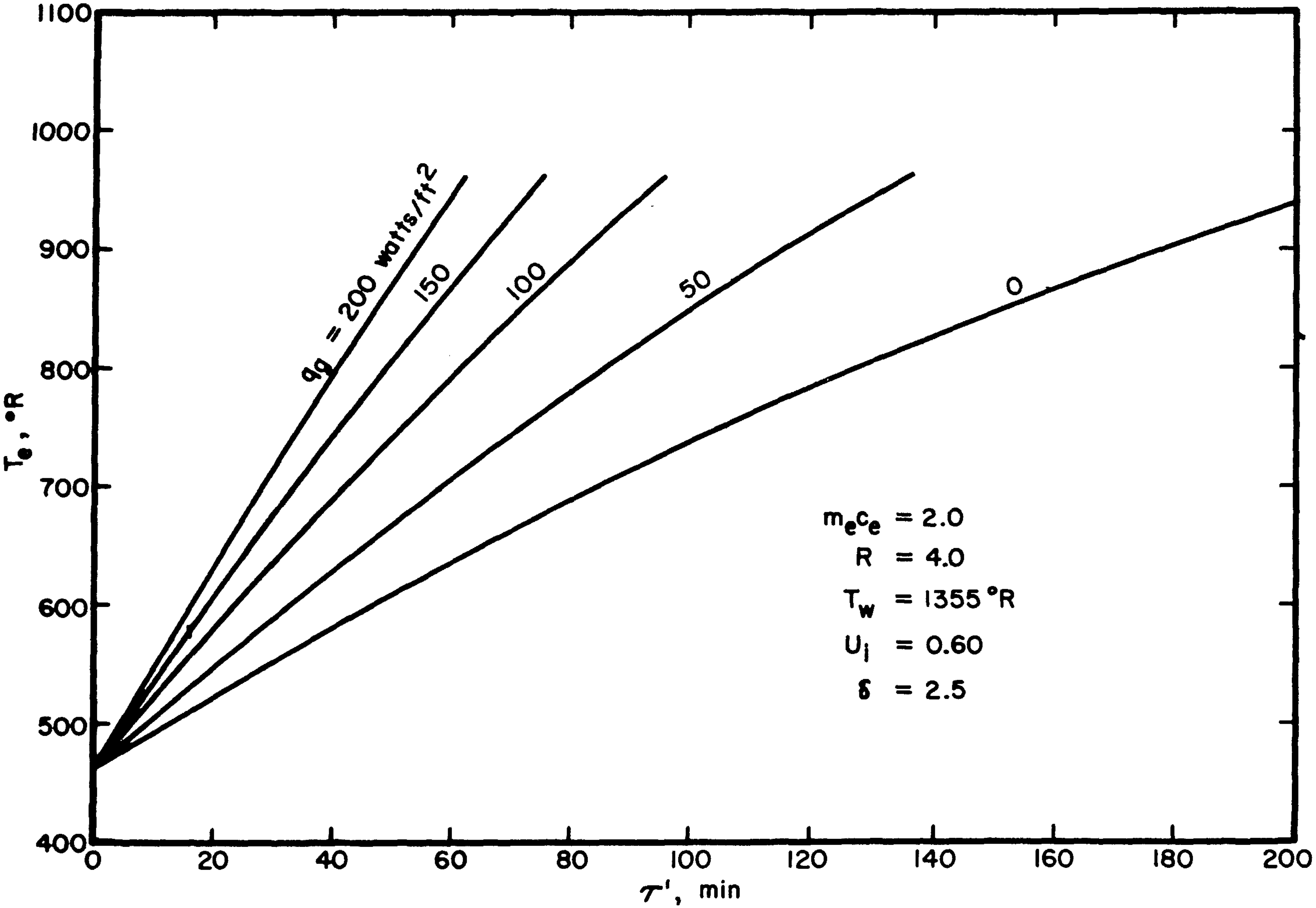

Figure V-6

Effect of Heat Generation on Equipment Temperature Rise

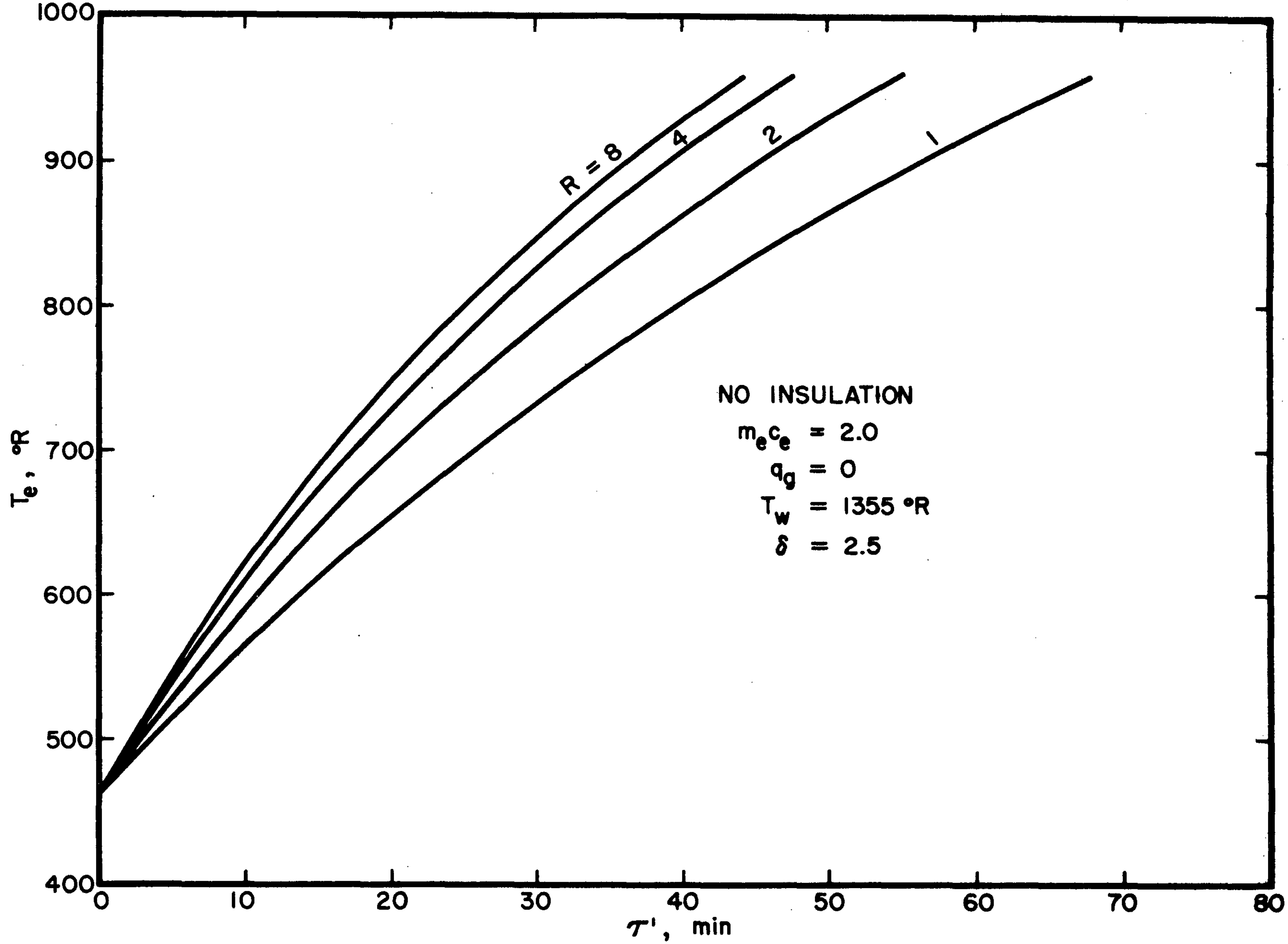

Figure V-7
Effect of Ratio of Free Convection to Radiation Heat Transfer Area on Equipment Temperature Rise

items, so arranged that much of their surface area is accessible to free convection, but not "seen" by the skin or skin insulation. The value of R is a factor which must be estimated for most installations, and it appears that the majority of practical cases would be in the range from R = 1 to R = 4. Equation (V-7) is used for free convection relationships in Figure V-7.

The plots of Figure V-7 show that temperature rise is more rapid for equipment which has greater area accessible to free convection heat transfer. This is particularly true for a compartment without insulation and without heat generation, where free convection heat transfer plays an important role in the determination of equipment temperature rise. Where free convection is relatively unimportant, as in cases with large heat generation rate, the importance of R is correspondingly less. In cases where free convection is important, some insulating effect might be achieved by grouping small components together so as to block some of their surface areas from air circulation. Another method would be to provide a large case to contain a number of smaller components wherever the value of R can be reduced in this way. The usefulness of these methods, however, is dependent upon the functions of equipment components, which may make common grouping or encasing impractical. R is therefore a factor of some importance in the compartment heat transfer scheme, but is not a factor which is subject to appreciable manipulation to achieve a desired performance result.

The plots of Figure V-7 can be used to represent cases with initial equipment temperatures above 460°R by means of shifting the time axis, as described earlier.

5. Compartment Air Pressure

The effect of compartment air pressure on the temperature rise characteristics of non-heat-generating equipment in a compartment without insulation is shown in Figure V-8. The initial equipment temperature is 460°R, and the skin temperature is 1355°R. The solid lines represent cases evaluated using equation (V-7) to describe free convection, while the dashed line represents a case using equation (V-9) with L taken as one foot.

It is apparent that the compartment air pressure has great influence on the rate of equipment temperature rise. This results from the fact that free convection heat transfer rates are proportional to $\delta^{2/3}$ or $\delta^{1/2}$, depending on whether equation (V-7) or equation (V-9) applies. A change of compartment pressure in the low pressure range is seen to affect the heating of equipment less markedly than in the higher pressure range, since in the former case radiation heat transfer, which is not affected by pressure, is a dominant factor. The choice of free convection coefficient for the single case shown (δ = 1.0) is seen to have little effect. A more extensive comparison of the two free convection relationships is made in Figure V-9.

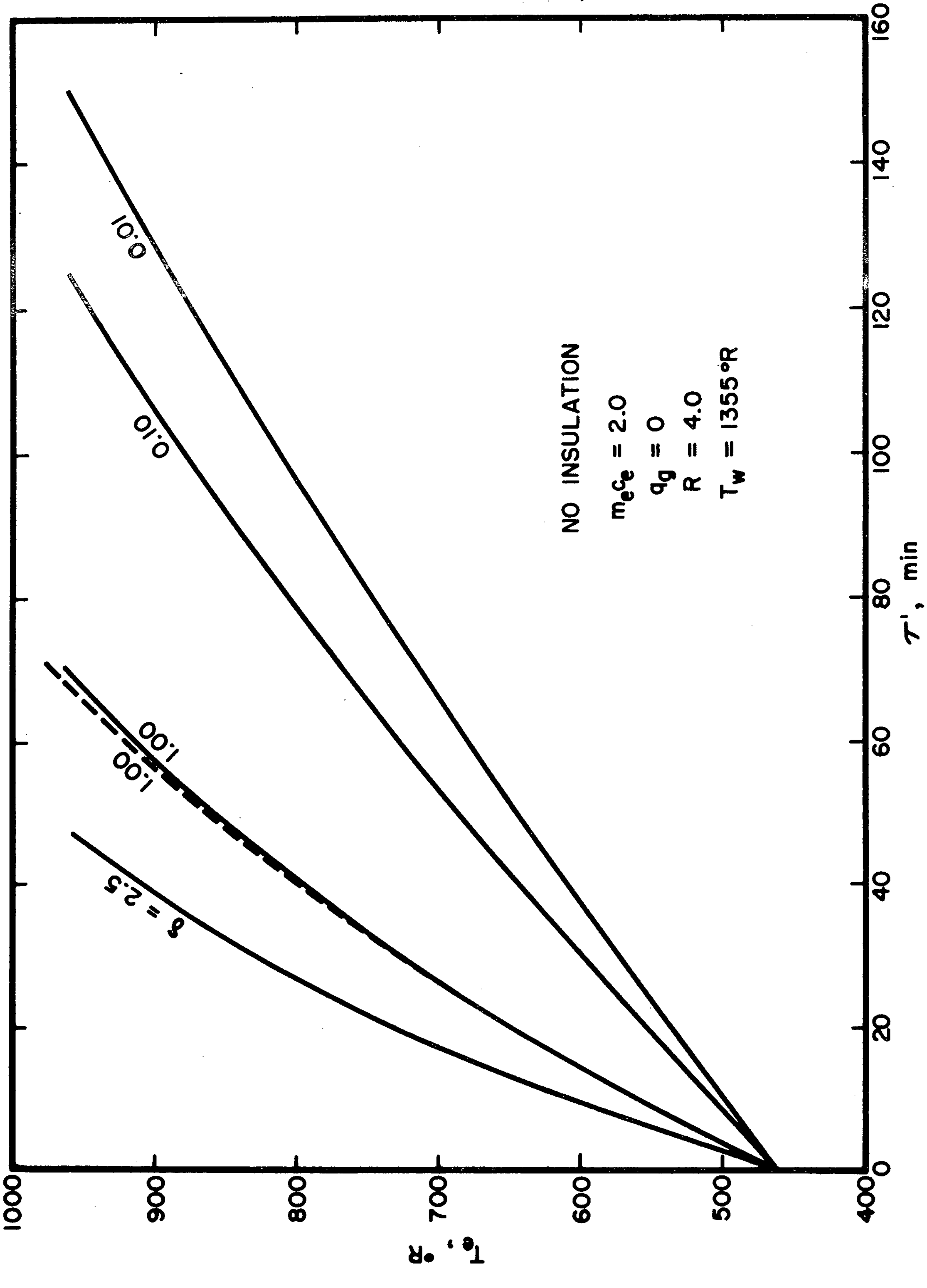

Figure V-8
Effect of Compartment Air Pressure on Equipment Temperature Rise

Figure V-9 is for the same conditions as Figure V-8, except that the compartment now has a skin insulation of $U_i = 0.60$ Btu/hr-ft^2 °R using rock wool. The solid lines represent use of equation (V-7) for free convection, while the dashed lines represent use of equation (V-9) with L of one foot. The effect of compartment air pressure in the insulated compartment is not so great as that for the uninsulated compartment in Figure V-8. This results from the lesser importance of free convection in the overall heat transfer scheme of the insulated compartment. The comparison of results for the two free convection equations indicates that it makes little difference which equation is used for the size of equipment considered, where L is about one foot. Figure V-10 indicates that this conclusion also applies for a considerable range of insulating effects.

The results given in Figures V-8 and V-9 show that the compartment air pressure exerts a strong influence on the rate of equipment temperature rise. Free convection heat transfer is the dominant part of the external heat load, so that the effect of compartment pressure on free convection might well be used to advantage in producing an insulating effect against external heat load. Therefore where equipment operation is not jeopardized, the use of low compartment pressures is indicated. A particular advantage of using low pressure to achieve insulating effect is that it does not impose the space and weight penalties of insulation materials. As with insulation, the method is effective only in reducing external heat load, and has limited value for equipment of large heat generation.

Figures V-8, -9, and -10 can represent cases with initial equipment temperatures above 460°R by modifications of the time scale, as described earlier.

6. Skin Temperature

Figure V-11 shows the effect of skin temperature on the rate of equipment temperature rise. The initial equipment temperature is 460°R in all the cases shown. Equation (V-7) is used to describe free convection, and rock wool insulation is used. The values of skin temperature are total temperatures corresponding to flight Mach numbers as shown for altitudes in the isothermal layer at atmospheric temperature of 393°R. In order to actually achieve this skin temperature, flight Mach numbers would have to be greater than those given to account for the recovery factor being less than unity and heat flux through the air film external to the skin.

For a given equipment temperature, a higher skin temperature gives greater temperature potential between skin and equipment. This results in greater external heat load, and a correspondingly faster equipment temperature rise for the higher skin temperature, as seen in Figure V-11. Inspection of the curves shows that the slope, or rate of equipment temperature rise with time, is about the same for equal values

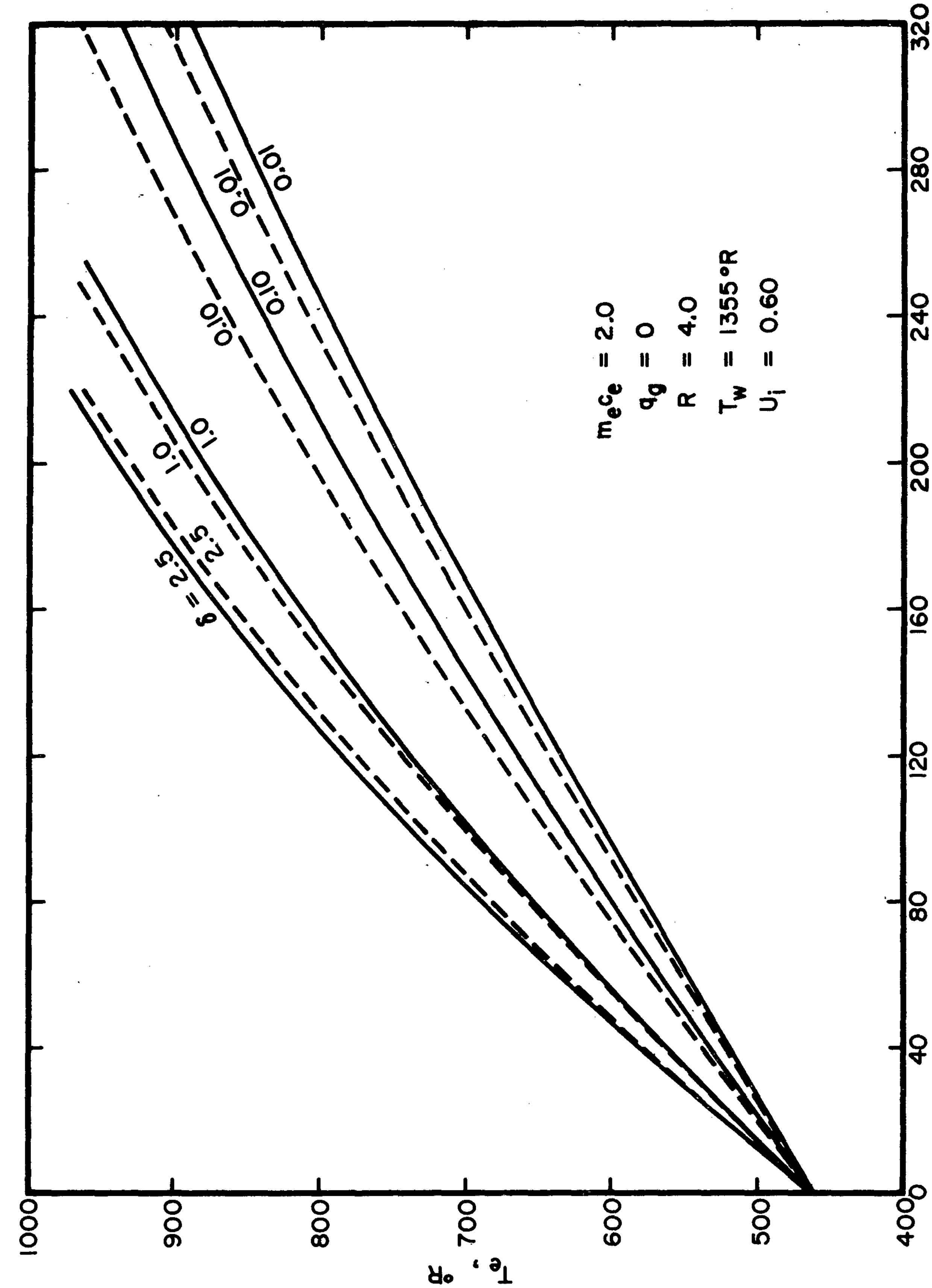

Figure V-9
Effect of Compartment Air Pressure on Equipment Temperature Rise

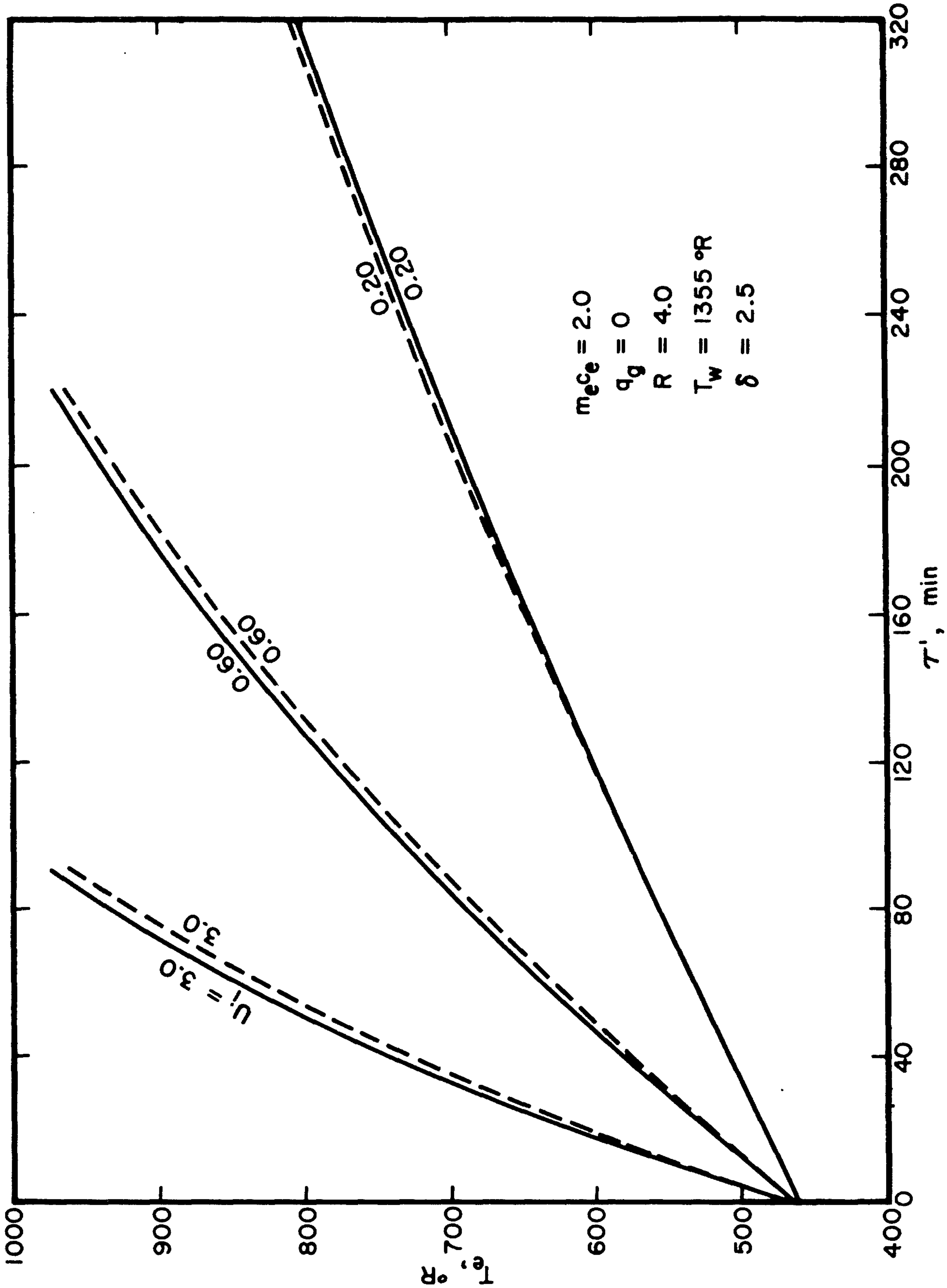

Figure V-10
Comparison of the Free Convection Equations for Different Insulation Conductances

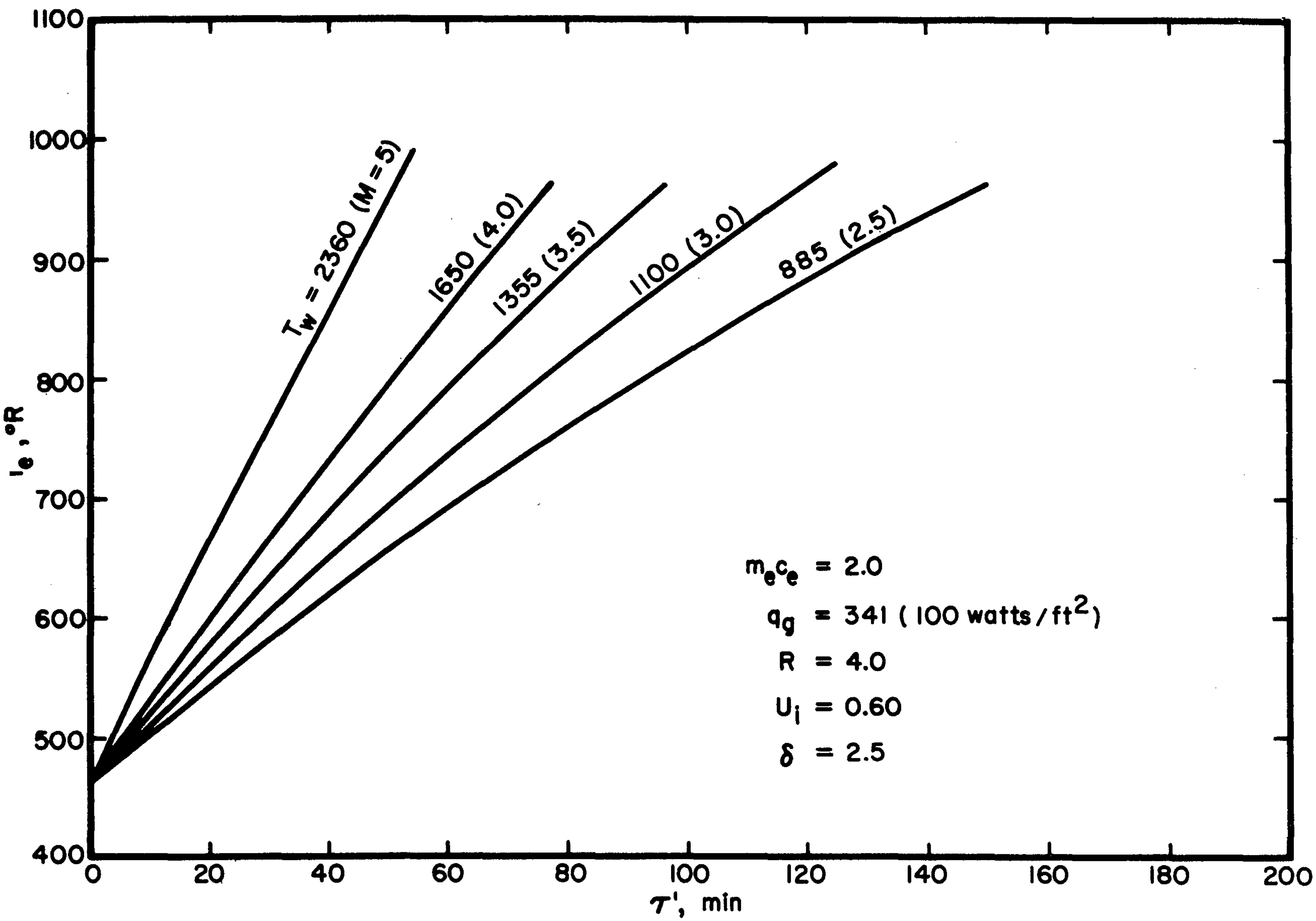

Figure V-11
Effect of Skin Temperature on Equipment Temperature Rise

of temperature potential $(T_w - T_e)$, where different skin temperatures are considered. For example, when the equipment of a compartment with a skin temperature of 1100°R is at T_e = 675°R, $(\Delta T_e / \Delta \mathcal{T})$ is nearly the same as for 885°R, and T_e = 460°R, since in each case the temperature potential is the same, and the generated heat loads are the same. This relationship is only approximate, however, since external heat load is not solely dependent on temperature potential, but is also a function of factors which vary with temperature level. Since the skin temperature affects only external heat load, high skin temperatures can be offset by use of insulation, low compartment pressures, and reflective shielding to reduce radiation heat load.

7. Surface Emissivity

Surface emissivities are not studied as a variable in the results presented, but their effect can easily be predicted in a qualitative sense. The heat transferred by radiation is proportional to the emissivity function given en equations (V-2) and (V-4) as

$$\frac{1}{\frac{1}{\epsilon_i} + \frac{1}{\epsilon_e} - 1}$$

Therefore the emissivity function exerts the same influence on radiant heat transfer that the compartment pressure function, $\delta^{2/3}$ or $\delta^{1/2}$, exerts on convective heat transfer. Accordingly, the surface emissivities will be important when the equipment and compartment characteristics are such as to make radiant heat transfer important in the overall compartment heat transfer scheme. This is likely to be the case where the compartment air pressure is low, so that little heat is transferred by free convection, and the sum of radiantion and free convection heat transfer is significant in magnitude compared to generated heat.

SIMPLIFIED ANALYSIS AND DESIGN OF INSULATION FOR AN UNCOOLED EQUIPMENT COMPARTMENT

1. Simplified Analysis

The variation of external heat load with equipment temperature has been evaluated for all of the calculated results shown thus far. If this quantity q_o is plotted versus T_e for a constant skin temperature, compartment pressure, and insulating effect, it is seen to be nearly a linear function of T_e. As an example, Figure V-12 shows the variation of q_o with T_e for a number of insulating effects, using rock wool, with T_w = 1355°R, and δ = 2.5. It is seen that q_o can be represented as a straight line function of T_e quite accurately for all of the insulated cases shown, and that it is a fairly good approximation in the case of

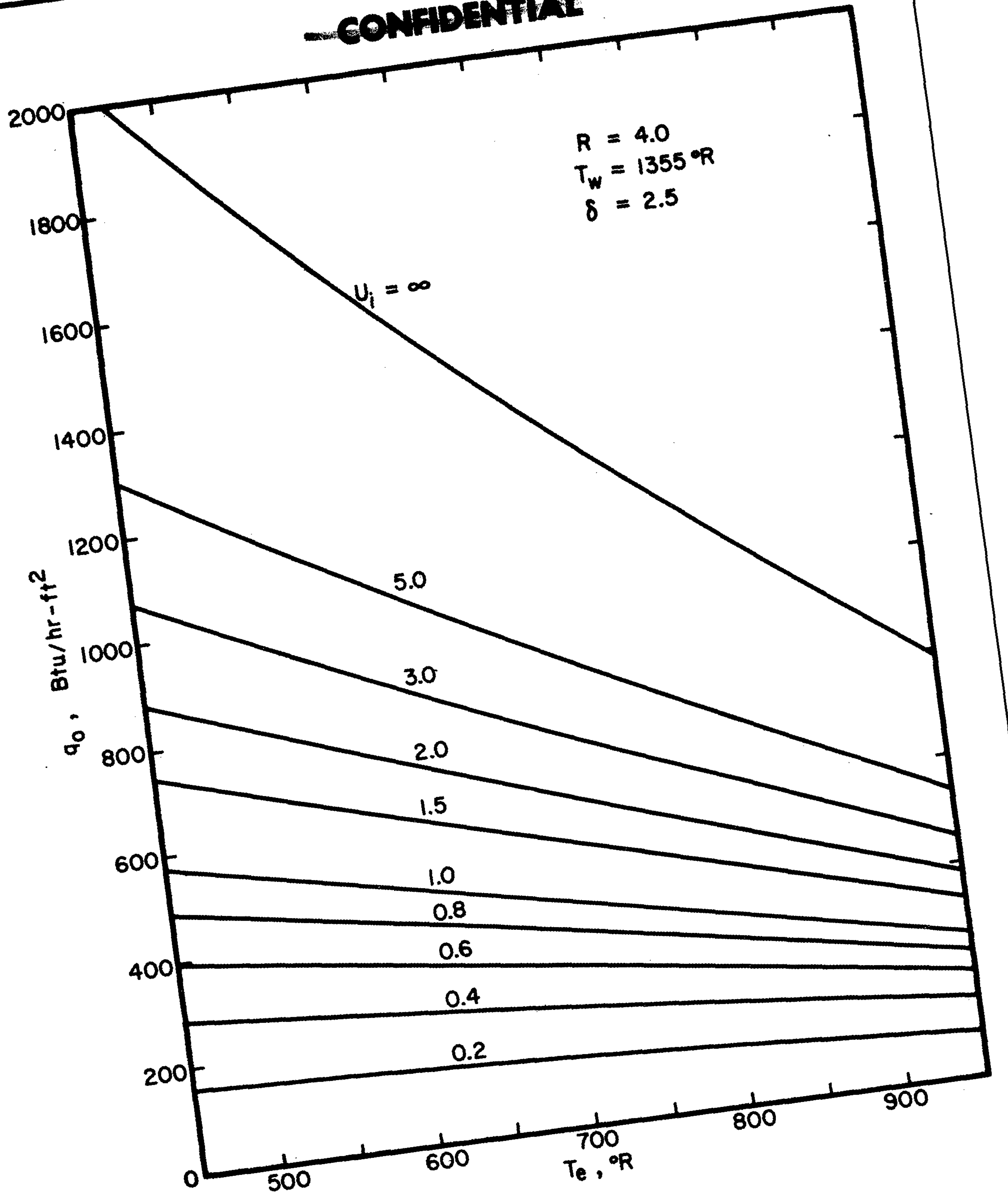

Figure V-12
External Heat Load to Equipment for Various Insulation Conductances

$U_i = \infty$. This fact permits determination of q_o for a given configuration by calculating q_o at the two extremes of T_e of interest, and interpolating linearly between them. A calculation procedure based on this approximation is considerably simpler than the trial and error procedures described earlier.

Since q_o can be represented quite well as a linear function of T_e, it is convenient to put it in the form

$$q_o = a - b\theta_e \tag{V-17}$$

where a and b are positive constants, and $\theta_e = (T_e - T_{eo})$, for T_{eo} at the beginning of a transient study. By substitution in equation (V-15), rearranging, and changing to the differential form gives

$$\frac{d\theta_e}{d\tau} + \left(\frac{b}{m_e c_e}\right)\theta_e = \frac{a+q_g}{m_e c_e}$$

which is a first order, linear differential equation with constant coefficients. This is solved to give

$$\theta_e = \left(\frac{a+q_g}{b}\right)\left[1 - e^{-\frac{b\tau}{m_e c_e}}\right] \tag{V-18}$$

The only trial and error calculations required to use equation (V-18) are those required for the determination of q_o for the initial and final values fo T_e of interest. This determines the constants a and b of equation (V-17), and permits application of equation (V-18) to determine θ_e, and hence T_e, at any time, τ.

Equation (V-18) can be solved for τ to give,

$$\tau = \left(\frac{m_e c_e}{b}\right) \log_e\left(\frac{a+q_g}{a - b\theta_e + q_g}\right)$$

From this it is apparent that the time required to heat equipment to any value of θ_e is directly proportional to the thermal capacity of the equipment as found earlier with equation (V-16).

2. <u>Design of Insulation for an Uncooled Equipment Compartment</u>

A method for selecting the proper insulation effect to use with an uncooled aircraft compartment is here described. The general problem of determining the suitability of an uncooled compartment as compared to a compartment with fuel jacketing or cooling effects is discussed in Section XI. It is assumed here that this problem has been dealt with and that the use of an uncooled compartment has been decided upon. It is also assumed that all of the factors which affect equipment

temperature rise other than the insulation effect have been established, and are not subject to much alteration. As examples, it is assumed that the compartment air pressure and equipment surface emissivities are known.

It is convenient to describe this design procedure in terms of a specific example. Suppose it is desired to select insulation for a compartment so that the equipment temperature will not exceed 900°R in 82 minutes flight time under the following conditions:

Initial equipment temperature	= 460°R
Skin temperature	= 1355°R
Compartment air pressure	= 2.5 atmospheres
Skin area associated with compartment	= 18 ft^2
Total weight of equipment in compartment	= 200 lbs
Average specific heat of equipment	= 0.18 Btu/lb-°R
Total heat generation rate of equipment	= 6150 Btu/hr = 1800 watts
Ratio of equipment free convection area to skin area of compartment	= 4

From the above, the heat generation and thermal capacity of equipment on a unit area basis are calculated.

$$q_g = \frac{Q_g}{A_w} = \frac{6150}{18} = 341.3 \text{ Btu/hr-ft}^2$$

$$m_e c_e = \frac{M_e c_e}{A_w} = \frac{200 \times .18}{18} = 2 \text{ Btu/°R-ft}^2$$

An approximation is used to determine a representative heat load to the equipment. It is assumed that the variation of T_e with τ is approximately linear. Since the variation of q_o with T_e is almost linear, it is easily shown that the average value of q_o occurs at the average value of T_e, and that both occur at the middle of the design time span. This time is,

$$\frac{82 \text{ min}}{60 \times 2} = 0.684 \text{ hr}$$

The average equipment temperature is,

$$T_{em} = \frac{900 + 460}{2} = 680°R$$

Since it is assumed that T_e varies with τ approximately as a straight line, equation (V-15) is used to determine the average heat load to the equipment from the skin,

$$q_{om} = m_e c_e \left(\frac{\Delta Te}{\Delta \tau}\right) - q_g$$

$$q_{om} = 2 \times \frac{900-460}{\frac{82}{60}} - 341.3 = 302.7 \text{ Btu/hr-ft}^2$$

A trial and error procedure is required to determine the insulation effect U_i required to give $q_{om} = 302.7$ Btu/hr-ft^2 when $T_{em} = 680°R$ and $T_w = 1355°R$. The procedure is carried out below, with values shown only for the final, successful trial. In this procedure, surface emissivities have been taken as $\epsilon_i = 0.10$ and $\epsilon_e = 0.20$, and equation (V-9) has been used with L = 1 ft. to describe free convection heat transfer.

1. Assume $T_i = 906°R$ (T_i is between T_w and T_{em})

2. Calculate $U_i = \frac{q_{om}}{(T_w - T_i)} = \frac{302.7}{1355-906} = 0.675$ Btu/hr-ft^2-°R

3. Assume $T_a = 734°R$ (T_a is between T_i and T_{em})

4. Calculate $h_r = 1.24 \times 10^{-4}$ B

   where $B = \dfrac{\left(\frac{T_i}{100}\right)^4 - \left(\frac{T_e}{100}\right)^4}{\left(\frac{T_i}{100}\right) - \left(\frac{T_e}{100}\right)}$

   from Figure AIV-1 B = 2030, $h_r = 0.252$ Btu/hr-ft^2-°R

5. Get $\left(\frac{a'' L^{1/4}}{\delta^{1/2}}\right)_i$ at $\frac{T_i + T_a}{2}$

   from Figure AIV-3

$$\left(\frac{a'' L^{1/4}}{\delta^{1/2}}\right)_i = 0.2505$$

6. Get $\left(\frac{a'' L^{1/4}}{\delta^{1/2}}\right)_e$ at $\frac{T_a + T_e}{2}$

from Figure AIV-3

$$\left(\frac{a'' \ L^{1/4}}{\delta^{1/2}}\right)_e = 0.262$$

7. $h_{ci} = \left(\frac{a'' \ L^{1/4}}{\delta^{1/2}}\right)_i \left(\frac{\delta^{1/2}}{L^{1/4}}\right) (T_i - T_a)^{1/4}$

$= 0.2505 \times 1.580 \times 3.62 = 1.432$ Btu/hr-ft^2-°R

8. $h_{ce} = \left(\frac{a'' \ L^{1/4}}{\delta^{1/2}}\right)_e \left(\frac{\delta^{1/2}}{L^{1/4}}\right) (T_a - T_e)^{1/4}$

$= 0.2615 \times 1.580 \times 2.71 = 1.12$ Btu/hr-ft^2-°R

9. $h_c = \dfrac{1}{\dfrac{1}{h_{ci}} + \dfrac{1}{Rh_{ce}}} = \dfrac{1}{\dfrac{1}{1.432} + \dfrac{1}{4 \times 1.12}} = 1.085$ Btu/hr-ft^2 °R

10. $(T_i - T_e) = \dfrac{q_{om}}{h_c + h_r} = \dfrac{302.7}{1.337} = 226.5$°R

11. $T_i = (T_i - T_e) + T_e = 226.5 + 680 = 906.5$°R

12. $(T_a - T_e) = \dfrac{h_c}{Rh_{ce}} (T_i - T_e) = \dfrac{1.085}{4.48} (226) = 54.6$°R

13. $T_a = (T_a - T_e) + T_e = 54.6 + 680 = 734.6$°R

Since the calculated results in steps 11 and 13 are in substantial agreement with the assumed values, the value of $U_i = 0.675$ Btu/hr - ft^2°R is correct.

The average insulation temperature is $(T_w + T_i/2)$, or 1130.5°R. From Appendix II the thermal conductivity of rock wool insulation at this temperature is $k_i = 0.058$ Btu/hr-ft-°R, so the insulation thichness is,

$$x_i = \frac{k_i}{U_i} = \frac{0.058}{0.675} = 0.086 \text{ ft.}$$

A set of charts is provided in the Appendix to this Section which permits making the above trial and error calculation to find U_i graphically. Figure V-13 is for conduction through insulation. For an assumed value of U_i, the chart is used by traveling parallel to the dashed-arrow lines to determine T_i. The next, Figure V-14, is for free convection in air, and is used with this value of T_i, and the pertinent values of T_e and δ, to find q_c. This convection chart is based on equation (V-7) to describe convection coefficients (unlike the example just worked) and on a standard value of R = 4. Since the difference between equations (V-7) and (V-9) is not great, the chart can be used for a good approximation even where equation (V-9) should be used. The next chart, Figure V-15, is for radiation heat transfer, and is in two parts to cover the low and high emissivity ranges. The chart is used with the previously determined value of T_i and the pertinent values of T_e and ϵ', to obtain q_r. The quantity ϵ' is

$$\frac{1}{\frac{1}{\epsilon_i} + \frac{1}{\epsilon_e} - 1}$$

as evaluated for the insulation and equipment surface emissivities. The resulas q_r and q_c from the last charts are then added, and if the sum agrees with q_o the value of U_i used in the trial is correct. Otherwise a new value of U_i must be assumed, and another trial made. If the sum $(q_c + q_r)$ is greater than q_o the value of U_i should be decreased for the next trial, and conversely.

With the value of insulation thickness found, it is necessary to make a transient evaluation of equipment temperature rise with time. This will be done by the method of using a linear variation of q_o with T_e, as in equation (V-17), and then applying equation (V-18). A trial and error calculation is required to determine the values of the constants a and b of equation (V-17). A sample of this calculation is carried out below, showing only the final trial calculation. This calculation must be made for two values of T_e, which in this case are taken at the beginning and end of the transient evaluation. The calculation shown is for $T_e = 460°R$

1. Assume $T_i = 740°R$ and $T_a = 526°R$

2. Calculate $h_r = 1.24 \times 10^{-4}$ B

$$\text{where B} = \frac{\left(\frac{T_i}{100}\right)^4 - \left(\frac{T_e}{100}\right)^4}{\frac{T_i}{100} - \frac{T_e}{100}}$$

from Figure AIV-1 B = 920

$h_r = 0.114$ Btu/hr-ft^2-°R

3. Get

$$\left(\frac{a'' \; L^{1/4}}{\delta^{1/2}}\right)_i \quad \text{at} \quad \frac{T_i + T_a}{2}$$

from Figure AIV-3

$$\left(\frac{a'' \; L^{1/4}}{\delta^{1/2}}\right)_i = 0.270$$

4. Get $\left(\frac{a'' \; L^{1/4}}{\delta^{1/2}}\right)_e$ at $\frac{T_a + T_e}{2}$

from Figure AIV-3

$$\left(\frac{a'' \; L^{1/4}}{\delta^{1/2}}\right)_e = 0.289$$

5. $$h_{ci} = \left(\frac{a'' \; L^{1/4}}{\delta^{1/2}}\right)_i \left(\frac{\delta^{1/2}}{L^{1/4}}\right) (T_i - T_a)^{1/4}$$

$$= 0.270 \times 1.580 \times 3.82 = 1.63 \text{ Btu/hr-ft}^2\text{-°R}$$

6. $$h_{ce} = \left(\frac{a'' \; L^{1/4}}{\delta^{1/2}}\right)_e \left(\frac{\delta^{1/2}}{L^{1/4}}\right) (T_a - T_e)^{1/4}$$

$$= 0.289 \times 1.58 \times 2.85 = 1.30 \text{ Btu/hr-ft}^2\text{-°R}$$

7. $$h_c = \frac{1}{\frac{1}{h_{ci}} + \frac{1}{Rh_{ce}}} = \frac{1}{\frac{1}{1.63} + \frac{1}{5.2}} = 1.24 \text{ Btu/hr-ft}^2\text{-°R}$$

8. $U_i = \frac{k_i}{x_i}$, for k_i at $\frac{T_w + T_i}{2} = 1048$°R

from Appendix II, $k_i = 0.053$ Btu/hr-ft-°R

9. then $U_i = \frac{0.053}{0.086} = 0.616$ Btu/hr-ft^2-°R

10. $$(T_w - T_i) = \frac{h_c + h_r}{U_i + h_c + h_r} (T_w - T_e)$$

$$(T_w - T_i) = \frac{1.354}{1.970} (895) = 615$$

11. $$T_i = T_w - (T_w - T_i) = 1355 - 615 = 740°R$$

12. $$(T_a - T_e) = \frac{h_c}{Rh_{ce}} (T_i - T_e)$$

$$= \frac{1.24}{5.2} (280) = 66.8$$

13. $$T_a = (T_a - T_e) + T_e = 66.8 + 460 = 526.8°R$$

Since the calculated results of steps 11 and 13 agree with assumed values, q_o can be determined for the condition $T_e = 460°R$

14. $$q_o = U_i (T_w - T_i) = 0.616 \times 615 = 379 \text{ Btu/hr-ft}^2$$

This same calculation when made for the condition $T_e = 900°R$, gives $q_o = 216.3$ Btu/hr-ft^2. Defining $\theta_e = T_e - 460$, equation (V-17) for the two cases becomes,

$$379 = a - b \times 0$$

$$216 = 2 - b \times 440$$

Solving gives $a = 379$, $b = 0.370$

Figures V-13, -14, and -15 of the Appendix to this Section can also be used to solve this type of trial and error calculation. For the assigned conditions, it is necessary to assume T_i, then evaluate U_i at the average insulation temperature, $(T_w + T_i)/2$, using the formula $U_i = (k_i/x_i)$ for the insulation material and thickness. Figure V-13 is then used by entering with T_i and traveling parallel to the dashed arrow lines down to the assigned T_w, across to the U_i determined above, and down to q_o. The free convection and radiation charts are then used as described previously, entering with the assumed value of T_i, and obtaining q_c and q_r. When the sum $(q_c + q_r)$ is equal to q_o, the value of q_o is correct. Otherwise a new value of T_i must be assumed, and another trial made. If the sum $(q_c + q_r)$ is greater than q_o the assumed value of T_i should be reduced for the next trial, and conversely. The free convection chart should be used only if R is about 4 as it is based on this value.

All of the information required for application of equation (V-18) has now been determined. Equation (V-18) is therefore used to determine T_e at the time = 1.368 hr (82 min),

$$\theta_e = \left(\frac{379 + 341.3}{0.370}\right)\left[1 - e^{-\left(\frac{0.370 \times 1.368}{2}\right)}\right]$$

$$\theta_e = 436$$

Then $T_{e\tau} = \theta_e + 460 = 896°R$

This result is quite close to the design value of 900°R, so that no further trials are required. If this had not been the case, it would be necessary to revise the value of x_i by estimation and repeat the calculations beginning with the determination of q_o at T_e = 460°R and T_e = 900°R. The value of x_i should be increased if $T_{e\tau}$ is much above 900°R, and decreased if $T_{e\tau}$ is much below 900°R.

The selection of rock wool insulation in the example is purely arbitrary. The physical properties of the insulation seclected determine the thickness required and the constants of equation (V-16) however, so that for other insulating materials recalculation of part of the design example would be required. The insulation thickness found, i.e. 0.086 feet or 1.03 inches, is a reasonable value for a compartment of large size, particularly since it might be difficult to utilize space very close to the walls of a compartment for installation of equipment. This would be the case where the space near walls is partially occupied by structural members, or where the equipment shape is not similar to the wall contour. If this is not the case, the designer should consider the use of additional thermal capacity with the equipment.

3. Use of Thermal Capacity as Compared to Insulation

It is interesting to make a brief comparison of the performance resulting from additional thermal capacity compared with insulation on the basis of weight and volume. For the compartment considered, 1.03 inches of insulation on the 18 square feet of skin area would occupy a volume of 1.545 cubic feet. For an insulation such as rock wool, having a bulk density of 12 lb/ft^3, this would give a weight of at least 18.55 pounds. If all the skin insulation is removed the constants a and b of equations (V-17) and (V-18) are found by calculation to be, a = 1750, b = 1.98. If the insulation is replaced by an equivalent volume of water added to the equipment, the water added would weigh 96.4 pounds, and would increase the thermal capacity of equipment per unit skin area by 5.35 Btu/°R-ft^2. Applying equation (V-18) for the total $m_e c_e$ value of 7.35 Btu/°R-ft^2 gives the equipment temperature at 82 minutes as 784°R, which is a considerable improvement over the performance offered by insulation alone. If the insulation is replaced by an equivalent weight of water added to the equipment, the water would weigh 18.55 pounds, and would increase the thermal capacity of equipment per unit skin area by 1.03 Btu/°R-ft^2. Applying

equation (V-18) for the total $m_e c_e$ value of 3.03 Btu/°R-ft^2 gives the equipment temperature at 82 minutes as 1083°R, which is inferior to the performance offered by insulation alone. For this design example then, superior performance could be obtained with increased thermal capacity, but at an expense in terms of weight. In other cases, having a higher ratio of generated heat load to external heat load, the thermal capacity effect would have increasing merit as compared to the insulation effect, since insulation is ineffective in reducing generated heat load. The use of thermal capacity with the equipment entails some difficulties, since for best effect it should be appropriately distributed among the equipment bodies. Furthermore, as indicated earlier, its true merit is dependent on the relative usefulness of space well inside the compartment to space near the walls. This relative usefulness is difficult to evaluate quantitatively.

APPENDIX TO SECTION V

1. Calculation Procedures for Temperature Rise of Equipment in an Uncooled Compartment

Calculation procedures are given here for the stepwise evaluation of equipment temperature rise in an uncooled aircraft compartment. The first procedure is for a compartment with skin insulation, and the second is for a compartment without skin insulation. In the first case a sample interval calculation is carried along with the procedure.

Procedure A: Compartment with Skin Insulation

Given Data:

T_w = 1355°R

δ = 2.5 atmospheres

U_i = 0.40 Btu/hr-ft^2°R   rock wool insulation

$m_e c_e$ = 2.0 Btu/ft^2-°R

R = 4

e_i = 0.1, e_e = 0.2

T_{e1} = 701°R

T_{a1} = 743°R

T_{i1} = 867°R

q_g = 0 Btu/ft^2-hr

1. Select time interval $\Delta\tau' = 15$ min

2. Assume T_{e2}, T_{a2}, T_{i2}

$$T_{e2} = 727°R$$
$$T_{a2} = 768°R$$
$$T_{i2} = 889°R$$

3. Calculate T_{em}, T_{am}, T_{im}

$$T_{em} = \frac{727 + 701}{2} = 714°R$$

$$T_{am} = \frac{768 + 743}{2} = 756°R$$

$$T_{im} = \frac{889 + 867}{2} = 878°R$$

4. Calculate $h_r = 17.4 \times 10^{-4} \left(\frac{1}{\frac{1}{\epsilon_i} + \frac{1}{\epsilon_e} - 1} \right) B$

Where $B = \dfrac{\left(\frac{T_{im}}{100}\right)^4 - \left(\frac{T_{em}}{100}\right)^4}{\left(\frac{T_{im}}{100}\right) - \left(\frac{T_{em}}{100}\right)}$

from Figure AIV-1

$$h_r = 17.4 \times 10^{-4} \times .0714 \times B = 1.24 \times 10^{-4} \times 2020 = 0.253$$

5. Get $(a'/\delta^{2/3})_i$ at $\frac{T_{im} + T_{am}}{2}$

from Figure AIV-2

$$\frac{T_{im} + T_{am}}{2} = \frac{878 + 756}{2} = 817°R$$

$$(a'/\delta^{2/3})_i = 0.1585$$

6. Get $(a'/\delta^{2/3})_e$ at $\frac{T_{am} + T_{em}}{2}$ from

Figure AIV-2

$$\frac{T_{am} + T_{em}}{2} = \frac{756 + 714}{2} = 735°R$$

$$(a'/\delta^{2/3})_e = 0.1697$$

7. $h_{ci} = (a'/\delta^{2/3})_i \ (\delta^{2/3}) \ (T_{im}-T_{am})^{1/3}$

$$h_{ci} = 0.1585 \times 1.84 \times (122)^{1/3} = 1.45 \text{ Btu/hr-ft}^2\text{-°R}$$

8. $h_{ce} = \left(\frac{a'}{\delta^{2/3}}\right)_e (\delta^{2/3}) \ (T_{am}-T_{em})^{1/3}$

$$h_{ce} = 0.1697 \times 1.84 \times (42)^{1/3} = 1.085 \text{ Btu/hr-ft}^2\text{-°R}$$

9. $h_c = \dfrac{1}{\frac{1}{h_{ci}} + \frac{1}{Rh_{ce}}} = \dfrac{1}{\frac{1}{1.45} + \frac{1}{4 \times 1.085}} = 1.087 \text{ Btu/hr-ft}^2\text{-°R}$

10. $h_c + h_r = 1.087 + 0.253 = 1.34 \text{ Btu/hr-ft}^2\text{-°R}$

11. $q_o + q_g = \left[(h_c + h_r)\ (T_{im} - T_{em}) + q_g\right] \dfrac{\Delta '}{60}$

$$= \left[1.34\ (164) + 0\right] .25 = 55 \text{ Btu/ft}^2$$

12 $\Delta T_e = \dfrac{q_o + q_g}{m_e c_e} = \dfrac{55}{2} = 27.5$

13. $T_{e2} = T_{e1} + \Delta T_e = 701 + 27.5 = 728.5°R$

14. Get U_i at T_{im} from

Figure AIV-4 for rock wool

$$U_i = 0.459 \text{ Btu/hr-ft}^2\text{-°R}$$

15. $$T_w - T_{i2} = \frac{h_c + h_r}{U_i + h_c + h_r}(T_w - T_{e2})$$

$$= \frac{1.34}{1.799}(626.5) = 467$$

16. $$T_{i2} = T_w - (T_w - T_{i2}) = 1355\text{-}467 = 888°R$$

17. $$(T_{a2} - T_{e2}) = \frac{h_c}{Rh_{ce}}(T_{i2} - T_{e2}) = \frac{1.087}{4.340}(159.5) = 40$$

18. $$T_{a2} = (T_{a2} - T_{e2}) + T_{e2} = 728.5 + 40 = 768.5°R$$

The calculated results of steps 13, 16, and 18 agree well with the assumed values, indicating that the calculation is correct for the interval shown. In using this calculation procedure, the values of T_{i1}, T_{a1}, and T_{e1} are taken as the values of T_{i2}, T_{a2}, and T_{e2} of the previous interval. To start a calculation from the initial assigned values of T_w and T_{e1}, it is necessary only to determine the initial values of T_{i1} and T_{a1}. This can be done by using the same calculation procedure without selecting a time interval, and omitting steps 11, 12, and 13.

Procedure B: Compartment Without Skin Insulation

Given Data:

T_w = ____ °R

δ = ____ atmosphere

$m_e c_e$ = ____ Btu/ft^2-°R

R = ____

ϵ_w = ____ ϵ_e = ____

T_{e1} = ____ °R

T_{a1} = ____ °R

q_g = ____ Btu/ft^2-hr

1. Select time interval $\Delta \tau' =$ ____ min

2. Assume T_{e2} and T_{a2} $T_{e2} =$ ____ °R

$T_{a2} =$ ____ °R

3. Calculate T_{em} and T_{am} $T_{em} =$ ____ °R

$T_{am} =$ ____ °R

4. Calculate $h_r = 17.4 \times 10^{-4} \left(\dfrac{1}{\dfrac{1}{\epsilon_w} + \dfrac{1}{\epsilon_e} - 1} \right) B$

$$\text{where } B = \frac{\left(\frac{T_w}{100}\right)^4 - \left(\frac{T_{em}}{100}\right)^4}{\left(\frac{T_w}{100}\right) - \left(\frac{T_{em}}{100}\right)}$$

from Figure AIV-1

$h_r =$ ____ Btu/ft^2-hr-°R

5. Get $(a'/\delta^{2/3})_w$ at $\dfrac{T_{wm} + T_{am}}{2}$

from Figure AIV-2

$(a'/\delta^{2/3})_w =$ ____

6. Get $(a'/\delta^{2/3})_e$ at $\dfrac{T_{am} + T_{em}}{2}$

from Figure AIV-7

$(a'/\delta^{2/3})_e =$ ____

7. $h_{cw} = (a'/\delta^{2/3})_w \, (\delta^{2/3}) \, (T_w - T_{am})^{1/3} =$ ____ Btu/hr-ft^2-°R

8. $h_{ce} = (a'/\delta^{2/3})_e \, (\delta^{2/3}) \, (T_{am} - T_{em})^{1/3} =$ ____ Btu/hr-ft^2-°R

9. $h_c = \dfrac{1}{\dfrac{1}{h_{cw}} + \dfrac{1}{Rh_{ce}}}$ $h_c =$ ____ Btu/hr-ft-°R

10. $h_c + h_r =$ ____ Btu/hr-ft^2-°R

11. $q_o + q_g = \left[(h_c + h_r)(T_w - T_{em}) + q_g\right]\left(\frac{\Delta \tau'}{60}\right)$

$(q_o + q_g) =$ ____ Btu/ft^2

12. $\Delta T_e = \frac{q_o + q_g}{m_e c_e}$ $\Delta T_e =$ ____ °R

13. $T_{e2} = T_{e1} + \Delta T_e$ $T_{e2} =$ ____ °R

14. $(T_{a2} - T_{e2}) = \frac{h_c}{Rh_{ce}}(T_w - T_{e2})$

$(T_{a2} - T_{e2}) =$ ____ °R

15. $T_{a2} = (T_{a2} - T_{e2}) + T_{e2}$ $T_{a2} =$ ____ °R

When the calculated results of steps 13 and 15 agree with the assumed values, the interval calculation is complete, and values of T_{e2} and T_{a2} are used as T_{e1} and T_{a1} for the next interval.

2. Graphical Solutions for Conduction, Free Convection, and Radiation

The equations describing heat oonduction through insulation, free convection, and radiation can be solved in graphical form. This is particularly desirable when a large number of calculations are to be made, and where extreme accuracy is not required. Figure V-13 is a graphical solution to equation (V-1). It is constructed by first plotting the function (T_w-T_i), using an abscissa scale for T_i, an ordinate scale for the function, and lines of constant T_w. Using the same ordinate scale for the function (T_w-T_i) an abscissa scale is laid off in values of q_o, and lines of constant U_i are plotted to fit the (T_w-T_i) and q_o scales. The chart can be used to find either q_o or U_i when the other three variables are known. Figure V-14 is a graphical solution to equation (V-12) and is constructed in a manner similar to Figure V-13. The ordinate scale of Figure V-14 (not shown) is laid off in units of the function

$$\frac{1}{(\delta)^{2/3}\;\frac{1}{h_{ci}} + \frac{1}{Rh_{ce}}}\,(T_i - T_e)$$

which is a function independent of pressure. Figure V-14 is constructed

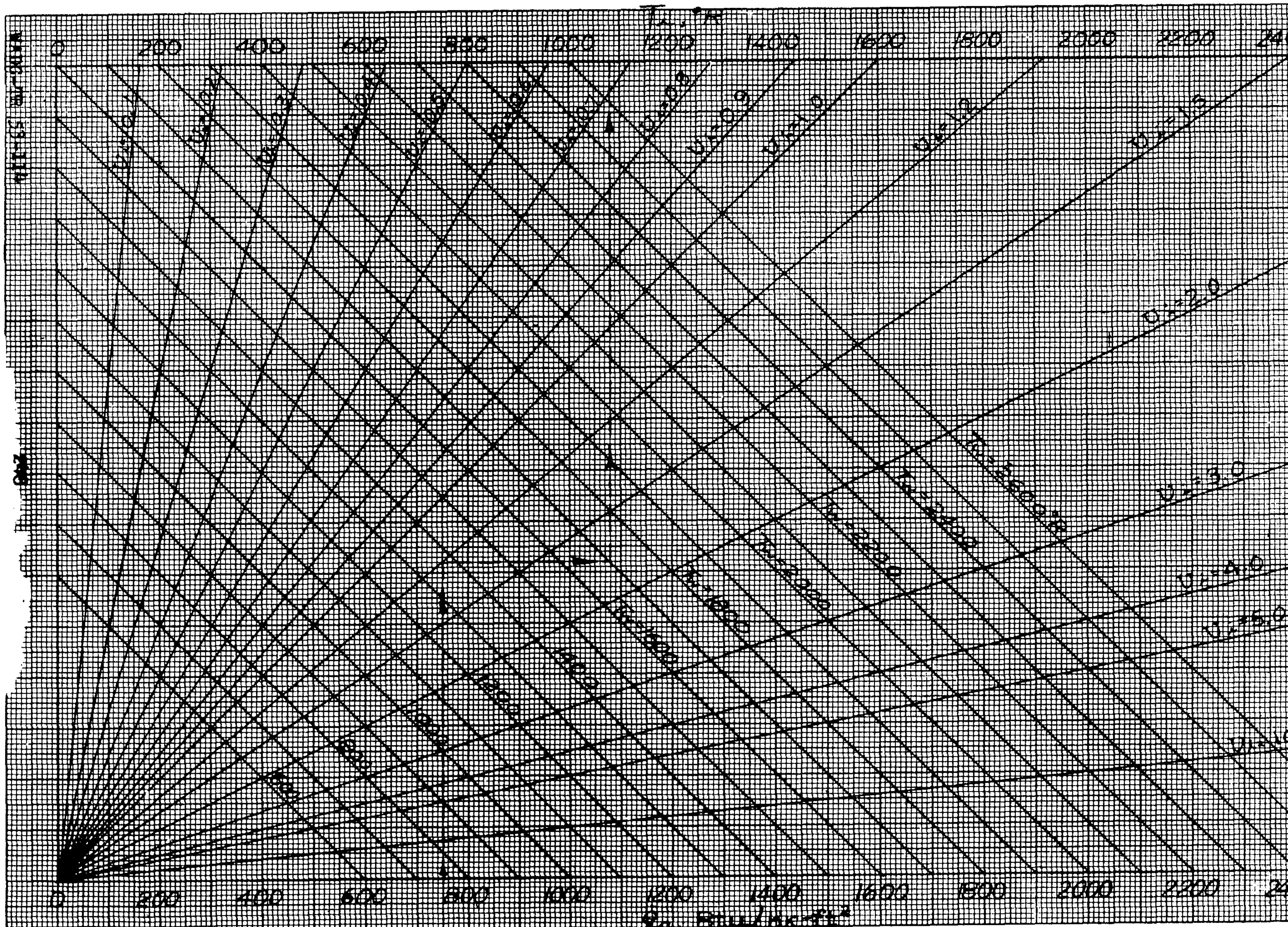

Figure V-13

Heat Conduction Through Insulation

CONFIDENTIAL

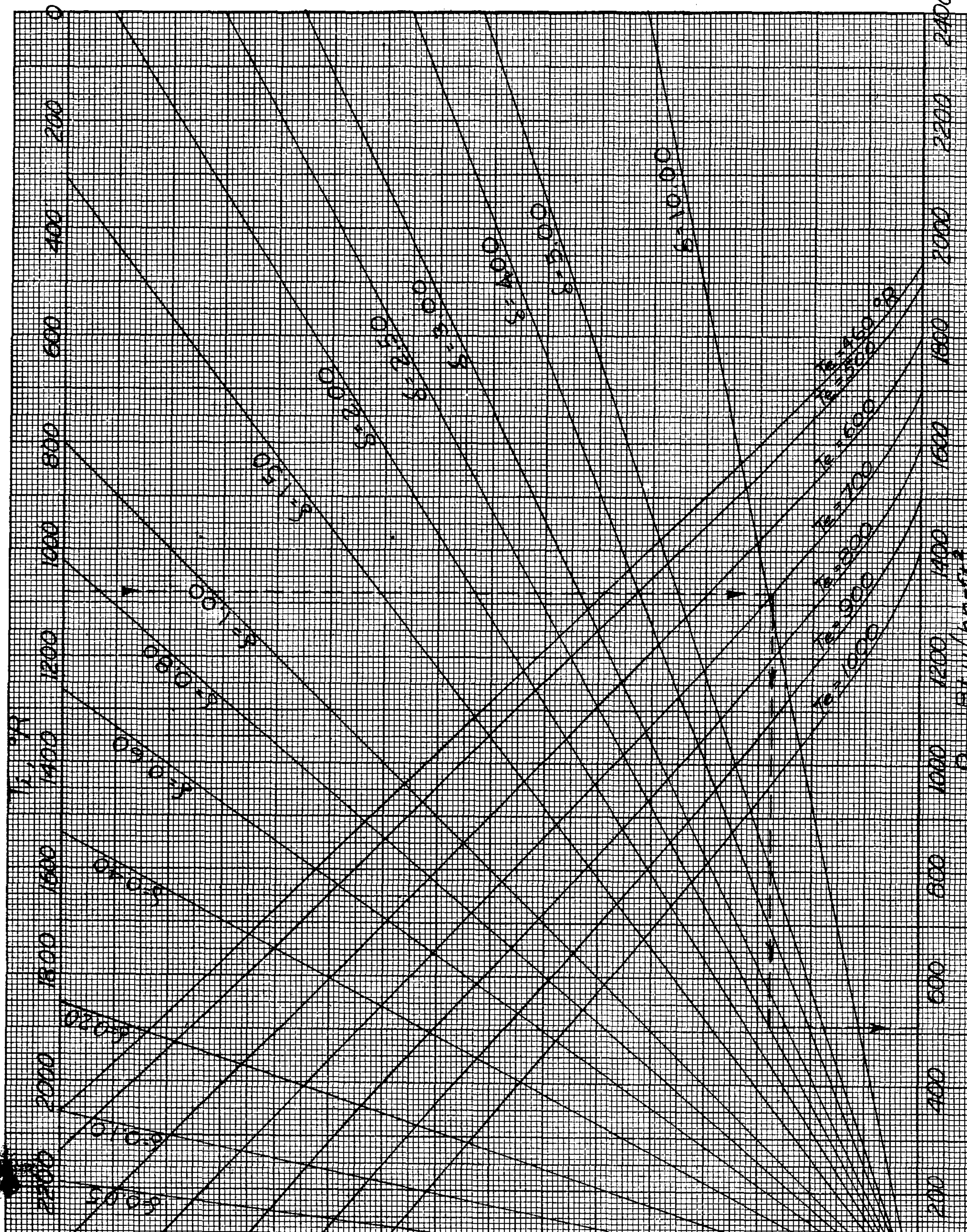

Figure V-14
Free Convection in Air

using a value of $R = 4$, and can be used with precision only for this value. For values near $R = 4$, it can be used as an approximation. Figure V-15 is a graphical solution of equation (V-3) with the ordinate scale (not shown) laid off to values of the function.

$$(17.4 \times 10^{-4}) \frac{\left(\frac{T_i}{100}\right)^4 - \left(\frac{T_e}{100}\right)^4}{\left(\frac{T_i}{100}\right) - \left(\frac{T_e}{100}\right)}$$

The function ϵ' is defined as

$$\epsilon' = \frac{1}{\frac{1}{\epsilon_i} + \frac{1}{\epsilon_e} - 1}$$

Figure V-15 is in two parts. Part a is for low values of emissivity function, while part b is for higher values of the emissivity function.

Two applications for the series of charts Figures V-13,-14, and -15 are given in the example of design of insulation for an uncooled compartment. In addition, they may be used to do an interval calculation of the type given in this Appendix. To calculate an interval, the value of T_{e2} is first assumed, and the value of T_{em} calculated. Then the value of T_{im} is assumed, and the value of $U_i = k_i/x_i$ is evaluated for the mean insulation temperature, either from a prepared chart of U_i versus T_{im} or by calculation for k_i at $(T_w + T_{im})/2$. The conduction chart is then used, entering with T_{im} and moving parallel but opposite to the dashed-arrow lines, to get q_o. The free convection chart is used next, entering with T_{im} and obtaining q_c corresponding to T_{em} and . The radiation chart is next used, entering with T_{im} and obtaining q_r for T_{em} and the appropriate

$$\epsilon' = \frac{1}{\frac{1}{\epsilon_i} + \frac{1}{\epsilon_e} - 1} .$$

When the sum $(q_c + q_r)$ equals the value of q_o, the value of T_{im} assumed is correct. The quantity q_o is then used in the equation,

$$\Delta T_e = \frac{(q_o + q_g)\,\Delta\tau}{m_e c_e}$$

This value of ΔT_e is then used to determine the value

$$T_{e2} = T_{e1} + \Delta T_e$$

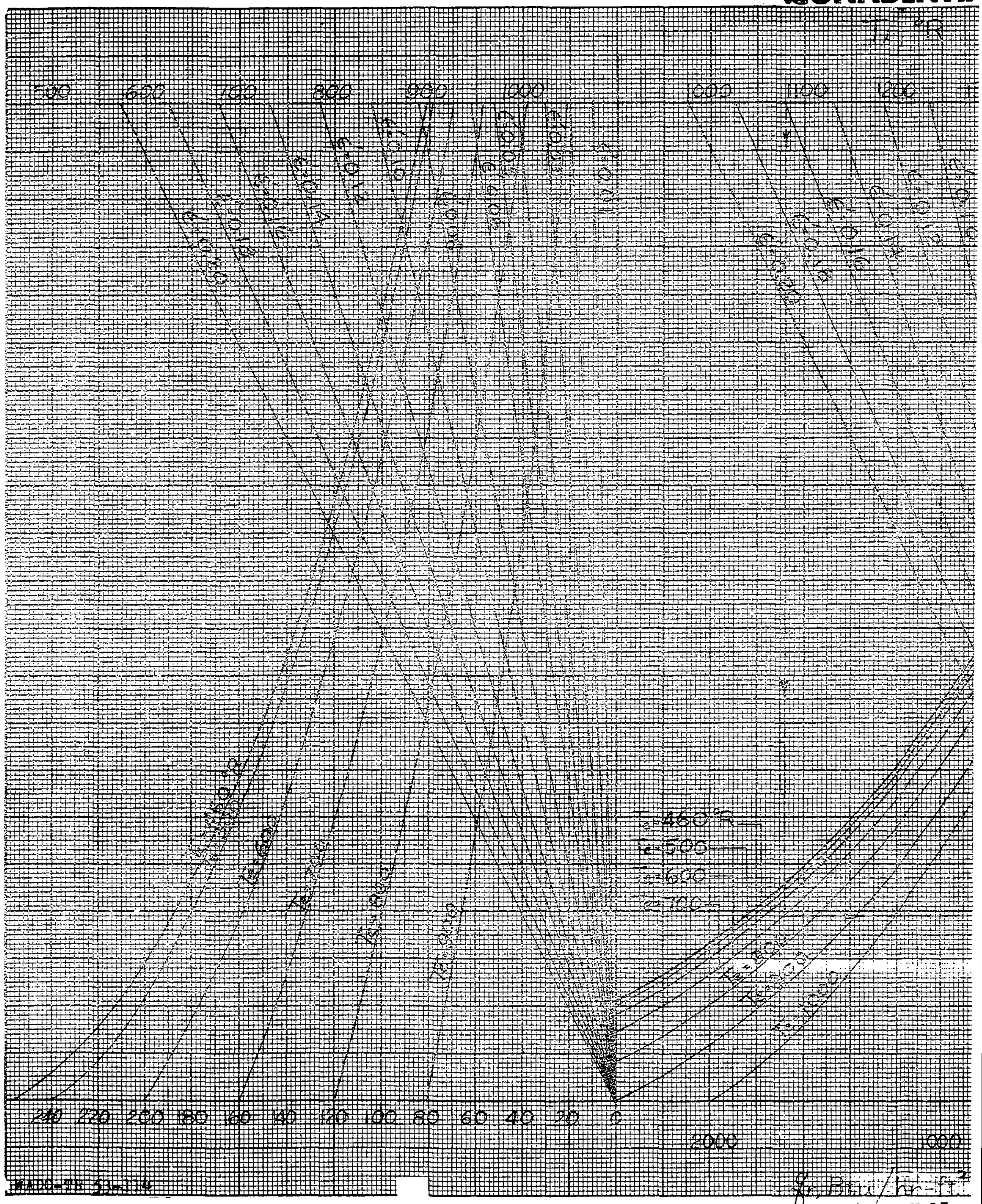

Figure V-15a
Radiation

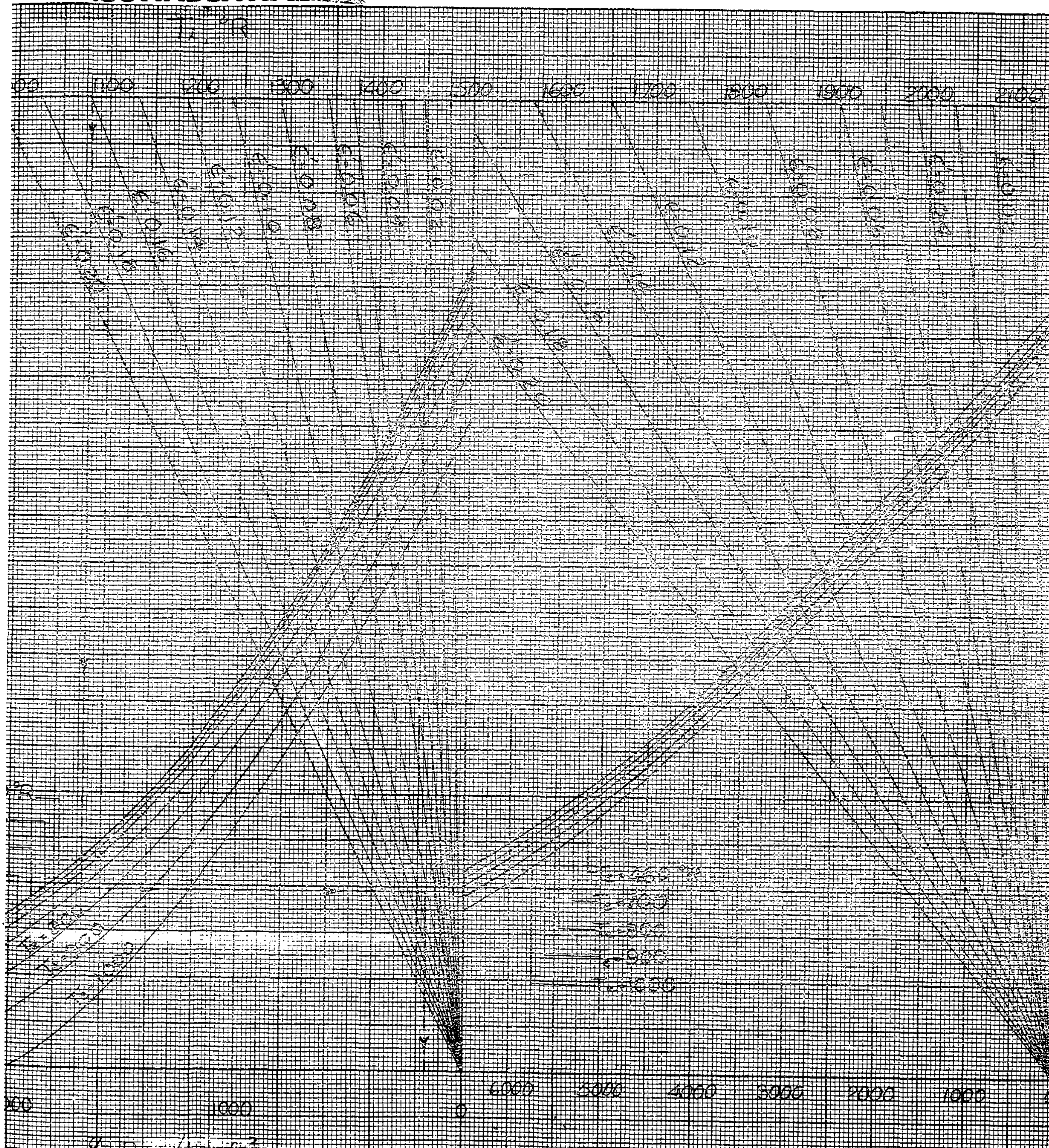

Figure V-15a
Radiation

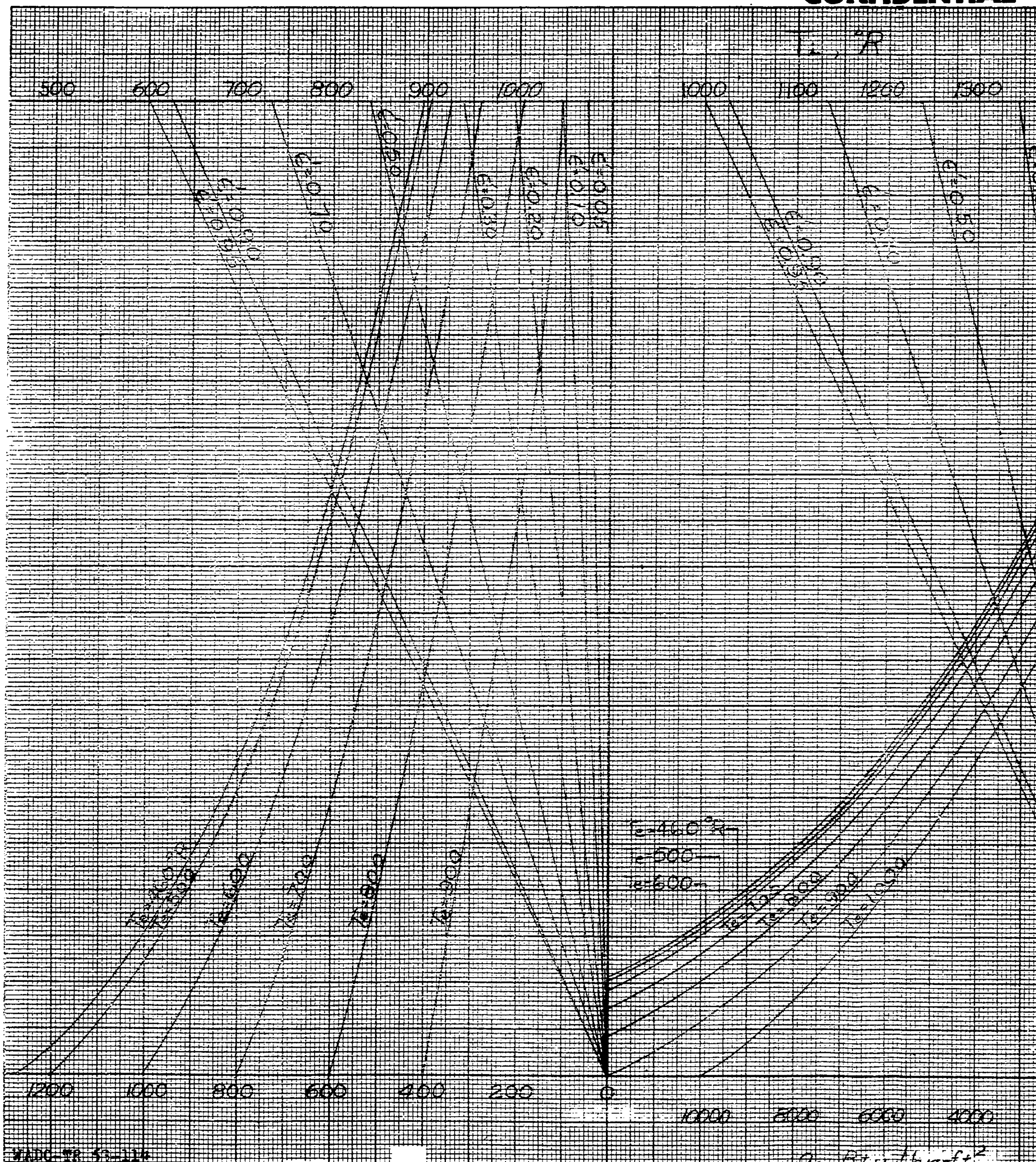

Figure V-15b
Radiation

(1)

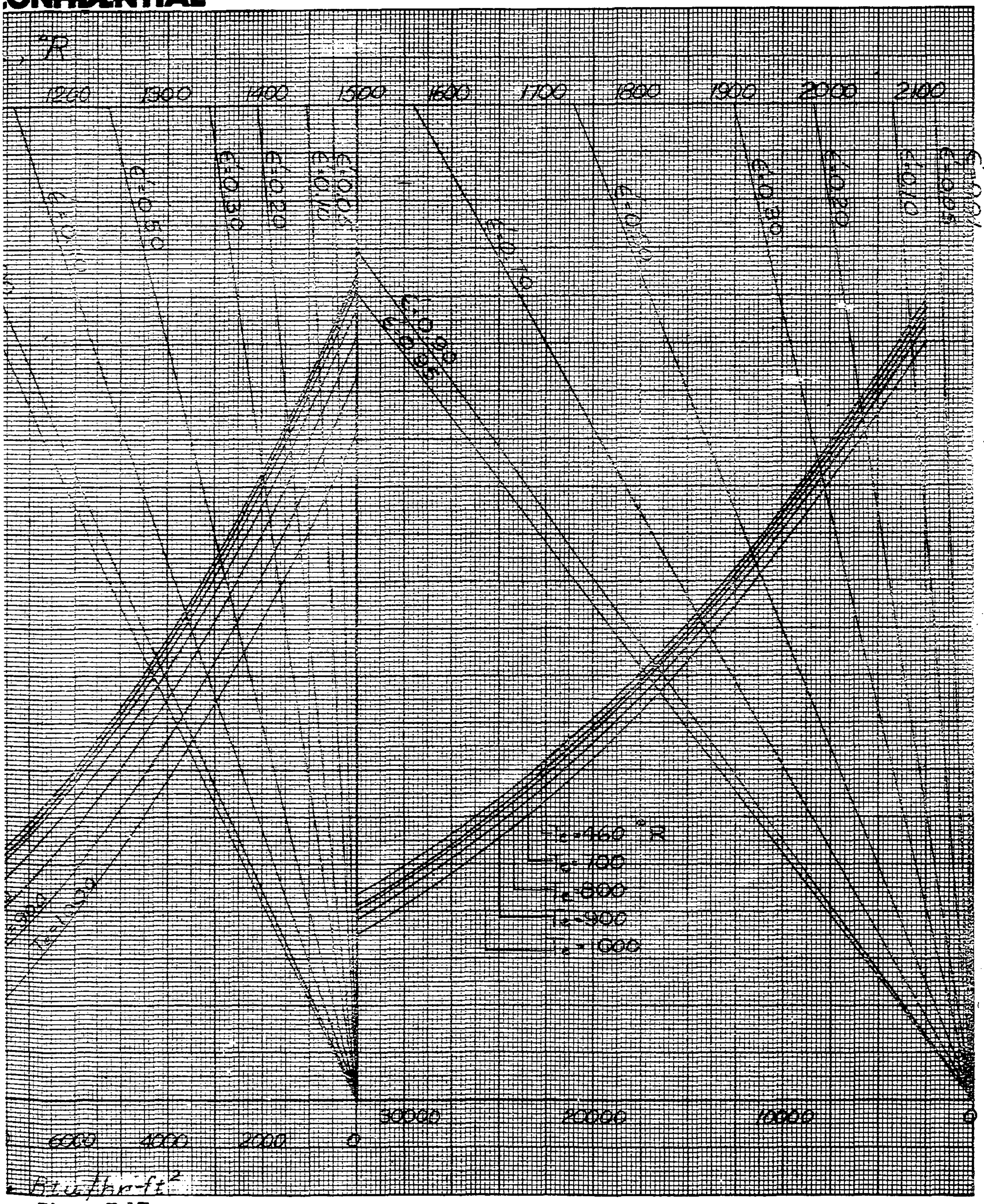

Figure V-15b

Radiation

If T_{e2} agrees with the assumed value, the interval calculation is completed, and is repeated for the next interval. All heat transfer rates, heat generation rates, and thermal capacities are on a unit skin area basis, as before. The charts are based on a value of R = 4, so should not be used in cases where the ratio of free convection to radiation area of equipment differs appreciably from that value.

These charts were actually designed for use in the calculations indicated in the design example, and hence are somewhat awkward for use in the calculation above. For most purposes it is more convenient to make a transient analysis of equipment temperature rise with equations (V-17) and (V-18), using the charts as indicated in the design example to establish the constants of equation (V-17).

3. Reference

(V-1) Brown, A. I. and Marco, S. M. Introduction to Heat Transfer. Second Edition, McGraw-Hill Book Company, Inc., New York, 1951.

SECTION VI

TEMPERATURE RISE OF EQUIPMENT IN A FUEL-JACKETED COMPARTMENT IN SUPERSONIC FLIGHT

By T. C. Taylor and Y. H. Sun

Compartment fuel jacketing is one method of preventing excessive temperature rise of equipment during supersonic flight. Flat ducts or tubes of fuel can be arranged along the inside of the skin insulation so as to absorb the external heat load entering through the skin. The external load insofar as interior equipment is concerned is then reduced to the heat transfer between the fuel ducts and the equipment by means of free convection and radiation. This heat transfer is a cooling effect if the fuel temperature is lower than the equipment temperature. This method of protecting equipment from excessive temperature rise is intermediate to the cases of an uncooled compartment and a compartment with internal cooling. The protection of equipment against external heat load in the fuel-jacketed compartment is almost perfect, and thus superior to the performance of insulation of any reasonable thickness. The jacketed compartment does not deal very effectively with generated heat, however, and in this respect is inferior to cooled compartments. Two salient advantages of fuel-jacketing are that it uses a coolant which is already present in any liquid-fuel burning aircraft, and that it uses it in a way which does not occupy valuable installation space near the center of the compartment. Tending to offset these are the constructional complications involved and the possible reduced accessibility of the compartment.

In this section, an analysis is developed to evaluate the temperature rise of equipment in a fuel-jacketed compartment. It is emphasized, however, that even where thermal performance would be satisfactory, constructional limitations may preclude the use of this method.

SUMMARY

The temperature rise of equipment in a fuel-jacketed compartment is considered. It is assumed that the compartment is fitted with flat fuel ducts at the inner face of the skin insulation. The fuel thus receives heat coming through the insulation from the skin, and exchanges heat with the equipment by free convection and radiation. Equations are developed to describe all of the heat transfer and heat storage mechanisms. A trial and error calculation procedure is developed from the equations, using a stepwise application of the equations to evaluate the temperature rise with time of equipment.

A design and a rapid evaluation procedure are given. The design procedure determines the thickness of skin insulation required to meet a maximum fuel temperature specification for the selected fuel duct

dimensions and fuel flow rate. A preliminary evaluation procedure is given which indicates whether in certain cases a fuel-jacketed compartment can give satisfactory equipment temperature performance. In other cases a more detailed evaluation procedure is required. The more detailed procedure involves trial and error calculations, but is based on simplifications of the general calculation procedure.

Equipment temperature rise characteristics are calculated for a variety of compartment and equipment characteristics. The salient conclusions based on the results of these calculations are summarized as follows:

1. The equipment temperature in a fuel-jacketed compartment must always be between the fuel temperature and that temperature which the equipment would attain if it exchanged no heat with its surroundings. The latter temperature is easily computed from the equipment thermal capacity and heat generation rate. Where the fuel temperature is above the equipment temperature some heat is transferred from the fuel to the equipment, but it is usually small compared to that which would be transferred without the fuel jacket, since fuel temperatures are less than skin temperatures for supersonic flight. When the fuel temperature is below the equipment temperature, the equipment is entirely protected from the external heating, and is cooled somewhat by transfer of heat to the fuel jacket.

2. As in the case of an uncooled compartment, equipment with greater heat generation has more rapid temperature rise. Therefore, when fuel temperatures are below equipment temperature, the equipment with higher heat generation furnishes greater temperature potential to transfer heat to the fuel, giving greater heat transfer rates.

3. In the range of fuel flow rates from 500 to 1000 lb/hr-ft^2, based on skin surface area, the fuel flow rates do not greatly affect the equipment temperature rise. For the two fuel rates studied, the lower one gives a slightly greater rate of equipment temperature rise with time. The small effect of fuel flow rate is due to two factors. First, the thermal capacity of the fuel is great compared to the heat it receives, resulting in a small temperature rise. Second, the resistance to heat flow on the fuel-side of the inner heat transfer surface is very small compared to the resistances to heat flow by free convection and radiation on the compartment-side of the inner heat transfer surface.

4. The ratio of free convection to radiation heat transfer area of the equipment has little effect on the rate of equipment temperature rise in a fuel-jacketed compartment. Modifications in the arrangement and extent of equipment surfaces therefore cannot be used as a means of reducing equipment temperature rise. Efforts to reduce temperature rise should concentrate on changes of surface emissivity of bodies exchanging heat by radiation, and on compartment air pressure, which has a dominant effect on heat transfer by free convection.

5. Insulation must be used between the skin and the fuel ducts for two reasons. First, the insulation prevents exposing the fuel to the high temperature of the skin. Second, the insulation reduces heat flow into the fuel from the skin, and thus reduces the temperature rise of the fuel. For a skin temperature of 1355°R and for available fuel flow rates of 500 to 1000 lb/hr-ft^2, the insulation thickness required to limit the fuel temperature rise to less than 8°R in about 0.3 in. for insulations like rock wool.

ANALYSIS

1. Assumptions for Analysis

The typical configuration of a fuel-jacketed compartment is shown schematically in Figure VI-1. The compartment shown is cylindrical in form, although the analysis is applicable to any shape.

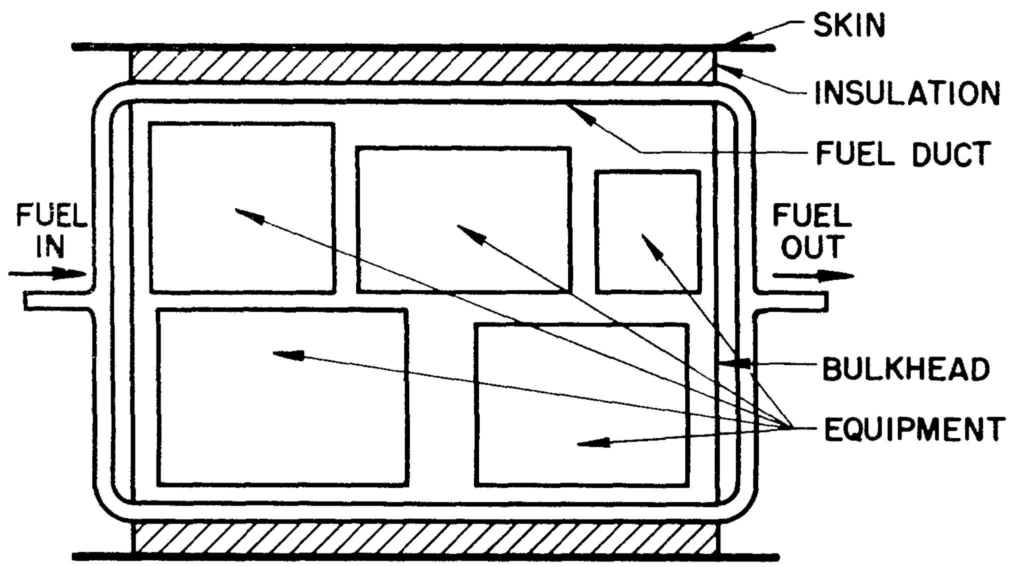

Figure VI-1. Schematic of Fuel-Jacketed Compartment

Heat flows inward from the high-temperature skin to the fuel coolant in the ducts. Insulation is provided between the skin and the ducts to prevent contact between hot skin and the fuel. The variation of insulation thermal conductivity with temperature is accounted for, but

insulation thermal capacity is neglected. The film heat transfer coefficient for fuel in the duct is included, assuming laminar flow conditions. This condition is most likely, since fuel ducts would be large in proportion to fuel flow rates so as not to produce objectionable pressure drop. The skin of the aircraft is assigned a constant temperature, a simplification which is explained in Section IV.

In addition to receiving heat from the skin, the fuel in the duct also exchanges heat with the equipment. Heat is transferred between the equipment and the inner surface of the fuel duct by free convection and radiation only, and between the duct surface and the fuel by forced convection through the fuel film.

The evaluation of free convection and radiation heat transfer is treated in the same manner as in Section V. An average equipment surface temperature is used, and the average inner fuel duct surface temperature is used for writing the heat transfer equations between these two surfaces. Average free convection coefficients are used, and the emissivities assigned to surfaces involved in radiant heat transfer are assumed to be constant with varying temperature.

2. Nomenclature

Symbol	Definition	Units
A	Area	ft^2
a'	Group of properties for free convection, used in equation (VI-6).	
B	Temperature function for radiation, used in equation (IV-5)	$°R^3$
b	Group of properties for forced convection over flat plates, defined for equation (VI-2)	
c	Specific heat	Btu/lb-°R
c_p	Specific heat at constant pressure	Btu/lb-°R
h	Heat transfer coefficient	Btu/hr-ft^2-°R
k	Thermal conductivity	Btu/hr-ft-°R
L	Length of fuel duct	ft
m	Weight per unit skin area	lb/ft^2

Symbol	Definition	Units
Pr	Prandtl modulus	dimensionless
Q	Volume flow rate	ft^3/hr
q	Heat transfer rate	$Btu/hr\text{-}ft^2$
R	Ratio of free convection to radiation area of equipment	dimensionless
Re	Reynolds modulus	dimensionless
T	Absolute temperature	°R
U	Thermal conductance	$Btu/hr\text{-}ft^2\text{-}°R$
V	Velocity	ft/hr
W	Weight flow rate per unit skin area	$lb/ft^2\text{-}hr$
x	Length	ft
$\propto$	Proportionality symbol	
γ	Weight density	lb/ft^3
δ	Pressure	dimensionless
ϵ	Emissivity	dimensionless
θ	Temperature potential	°R
μ	Viscosity	lb/ft-hr
τ	Time	hr
τ'	Time	min.

Subscripts

a	Denotes air
c	Refers to convection
d	Denotes duct wall spacing
e	Denotes equipment

Subscripts	Definition
f	Denotes fuel
fe	Denotes fuel at entrance to duct
fL	Denotes fuel at exit of duct
i	Denotes insulation
if	Denotes heat transfer from insulation to fuel
it	Denotes insulation of fuel tank
m	Denotes average value
o	Denotes external value
p	Denotes previous interval
r	Refers to radiation
s	Denotes inner duct surface
sf	Denotes surface to fuel
w	Denotes skin
1,2	Denotes initial and final values of an interval

3. Derivation of Equations

a. Heat Conduction through Insulation

An equation for heat transfer rate through the insulation, based on a unit skin area, is,

$$q_o = U_i(T_w - T_i) \tag{VI-1}$$

where $U_i = k_i/x_i$. The method of accounting for variation of thermal conductivity with temperature in a stepwise calculation is given in Appendix II.

b. Forced Convection Heat Transfer in the Fluid Ducts

Since a construction using flat ducts for fuel is assumed, a flat plate heat transfer coefficient is used. Reference (VI-1) gives an expression for the heat transfer coefficient where fluid flows in

laminar flow parallel to a flat plate as,

$$h_f = 0.66 \frac{\gamma c_p}{(Re)^{1/2}(Pr)^{2/3}} V_f$$

which is suitable for Re = 300,000 and below. This is put in the form,

$$h_f = 0.66\ b\ V_f^{0.5} \qquad \text{(VI-2)}$$

where

$$b(x)^{0.5} = \frac{\gamma c_p}{(\frac{\gamma}{\mu})^{0.5}(\frac{c_p \mu}{k})^{0.67}}$$

Values of $b(x)^{0.5}$ are plotted as a function of temperature in Figure VI-9 contained in the Appendix to this Section, for use in calculations involving equation (VI-2). Values of $b(x)^{0.5}$ as taken from the plot are divided by $(x)^{0.5}$, to obtain b of equation (VI-2). The length x represents the characteristic dimension of the flat duct, which is taken as its length. The use of the flat plate equation and the duct length to define characteristic length for a flat duct is rigorous only if the spacing between duct walk is somewhat greater than twice the thickness of a fluid boundary layer. For very narrow ducts it is used as an approximate method of defining the heat transfer coefficient.

The value of b for use in equation (VI-2) should be determined at the average temperature of the fluid film. In the case of the fluid film at the duct wall facing the insulation, this average temperature is $(T_i+T_f)/2$, as based on instantaneous temperatures at the insulation face and of the fuel. For the fluid film at the interior duct wall, the average temperature is $(T_f+T_s)/2$, as based on instantaneous values. Heat transfer rates through the fluid films, per unit skin area, are described by the equations,

$$q_o = q_{if} = h_{if}(T_i - T_f) \qquad \text{(VI-3)}$$

for the insulation-side duct surface, and,

$$q_{sf} = h_{sf}(T_s - T_f) \qquad \text{(VI-4)}$$

for the inner duct surface.

c. <u>Radiation Heat Transfer</u>

In keeping with the practice of Section V, the radiation heat transfer rate based on a unit skin area is given by,

$$q_r = h_r(T_e - T_s) \qquad \text{(VI-5)}$$

where

$$h_r = 17.4 \times 10^{-4} \left(\frac{1}{\frac{1}{\epsilon_s} + \frac{1}{\epsilon_e} - 1} \right) \left[\frac{\left(\frac{T_e}{100}\right)^4 - \left(\frac{T_s}{100}\right)^4}{\left(\frac{T_e}{100}\right) - \left(\frac{T_s}{100}\right)} \right]$$

The function of temperatures is given as B in Figure A-IV-1.

The emissivity values, ϵ_s and ϵ_e, are chosen to represent the surfaces exchanging heat by radiation. For this analysis, values of $\epsilon_s = 0.1$ and $\epsilon_e = 0.2$ are used in describing h_r. The values of emissivity for a large variety of surface conditions and materials are given in Reference (VI-2). The form of the emissivity factor given in h_r above is for the case of radiation heat exchange between a body and its enclosure when the body is large compared to the enclosure. This is likely to be the case in an aircraft compartment filled with equipment.

d. Free Convection Heat Transfer

An expression for the free convection heat transfer coefficient in the compartment air is developed in Section V as,

$$h_c = \left(\frac{a'}{\delta^{2/3}} \right) \delta^{2/3} \quad \theta^{1/3} \tag{VI-6}$$

where $(a'/\delta^{2/3})$ is a group of physical properties for air, given as a function of air temperature in Figure A-IV-2. The average film temperature is used to evaluate $(a'/\delta^{2/3})$. Thus, the temperature potential θ for the coefficient at the equipment surface is $(T_e - T_a)$ and the average film temperature is $(T_e + T_a)/2$. The temperature potential θ for the coefficient at the duct surface is $(T_a - T_s)$, and the average film temperature is $(T_a + T_s)/2$.

Using equation (VI-6) with the appropriate temperature potential, the free convection heat transfer rate, based on a unit skin area is

$$q_c = Rh_{ce}(T_e - T_a) \tag{VI-7}$$

for the equipment surfaces,
and,

$$q_c = h_{cs}(T_a - T_s) \tag{VI-8}$$

for the duct surface.

The factor R is the ratio of effective free convection to radiation surface area of the equipment.

e. Heat Balance for Equipment

The overall equation for free convection heat transfer between the equipment and the duct surface is found by combining equations (VI-7) and (VI-8) to give,

$$q_c = \frac{1}{\frac{1}{h_{cs}} + \frac{1}{Rh_{ce}}} (T_e - T_s)$$

where an overall free convection heat transfer coefficient is defined to give

$$q_c = h_c(T_e - T_s) \qquad \text{(VI-9)}$$

Equations (VI-5) and (VI-9) are then combined to give the total heat transfer rate between the equipment and duct surfaces,

$$q_c + q_r = (h_c + h_r)(T_e - T_s) \qquad \text{(VI-10)}$$

A heat balance equation is next written for the equipment, describing the change of equipment temperature with time. For heat generating equipment, this heat balance is,

$$q_g = m_e c_e \frac{\Delta T_e}{\Delta \tau} + (h_c + h_r)(T_e - T_s) \qquad \text{(VI-11)}$$

In this equation, the generated heat, q_g, and the equipment thermal capacity, $m_e c_e$, must be expressed on a unit skin area basis, as explained in the Analysis portion of Section V.

f. Heat Balance for the Fuel

The overall heat transfer between the skin and the fuel is found by combining equations (VI-1) and (VI-3) to give

$$q_{if} = q_o = \frac{1}{\frac{1}{U_i} + \frac{1}{h_{if}}} (T_w - T_f) \qquad \text{(VI-12)}$$

The heat transfer between the inner duct surface (facing the equipment) and the fuel is given by equation (VI-4). Using equations (VI-12) and (VI-4), a heat balance equation is written for the fuel,

$$q_o + q_{sf} = W_f c_f \Delta T_f \qquad \text{(VI-13)}$$

where W_f is the weight flow rate of fuel per unit time, based on a unit skin area for the compartment.

The fuel temperature, T_f, appearing in equations (VI-3, -4, -12 and -13) is in general variable with time because of fuel heating at its source, or in the storage tank. The temperature rise of the fuel in storage tanks during supersonic flight is treated in Appendix III. Some of the results given there are used in the calculation procedures for evaluating equipment temperature rise in a fuel-jacketed compartment.

3. Procedure for Calculation of Equipment Temperature Rise with Time

a. General Method

The derived heat balance equations (VI-11) and (VI-13) must be satisfied simultaneously to determine the equipment temperature T_e for any assigned time τ. A direct solution is not feasible because of the functions required to describe forced convection, free convection, and radiation coefficients, the independent variation of fuel temperature with time, and the complex interdependence of temperatures. It is therefore necessary to use a stepwise calculation procedure. Two methods of stepwise calculation are applicable to this problem. The first uses the heat transfer rate and heat balance equations in their stated form, evaluating all heat transfer coefficients at the initial values of temperature for the interval, and solving equation (VI-11) for T_e, the equipment temperature at the end of the interval. This method is not accurate for large time intervals $\Delta\tau$. The second method is to use average values of temperatures during a time interval for the evaluation of all heat transfer coefficients and heat transfer rates. Since the average temperature for an interval is unknown at the start of an interval calculation, this method requires a trial and error solution based on assumed values. This method involves more work, but is more accurate for an interval of given size. The trial and error method, is described here, since it is more generally applicable. The method based on initial temperatures is an obvious simplification of the described method.

For any set of conditions, describing the compartment and equipment characteristics, there are six temperatures which define the thermal condition of the compartment. The first of these is T_w, which is assumed constant and the others are T_i, T_f, T_s, T_a, and T_e, which are all variable with time. A trial and error calculation involving so many variable temperatures would be extremely difficult were it not for the fact that certain of these temperatures are rather closely restricted in value. The entrance temperature of the fuel T_{fe} is known for any instant of time from a plot of fuel temperature vs. time (See Appendix III). The average entrance temperature T_{fem} can then be found at the middle of any time interval $\Delta\tau$ from such a plot. The mean temperature of the fuel is not this mean entrance temperature, however, but is somewhat higher due to heat received by the fuel. This heat, q_{if} can be found very accurately by estimate and varies only slightly, so that T_{fm} can be predicted with ease. The temperatures T_i and T_s are both quite close to T_{fm}, and differ from it by amounts which vary slowly, so that they may also be predicted

with ease. The remainder of the temperatures, T_a and T_e are then the only ones which could vary with sufficient rapidity to offer any difficulty in assuming values.

The calculation procedure is described in principle here. A detailed calculation procedure and sample calculation are given in the Appendix to this section. The procedure is described on the basis of calculating one time interval $\Delta\tau$ where the subscripts 1, 2, and m refer to values at the beginning, end and middle of the interval, respectively, and where the average value for any quantity, for example T_f, is always found from a form such as

$$T_{fm} = \frac{T_{f1}+T_{f2}}{2}$$

The initial temperatures that must be found at the very beginning of a calculation are found by a simplified procedure, omitting many of the steps of the standard interval procedure. The simplifications allowed are indicated in the Appendix to this section.

b. Calculation of an Interval

After finding T_{fem} for the middle of the time interval from the fuel time temperature plot, the value of h_f is found from equation (VI-2), evaluating b at T_{fem}. For this purpose V_f must be known from the fuel duct design and the fuel flow rate. Then, q_{if} can be estimated from a modification of equation (VI-12) in the form,

$$q_{if} = \left(\frac{1}{\frac{1}{U_i}+\frac{1}{h_f}}\right)\left(T_w-T_{fcm}\right)$$

where U_i is taken from the previous interval. Equation (VI-13) is next solved for ΔT_f, using q_{sfm} from the previous interval, since q_{sfm} is generally quite small compared to $q_o=q_{if}$. The value of c_f for equation (VI-13) is taken from Figure AT-2 at T_{fem}. The mean temperature of the fuel is next estimated from,

$$T_{fm} = T_{fem}+\frac{\Delta T_f}{2}$$

The value of T_{i2} is next assumed, where $(T_{i2}-T_{i1}) \approx (T_{fe2}-T_{fe1})$

Then T_{im} is calculated as,

$$T_{im} = \frac{T_{i2}+T_{i1}}{2}$$

Then the film temperature $(T_{im}+T_{fm})/2$ is calculated, and a more accurate

evaluation of the film heat transfer coefficient h_{ifm} is based on this film temperature, using equation (VI-2). The more accurate calculation of external heat load to the fuel q_{ifm} is then made from

$$q_{ifm} = \left(\frac{1}{\frac{1}{U_i} + \frac{1}{h_{ifm}}} \right) (T_w - T_{fm})$$

with U_i based on the value of T_{im} recently found. If q_{ifm} agrees with q_{if} sufficiently close that ΔT_f would not be changed more than 3°R by using q_{ifm}, the calculation need not be repeated; otherwise the calculation is repeated from the determination of ΔT_f onward. This rarely is necessary.

T_{sm} is next approximated from

$$T_{sm} \approx T_{fm} + \left(\frac{q_{stm}}{h_{sfm}} \right)_p$$

where the subscript p denotes the previous interval. T_{e2} and T_{a2} are assumed, and the values of T_{em} and T_{am} are calculated. If T_e and T_f are about equal, initially or at any other time during the calculation, T_{e2} can be estimated from

$$T_{e2} \approx T_{e1} + \frac{q_g \Delta \tau}{m_e c_e}$$

Otherwise T_{e2} will be less than that found by this estimation formula for $T_e > T_f$, and greater than given by the formula for $T_e < T_f$.

The value of h_r is next determined, as based on T_{sm} and T_{em}, and the value of q_r determined from equation (VI-5) based on these same temperatures. Using T_{sm}, T_{am}, and T_{em}, values of h_{ce} and h_{cs} are found as in Section V, and the value of h_c is calculated for use in equation (VI-9). Then, q_c is calculated from equation (VI-9) and q_{sfm} is calculated from,

$$q_{sfm} = \left(\frac{1}{\frac{1}{h_{fsm}} + \frac{1}{h_c + h_r}} \right) (T_{em} - T_{fm})$$

Equation (VI-4) is solved, using all quantities with m subscripts, as a check on T_{sm}. This calculated result should agree closely with the value estimated earlier. If not, recalculation is required, using the first calculated result as the estimated value. Agreement within 1°R is sufficient, and very easily achieved by the estimation formula given, so that recalculation is rarely necessary.

Equation (VI-11) is next solved for ΔT_e, using coefficients and temperatures at the average value (subscript m). T_{e2} is given by,

$$T_{e2} = T_{e1} + \Delta T_e$$

T_{a2} is calculated from the heat balance,

$$(T_{am}-T_{em}) = \frac{h_c}{h_{ce}R} \quad (T_{sm}-T_{em})$$

where $$T_{am} = T_{em} + (T_{am}-T_{em})$$

and $$T_{a2} = T_{a1} + 2\,(T_{am}-T_{a1})$$

The calculated values of T_{a2} and T_{e2} should agree within 3°R of the assumed values, otherwise the calculated values should be used as the assumed values for the repeated trial. When agreement is within 3°R, the calculated values are very accurate, and can be used as values of T_{e1} and T_{a1} for the next interval calculation.

The time interval used for any interval should be restricted to a value which corresponds to a rise in entrance temperature of the fuel $(T_{fe2}-T_{fe1})$ of 20°R.

EFFECTS OF COMPARTMENT AND EQUIPMENT CHARACTERISTICS ON THE TEMPERATURE RISE OF EQUIPMENT IN A FUEL JACKETED COMPARTMENT

The calculation procedure of the Appendix to this Section has been used to evaluate the temperature rise of equipment in a fuel-jacketed compartment for a number of conditions. The results of these evaluations are given here, together with a discussion of the significant variables and salient conclusions.

1. General Temperature Performance

An indication of the temperature rise characteristics of equipment in a fuel-jacketed compartment is given in Figure VI-2. The equipment in a jacketed compartment is compared with the same equipment in a compartment without a fuel jacket but the same insulating effect, and with the same equipment in a compartment having perfect insulation. The compartment and equipment characteristics are indicated in Figure VI-2. The characteristic length used in evaluating the laminar flow heat transfer coefficient in the fuel duct is one foot.

This could be interpreted to represent a cylindrical compartment one foot in axial length, with the peripheral fuel jacket made up of flat ducts one foot in length and running parallel to the axis

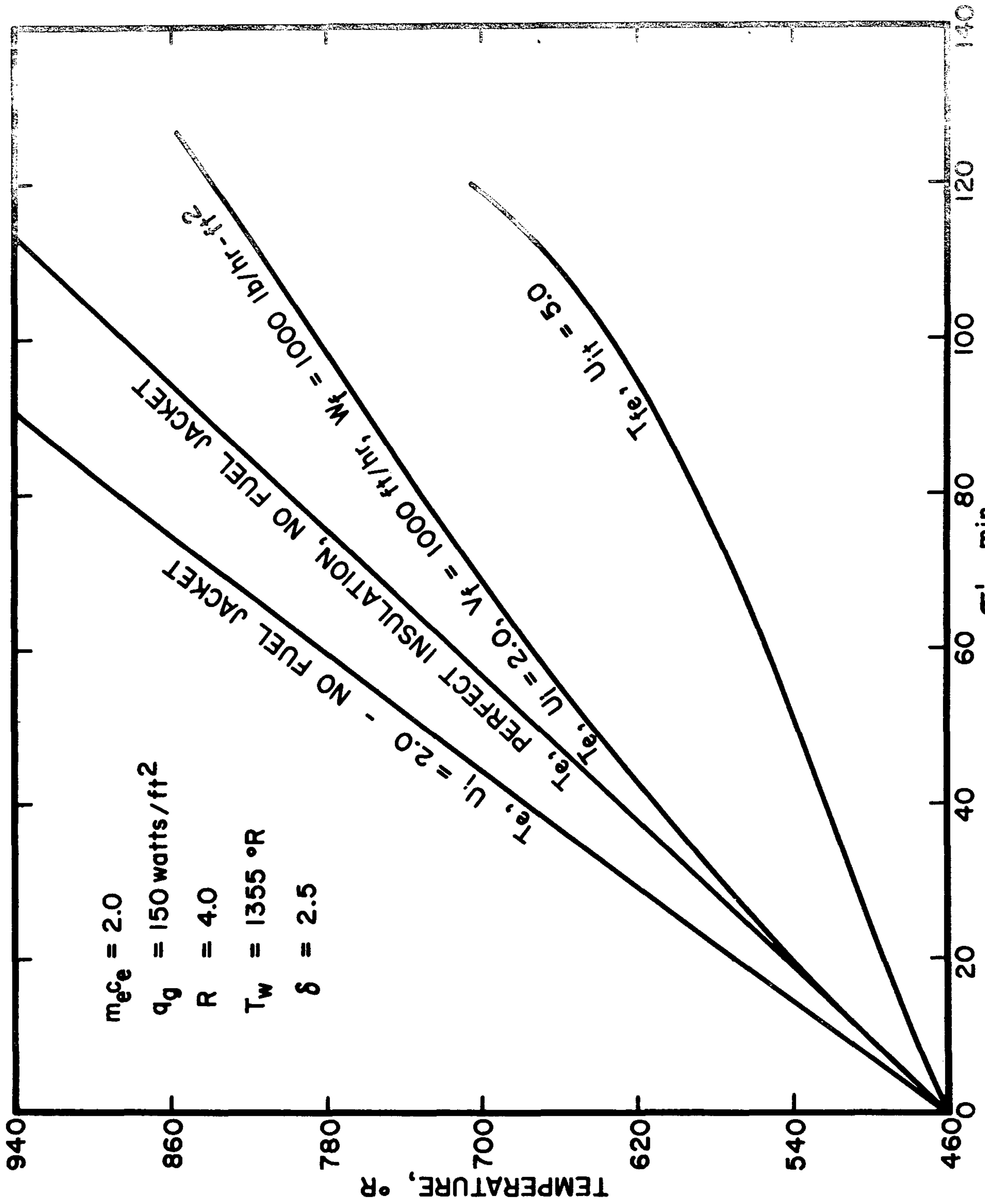

Figure VI-2
Temperature Rise of Equipment in a Fuel-Jacketed Compartment

of the compartment, with the duct thickness and fuel flow rates so proportioned that V_f = 1000 ft/hr and W_f = 1000 lb/hr-ft^2.

From Figure VI-2 it is seen that the equipment in the fuel-jacketed compartment has the lowest temperature rise of the three cases considered. It is interesting to compare the performance with that of the perfectly insulated compartment. In a perfectly insulated compartment, the equipment is protected completely from external heat load, and the equipment temperature rise is linear with time due to the constant heat generation rate, as shown. This would be the performance of a fuel-jacketed compartment if there were no heat exchange between the equipment and the fuel jacket. In the case shown, however, the fuel temperature (taken from Figure AIII-9) is always below the temperature which the equipment would assume without heat exchange. Therefore heat is transferred from the equipment to the fuel jacket by free convection and radiation, giving some cooling effect to the equipment. It is thus apparent that for the condition of fuel temperature lower than equipment temperature, the fuel jacket not only performs the function of a perfect insulator, but gives a slight cooling effect as well. Strictly speaking, the equipment is exposed to fuel jacket temperatures slightly higher than those shown, since the temperatures plotted in Figure VI-2 are entrance temperatures of the fuel. The fuel will be a few degrees hotter because of heat received through the skin insulation, and heat received from the equipment. If the fuel in the jacket were at all times at a temperature equal to the equipment temperature, the jacket would function only as a perfect insulator.

The plot for equipment temperature in a compartment having U_i = 2.0 Btu/hr-ft^2-°R and no fuel jacket is taken from a calculation using the analytical methods of Section V for equipment in an uncooled compartment. In this case the equipment is exposed to some external heat load as well as the generated heat load, so that its rate of temperature rise exceeds that for the perfectly insulated compartment.

Figure VI-3 compares equipment temperature rise of two cases having different fuel temperature characteristics. These fuel temperature plots are taken from Figure A-III-9. The case of perfect insulation, as before, represents equipment temperatures that would prevail if only the generated heat were absorbed by the equipment, and if there were no external heat transfer to or from the equipment. For an insulating effect on the fuel tank of U_{it} = 5.0 Btu/hr-ft^2-°R the fuel temperature as received from the storage tank is about equal to or higher than the temperature of perfectly insulated equipment. For the other case, where U_{it} = 1.0 Btu/hr-ft^2-°R the fuel temperature at entrance to the ducts is less than the temperature of perfectly insulated equipment. As found before in Figure VI-2, the equipment is not only protected from external heat, but is cooled somewhat by fuel temperatures below what might be called the "adiabatic" equipment temperature. The other case, for U_{it} = 5.0 shows that the equipment is heated somewhat by the fuel jacket when the fuel temperatures run above the adiabatic equipment temperature. As explained earlier, the true fuel temperatures are a little above the entrance fuel temperatures

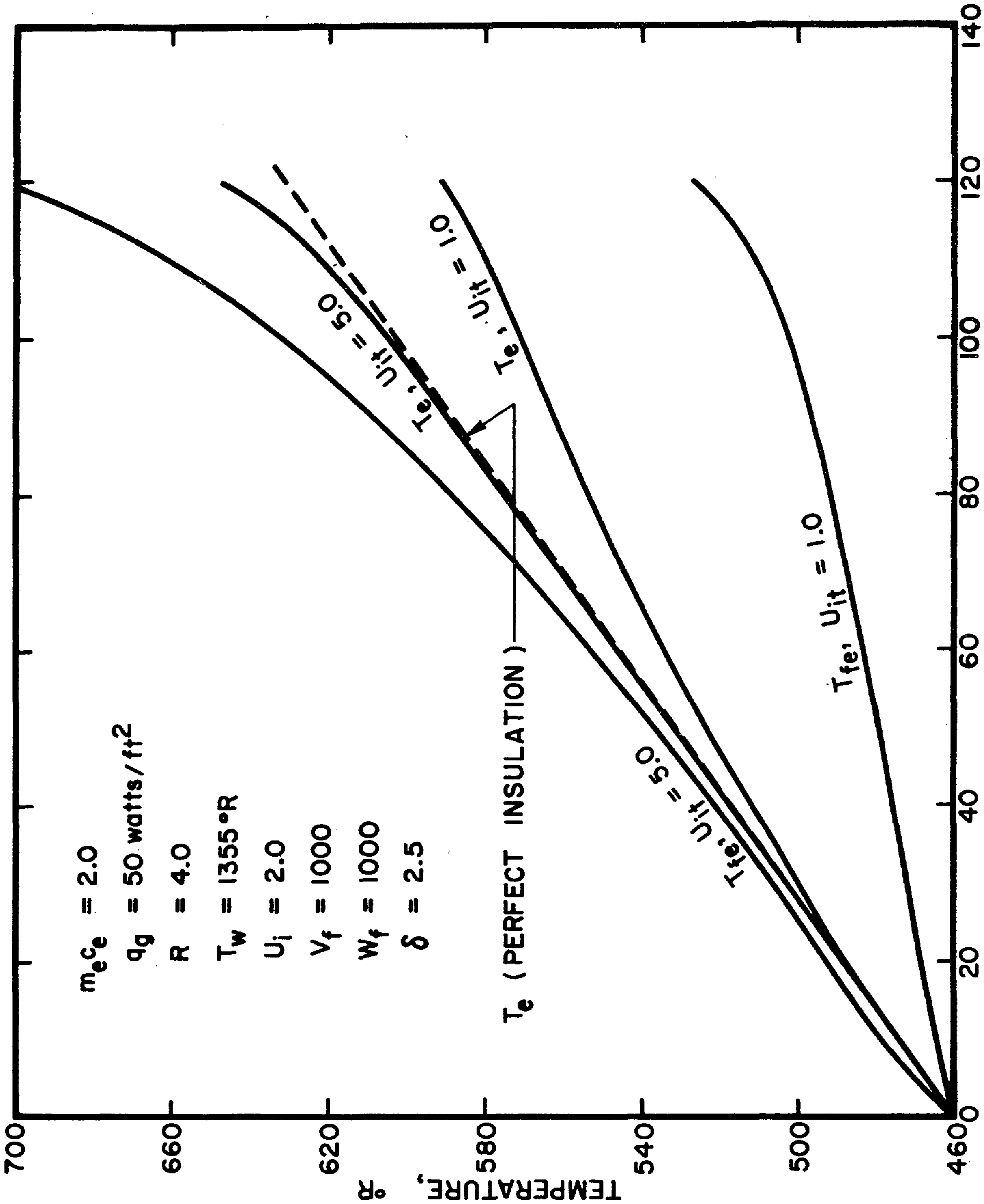

Figure VI-3
Temperature Rise of Equipment for Different Fuel Temperatures

shown because of heat gain to the fuel, hence there is some equipment heating even where the entrance fuel temperature is about equal to adiabatic equipment temperature.

An important conclusion can be drawn from the plots of Figures VI-2 and VI-3 for aiding the prediction of temperature rise performance of equipment in a fuel jacketed compartment. It is apparent from the results shown and from analytical considerations that the equipment temperature must always be between the adiabatic equipment temperature and the entrance fuel temperature. Since the entrance fuel temperature plot can be determined, and the adiabatic equipment temperature line is defined by

$$\frac{\Delta T_e}{\Delta \tau} = \frac{q_g}{m_e c_e}$$

definite limits are easily placed on the equipment temperature. The designer can therefore use these limits to predict the range of possible equipment temperatures for a fuel-jacketed compartment.

2. Heat Generation

The effects of heat generation by equipment on the temperature rise of equipment in a fuel-jacketed compartment are shown in Figure VI-4. The compartment and equipment characteristics are indicated in the figure. A characteristic length of one foot is used in evaluating the fuel heat transfer coefficients. The dashed line tangent to each temperature curve at 460°R indicates adiabatic equipment temperature. The line representing adiabatic equipment temperature is not shown for the case q_g = 50 Watts/ft^2, since it nearly coincides with the T_e plot. The fuel temperature plot shown is for U_{it} = 5.0, and is taken from Figure A-III-9.

The case of q_g = 50 Watts/ft^2 in Figure VI-4 is one in which the fuel temperature is very close to the adiabatic equipment temperature. Therefore, there is very little heat exchange between the fuel jacket and the equipment, so that the equipment temperature is close to the temperature for a perfectly insulated equipment. In the cases with higher heat generation, the temperature lines for perfectly insulated equipment lie considerably above the fuel temperature plot. Therefore, for all of cases with q_g > 50 Watts/ft^2 some cooling takes place and the T_e-plots lie between the T_f-plot and the adiabatic line for the particular case.

Since the rate of heat transfer increases with increased temperature potential, the cases of Figure VI-4 having greater temperature potentials (T_e-T_f) discharge more heat to the cooling jacket. This is clearly shown in Figure VI-5 where the heat transferred to the cooling jacket is plotted against time for each of the cases of Figure VI-4. Although the cases

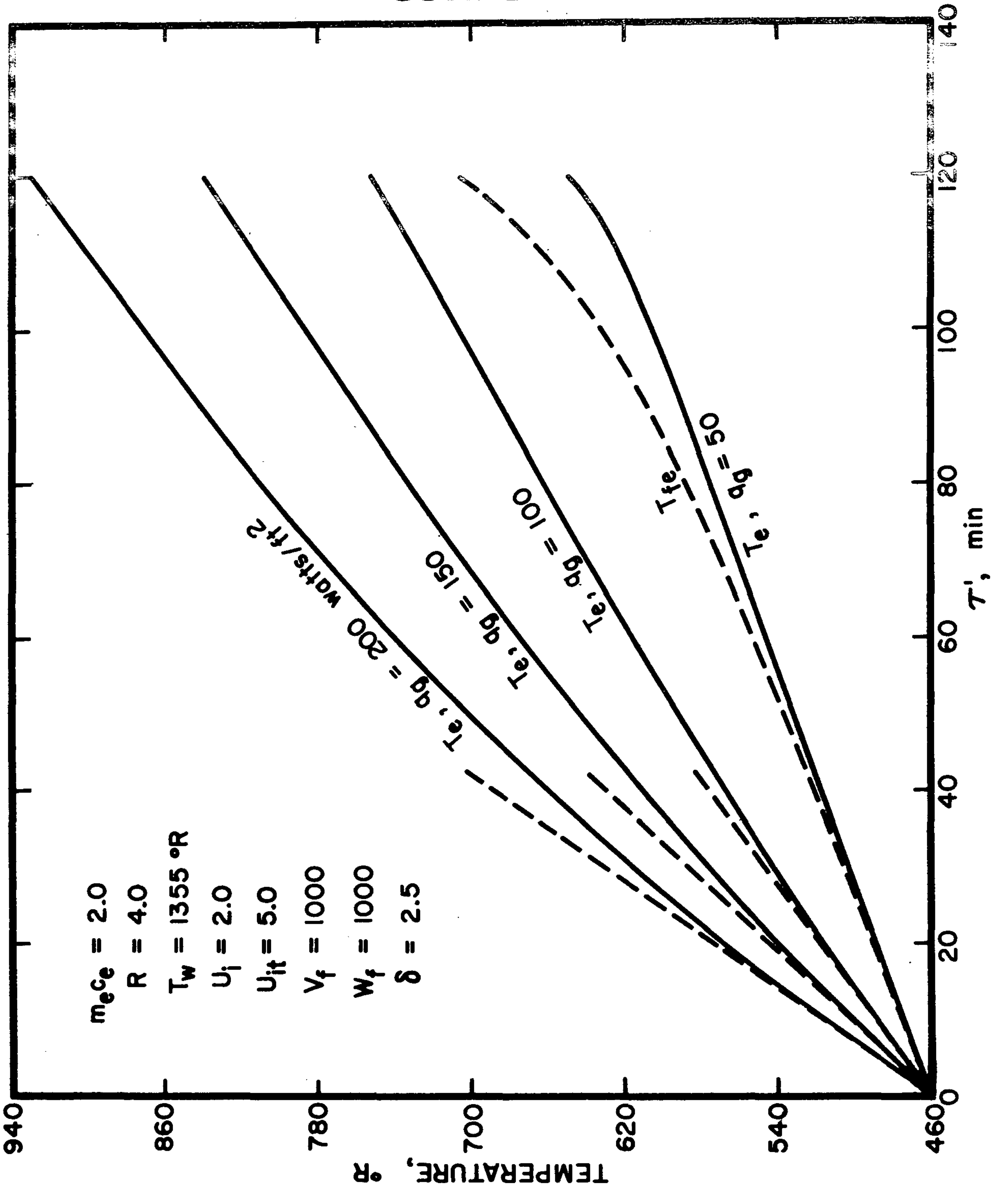

Figure VI-4
Effect of Heat Generation on Equipment Temperature Rise

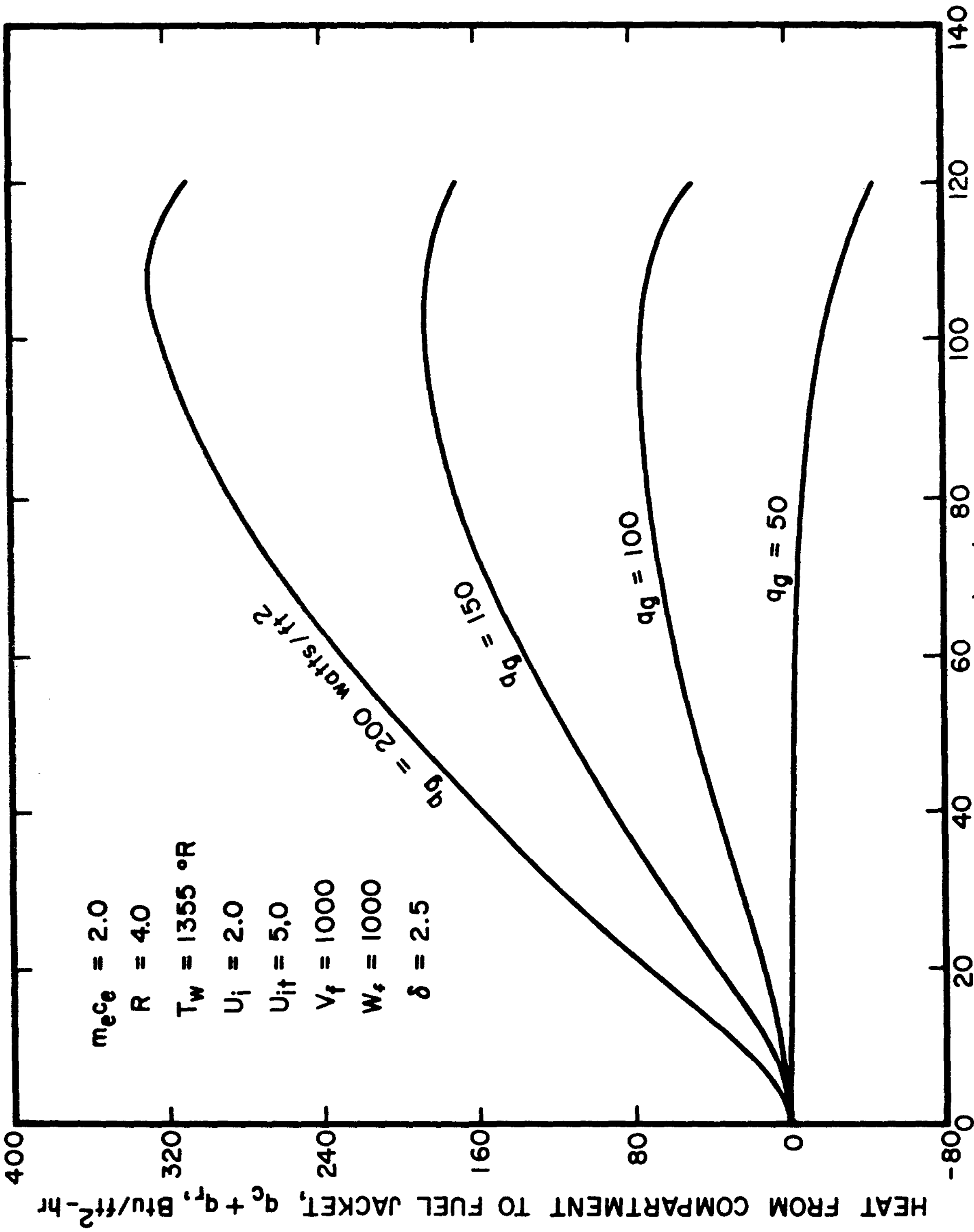

Figure VI-5
Heat Transfer Between Equipment and Fuel Jacket

with greater heat generation have a more rapid rise of temperature and a greater overall temperature rise, they are somewhat compensated in that they are cooled more by the fuel jacket. It is noted, however, that the greatest heat exchange rate of Figure VI-5 is only 328 Btu/hr-ft^2, or 48 percent of the corresponding heat generation rate of 200 Watts/ft^2. The deliberate use of surfaces with higher emissivity to improve radiation heat transfer, and higher compartment air pressures to improve free convection heat transfer, would augment this cooling action somewhat. For cases such as that with q_g = 50 watts/ft^2 it is desirable to use low emissivity surfaces and low compartment pressures, since the jacket heats the equipment somewhat, as indicated by Figure VI-5.

Since forced convection is a more efficient heat transfer process then free convection, the cooling effects of a low temperature jacket could be greatly improved by using a blower or fan to circulate air over the equipment and along the wall of the fuel duct. This would introduce some additional heat generation in the compartment due to the blower motor. Such a system actually is a forced air heat exchanger system, where the heat exchanger surface is the duct wall, and where the secondary coolant, or transfer fluid, is the circulated air. This is not a very efficient heat exchanger system, however, since the heat transfer coefficients in forced convection over flat surfaces are not very large for a given volume rate of air circulation. Further, if a forced air circulation system is desired, it is usually preferred to use a compact exchanger located within the compartment. Such an exchanger eliminates the structural difficulties and compartment accessibility drawbacks of a peripheral fuel jacket. The subject of cooling with compact central heat exchangers is covered in Section VII.

The initial slopes $(\Delta T_e/\Delta\tau)$ of Figure VI-4 are all approximately equal to the slopes of the corresponding lines for adiabatic equipment temperature rise. This condition exists only when the initial equipment temperature equals the initial fuel temperature.

3. Fuel Flow Rates

The temperature rise plots of equipment in a fuel jacketed compartment for two fuel flow rates are shown in Figure VI-6. Compartment and equipment characteristics are given in the figure.

It is apparent that the temperature rise of equipment is not greatly affected by the fuel flow rate in the range of flow rates from 500 to 1000 lb/ft^2-hr. There are two reasons for this. First, both flow rates are sufficient that the temperature rise of the fuel due to the heat it receives is small, having little effect on the temperature of the fuel duct exposed to the equipment. Second, the fuel heat transfer coefficient inside of the duct is quite large compared to the radiation and free convection coefficients inside the compartment. The temperature potential across the fuel film is therefore very small, and its variation over the

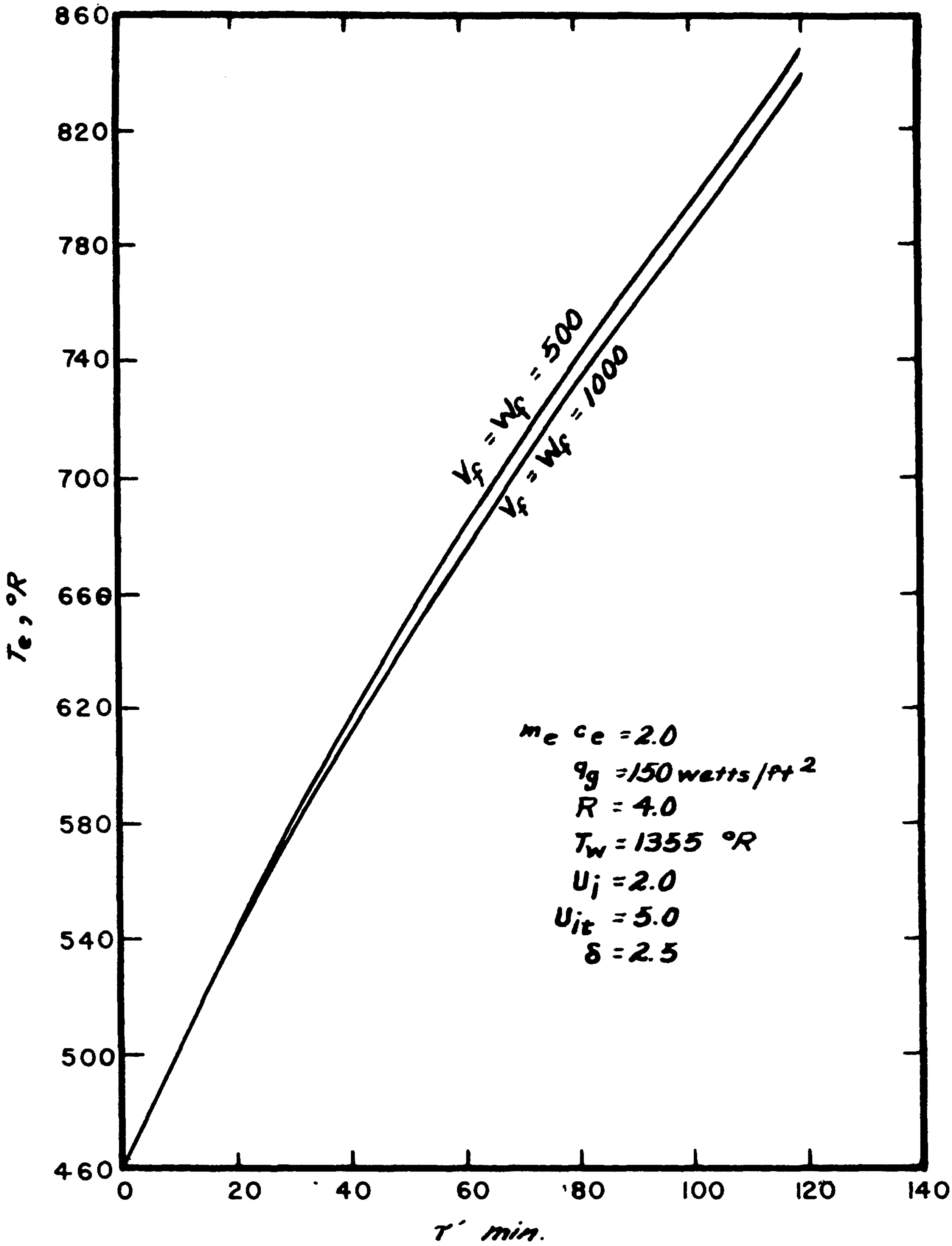

Figure VI-6
Effect of Fuel Flow Rate on Equipment Temperature Rise

range of flow rates considered has a negligible effect on the duct temperature exposed to the equipment. The fuel flow rate would be of more importance in determining equipment temperature performance at very low flow rates, since the temperature rise of the fuel would be large and the fuel film coefficient would be small.

4. Ratio of Free Convection to Radiation Heat Transfer Surface Area

The effect of the ratio of free convection to radiation heat transfer surface on the temperature rise of equipment is shown in Figure VI-7. Compartment and equipment characteristics are given in the figure.

It is apparent that the area ratio has little effect on the temperature rise performance of the equipment. This area ratio is significant only to the free convection heat transfer process. The higher values of R signify greater heat transfer by free convection, and result in greater reductions of equipment temperature below the adiabatic temperature. However, the equipment temperature is influenced so heavily by other variables such as generated heat and thermal capacity that changes in free convection due to rearrangement of equipment surfaces have little effect. It is therefore concluded that changes of heat transfer rates and temperature rise rates in a jacketed compartment should be effected by manipulation of the more dominant variables, such as air pressure, surface emissivities, and equipment thermal capacity.

5. Temperature Rise of the Fuel

The insulation between the skin and the fuel duct as shown in Figure VI-1 serves two purposes. Its first purpose is to prevent contact between the fuel and the high temperature skin, since the skin temperatures of interest in supersonic flight may be far above the maximum allowable fuel temperature. Its second purpose is to reduce the overall heat transfer coefficient between the skin and the fuel. This reduces the amount of heat from the skin which is absorbed by the fuel, and consequently reduces the temperature rise of the fuel. For the calculation cases considered earlier, the value of h_{ifm} is about 20 Btu/hr-ft^2-°R for the cases with $V_f = 1000$ ft/hr and is about 15 Btu/hr-ft^2-°R for the case with $V_f = 500$ ft/hr. If no skin insulation were provided, this would be the overall heat transfer coefficient between the skin and the fuel (in the actual case, h_{ifm} would be a little greater because of the temperature effect on the value of b, as indicated by Figure VI-9). From inspection of equations (VI-12) and (VI-13) it is seen that this condition would give excessive temperature rise of the fuel. For example, for $T_w = 1355$°R, $T_f = 600$°R, $W_f = 500$ lb/hr-ft^2 and $h_{ifm} =$ 15 Btu/hr-ft^2-°R, the fuel temperature rise would be 42.8°F due to heat received from the skin. For the same conditions, but using an insulating effect of $U_i = 2.0$ Btu/hr-ft^2-°R between the duct and the skin, the temperature rise is only 5°F. For all of the cases shown in the

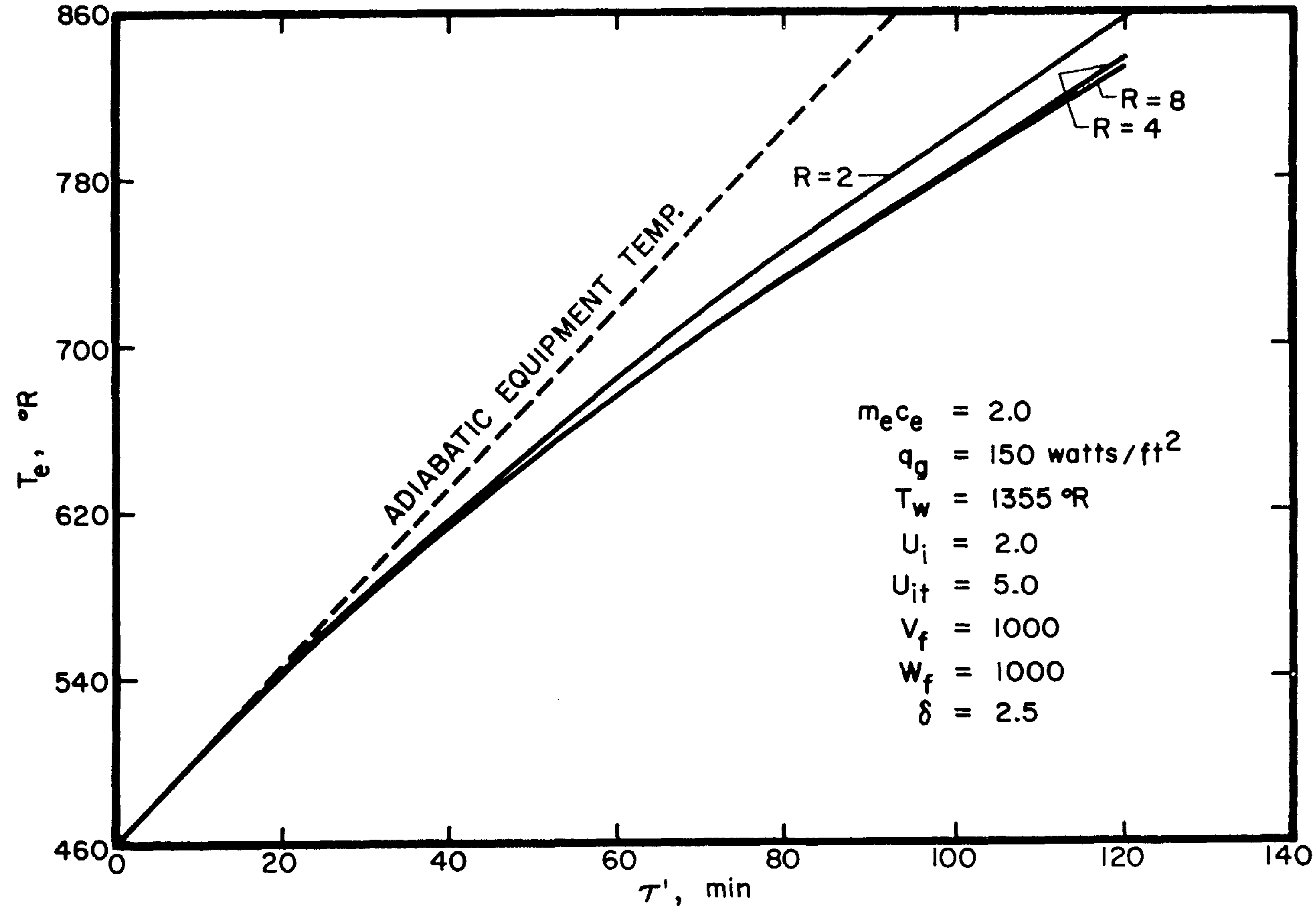

Figure VI-7
Effect of Ratio of Free Convection to Radiation Heat Transfer Surface Area on Equipment Temperature Rise

preceding plots, the fuel temperature rise is less than 8°F, and for nearly all cases less than 4°F. Since an insulating effect of $U_i = 2$ does not represent much by way of insulation thickness, it is apparent that the fuel temperature rise due to heat from the skin can easily be restricted to small values.

The actual temperature rise of the fuel is not so important as the maximum temperature it achieves. This highest temperature occurs at the fuel film which touches the insulation side of the fuel duct. The temperature at this point must be held below values at which fuel deterioration due to overheating occurs. A design example is given later, showing the method of selecting a proper skin insulating effect to limit the greatest fuel temperature to any desired value.

DESIGN PROCEDURE FOR A FUEL-JACKETED COMPARTMENT

Procedures are given here for the evaluation of temperature rise performance and the design of insulation and fuel ducts for a fuel jacketed compartment. The question of whether or not to use a fuel jacketed compartment to achieve a desired performance depends on many factors, and can be answered only by comparison of the fuel jacketed compartment with other compartment types capable of producing the same temperature rise performance. A method of dealing with the general question is described in Section XI.

1. Preliminary Performance Evaluation

The first problem in determining the suitability of a fuel jacketed compartment is to determine whether it is capable of providing the proper variation of equipment temperature with time. It is assumed that the temperature-time plot for the fuel is already known or is calculated by the methods of Appendix III. The next step is to construct the adiabatic equipment temperature line, which describes the equipment temperature as a function of time, assuming that the equipment is heated by generated heat, but does not exchange heat with any other body. The slope of this line is given by,

$$\frac{\Delta T_e}{\Delta \tau} = \frac{q_g}{m_e c_e}$$

A line having this slope, and beginning at the known initial equipment temperature is constructed on the same grid with the fuel temperature plot. All of the possible plots of equipment temperature versus time must lie between the fuel temperature plot and the adiabatic equipment temperature line as found in Figures VI-2,-3, and -4. An example of a preliminary performance evaluation plot is given in Figure VI-8. All of the possible temperature-time curves for the equipment lie within the shaded region. It is impossible to produce an equipment temperature

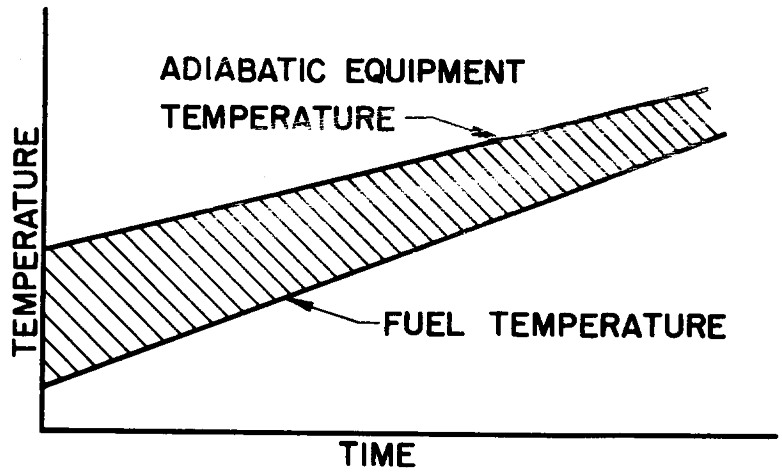

Figure VI-8

Schematic of Performance Evaluation Plot

outside of this region, using a fuel jacketed compartment. Of course, if the allowable equipment temperatures lie above the shaded region and lower temperatures are not detrimental to operation, the fuel-jacketed compartment may be used. Where this is the case, the designer's work is finished after using the design procedures for determining fuel duct dimensions and required insulation thickness. If the allowable maximum equipment temperatures lie in the shaded region, a more detailed performance evaluation must be made. In order to do this, the insulation and duct system must be designed first.

2. Design of Insulation and Fuel Ducts

a. Dimensions of Fuel Duct

The spacing between the fuel duct walls should be made as small as possible in the interest of conserving space occupied by both the fuel duct and the skin insulation. From equation (VI-2)

$$h_f \propto (V_f)^{0.5} = \left(\frac{Q}{A_f}\right)^{0.5} \propto \left(\frac{1}{x_d}\right)^{0.5}$$

Therefore, the film heat transfer coefficient increases with reduced wall spacing in the duct for a given fuel flow rate. For given temperature conditions, this gives increased heat flow to the fuel q_{if}. Therefore from the heat flow equation

$$q_{if} = \frac{k_i}{x_i} \quad (T_w - T_i)$$

it is apparent that the insulation thickness required is reduced. This qualitative analysis is based on assumed given temperature conditions, where the skin temperature T_w is known and the maximum allowable fuel temperature is known. Since one wall of the fuel duct contacts the insulation face, T_i must be limited to the maximum allowable fuel temperature.

b. Thickness of Insulation

As pointed out in the preceding paragraph, the insulation thickness required is dependent on the particular temperature conditions and on the flow velocity in the fuel ducts. The procedure for selecting the skin insulation to meet given design conditions is given here, together with an example design problem.

Given data:

(1) Compartment is cylindrical 2 ft diameter and 2 ft long. Ducts run entire length. Skin surrounds the cylindrical surface only.

(2) A total fuel flow rate of 10,000 lb/hr is available to the jacket ducts.

(3) Maximum allowable fuel temperature is 640°R (therefore design T_i = 640°R).

(4) Insulation having the physical properties of rock wool is used.

(5) Spacing between the duct faces x_d is 1/4 inch or 0.0208 ft.

T_w = 1355°R

q_g = 150 watts/ft^2 = 511 Btu/hr-ft^2

$m_e c_e$ = 2 Btu/°R-ft^2

$R = 4$

$\delta = 2.5$

Fuel temperatures on entrance to the duct are taken from Figure A-III-9, for $U_{it} = 5.0$ Btu/hr-ft^2-°R

The flight time is $\tau' = 80$ min.

Calculation:

1. Calculate the total area of skin for the compartment

$$A_w = \pi x2x2 = 12.6 \text{ ft}^2$$

2. Calculate the fuel flow rate per square foot of skin

$$W_f = \frac{10,000}{12.6} = 794 \text{ lb/hr-ft}^2$$

3. Get T_{fe} at terminal flight time from Figure A-III-9

$$T_{fe} = 588°R$$

4. Calculate $V_f = \left(\frac{W_f}{\gamma}\right)\left(\frac{L}{x_d}\right)$

duct length L = 2 ft

for fuel at 588°R, Figure AI-2, $\gamma = 47.1$ lb/ft^3

$$V_f = \frac{794}{47.1} \; \frac{2}{0.0208} = 1620 \text{ ft/hr}$$

5. Calculate $R_e = \frac{\gamma V_f x}{\mu}$

μ from Figure AI-2

for $T_f = 588°R$, $\mu = 1.18$ lb/ft-hr

$$R_e = \frac{47.1x1620x2}{1.18} = 129,000$$

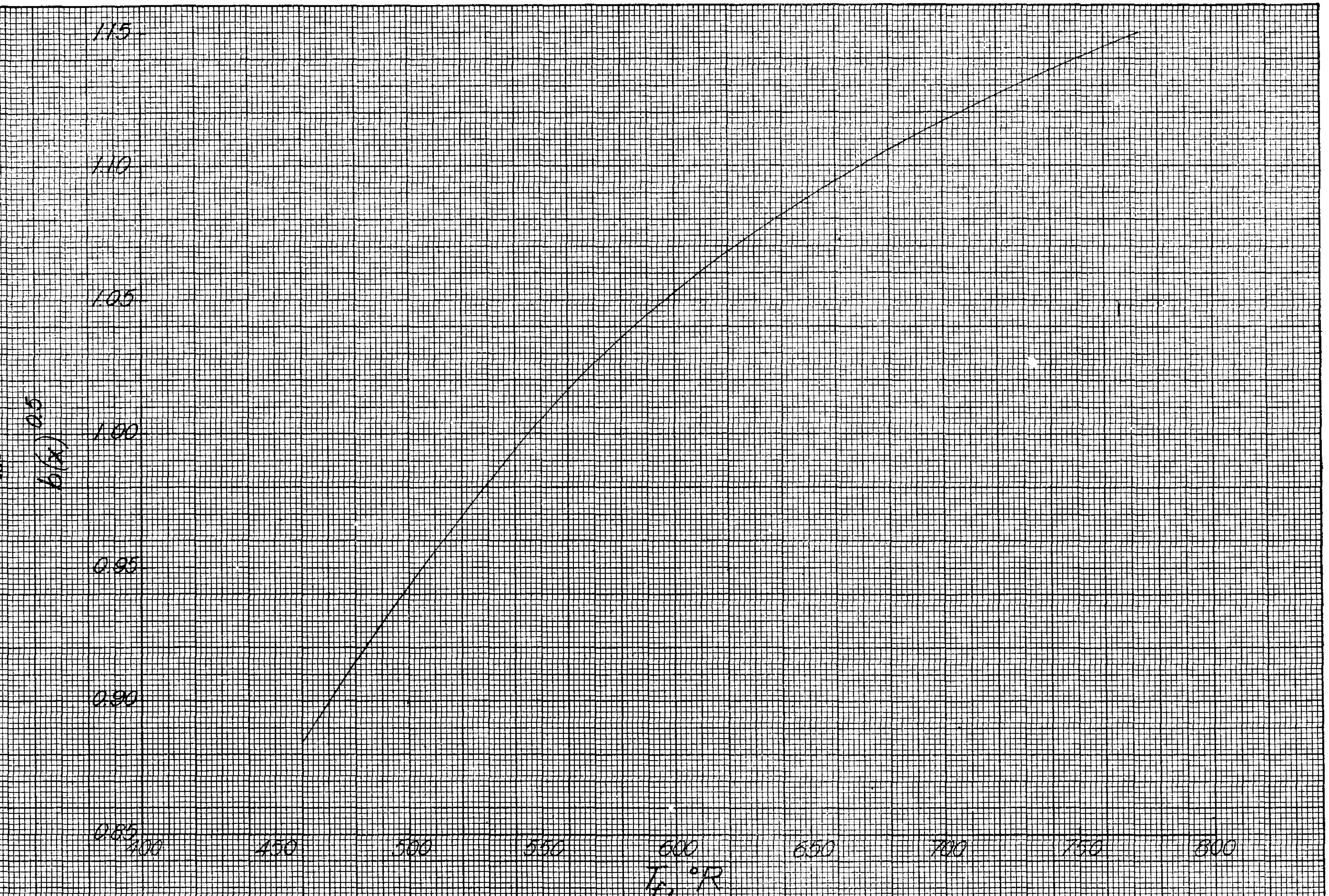

Figure VI-9
Calculation Chart for Equation VI-11 Based on JP-3 Fuel and < 300,000

(Reference VI-1 gives R_e = 300,000 as the value for change from laminar to turbulent flow. The figure above therefore represents laminar flow, indicating the validity of this procedure for this case.)

6. Calculate $h_{if} = 0.66\ b\ (V_f)^{0.5}$ evaluating b with Figure VI-9 in the appendix to this Section.

$$b\left(\text{for } T_f = 588°R\right) = \frac{1.046}{(2)^{0.5}} = 0.739$$

(using the duct length, L = 2 ft for x)

$$h_{if} = 0.66 x 0.739 x (1620)^{0.5} =$$

$$19.6\ \text{Btu/hr-ft}^2\text{-°R}$$

7. Write the equation $q_{if} = h_{if}(T_i - \frac{T_{fe}+T_{fL}}{2})$

where T_i is equal to the maximum allowable fuel temperature

$$q_{if} = 19.6\ (346 - \frac{T_{fL}}{2})$$

8. Write the equation $q_{if} = W_f c_f (T_{fL} - T_{fe})$

for c_f from Figure AI-2

$$c_f \text{ at } 588°R = 0.524\ \text{Btu/lb-°R}$$

$$q_{if} = 417\ (T_{fL} - 588)$$

9. Solve equations from 7 and 8 for T_{fL}

$$T_{fL} = 591°R$$

10. Calculate $q_{if} = h_{if}\ (T_i - \frac{T_{fe}+T_{fL}}{2})$

$$\frac{T_{fe}+T_{fL}}{2} = \frac{588+591}{2} = 589.5°R$$

$$q_{if} = 19.6\ (640-589.5) = 1010\ \text{Btu/hr-ft}^2$$

11. Get k_i for insulation at

$$\frac{T_w+T_i}{2}$$

$$k_i = 0.0502 \text{ Btu/hr-ft-°R}$$

12. Calculate $x_i = \dfrac{k_i}{q_{if}} (T_w-T_i)$

$$x_i = \frac{0.0502}{1010} (1355-640) = 0.0355 \text{ ft.}$$

$$\text{or } x_i = 0.0355 \text{x} 12 = 0.427 \text{ in}$$

which, to be conservative, should be increased to 1/2 inch.

It should be noted that this design calculation neglects heat received by the fuel from the equipment. This assumes that the heat flow rate from the equipment is not great enough to affect the fuel temperature appreciably.

3. Detailed Performance Evaluation

After designing the fuel ducts and insulation, a more detailed performance evaluation is made. This can be done quite accurately by a simplified procedure based on the following assumptions:

a. The fuel temperature is determined principally by the entrance fuel temperature and the heat received through the skin insulation. Heat received from the equipment is neglected.

b. The fuel film coefficients are so large compared to free convection and radiation coefficients that the fuel jacket surface facing the equipment can be considered to be at fuel temperature.

c. The compartment air temperature can be approximated by the arithmetic mean of fuel jacket temperature and equipment temperature at any time.

Using the first of these assumptions, a plot of fuel temperature versus time is constructed by the following procedure.

Procedure A: Calculation for Fuel Temperature Plot

Given Data:

insulation material __________ , x_i = ________ ft

length of fuel ducts x = ______ ft

fuel flow rate W_f = __________ lb/ft^2-hr

skin temperature T_w = ________ °R

spacing between duct walls x_d = ________ ft.

plot of entrance fuel temperature versus time

Calculation:

This calculation should be made for several instants of time τ one at the beginning of the design flight time, one at the end, and sufficient intermediate points to establish the shape of the fuel temperature plot.

1. Select τ and assume T_i

T_i = ______ °R

2. Get k_i at $\frac{T_w+T_i}{2}$

k_i = ______ Btu/hr-ft-°R

3. Calculate $q_{if} = \frac{k_i}{x_i} \quad (T_w-T_i)$

q_{if} = _____ Btu/hr-ft^2

4. Get T_{fe} at τ and c_f at T_{fe}

T_{fe} = ______ °R

c_f = ______ Btu/lb-°R

5. Calculate $\Delta T_f = \frac{q_{if}}{W_f c_f}$

ΔT_f = _____ °R

6. Calculate $T_{fm} = T_{fe} + \frac{\Delta T_f}{2}$

T_{fm} = _____ °R

7. Get γ, c_f, μ, P_r at T_{fm}

γ = _______ lb/ft³

c_f = _______ Btu/lb-°R

μ = _______ lb/ft-hr

P_r = _______

8. Calculate $V_f = \left(\frac{W_f}{\gamma}\right)\left(\frac{x}{x_d}\right)$

V_f = _______ ft/hr.

9. Calculate $h_{if} = \frac{0.66}{\sqrt{\frac{x\gamma}{\mu}}} \left[\frac{\gamma c_f}{(P_r)^{2/3}}\right] (V_f)^{0.5}$

h_{if} = _________ Btu/hr-ft²-°R

10. Calculate $T_i = \frac{q_{if}}{h_{if}} + T_{fm}$ = _________ °R

Repeat procedure for agreement between assumed T_i and calculated result.

In using a procedure such as this, agreement of assumed and calculated values of 2 or 3°R is entirely sufficient, since slide rule calculation and chart reading introduces at least this much error.

After determining the plot of T_{fm} versus τ, the last two assumptions are used in a procedure to determine equipment temperature rise with time as given below.

Procedure B: Calculation of Equipment Temperature Rise

Given Data:

fuel temperature plot from Procedure A

R = ______

q_g = ______ Btu/hr-ft^2

δ = ______

ϵ_s = ______ , ϵ_e = ______

T_{e1} = ______ °R

Calculation:

1. Select $\Delta\tau$, assume T_{e2}

$\Delta\tau$ = ___ hr

T_{e2} = ___ °R

2. Calculate $T_{em} = \dfrac{T_{e1}+T_{e2}}{2}$

T_{em} = ___ °R

3. Get T_{fm} at middle of $\Delta\tau$

T_{fm} = ____ °R

4. Calculate $h_r = 17.4 \times 10^{-4} \left(\dfrac{1}{\frac{1}{\epsilon_s}+\frac{1}{\epsilon_e}-1}\right) B$

$$\text{where } B = \frac{\left(\frac{T_e}{100}\right)^4 - \left(\frac{T_s}{100}\right)^4}{\left(\frac{T_e}{100}\right) - \left(\frac{T_s}{100}\right)}$$

from Figure AIV-1

h_r = ______ Btu/hr-ft^2-°R

5. Calculate $T_{am} \approx \dfrac{T_{fm}+T_{em}}{2}$

T_{am} = ______

6. Get $\left(\frac{a'}{\delta^{2/3}}\right)_s$ at $\frac{T_{sm}+T_{am}}{2}$

Figure AIV-2 $\left(\frac{a'}{\delta^{2/3}}\right)_s =$ ______

7. Get $\left(\frac{a'}{\delta^{2/3}}\right)_e$ at $\frac{T_{am}+T_{em}}{2}$

$\left(\frac{a'}{\delta^{2/3}}\right)_e =$ ______

8. Calculate $h_{cs} = \left(\frac{a'}{\delta^{2/3}}\right)_s (\delta^{2/3}) \quad (T_{am}-T_{sm})^{1/3}$

$h_{cs} =$ ____ Btu/hr-ft^2-°R

9. Calculate $h_{ce} = \left(\frac{a'}{\delta^{2/3}}\right)_e \quad (\delta^{2/3}) \quad (T_{em}-T_{am})^{1/3}$

$h_{ce} =$ ___ Btu/hr-ft^2-°R

10. Calculate

$$h_c = \frac{1}{\frac{1}{h_{cs}} + \frac{1}{Rh_{ce}}}$$

$h_c =$ ______ Btu/hr-ft^2-°R

11. Calculate

$$\Delta T_e = \frac{(h_c+h_r)(T_{em}-T_{sm})\ \Delta\tau}{m_e c_e}$$

$\Delta T_e =$ ______ °R

12. Calculate $T_{e2} = T_{e1} + \Delta T_e$

$T_{e2} =$ ____ °R

Repeat procedure for each time interval until assumed and calculated values of T_{e2} agree within about 6°R, then calculated result is correct.

The procedure is continued for successive time intervals until the flight duration of the design is covered. When the calculation is completed the designer will have an accurate indication of the temperature rise performance of equipment in a fuel-jacketed compartment of the proposed design.

In designing a compartment for performance within the shaded region of Figure VI-8, the effects of surface emissivities and compartment air pressures should be kept in mind. If the upper boundary of the shaded region is the fuel temperature curve, the emissivities and pressure should be low. If the upper boundary of the shaded region is the adiabatic temperature, the reverse is true.

APPENDIX TO SECTION VI

1. Calculation Procedure for Temperature Rise of Equipment in a Fuel-Jacketed Compartment

The calculation procedure given below is for the stepwise calculation of equipment temperature rise with time in a fuel-jacketed compartment. An example interval calculation is carried along with the procedure.

Given Data:

$T_w = 1355°R$

$\delta = 2.5$ atmospheres

$U_i = 2.0$ Btu/hr-ft^2-°R (rock wool)

$m_e c_e = 2.0$ Btu/ft^2-°R

$R = 4$

$\epsilon_s = 0.1$, $\epsilon_e = 0.2$

$T_{e1} = 820.1°R$

$T_{a1} = 775.3°R$

$T_{i1} = 758.3$

$q_g = 150$ watts/ft^2 = 511 Btu/hr-ft^2

$V_f = 1000$ ft/hr

$W_f = 1000$ lb/hr-ft^2

Fuel temperature from Figure AIII-9 with $U_{it} = 5$ Btu/hr-ft^2-°R

$x = 1$ ft

1. Select $\Delta\tau$ and get T_{fem} at middle of $\Delta\tau$ from Figure AIII = 9

$$\Delta\tau = 0.1168 \text{ hr}$$
$$T_{fem} = 686.6°R$$

2. Calculate $h_f = 0.66\, b(V_f)^{0.5}$

where $b(x)^{0.5}$ is from Figure VI-9

at T_{fem}, and $b = b(x)^{0.5}/(x)^{0.5}$

$$b = 1.11$$

$$h_f = 0.66x1.11x31.62 = 23.18 \text{ Btu/hr-ft}^2\text{-°R}$$

3. Calculate $q_{if} = \left(\dfrac{1}{\frac{1}{U_i} + \frac{1}{h_f}}\right)(T_w - T_{fem})$

using U_i from previous interval, step 11

$$q_{if} = \frac{(1355 - 686.6)}{\frac{1}{2.276} + \frac{1}{23.18}} = 1381 \text{ Btu/hr-ft}^2$$

4. Get c_f at T_{fem} from Figure AI-2

$$c_f = 0.5886 \text{ Btu/lb-°R}$$

5. Calcu' :te $\Delta T_f = \dfrac{q_{if} + q_{sfm}}{w_f c_f}$

using q_{sfm} from previous interval

$$\Delta T_f = \frac{138 + 170}{1000x0.5886} = 2.64\ °R$$

6. Calculate $T_{fm} = T_{fem} + \dfrac{\Delta T_f}{2}$

$$T_{fm} = 686.6 + 1.32 = 687.9\ °R$$

7. Get $(T_{fe2} - T_{fe1})$ from Figure AIII-9

Calculate $T_{i2} \approx T_{i1} + (T_{fe2} - T_{fe1})$

$$T_{i2} \approx 758.3 + 33.6 = 791.9°R$$

8. Calculate $T_{im} = \dfrac{(T_{i1} + T_{i2})}{2}$

$$T_{im} = 775.1°R$$

9. Calculate film temperature

$$\left(\frac{T_{im} + T_{fm}}{2}\right) = 731.5°R$$

10. Calculate $h_{ifm} = 0.66\, b(V_c)^{0.5}$

using Figure VI-9 and film temperature of step 9

$$b = 1.133$$

$$h_{ifm} = 0.66 \times 1.133 \times 31.62 = 23.7 \text{ Btu/hr-ft}^2\text{-°R}$$

11. Get U_i at T_{im} from Figure AIV-4

$$U_i = 2.308 \text{ Btu/hr-ft}^2\text{-°R}$$

12. Calculate

$$q_{ifm} = \left(\frac{1}{\frac{1}{U_i} + \frac{1}{h_{ifm}}}\right)(T_w - T_{fm})$$

$$q_{ifm} = \frac{(1355 - 687.9)}{\frac{1}{2.308} + \frac{1}{23.7}} = 1400 \text{ Btu/hr-ft}^2\text{-°R}$$

Recalculate ΔT_f in step 5 using this result. If result agrees with original within 2°R, continue to step 13, otherwise recalculate from 5 on.

13. Calculate $T_{sm} \approx T_{fm} + \left(\frac{q_{sfm}}{h_{sfm}}\right)_p$

where subscript p refers to previous interval.

$$T_{sm} \approx 687.9 + 7.5 = 695.4°R$$

14. Assume T_{e2} and T_{a2}

Calculate T_{em} and T_{am}

if $T_e \approx T_f$,

$$T_{e2} \approx T_{e1} + \frac{q_g \Delta\tau}{m_e c_e}$$

$$T_{e2} = 839.2°R$$

$$T_{a2} = 811.5°R$$

$$T_{em} = 829.6°R$$

$$T_{am} = 793.4°R$$

15. Calculate $h_r = 17.4 \times 10^{-4}\left(\frac{1}{\frac{1}{\epsilon_s} + \frac{1}{\epsilon_e} - 1}\right)$ B

taking B from Figure AIV-1 for T_{sm} and T_{em}

where $B = \dfrac{\left(\frac{T_{em}}{100}\right)^4 - \left(\frac{T_{sm}}{100}\right)^4}{\frac{T_{em}}{100} - \frac{T_{sm}}{100}}$

$B = 1780$

$h_r = 1.24 \times 1780 \times 10^{-4} = 0.221$ Btu/hr-ft^2-°R

16. Calculate $\dfrac{T_{sm} + T_{am}}{2}$ and get

$\left(\dfrac{a'}{\delta^{2/3}}\right)_s$ from Figure AIV-2

at this temperature $\left(\dfrac{a'}{\delta^{2/3}}\right)_s = 0.1681$

17. Calculate $\dfrac{T_{am} + T_{sm}}{2}$ and get

$\left(\dfrac{a'}{\delta^{2/3}}\right)_e$ from Figure AIV-2

at this temperature $\left(\dfrac{a'}{\delta^{2/3}}\right)_e = 0.1591$

18. Calculate $h_{cs} = \left(\dfrac{a'}{\delta^{2/3}}\right)_s \left(\delta^{2/3}\right) (T_{am} - T_{sm})^{1/3}$

$h_{cs} = 0.1681 \times 1.841 \times (793.4 - 695.4)^{1/3} = 1.43$ Btu/hr-ft^2-°R

19. Calculate $h_{ce} = \left(\dfrac{a'}{\delta^{2/3}}\right)_e \left(\delta^{2/3}\right) (T_{em} - T_{am})^{1/3}$

$h_{ce} = 0.1591 \times 1.841(829.6 - 793.4)^{1/3} = 0.971$ Btu/hr-ft^2-°R

20. Calculate $h_c = \dfrac{1}{\frac{1}{h_{cs}} + \frac{1}{h_{ce}R}}$

$h_c = \dfrac{1}{\frac{1}{1.43} + \frac{1}{4 \times 0.971}} = 1.046$ Btu.hr-ft^2-°R

21. Calculate $\frac{T_{sm} + T_{fm}}{2}$

and $h_{sfm} = 0.66\ b(V_f)^{0.5}$

using Figure VI-9 at this average film temperature

$$b = 1.113$$

$$h_{sfm} = 0.66 \times 1.113 \times 31.62 = 23.22 \text{ Btu/hr-ft}^2\text{-°R}$$

22. Calculate $q_{sfm} = \left(\frac{1}{\frac{1}{h_{sfm}} + \frac{1}{h_c+h_r}} \right) (T_{em} - T_{fm})$

$$q_{sfm} = \frac{829.6 - 687.9}{\frac{1}{23.22} + \frac{1}{1.046+0.221}} = 170 \text{ Btu/hr-ft}^2$$

23. Calculate $T_{sm} = T_{fm} + \frac{q_{sfm}}{h_{sfm}}$

$$T_{sm} = 687.9 + \frac{170}{23.22} = 695.2\text{°R}$$

Result should agree within 1°R of step 13, otherwise repeat, using result of 23 as T_{sm}, from step 13 onward.

24. Calculate

$$\Delta T_e = \left[\frac{q_g - (h_c+h_r)(T_{em}-T_{sm})}{m_e c_e} \right] \Delta\tau$$

$$\Delta T_e = \frac{(511 - 1.267 \times 134.4) \times 0.1168}{2} = 19.9\text{°R}$$

25. Calculate $T_{e2} = T_{e1}+\Delta T_e$

$$T_{e2} = 820.1 + 19.9 = 840\text{°R}$$

26. Calculate

$$(T_{em}-T_{am}) = \frac{h_c}{h_{ce}R} (T_{em}-T_{sm})$$

$$(T_{em}-T_{am}) = \frac{1.046}{0.971\text{x}4} (830-695.4) = 36.2\text{°R}$$

27. Calculate $T_{am} = T_{em} - (T_{em}-T_{am})$

$$T_{am} = 830 - 36.2 = 793.8°R$$

28. Calculate $T_{a2} = T_{a1} + 2(T_{am}-T_{a1})$

$$T_{a2} = 775.3 + 2x18.5 = 812.3°R$$

The calculated results of steps 25 and 28 should agree within 3°R of assumed values of step 14, otherwise recalculate from 14 onward until such agreement is reached, then use calculated results as values of T_{e1} and T_{a1} of the next interval.

In using the above calculation procedure, proper attention must be paid to the signs of the various heat rate quantities and temperature potentials. A negative value should be carried with its negative sign, following the rules of algebra. Negative signs encountered in the determination of a heat transfer coefficient are ignored, however, using the absolute value of the quantity, since heat transfer coefficients are always positive. For example, in step 18 the term $(T_{am}-T_{sm})$ may be negative, but its absolute value is used to determine the value of h_{cs}, which is always positive.

If calculation for a fuel-jacketed compartment is just beginning, it is necessary to determine values of T_i, T_{fm}, T_s, and T_a corresponding to the initial assigned values of T_w, T_{fe}, and T_e. This can be done by trial and error calculation, using this same procedure for $\Delta\tau = 0$. Special modifications are as follows for the same step numbers. Steps not mentioned remain essentially unchanged.

1. $\Delta\tau = 0$
2. Evaluate at T_{fe} for $\tau = 0$
3. Take initial assigned value of U_i
5. Take $q_{sfm} = 0$ as first try (true if $T_e = T_f$, then $T_a = T_e$)
7. Calculate $T_i = T_w - \dfrac{q_{if}}{U_i}$
8. Omit
9. Calculate $\dfrac{T_i + T_{fm}}{2}$
11. Omit, used assigned value
13. Assume $T_s = T_{fm}$
14. Work with T_e and T_a, omitting time subscripts in steps 14 through 23.

(note that T_{fm} has already been determined, and that its subscript m is not a time subscript).

24. Omit.

25. Omit.

26. Use T_s, T_a, and T_e as assigned or assumed.

28. Omit.

Repeat to convergence of assumed and calculated values.

2. References

(VI-1) Jakob, M. and Hawkins, G. A. Elements of Heat Transfer and Insulation. Second Edition. John Wiley and Sons, Inc., New York, 1950, pp. 220-21.

(VI-2) Brown, A. I. and Marco, S. M. Introduction to Heat Transfer. Second Edition. McGraw-Hill Book Company, Inc., New York, 1951, pp. 52-55.

SECTION VII

TEMPERATURE RISE OF EQUIPMENT IN A COMPARTMENT COOLED BY AN AIR-TO-LIQUID HEAT EXCHANGER

By T. C. Taylor and Y. H. Sun

There are many cases in which the combination of external and generated heat loads is so severe that an uncooled or fuel-jacketed compartment is unsatisfactory. In such cases an effective cooling method must be employed to limit the equipment temperature rise. One method would employ a primary cooling fluid, a heat exchanger, and a secondary coolant, or transfer fluid, which is used to convey heat from the equipment to the heat exchanger. The use of a system of this type has the outstanding advantage of wide freedom in the choice of a primary coolant, since only the secondary coolant contacts the equipment.

This Section is concerned with the characteristics of practical systems in which the transfer fluid is air, the compartment atmosphere, and the primary coolant is a liquid. The study is specifically concerned with the use of fuel as the primary coolant, although the methods used are sufficiently general to be applicable to other fluids as well.

Compartments with direct cooling systems incorporating an air-to-liquid heat exchanger are physically more complex than uncooled or fuel-jacketed compartments. Space and weight requirements are added for the heat exchanger, the air circulating blower and motor, and the duct work. These complications are justified only where the simpler systems discussed in Sections V and VI are unsatisfactory. Therefore, the cooling system analyzed in this Section should be used only when it has been definitely established that the simpler systems are inadequate for the limitation of equipment temperature in a particular application.

The analysis of transient thermal performance of compartments with direct cooling systems is complicated by the evaluation of the variable cooling performance resulting from the variations of equipment and coolant temperatures with time. However, these factors and thermal storage capacity must be considered for the purpose of designing a heat exchange system of minimum size for a given application having a specified equipment temperature limit.

SUMMARY

The temperature rise of equipment in a compartment cooled with a heat exchanger is considered. It is assumed that a heat exchanger using a liquid primary coolant is located in the compartment, and that air is forced over the equipment and through the heat exchanger in a closed circuit.

Fuel is principally considered as coolant. The location of the heat

exchanger is assumed to be central and near the fuel line, thus not impeding the accessibility of the compartment. However, the equipment is directly exposed to external heat loads by radiation and free convection.

In addition to external heat gain and the heat generated by the equipment itself, the power requirements of the circulating blower of the forced air system is included in the equipment heat balance. The entire group of equipment bodies is considered as a heat generating heat exchanger, and a constant value of heat exchange effectiveness is assigned to the group. Only the air side of the cooling heat exchanger is analyzed, it being assumed that the primary coolant is used in such a way as to give a very high heat transfer coefficient on the liquid side, and negligible temperature rise of the primary coolant. A constant compartment air pressure is assumed, and the thermal capacities of the air and the skin insulation are neglected. The skin temperature is assumed constant, as justified for many cases in Section IV.

Equations are developed to describe the external heat load and the heat exchanger cooling action, and the power requirements of the blower motor. These equations are combined with those for the generated heat load and the effect of equipment thermal capacity to give a complete heat balance for the system. A general calculation procedure based on these equations is developed, and is used to evaluate the equipment temperature rise in supersonic flight. The heat rates and characteristics of the compartment, the equipment, and the cooling apparatus are all expressed on the basis of unit skin area. This permits application of the calculation procedure to compartments of any shape.

A simplified analysis is given, based on linear relationship between external heat load and equipment temperature. For a linear relationship between the primary coolant temperature and time, this analysis results in a differential equation involving the equipment temperature and time which is formally integrated. The solution can be used over fairly large ranges of equipment temperature to obtain a rapid, approximate evaluation of the equipment temperature rise.

A procedure and example are given to show the method of determining the design conditions for the heat exchange system on the basis of transient performance and of designing for the optimum combination of a heat exchanger and skin insulation. For a given desired temperature performance of the equipment, the design can be either for minimum space requirements or minimum weight requirements, whichever is critical. In the example given, the optimum designs for these two criteria are substantially the same.

Equipment temperature-rise performance is calculated for a number of compartment, equipment, and cooling apparatus characteristics. The cases studied are confined to the use of JP-3 fuel as a primary coolant. The salient conclusions based on the results of these calculations are as follows.

1. Following an initial period of adjustment, the heat exchanger in a cooled compartment maintains a nearly constant temperature difference

between the equipment and the primary coolant used. The equipment temperature is sufficiently above the coolant temperature to transfer all heat except that which is stored in the equipment itself. The equipment stores heat when necessary to raise the equipment temperature in keeping pace with the change of primary coolant, or fuel temperature. The temperature difference required to maintain the parallel relationship between the equipment temperature and the coolant temperature increases with increased heat loads and decreases with increased thermal capacity of the equipment.

2. The heat exchange effectiveness of both the heat exchanger and the equipment are important factors in determining how closely the equipment temperature may be made to approach the fuel temperature. An increase of either of these effectiveness values decreases the temperature difference required for a given heat removal, or cooling effect. The temperature difference is also inversely proportional to the flow rate of the air used as a secondary coolant. If increased heat exchanger effectiveness is used to obtain better cooling effects, the heat exchanger size and weight increase, and the air power requirements increase. If increased air flow rate is used to improve the cooling effect, the result is at least partially offset by increased air power requirements. The effect can be quite serious, since the power requirements are proportional to the third power of the air flow rate. Equipment should be arranged wherever possible so as to have the highest possible effectiveness as a heat exchange device.

3. In order to design a heat exchanger system which maintains a specified difference between the equipment temperature and the fuel temperature, the heat storage rate of the equipment must be properly accounted for. This heat storage rate is subtracted from the sum of external, generated, and blower power loads, since it is not actually handled by the heat exchanger. The heat storage rate can be determined in advance of the other design calculations by making use of the approximately constant temperature difference (T_e-T_f) observed from the calculation study. The importance of accounting for the heat storage rate in a transient design is illustrated by an example in which a steady-state design procedure gives a heat exchanger over twice as large as the one actually required for transient operation.

Infinitely many heat exchanger designs are possible for a given performance, depending upon the heat exchanger effectiveness and the ratio of blower power to cooling load selected. A low-effectiveness heat exchanger can be made to do the same job as a more effective exchanger, but a higher air flow rate is required, giving higher air power requirements. The heat exchanger of lower effectiveness is smaller, however, and therefore offers some advantage.

ANALYSIS

1. Assumptions for Analysis

This analysis of equipment cooled by an air-to-liquid heat exchanger makes use of a compartment similar to that described in Section V. Both the equipment and cooling apparatus are enclosed in a constant-pressure compartment, either with or without skin insulation. Since the heat exchanger is centrally located with the equipment, both are exposed to the external heat loads by radiation and free convection. This requires more effective cooling of the equipment than would be required if the heat exchanger surrounded the equipment. The centrally located exchanger offers the important advantages of greater compartment accessibility and fewer structural complications, however. In addition, the total heat load to the fuel or primary coolant is much less for a central heat exchanger than for one which surrounds the equipment. This is important, since the allowable heat addition to the fuel may be severely limited. A closed air circuit is used, consisting of the ductwork, the equipment casing, the blower casing, and the heat exchanger. Although air in the closed circuit is under forced circulation, it is assumed to be at substantially the same pressure as the compartment air surrounding the equipment. A schematic drawing of the arrangement of equipment components and cooling apparatus as they might be placed in a cylindrical compartment is shown in Figure VII-1. In the figure, the individual equipment bodies are shown connected in series in the closed air circuit, although parallel and combinations of series-parallel circuits are just as likely.

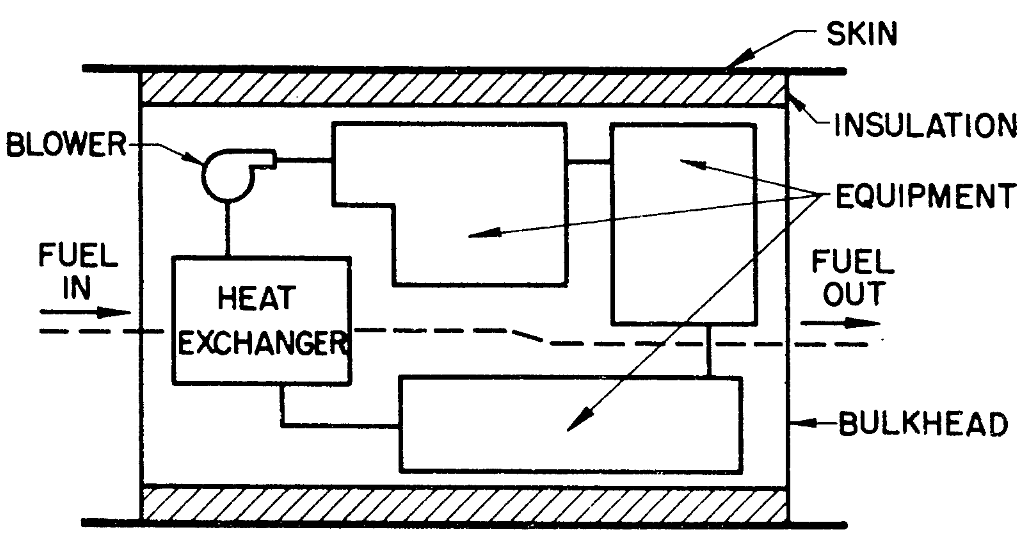

Figure VII-1. Schematic of Compartment With an Air-to-Liquid Heat Exchanger

As in Section V, the equipment is assumed to receive external heat from the aircraft skin by free convection and radiation only. It is also assumed that an average surface temperature can be used to represent all equipment surfaces in describing the heat transfer processes in the compartment. This applies to both heat received from the skin and heat removed in the forced air circuit. It is convenient to consider the entire group of equipment bodies as a heat generating exchanger. This permits the use of the concept of heat exchange effectiveness (to be defined later) in constructing analytical relationships between the equipment temperature and other variables of the system. It is assumed that this heat exchange effectiveness of the equipment is substantially constant with changes of equipment temperature. This assumption is reasonably accurate, since the heat exchange effectiveness of any surface is principally a function of its physical dimensions, shape, and flow rates, and is affected only slowly by changes of fluid properties due to changes of temperature.

Equipment usually cannot be designed in such a way as to give high priority to its performance as a heat exchange device. It is therefore reasonable to assume that the effectiveness of the equipment as a heat exchanger is low, and consequently that the pressure drop due to forced air flow through the equipment is low. Thus, in analyzing pressure drop and air flow power requirements of the system, it is assumed that the principal pressure loss of the forced air circuit occurs in the heat exchanger, and that losses occurring elsewhere are negligible. In most of the analysis, the type of heat exchanger considered has air flow through tubes so that the air pressure drop is based on data for straight, smooth tubes, with an appropriate allowance for entrance and exit losses. The pressure loss and air flow rate are used to establish air power requirements. In determining the heat load on the system due to energy input for air circulation, it is assumed that the over-all efficiency of the blower-motor unit is 25 percent. It is assumed that the blower's discharge volume remains constant during the entire flight time, irrespective of changes in air temperature.

The film coefficient on the liquid side of the heat exchanger is not considered in this analysis. It is assumed that the liquid coolant is circulated around the outside of the tubes at high velocity, giving a large heat transfer coefficient and negligible temperature drop between the liquid and the tube surface. Temperature drop through the metal tube wall is also neglected. It is also assumed that the liquid flow rate is so high that the temperature rise of the liquid can be neglected, and the entire tube surface in the heat exchanger can be considered at the same temperature. Thus, the liquid temperature is at all times taken as substantially equal to its temperature on entering the heat exchanger. The primary coolant temperature may therefore vary with time depending on factors which affect its temperature at its source, but the primary coolant temperature is independent of the heat exchange process within the compartment. The conditions of very large heat transfer coefficient on the liquid side and negligible temperature change of the liquid coolant are possible in a practical application. These conditions would be fulfilled by using as primary coolant the fuel consumed by a large ram-jet engine, providing the cooling load were not exceptionally great. They would also be fulfilled when using an evaporative coolant on the liquid side of the heat exchanger.

As in the case of previous analyses, thermal capacities of the compartment air and insulation are neglected. The thermal capacities and heat transfer surface areas based on a unit skin area associated with the compartment are now considered to include the ducts and other cooling apparatus in the compartment. The heat exchanger itself is not included. Any external heat load by convection and radiation to the heat exchanger is transferred to the primary coolant without entering the air circuit and therefore is not a part of the heat loads in the equipment cooling problem.

All heat transfer and heat generation rates are expressed on a unit skin area basis. The same is true of the equipment thermal capacity. It therefore follows that the principal variables describing the heat exchanger and the cooling performance are on a unit skin area basis. For example, in the case of a tube-type heat exchanger with air flow through the tubes, the number of tubes specified and the total air-flow rate are expressed as the number of tubes per unit area and the cubic feet per hour and per unit area, respectively. A heat exchanger serving a compartment having several units of skin area would consist of the same length tubes, but the total number of tubes would be the number per unit skin area times the total number of skin area units associated with the compartment.

2. Nomenclature

Symbol	Definition	Units
A	Area	ft^2
a,b,c,d	Empirical constants defined by equations (VII-19 and -20)	
a'	Convection group used in equation (VII-3)	
B,C	Substitution constants for equation (VII-22)	
c	Specific heat	Btu/lb-°R
c_p	Specific heat at constant pressure	Btu/lb-°R
D	Diameter	ft
E	Constant of integration	
F	Relative use factor	dimensionless
f	Friction factor	dimensionless
G	Substitution constant for equation (VII-22)	
g	Gravitational constant = 4.17×10^8	ft/hr^2
H	Substitution variable defined in Figure VII-9	

Symbol	Definition	Units
h	Heat transfer coefficient	Btu/hr-ft^2-^{o}R
K	Coefficient for entrance and exit losses	dimensionless
k	Thermal conductivity	Btu/hr-ft^2-^{o}R
M	Substitution constant for equation (VII-22)	
m	Weight based on unit skin area	lb/ft^2
n	Number of tubes or number of frontal area units in heat exchanger core based on unit skin area	dimensionless
n'	Total number of tubes or number of frontal area units in heat exchanger	dimensionless
Pr	Prandtl modulus	dimensionless
p	Pressure	lb/ft^2
Q	Volume flow rate based on unit skin area	ft^3/hr-ft^2
q	Heat transfer rate	Btu/hr-ft^2
R	Ratio of free convection to radiation heat transfer surface area	dimensionless
Re	Reynolds modulus	dimensionless
r	Radius	ft
T	Absolute temperature	^{o}R
U	Conductance	Btu/hr-ft^2-^{o}R
V	Velocity	ft/hr
W	Weight flow rate based on a unit skin area	lb/hr-ft^2
w	Weight	lb
x	Length or thickness	ft
α	A ratio of motor power to heat exchanger capacity	dimensionless
γ	Weight density	lb/ft^3
δ	Pressure	atmospheres (dimensionless)

Symbol	Definition	Units
ϵ	Radiation emissivity	dimensionless
μ	Viscosity	lb/ft-hr
σ	Heat exchanger effectiveness	dimensionless
τ	Time	hr
τ'	Time	min

SUBSCRIPTS

a	Refers to air
ai	Denotes air entering equipment
ao	Denotes air leaving equipment
al	Denotes air entering tube
ax	Denotes air leaving tube of length x
c	Denotes convection when used with heat transfer coefficient Denotes free flow area of core when used with area
ce	Denotes convection at equipment surface
ci	Denotes convection at insulation surface
d	Denotes design value
e	Refers to equipment
f	Refers to fuel
g	Denotes generated value
H	Refers to heat exchanger
h	Denotes hydraulic radius
i	Refers to insulation
it	Refers to insulation on fuel tanks
m	Denotes average value

SUBSCRIPTS

o	Denotes external value
p	Denotes power requirement of blower motor
r	Denotes radiation value
s	Refers to heat exchanger shell
se	Denotes equipment heat storage
sh	Refers to heat exchanger tube sheets
t	Refers to heat exchanger tubes
tot	Denotes total value
w	Refers to skin
1,2	Denotes initial and final value for a time interval, respectively
(1/2)	Denotes value at middle of flight time

3. Derivation of Equations

a. External Heat Load to the Equipment

The external heat load to the equipment is transferred by conduction through the skin insulation, and by free convection and radiation inside of the compartment. The rate of heat transfer by conduction through the insulation is given by

$$q_o = \frac{k_i}{x_i} (T_w - T_i) \qquad \text{(VII-1)}$$

The rate of heat transfer from the insulation to the equipment by radiation is given by

$$q_r = h_r (T_i - T_e) \qquad \text{(VII-2)}$$

where

$$h_r = 17.4 \times 10^{-4} \left(\frac{1}{\frac{1}{\epsilon_i} + \frac{1}{\epsilon_e} - 1} \right) \left[\frac{\left(\frac{T_i}{100}\right)^4 - \left(\frac{T_e}{100}\right)^4}{\left(\frac{T_i}{100}\right) - \left(\frac{T_e}{100}\right)} \right]$$

as explained in Section V.

The rate of heat transfer from the insulation to the equipment by free convection is given by

$$q_c = h_c (T_i - T_e) \qquad \text{(VII-3)}$$

where

$$h_c = \frac{1}{\frac{1}{h_{ci}} + \frac{1}{Rh_{ce}}}$$

and where

$$h_{ci} = \left(\frac{a'}{\delta^{2/3}}\right)_i (\delta)^{2/3}(T_i - T_a)^{1/3}$$

for $\left(\frac{a'}{\delta^{2/3}}\right)_i$ evaluated at $\frac{T_i + T_a}{2}$ and similarly for h_{ce}.

The reader is referred to the analysis of Section V for complete details concerning the equations for conduction, radiation, and free convection.

b. Heat Transfer Between the Equipment and the Primary Coolant

Heat exchange between the equipment and the air-to-liquid heat exchanger is most conveniently considered in terms of the heat exchanger effectiveness, and the equivalent heat exchanger effectiveness of the equipment. The definition of heat exchanger effectiveness used for this purpose is the ratio of actual temperature rise of the secondary coolant in the equipment to the greatest possible temperature rise of that fluid when exposed to the equipment surface temperature. According to this definition, the effectiveness for the equipment can be written,

$$\sigma_e = \frac{(T_{ao} - T_{ai})}{(T_e - T_{ai})} \qquad \text{(VII-4)}$$

where T_{ai} and T_{ao} are the air temperatures on entering and leaving the equipment, respectively. Similarly, the effectiveness for the heat exchanger can be written,

$$\sigma_H = \frac{(T_{ao} - T_{ai})}{(T_{ao} - T_f)} \qquad \text{(VII-5)}$$

Equations (VII-4) and (VII-5) can be combined and rearranged to give

$$\frac{\sigma_e}{\sigma_H} + 1 = \frac{(T_e - T_f) + (T_{ao} - T_{ai})}{(T_e - T_{ai})}$$

By a heat balance equation

$$q_f = W_a c_p (T_{ao} - T_{ai})$$

or

$$q_f = W_a c_p \sigma_e (T_e - T_{ai})$$

Combining the last three equations to eliminate T_{ao} and T_{ai}, and rearranging gives

$$q_f = \left(\frac{1}{\frac{1}{\sigma_H} + \frac{1}{\sigma_e} - 1}\right)(W_a c_p)(T_e - T_f) \qquad \text{(VII-6)}$$

Equation (VII-6) shows that the heat transfer rate between the equipment and the primary coolant is directly proportional to the over-all temperature potential, the thermal capacity rate of the secondary coolant, and a function of the effectiveness values for the heat exchanger and the equipment. As explained earlier, the effectiveness of the equipment is taken as constant.

c. Effectiveness of the Heat Exchanger

An expression for the effectiveness of a straight-tube heat exchanger can be derived from the definition of effectiveness and a heat balance equation. For air flowing through n tubes and exchanging heat with the tube surfaces, the heat balance is,

$$(Q_a \gamma_a c_p) dT_a = \left[h_a (T_s - T_a) n\pi D\right] dx$$

By rearranging, this becomes

$$\frac{dT_a}{(T_s - T_a)} = \left(\frac{h_a n\pi D}{Q_a \gamma_a c_p}\right) dx,$$

and may be integrated for constant T_s and Q_a, and for a suitable constant mean value of heat transfer coefficient h_a and air properties. The result is

$$x = \left(\frac{Q_a \gamma_a c_p}{h_a n\pi D}\right) \log_e \left(\frac{T_w - T_{a1}}{T_w - T_{ax}}\right) \qquad \text{(VII-7)}$$

Using the definition of σ_H, and observing that by previous definition $T_w = T_f$, $T_{a1} = T_{ao}$, and $T_{ax} = T_{ai}$, equation (VII-7) becomes

$$x = \left(\frac{Q_a \gamma_a c_p}{h_a n\pi D}\right) \log_e \left(\frac{1}{1 - \sigma_H}\right) \qquad \text{(VII-8)}$$

This is solved for the effectiveness to give

$$\sigma_H = 1 - (e)^{-\left(\frac{h_a \pi D n x}{Q_a \gamma_a c_p}\right)} \qquad \text{(VII-9)}$$

Equation (VII-9) is for a straight-tube type exchanger with air flow through the tubes. It is easily shown that for any type of heat exchanger core,

$$\sigma_H = 1 - (e)^{-\left(\frac{h_a A n x}{Q_a \gamma_a c_p}\right)} \qquad \text{(VII-10)}$$

where A is the heat transfer area per unit length parallel to the flow and per unit frontal area normal to the flow, and where n is the number of such frontal area units.

The heat transfer coefficients h_a used in equations (VII-9) and (VII-10) are for forced convection through the heat exchanger core. For a straight tube, Reference (VII-1) gives an expression suitable for cooling of air as,

$$h_a = 0.0265 \left(\frac{k}{D}\right) \left(\frac{D\, V_a \gamma_a}{\mu}\right)^{0.8} \left(\frac{c_p \mu}{k}\right)^{0.3} \qquad \text{(VII-11)}$$

which is appropriate for use in equation (VII-9). For use in equation (VII-10), a value of h_a appropriate to the particular heat exchanger core must be selected. Reference (VII-2) gives graphical data on heat transfer coefficients for a large number of heat exchanger cores.

d. Power Requirements of the Closed Air Circuit

As assumed earlier, the pressure drop of all parts of the system other than the heat exchanger is neglected. By use of the Darcy equation (Ref. VII-3), the pressure drop for a straight tube is given by

$$\Delta p = \gamma_a \left(\frac{V_a^2}{2g}\right) \left(1.5 + \frac{fx}{D}\right)$$

where the term 1.5 allows for entrance and exit losses to the heat exchanger. The power requirement is the product of this pressure drop times the total volume flow rate of circulated air. Converting from mechanical units to thermal units, and allowing for a 25 percent over-all fan and motor efficiency, the total heat load imposed by operation of the air circulation system is

$$q_p = \left(\frac{4}{778}\right) (Q_a \gamma_a) \left(\frac{V_a^2}{2g}\right) \left(1.5 + \frac{fx}{D}\right)$$

or,

$$q_p = \left(\frac{Q_a \gamma_a V_a^2}{1621x10^8}\right)\left(1.5 + \frac{fx}{D}\right) \qquad \text{(VII-12)}$$

Equation (VII-12) is for a system using a straight tube heat exchanger core, with air flow through the tubes. It is similarly shown that for any type heat exchanger core

$$q_p = \left(\frac{\gamma_a Q_a^3}{1621x10^8 \; n^2 \; A_c^2}\right)\left(K + \frac{fx}{4r_h}\right) \qquad \text{(VII-13)}$$

where A_c is the free area available to flow per unit frontal area of the core, and r_h is the hydraulic radius of the core defined as

$$r_h = \frac{A_c \; x}{A} \qquad \text{(VII-14)}$$

The term K of equation (VII-13) allows for entrance and exit losses to the heat exchanger.

The friction factor f of equations (VII-12, and -13) is a function of the Reynolds number. For turbulent flow in a smooth tube, f is obtained using equation (VII-23), p. VII-27, where

$$Re = \frac{\gamma_a \; VD}{\mu} \qquad \text{(VII-15)}$$

Or it may be obtained from plots of f versus Re, such as Figure VII-10. Reference VII-2 gives values of f plotted versus Re for a large number of other heat exchanger cores. The Reynolds number as defined for any core is

$$Re = \frac{4r_h \gamma_a \; V}{\mu} \qquad \text{(VII-16)}$$

Caution should be exercised in the use of friction factors. Those given in Reference VII-2 are Fanning friction factors rather than Darcy friction factors. Values taken from this reference should therefore be multiplied by four for use in equation (VII-13).

e. Heat Balance for the Compartment

A heat balance may be written for the compartment, wherein the sum of all heat loads minus the cooling effect is set equal to the rate of heat stored in the equipment. This is given by the equation

$$q_{se} = q_o + q_p + q_g - q_f \qquad \text{(VII-17)}$$

The rate of heat storage in the equipment is given by,

$$q_{se} = m_e c_e \left(\frac{\Delta T_e}{\Delta \tau}\right) \qquad \text{(VII-18)}$$

where the thermal capacity product $m_e c_e$ is expressed on a unit skin area basis (for skin area associated with the compartment), as are all the other heat rate quantities of equation (VII-17).

The equations here derived are sufficient to describe completely the heat exchange processes and temperature rise of equipment in a cooled compartment.

4. Procedure for Calculating Equipment Temperature Rise with Time

a. General Method

Because of the large number of heat loads in the compartment studied in this Section, it is convenient to divide the calculation procedure into two parts. The first part is concerned with calculating the external heat load q_o over a range of temperature values for the equipment. Results of this calculation are then prepared as a plot of q_o versus T_e and used for the second part of the calculation. The calculation of external heat loads is covered extensively in Section V and is therefore not given here. A description is given here of the second part of the calculation, which is concerned with calculating the equipment temperature rise with time. A detailed calculation procedure and a sample calculation are given in the Appendix to this Section.

A stepwise calculation procedure is required, since the expression for heat exchanger effectiveness, equation (VII-9) is derived assuming constant values of heat transfer coefficient and air properties. This assumption is reasonable only for small temperature ranges. The stepwise calculation can be made using the initial temperature conditions of a time interval for calculating temperature rise, in which case the interval calculation is direct. If average interval temperatures are used, the calculation is more accurate for intervals of given size, but the procedure involves trial and error. The second method is described here, since it is more generally valid. The procedure described is for the use of the straight-tube type of heat exchanger core.

b. Procedure

To begin calculation, a number of compartment and equipment characteristics must be known, in addition to those required to calculate the external heat load. To describe heat exchanger performance, Q_a, x, δ, V_a, D, and n must be known, and a temperature-time plot for the coolant or fuel must be available. This procedure assumes the use of JP-3 fuel as a liquid coolant, and fuel. Temperature-time plots are taken from Appendix III. The equipment must be described in terms of σ_e, q_g, and $m_e c_e$.

Calculation of an interval begins by assuming a value of T_{e2} corresponding to a selected time interval $\Delta\tau$. The value of T_{fm} is then obtained from the fuel temperature plot at the middle of $\Delta\tau$, and the value of T_{em} is calculated as

$$T_{em} = \frac{(T_{e1} + T_{e2})}{2}$$

By a combination of equations (VII-4, -6) and the equation,

$$q_f = W_a c_p (T_{ao} - T_{ai}),$$

the equation

$$T_{ai} = T_{em} - \frac{(T_{em} - T_{fm})}{\sigma_e \left(\frac{1}{\sigma_H} + \frac{1}{\sigma_e} - 1\right)}$$

is obtained. This is used to calculate T_{ai} as based on σ_H from the previous interval. Equations (VII-4 and -5) are next combined to give

$$T_{ao} = (T_{em} - T_{ai}) \left(\frac{\sigma_e}{\sigma_H}\right) + T_{fm}$$

which is used to calculate T_{ao} as based on σ_H from the previous interval. Then T_{am} is calculated as

$$T_{am} = \frac{T_{ao} + T_{ai}}{2}$$

and values of γ_a and c_p are found for air at T_{am}.

Equation (VII-6) is used to calculate q_f, using the relationship

$$W_a c_p = Q_a \gamma_a c_p$$

and using temperatures at their mean values (subscript m).

The heat transfer coefficient h_a is evaluated at T_{am} next. This is conveniently done using Figure VII-8, where h_a is given as

$$h_a = H \times 10^{-4} (\delta V_a)^{0.8}$$

based on equation (VII-11). The value of H is read from the Figure at T_{am} and then used in the above equation to calculate h_a.

The value of σ_H is then calculated from equation (VII-9), and equation (VII-6) is again used to calculate q_f. The most recently calculated value of q_f for the interval should agree within one percent of the value obtained earlier. Otherwise the calculation is repeated, using the calculated value

of σ_H in preference to the value from the previous interval.

When q_f is sufficiently accurate, the power requirement may be calculated. The Reynolds number is evaluated using equation (VII-15) and taking fluid properties at T_{am}. If the compartment is at other than standard atmospheric pressure, the value of γ_a must be adjusted accordingly, since it is directly proportional to pressure for a perfect gas. The value of f is then obtained from equation (VII-23), p. VII-27, corresponding to Re, or from a plot, such as Figure VII-11, and q_p is calculated with equation (VII-12).

Equation (VII-17) is used to calculate q_{se}, and equation (VII-18) is used to calculate ΔT_e. T_{e2} is then given by

$$T_{e2} = T_{e1} + \Delta T_e$$

T_{e2} as calculated with the above equation should agree closely with the value assumed at the beginning of the interval calculation. It is not difficult to obtain agreement between the assumed and calculated ΔT_e of one or two percent.

On completion of the interval calculation, the value of T_{e2} obtained is used as the value of T_{e1} for the next interval, and the entire process is repeated. The procedure required to establish the initial value of σ_H for use in the first interval is indicated in the Appendix of this Section.

c. Selection of the Time Interval

The size of time interval to use varies depending on the amount of curvature in the plot of T_e versus τ. A large time interval should not be used where the slope of this plot is changing rapidly. It is recommended that occasional checks be made to determine whether the size of time interval being used is small enough. This is readily done by dividing an interval in two, and recalculating with the two half-size intervals to determine if substantially the same end temperature is achieved. If not, the interval being used is too large. It is then necessary to determine by trial the size of the largest accurate interval.

EFFECTS OF COMPARTMENT, EQUIPMENT, AND HEAT EXCHANGER CHARACTERISTICS ON EQUIPMENT TEMPERATURE RISE

1. General Performance. Coolant Temperature

Typical equipment temperature curves for equipments located in a compartment with an air-to-fuel heat exchanger are shown in Figure VII-2. Fuel JP-3 is used as the liquid coolant, and the plots of fuel temperature are taken from Figure AIII-9. The characteristics of the compartment, the equipment, and the heat exchanger are given in the figure. The two cases plotted are for identical conditions, except that a different coolant tem-

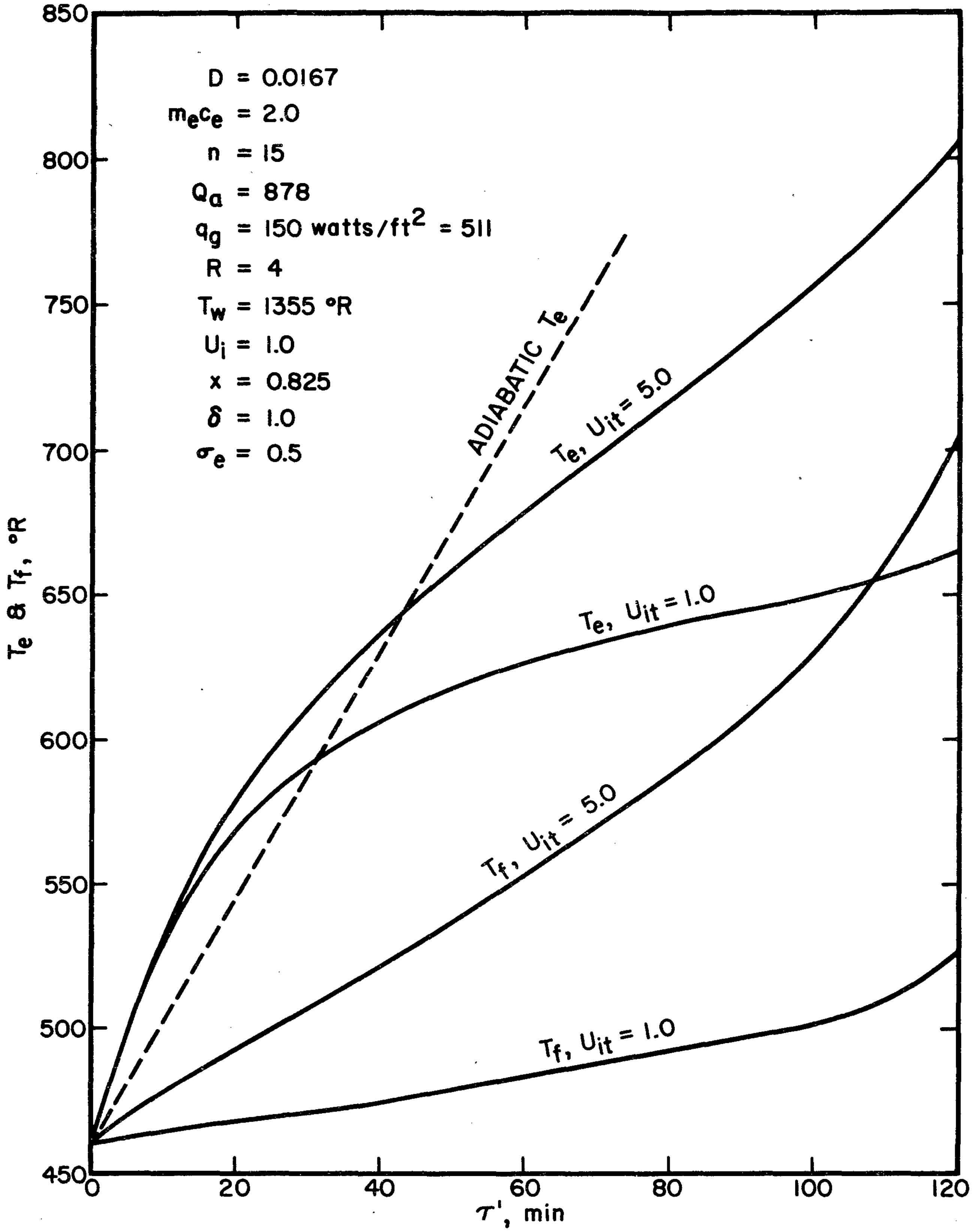

Figure VII-2

Typical Performance, Temperature Rise of Equipment in a Compartment Cooled by an Air-to-Fuel Heat Exchanger.

perature schedule is used. The line labeled as "adiabatic T_e" represents the temperature plot for the same heat generating equipment, but without any heat exchange, neither heating nor cooling. Physically, it represents equipment which is perfectly insulated from its surroundings.

The two plots of T_e in Figure VII-2 show that after an initial period of rapid temperature rise, the equipment temperature plot runs approximately parallel to the fuel coolant temperature plot, or $(\Delta T_e/\Delta\tau) \approx (\Delta T_f/\Delta\tau)$. The initial rate of temperature rise is greater than for the perfectly insulated equipment because in the arrangement analyzed, external heat loads are directly applied to the equipment. Since equipment and fuel temperatures are initially equal, the equipment must first achieve a temperature sufficiently higher than the fuel to provide the necessary potential to transfer a portion of the various heat loads to the primary coolant. In order to do this, it is necessary for the equipment to store some of the heat it receives, or generates. Later, as (T_e-T_f) becomes large enough, the cooling action of the heat exchanger predominates and the difference between the equipment temperature and its adiabatic value becomes progressively greater. For the cases shown, the use of cooling appears to be desirable only for flight times longer than 30 minutes since only thereafter the equipment would be cooler than if it were perfectly insulated.

It is shown in Section V, that for a constant skin temperature, higher external heat loads occur at lower equipment temperatures. Therefore, in the case of lower equipment temperature ($U_{it} = 1.0$) a greater temperature potential $(T_e - T_f)$ is maintained than in the case where $U_{it} = 5.0$. Another reason for this greater value of $(T_e - T_f)$ is that in the case of more slowly rising temperatures less heat is stored in the equipment per unit time, requiring that more of the heat be transferred to the fuel. It is apparent from Figure VII-2 that the parallel relationship between the equipment temperatures and the fuel temperatures does not hold where the $(\Delta T_f/\Delta\tau)$ is changing rapidly, as occurs at $\tau' = 100$ min and beyond. Under these circumstances the equipment thermal capacity provides an inertia effect, tending to prevent comparatively sudden changes of $(\Delta T_e/\Delta\tau)$.

Equipment with different thermal capacity than the cases shown would behave in a similar fashion. For smaller equipment thermal capacity, the initial equipment temperature rise would be more rapid, since the heat load conditions would be the same, but the equipment is able to store less heat per unit temperature rise. In the region where $(\Delta T_e/\Delta\tau) \approx (\Delta T_f/\Delta\tau)$, the equipment would maintain a greater temperature potential $(T_e - T_f)$, since a greater portion of the heat loads would have to be transferred to the fuel because of the reduction in q_{se} due to lower thermal capacity. Cases with greater equipment thermal capacity would behave in the reverse manner.

2. Heat Exchanger Effectiveness

The effect of heat exchanger effectiveness in terms of tube length on the equipment temperature rise is shown in Figure VII-3. Characteristics of the compartment, the equipment, and the heat exchanger are

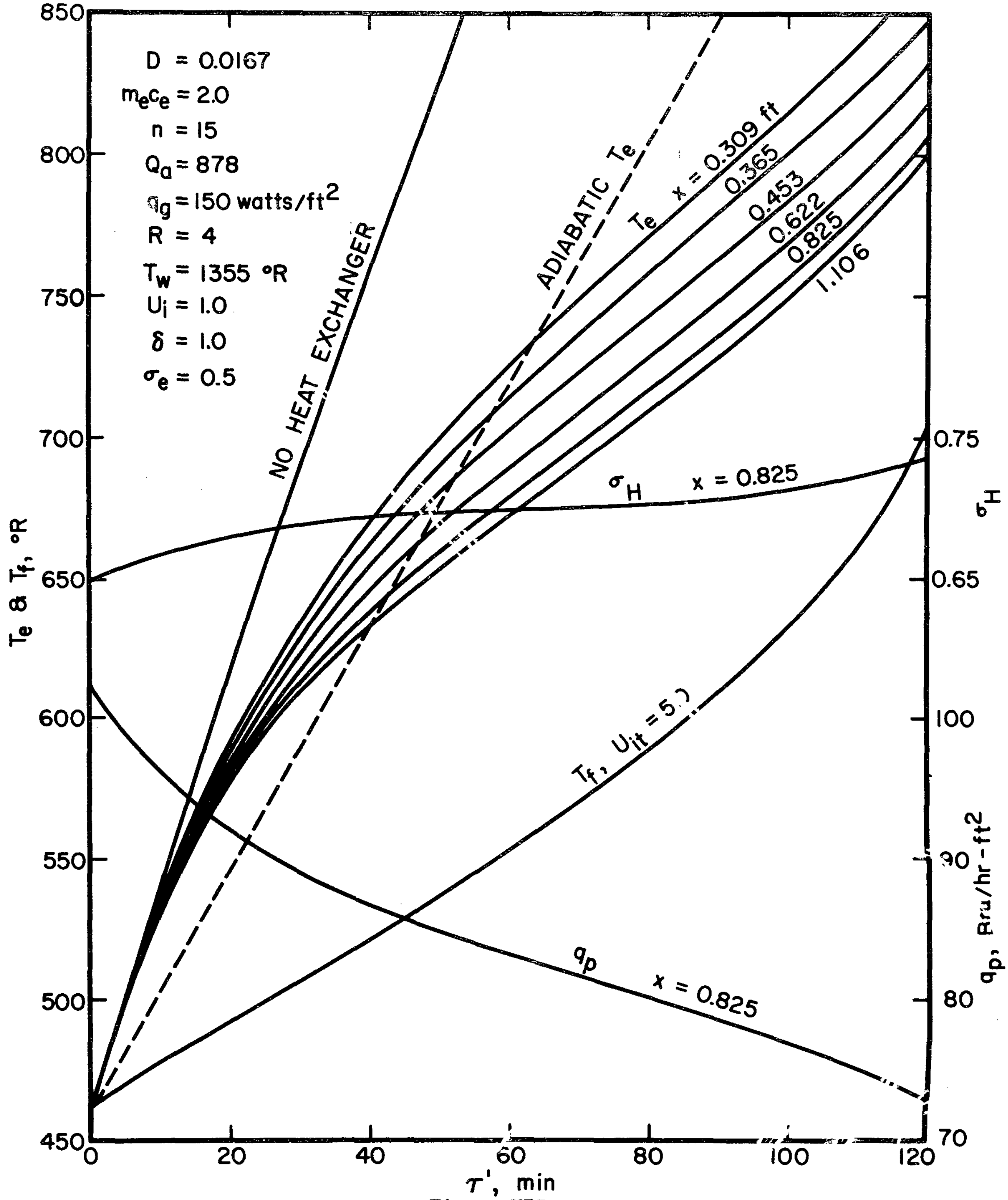

Figure VII-3

Effect of Heat Exchanger Effectiveness on the Temperature Rise of Equipment in a Cooled Compartment

given in the figure. Fuel is used as the primary coolant, with the fuel temperature plot taken from Figure AIII-9. All the cases plotted in Figure VII-3 are identical, except that the length of the tubes in the heat exchanger is varied. The plot labeled "adiabatic T_e", as before, represents the temperature of perfectly insulated equipment. The plot labeled "no heat exchanger" is the result of a calculation based on the methods of Section V. It represents the same equipment and the same compartment, except that there is no heat exchanger and no forced air circulating system.

It is immediately seen from Figure VII-3 that the longer the heat exchanger tubes, the greater the cooling effect. This results from the dependence of heat exchanger effectiveness on tube length. Equation (VII-9) indicates clearly that the heat exchanger effectiveness σ_H increases with tube length. The significance of this to the plots of Figure VII-3 can be seen from equation (VII-6), where increased σ_H indicates that a smaller value of (T_e-T_f) is required per unit of heat transfer rate q_f. Therefore, for all other factors constant, as the effectiveness of the heat exchanger is increased, the equipment is brought closer to the primary coolant temperature. The improvement in performance is paid for in terms of the longer tubes, which weigh more, have greater pressure drop, and occupy more space. Due to changes in temperature, the power requirements for circulating the air vary from the beginning to the end of a flight. For the beginning of flight, however, the value of q_p ranges from 70.5 Btu/hr-ft^2 for the shortest tube length of 0.309 ft to 120.1 Btu/hr-ft^2 for the greatest tube length of 1.106 ft. It is therefore clear that the use of a more effective heat exchanger imposes greater power requirements for its operation, as well as the greater space and weight requirements. Values of σ_H are not given in Figure VII-3, since they vary with temperature. As based on equation (VII-9) for the beginning of flight, however, the range represented is from $\sigma_H = 0.327$ for $x = 0.309$ ft to $\sigma_H = 0.751$ for $x = 1.106$ ft.

In Figure VII-3, the variations of heat exchanger effectiveness and power requirements with time are shown for one of the tube lengths. Although the value of σ_H is principally dependent on the tube length, it increases somewhat for constant volume flow because of the reduction of air density and changes of other physical properties with increased air temperature. The circulating power requirement decreases because of the reduced air density.

Equation (VII-6) shows that the equipment effectiveness σ_e has the same influence on performance as σ_H. This points to the desirability of arranging the equipment to act as an effective heat exchange device wherever possible. One method of doing this would be to arrange the equipment components so they receive the cooling air from the heat exchanger in series, giving a greater length effect to the equipment. This would have a disadvantage, however, in that the equipment components which received the air last would operate at higher temperature for a given heat dissipation than the others. The value of T_e used in this analysis might therefore represent a great range of temperatures, with actual values at extremes considerably above and below the average value as indicated by T_e.

3. Heat Load

The effects of generated heat load on the equipment temperature rise are shown for three lengths of heat exchanger tube for each heat generation rate in Figure VII-4. The characteristics of the compartment, the equipment, and the heat exchanger are given in the figure. The heat exchangers of the same tube length have the same effectiveness, or σ_H value for given temperature conditions, since the air flow rates are directly proportional to the number of heat exchanger tubes. The number of heat exchanger tubes is proportioned approximately to the total heat load on the equipment for the two cases of different heat generation.

It is interesting to note that the cases with lower heat generation are held to smaller values of $(T_e - T_f)$, in spite of the fact that the heat exchangers are proportioned in size to the total heat load. The reason for this can be found by examination of the heat balance, equation (VII-17). By rearranging this equation it can be shown that the cooling effect q_f is equal to the sum of the external, generated, and motor heat loads minus the heat storage rate q_{se}. In designing the heat exchangers for the cases in Figure VII-4 this heat storage rate was not subtracted from the sum of the heat loads. Therefore the cases with a smaller heat generation rate have a larger cooling capacity as compared to that needed under given temperature conditions, and so operate with a smaller value of the temperature difference $(T_e - T_f)$.

An important conclusion can be drawn from the foregoing. In order to design a heat exchanger to provide a specified equipment temperature rise, the capacity of the heat exchanger must be proportioned to the quantity

$$(q_o + q_p + q_g) - q_{se}$$

where the heat stored due to thermal capacity is subtracted from the total heat load. This procedure is followed in the design method given later. The value of q_{se} to be used for this purpose can be calculated, since it was noted earlier that $(\Delta T_e / \Delta \tau) \approx (\Delta T_f / \Delta \tau)$ permitting the use of equation (VII-18) for the calculation. The importance of allowing for the heat storage rate in a transient heat exchanger design is illustrated by the following example. In Figure VII-3 it is seen that for a heat exchanger with $x = 0.309$ ft the equipment reaches $T_e = 815^oR$ at $\tau' = 100$ min. If a heat exchanger is designed for the heat loads corresponding to this equipment temperature and the fuel temperature at $\tau' = 100$ min, but, neglecting the value of q_{se}, the tube length is found to be $x = 0.725$ ft. All of the other factors, such as air flow rate, are the same as in Figure VII-3. This steady-state design procedure is thus seen to indicate a heat exchanger over twice as big as that actually required to achieve the design equipment temperature. Furthermore, by interpolation in Figure VII-3, it is found that a heat exchanger with $x = 0.725$ ft would overcool by more than 50^oF assuming that $T_e = 815^oR$ were desired as the equipment temperature.

A design procedure is given later which uses the principles found in this calculation study to design heat exchangers for desired transient performance characteristics.

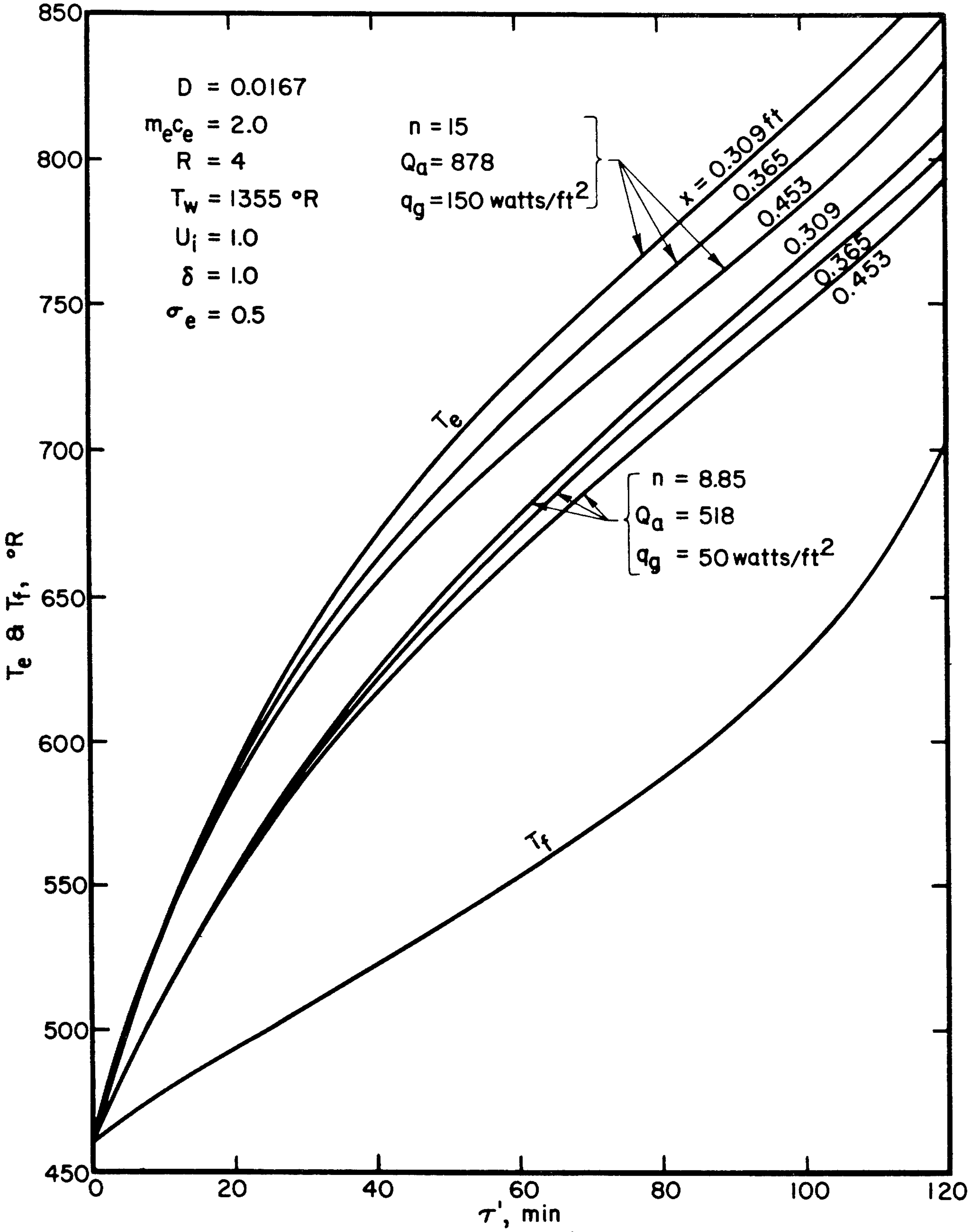

Figure VII-4

Effect of Generated Heat Load and Heat Exchanger Effectiveness on the Temperature Rise of Equipment in a Cooled Compartment

SIMPLIFIED ANALYSIS

In Section V, it is shown that the external heat loads on the equipment due to radiation and free convection can be closely approximated with a linear function of T_e. This simplification can be used to develop an approximate expression for the temperature rise of equipment in a compartment with a heat exchanger.

The external heat load is written,

$$q_o = a - b\,T_e \qquad \text{(VII-19)}$$

which is a different form than that used in Section V.

By combination of equations (V-6, -17, -18, and -19), and by changing to differential form,

$$a - bT_e + q_g + q_p = m_e\,c_e\,\frac{dT_e}{d\tau} + \left(\frac{Q_a\,\gamma_a\,c_p}{\frac{1}{\sigma_H} + \frac{1}{\sigma_e} - 1}\right)(T_e - T_f)$$

where a, b, q_g, $m_e c_e$, Q_a, and σ_e are constants. From Figure VII-4 it appears that σ_H is substantially constant if the temperature range is not too great. The product $\gamma_a c_p$ is also fairly constant for small temperature ranges ($\gamma_a c_p = 0.012$ at 800°R, $\gamma_a c_p = 0.099$ at 1000°R). Figure VII-3 shows some variation of q_p, but its magnitude is small compared to the other terms, and it is therefore considered constant. The equation is next restricted to regions of time short enough that the variation of fuel temperature with time can be expressed as a linear function of time, i.e.,

$$T_f = c + d\tau \qquad \text{(VII-20)}$$

Then making the substitution

$$M = \frac{Q_a\,\gamma_a\,c_p}{\frac{1}{\sigma_H} + \frac{1}{\sigma_e} - 1}$$

the equation becomes

$$\frac{dT_e}{d\tau} + \frac{M + b}{m_e\,c_e}\,T_e = \left(\frac{a + q_g + q_p + Mc}{m_e\,c_e}\right) + \left(\frac{Md}{m_e\,c_e}\right)\tau$$

Substituting again, let

$$B = \frac{M + b}{m_e\,c_e}$$

$$C = \frac{a + q_g + q_p + Mc}{m_e\,c_e}$$

$$G = \frac{Md}{m_e\,c_e}$$

Then

$$\frac{dT_e}{d\tau} + B\,T_e = C + G\tau \qquad \text{(VII-21)}$$

Equation (VII-21) is a linear differential equation, which is readily solved (Ref. VII-4) to give

$$T_e = \frac{C}{B} + \frac{G}{B}\tau - \frac{G}{B^2} + \frac{E}{e^{B\tau}}$$

where E is the arbitrary constant of integration. Using the boundary condition that $T_e = T_{e1}$ when $\tau = 0$ to evaluate E gives

$$T_e = \frac{C}{B} + \frac{G}{B}\tau - \frac{G}{B^2} + \frac{T_{e1} - \frac{C}{B} + \frac{G}{B^2}}{e^{B\tau}} \qquad \text{(VII-22)}$$

When the constant terms of equation (VII-22) are evaluated for any particular case, the equation can be used to obtain a direct solution for T_e corresponding to any time τ. Values of terms such as σ_H and q_p can be evaluated with equations (VII-9 and -12) respectively, using an estimated average temperature of the air for the fluid properties.

It is interesting to note that for large values of τ equation (VII-22) becomes

$$T_e \approx \frac{C}{B} + \frac{G}{B}\tau - \frac{G}{B^2}$$

which is a straight line function of τ. The slope of the line is

$$\frac{G}{B} = \frac{Md}{M + b}$$

Since b is quite small compared to M, this becomes

$$\frac{G}{B} \approx d$$

This shows that as τ increases, the plot of T_e versus τ approaches the slope of T_f versus τ, since d is the slope in equation (VII-20). This is an analytical confirmation of the plot characteristics noted in Figures VII-2, -3, and -4.

DESIGN OF HEAT EXCHANGER AND INSULATION FOR COOLED EQUIPMENT

1. Design Example

A design procedure and a design example are given here for the selection of a heat exchanger system and insulation for a compartment. Using this procedure, it is possible to select the optimum combination of heat exchanger and insulation, corresponding to either minimum space requirements or minimum weight requirements. After such an optimum design has been achieved, it can be compared to any other compartment systems which are capable of giving the same temperature-time performance of the equipment. By means of such a comparison, the system best suited to all the requirements of the cooling problem may be selected. Section XI describes the general procedure for selection of systems.

It is noted earlier in this Section that the plot of T_e versus τ tends to run parallel to the plot of T_f versus τ after an initial period of rapid temperature rise of the equipment. This fact is of use in the design procedure given here, since it makes possible the selection of appropriate temperatures for designing the heat exchanger. As an example, a design is given to meet the following specifications:

initial equipment temperature = $460^\circ R$

maximum permissible equipment temperature = $757^\circ R$

flight time required = 100 min

skin temperature = $1355^\circ R$

compartment air pressure δ = 1.0

equipment thermal capacity $m_e c_e$ = 2.0 Btu/$^\circ$R-ft^2

heat generation q_g = 150 watts/ft^2 = 511 Btu/hr-ft^2

ratio of free convection to radiation heat transfer area R = 4

fuel temperatures from Figure AIII-9 where U_{it} = 5.0 Btu/hr-ft^2-$^\circ$R

From Figure AIII-9 it is seen that the fuel temperature plot is reasonably straight. The plot of T_e versus τ will therefore have about the same slope during the last part of the design time span. The temperature potential between the equipment and the fuel at the end of flight is $(T_e-T_f)_d$ = $(757-632) = 125^\circ R$. Assuming the system will hold an approximately constant value of (T_e-T_f) during the last half of the flight time, an average equipment temperature for this period is

$$T_e = 125 + \frac{T_{f50} + T_{f100}}{2}$$

$$\text{or} \quad T_e = 125 + \frac{632 + 537}{2} = 709.5^\circ R$$

The average fuel temperature for the same period is

$$T_f = \frac{632 + 537}{2} = 584.5^\circ R$$

The heat exchanger and insulation system can be designed for these temperatures, since they represent average temperature conditions that must be achieved in the final design.

Since the external heat load is one of the quantities involved in a heat exchanger design, it is determined next. As yet the amount of insulation to be used is unknown. It is therefore necessary to assume a range of insulating effects, and determine the external heat load corresponding to each of them. The external heat load is conveniently determined by the methods described in the design example of Section V. Making calculations of this type for a range of insulating effects, and based on the use of rock wool insulation, the following data are obtained, assuming $\epsilon_i = 0.1$ and $\epsilon_e = 0.2$.

$$T_w = 1355^\circ R$$

$$T_e = 709.5^\circ R$$

U_i	$\frac{T_w+T_i}{2}$	k_i	$x_i = \frac{k_i}{U_i}$	q_o
0.2	1098	0.0560	0.0280	102.5
0.6	1157	0.0592	0.0987	237.5
1.0	1191	0.0612	0.0612	328.0
2.0	1238	0.0639	0.0319	467.0
5.0	1292	0.0668	0.0167	647.5

A heat exchanger for the compartment can now be designed corresponding to each insulating effect. In order to do this, it is necessary to assume values for the effectiveness of the heat exchanger and the equipment, and the ratio of power requirements to heat exchanger capacity. A value of $\sigma_H = 0.70$ is in keeping with good practice, and a value of $\sigma_e = 0.50$ is assumed. It is also assumed that the ratio of power requirement to heat exchanger capacity of $(q_p/q_f) = 0.1$ is satisfactory. Then the over-all heat balance for the heat exchanger is

$$q_o + q_g + q_p = q_f + q_{se}$$

But since $q_p = \alpha q_f$, where $\alpha = 0.1$, the heat balance can be written,

$$q_f = \frac{(q_o + q_g - q_{se})}{(1 - \alpha)}$$

where

$$q_{se} = (m_e c_e) \frac{(T_{f100} - T_{f50})}{\left(\frac{\Delta\tau'}{60}\right)}$$

Then

$$q_{se} = \frac{2 \times (632-537)}{0.833} = 228 \text{ Btu/hr-ft}^2$$

Using the assigned values of α and q_g

$$q_f = 1.11\, q_o + 314$$

The various values of q_o are next used to design heat exchangers, using the procedure given below. This procedure is based on the equation

$$f = \frac{0.184}{(Re)^{0.2}} \qquad \text{(VII-23)}$$

for the Darcy friction factor in smooth tubes (Ref. VII-1, p. 121).

Given Data

q_o = ______ Btu/hr-ft²
q_f = $(1.11\, q_o + 314)$ = ______ Btu/hr-ft²
σ_H = ______
σ_e = ______
$(q_p/q_f) = \alpha$ = ______
D = ______ ft
T_e = ______ °R
T_f = ______ °R

1. Calculate

$$T_{am} = \frac{T_e + T_f}{2} - \frac{(T_e - T_f)\,(\sigma_H - \sigma_e)}{2\sigma_e\sigma_H\left(\frac{1}{\sigma_H} + \frac{1}{\sigma_e} - 1\right)}$$

2. Get γ_a, c_p, μ, k, Pr at T_{am}. If γ for air is taken from a figure or table based on one atmosphere, then $\gamma_a = \delta\gamma$.

γ_a = lb/ft³
c_p = Btu/lb-°R
μ = lb/ft-hr
k = Btu/hr-ft-°R
Pr =

3. Calculate

$$Q_a = \frac{q_f\left(\frac{1}{\sigma_e} + \frac{1}{\sigma_H} - 1\right)}{\gamma_a\, c_p\, (T_e - T_f)}$$

$Q_a =$ ft^3/hr

4. Calculate

$$\frac{fx}{D} = \left[\frac{(Pr)^{0.7}}{(0.576)}\right] \log_e \left(\frac{1}{1 - \sigma_H}\right)$$

$\frac{fx}{D} =$

5. Calculate

$$n^2 = \frac{Q_a{}^3 \gamma_a}{\left(\frac{\pi}{4} D^2\right)^2 x 1621 x 10^8 x q_p} \left(1.5 + \frac{fx}{D}\right)$$

$n^2 =$

$n =$

6. Calculate

$$V_a = \frac{Q_a}{n\left(\frac{\pi}{4} D^2\right)}$$

$V_a =$ ft/hr

7. Calculate

$$Re = \frac{D\, V_a \gamma_a}{\mu}$$

$Re =$

This value should lie in the range 5000 to 2×10^5 for proper use of the equation for f used in deriving the procedure.

8. Calculate

$$x = \left(\frac{D}{0.184}\right)\left(\frac{D\, V_a \gamma_a}{\mu}\right)^{0.2} \left(\frac{fx}{D}\right)$$

$x =$ ft

This procedure determines the number of tubes required and their length. In order to determine the actual size or volume requirements of a heat exchanger, the tube arrangement must be decided upon. It is assumed here that the tubes of 0.20-inch internal diameter are located with a 0.45-inch equilateral-triangular pitch. The header sheet area for each tube then is

$$0.45 \times 0.45 \sin 60^\circ = 0.1755 \text{ in}^2$$

The volume requirement of the entire tube bundle in cubic inches, for one square foot of skin, is then 0.1755 x 12(xn). It is reasonable to assume that the volume of the heat exchanger is about 130 per cent that of the tube bundle. This makes allowance for the shell, tube header sheets, and the like. The actual heat exchanger volume, expressed in cubic inches, then becomes 1.3 x 0.1755 x 12(xn) = 2.74 xn.

Using this method of determining the heat exchanger volume, the results of the heat exchanger designs corresponding to the various insulating effects are summarized as follows:

q_o	x	n	(2.74 xn)
102.5	0.807	9.87	21.84
237.5	0.807	13.30	29.40
328.0	0.807	15.69	34.60
467.0	0.807	19.22	42.50
647.5	0.807	23.85	52.70

The last column gives the heat exchanger volume, in cubic inches, for each square foot of skin surface area associated with the compartment. This volume can be added to the volume of insulation on one square foot of skin area, to give the total installation volume of the heat exchanger and insulation. If desired, an additional factor may be applied to the heat exchanger volume in order to account for the volume requirements of the motor and blower.

In order to make a just evaluation of the space requirements, it is necessary to account for the relative value of the space occupied by the insulation and that occupied by the heat exchanger. In a cylindrical compartment, for instance, the peripheral space where the insulation is located may be already obstructed to some extent by structural ribs or members, making its use for equipment impractical. Furthermore, the shape of equipments may be such that space near the compartment walls cannot be used effectively. Under such circumstances, the use of this space for insulation would not impose as severe a penalty on the free installation space of the compartment as the actual volume of the insulation would seem to indicate. It is therefore advisable to apply a "relative use factor" to the insulation volume requirements before comparing them with the heat exchanger volume requirements. The actual relative use factor applying to any specific case must be determined by the designer. If the designer decides he can use all of the space near the skin for installation of equipment, the relative use factor is one, and the insulation volume requirement is taken as $12x_i$, for the cubic inches of insulation on each square foot of skin. For most practical cases the relative use factor is less than one, and the insulation volume requirement should be taken as $12Fx_i$. The total volume requirements of both the insulation and the heat exchanger of the design example and for a number of relative use factors are given below:

Total Volume Requirements

U_i	(F=0.1)	(F=0.2)	(F=0.3)	(F=0.5)
0.2	70.2	118.3	166.8	263.8
0.6	46.5	63.5	80.6	114.7
1.0	45.2	55.8	66.4	87.4
2.0	48.0	53.5	59.0	70.0
5.0	55.6	58.4	61.4	67.1

These results are plotted in Figure VII-5. The abscissa represents U_i, or the insulating effect. The insulation thickness is inversely proportional to U_i, as indicated by the relationship $U_i = (k_i/x_i)$. At a value of $U_i =$ 0.20, corresponding to about 3-3/8 inches of insulation, the heat exchanger required is small, but the insulation occupies so much space that the total volume is large, indicating that too much insulation is being used. As the insulation thickness is reduced, the size of the heat exchanger increases, but not very rapidly. This gives a point of minimum volume requirements, with a very slow increase in the direction of less insulation. The minimum point represents an optimum design condition, and corresponds to greater insulation thicknesses for smaller values of relative use factor. This indicates that if peripheral space cannot be used for equipment, it is profitable to utilize it for thick insulation.

If for the design example it is assumed that the F = 0.12, Figure VII-5 indicates that the optimum design would have compartment insulation with $U_i = 1.1$ Btu/hr-ft^2-^{o}R. By plotting the values of q_o versus U_i as determined earlier, it is found that at optimum design conditions the value of q_o is about 343 Btu/hr-ft^2. When this value is used in the heat exchanger design procedure, the following values are determined.

$$Q_a = 895 \text{ ft}^3/\text{hr}$$
$$x = 0.806 \text{ ft}$$
$$n = 16.11$$

This heat exchanger design is next used together with the compartment conditions given at the beginning of the example to make an evaluation of equipment temperature rise. The calculation method of the Appendix to this Section is used for this. The result of this calculation is shown in Figure VII-6. Whereas the original design specifications required that T_e would not exceed 757^{o}R in 100 minutes of flight time, the actual evaluation indicates that the temperature at the end of the flight would be 754^{o}R. The difference is small and certainly within the accuracy of the analytical evaluation methods used. It should be pointed out that the determined optimum value of $U_i = 1.1$ corresponds to insulation properties at the design temperature conditions. Since the thermal conductivity of rock wool insulation increases with temperature, the value of U_i must be reduced a little in order to use it in the evaluation procedure of the Appendix. As defined for that procedure, U_i is assigned a value corresponding to the temperature conditions at the start of the calculation. The adjustment can readily be made by estimate. For the design example the value was reduced to $U_i = 1.0$.

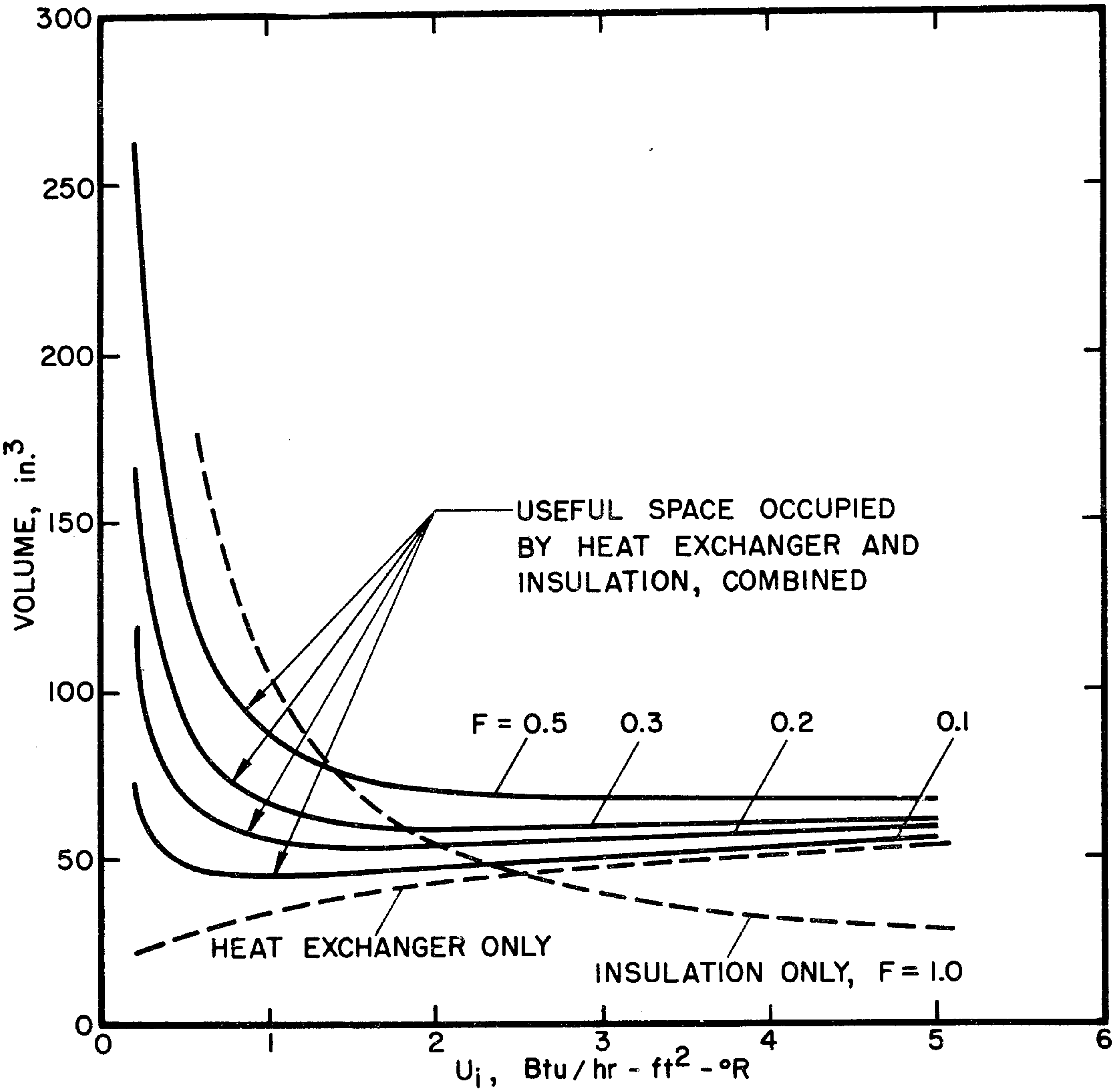

Figure VII-5

Evaluation of Volume Requirements for the Heat Exchanger and Compartment Insulation

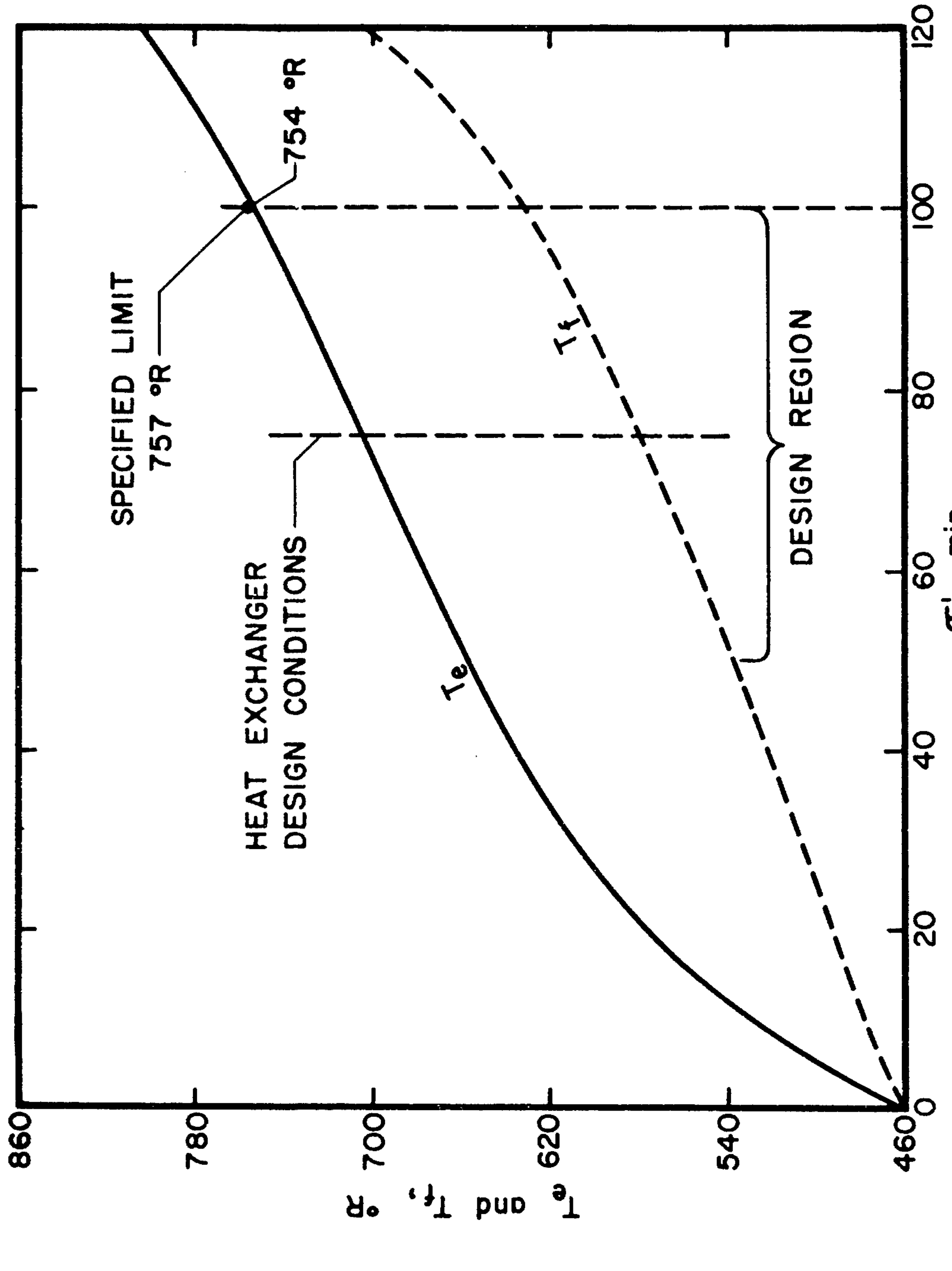

Figure VII-6

Calculated Performance Verification
of Heat Exchanger Design

It is conceivable that in some design problems the nature of conditions would be appreciably different from the design example. For instance, the allowable difference between the terminal fuel temperature and the terminal equipment temperature could be so large that even at the end point the rate of temperature rise of the equipment would be appreciably greater than that of the fuel. In such a case the design procedure given would not give results so close to the design specifications on the first try. The procedure for evaluating the equipment temperature rise can be repeated however, making small changes in the insulating effect or the heat exchanger to modify the results in the desired direction.

The example as given thus far has been concerned only with determining the optimum design from the standpoint of the minimum space requirements of the heat exchanger and insulation. It is also worthwhile to consider the design from the standpoint of the total weight requirements. To do this, it is assumed that the heat exchanger is made of aluminum alloy having a density of 0.10 lb/in^3, and that the tube wall thickness is 0.05 in. The weight per tube is then

$$\frac{\pi}{4}\left(\overline{0.30}^2 - \overline{0.20}^2\right) \times 9.7 \times 0.1 = 0.0382 \text{ lb}$$

The tube bundle weight is then

$$w_t = 0.0382\, n'$$

where n' is the number of tubes required for all the skin area of the compartment. Where the total skin area is A_w, this is given by

$$n' = n\, A_w$$

It is next assumed that the shell of the heat exchanger is 0.25 in. thick. Then the shell size is estimated as follows. Each tube in the bundle requires 0.1755 in^2 of sheet area, so the total end area is 0.1755 n'. Then for a round exchanger

$$\frac{\pi D_s^2}{4} = 0.1755\, n'$$

or

$$D_s = \sqrt{0.2238\, n'}$$

The shell weight is therefore given by

$$w_s = \pi D_s \times 9.7 \times 0.25 \times 0.1$$

or

$$w_s = 0.763\, D_s$$

The tube sheets of the exchanger are evaluated next. Assuming a sheet thickness of 0.25 in, the net area of the tube sheet for each tube is

$$0.1755 - \frac{\pi}{4}(0.3)^2 = 0.1047 \text{ in}^2$$

Therefore the weight of the two end sheets is given by

$$w_{sh} = 0.1047 \, n' \times 0.25 \times 2 \times 0.1$$

or

$$w_{sh} = 0.00525 \, n'$$

Since the heat exchanger is probably filled with fuel at the end of a flight, the weight of this fuel must also be considered. The fuel temperature at the end of the flight is 632°R, corresponding to a density of 45.9 lb/ft^3. The weight is therefore

$$w_f = \frac{0.1047 \, n' \times 9.7}{1728} \times 45.9$$

or

$$w_f = 0.027 \, n'$$

To the total of all weights as determined above is added two pounds as an allowance for fittings, end flanges, and the like. The total weight of the heat exchanger is then given by

$$w_{tot} = w_t + w_s + w_p + w_f + 2$$

Based on a two-foot diameter centerbody compartment, five feet long, with skin area only on the cylindrical portion of the surface, the weights of the heat exchanger designs determined earlier are:

U_i	w_{tot}
0.2	30.2
0.6	38.8
1.0	44.7
2.0	53.3
5.0	64.6

The insulation weight requirements are determined next, assuming that the rock wool insulation used is of the batt type, having a density of 12 lb/ft^3. For the insulation thicknesses determined earlier, this gives

U_i	w_i
0.2	105.5
0.6	37.2
1.0	23.0
2.0	12.0
5.0	6.3

where the insulation weights are based on the same centerbody compartment size as were the heat exchanger weights. The results of these weight calculations are shown in Figure VII-7. An optimum design from the standpoint of weight exists when U_i is 1.8 Btu/hr-ft^2-^{o}R as based on the design temperature conditions. However, reducing U_i to 1.1, the point where optimum space requirements exist, introduces a negligible weight penalty, thus justifying the design based on optimum space requirements.

In the example given, the weight requirements and the space requirements of the blower and its drive motor have been neglected, since they are small compared to the other factors involved.

2. General Design Procedure for a Heat Exchanger

The preceding design example is based on the case of a tubular-type air-to-liquid heat exchanger, where the air is forced through the tubes and the liquid surrounds the tubes. It is possible to give a design procedure which is more generally applicable, and which is based on graphical data in the form commonly determined for heat exchanger cores. The procedure as given here assumes that a plot is available showing both the Darcy friction factor and the heat transfer coefficient as functions of the Reynolds number. Reference VII-2 reports data on a large number of heat exchanger cores in a manner similar to this, except that the Fanning friction factor is used. The Darcy friction factor is simply four times as great as the Fanning friction factor.

Assigned Data

flight time, τ_d = hr
maximum allowable equipment temperature, T_{ed} = ^{o}R
heat generation rate, q_g = Btu/hr-ft^2
equipment thermal capacity, $m_e c_e$ = Btu/^{o}R-ft^2
skin temperature, T_w = ^{o}R
skin insulation, U_i = Btu/hr-ft^2-^{o}R
compartment air pressure, δ =
ratio of free convection to radiation heat transfer area, R =
ratio of blower motor power to heat exchanger capacity, α =
heat exchanger effectiveness, σ_H =
equipment effectiveness, σ_e =
time-temperature schedule of the liquid coolant
core hydraulic radius, r_h = ft
heat transfer area per unit frontal area and per unit length, A = ft^2
free flow area of core per unit frontal area, A_c = ft^2

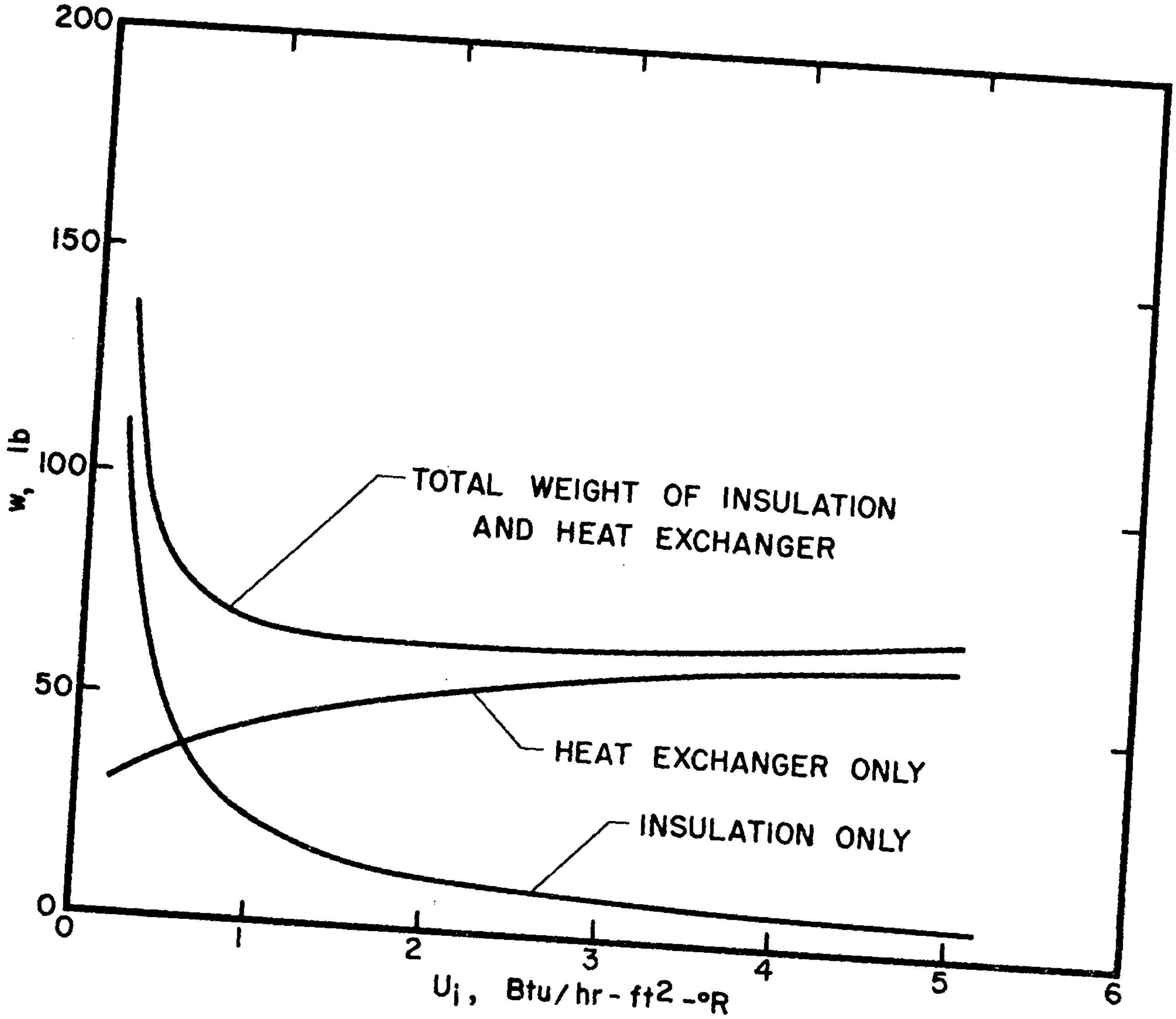

Figure VII-7

Evaluation of Weights of Heat Exchanger and Compartment Insulation

1. Get T_{fd} at the end of flight time

T_{fd} = ^oR

2. Get $T_{f(1/2)}$ at the middle of the flight time

$T_{f(1/2)}$ = ^oR

3. Calculate $(T_{fd} - T_{f(1/2)})$= ^oR

4. Calculate $q_{se} = m_e c_e \, (T_{fd} - T_{f(1/2)})$

q_{se} = Btu/hr-ft^2

5. Calculate

$$T_{em} = (T_{ed} - T_{fd}) + \frac{T_{fd} + T_{f(1/2)}}{2}$$

for T_{em} = ^oR

6. Get q_o, using the calculation methods of Section V, and using the given values of U_i, δ, R, T_w, T_{em}.

7. Calculate $(q_o + q_g - q_{se})$ =

8. Calculate

$$\frac{(\sigma_H - \sigma_e)}{(2\sigma_H\sigma_e)\left(\frac{1}{\sigma_H} + \frac{1}{\sigma_e} - 1\right)} =$$

9. Calculate

$$\frac{T_{em} + T_{fm}}{2} = \ ^oR$$

10. Calculate

$$T_{am} = \frac{T_{em} + T_{fm}}{2} - \frac{(T_{ed} - T_{fd})\,(\sigma_H - \sigma_e)}{(2\sigma_H\sigma_e)\left(\frac{1}{\sigma_H} + \frac{1}{\sigma_e} - 1\right)}$$

T_{am} = ^oR

11. Get γ_a, c_p, μ, Pr, and k at T_{am} as from Figure AI-1. (Recall that $\gamma_a = \delta\gamma$ for γ at one atmosphere pressure as given in the figure.)

γ_a = lb/ft^3
c_p = Btu/lb-^oR
μ = lb/ft-hr
Pr =
k = Btu/hr-ft-^oR

12. Calculate

$$q_f = \frac{(q_o + q_g - q_{se})}{(1 - \alpha)}$$

$q_f =$ Btu/hr-ft^2

13. Calculate

$$Q_a = \frac{q_f \left(\frac{1}{\sigma_H} + \frac{1}{\sigma_e} - 1\right)}{\gamma_a \, C_a \, (T_{ed} - T_{fd})}$$

$Q_a =$ ft^3/hr

14. Calculate $q_p = \alpha \, q_f$

$q_p =$ Btu/ft^2-hr

15. Calculate

$$hAnx = (Q_a \gamma_a \, c_p) \log_e \left(\frac{1}{1 - \sigma_H}\right)$$

$hAnx =$

16. Assume the value of n

$n =$

17. Calculate

$$V_a = \frac{Q_a}{h \, A_c}$$

$V_a =$ ft/hr

18. Calculate

$$Re = \frac{\gamma_a \, V_a \, 4r_h}{\mu}$$

$Re =$

19. Get f from the chart of f versus Re for the core being used.

$f =$

20. Get h_a from the chart of h_a versus Re for the core being used. This may require using Pr, and k as found earlier.

$h_a =$ Btu/hr-ft^2-^{o}R

21. Calculate h_a An =

22. Calculate

$$x = \frac{h_a\ Anx}{h_a\ An}$$

(See step 15.)

$x =$ ft

23. Calculate

$$\frac{fx}{4r_h} + K =$$

where K is an appropriate allowance for entrance and exit losses in the heat exchanger core.

24. Calculate

$$n^2 = \frac{4\ \gamma_a\ Q_a{}^3}{2g \times 778\ q_p\ (A_c)^2}\left(\frac{fx}{4r_h} + K\right)$$

$n^2 =$

$n =$

where the factor 4 allows for an over-all blower-motor efficiency of 25 percent.

It is now necessary to repeat from step 16 onward until the assumed and calculated values of n agree. The calculated result may be used as the assumed value in the next trial, unless computing experience makes it possible to assume a more accurate value.

APPENDIX TO SECTION VII

1. Calculations for Temperature Rise of Equipment in a Compartment with an Air-to-Fuel Heat Exchanger

A calculation procedure is given here for the stepwise evaluation of equipment temperature rise in a compartment cooled by a fuel to air heat exchanger. The procedure form includes a sample interval calculation. This sample calculation is based on an earlier calculation of the external heat load q_o, using the method described in the design portion of Section V. Results of this earlier calculation are used to construct the q_o versus T_e plot given in Figure VII-9.

Given Data

$x = 0.825$ ft
$n = 12$
$D = 0.0167$ ft
$Q_a = 690\ ft^3/hr$

$$V_a = \frac{Q_a}{\frac{\pi}{4}\ nD^2} = 263{,}800\ ft/hr$$

$\sigma_e = 0.5$

$\delta = 1$ atmosphere

$q_g = 150$ watts/ft^2 $= 511$ Btu/hr-ft^2

$m_e c_e = 2$ Btu/^{o}R-ft^2

$U_i = 1$ Btu/hr-ft^2-^{o}R

$\epsilon_i = 0.10$, $\epsilon_e = 0.20$

$T_w = 1355^o$R

$T_{e1} = 460^o$R

Fuel temperatures from Figure AIII-9 where $U_{if} = 5.0$ Btu/hr-ft^2-^{o}R

1. Select $\Delta\tau$

$$\Delta\tau = 0.0834 \text{ hr}$$

2. Assume T_{e2} and calculate

$$T_{em} = \frac{(T_{e1} + T_{e2})}{2}$$

$$T_{e2} = 500^oR$$
$$T_{em} = 480^oR$$

3. Get T_{fm} at middle of $\Delta\tau$ from Figure AIII-9

$$T_{fm} = 466^oR$$

4. Using σ_H from previous interval, calculate

$$T_{ai} = T_{em} - \frac{(T_{em} - T_{fm})}{\sigma_e\left(\frac{1}{\sigma_H} + \frac{1}{\sigma_e} - 1\right)}$$

$$T_{ai} = 480 - \frac{14}{0.5\left(\frac{1}{0.648} + \frac{1}{0.5} - 1\right)} = 469^oR$$

5. Using σ_H from previous interval, calculate

$$T_{ao} = (T_{em} - T_{ai})\left(\frac{\sigma_e}{\sigma_H}\right) + T_{fm}$$

$$T_{ao} = 11\left(\frac{0.5}{0.648}\right) + 466 = 474.5^oR$$

6. Calculate

$$T_{am} = \frac{(T_{ai} + T_{ao})}{2}$$

$$T_{am} = 471.8^oR$$

7. Get γ_a and c_p for air at T_{am} from Figure AI-1 where $\gamma_a = \delta \gamma$.

$$\gamma_a = 0.0848 \text{ lb/ft}^3$$
$$c_p = 0.2392 \text{ Btu/lb-}^{\circ}\text{R}$$

8. Calculate

$$q_f = \frac{Q_a \gamma_a c_p (T_{em} - T_{fm})}{\frac{1}{\sigma_H} + \frac{1}{\sigma_e} - 1}$$

$$q_f = \frac{14\ (480 - 466)}{\frac{1}{0.648} + \frac{1}{0.5} - 1} = 77.2 \text{ Btu/hr-ft}^2$$

9. Get H at T_{am} from Figure VII-8.

$$H = 13.10$$

10. Calculate $h_a = H \times 10^{-4}\ (\delta V_a)^{0.8}$

$$h_a = 13.1 \times 10^{-4} \times 21700 = 28.4 \text{ Btu/hr-ft}^2\text{-}^{\circ}\text{R}$$

11. Calculate

$$\frac{h_a\ \pi D n x}{Q_a \gamma_a c_p} = 1.052$$

12. Calculate

$$\sigma_H = 1 - (e)^{-\frac{h_a \pi D n x}{Q_a \gamma_a c_p}}$$

$$\sigma_H = 1 - 0.348 = 0.652$$

13. Using result of step 12, calculate

$$q_f = \frac{Q_a \gamma_a c_p (T_{em} - T_{fm})}{\frac{1}{\sigma_H} + \frac{1}{\sigma_e} - 1}$$

$$q_f = \frac{14 \times 14}{\frac{1}{0.652} + \frac{1}{0.5} - 1} = 77.3 \text{ Btu/hr-ft}^2$$

This result should agree within one percent with the value of step 8. If not, repeat from step 8 onward using the result of step 12.

14. Get μ from Figure AI-1 at T_{am}.

$$\mu = 0.0405 \text{ lb/ft-hr}$$

15. Calculate

$$Re = \frac{\gamma_a V_a D}{\mu}$$

$$Re = \frac{1 \times .0848 \times 263,800 \times .0167}{.0405} = 9150$$

16. Get f for Re from Figure VII-10.

$$f = 0.0312$$

17. Calculate

$$q_p = \frac{Q_a \gamma_a V_a^2}{1621 \times 10^8} \left(1.5 + \frac{fx}{D}\right)$$

$$q_p = 25 \times 3.04 = 76 \text{ Btu/hr-ft}^2$$

18. Using q_o from external heat load calculation for T_{em}, calculate

$$q_{se} = (q_o + q_p + q_g) - q_f$$

$$q_{se} = (454.5 + 76 + 511) - 77.3 = 964.2 \text{ Btu/hr-ft}^2$$

19. Calculate

$$\Delta T_e = \left(\frac{q_{se}}{m_e c_e}\right) \Delta \tau$$

$$\Delta T_e = \frac{964.2}{2} \times 0.0834 = 40.1^\circ R$$

20. Calculate $T_{e2} = T_{e1} + \Delta T_e$

$$T_{e2} = 460 + 40.1 = 500.1^\circ R$$

This should agree within 2 or 3°R of the assumed value in step 2. If not, the interval calculation must be repeated, using the calculated value as the assumed T_{e2} of the next trial.

It should be observed that the computer can usually notice the trend of values of σ_H after working several intervals. It is therefore possible to improve the accuracy of steps 4 and 5 by assuming a value of σ_H in accordance with this trend, rather than using the value from the previous interval.

In order to calculate the first time interval, it is necessary to establish the value of σ_H corresponding to the initial values of T_e and T_f. This is done by assuming a value of T_{am} and calculating σ_H with steps 7, 9, 10, 11, and 12. Then steps 4, 5, and 6 are used to calculate T_{am}, and the

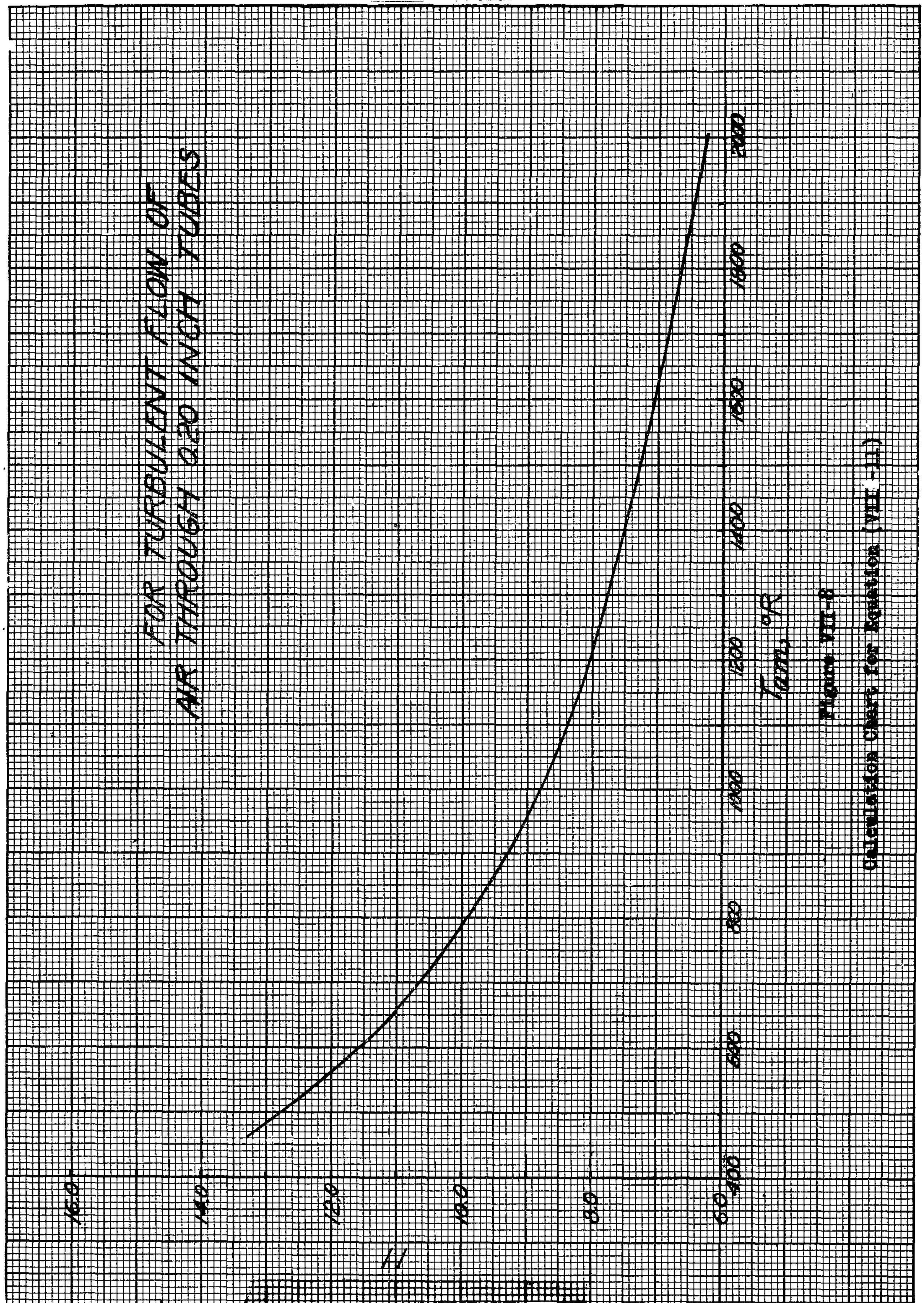

Figure VII-8

Calculation Chart for Equation (VII-11)

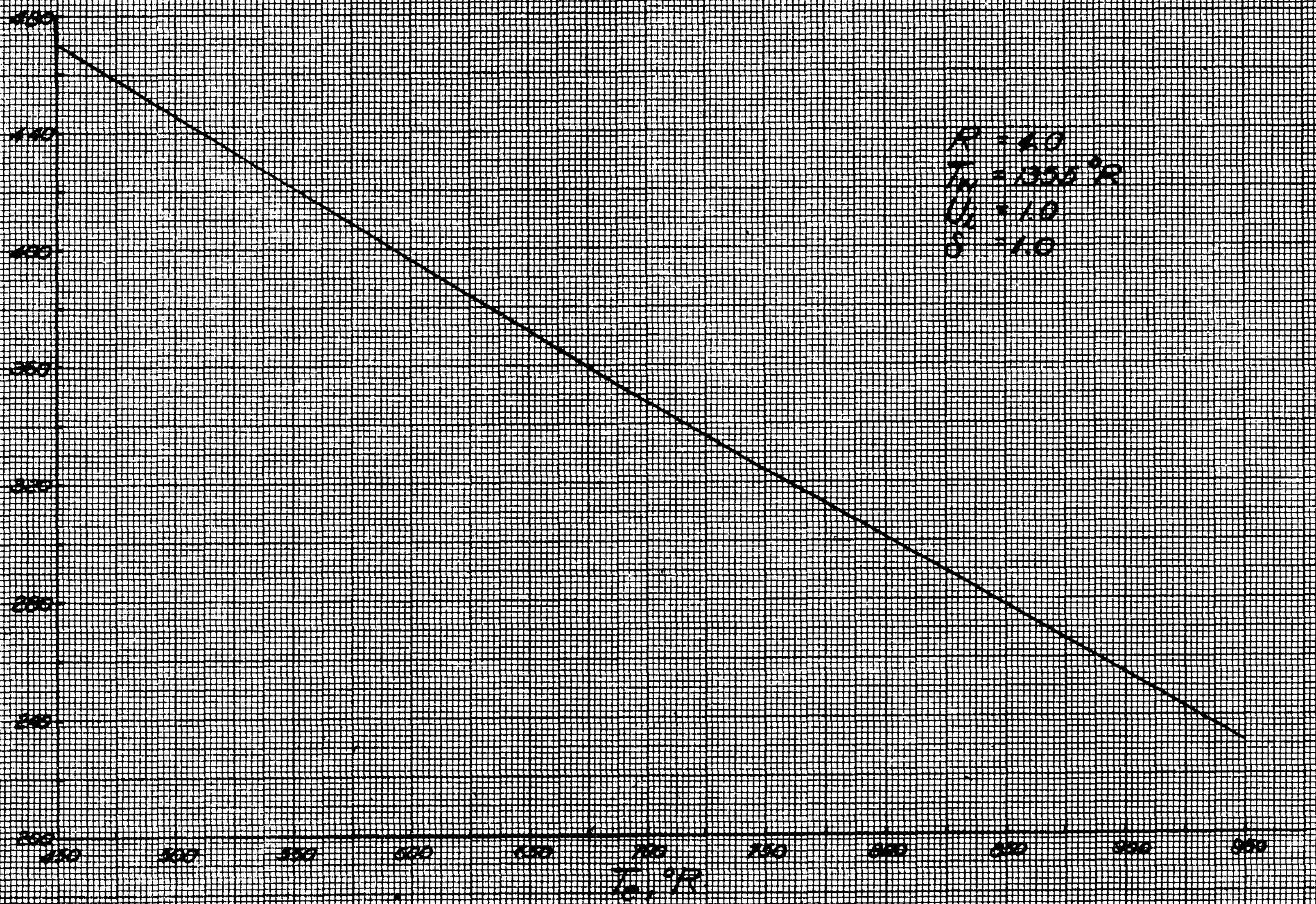

Figure VII-9

Typical Variation of Outside Heat Load with Equipment Temperature

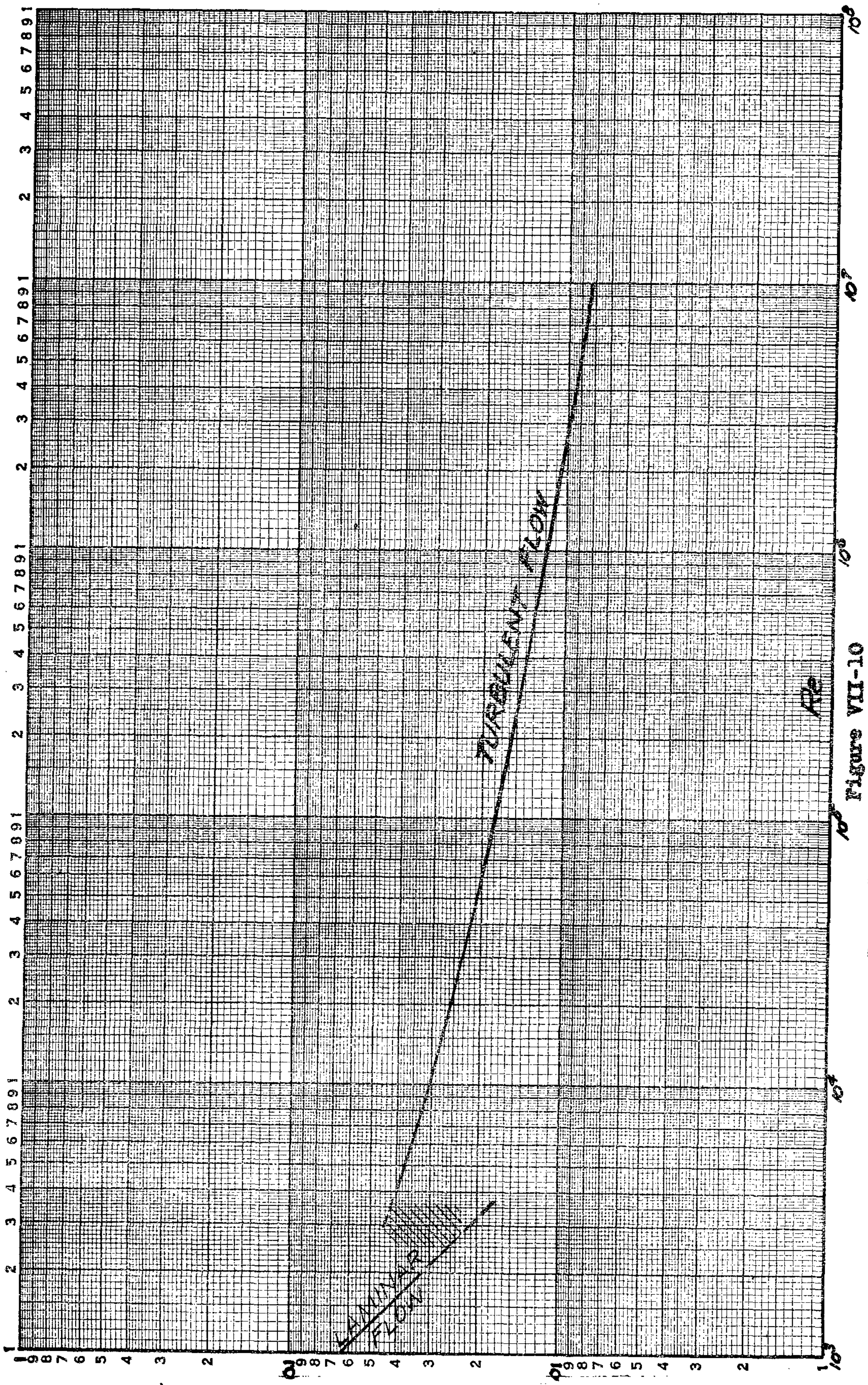

Figure VII-10
Darcy Friction Factor for Flow Through
Hydraulically Smooth Tubes

process is repeated until assumed and calculated values of T_{am} agree within 2 or $3^{o}R$, at which time σ_H is substantially correct. The initial values of T_e and T_f are used in this calculation without regard to subscripts as given in the numbered steps.

2. References

(VII-1) Brown, A. I. and Marco, S. M. Introduction to Heat Transfer. Second Edition. McGraw-Hill Book Company, Inc., New York, 1951.

(VII-2) Kays, W. M. et.al. Gas Turbine Plant Heat Exchangers. A.S.M.E. New York, April, 1951.

(VII-3) Vennard, John K. Elementary Fluid Mechanics. Second Edition. John Wiley and Sons, Inc., New York, April, 1949, p. 157.

(VII-4) Murray, Daniel A. Introductory Course in Differential Equations. Longmans, Green and Co., New York, Sept., 1945, pp. 26-27.

SECTION VIII

TEMPERATURE RISE OF EQUIPMENT MOUNTED ON FUEL-COOLED SURFACES

by T. C. Taylor and Y. H. Sun

One very straightforward method of cooling equipments consists of mounting them directly to fuel-cooled surfaces. In this way the heat generated or received by the equipment is provided with a direct path for solid conduction heat transfer to the fuel coolant. This is the most direct application of the coolant that can be achieved short of actually immersing the equipment in the coolant, and therefore makes it possible to hold the cooled equipments to a temperature only a little above the available coolant temperature. In addition to this primary advantage from the standpoint of cooling performance, this cooling method possesses physical advantages. The most obvious is that it uses a coolant which is already available on any aircraft using liquid fuel. In addition, it does not require the use of secondary coolants or their attendant ductwork and circulating pumps or blowers. The equipment is therefore unencumbered by enclosures for a secondary coolant. This is particularly important for mechanical equipments which act on other fairly distant equipments through moving linkages.

Possible disadvantages of this cooling method are the pressure drop required to circulate the fuel through the passages which cool the mounting surface, and the temperature rise resulting from heat addition to the fuel. The first of these may not be objectionable since cooling plates of high capacity can often be designed to operate with quite small pressure drop. The second disadvantage does not apply if fuel is available in sufficient quantity at temperatures a little below the maximum allowed for proper functioning of the power plant. Another possible disadvantage is the requirement of this cooling method that the cooled components be designed to give good heat conduction from all of their parts to the surfaces in contact with the cooling plate, or mounting surface. For mechanical equipments this need present no problem and may not require re-design. For components which are assemblies of smaller heat-generating bodies, such as electronic components, special design is probably required if adequate cooling is to be achieved by this method. Therefore, this cooling method may not be suited to existing equipments.

In this Section the two possible types of fuel flow, laminar and turbulent, are considered in their application to the problem of cooling equipment mounting surfaces. With a modification in the method of determining the external heat load to the mounted equipment, fuel-cooled surfaces can be considered either as a method for cooling individual critical equipment components or as a method for cooling all of the equipment in a compartment.

SUMMARY

The use of fuel-cooled mounting surfaces for equipment is considered. It is assumed that the equipment items are attached to the fuel-cooled surface in a manner which gives high thermal conductance between the equipment and the surface, so that they may be considered to be substantially at the same temperature. The external heat load to the cooled equipment is assumed to consist entirely of free convection and radiation from the environment within the compartment. In addition to the external load the equipment itself may generate heat. The fuel-cooled surface is assumed to have internal passages for flow of the fuel. Two fundamentally different passage types and flow conditions are considered. In the first, a single, serpentine passage winds back and forth through the plate, and the fuel flow rate is great enough to give turbulent flow conditions. In the second, a number of straight, parallel passages are provided, with the flow rate per passage small enough to give laminar flow conditions.

Methods are given for calculating the external heat load to equipment mounted on a fuel-cooled surface in two types of application. In the first, all of the equipment of the compartment is cooled by this means, and the external heat load to the equipment can be expressed as a function of the temperature of the cooled equipment. In the second, only a small portion of the equipment is cooled by means of the fuel-cooled surface, with the remaining equipments uncooled. The environmental temperatures of the compartment are therefore determined by the uncooled equipment, and the external heat load to the cooled equipment is a function of both these temperatures and that of the cooled equipment itself.

Equations are developed which describe the heat transfer between the fuel-cooled plate and the fuel in the internal passages of the plate. The equations are somewhat different in detail for the two types of fuel passages, because of the fundamentally different flow situations. Only fuel passages of circular cross-section are considered. Equations are also developed for calculating the fuel pressure drop requirements of the two types of cooling plate. The heat transfer and pressure drop equations are arranged in the form of calculation procedures which can be used to determine the significant design features required in the fuel passages to meet an assigned set of operating specifications. The design of the cooling plate itself depends on knowing the cooling capacity required, the temperature rise which can be tolerated in the available coolant, the desired logarithmic mean temperature difference between the coolant and the equipment it cools, the allowable fuel pressure drop, and the general size and shape of plate required. By a suitable determination of the cooling capacity for the design, it may apply to transient operation.

A design example is given, in which all of the equipment in a compartment is cooled with a cooling plate, and in which the available coolant temperature varies with time. It is shown that a design method in which the heat storage rate (due to thermal capacity of the equipment and the cooling plate) is subtracted from the total heat load for determining the required cooling capacity leads to a prediction of transient performance. A procedure for calculating this transient performance is given.

Two sets of charts are provided which permit designing either of the two cooling plate types without recourse to the detailed calculation procedure. These charts give a graphical solution based on the use of JP-3 fuel as the coolant. In the case of the serpentine-passage plate, the charts give an approximate design which is conservative in that it provides a somewhat smaller value of temperature difference between the equipment and the coolant than that designed for. The conservative feature results from some analytical simplifications which are required to put the equations for this case in graphical form. In the case of the parallel-passage plate, the charts are an exact graphical representation of the heat transfer equations.

A number of calculations are made with the heat transfer equations to demonstrate the characteristics of cooling plate designs. Significant findings are summarized as follows.

1. A serpentine-passage cooling plate of fixed physical dimensions and operating on a fixed temperature rise of the fuel can provide various cooling capacities for corresponding fuel flow rates. As the cooling capacity is increased, however, the logarithmic mean temperature difference between the plate and the fuel increases, so that the cooled equipment operates at a higher temperature with respect to the coolant.

2. For a serpentine-passage plate of fixed cooling capacity and fuel flow rate, the pressure drop of the fuel and the plate thickness are conflicting factors, since a reduction of pressure drop cannot be achieved without increasing the fuel-passage diameter. Furthermore, any reduction of pressure drop requires an increase in the temperature difference between the equipment and the coolant.

3. A serpentine-passage cooling plate of fixed physical dimensions and fixed cooling capacity can operate with various fuel flow rates and corresponding fuel temperature rises. As the flow rate is decreased, however, the pressure drop of the fuel is reduced and the temperature difference between the plate and the coolant is increased. This temperature difference can be maintained constant for an increased fuel temperature rise (reduced flow rate) only by reducing the passage diameter, which gives an increase of fuel pressure drop.

4. A serpentine-passage cooling plate can be designed for fixed cooling capacity, fuel flow rate, fuel temperature rise, and temperature difference between the plate and the coolant, with wide latitude in the fuel pressure drop requirements. However, lower pressure drop requires an increased number of passage bends and a larger passage diameter. The latter, in turn, requires a thicker plate.

5. The heat transfer processes in a parallel-passage cooling plate are not affected by the fuel-passage diameter so long as the fuel flow is laminar. Thus passages of very small diameter may be used

so long as the resulting fuel pressure drop is not objectionable.

6. A parallel-passage cooling plate of fixed fuel temperature rise and fixed number of fuel passages can provide a range of cooling capacities for corresponding fuel flow rates. As the cooling capacity is increased, however, the pressure drop and the temperature difference between the plate and the coolant increase. The pressure drop and the temperature difference can be held constant if the number of cooling passages is changed in direct proportion to a change in cooling capacity.

7. For a given set of design conditions, the parallel-passage cooling plate requires a rather large number of fuel passages for small temperature differences between the plate and the coolant. Therefore where the plate must be maintained at temperatures close to the coolant, it is advisable to use a serpentine-passage cooling plate. For example, a particular parallel-passage design for a temperature difference of 20°F between plate and coolant with a cooling capacity of 2555 Btu/hr requires over 50 passages. For the same capacity and a temperature difference of 10°F, the passage number required is 150. The numbers involved are proportionately greater at higher cooling capacities. Large numbers of passages such as these would be likely to give manufacturing difficulties.

8. A parallel-passage plate with a fixed number of fuel passages and a fixed cooling capacity can be used with a range of fuel flow rates and corresponding values of temperature rise of the fuel. As the flow rate is reduced, the pressure drop is reduced and the temperature difference between the plate and the coolant is increased. The temperature difference can be held constant with decreasing fuel flow rate only by increasing the number of fuel passages.

9. Both types of cooling plate are effective cooling methods in that they supply a cooling effect with an unusually small temperature potential required between the cooled equipment and the coolant. For very small temperature potentials, the serpentine-passage plate is preferred, since the parallel-passage type requires a very large number of passages. The parallel-passage plate, on the other hand, possesses an advantage of smaller size when designs of lower cooling capacity are considered. For example, in one design example for a plate of 2555 Btu/hr cooling capacity, a parallel-passage plate having a total thickness of about 0.1875 in. is satisfactory, while a serpentine-passage plate for the same job would be about 0.925 in. thick and weigh correspondingly more. In both cases the fuel pressure drop is very small, being of the order of 0.2 lb/in^2 for the parallel-passage plate and even less for the other. In general the parallel-passage plate required more passages and greater thickness for higher cooling capacities, while the thickness requirements of serpentine-passage plates are reduced at higher cooling capacities.

ANALYSIS

1. Assumptions for Analysis

A typical example of the use of a fuel-cooled surface to cool equipment located in an aircraft compartment is shown schematically in Figure VIII-1. The compartment shown is cylindrical in shape, although the analysis is suited to any shape of the compartment. In the example of the figure, all of the equipment items are shown mounted on the cooled surface, although this need not be the case, since in many applications only a few critical items may need cooling. The fuel-cooled plate shown is assumed to

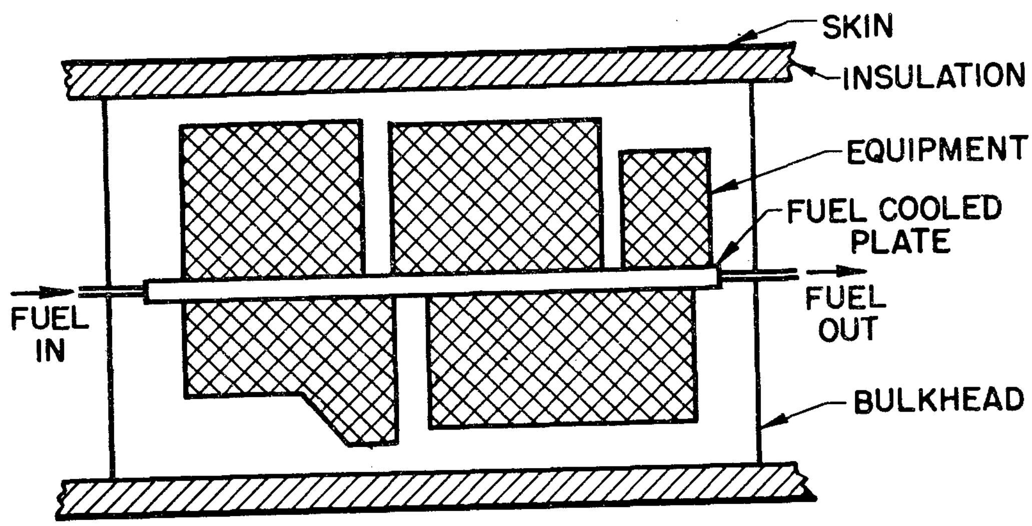

Figure VIII-1. Schematic of Compartment with Equipment Mounted on a Fuel-Cooled Surface

have internal passages for the fuel, and the passages may either convey the entire throughput of the fuel line or simply be arranged in a parallel branch to the fuel line. The selection of flow arrangement depends on the cooling capacity required by the equipment.

It is assumed that the equipments shown are mounted to the plate in a manner which gives very good thermal contact. If shock-mounting of the equipment is required, the entire cooling plate should be shock mounted, so that the equipments may be directly mounted to the plate. This would require flexible fuel connections for inlet and outlet. It is also assumed that the equipment components are designed so as to give good heat conduction from all of their parts to their surfaces in contact with the cooling plate. Components such as electronic assemblies should therefore be modified in design to give this effect. If not, this cooling method loses some of its effectiveness due to a temperature potential required to transfer heat through the parts of the component to the plate. Although some temperature difference between parts of the component and the plate

is always required for cooling to occur, the difference can be made negligibly small by means of proper construction. It is therefore assumed that the equipment is at substantially the same temperature as the plate. This temperature is used both in describing heat transfer from the plate to the fuel in it, and in describing the external heat load to the equipment.

The external heat load is assumed to consist entirely of free convection and radiation. The equipment receives heat from the compartment air by free convection, and from the skin insulation by radiation. The sum of these two is the external heat load. In addition, the equipment may generate heat.

The assumptions given are sufficient to describe the heat transfer processes in the compartment from the surface of the cooling plate outward. In addition to these, certain assumptions are required to analyze the heat transfer process between the plate and the fuel in its internal passages. The nature of the analysis for this process differs for the two types of flow passages considered. Certain other assumptions and system descriptions are therefore given with the derivation of equations for each case. The first case considered is that in which the cooling plate is equipped with a single internal fuel passage which winds back and forth in serpentine fashion, and in which the fuel flow is turbulent. The second case is that in which a number of straight-through, parallel passages are used, with laminar flow of the fuel in them. The two types of plate can be used to do the same job in many instances, although they have dimensional and pressure-drop characteristics which differ.

2. Nomenclature

Symbol	Definition	Units
A	Area	ft^2
a'	Convection group, defined for equation (VIII-2)	
c	Specific heat	Btu/lb-^oR
c_p	Specific heat at constant pressure	Btu/lb-^oR
D	Diameter	ft
f	Friction factor	dimensionless
g	Gravitational constant = 4.17×10^8	ft/hr^2
h	Heat transfer coefficient for flow through straight tube	Btu/hr-ft^2-^oR
h'	Average heat transfer coefficient	Btu/hr-ft^2-^oR

Symbol	Definition	Units
K	Pressure loss coefficient for bends, defined by equation (VIII-7)	dimensionless
k	Thermal conductivity	Btu/hr-ft-^{o}R
L	Characteristic length for free convection	ft
M	Weight	lb
M'	A group used in Figures VIII-10a and -10b	
m	Weight on unit skin area basis	lb/ft^2
N	A group used in the transient calculation procedure, Part 2 of the Appendix to this Section	
n	Number of straight runs in serpentine-passage plate or number of passages in parallel-passage plate	dimensionless
P	Pressure	lb/ft^2
Pr	Prandtl modulus	dimensionless
p	Pressure	lb/in^2
Q	Flow rate	ft^3/hr
q	Heat flux	Btu/hr-ft^2
q'	Heat transfer rate	Btu/hr
R	Ratio of free convection to radiation surface area	dimensionless
R_b	Bend radius	ft
Re	Reynolds modulus	dimensionless
r	Cooling plate dimension	ft
s	Cooling plate dimension	ft
T	Absolute temperature	^{o}R
U	Insulation conductance	Btu/hr-ft^2-^{o}R
V	Velocity	ft/hr
W	Weight flow rate	lb/hr

Symbol	Definition	Units
w	Cooling plate dimension	ft
x	Length	ft
γ	Weight density	lb/ft^3
δ	Pressure	atmospheres (dimensionless)
ϵ	Emissivity	dimensionless
θ	Temperature difference	^oF
μ	Viscosity	lb/ft-hr
τ	Time	hr
τ'	Time	min
ϕ	A factor for heat transfer coefficients in curved tubes	dimensionless

SUBSCRIPTS

a	Denotes air in compartment
b	Denotes bend in fuel passage
c	Denotes convection value
e	Denotes equipment
f	Denotes fuel or coolant
fe	Denotes entrance temperature of fuel
fo	Denotes outlet temperature of fuel
fm	Denotes average of inlet and outlet temperatures
g	Denotes generated value
i	Denotes insulation
it	Denotes insulation on fuel tank
lm	Denotes logarithmic mean value of θ
m	Denotes average value

Subscripts (continued)

Symbol	
o	Denotes external value
r	Denotes radiation value
s	Denotes value at surface of fuel passage
w	Denotes skin
1,2	Denote initial and final values for a time interval, respectively.

3. Derivation of Equations

a. External Heat Load

The external heat load to equipment mounted on a fuel-cooled surface must be analyzed in a manner which is appropriate to the application. If all of the equipment in a compartment is thus mounted, the temperature of the cooled equipment plays an important part in determining the environmental temperatures of the compartment. If only a few equipment components are cooled in this manner, the environmental temperatures are dominated by the average temperature of the uncooled components. Methods for calculating the heat load to the cooled equipment in each case are described here.

When all of the equipment in a compartment is fixed to the fuel cooled surface, the temperature of all equipments is essentially the same. This temperature is therefore used in the radiation and free convection heat transfer equations exactly as they appear in Section V. Corresponding to each value of equipment temperature there are values of the insulation face temperature and of the compartment air temperature which must be determined by a trial and error calculation. As in the analysis of Section VII, it is most convenient in a calculation of equipment temperature rise to prepare in advance a plot of values of q_o vs. T_e as based on the methods of Section V. When performing this calculation, the surface areas of the cooled plate which are not covered by equipment must be included in the value of R, since they are heat-receiving surfaces just as those of the equipment are. Similarly, the average thermal capacity of the equipment $m_e c_e$ is interpreted to include the thermal capacity of the cooled plate along with that of the equipment.

When only a few critical equipment components are mounted on a fuel-cooled surface, the calculation of the external heat load to these cooled items is somewhat different. It is assumed that the uncooled equipments in the compartment dominate the heat transfer processes between the skin and the equipment. It is therefore possible to analyze the heat transfer from the skin to the uncooled equipments using the methods of Section V.

By this means the skin insulation temperature and the compartment air temperature can be determined. These are plotted versus time and used to describe the environmental temperatures for the cooled components.

With these environmental temperatures known, the radiation heat load to the cooled components is given by

$$q_r' = h_r A_r (T_i - T_e) \tag{VIII-1}$$

where

$$h_r = 17.4 \times 10^{-4} \left(\frac{1}{\frac{1}{\epsilon_i} + \frac{1}{\epsilon_e} - 1} \right) \left[\frac{\left(\frac{T_i}{100}\right)^4 - \left(\frac{T_e}{100}\right)^4}{\left(\frac{T_i}{100}\right) - \left(\frac{T_e}{100}\right)} \right]$$

It is assumed in using this equation that most of the radiation heat transfer to the cooled equipment comes from the skin insulation, and radiation between the cooled equipment and the uncooled equipments is neglected. The value of A_r for use in equation (VIII-1) should be limited to those areas of the cooled equipment and the cooling plate which "see" the skin insulation, and which are essentially parallel to the insulation. Areas which are approximately perpendicular to the insulation are not very effective in radiant heat transfer. Areas of the cooled equipment or plate which have obstructions between them and the insulation are also prevented from direct radiation and are rather ineffective. The above statements are given as general guides for the estimation of A_r.

The compartment air temperature is used in computing the free convection heat load to the cooled equipment with the equation

$$q_c' = h_c A_c (T_a - T_e) \tag{VIII-2}$$

where

$$h_c = \left(\frac{a' L^{1/4}}{\delta^{1/2}} \right) \left(\frac{\delta^{1/2}}{L^{1/4}} \right) (T_a - T_e)^{1/4}$$

and where the quantity $(a' L^{1/4} / \delta^{1/2})$ is evaluated from Figure AIV-3 at the film temperature $(T_a + T_e)/2$. The value for A_c in equation (VIII-2) is the area of the cooled equipment and the cooled plate which is effective in free convection heat transfer. In general, this consists of the entire surface of the equipment and plate facing on the compartment air, except for those areas which are obstructed from free air circulation. Any area which faces on a gap formed by that area and the surface of another equipment where the gap is less than 3/8 in. wide may be considered obstructed in this sense. If the area faces such a narrow gap formed together with the skin insulation, the heat transfer to this surface through the air should be somewhere between the value for free convection and that for gaseous conduction. The value for L, the characteristic length for free convection, must be estimated for the shape and size of the cooled equipment and cooling plate com-

bination. This subject is discussed in some detail in Section V.

b. <u>Heat Transfer to the Fuel in a Plate with a Serpentine Turbulent-Flow Passage</u>

The general arrangement of passages in a fuel cooled plate of the serpentine-passage type is shown schematically in Figure VIII-2. The passage is assumed to be circular in cross-section.

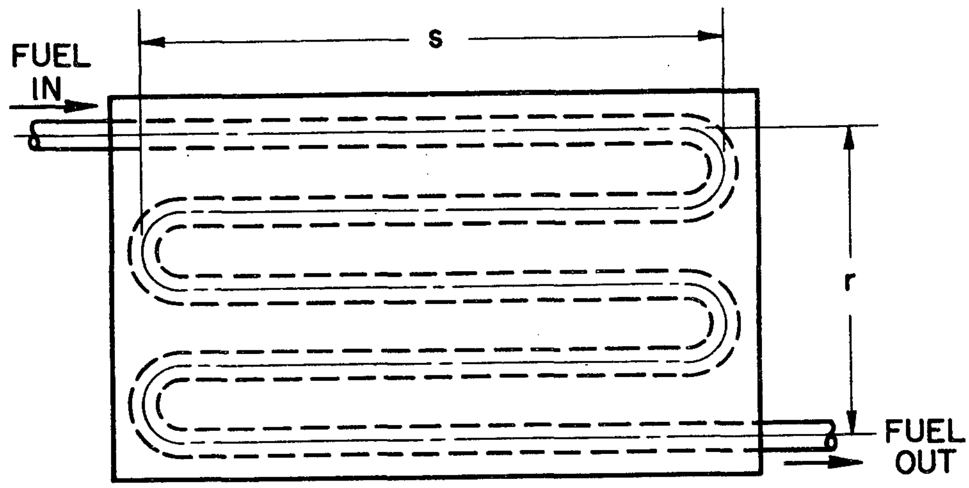

Figure VIII-2. Schematic of a Fuel-Cooled Plate with a Serpentine Fuel Passage

It is assumed that the plate itself is of metal and is thick enough that temperature gradients are negligible, giving a constant-temperature plate (recall that it was also assumed earlier that a construction is used which makes the plate temperature and cooled equipment temperature equal). T_e is therefore taken as the temperature of the plate, and the equation for heat transfer between the plate and the fuel is

$$q_f' = h_f' A_f \theta_{lm} \tag{VIII-3}$$

where A_f is the entire surface area inside of the serpentine fuel passage, and h_f' is a forced convection coefficient appropriate to the flow and temperature conditions of the fuel. For the assumed conditions, the temperature difference is given by

$$\theta_{lm} = \frac{(T_{fo} - T_{fe})}{\log_e \left(\frac{T_e - T_{fe}}{T_e - T_{fo}}\right)} \tag{VIII-4}$$

A suitable value of h_f for straight passages is given by Reference (VIII-1) as

$$h_f = 0.023\left(\frac{k}{D}\right)\left(\frac{\gamma VD}{\mu}\right)^{0.8}\left(\frac{c_p\mu}{k}\right)^{0.4} \qquad \text{(VIII-5)}$$

Little is known about the effects of passage curvature on heat transfer coefficients, so that it is necessary to use an approximation to allow for the effect of the return bends. Jakob (Ref. VIII-2) indicates that the value of h_f for a straight tube should be multiplied by the factor

$$\phi = 1 + 3.54\left(\frac{D}{2R_b}\right)$$

to obtain the heat transfer coefficient during turbulent flow in a curved tube. Using equation (VIII-5), it is apparent that the product $h_f'A_f$ of (VIII-3) is given by

$$0.023\left(\frac{k}{D}\right)\left(\frac{\gamma VD}{\mu}\right)^{0.8}\left(\frac{c_p\mu}{k}\right)^{0.4}\left[n\pi Dx + \left(1+1.77\,\frac{D}{R_b}\right)(n-1)\pi^2 DR_b\right]$$

if it is assumed that the factor for curved tubes applies only to the curved portions. Since the effect of a curved section followed by a straight run is not the same as that of a continuous curved section, this is only an approximation.

Using the dimensional notation of Figure VIII-2 it is apparent that

$$R_b = r/2(n-1)$$

and

$$x = s - 2R_b$$

Substituting this expression for R_b, and combining and rearranging from equation (VIII-3) onward gives

$$\theta_{lm} = \frac{q_f'}{h_f\left[n\pi Dx + \left(\frac{r}{2}\right)\pi^2 D + 1.77(n-1)\pi^2 D^2\right]} \qquad \text{(VIII-6)}$$

By equation (VIII-6) it is possible to calculate the temperature difference θ_{lm} for a cooling plate of given passage dimensions and fuel flow rate, when producing a cooling effect q_f'. Because of the relationship for h_f, equation (VIII-6) is accurate for smooth tubes of small diameter only for values of the Reynolds modulus ($\gamma VD/\mu$) of about 10,000 and higher. It can be applied with decreasing accuracy down to Re = 2300.

c. Pressure Drop of the Fuel in a Serpentine Passage

By application of the Darcy equation for pipe friction pressure losses, and using the method of accounting for bend pressure loss given by Reference (VIII-3), the pressure loss for fuel flow through the serpentine passage is

$$\Delta P = \gamma\left(\frac{V^2}{2g}\right)\left[n\left(\frac{fx}{D}\right) + (n-1)\left(\frac{f\pi R_b}{D}\right) + (n-1)K_b\right] \qquad \text{(VIII-7)}$$

where the Darcy friction factor f is a function of the Reynolds number Re = ($\gamma VD/\mu$). The value of K_b for bends in passages depends on the characteristic dimensionless ratio for the bend (R_b/D). Values of K_b are shown in Figure VIII-12.

d. Heat Transfer to the Fuel in a Plate with Straight, Parallel, Laminar Flow Passages

The general arrangement of passages in a fuel-cooled plate of the parallel passage type is shown schematically in Figure VIII-3. The passages are assumed to be circular in cross-section.

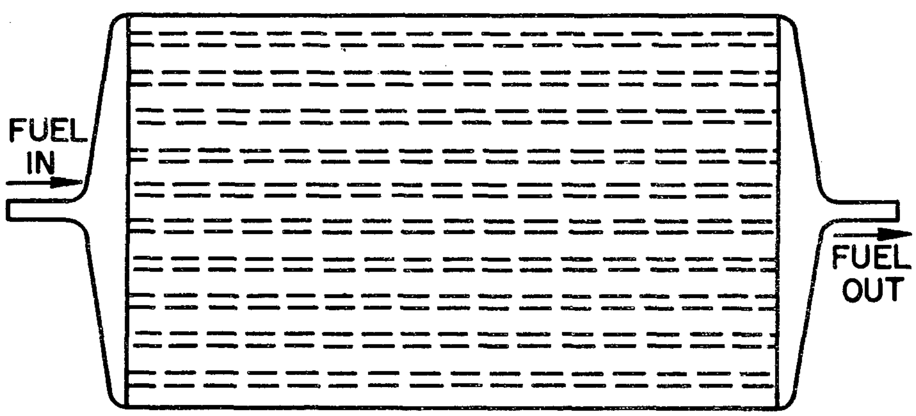

Figure VIII-3. Schematic of a Fuel-Cooled Plate with Straight, Parallel Fuel Passages

It is again assumed that the plate is at a constant temperature. The equation for heat transfer between the plate and the fuel is again given by equation (VIII-3), except that $h_f' = h_f$ for the straight passages. An expression suitable for h_f under laminar flow conditions is given by Reference (VIII-1) as

$$h_f = 1.86\left(\frac{k}{D}\right)\left(\frac{\gamma VD}{\mu}\right)^{1/3}\left(\frac{c_p\mu}{k}\right)^{1/3}\left(\frac{D}{x}\right)^{1/3}\left(\frac{\mu}{\mu_s}\right)^{0.14} \qquad \text{(VIII-8)}$$

where the Reynolds modulus ($\gamma VD/\mu$) must be less than 2300 for proper application. However, the expression can be used with decreasing accuracy up to Re $\approx$ 10,000. The flow velocity for this case is given by

$$V = \frac{4\,W_f}{n\pi\gamma D^2}$$

By using this substitution, combining and rearranging equations (VIII-3 and -8),

$$\theta_{lm} = \frac{q_f^{\dagger}}{1.86\,k^{2/3}\,(4W_f c_p)^{1/3}\left(\frac{\mu}{\mu_s}\right)^{0.14}(n\pi x)^{2/3}} \qquad \text{(VIII-9)}$$

With equation (VIII-9) it is possible to calculate the temperature difference θ_{lm} for a cooling plate of given passage dimensions and fuel flow rate, when producing a cooling effect given by $q_f^{\dagger}$. It is particularly interesting to note that the equation does not involve the passage diameter, the only physical characteristics of the passages of importance being the number of passages and their length. This makes it possible to assign any convenient diameter to the passages, permitting wide latitude in the plate thickness and fuel pressure drop.

e. Pressure Drop of the Fuel in a Straight Passage

The fuel pressure drop may be calculated with the Darcy equation as before. In this case an allowance of 1.5 velocity heads is made to account for the loss in pressure due to entering and leaving the tubes, and flow in the inlet and outlet manifolds.

$$\Delta P = \gamma\left(\frac{V^2}{2g}\right)\left[\frac{fx}{D} + 1.5\right]$$

Using the expression for velocity developed earlier, and making use of the fact that for laminar flow $f = (64\,\mu/\gamma VD)$ the above equation becomes

$$\Delta P = \left(\frac{W_f}{n\pi\gamma D^4 g}\right)\left[128\mu x + \frac{12W_f}{n\pi}\right] \qquad \text{(VIII-10)}$$

f. Heat Balance for Equipment on a Fuel-Cooled Plate

The heat balance equation for equipment mounted on a fuel-cooled surface is similar to that used in Section VII to describe equipment

cooled by a forced air system. In the case of the cooling plate, however, there is no power term, since there is no secondary coolant. Another difference is that it is now more convenient to write a heat balance equation which applies for all of the cooled equipment, rather than basing the equation on a unit of skin area. The equation is therefore

$$q_o' + q_g' - q_f' = M_e c_e \left(\frac{\Delta T_e}{\Delta \tau}\right) \qquad \text{(VIII-11)}$$

and simply indicates that all of the heat received or generated by the equipment is either transferred to the cooling fluid or stored in the thermal capacity of the equipment, causing temperature rise. As indicated earlier, q_o' is assumed to include the external heat loads to any part of the cooling plate which is not covered by the cooled equipment, and the term M_e includes all of the thermal capacity of both the cooled equipment and the plate. If q_o is calculated instead of q_o', as recommended earlier for cases where all of the equipments in the compartment are cooled, it is necessary to express the result in terms of q_o', as

$$q_o' = q_o A_w$$

The expression used for q_f' must, of course, correspond to the type of passages used in the cooling plate.

4. Calculation Procedures for the Steady State Operation of Fuel-Cooled Mounting Plates

The calculation procedures described here are used in evaluating the steady-state characteristics of fuel-cooled mounting plates of both the types described earlier. The calculation procedure required to evaluate the temperature rise of equipments mounted on fuel-cooled plates in a typical transient case is given in the Appendix to this Section. The emphasis is placed on steady-state characteristics in the calculation procedures given here for two reasons. First, the unique nature of the fuel-cooled surface makes it necessary to develop an understanding of the effects of the principal design variables on its steady-state performance and pressure drop characteristics. Second, the transient temperature rise characteristics of equipment cooled by this method are easily predicted, and are very similar to those noted for equipments cooled by the method described in Section VII.

a. Steady-State Calculation for the Plate with a Serpentine Passage and Turbulent Flow

The procedure described here is used to calculate the principal performance characteristic of a fuel-cooled surface for a given set of plate dimensions and operating conditions. For this purpose, the principal performance characteristic is defined to be Θ_{lm}, or the temperature potential required for a given apparatus to accomplish the cooling job at hand. A small value of Θ_{lm} represents a very effective cooling plate, since it

accomplishes the given heat removal job and at the same time maintains the equipment at very near the average available coolant temperature. In other words, the cooling apparatus itself imposes little temperature barrier for the transfer of heat. A large value of Θ_{lm} required by another plate which removes the same amount of heat represents an apparatus which does the job at hand less efficiently.

In specifying any cooling problem where fuel-cooled plates are to be used, it is assumed that the two principal dimensions of the plate are known. The rectangular plate must be of such size and shape as to properly accommodate the equipments to be fastened to it. It is also assumed that the available coolant temperature is known, and that either the amount of coolant (fuel) that is to be used for this purpose or its maximum allowable temperature rise is known. Since the cooling effect required consists of the sum of the external heat loads and the generated heat load (for steady-state only), the cooling effect, fuel rate, and fuel temperature rise are related by the equation

$$q_f' = q_o' + q_g' = W_f \, c_p \, (T_{fo} - T_{fe})$$

where the left-hand member is known, and two of the factors of the right-hand member must be known.

With all of the above characteristics established, it is possible to proceed with the calculation of Θ_{lm} after establishing the remaining physical characteristics n and D. The passage diameter D may have a maximum limit due to limitations on the over-all thickness of the plate, or otherwise may be assumed for a first trial. The value of n should be established so as to give a good distribution of the cooling effect over all the surface of the plate. For a given cooling capacity, large values of n lead to large passage diameters, as will be shown later.

The physical properties of the fuel are next evaluated at $(T_{fe}+T_{fo})/2$, and a direct application of equation (VIII-6) made to determine Θ_{lm}. Equation (VIII-7) is then applied to calculate the pressure drop. If the value of Θ_{lm} obtained is too large, the calculation may be repeated using a smaller value of D or a larger value of n, or both, until a satisfactory design is achieved. Either change leads to a higher pressure drop requirement. A detailed procedure and an example calculation for this type cooling plate are given in the Appendix to this Section.

b. Steady-State Calculation for the Plate with Straight Parallel Passages and Laminar Flow

The general remarks given for calculating Θ_{lm} for the serpentine-passage plate apply here as well, except that the passage diameter is not a significant variable. For a given set of fuel temperature and flow conditions, and an arbitrarily assigned value of n, Θ_{lm} is calculated directly from equation (VIII-9) by taking $(\mu/\mu_s)^{0.14} \approx 1$ and evaluating the fuel properties at $(T_{fe}+T_{fo})/2$. If Θ_{lm} is large, μ_s should be evaluated at $(T_{fe}+T_{fo})/2 + \Theta_{lm}$, and a recalculation made including the proper

value of $(\mu/\mu_s)^{0.14}$ in the equation. The calculation may be done in a different order by assigning a value of θ_{lm} for equation (VIII-9) and calculating the value of n required. This latter method is more appropriate to design, where a performance in terms of θ_{lm} is desired and the physical characteristics necessary to achieve it are sought.

Although the diameter is not involved in the thermal performance of this type cooling plate, it must be assigned to determine the pressure drop for the fuel. If very small diameters are used the plate thickness is small and space is saved, but large pressure drops may be encountered. With an assigned diameter, the pressure drop is determined with equation (VIII-10).

A detailed procedure and example calculation are given in the Appendix to this Section for determining the number of passages required and the fuel pressure drop in a parallel-passage plate.

EFFECTS OF FUEL TEMPERATURE RISE, COOLING CAPACITY, AND PASSAGE DESIGN ON THE SIZE AND PERFORMANCE OF FUEL-COOLED MOUNTING PLATES

1. The Serpentine Passage Plate with Turbulent Flow of the Fuel

a. Effect of Cooling Capacity

The effect of cooling capacity on the design and performance of a fuel-cooled mounting plate of the serpentine-passage type is shown in Figure VIII-4. The plate is assumed to have six straight runs to the fuel passage, and a fuel temperature rise in operation of 20°F. The coolant used is JP-3 fuel at an average temperature of 600°R, or $T_{fe} = 590$°R, $T_{fo} = 610$°R. The nominal surface area of the plate on one side is 1.5 ft^2, this being the rectangular area enclosed by the centerlines of the passages, or (rxs) as shown in Figure VIII-2.

It is apparent from Figure VIII-4 that an increase of cooling capacity for a plate with a given diameter passage requires an increase in temperature difference between the plate and the coolant. For the constant fuel temperature rise, an increase of cooling capacity requires a proportionate increase in the fuel flow rate. The heat transfer coefficient in the passage only increases as $(V)^{0.8}$, however, so that the cooling capacity does not keep pace with the fuel rate unless the temperature difference for heat transfer θ_{lm} is also increased. The increased fuel flow rate also requires greater pressure drop, as seen in the figure. If a plate having increased cooling capacity but no increase of pressure drop is required, it is necessary to increase the passage diameter. This would involve an increase in thickness and space requirements for the plate. An increase of cooling capacity with a reduction of pressure drop requires a more rapid increase of passage diameter with the increased capacity.

For any given cooling capacity, it is possible to vary the passage diameter (and hence the plate thickness) over a wide range, giving changes in the temperature difference θ_{lm} and the pressure drop. As the passage

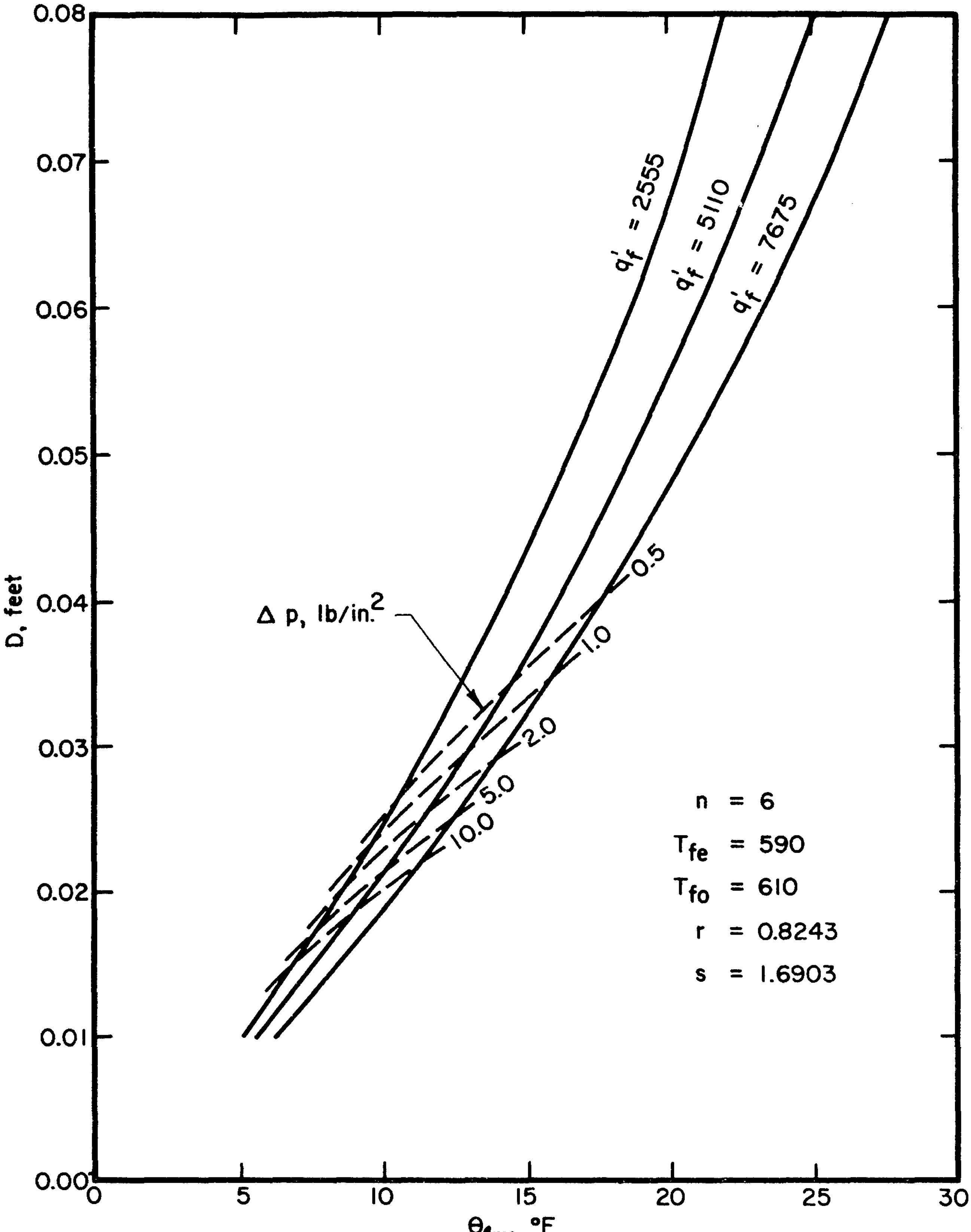

Figure VIII-4
Effect of Cooling Capacity on the Design and Performance of a Serpentine-Passage Cooling Plate

diameter is increased, θ_{lm} increases, and the pressure drop is reduced. Higher values of θ_{lm} represent a progressively less efficient cooling plate, since the equipment mounted thereon is farther above the available coolant temperature. If an increase of pressure drop can be tolerated, the passage diameter can be reduced to bring the plate temperature close to the coolant temperature and still retain the same cooling capacity. For a given capacity plate the pressure drop and space requirements are therefore in conflict, since a reduction of either requirement involves an increase in the other. Furthermore, the pressure drop and temperature potential are in conflict, since a reduction in either requires an increase of the other.

b. Effect of Fuel Temperature Rise

The effect of fuel temperature rise on the design and performance of a fuel-cooled mounting plate is shown in Figure VIII-5. As before, the plate is assumed to have a nominal area of 1.5 ft^2, and use JP-3 fuel as coolant, with an average temperature of 600^oR and entrance and exit temperatures corresponding to the fuel temperature rise assigned. Other characteristics are indicated in the figure.

For a plate with a fixed-diameter fuel passage, and fixed cooling capacity, an increase of fuel temperature rise corresponds to a decrease of fuel velocity and weight flow rate. As expected, the figure shows a corresponding increase required in the temperature difference θ_{lm}, and a reduction of pressure drop. If the value of θ_{lm} must be held constant, it is necessary to reduce the passage diameter and suffer increased pressure drop as ΔT_f is increased.

For a fixed allowable fuel temperature rise, it is noted as before that space and pressure drop requirements are in conflict, since a reduction of passage diameter or plate thickness requires an increase of pressure drop.

c. Effect of the Number of Bends in the Passage

The effect of the number of fuel passage bends on the passage diameter in a serpentine-passage cooling plate is shown in Figure VIII-6. The design characteristics are given in the figure.

Since n (the number of bends is (n-1)) is varied while the cooling capacity and other significant factors are held constant, it follows that the passage diameter increases with increased n. When more bends are used, the length of the passage is greater, and the heat transfer coefficient must be reduced. This is accomplished by increasing the passage diameter, which lowers the heat transfer coefficient rapidly enough to offset the increase of passage surface area. Figure VIII-6 also shows that the pressure drop for the fuel is decreased for greater n. Therefore, by using a larger number of bends and a larger passage diameter the pressure drop requirements of a plate may be reduced, while keeping all other performance characteristics the same.

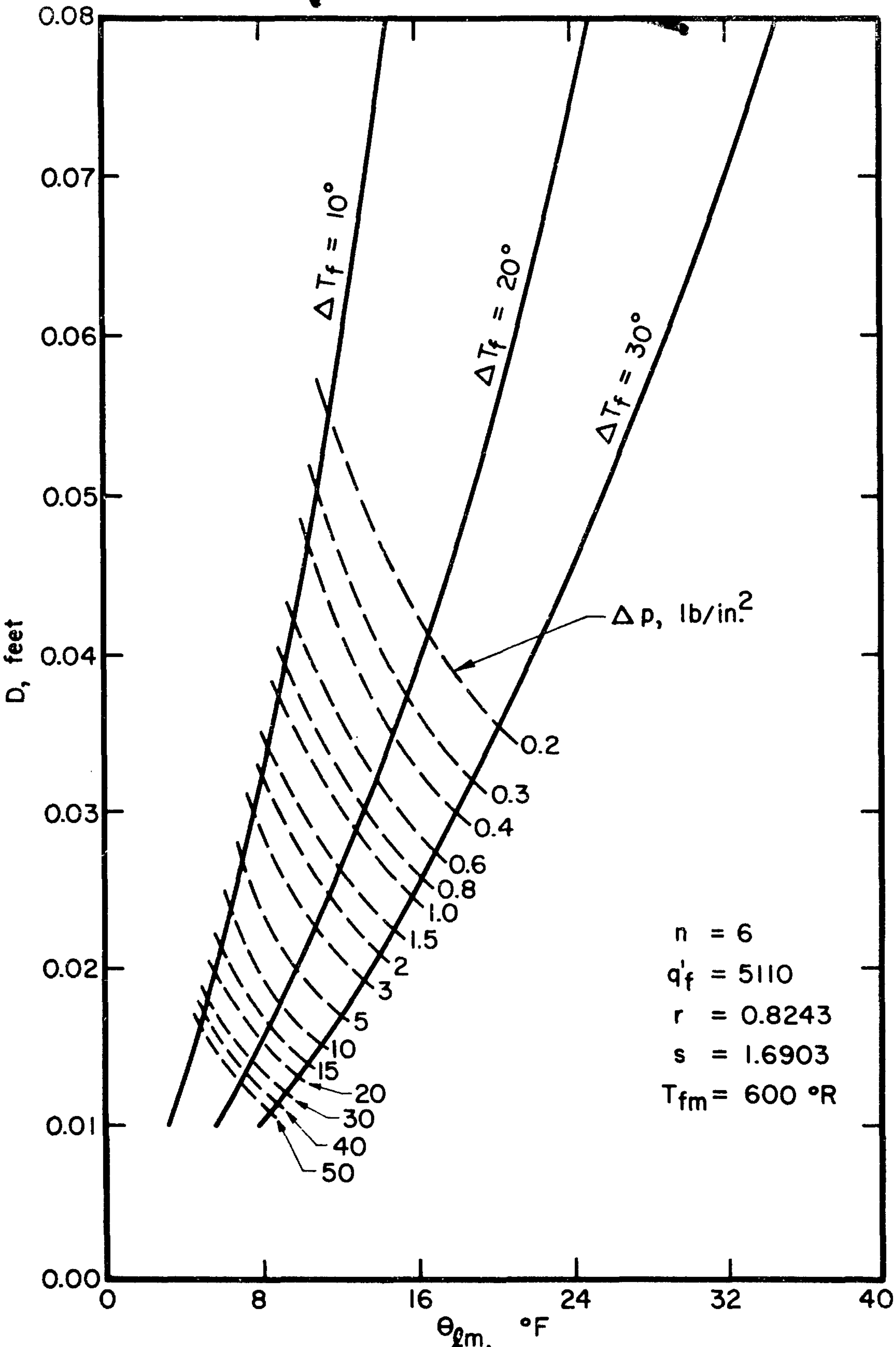

Figure VIII-5
Effect of Fuel Temperature Rise on the Design and Performance of a Serpentine-Passage Cooling Plate

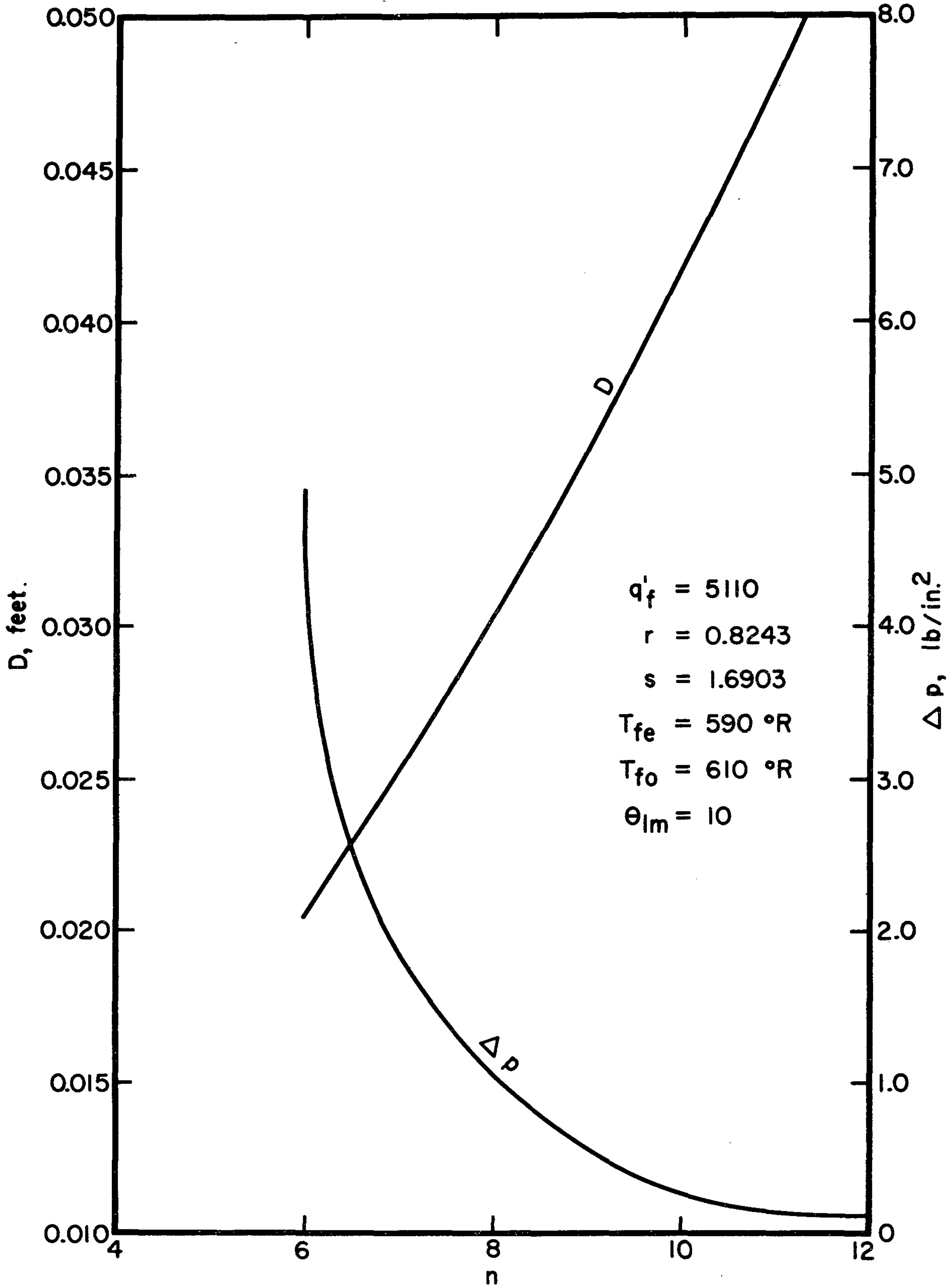

Figure VIII-6
Effect of Number of Bends (n-1) on the Design and Pressure Drop of a Serpentine-Passage Plate

2. The Parallel-Passage Plate with Laminar Flow of the Fuel

a. Effect of Cooling Capacity

The effect of cooling capacity on the design and performance of a fuel-cooled mounting plate of the parallel passage type is shown in Figure VIII-7. The nominal area of the plate is 1.5 ft^2, this being the product of the passage length and the distance between centerlines of the outermost passages. Other specifications for the plate are given in the figure. As shown in the analysis of this Section, the thermal performance of a plate of this type is not affected by the fuel passage diameter, so that the relationships shown for n, q_f and Θ_{lm} are valid for any diameter of the fuel passage which gives laminar flow. The pressure drop depends on the passage diameter, however, and the values shown are for a value of D = 0.00521 ft or 1/16 in.

The plot shows that a plate with a fixed number of fuel passages can give increased cooling capacity only by operating at a higher temperature above the temperature of the coolant. Since the cases shown are for a constant fuel temperature rise of 20°F, an increase of capacity requires an increase of fuel flow rate, and greater pressure drop. It is significant to note that the change in Θ_{lm} with change of capacity is less for plates with a large number of passages than for those with fewer fuel passages.

Considerable freedom of design exists for a cooling plate of constant capacity. The figure shows that the number of passages can be reduced to comparatively few if large values of Θ_{lm} are not objectionable. With fewer passages the pressure drop increases, but the pressure drop is always quite small compared to the values found earlier for serpentine-passage plates with small passages. It should be noted that the parallel passage plate is rather unsuited to service requiring small values of Θ_{lm}, since the number of passages required becomes quite large. It would therefore seem advisable to use a serpentine-passage plate where small Θ_{lm} is required, unless the cooling capacity is rather low.

b. Effect of Fuel Temperature Rise

The effect of fuel temperature rise on the design and performance of a parallel-passage cooling plate is shown in Figure VIII-8. Operating and design specifications are given in the figure.

For a plate with a fixed number of passages, an increase of fuel temperature rise results in increased Θ_{lm}. Since the cooling capacity is constant, the fuel flow rate is decreased for increased ΔT_f, giving a smaller heat transfer coefficient and therefore increasing the temperature potential required. The lower fuel flow rate also leads to a smaller pressure loss for the fuel. For a fixed temperature rise, the characteristics are the same as noted in Figure VIII-7.

If a cooling plate which requires a large number of passages is needed, it may be necessary to place the passages in staggered rows and, therefore,

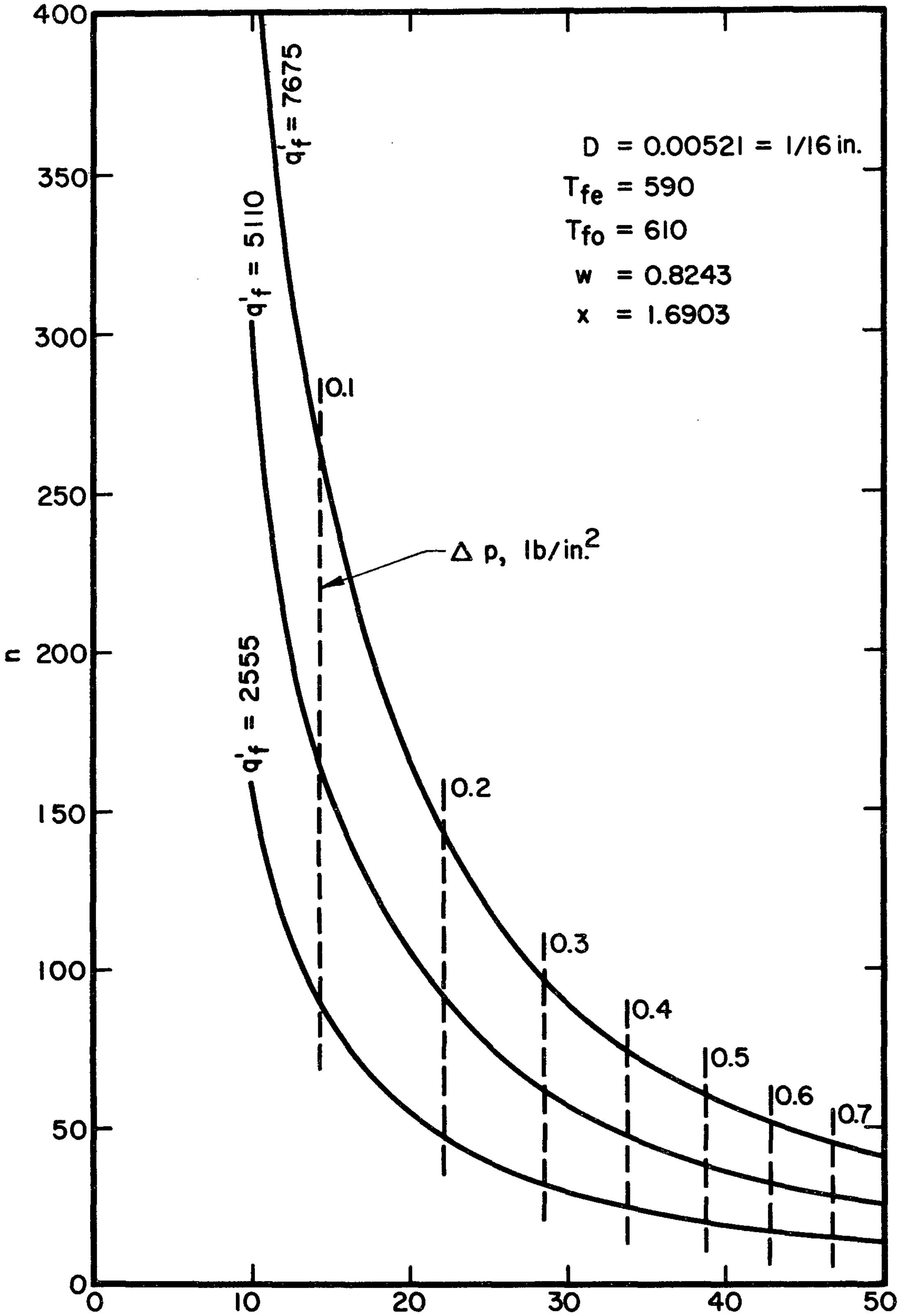

Figure VIII-7
Effect of Cooling Capacity on the Design and Performance of a Parallel-Passage Cooling Plate

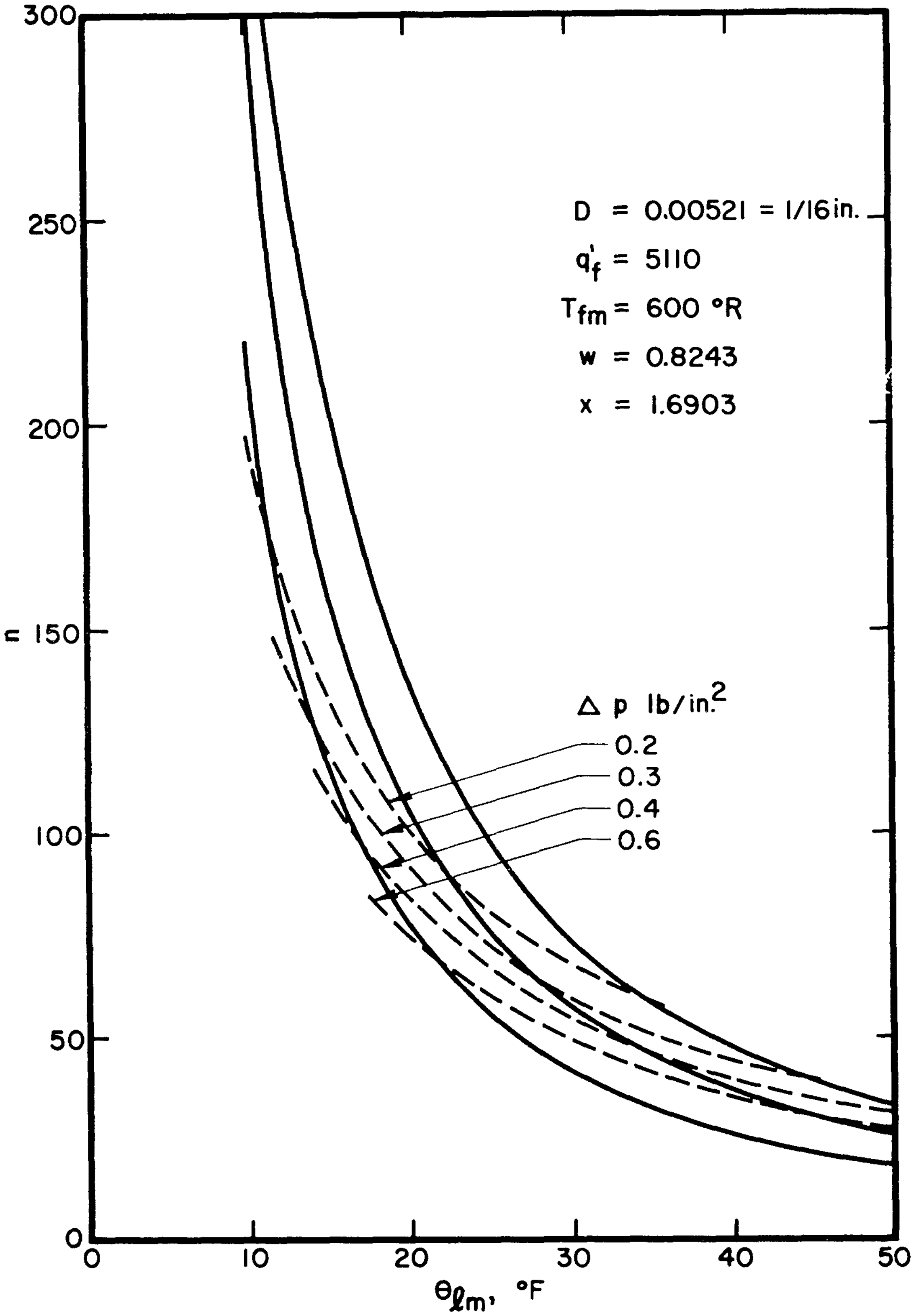

Figure VIII-8
Effect of Fuel Temperature Rise on the Design and Performance of a Parallel-Passage Cooling Plate

use a thicker plate. This complication seems unwarranted, however, in view of the better suitability of the serpentine-passage plate in the range of low Θ_{1m}. An important advantage of the parallel-passage plate over the serpentine-passage plate is noted from inspecting Figures VIII-4 and -7. For design specifications of $\Theta_{1m} = 20^{o}F$, $\Delta T_f = 20^{o}F$, and $q_f' = 2555$ Btu/hr, the parallel passage plate requires only 55 passages. If 1/16 in. passages were used, with 1/16 in. wall thickness, this would give a total plate thickness of 0.1875 in. if high structural rigidity is not required. For the same specifications a serpentine-passage plate would be about 0.925 in. thick, and weigh correspondingly more. As designs for higher cooling capacity are considered, the number of passages required for the parallel-passage plate increases. This in turn may require a thicker plate when it becomes necessary to use a double or triple row of passages. With the serpentine-passage plate, on the other hand, the higher cooling capacities require smaller passages and a thinner plate. Although for the design cited above the pressure drop is not given in Figure VIII-4, it is seen that for both type plates the pressure drop is very small, being at most 0.2 lb/in.^{2} If the cooling capacity is increased with all other specifications unchanged, the serpentine-passage plate requires higher fuel pressure drop, while that for the parallel passage plate is constant. Although these factors must be compromised in a design selection, it appears that the parallel-passage plate offers a size and weight advantage in the lower cooling capacity range. The serpentine-passage plate, however, offers structural simplicity at sacrifice in pressure drop in the higher cooling capacity range.

DESIGN OF A FUEL-COOLED MOUNTING PLATE FOR TRANSIENT SERVICE

The analysis to this point has concentrated on the characteristics of cooling plates of a given cooling capacity for one coolant temperature. In actual service in a high speed aircraft, it is probable that both the fuel temperature and the equipment heat loads would vary during flight. It is therefore desirable to consider the transient performance characteristics of equipment mounted on fuel-cooled plates so as to develop a method of designing the plates for transient service applications.

It was noted earlier that the heat balance equation for equipment mounted on a fuel-cooled plate is similar in form to that for equipment cooled by the system described in Section VII. It can therefore be expected that a plot of T_e vs. τ for equipment cooled by a plate would show characteristics which are similar to those found in Section VII. The most important of these characteristics from the design viewpoint is the nearly parallel relationship between the plots of T_e vs. τ and T_f vs. τ. Assuming that this characteristic holds, the general design procedure for a fuel-cooled mounting plate is the same as that used for the heat exchanger design of Section VII. The equations which involve details of the particular cooling apparatus are, of course, different. An example to illustrate the transient design technique as applied to cooling plates is given here. It is assumed that a serpentine-passage plate is used, since it is desired to hold the equipment very close to the fuel temperature. The first part of the design consists of finding the cooling capacity required, and the second consists of finding the design details for the particular cooling plate to

be used.

1. Design Example

Part A: Determining the Cooling Capacity Required of a Cooling Plate for Transient Service

It is assumed that it is desired to cool all of the equipment in a cylindrical aircraft compartment by mounting it on a cooling plate. The general characteristics of the compartment, the equipment, and the available coolant are as follows:

skin temperature of compartment $T_w = 1355^oR$

skin insulation of rock wool, $U_i = 0.60$ when $T_e = 460^oR$ and $T_w = 1355^oR$

dimensions of compartment, diameter = 2.0 ft, length = 0.866 ft, skin area = $\pi \times 2.0 \times 0.866 = 5.45$ ft^2

heat generation of equipment $q_g' = 5110$ Btu/hr

Cooling plate should have a total of 3 ft^2 of mounting surface (both sides), with a two to one side ratio.

ratio of free convection to radiation surface area of equipment and cooling plate assembly, $R = 4$

emissivities, skin insulation $\epsilon_i = 0.10$, equipment $\epsilon_e = 0.20$

Thermal capacity of equipment and cooling plate assembly will be approximately $M_e c_e = 2.0$ Btu/^oR (assuming the total weighs about 14 lb and has an average specific heat of 0.143 Btu/lb-^oR; very light equipment).

compartment air pressure $\delta = 2.5$

coolant JP-3 fuel, temperatures taken from Figure AIII-9, $U_{it} = 5.0$ Btu/hr-ft^2-^oR

It is next assumed that it is desired to prevent the equipment from exceeding $T_e = 644^oR$ in 100 minutes of flight time. The equipment is initially at 460^oR. Reference to Figure AIII-9 indicates that the entrance fuel temperature to the plate is 632^oR when $\tau' = 100$ min, so that the difference between the equipment and entering fuel temperatures at the end of flight is 12^oF. Since the fuel temperature and equipment temperature maintain approximately constant spacing, the value of the slope of the equipment temperature during the last half of the flight is estimated as

$$\left(\frac{\Delta T_e}{\Delta \tau}\right) \approx \left(\frac{\Delta T_f}{\Delta \tau}\right) = \frac{(632-537)}{(50/60)} = 114^oR/hr$$

The heat storage rate in the equipment and plate thermal capacities is therefore

$$M_e \, c_e \left(\frac{\Delta T_e}{\Delta \tau}\right) = 228 \text{ Btu/hr}$$

Next it is necessary to calculate the external heat load to the equipment and cooling plate assembly. This is conveniently done by the methods of Section V, after expressing the significant heat transfer characteristics in this example on a unit skin area basis. In keeping with earlier practice, the design value of external heat load is calculated for the equipment temperature occurring at the middle of the second half of the flight span. Since $T_{fe} = 578^{\circ}R$ at this time, the equipment temperature would be

$$T_e = T_{fe} + 12^{\circ}F = 590^{\circ}R$$

The details of calculating the external heat load based on this temperature and the assigned characteristics are not given here. Using the methods of Section V, the value is found as $q_o = 342$ Btu/hr-ft^2. For the entire compartment, this therefore gives

$$q_o' = 342 \times 5.45 = 1862 \text{ Btu/hr}$$

Applying the heat balance of equation (VIII-11)

$$q_f' = q_o' + q_g' - M_e c_e \left(\frac{\Delta T_e}{\Delta \tau}\right)$$

$$q_f' = 1862 + 5110 - 228 = 6744 \text{ Btu/hr}$$

This is the cooling capacity for which the cooling plate must be designed. The temperature difference between the plate and the fuel is assumed to be substantially the same as that between the equipment and the fuel. Since the fuel temperatures referred to until this point are entrance temperatures to the plate, θ_{lm} is something less than $12^{\circ}F$. As noted in connection with Figures VIII-7 and -8, this requires the use of a serpentine-passage plate to avoid the very large number of passages of a parallel-passage plate.

Part B: Design of the Cooling Plate

In addition to the characteristics given above, the following specifications and design details are assumed for the cooling plate.

Pressure drop of the fuel must be less than 15 lb/in.^{2}

Temperature rise of fuel $\Delta T_f = 10^{\circ}F$ (this will give a maximum fuel temperature of $632+10 = 642^{\circ}R$ or $182^{\circ}F$ at the end of flight

The passage centerlines come to within 1/4 in. of the edge of the plate, thus $r = 0.866-0.042 = 0.824$ ft and $s = 1.732-0.042 =$

1.690 ft. (plate external dimensions are 1.732x0.866 = 1.5 ft^2)

Design temperature for the fuel T_{fe} = 578°R corresponding to T_e = 590°R

Design of the plate is now a direct calculation except that n, the number of straight runs in the passage is unknown. This is therefore assumed, and another value used later if the pressure drop is unsatisfactory (recall the effect of n on pressure drop, as shown in Figure VIII-6).

1. Assume n $\qquad$ $n = 8$

2. Calculate $R_b = r/2(n-1)$ and $x = s - 2R_b$

$$R_b = \frac{0.824}{2 \times (8-1)} = 0.0588 \text{ ft}$$

$$x = 1.69 - 2 \times 0.0588 = 1.572 \text{ ft}$$

3. Calculate $T_{fm} = T_{fe} + (\Delta T_f/2)$ and evaluate γ, μ, k, c_p, Pr for the fuel at T_{fm} (use Figure AI-2 for JP-3 fuel)

$$T_{fm} = 578 + (10/2) = 583°R$$

$$\gamma = 47.22 \text{ lb/ft}^3$$

$$\mu = 1.21 \text{ lb/ft-hr}$$

$$k = 0.0855 \text{ Btu/hr-ft-°R}$$

$$c_p = 0.52 \text{ Btu/lb-°R}$$

$$Pr = 7.32$$

4. Calculate

$$Q_f = \frac{q_f}{\gamma \, c_p \, (\Delta T_f)}$$

$$Q_f = \frac{6744}{24.6 \times 10} = 27.4 \text{ ft}^3/\text{hr}$$

5. Calculate

$$\theta_{lm} = \frac{T_{fo} - T_{fe}}{\log_e \left(\frac{T_e - T_{fe}}{T_e - T_{fo}}\right)}$$

$$\theta_{lm} = \frac{10}{\log_e \left(\frac{590-578}{590-588}\right)} = 5.59°F$$

6. Assume D $D = 0.0268$ ft

7. Calculate $V = (4Q_f/\pi D^2)$

$V = 48{,}500$ ft/hr

8. Calculate $N = \left[n\pi Dx + \frac{r}{2}\pi^2 D + 1.77(n-1)\pi^2 D^2\right]$

$N = 1.06 + 0.109 + 0.0878 = 1.257$

9. Calculate

$$h_f = 0.023\left(\frac{k}{D}\right)\left(\frac{\gamma VD}{\mu}\right)^{0.8}(Pr)^{0.4}$$

$$h_f = 0.023\left(\frac{0.0855}{0.0268}\right)(50{,}700)^{0.8}(7.32)^{0.4} = 946 \text{ Btu/hr-ft}^2\text{-}^\circ\text{R}$$

10. Calculate $q_f' = h_f N \theta_{1m}$

$q_f' = 6640$ Btu/hr

If q_f' as calculated agrees with the cooling capacity requirement found earlier, D is correct, otherwise assume another D and recalculate to convergence. If q_f' as found in step 10 is too large, assume a larger value of D for the next trial, and conversely. (In the example calculation, the result of $q_f' = 6640$ is sufficiently close to the required $q_f' = 6744$ to make recalculation unnecessary.)

11. Calculate (R_b/D) and get K_b from Figure VIII-12.

$(R_b/D) = 2.195$

$K_b = 0.22$

12. Calculate $Re = (\gamma VD/\mu)$ and get f from a chart of friction factor (Darcy) vs. Re for smooth tubes (such as Figure VII-10).

$Re = 50{,}700$

$f = 0.0208$

(The use of this design procedure should properly be confined to cases where $Re \approx 10{,}000$, although it may be applied with decreasing accuracy down to $Re = 2300$.)

13. Calculate

$$\Delta P = \left(\frac{\gamma V^2}{2g}\right)\left[n\left(\frac{fx}{D}\right) + (n-1)\left(\frac{f}{D}\right)(\pi R) + (n-1)K_b\right]$$

$$\Delta P = 133 \times [9.77 + 1.002 + 1.54] = 1640 \text{ lb/ft}^2$$

$$\text{or} \quad \Delta p = 11.4 \text{ lb/in}^2$$

If the pressure drop is too great, assume a larger value of n and repeat the design procedure.

This completes the design of the cooling plate for the example design problem. It is now possible to make an analysis of the transient performance to confirm the suitability of the cooling plate design. Such an analysis requires a stepwise calculation process applied for short intervals over the flight time of interest. The procedure and an example calculation for one time interval are given in the Appendix to this Section. The results for such a calculation for the design example above are shown in Figure VIII-9, where it is seen that the equipment temperature at $\tau' = 100$ min is 642°R, compared to the intended value of 644°R. The design for the cooling plate is therefore satisfactory.

If a parallel-passage plate with laminar flow of the fuel is used, the determination of the required cooling capacity is the same as in Part I above. The second part simply requires solving equation (VIII-9) for n, which is a direct calculation requiring no assumptions.

2. Design Charts for Cooling Plates

After the required cooling capacity of a cooling plate has been determined, it is convenient to use a chart for the calculations required in Part B of the design. Charts have been developed for this purpose to design both serpentine-passage plates and parallel-passage plates. A brief description of these charts and their use is given here. They are based on the use of JP-3 fuel as coolant, and cannot be used for other coolants.

a. Charts for the Design of a Serpentine-Passage Plate

In any cooling plate design problem, it is assumed that the designer knows the plate dimensions r and s (see Figure VIII-2), the cooling capacity $q_{\downarrow}$, the allowable fuel temperature rise ΔT_f, and the temperature of the available fuel T_{fe}. In addition, it is necessary in using charts that the designer assume a value of θ_{1m} which can be regarded as a measure of the mean temperature difference between the plate (or equipment) and the coolant. With all of these values established, the charts given here can be used to determine the passage diameter and the fuel pressure drop for an assumed value of n (number of straight runs in the serpentine passage). If the resulting pressure drop is too great, the value of n is increased and the procedure is repeated until a satisfactory design is achieved.

The design charts for a serpentine-passage plate are based on a somewhat simplified analysis of the heat transfer process between the plate and the fuel. It is assumed that the passage can be considered straight for determining the heat transfer coefficient, thus neglecting the factor

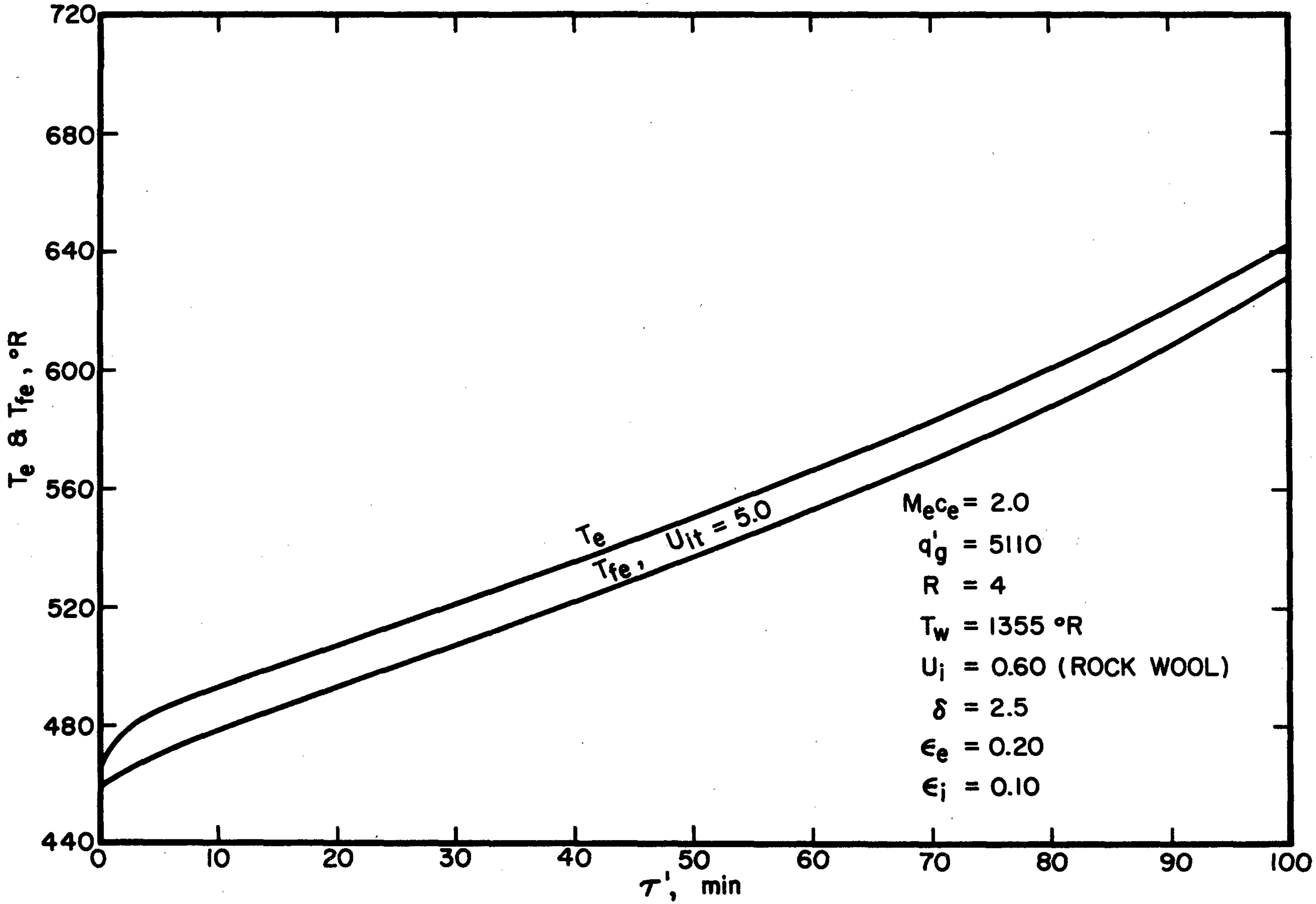

Figure VIII-9
Calculated Performance Verification for Cooling Plate Design

$\phi = 1+3.54(D/2R_b)$. The true length and surface area of the passage is used, however. Under this assumption, equation (VIII-6) is rewritten as

$$q_f^{\prime} = \Theta_{1m}\left[0.023k(Pr)^{0.4}(Re)^{0.8}\right]\left[n\pi s+r\left(\frac{\pi^2}{2}-\frac{n\pi}{(n-1)}\right)\right]$$

All of the variables in this equation are known or can be determined from the assigned design conditions, except the passage diameter D which is involved in the Reynolds modulus Re. The system of charts given in Figure VIII-10a is used to solve for this diameter. For clarity of description, the last bracketed term of the equation above is denoted by M'.

The charts are entered in quadrant I by drawing a horizontal line starting at the value of n on the right-hand scale. The intersections of this line with the proper line of constant s and the proper line of constant r are found. From these intersections, lines are projected vertically downward into quadrant II. The line from the intersection with s is projected horizontally from its intersection with the diagonal of quadrant II until it intersects the line projected downward from its original intersection with r. The intersection of these two lines determines M'. From this point, a line is projected parallel to the lines of constant M' until it reaches the left edge of quadrant III. From this point the line is projected horizontally into quadrant III until it intersects the proper line of constant ΔT_f, then vertically until it intersects the proper line of constant Θ_{1m}. From this point the line is projected horizontally into quadrant IV until it intersects the proper line of constant $q_f^{\prime}$, and thence vertically until it intersects the proper line of constant T_{fm}. T_{fm} is defined as $T_{fe} + (\Delta T_f/2)$, and should be calculated before using the charts. From the last named intersection the line is projected horizontally to the right until it intersects the scale of diameters, where the answer is read. An example of using the charts according to the above description is indicated in Figure VIII-10a by the dashed lines with arrows.

The charts for calculating the pressure drop in a serpentine passage are also based on a simplified analysis. If a constant value of $K_b = 0.25$ is used, equation (VIII-7) can be written as

$$\Delta P = \left(\frac{\gamma V^2}{2g}\right)\left[\left(\frac{M'}{\pi}\right)\left(\frac{f}{D}\right) + 0.25(n-1)\right]$$

This equation is solved using the charts of Figure VIII-10b. Quadrants V, VI, and VII are used first to determine the fuel velocity and the Reynolds modulus. These values are then recorded and used later. Quadrant V is entered by projecting a line horizontally to the right, starting from the value of $q_f^{\prime}$ on the left-hand scale. This line is continued until it intersects with the proper line of constant ΔT_f. From this intersection, the line is projected vertically to intersect with the proper line of constant T_{fm}, and then projected horizontally into quadrant VI. The scale on the left of quadrant VI gives the fuel flow rate Q_f. This flow rate must be supplied to the plate to satisfy the design conditions. The line is continued horizontally into quadrant VI until intersection with the proper line of constant D. The line is then projected vertically downward from this

intersection to give the velocity of the fuel on the bottom scale of quadrant V. The intersection of this last vertical projection with the proper line of constant T_{fm} is next used as a starting point to project horizontally into quadrant VII until intersecting the line of constant D for the design case at hand. The value of Re is then given by the scale at the bottom of quadrant VII directly beneath this last intersection.

With the values of V and Re established, the designer enters quadrant VIII with the value of M' as found in quadrant II. Quadrants VIII, IX, and X are then used, in that order, to complete the calculation of the pressure drop. The intersections are to be made in the order indicated by the example shown by the dashed lines with arrows. The final result is given as Δp in units of $lb/in.^2$

The simplifications used in constructing these charts lead to different design results than when the original equations are used unaltered. Since the effect of the bends on increasing the heat transfer coefficient is neglected, the chart design indicates the need of a smaller passage diameter than that found by the original equation. The smaller diameter results in increased fuel velocity, and a higher value of the straight-passage heat transfer coefficient. It is readily seen that this gives a conservative effect to the design, since it should give a performance value of Θ_{1m} which is less than the design value. As a result of the smaller passage diameter, a cooling plate designed by the chart would require greater fuel pressure drop than one designed with the procedure given in Part B of the design example.

It is emphasized that the charts are for turbulent flow. Thus, Re as found in quadrant VII should be greater than 10,000 for proper use of the charts, although they may be used with diminishing accuracy down to Re = 2300.

b. Charts for the Design of a Parallel-Passage Plate

For the design of a parallel-passage cooling plate, the same quantities must be known as for the serpentine passage plate, except that the passage diameter D is unimportant to the thermal performance, and the number of passages n is calculated rather than assumed. Only one simplification to the heat transfer relationship of equation (VIII-9) is required for the parallel-passage charts. It is assumed that the quantity $(\mu/\mu_s)^{0.14} = 1$. This assumption is quite accurate unless very large values of Θ_{1m} are used.

Figure VIII-11a is the set of charts required for solving equation (VIII-9) for n. Quadrant I is entered from the left at the value of cooling capacity required. A line is then projected successively to intersections with the appropriate values of ΔT_f, Θ_{1m}, x, T_{fm}, and thence to the result n. An example is indicated by the dashed-arrow line.

The pressure drop calculation required by equation (VIII-10) is solved by the charts of Figure VIII-11b. The charts are entered at quadrant III

by projecting from the cooling capacity scale successively to intersections with the proper values of ΔT_f, T_{fm} and n in quadrant IV. A line is then projected from the intersection with the line of constant n directly down to quadrant V to intersect with the single line plotted there. From this intersection a line is projected horizontally into quadrant VI to intersect with the value of D and thence vertically to the value of T_{fm}. From the intersection with T_{fm}, the line is projected horizontally across to quadrant VIII, as shown by the dashed-arrow line. The designer then returns to quadrant IV and locates the intersection of his original vertical projection with the proper value D. From this point a line is projected horizontally into quadrant VII to intersect with the line for T_{fm}, and thence vertically to intersect with x. From this last point, a line is projected horizontally to the right edge of the quadrant. A circular arc is then swung, using the lower right corner of the quadrant as a center, and locating the entry point on the upper edge of quadrant VIII. A line is next projected vertically downward from this point to intersect with the line projected horizontally into quadrant VIII earlier. The intersection of the two determines the pressure drop of the fuel in lb/in.^{2} It should be noted that the fuel flow rate is also given by the chart at the right of quadrant III, where the scale is read at the point where the horizontal projection line passes through it.

This set of charts given in Figures VIII-11a and -11b is for laminar flow of the fuel. It is recommended that Re = $(4W_f/n\pi D\mu)$ be calculated after completing the design to determine if Re is properly below 2300. If not, the chart design may still be used, but with diminishing accuracy, up to Re $\approx$ 10,000. In this transition range between laminar and turbulent flow, a performance value of θ_{lm} smaller than the design value may be expected, and an actual pressure drop greater than the design value is likely.

APPENDIX TO SECTION VIII

1. Calculation Procedures for the Steady-State Operation of Fuel-Cooled Mounting Plates

a. The Serpentine-Passage Plate with Turbulent Flow of the Fuel

The calculation procedure and example calculation given below illustrate the determination of θ_{lm} and Δp for a serpentine-passage plate of known dimensions and operating conditions. The example uses JP-3 fuel as the coolant.

Given Data:

plate dimensions (see Figure VIII-2) s = 1.69 ft, r = 0.824 ft

cooling capacity required $q_f' = 5110$ Btu/hr

number of straight runs in the passage n = 6

entrance temperature of fuel $T_{fe} = 590°R$

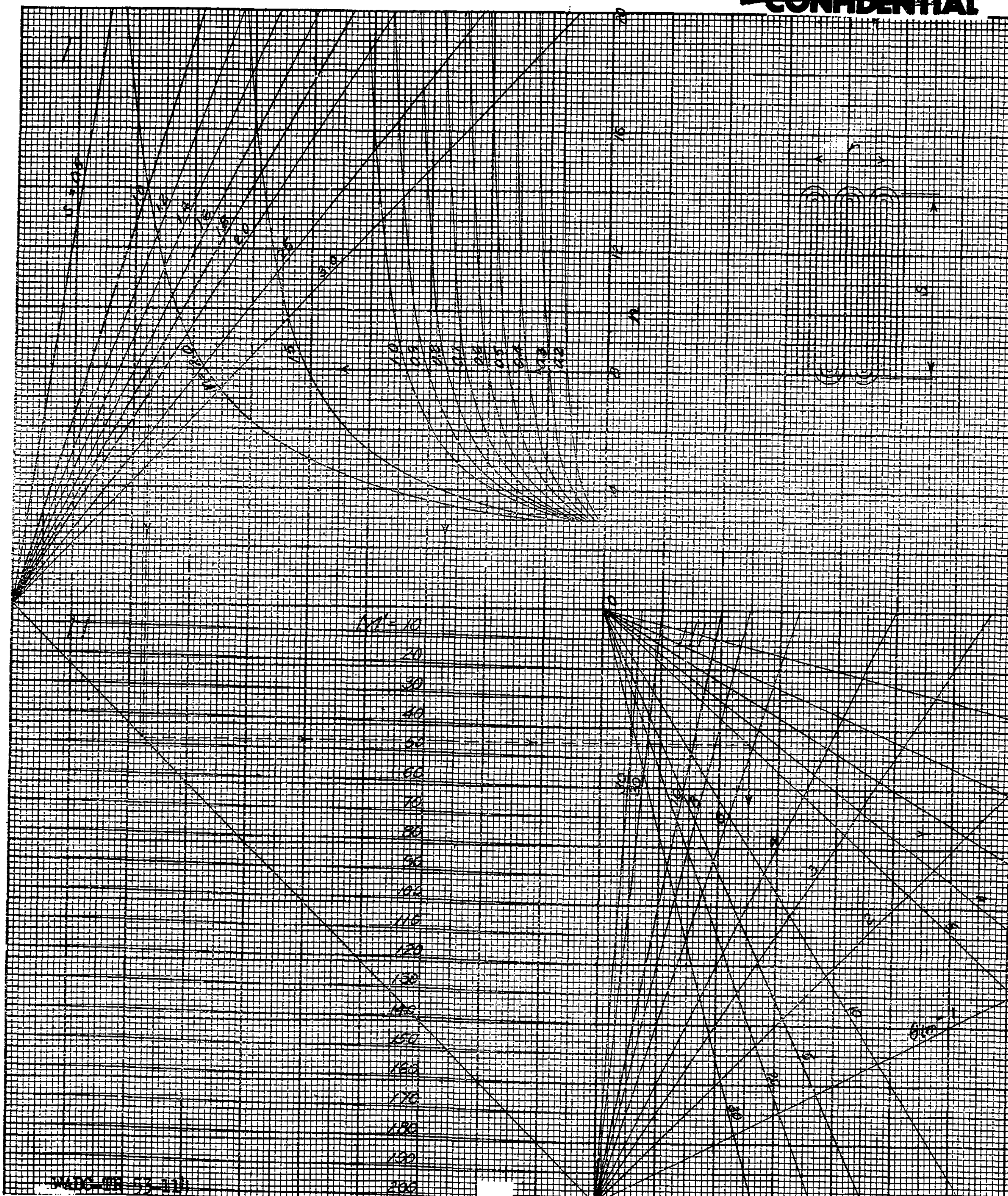

Design Chart for Serpentine-Passage Cooli

Figure VIII-10a

CONFIDENTIAL

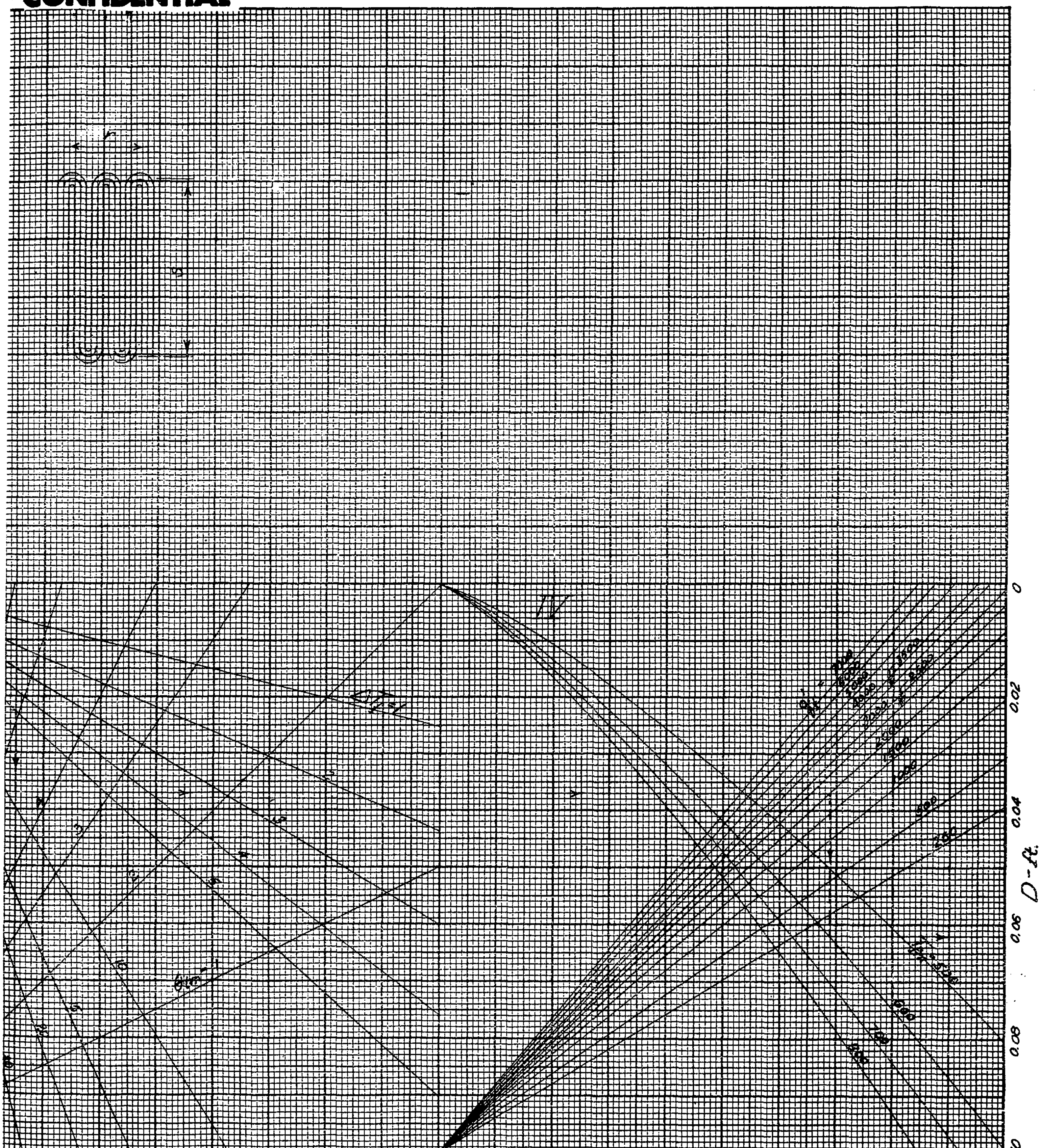

for Serpentine-Passage Cooling Plate
Figure VIII-10a

CONFIDENTIAL

375

2

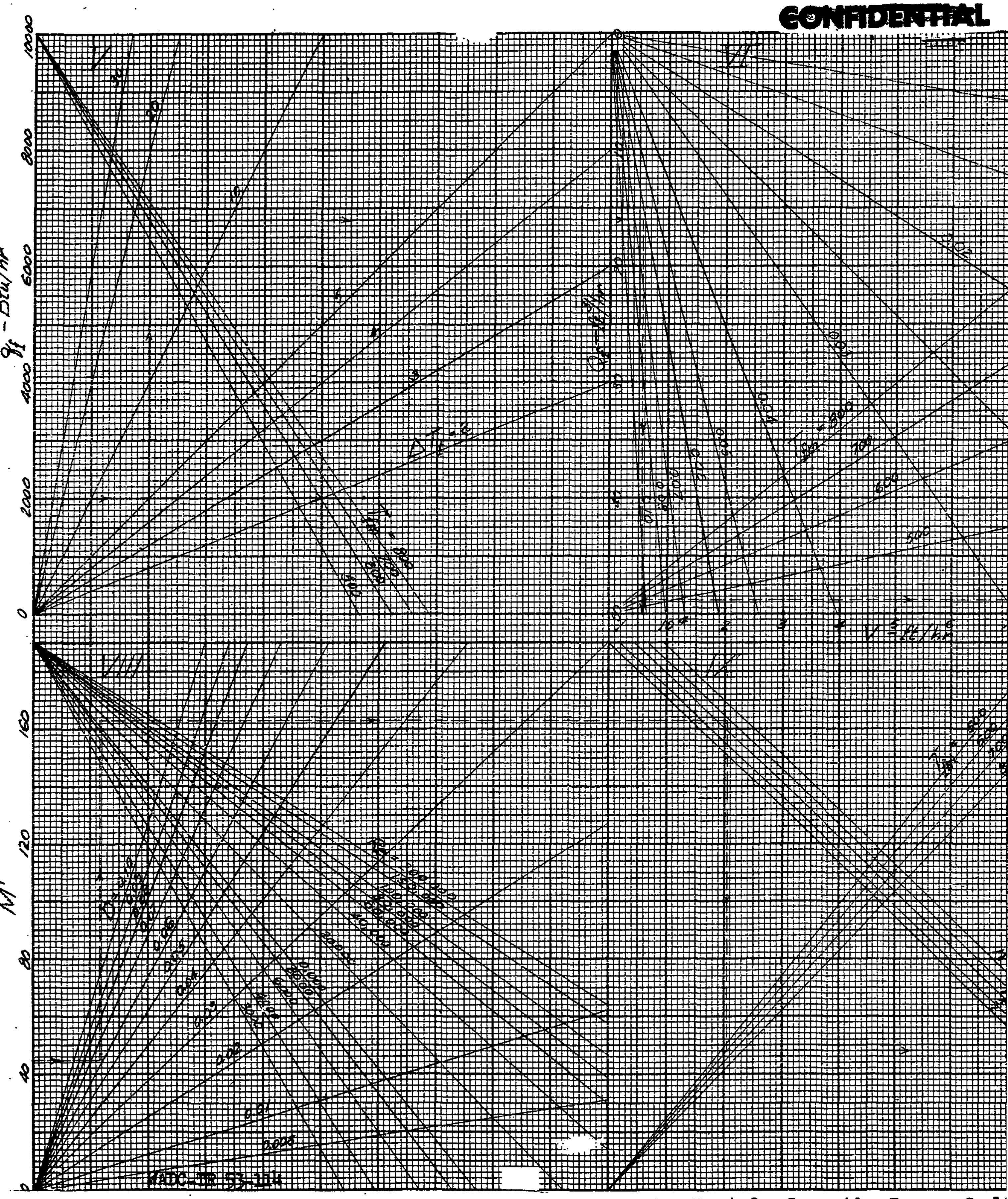

Design Chart for Serpentine-Passage Cool:

Figure VIII-10b

CONFIDENTIAL

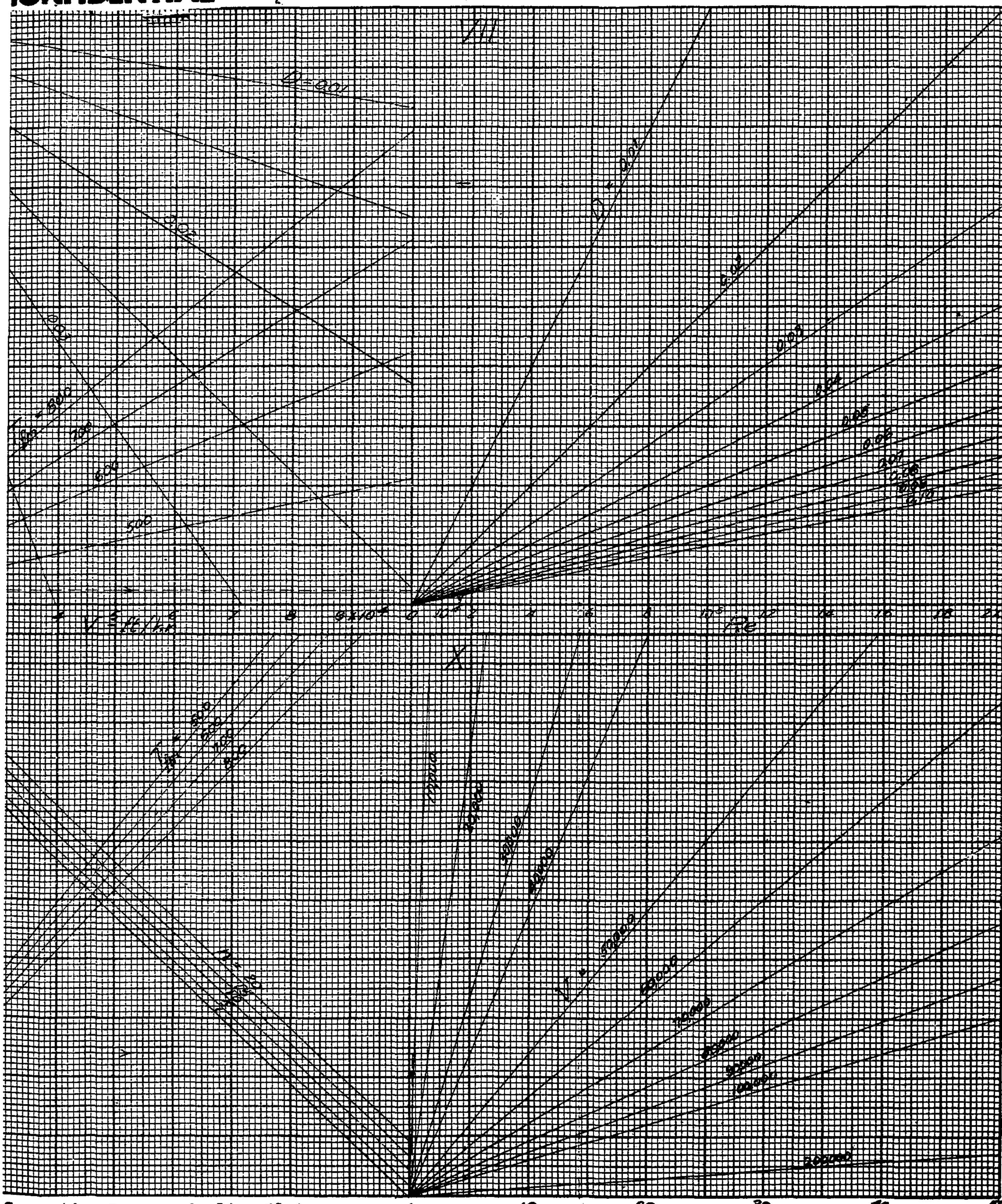

Serpentine-Passage Cooling Plate
Figure VIII-10b

CONFIDENTIAL

(2)

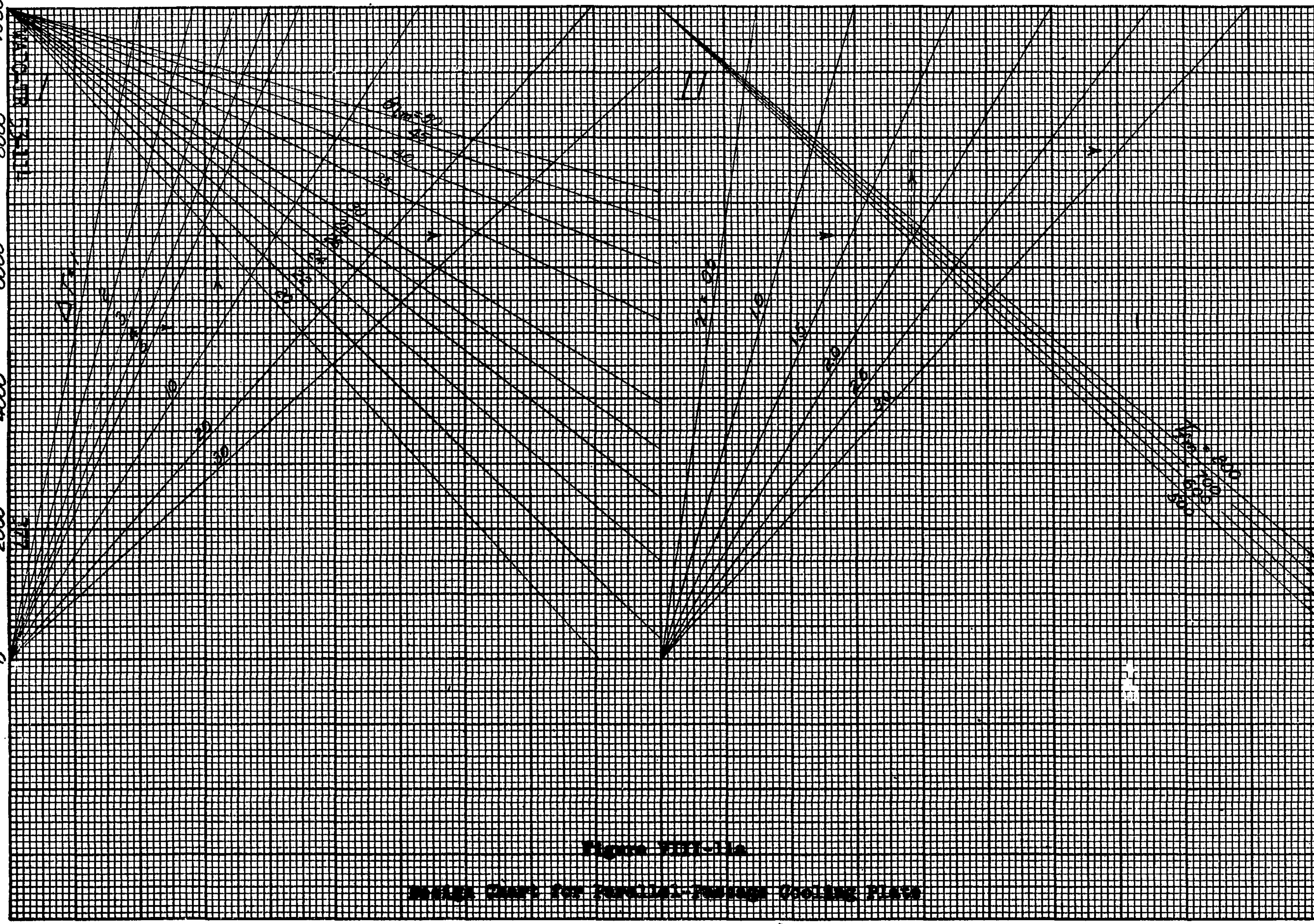

Figure VIII-11a.

Design Chart for Parallel-Passage Cooling Plate

L.L.C

377

(1)

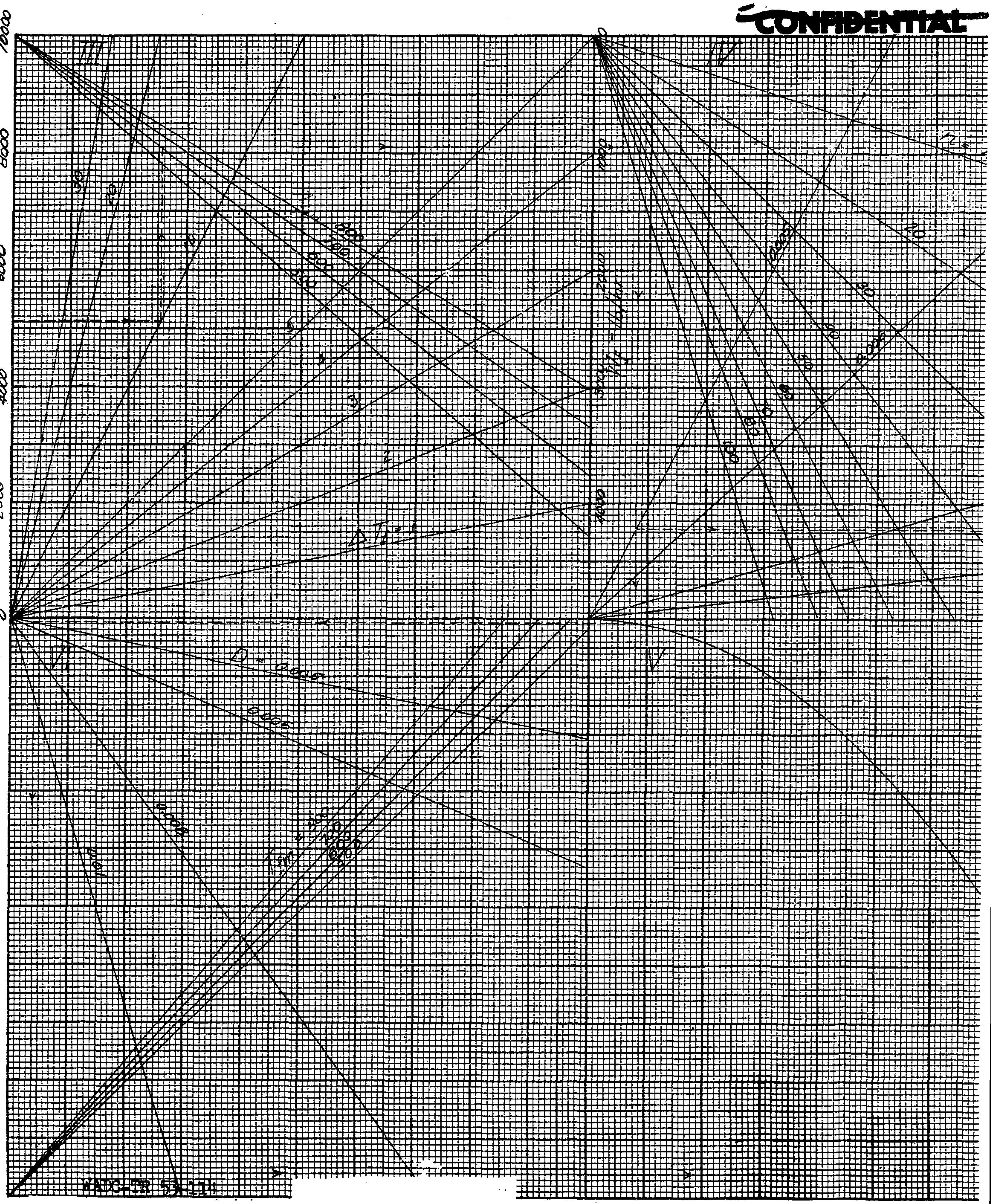

Design Chart for Parallel-Passage Cooli
Figure VIII-11b

CONFIDENTIAL

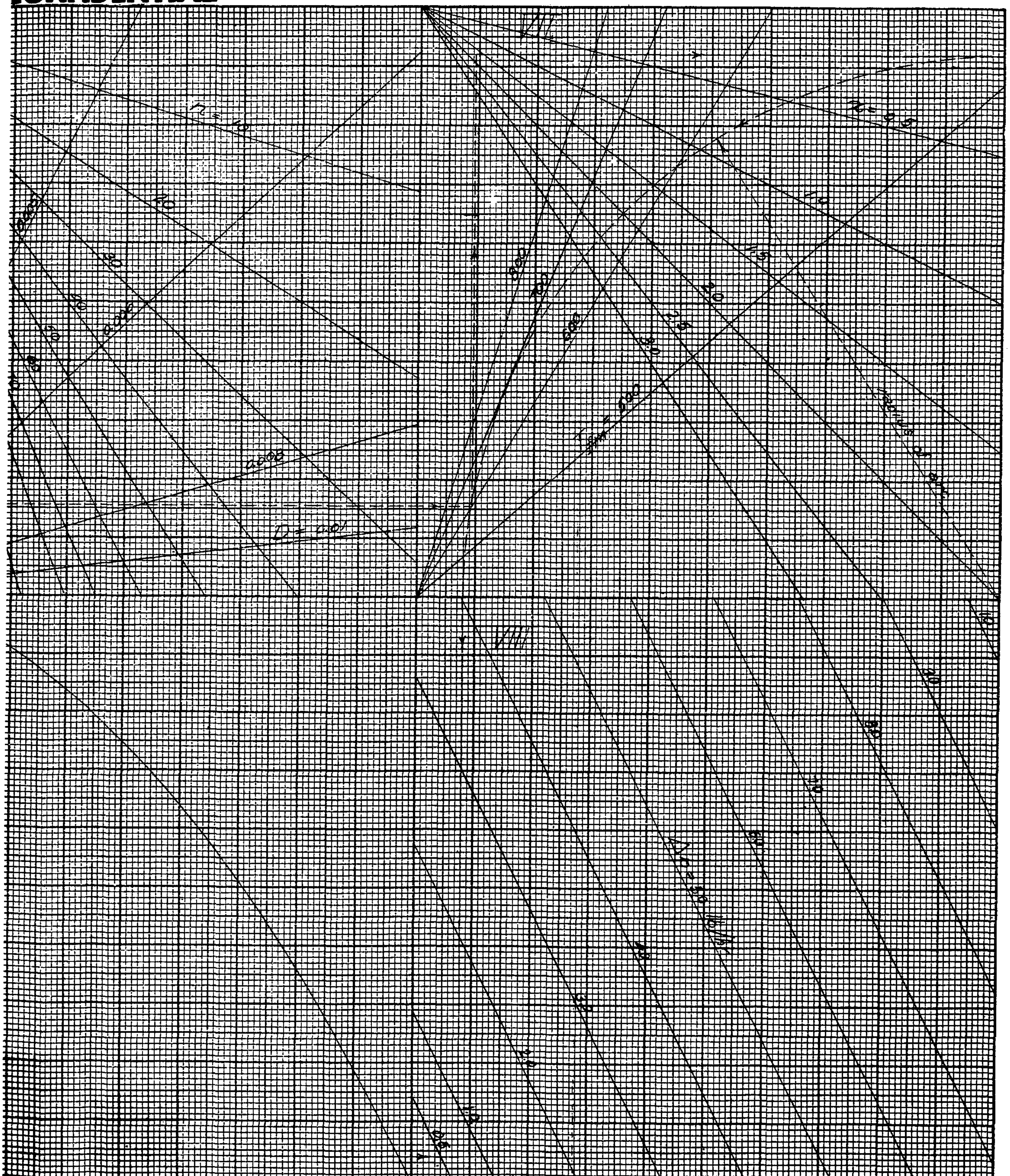

r Parallel-Passage Cooling Plate
Figure VIII-11b

ONFIDENTIAL

(2)

allowable temperature rise of fuel $\Delta T_f = 20^oF$, $T_{fo} = 610^oR$

diameter of circular fuel passage $D = 0.02$ ft

Calculate:

θ_{lm}, the logarithmic mean temperature difference between the fuel and the plate, and the fuel pressure drop.

1. Calculate $(T_{fe} + T_{fo})/2$ and evaluate γ, c_p, μ, k, and Pr for the fuel at this temperature (for JP-3 fuel, use Figure AI-2)

$\gamma = 46.78 \text{ lb/ft}^3$

$c_p = 0.532 \text{ Btu/lb-}^oR$

$\mu = 1.1 \text{ lb/ft-hr}$

$k = 0.085 \text{ Btu/hr-ft-}^oR$

$Pr = 6.88$

2. Calculate $R_b = \frac{r}{2(n-1)}$ and $x = s - 2R_b$

$R_b = 0.0824$ ft

$x = 1.5252$ ft

3. Calculate $W_f = \frac{q_f'}{c_p\,(T_{fo}-T_{fe})}$

$$W_f = \frac{5110}{0.532(20)} = 480 \text{ lb/hr}$$

4. Calculate $V = \frac{4W_f}{\pi D^2 \gamma}$

$V = 32600$ ft/hr

5. Calculate

$$h_f = 0.023\left(\frac{k}{D}\right)\left(\frac{\gamma VD}{\mu}\right)^{0.8}(Pr)^{0.4}$$

$$h_f = 0.023\left(\frac{0.085}{0.02}\right)(27700)^{0.8}(6.88)^{0.4} = 758 \text{ Btu/hr-ft}^2\text{-}^oR$$

6. Calculate

$$h_f A_f = h_f\left[n\pi Dx + \left(\frac{r}{2}\right)\pi^2 D + 1.77(n-1)\pi^2 D^2\right]$$

$$h_f A_f = 758\left[6x3.141x0.02x1.525 + \left(\frac{0.824}{2}\right)(3.141)^2 0.02 + 1.77x5x(3.141)^2(0.02)^2\right] = 525 \text{ Btu/hr-}^oR$$

7. Calculate

$$\theta_{lm} = \frac{q_f'}{h_1 A_f}$$

$$\theta_{lm} = \frac{5110}{525} = 9.75^{\circ}F$$

8. Get f from a chart of friction factors at Re = ($\gamma VD/\mu$) for smooth tubes (see Figure VII-10)

$$Re = 27{,}700$$
$$f = 0.0238$$

(This procedure is based on turbulent flow conditions in the fuel and is therefore accurate only if Re $\approx$ 10,000. It may be used with decreasing accuracy down to Re = 2300.)

9. Calculate (R_b/D) and get K_b from Figure VIII-12.

$$(R_b/D) = 4.12$$
$$K_b = 0.199$$

10. Calculate

$$\Delta P = \left(\frac{\gamma V^2}{2g}\right)\left[n\left(\frac{fx}{D}\right) + (n-1)\left(\frac{f}{D}\right)(\pi R_b) + (n-1)K_b\right]$$

$$\Delta P = 59.55\left[10.89 + 1.54 + .995\right] = 801 \text{ lb/ft}^2$$

b. The Straight, Parallel Passage Plate with Laminar Flow of the Fuel

The calculation procedure and example calculation given below illustrate the determination of the number of passages required and the pressure drop for a parallel passage plate of known dimensions and operating conditions. The example uses JP-3 fuel as the coolant.

Given Data:

plate dimensions, length x = 1.69 ft and width w = 0.824 ft

passage length x = 1.69 ft

cooling capacity required q_f' = 5110 Btu/hr

entrance temperature of fuel T_{fe} = 590°R

allowable temperature rise of fuel ΔT_f = 20°F, T_{fo} = 610°R

logarithmic mean temperature difference between the fuel and the plate $\theta_{1m} = 30^{\circ}F$

Calculate:

n, the number of passages required, and the pressure drop, assuming $D = 0.00521 \cdot ft$

1. Calculate $(T_{fe}+T_{fo})/2$ and get γ, k, μ, and c_p for the fuel at this temperature (for JP-3 fuel use Figure AI-2)

$$\gamma = 46.78 \text{ lb/ft}^3$$
$$k = 0.085 \text{ Btu/hr-ft-}^{\circ}R$$
$$\mu = 1.1 \text{ lb/ft-hr}$$
$$c_p = 0.532 \text{ Btu/lb-}^{\circ}R$$

2. Get μ_s at $\left[(T_{fe}+T_{fo})/2\right]+\theta_{1m}$

$$\mu_s = 1.09 \text{ lb/ft-hr}$$

3. Calculate $W_f = \dfrac{q_f^{\dagger}}{c_p(T_{fo}-T_{fe})}$

$$W_f = \frac{5110}{0.532 \times 20} = 480 \text{ lb/hr}$$

4. Calculate

$$(n\pi x) = \left[\frac{q_f^{\dagger}}{1.86(k)^{2/3}\,(4W_f c_p)^{1/3}\,\left(\frac{\mu}{\mu_s}\right)^{0.14}\,\theta_{1m}}\right]^{3/2}$$

$$(n\pi x) = \left[\frac{5110}{1.86 \times 0.194 \times 10.1 \times 1 \times 30}\right]^{3/2} = 320 \text{ ft}$$

5. Calculate $n = (n\pi x/\pi x)$

$$n = 60.2$$

6. Calculate

$$\Delta P = \left(\frac{W_f}{\pi\,\gamma\,D^4 g n}\right)\,128\,\mu\,x + 12\,\frac{W_f}{n\pi}$$

$$\Delta P = 0.1765\,(238 + 30.4) = 47.5 \text{ lb/ft}^2$$

$$p = 0.33 \text{ lb/in}^2$$

7. Calculate $Re = \frac{4W_f}{n\pi D\mu}$

$Re = 1770$

(Re should be less than 2300 for proper use of this procedure, since laminar flow of the fuel is assumed. It may be used, however, with decreasing accuracy up to a value of $Re \approx 10{,}000$.)

2. Calculation Procedure for Evaluating the Temperature Rise of Equipment Mounted on a Fuel-Cooled Plate

The procedure given here is for the calculation of equipment temperature rise for a single time interval. It is assumed that the equipment is mounted to a plate having a single, serpentine fuel passage through which the fuel flow is turbulent. As with the transient analyses of Section VII, this procedure assumes that the methods given in Section V have been used to construct a plot of q_o vs. T_e, which is then used as indicated below. The list of compartment, equipment, fuel temperature, and cooling plate characteristics are not given, since they are given for the design example (pp. VIII-26 to -30 and Figure VIII-9) to which this calculation applies. The example here is for the time interval beginning at $\tau = 1$ hr and ending at $\tau = 1.0833$ hr. T_e at the beginning of this time interval is 566°R.

1. Select $\Delta\tau$ and assume T_{e2}

$\Delta\tau = 0.0833$ hr
$T_{e2} = 573°R$

2. Calculate $\Delta T_e = T_{e2} - T_{e1}$ and $T_{em} = T_{e1} + (\Delta T_e/2)$

$\Delta T_e = 7°R$
$T_{em} = 569.5°R$

3. Get q_o from outside heat load calculation at T_{em}

$q_o = 350$ Btu/hr-ft^2

4. Calculate $q_o' = q_o A_w$ where A_w is total skin area of the compartment

$q_o' = 350 \times 5.45 = 1908$ Btu/hr

5. Calculate $q_f' = q_o' + q_g' - M_e c_e \left(\frac{\Delta T_e}{\Delta\tau}\right)$

$q_f' = 6850$ Btu/hr

6. Get T_{fe} at the middle of $\Delta\tau$ from the plot of T_f vs. τ. (In this

example, JP-3 fuel is used, T_f from Figure AIII-9, $U_{it} = 5.0$.)

$T_{fe} = 557^\circ R$

7. Assume T_{fo}, and get c_p and γ at $(T_{fe}+T_{fo})/2$ (for JP-3 use Figure AI-2)

$T_{fo} = 567^\circ R$

$c_p = 0.506$ Btu/lb-°R

$\gamma = 47.8$ lb/ft³

8. Calculate $T_{fo} = (q_f'/c_p \gamma Q_f)+T_{fe}$

$T_{fo} = 567.3^\circ R$

If this does not agree with the value assumed in step 7, repeat 7 and 8 to agreement.

9. Get μ, k, Pr at the correct value of $(T_{fe}+T_{fo})/2$

$\mu = 1.38$ lb/ft-hr

$k = 0.08604$ Btu/hr-ft-°R

$Pr = 8.1$

10. Calculate

$$h_f = 0.023\left(\frac{k}{D}\right)\left(\frac{\gamma VD}{\mu}\right)^{0.8}(Pr)^{0.4}$$

(from the design calculation $V = 48{,}500$ ft/hr, $D = 0.0268$ ft)

$h_f = 0.023(3.21)(45{,}000)^{0.8}(8.1)^{0.4} = 895$ Btu/hr-ft²-°R

11. Calculate $N = \left[n\pi Dx + \left(\frac{r}{2}\right)\pi^2 D + 1.77(n-1)\pi^2 D^2\right]$

$N = 1.257$

12. Calculate $\theta_{lm+d} = (q_f'/h_f N)$

$\theta_{lm+d} = 6.08^\circ F$

13. Calculate

$$\theta_{lm} = \frac{(T_{fo} - T_{fe})}{\log_e\left(\frac{T_{em} - T_{fe}}{T_{em} - T_{fo}}\right)}$$

$\theta_{lm} = 5.93^\circ F$

Repeat interval calculation until steps 12 and 13 agree by assuming new values of T_{e2}. If $(\theta_{1m})_{13} > (\theta_{1m})_{12}$ T_{e2} should be decreased and conversely.

This calculation procedure offers no special difficulty except during the first few intervals, when T_e has not assumed its equilibrium value with respect to T_f. Very short time intervals should therefore be used at first in order to insure a smooth plot of the values of T_e. The calculation shown applies only when all of the equipment in the compartment is mounted on the fuel-cooled surface. If this is not the case, a different method of describing the external heat load to the equipment must be used, as described in the analysis of this Section.

3. References

(VIII-1) Jakob, M. and Hawkins, G. A. Elements of Heat Transfer and Insulation. Second Edition, John Wiley and Sons, Inc., New York, 1950. pp. 113-14.

(VIII-2) Jakob, M. Heat Transfer Vol. I. John Wiley and Sons, Inc., New York, 1949. p. 548.

(VIII-3) Cox, G. N. and Germano, F. J. Fluid Mechanics. D. Van Nostrand Company, Inc., New York, 1941. p. 193.

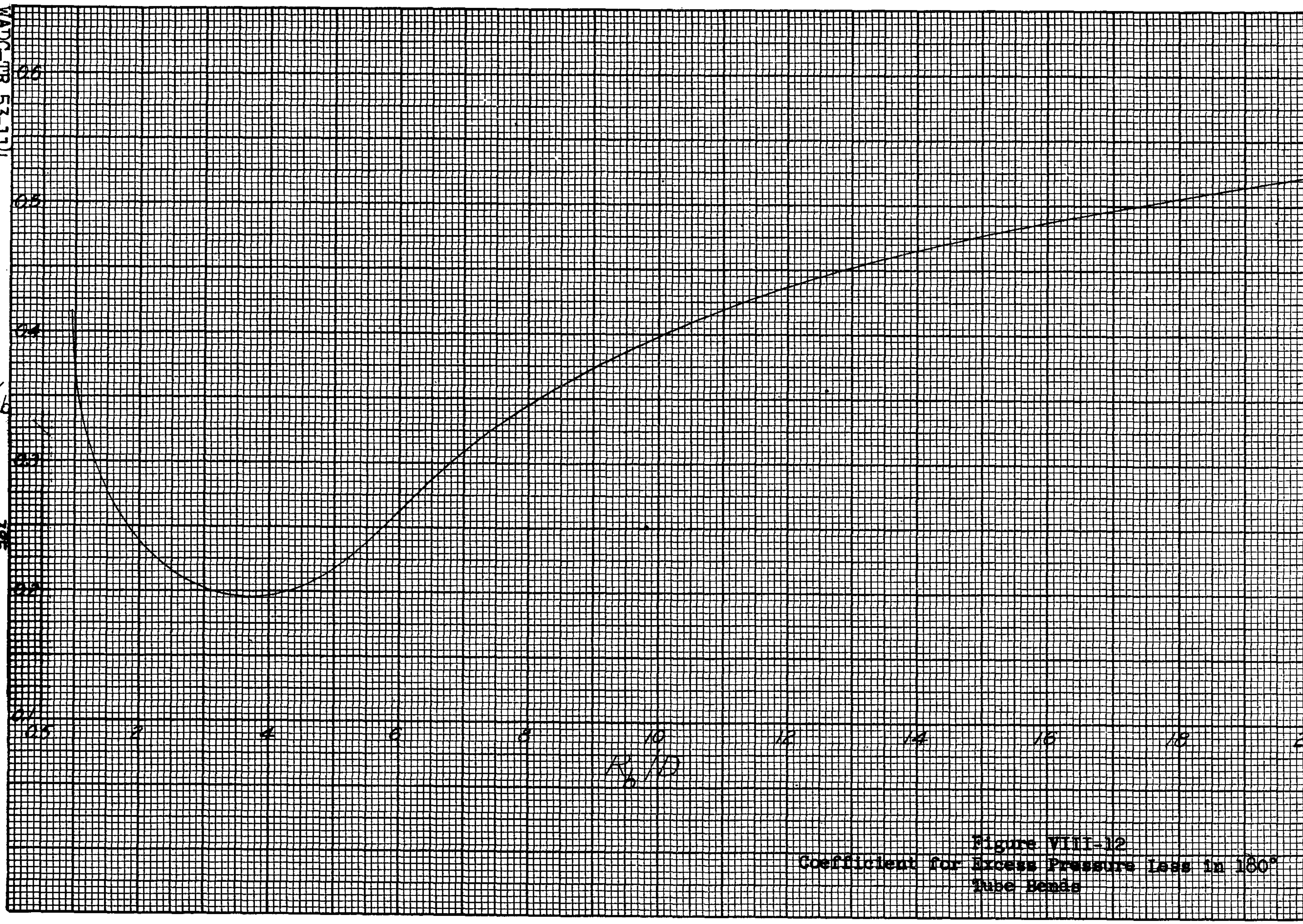

Figure VIII-12
Coefficient for Excess Pressure Loss in 180° Tube Bends

SECTION IX

TEMPERATURE RISE OF EQUIPMENT COMPONENTS COOLED BY AN EXPENDABLE EVAPORATIVE COOLANT

By T. C. Taylor and Y. H. Sun

It is possible that in many installations of aircraft equipment only a few critical items are subject to severe temperature rise limitations. In these cases it would be wasteful to cool the entire compartment, since savings in space and weight can be effected if cooling is applied only to those items which need it. One method of applying this individualized cooling effect is to use an evaporative coolant. In this method, a supply of the coolant is attached in good thermal contact with the equipment to be cooled. Heat is therefore transferred from the equipment to the coolant which is boiled off and discharged from the aircraft. By this means the equipment is maintained at very nearly the temperature of evaporation so long as the supply of coolant lasts. The equipment must be slightly above the evaporation temperature to provide temperature potential for transferring the heat to the coolant. Since the evaporation temperature of any coolant is a function of the pressure, this cooling method is readily controlled by using pressure regulators for the coolant container. In addition to its usefulness as a means of limiting the temperature rise of critical equipments, the evaporative coolant can be used to dispose of one or more severe generated heat loads, thus reducing the heat load to all of the equipments in the compartment. The use of evaporative coolant in these applications derives advantage from the comparatively great heat-absorbing capacity of a substance as it changes from the liquid to the vapor state. The weight and space requirements of this type of expendable coolant are therefore low. In addition, the apparatus required for this cooling method is small, light, and simple compared to that required by other methods.

Methods are developed in this Section to evaluate the temperature rise of individual equipments or equipment groups which are protected with an evaporative coolant. A method is also included for evaluating the temperature rise of an individual equipment component without special protection and not conforming to the average characteristics for all of the equipment in the compartment.

SUMMARY

The application of evaporative coolants to the protection of individual equipment items is considered. It is assumed that one or more critical items to be cooled are located in an otherwise uncooled compartment. The uncooled equipment items are assumed to dominate the heat transfer processes of the compartment and therefore determine the environment temperature-time history, which in turn determines the external heat load to the cooled items. It is assumed that the evaporative coolant is placed in good thermal contact with the item to be cooled, and the temperature difference between the equipment

item and the coolant is therefore neglected. Two methods for controlling the evaporation temperature of the coolant are analyzed. In the first, the coolant is vented through a pressure regulator which maintains a constant pressure in the evaporative coolant container. This gives a constant evaporation temperature irrespective of the variation of heat loads to the equipment. In the second control method, the coolant vapor is discharged to a constant pressure region, but passes through a convergent nozzle which causes a pressure build-up upstream of the nozzle. This method gives an increasing evaporation temperature for increasing heat loads to the cooled equipment. The external heat loads to the cooled equipment are assumed to consist only of the free convection heat transfer with the compartment air and radiation heat transfer with the skin insulation. Radiation heat transfer between bodies in the compartment is neglected.

Equations are given for calculating the external heat loads and for describing the temperature rise of the cooled equipment during periods when no coolant is evaporating. Equations are also developed to describe the coolant evaporatinn rate, and for the second method of control, the equipment temperature rise during periods of coolant evaporation. Calculation procedures are given which use these equations to calculate the over-all temperature rise of an equipment protected with evaporative coolant. One procedure is given for each of the evaporation control schemes. These procedures use a stepwise calculation method which requires trial and error calculations of some of the quantities involved. However, the procedures are not unduly complicated or difficult.

A design procedure and design example are given, showing how to select the proper amount of coolant to meet a desired temperature-flight plan for the cooled equipment. Although the design method is based on a number of approximate assumptions, it is found to give quite accurate results in the example. The problem of selecting the evaporative coolant for a design is not considered.

A number of calculations are made to study the temperature rise of individual equipments, both cooled and uncooled, in a compartment with constant skin temperature. All of these calculations assume water for the coolant. The salient conclusions reached from studying the results of these calculations are summarized as follows:

1. There are a variety of conditions which can require special cooling for some of the equipment items in an otherwise uncooled compartment. The first and most obvious condition is when the temperature of a particular piece of equipment must be restricted to lower values than that of the average uncooled equipment. Special cooling may also be desired if there is a concentrated source of generated heat, since the cooling effect can both reduce the local temperature rise and eliminate this heat source from the over-all compartment heat load. In addition, equipment which does not generate heat and which can tolerate the average equipment temperatures may require special cooling because of thermal characteristics which are out of line with the average. In one example it was found that equipment which has an exceptionally high surface emis-

sivity and a thermal capacity one-half of the average value may be as much as 70°F above the average equipment temperature.

2. When an individually cooled equipment is controlled so that its coolant boils at constant temperature, the plot of equipment temperature vs. time shows three distinct periods. In the first, the equipment temperature rises due to storage of heat in the thermal capacities of the equipment and the liquid coolant. The temperature rises until the coolant is at the saturation temperature corresponding to its pressure. At this temperature, the coolant begins to boil and maintains the equipment at a constant temperature as long as the expendable coolant lasts. This constant temperature effect is based on the assumption of a very large heat transfer coefficient to the boiling liquid and a high conductance for any heat conduction path between the equipment and the coolant. These conditions are easily approximated in an actual case. In the final period after all of the coolant is boiled off, the temperature again rises due to storage of heat in the equipment. An increase in the amount of coolant provided extends the flight time below a limiting temperature in two ways. First, the added thermal capacity of the coolant prolongs the initial period of temperature rise. Second, the added coolant provides more heat absorption capacity due to boiling, prolonging the period of constant temperature operation. The added flight time resulting from added coolant is not proportional to the amount of coolant added, however, since the average external heat load is greater for longer flight durations. This increase of average external heat load is due to an increase of environment temperatures with time in an uncooled compartment.

3. The effect of raising the evaporation temperature when using a coolant evaporating at constant temperature is to prolong the time before the coolant is all boiled off. This effect is due principally to two conditions. First, added use is made of the equipment and liquid thermal capacities by storing heat in them over a longer initial period of temperature rise. Second, constant temperature operation at higher temperatures involves smaller external heat loads to the coolant. This second effect is at least partially offset by a decrease in the latent heat of vaporization for the coolant as the temperature is increased. The combination of these effects indicates that for most efficient use of a given amount of coolant, the evaporation temperature should be chosen as high as possible consistent with reliable operation of the equipment.

4. When a convergent nozzle of small enough size is used to control the discharge of the coolant vapor, the coolant and equipment temperatures rise during the evaporation period. The temperature rise is initially rapid while building up sufficient pressure to discharge enough coolant vapor to dissipate the heat loads. Thereafter the temperature rise is more gradual to accommodate the increase of external heat load with time. The use of this method of

control offers no significant advantage over using the method of constant-temperature evaporation when the average equipment temperatures during the evaporation period are comparable.

ANALYSIS

1. Assumptions for Analysis

A typical configuration for a compartment containing a number of equipment items, one of which is protected by evaporative coolant, is shown in Figure IX-1. The particular compartment shown is cylindrical in shape, and no other cooling method is used in the compartment. The single item which is cooled is assumed to consist of a box which contains one or more equipment items. On the interior of the box is a flask or container of evaporative coolant, so placed that it is in good thermal contact with the box and the equipment inside of the box. If it is not detrimental to opera-

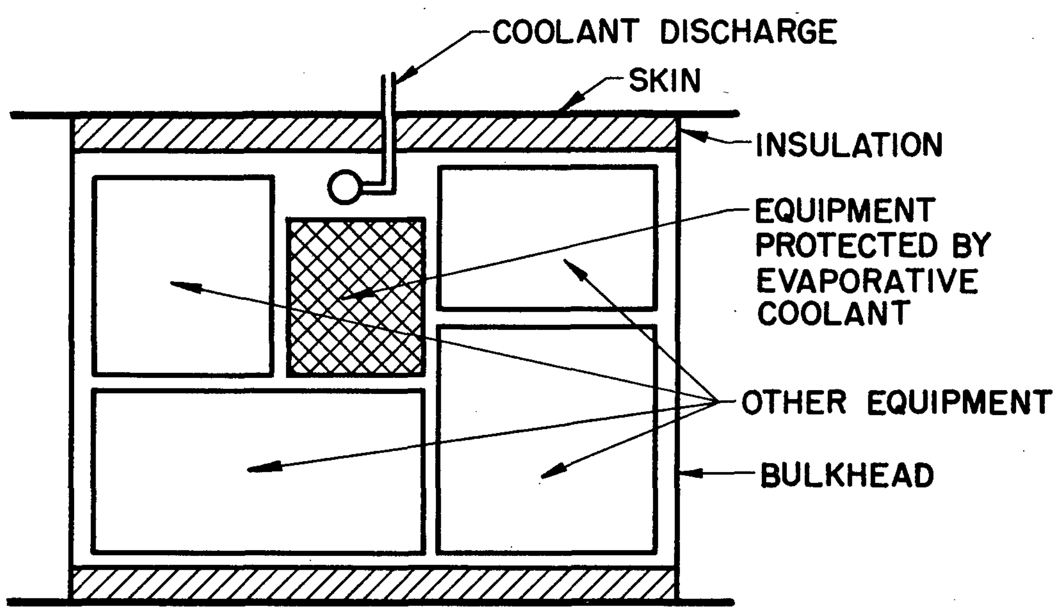

Figure IX-1. Schematic of a Compartment with an Equipment Protected by Evaporative Coolant

tion, the entire box may be filled with evaporative coolant, completely immersing the equipment. The box is fitted with a discharge line for disposing of the vapor. By means of this line, the coolant is vented to a pressure which establishes the evaporation temperature. Two methods of control are assumed for the analysis. In one case, it is assumed that the vent or discharge line for the coolant contains a pressure regulator which

maintains the coolant at constant pressure. The evaporation temperature of the coolant is therefore constant. In the second method of control, it is assumed that the coolant is vented to a constant pressure region but the vent line contains a convergent nozzle as a restriction which offers resistance to the flow of the discharging vapor. The pressure of the coolant and the evaporation temperature therefore rise for an increase in evaporation rate.

The external heat loads to the cooled box of equipment are assumed to be those due to radiation from the skin insulation and free convection of the compartment air only. In addition, the cooled equipment may generate heat. The sum of the external and generated heat loads of the box is dissipated by the evaporative coolant. Although a slight temperature difference is required to transfer generated and received heat from the equipment to the evaporative coolant, it is assumed that this is negligible, and that the equipment and coolant are at the same temperature. For purposes of determining the external heat load to the box, it is assumed that the cooled equipment itself has negligible effect on the compartment temperatures. The compartment air temperature and the insulation face temperature are therefore established by the heat transfer processes between the skin and all of the other equipment in the compartment. This assumption is accurate in the case where the cooled box or boxes are a small portion of the entire contents of the compartment.

The only insulation used in this analysis is that on the inside of the compartment skin. The use of insulation on individual equipment boxes is considered in Section X. The radiation portion of the external heat load is assumed to consist only of radiant heat transfer between the box and the compartment skin or skin insulation. The temperature difference between the cooled box and nearly uncooled bodies is assumed to be sufficiently small that radiant heat interchange between them can be neglected.

2. Nomenclature

Symbol	Definition	Units
A	Surface area	ft^2
a	Flow area	in^2
a'	A convection group, used in equation (IX-4)	
c	Specific heat	Btu/lb-^oR
H	Enthalpy	Btu/lb
h	Heat transfer coefficient	Btu/hr-ft^2-^oR
K	Nozzle coefficient	dimensionless

Symbol	Definition	Units
L	Characteristic length for free convection	ft
M	Weight	lb
m	Weight on unit skin area basis	lb/ft^2
p	Pressure	lb/in^2
q	Heat transfer, storage, or generation rate based on unit skin area	$Btu/hr\text{-}ft^2$
q'	Heat transfer, storage, or generation rate	Btu/hr
R	Ratio of free convection to radiation heat transfer area	dimensionless
T	Absolute temperature	^oR
U	Insulation conductance	$Btu/hr\text{-}ft^2\text{-}^oR$
V	Volume	ft^3
v	Specific volume	ft^3/lb
W	Weight flow rate	lb/hr
x	Fraction of coolant in the vapor state	dimensionless
δ	Pressure	atmospheres (dimensionless)
ϵ	Emissivity	dimensionless
τ	Time	hr
τ'	Time	min

SUBSCRIPTS

a	Denotes air	
b	Denotes time of initial evaporation	
c	Denotes convection value	
ch	Denotes chord to curve segment	

Subscripts (continued)

d	Denotes design value
e	Denotes equipment
evap	Denotes evaporation
f	Denotes coolant in general, or liquid value of enthalpy or specific volume
fg	Denotes value for change of state from liquid to vapor
g	Denotes generated value with heat rate, or vapor state value with enthalpy
i	Denotes insulation
m	Denotes average value for a time interval
n	Denotes the n-th interval of time
o	Denotes external value for heat load and original value if used as a second subscript, i.e., T_{eo}
r	Denotes radiation value
s	Denotes storage value for heat rate
t	Denotes tangent to curve segment
th	Denotes throat of nozzle
v	Denotes vapor heat rate
w	Denotes skin
1,2	Denotes initial and final values for a time interval; also denotes upstream and downstream values for a nozzle

3. Derivation of Equations

a. External Heat Load to the Cooled Box

To determine the external heat load by radiation and free convection to the cooled box, it is necessary to define the environmental conditions of the compartment. Since no other cooling is used in the compartment, and since most of the compartment heat transfer processes are domi-

nated by the uncooled equipment, the methods of Section V are used. A calculation for the compartment as a whole is made exactly as in Section V, the only difference being that the insulation face temperature and compartment air temperature are the results of principal interest rather than the equipment temperature. A plot of insulation face temperature and air temperature versus time is then used to define the external heat load to the cooled box by means of the equations which follow. No additional compartment or equipment characteristics for the uncooled equipment are required beyond those used in the method of Section V.

In keeping with the practice of Section V, the radiation heat load to the cooled equipment is defined by

$$q_r' = A_r\, h_r\, (T_i - T_e) \qquad \text{(IX-1)}$$

where A_r is that amount of the surface area of the box which "sees" the insulation and therefore exchanges heat with it by radiation. The radiation coefficient is defined as

$$h_r = 17.4\text{x}10^{-4}\left(\frac{1}{\frac{1}{\epsilon_i} + \frac{1}{\epsilon_e} - 1}\right)\left[\frac{\left(\frac{T_i}{100}\right)^4 - \left(\frac{T_e}{100}\right)^4}{\left(\frac{T_i}{100}\right) - \left(\frac{T_e}{100}\right)}\right] \qquad \text{(IX-2)}$$

where the function of temperatures is given by Figure AIV-1. The use of this form of the radiation coefficient for a single equipment body assumes that the surface which "sees" the insulation is essentially parallel to it. The value of T_i for equation (IX-1) is a function of time, as determined for the uncooled equipment. The free convection heat load to the cooled equipment is given by

$$q_c' = A_c\, h_c\, (T_a - T_e) \qquad \text{(IX-3)}$$

where the area A_c refers to the entire surface of the cooled box if it is all exposed to free air circulation. If some of the surface area is obstructed from free air circulation, that portion is not included in A_c. Surfaces facing gaps of 3/8-inch width and less are usually considered obstructed when the gaps are bounded by other equipments. If such a gap is bounded on the other side by the skin surface, or its insulation, the heat transferred across it should be estimated as somewhere between that which occurs for free convection and that which occurs for gaseous conduction. To be conservative the larger value should be used. The convection coefficient of equation (IX-2) is defined as

$$h_c = \left(\frac{a' L^{1/4}}{\delta^{1/2}}\right)\left(\frac{\delta^{1/2}}{L^{1/4}}\right)(T_a - T_e)^{1/4} \qquad \text{(IX-4)}$$

The total external heat load to the cooled box is the sum of the radiation and the free convection heat transfer loads.

b. Heat Balance for the Cooled Box

There are two heat balance equations which apply to the cooled equipment box. The first equation is for the time when no coolant is being evaporated, as occurs if the temperature is less than that corresponding to evaporation pressure, or if the coolant has already been completely used up. During operation of this type, all of the heat received by or generated in the cooled equipment is stored in the combined thermal capacities of the equipment and the coolant in the liquid state. The heat balance equation is therefore

$$(q_o' + q_g')\,\Delta\tau = (M_e c_e + M_f c_f)\,\Delta T_e \tag{IX-5}$$

The second heat balance equation applies to that time when coolant is evaporating. The equation is different in form for the two different types of coolant control. If the coolant is vented through a pressure regulator, the evaporation and equipment temperatures are constant, and the heat balance simply equates the external and generated heat loads to the evaporation rate times the latent heat of the coolant, giving

$$q_o' + q_g' = H_{fg}\left(\frac{\Delta M_f}{\Delta\tau}\right) \tag{IX-6}$$

where H_{fg} is the enthalpy of vaporization of the coolant at the temperature of evaporation.

If the coolant is vented to a constant pressure through a line which contains a flow restriction, such as a convergent nozzle, the heat balance is more complicated. The pressure, and hence the temperature at which coolant evaporation takes place, depends on the pressure drop across the flow restriction, and this, in turn, depends on the evaporation rate. Since the evaporation rate varies with external heat load, the temperature of evaporation varies, and equipment and coolant thermal capacities are involved. The equations describing the flow of saturated steam through a convergent nozzle are (e.g. Ref. IX-1),

$$\frac{W_f}{a_{th}K} = 1080\sqrt{\frac{p_1}{v_1}} \tag{IX-7}$$

for $(p_2/p_1) \leqq 0.58$, and

$$\frac{W_f}{a_{th}K} = 7090\sqrt{\left(\frac{p_1}{v_1}\right)\left[\left(\frac{p_2}{p_1}\right)^{1.77} - \left(\frac{p_2}{p_1}\right)^{1.89}\right]} \tag{IX-8}$$

for $(p_2/p_1) > 0.58$.

For any given discharge pressure p_2 these equations can be used to construct a plot of $(W_f/a_{th}K)$ versus T_e, where the values of T_e are saturation temperatures for water vapor corresponding to values of p_1. A plot of this form can then be used to facilitate calculation with the heat balance equa-

tions. For other coolants than water, similar equations with appropriate empirical constants must be used.

The quantity of coolant remaining in the container at the end of any time interval during the evaporation process is given by

$$(M_{f2})_n = (M_{f2})_{n-1} - \left[\left(\frac{W_f}{a_{th}K}\right)(a_{th}K)\,\Delta\tau\right]_n$$

where $(W_f/a_{th}K)$ is found for the current interval as based on the average value of T_e during the interval, and where n refers to the current interval, while (n-1) refers to the previous interval.

Because of changes in pressure and temperature of the coolant, it is necessary to account for changes of coolant enthalpy in both the liquid and the vapor states. To do this, it is convenient to define the quantity x as the portion of the coolant still within the container but in the vapor state. Then for a total container volume V,

$$V = M_{f2}\left[x(v_f + v_{fg}) + (1 - x)v_f\right]$$

or

$$V = M_{f2}\,(v_f + x\,v_{fg}) \qquad \text{(IX-9)}$$

If v_f and v_{fg} are evaluated for the temperature at the end of the interval, or T_{e2}, equation (IX-9) can be solved for x, since M_f for the end of a time interval is known from the previous equation. This permits computing the enthalpy of all the coolant in the container at the end of an interval as

$$M_{f2}H_c = M_{f2}\,(H_f + x\,H_{fg}) \qquad \text{(IX-10)}$$

where H_f and H_{fg} are evaluated at T_{e2}.

The heat stored in both the equipment and the coolant during any interval of time and temperature change is therefore given by

$$(q_s')\,\Delta\tau = \left[(M_{f2}H_c)_n - (M_{f2}H_c)_{n-1}\right] + M_e c_e\,\Delta T_e \qquad \text{(IX-11)}$$

The heat escaping with the vapor during a time interval is given by

$$(q_v')\,\Delta\tau = \left(\frac{W_f}{a_{th}K}\right)(a_{th}K)\,H_g\,\Delta\tau \qquad \text{(IX-12)}$$

where the value of H_g is taken for the average temperature of the interval.

The complete heat balance for the cooled equipment box is therefore given by

$$(q_o' + q_g')\,\Delta\tau = (q_s' + q_v')\,\Delta\tau \qquad \text{(IX-13)}$$

The equations developed are sufficient to describe all of the heat transfer and heat storage processes occurring, and are used in the calculation procedure described next.

4. Calculation Procedure for Determining the Temperature Rise of Equipment Protected by an Evaporative Coolant

a. General Method

As indicated by the form of the equations developed, it is necessary to employ a stepwise calculation method for this temperature rise evaluation. The calculation method described here is based on the evaluation of heat transfer and storage rates at the average temperature conditions of an interval. A less accurate method can be used based on temperature conditions at the beginning of an interval, but it is not described here. The method described requires trial and error calculations, since the evaluation temperatures used are unknown at the start of an interval, and therefore must be assumed and then checked later. Detailed procedures and examples of interval calculations are given in the Appendix to this Section.

b. Calculation of Compartment Environment Temperatures

Before subsequent calculations can be made to evaluate the temperature rise of cooled equipment, it is necessary to determine the variation of skin insulation temperature and compartment air temperature with time. This is most readily done by using the general calculation procedure for evaluating the temperature rise of uncooled equipment, as given in Section V. The same compartment and equipment characteristics as indicated in Section V must be known, and should be established based on the entire contents of the compartment except the specially cooled items. After completing the calculation, a plot is prepared showing the values of T_i and T_a for the time range of interest, and this plot is used in the subsequent calculations for determining the external heat load to the cooled equipment box. For further details of determining the compartment environment temperatures, the reader is referred to the Appendix to Section V.

c. Calculation for Periods when No Coolant Evaporates

The calculation procedure described here is used to evaluate the temperature rise of equipment which is protected by evaporative coolant when no evaporation is taking place. This condition exists during the initial heating-up period, when the equipment has not yet reached evaporation temperature, and also applies during the final period, when all of the coolant has evaporated. Since the compartment air temperature and the insulation face temperature have been determined by previous calculation, and plotted in a chart of T_a and T_i versus time, their values are available for any time interval of the calculation. For a selected time interval for which the initial temperatures are known as T_{a1} and T_{i1}, the values at the

end of the interval, T_{a2} and T_{i2}, are found from the plot. The average values are then calculated as $T_{am} = (T_{a1}+T_{a2})/2$, and similarly for T_{im}. It is then necessary to assume the only unknown temperature for the end of the interval, which is T_{e2}. T_{em} is then calculated, and equations (IX-1 and -2) are used, based on the average temperatures for the interval, to determine q_r'. Equations (IX-3 and -4) are used next to evaluate q_c', basing the determination of the quantity $(a'L^{1/4}/\delta^{1/2})$ from Figure AIV-3 on the average air film temperature of $(T_{am}+T_{em})/2$. The value used as A_r is that portion of the surface of the equipment box which "sees" the insulation face and is involved in radiant heat transfer. This value must be estimated and should be principally restricted to those surfaces of the box which are approximately parallel to the insulation face and have no intervening obstructions between them and the insulation. Surfaces of the box which are approximately perpendicular to the insulation face are not very effective in radiant heat transfer, particularly when they are facing nearly parallel faces of other equipments. As mentioned earlier, the convection area A_c consists of the entire box surface except those portions which face gaps of 3/8 inch and less formed together with other equipments. An individually cooled equipment box should not be butted in direct thermal communication with another equipment box, since it then receives heat by thermal conduction from the other equipment, thus subjecting the coolant fluid to unintended heat loads. After determining q_c' and q_r', equation (IX-5) is solved for ΔT_e, and T_{e2} is calculated from the equation

$$T_{e2} = T_{e1} + \Delta T_e$$

The calculated value of T_{e2} should agree within 5 or 6°R of the value originally assumed, in which case the calculated value is very accurate, and is used as the value of T_{e1} for calculation of the next time interval. If this degree of agreement is not achieved, the calculated value of T_{e2} is used as the assumed value for a second trial, in which the entire calculation procedure for the interval is repeated.

The calculation just described is an easy one, inasmuch as there is only one unknown temperature involved. The assumption of the value of T_{e2} for an interval is facilitated by keeping a running plot of the values of T_{e2}, and extrapolating the plot for the assumed values. Quite accurate results can be expected from the procedure if the time intervals $\Delta\tau$ are selected so as to limit the values of ΔT_e to a maximum rise of 40°R during the interval. When using this procedure to calculate the last time interval prior to initial evaporation of the coolant, the time interval must be such that the value of T_{e2} is the assigned evaporation temperature. This may require several trials. When the procedure is used for the period after coolant evaporation is completed, the value of M_f for equation (IX-5) is zero.

d. <u>Calculation for Periods of Coolant Evaporation at Constant Temperature</u>

The calculation described here applies to periods of coolant evaporation, when the coolant is maintained at a constant pressure. Opera-

tion under these conditions is at constant equipment temperature for the cooled box. For any time interval both the initial and final values of all temperatures are known, making possible the direct calculation of q_c' and q_r' using equations (IX-1, -2, -3, and -4), based on T_{im} and T_{am}. Equation (IX-6) is then solved for ΔM_f, which completes the interval calculation. This is repeated for succeeding intervals, calculating $\sum(\Delta M_f)_n$ for each interval until

$$\sum(\Delta M_f)_n = M_f$$

at which time all of the coolant has been evaporated. It is necessary to find the length of the final evaporation interval by trial such that the coolant is just used up at the end of the interval. The calculation gives very accurate results for time intervals selected such that $(T_{i2}-T_{i1}) \lessapprox 40°R$ (or °F).

e. Calculation of Temperature Rise for Periods of Coolant Evaporation Controlled by a Convergent Nozzle

The procedure described here applies to periods of coolant evaporation when the coolant is vented to a constant pressure region by a line which contains a convergent nozzle. It is assumed that the nozzle is small enough to offer something more than negligible flow resistance to the vapor discharging through it. Before starting the calculation of the equipment temperature rise, equations (IX-7 and -8) are used to construct a plot of the function $(W_f/a_{th}K)$ versus T_e. Since the vapor is discharged in a saturated condition, T_e is the saturation temperature corresponding to p_1; p_2 is the constant throat or discharge pressure of the nozzle. The plot is prepared by evaluating the equations for a range of selected values of p_1, corresponding to the range of values of T_e of interest. The lowest temperature of this range is the saturation temperature of the coolant corresponding to p_2. Equations (IX-7 and -8) are applicable only to the use of water as the evaporative coolant. If other coolants are used, equations for their flow must be used in constructing the plot of $(W_f/a_{th}K)$ versus T_e.

The first part of the temperature rise evaluation consists of selecting the time interval, assuming T_{e2}, and determining T_{im}, T_{am}, and T_{em}. Equations (IX-1, -2, -3, and -4) are used as before to determine q_r' and q_c'. The value of $(W_f/a_{th}K)$ is then taken from the plot corresponding to T_{em}, and W_f is calculated for the assigned $(a_{th}K)$. Since the throat area a_{th} of the nozzle is constant, the only variation of this product is due to change of the coefficient of discharge K, which is a function of the Reynolds number of flow. As an approximation, the value of K is assumed constant in this procedure. Using W_f and the value of H_g for T_{em}, q_v' is calculated from equation (IX-12).

Equation (IX-9) is used next, with specific volumes corresponding to T_{e2}, to calculate x, the portion of coolant inside the container, but in the vapor state, at the end of the interval. This requires using the value of $W_f \Delta\tau$ for the current interval, and M_{f2} for the previous interval to find the current value of M_{f2}. After finding x, the value of $(M_{f2}H_c)$ is

found from equation (IX-10), using enthalpies at T_{e2}. Equation (IX-13) is then used with q_s' expressed in the form of equation (IX-11). This is solved for ΔT_e, and T_{e2} is calculated. This calculated result should agree with the value of T_{e2} originally assumed. If not, the interval calculation is repeated until agreement to any desired degree of accuracy in ΔT_e is achieved. The evaporation process is completed when

$$\sum (W_f \Delta\tau)_n = M_{fo}$$

where M_{fo} is the initial value of M_f for the container. When using this procedure at the end of evaporation, the interval size must be found by trial such that the coolant is just used up at the end of the interval.

The calculation described above is a rather difficult one. The time intervals can be selected only from experience, and must be rather small when the plot of T_e vs. τ is changing slope rapidly. Otherwise the results tend to plot a zig-zag course above and below the true values of T_e. An example of an interval calculation using this method is given in the Appendix to this Section.

EFFECTS OF EQUIPMENT CHARACTERISTICS AND EVAPORATIVE COOLANT ON THE TEMPERATURE RISE OF INDIVIDUAL EQUIPMENTS

1. Temperature Rise of Individual Equipments as Compared to the Average

Before considering the application of evaporative cooling to individual equipments, it is interesting to examine briefly the temperature rise of individual uncooled equipments in an uncooled compartment. This will serve to point out some of the important applications of individualized evaporative cooling. In Section V methods are developed and used to predict the average temperature rise of all equipments in an uncooled compartment. It is obvious that each equipment item will not in general conform to the average temperature rise so determined. Equipments may have an unusually high surface emissivity, a low thermal capacity, a greater than average heat generation, or other factors which cause the individual temperature rise to be greater than the average. In order to study some of these effects, calculations have been made using Procedure A of the Appendix to this Section. The results are shown in Figure IX-2. The characteristics of the compartment and the average characteristics for all of the equipment are given in the figure.

The individual equipments studied in Figure IX-2 all consist of a cubic box, one foot on an edge and having a total surface area of six square feet. It is assumed that the ratio of free convection to radiation heat transfer area is R = 4, which gives $A_r = 1.5$ ft^2 and $A_c = 6$ ft^2. For a body having $A_r = 1.5$ ft the thermal capacity would be $M_e c_e = 3.0$ Btu/^{o}R if it conformed to an average of $m_e c_e = 2$ Btu/^{o}R-ft^2. The plots a and b of the figure therefore compare the temperature rise of a box having the average characteristics of all the equipment with that of a box having only half the average value of thermal capacity. With a lower value of thermal capacity the

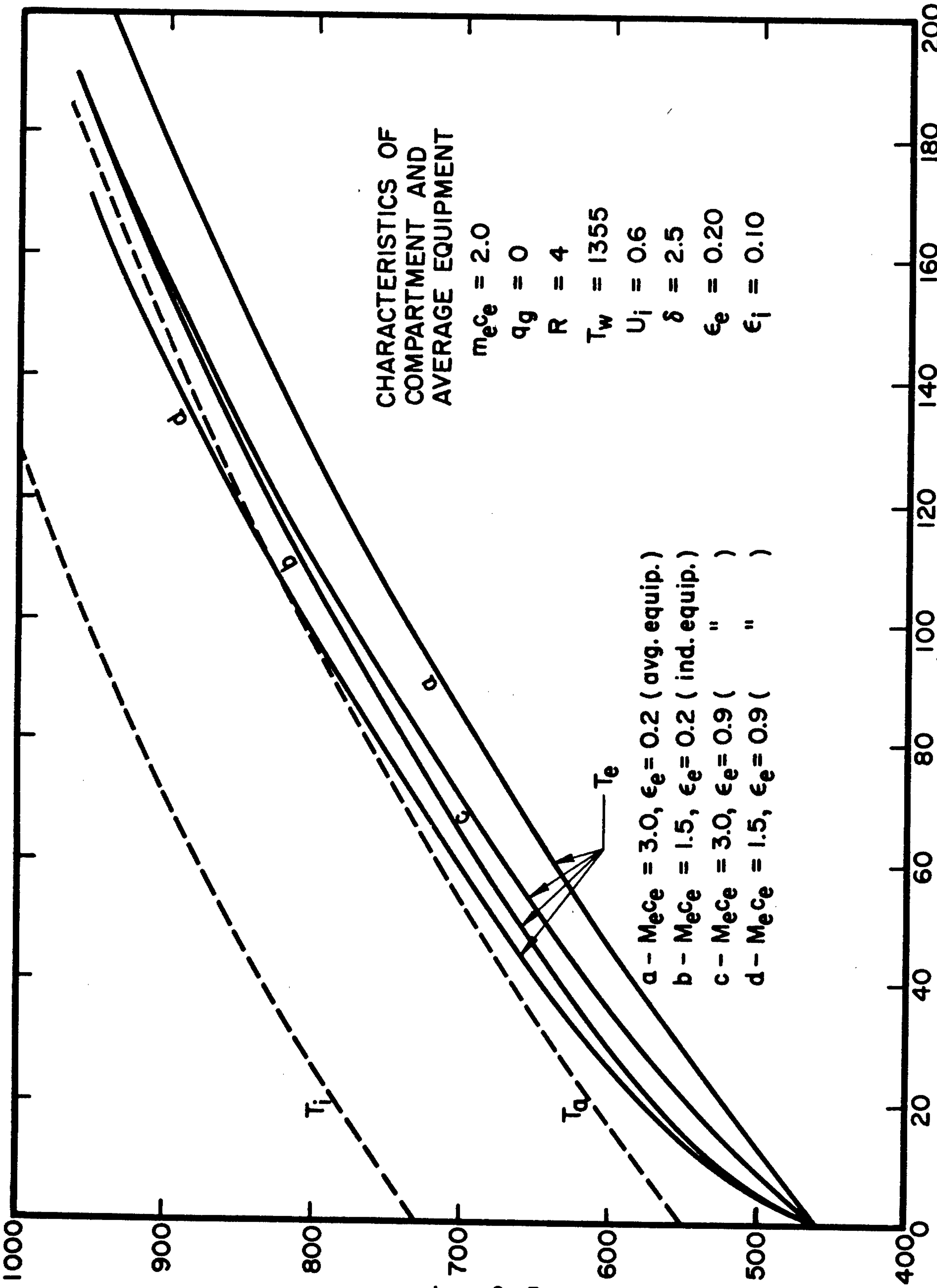

Figure IX-2

Temperature Rise of Individual Equipments Compared to the Average

box can approach the average air temperature and insulation temperature more closely than the average piece of equipment. The smaller values of (T_i-T_e) and (T_a-T_e) result directly from the fact that the box represented by b stores less heat per unit temperature rise than that represented by a. Therefore, for about the same rate of temperature rise the temperature difference for heat transfer is less for b than it is for a.

The plot c represents a box having the average thermal capacity but a higher than average surface emissivity. Whereas the average value for the equipment is $\epsilon_e = 0.2$, plot c is obtained using $\epsilon_e = 0.9$. Both cases assume $\epsilon_i = 0.1$. The strong influence of radiant heat transfer on the equipment temperature rise is evident. This effect would be more pronounced in a compartment having less insulation, since T_i would be greater for a given skin temperature. The plot d represents a box for which $\epsilon_e = 0.9$ and $M_e c_e = 1.5$ are assumed. In this case the individual equipment exceeds the average equipment temperature by as much as 70^oF. Due to its high surface emissivity and low thermal capacity, the individual box of equipment eventually attains a higher temperature than the compartment air. It is important to note that a difference in temperature rise of as much as 70^oF greater than the average can exist in non heat generating equipment. Even greater differences can therefore be expected for individual equipments which have a greater than average heat generation rate.

From the above results it is concluded that individualized cooling of critical equipments has many possible applications. It is particularly applicable where most of the equipment items in a compartment do not need cooling, but where certain critical items do. An item may be critical because of thermal characteristics which cause it to have a greater temperature rise than the average, or it may be critical in that it must be held to lower temperature limits than the average. The increase in temperature rise for cases b, c, and d of Figure IX-2 is a little greater than would actually occur due to neglecting the radiation heat transfer between individual equipments.

2. <u>General Performance with a Coolant Evaporating at Constant Temperature</u>

The general performance in terms of temperature rise is shown for two cases of an equipment using water as the evaporative coolant in Figure IX-3. The characteristics of the compartment and of both the individually cooled and the uncooled equipments are given in the figure. In this and all succeeding figures, the emissivity of the insulation face is taken as $\epsilon_i = 0.10$, while the emissivity of both the cooled and uncooled equipment surfaces is assumed to be $\epsilon_e = 0.20$. In particular, the cooled equipment is assumed in the form of a cubic box, one cubic foot in volume. The coolant is assumed to be vented so as to evaporate at a constant temperature. The initial temperature of the equipment and its coolant is taken as 492^oR so as to avoid the complication of a change of state of the coolant from ice to water. This effect could be included if the initial equipment temperature were below 492^oR, but is omitted here to avoid unnecessary complication.

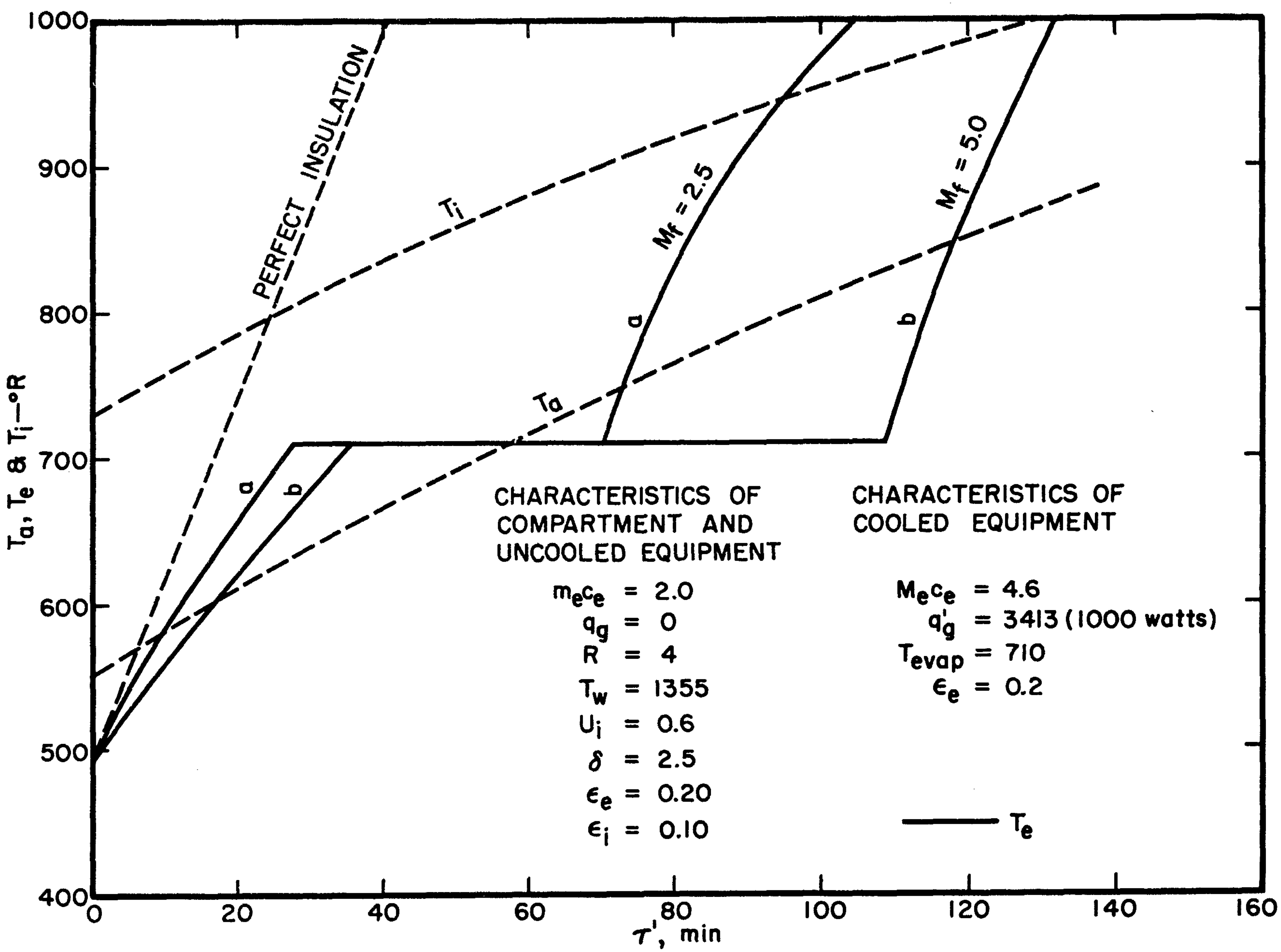

Figure IX-3
General Performance Characteristics for
Constant Temperature Evaporation

From the figure, it is seen that the equipment undergoes an initial heating period, where the temperature rises rapidly due to the combination of radiation, convection, and generated heat loads, all of which are stored in the equipment and coolant thermal capacity with rise in temperature. During this initial period the air temperature is exceeded, indicating that the convection action thereafter gives a cooling effect. As soon as the temperature reaches the saturation temperature for water corresponding to the water pressure, evaporation or boiling of the coolant starts. The combined heat loads are then dissipated by boiling of the water and discharge of the vapor as long as the water lasts. When all of the water is evaporated, the equipment temperature rises, since the heat loads are again stored by the equipment thermal capacity. The duration of the boiling or cooling period depends on the amount of coolant provided and the magnitude of the heat loads to the cooled equipment. Although one case has twice as much coolant as the other, the duration of its constant temperature period is not twice as great, since the average of the convection and radiation heat loads is greater. This is established by inspection of the relative positions of the T_i, T_a, and T_e plots. It is interesting to note that the extended duration of the constant-temperature period is not the sole benefit of more coolant. During the initial heating period, the presence of the greater amount of coolant results in more thermal capacity and a slower temperature rise.

The strong effect of the evaporative coolant is indicated by comparison of the temperature rise plots with the plot for perfect insulation. The latter represents the same equipment if it were provided with no coolant and were perfectly insulated from its surroundings, so that its temperature rise is entirely due to generated heat. The actual rate of temperature rise without any coolant would be even greater than shown for perfect insulation because of external heat loads to the equipment box.

3. Effect of Evaporation Temperature on Equipment Temperature Rise

The effect of evaporation temperature of the coolant on the temperature rise of cooled equipment is shown in Figure IX-4. The characteristics of the compartment, the uncooled equipment, and the cooled equipment are given in the figure. It is assumed that the coolant vapor is vented to a constant pressure discharge in a manner which gives a constant evaporation or boiling temperature for the coolant. The same amount of coolant (water) is provided in all of the cases shown.

Figure IX-4 shows clearly that the time required for the cooled equipment to reach any temperature beyond its coolant evaporation temperature is increased by using a higher coolant evaporation temperature. This is principally due to the increased use of the equipment thermal capacity to store heat during the initial period before boiling of the coolant takes place. There is, however, a small effect due to a lengthening of the period of evaporation at the higher operating temperatures. When a higher evaporation temperature is used, the equipment is at a higher temperature with respect to the compartment air and insulation face temperatures. This results in less external heat load and hence less heat dissipation to be provided by

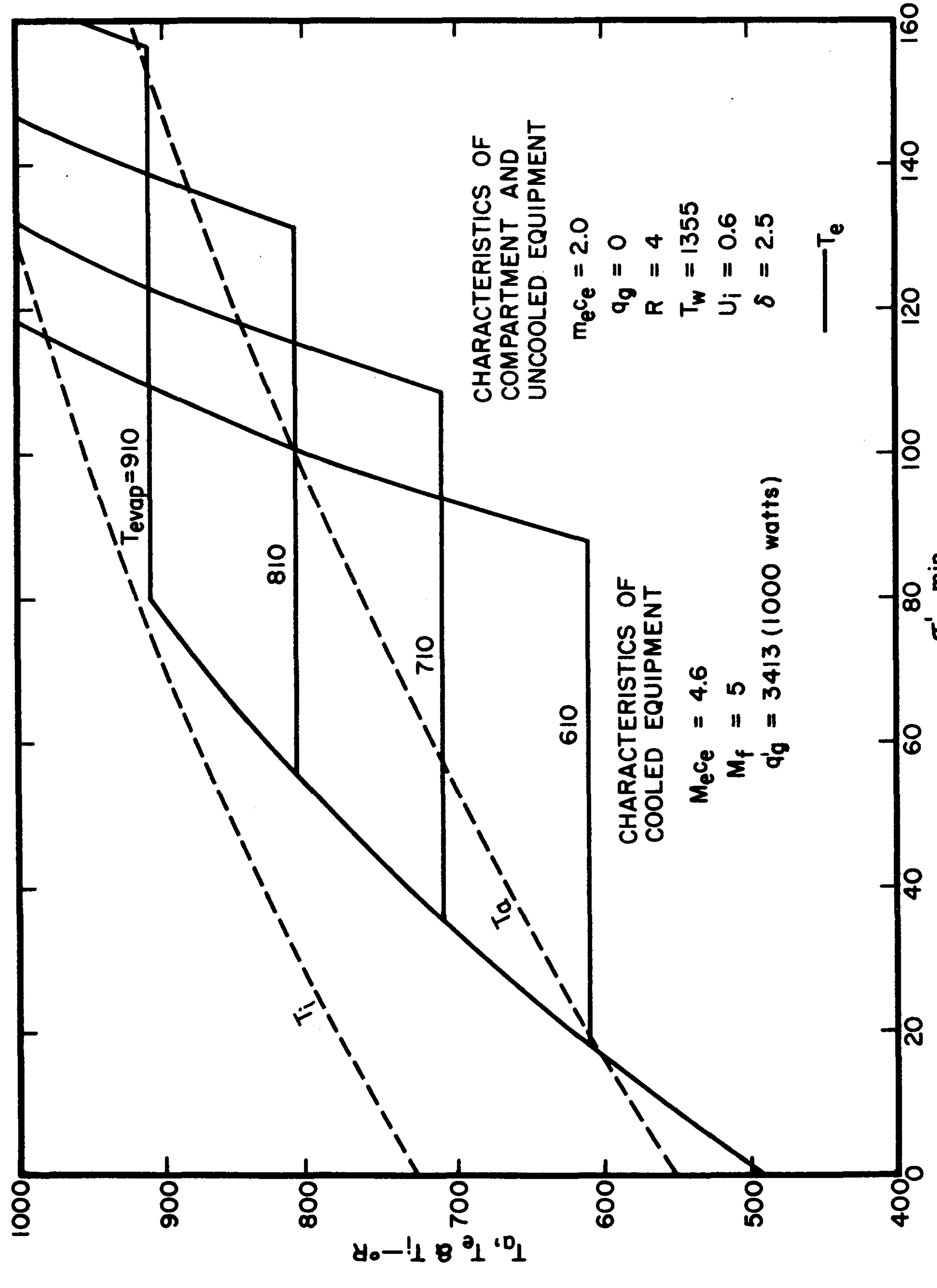

Figure IX-4

Effect of Evaporation Temperature on Equipment Temperature Rise

the coolant. Although the effect of the boiling temperature on the duration of the constant-temperature period is slight for the cases of Figure IX-4, it would be more pronounced for cases of a lower heat generation rate. The tendency for the evaporation period to be prolonged at higher temperatures due to the reduced heat loads may be partially or entirely offset by a reduction in the latent heat of vaporization for the coolant at higher temperatures.

Figure IX-4 shows that in order to achieve the longest possible flight time for a given amount of coolant, an evaporation temperature should be chosen as close as possible to the maximum allowable temperature for the equipment. Since many equipments have a useful operating life that is affected inversely by temperature even when below the maximum allowable temperature, the principle must be applied with caution. An optimum utilization of the coolant occurs when the useful life of the equipment expires at the end of the coolant evaporation period. This optimum condition is an ideal which cannot be realized for equipments except at great risk in the operating reliability. In actual practice, an evaporation temperature should be chosen such that the useful life of the equipment at that temperature somewhat exceeds the duration of the evaporation period. As the factor of safety in this regard is increased, the efficiency in the use of a given amount of coolant is reduced.

It may sometimes be desired to cool several items of equipment by application of an evaporative coolant: If it is desired to use different evaporation temperatures but the same common line for vapor discharge, special pressure regulators must be used in the branches of this line leading from the equipments which operate at the higher temperatures. The main discharge line is then vented through a regulator to a pressure which permits achieving the lowest evaporation temperature of interest. In this way it may be possible to reduce the length and size of piping from that which would be required if each cooled equipment would have a separate vapor discharge line.

4. Effect of Heat Generation Rate of the Cooled Equipment

The effect of heat generation by the cooled equipment on its temperature rise for a given amount of coolant is shown in Figure IX-5. The coolant is water, vented so as to evaporate at a constant temperature of 710°R. The characteristics of the compartment, the cooled equipment, and the uncooled equipment are shown in the figure.

As might be expected, in the cases with a higher heat generation rate the coolant is used up in a shorter time. It should be noted, however, that there is no direct relationship between the time the coolant is all used and the heat generation rate. This is due to the varying effect of the external heat loads as the heat generation rate is changed. For example, in the case where $q_g' = 0$ the equipment temperature is always well below both the compartment air temperature and the insulation face temperature, indicating a substantial external heat load. In the case where $q_g' = 3413$ Btu/hr the equipment temperature is usually above the air temperature, indicating some

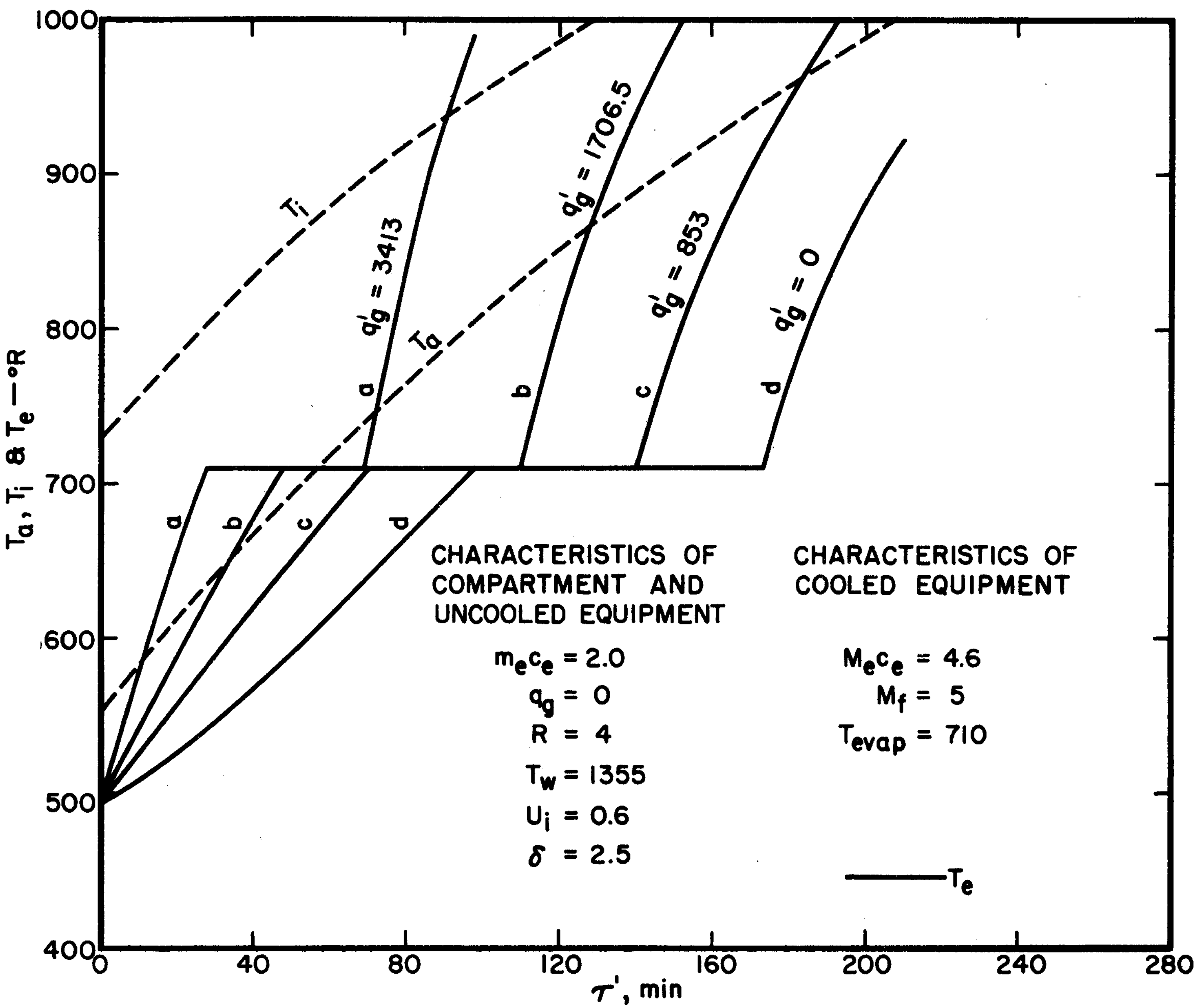

Figure IX-5

Effect of Heat Generation by the Cooled Equipment on Equipment Temperature Rise

cooling due to convection. Since the external heat load is a substantial portion of the total heat load in cases with lower heat generation rates, its variability precludes the use of any simple and direct method of determining coolant requirements. It is therefore necessary to use a design procedure involving trial and error calculations, as discussed later in this Section. It should also be noted from Figure IX-5 that the temperature plot during the initial heating period may be one of increasing or decreasing rate of temperature rise. This variability must be accounted for in a design procedure, since the initial heating period is a significant portion of the total flight time.

5. Effect of Using a Convergent Nozzle to Control the Evaporation Temperature

The effect of using a convergent nozzle to control the coolant evaporation temperature is shown in Figure IX-6. Characteristics of the compartment, the cooled equipment, and the uncooled equipment are shown in the figure. Water is used as the coolant, and the product $a_{th}K$ for the nozzle is assumed to be constant. For the two nozzle sizes shown, it is assumed that the discharge pressure is always 3.718 lb/in.^{2} abs. This gives an initial boiling temperature of 610^{o}R.

To consider either nozzle, as boiling begins the discharge of vapor through the nozzle causes a build-up of pressure on the upstream side. This requires that the temperature of the coolant and the equipment rise so that evaporation may continue. This temperature rise proceeds quite rapidly until the upstream pressure to the nozzle is great enough that the vapor discharge rate and consequently the heat dissipation rate is enough to flatten out the temperature plot. The temperature then rises more slowly as the external heat load rises, until all of the coolant is boiled away. It is seen in the figure that the temperature level at which the slower temperature rise takes place is determined by the nozzle size. A smaller nozzle requires greater upstream pressure to discharge vapor at a given rate, thus requiring a higher operating temperature for similar cooling effects.

Figure IX-6 also shows a comparison of performance for the nozzle-controlled vapor discharge with that for constant pressure evaporation. The lower plot is for constant temperature evaporation at 610^{o}R, which is the temperature where evaporation begins for the nozzle-controlled cases. The upper plot represents constant-temperature evaporation at 714^{o}R, which is the point of coolant exhaustion for the smaller nozzle. These four plots illustrate the same principle as was seen in Figure IX-4. The coolant lasts longer if it is used to dissipate heat at a higher temperature. Further, added use is made of both the equipment and the coolant thermal capacity in the course of heating to greater evaporation temperatures. Since all of the cases of Figure IX-6 have the same amount of coolant, the end points of the periods of coolant evaporation indicate directly the merits of the higher operating temperatures from a coolant standpoint. From the standpoint of equipment reliability, as discussed earlier, operating at lower temperatures may be mandatory.

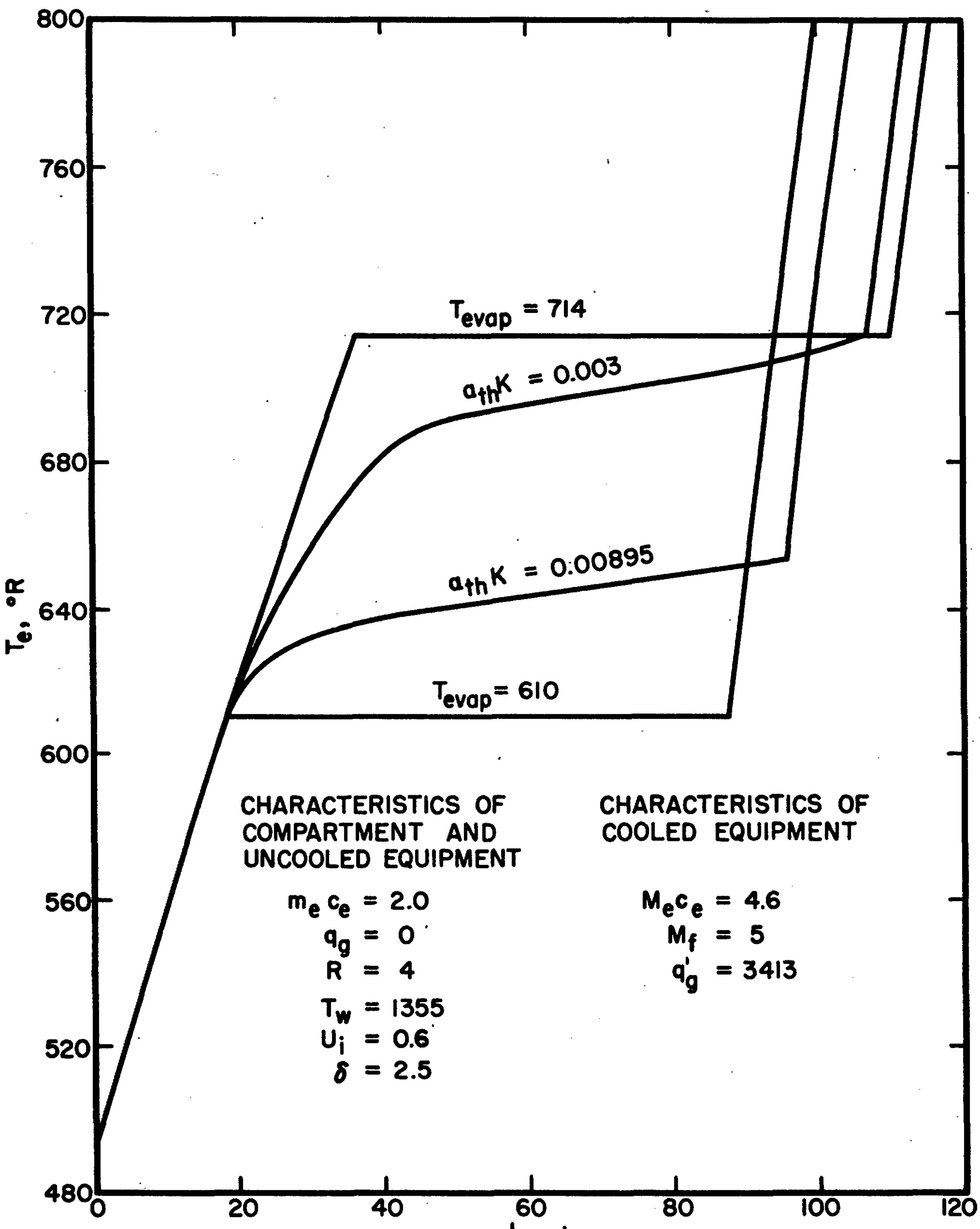

Figure IX-6

Effect of Using a Convergent Nozzle to Control the Evaporation Temperature

It should be pointed out that while the convergent nozzle is a simple control device, a pressure regulator is also simple and quite reliable. There seems, therefore, little reason to use the nozzle-control method in preference to the constant-pressure method. This is particularly true since there is but little difference in flight time afforded for a given amount of coolant when the average operating temperatures for the cooled equipment are comparable in the two control methods.

DESIGN PROCEDURE AND EXAMPLE FOR DETERMINING THE AMOUNT OF COOLANT TO USE

A design procedure and design example are given here for the determination of the amount of coolant required in an application of individualized evaporative cooling. This procedure assumes that the suitability of individualized cooling has already been established, and that the coolant to be used has been selected. Section XI discusses the general problem of selecting cooling systems and should be consulted to determine if this system is suitable before applying the design methods used here. The selection of an evaporative coolant is dependent on many suitability criteria such as latent heat of evaporation, dielectric strength and freezing point. For an extensive discussion of these and other factors the reader is referred to Reference (IX-3). The procedure and example given here are confined to the case of coolant evaporation at a constant temperature.

1. General Description of the Procedure

It should be recalled that the temperature-time plot for an equipment protected by evaporative coolant consists of three parts as shown in Figure IX-7. This design procedure neglects the final part after all of the coolant has evaporated, and assumes that it is desired to select the proper amount of coolant to evaporate at a particular temperature and last to a designated time.

Although the general shape of the temperature-time plot and the design time τ_d are known, the point of initial evaporation b is unknown, and must be assumed. After assuming this point, it is possible to calculate approximately the amount of coolant required to dissipate the heat loads during the constant temperature portion of the flight by using equation (IX-6) in the form

$$M_f = \frac{(q_o' + q_g')(\tau_d - \tau_b)}{H_{fg}} \qquad \text{(IX-14)}$$

and basing the evaluation of q_o' on T_{evap} and T_i and T_a at $(\tau_d+\tau_b)/2$. The determination of the amount of coolant required to give the temperature rise indicated before point b is somewhat more involved. It was noted in connection with Figure IX-5 that the first portion of the plot may be either concave or convex upward. This presents a difficulty in determining an appropriate average equipment temperature to represent the equipment in calculating the external heat load. The method used is based on the geometric principle that a curved line segment of this type must lie between a chord

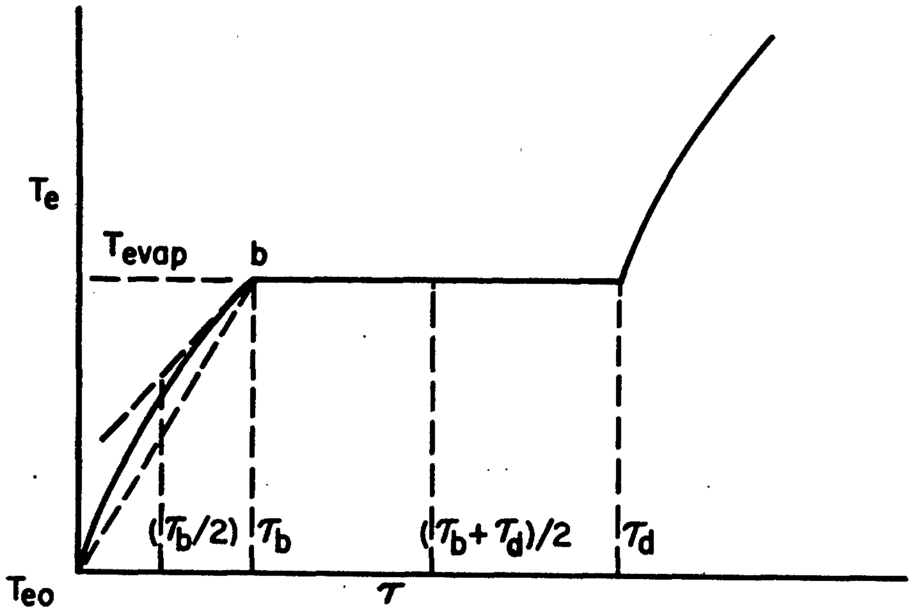

Figure IX-7. Schematic Temperature-Time Plot

to the segment and a tangent to the segment at either of its ends. The equation of the chord line for the example of Figure IX-7 is simply

$$T_{ch} = \left(\frac{T_{evap} - T_{eo}}{\tau_b}\right)\tau + T_{eo}$$

The tangent line for the end of the segment at b requires calculating q_o' as based on T_{evap} and T_i and T_a at τ_b, and is given by

$$T_t = T_{evap} - \frac{(q_o' + q_g')(\tau_b - \tau)}{(M_e c_e + M_f c_f)}$$

It is next assumed that the true equipment temperature lies halfway between T_{ch} and T_t, and that the average of all such values appropriate for determining q_o' in the initial heating period occurs at $\tau = (\tau_b)/2$. When this is done the coolant required for the initial heating period is given approximately by

$$M_f = \frac{(q_g' + q_o')\tau_b}{c_f(T_{evap} - T_{eo})} - \frac{M_e c_e}{c_f} \qquad \text{(IX-15)}$$

If all of the assumptions made in this design procedure were fulfilled,

and if the point b were assumed at its true time, the value of M_f determined by equation (IX-15) would agree with that found by equation (IX-14). When they do not agree, it is necessary to assume a new point b and recalculate until substantial agreement of M_f is reached. If the M_f of equation (IX-15) is greater than that of equation (IX-14) b should be moved to the left, and conversely. When agreement in values of M_f is reached the calculation procedure of the Appendix to this Section (Procedures A and B) are used to obtain an accurate temperature rise evaluation as a check. If the desired performance is not achieved, slight alterations in the amount of coolant can be made for recalculation, although this is usually not necessary.

2. Design Example

An example of the use of the above procedure is given here. The example is used to select the amount of coolant, using water, for the case plotted with $T_{evap} = 910^oR$ in Figure IX-4. This will permit a comparison of the amount of coolant determined by the design procedure with that amount which is known to give the performance desired.

Compartment Characteristics:

constant skin temperature $T_w = 1355^oR$

compartment air pressure $\delta = 2.5$

skin insulation of rock wool, at initial temperature conditions $U_i = 0.6$ Btu/hr-ft^2-^oR

insulation face emissivity $\epsilon_i = 0.10$

Uncooled Equipment Characteristics:

thermal capacity $m_e c_e = 2.0$ Btu/^oR-ft^2

no heat generation, $q_g = 0$ Btu/hr-ft^2

surface emissivity $\epsilon_e = 0.2$

ratio of free convection to radiation heat transfer area R = 4

Cooled Equipment Characteristics:

heat generation $q_g' = 3413$ Btu/hr

coolant evaporation temperature $T_{evap} = 910^oR$

latent heat of coolant $H_{fg} = 774.5$ Btu/lb

thermal capacity $M_e c_e = 4.6$ Btu/^oR

surface area of equipment for free convection heat transfer

$A_c = 6.0 \ ft^2$

surface area of equipment for radiation heat transfer $A_r = 3.96 \ ft^2$

surface emissivity $\epsilon_e = 0.20$

Design Performance:

Equipment is initially at 492^oR.

Water must last for a flight time of 156 minutes.

Calculation:

The compartment air and insulation face temperatures are calculated as explained in the Appendix to this Section. The results of such a calculation are plotted in Figure IX-4 and are used in the example below.

1. Assume the time at which point b occurs.

$$\tau_b = 1.333 \text{ hr}$$

2. Get T_i and T_a at $(\tau_b+\tau_d)/2$

$$(\tau_b+\tau_d)/2 = (1.33+2.6)/2 = 1.965 \text{ hr}$$

or 118 min

$$T_i = 982^oR$$

$$T_a = 845^oR$$

3. Calculate q_o' as based on T_{evap}, T_i, and T_a (details are given in the Appendix to this Section).

$$q_o' = -312 \text{ Btu/hr}$$

(the negative sign indicates heat flow from the equipment to the environment)

4. Calculate

$$M_f = \frac{(q_o' + q_g')(\tau_d - \tau_b)}{H_{fg}}$$

$$M_f = \frac{(-312+3413)(2.60-1.33)}{774.5} = 5.08 \text{ lb}$$

5. Get T_i and T_a at b

$$T_i = 920^oR$$
$$T_a = 765^oR$$

6. Calculate q_o' as based on T_{evap}, T_i, and T_a at b (details are given in the Appendix to this Section)

$$q_o' = -1165 \text{ Btu/hr}$$

7. Calculate

$$T_t = T_{evap} - \frac{(q_o' + q_g')(\tau_b - \tau)}{(M_e c_e + M_f c_f)} \quad \text{at } \tau = (\tau_b)/2$$

$$T_t = 910 - \frac{(-1165+3413)(.667)}{(4.6+5.0)} = 754^oR$$

8. Calculate

$$T_{ch} = \left(\frac{T_{evap} - T_{eo}}{\tau_b}\right)\tau + T_{eo} \quad \text{at } \tau = (\tau_b/2)$$

$$T_{ch} = \frac{910-492}{2} + 492 = 701^oR$$

9. Calculate $T_e = (T_{ch} + T_t)/2$

$$T_e = 728^oR$$

10. Get T_i and T_a at $\tau = (\tau_b/2)$

$$T_i = 835^oR$$
$$T_a = 663^oR$$

11. Calculate q_o' based on T_i, T_a, and T_e from step 9 (details are given in the Appendix to this Section)

$$q_o' = -359 \text{ Btu/hr}$$

12. Calculate

$$M_f = \frac{(q_g' + q_o')\tau_b}{c_f(T_{evap} - T_{eo})} - \frac{M_e c_e}{c_f}$$

$$M_f = \frac{(3413-359)(1.333)}{(910-492) \times 1} - \frac{4.6}{1} = 5.15 \text{ lb}$$

Since the values of step 12 and step 4 are in close agreement, the procedure need not be repeated, and the average of the two values $M_f = 5.12$ lb can be used. Since this example was based on the case of $T_{evap} = 910^oR$ in Figure IX-4, it is apparent that the design procedure is quite accurate in spite of the simplifying assumptions used. As compared to the actual value

of $M_f = 5$ lb, the design value of $M_w = 5.12$ lb is in error by only 2.5 percent.

Some of the calculation labor of the foregoing procedure can be eliminated by using the tangent to the plot of the initial heating period at T_{eo} instead of at b. The equation for this line need not be recalculated for successive values of b. It has been found by experience, however, that this gives less accurate results than the procedure above.

APPENDIX TO SECTION IX

1. Calculation Procedures

Calculation procedures and example calculations are given here for the interval calculations required to evaluate the temperature rise of equipment protected by evaporative coolant. The procedures apply to individually cooled items only, and it is assumed that these items are located in a compartment where there are no other cooling methods employed. The procedures also apply only where the individually cooled equipments represent a small portion of the total contents of the compartment.

The determination of the compartment air temperature and the insulation face temperature is done by the general calculation method in the Appendix to Section V, and is not repeated here. Figure IX-8 shows the environment temperatures determined by such a calculation, using the general compartment and equipment characteristics listed in the figure. This plot is used as the basis for calculating the external heat loads to the equipment with evaporative coolant in all of the subsequent examples.

Procedure A: Calculation for Periods when no Coolant Evaporates

Given Data:

compartment and uncooled equipment characteristics as shown in Figure IX-8

thermal capacity of cooled equipment $M_e c_e = 4.6$ Btu/^oR

heat generation of cooled equipment $q_g' = 3413$ Btu/hr

weight of coolant (water) $M_f = 5.0$ lb

total surface area of box available to free convection $A_c = 6.0$ ft^2

total surface area of box available to radiation $A_r = 3.96$ ft^2

surface emissivities $\epsilon_i = 0.10$, $\epsilon_e = 0.20$

characteristic dimension of cooled box $L = 1$ ft

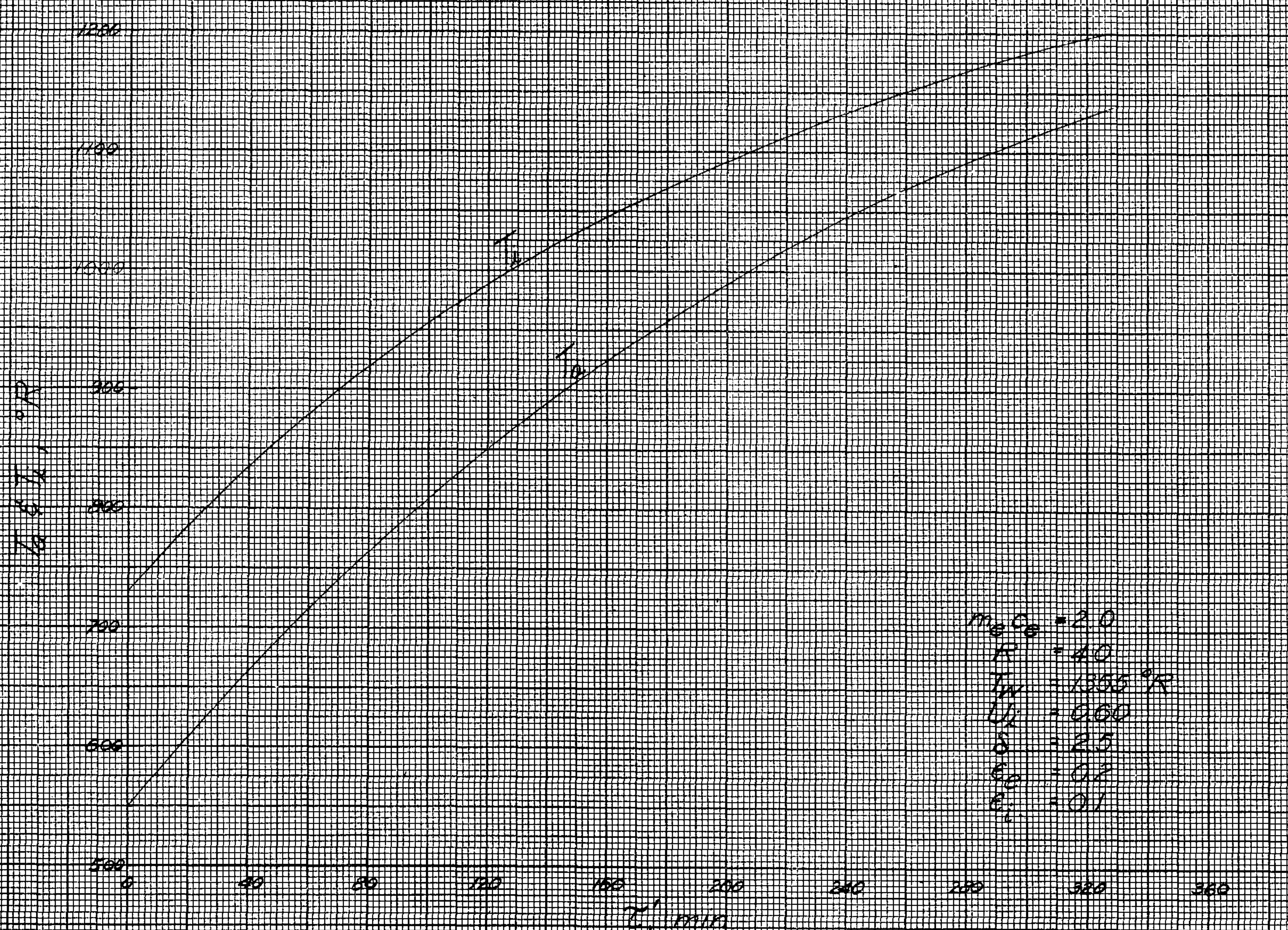

Figure IX-8

Environmental Temperatures for Use in Calculations

compartment pressure $\delta = 2.5$

$T_{e1} = 492^\circ R$ when $\tau = 0$

1. Select τ and assume T_{e2}

$$\tau = 0.0834 \text{ hr}$$
$$T_{e2} = 525.5^\circ R$$

2. Calculate $T_{em} = \dfrac{T_{e1} + T_{e2}}{2}$

$$T_{em} = 508.7^\circ R$$

3. Get T_{i1}, T_{a1}, T_{i2} and T_{a2} from Figure IX-8.

$$T_{i1} = 731^\circ R$$
$$T_{a1} = 551^\circ R$$
$$T_{i2} = 743^\circ R$$
$$T_{a2} = 565^\circ R$$

4. Calculate $T_{im} = \dfrac{T_{i1} + T_{i2}}{2}$ and $T_{am} = \dfrac{T_{a1} + T_{a2}}{2}$

$$T_{im} = 737^\circ R$$
$$T_{am} = 558^\circ R$$

5. Calculate

$$h_r = 17.4\text{x}10^{-4}\left(\frac{1}{\frac{1}{\epsilon_i} + \frac{1}{\epsilon_e} - 1}\right) B$$

taking B from Figure AIV-1 based on T_{im} and T_{em}

$$h_r = 17.4\text{x}10^{-4}\text{x}.0715\text{x}1000 = 0.124 \text{ Btu/hr-ft}^2\text{-}^\circ R$$

6. Calculate $q_r' = h_r A_r (T_{im} - T_{em})$

$$q_r' = .124\text{x}4\text{x}228.3 = 113.2 \text{ Btu/hr}$$

7. Calculate $(T_{am}+T_{em})/2$ and get $(a'L^{1/4}/\delta^{1/2})$ at this mean temperature from Figure AIV-3.

$$\frac{a'L^{1/4}}{\delta^{1/2}} = 0.2832$$

8. Calculate $h_c = \left(\dfrac{a'L^{1/4}}{\delta^{1/2}}\right)\left(\dfrac{\delta^{1/2}}{L^{1/4}}\right)(T_{am}-T_{em})^{1/4}$

$$h_c = .02832\text{x}1.58\text{x}49.3^{1/4} = 1.185 \text{ Btu/hr-ft}^2\text{-}^\circ R$$

9. Calculate $q_c' = h_c A_c (T_{am} - T_{em})$

$$q_c' = 1.185 \times 6 \times 49.3 = 350 \text{ Btu/hr}$$

10. Calculate $q_o' = q_r' + q_c'$

$$q_o' = 463.2 \text{ Btu/hr}$$

11. Get c_w at T_{em} from Figure IX-9.

$$c_w = 1.00 \text{ Btu/lb-}^{\circ}\text{R}$$

12. Calculate

$$\Delta T_e = \frac{(q_o' + q_g')\,\Delta\tau}{(M_e c_e + M_f c_f)}$$

$$\Delta T_e = \frac{3876.2 \times 0.0834}{4.6+5} = 33.7^{\circ}\text{R}$$

13. Calculate $T_{e2} = T_{e1} + \Delta T_e$

$$T_{e2} = 525.7^{\circ}\text{R}$$

This result should agree with the value assumed in step 1 within 6°R, otherwise repeat the calculation, using the calculated value as the assumed value in the next trial.

The value of M_f is taken as zero if no coolant is present, as, for instance, during the period after all of the coolant has evaporated.

Procedure B: Calculation for Periods of Coolant Evaporation at Constant Temperature

Given Data:

All data are the same as in Procedure A. In addition, the coolant (water) is vented such that its boiling temperature is 710°R.

enthalpy of vaporization at 710°R $H_{fg} = 945.5$ Btu/lb

Steps 1 through 10 are identical to Procedure A, except that T_e is constant. Making the calculation for q_o' as based on the time interval from $\tau = 0.5935$ hr to $\tau = .75$ hr gives $q_o' = -156$ Btu/hr as the result to step 10.

11. Calculate $\Delta M_f = \dfrac{(q_g' + q_o')\,\Delta\tau}{H_{fg}}$

$$\Delta M_f = \frac{(3413-156)\ .1565}{945.5} = 0.54 \text{ lb}$$

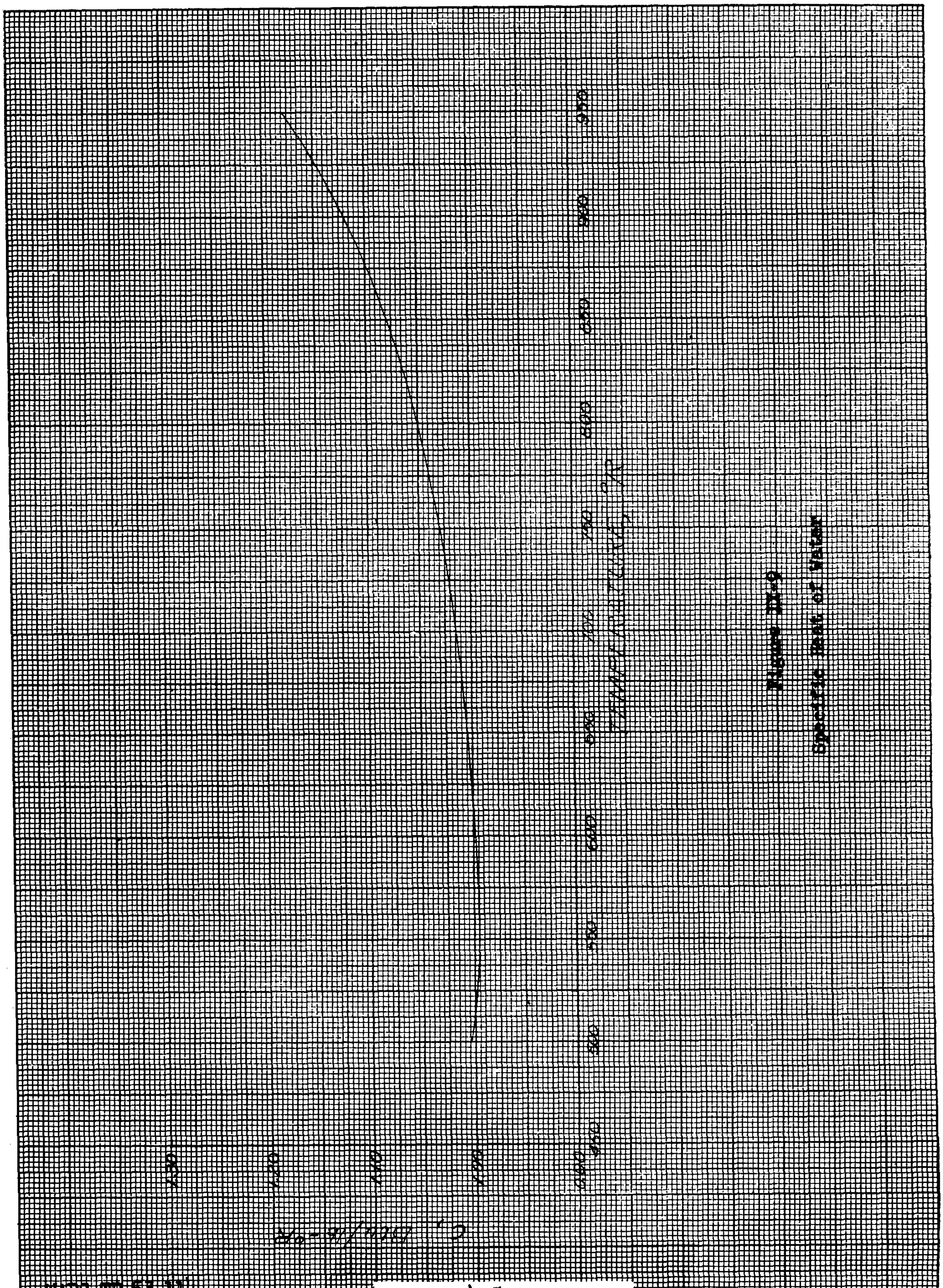

Figure IX-9

Specific Heat of Water

12. Calculate $\sum(\Delta M_f)_n$ for the n intervals calculated during evaporation, ending with the current one. When the sum equals M_f of the given data the evaporation process is completed.

Procedure C: Calculation of Temperature Rise for Periods of Coolant Evaporation Controlled by a Convergent Nozzle

Given Data:

All data are the same as in Procedure A. In addition, the coolant is vented such that the initial boiling temperature is $610^\circ R$. The discharging coolant vapor passes through a convergent nozzle for which $(a_{th}K) = 0.003\ in^2$. Data on the properties of steam and water are taken from Reference (IX-2).

Volume of coolant container $V = .0817\ ft^3$

Part 1: Determination of the Nozzle Performance Curve

Given Data:

$p_2 = 3.718\ lb/in^2$

1. Select a value of $p_1 > p_2$ at desired intervals

$$p_1 = 4.519\ lb/in^2$$

2. Get v_1 corresponding to saturated steam at p_1 from a chart or steam tables.

$$v_1 = 80.84\ ft^3/lb$$

3. Get T_e as the saturation temperature corresponding to p_1

$$T_e = 618^\circ R$$

4. Calculate (p_2/p_1)

$$(p_2/p_1) = .08224$$

5. If $(p_2/p_1) > 0.58$, calculate

$$\frac{W_f}{a_{th}K} = 7090\sqrt{\left(\frac{p_1}{v_1}\right)\left[\left(\frac{p_2}{p_1}\right)^{1.77} - \left(\frac{p_2}{p_1}\right)^{1.89}\right]}$$

$$\frac{W_f}{a_{th}K} = 214\ lb/hr\text{-}in^2$$

6. If $(p_2/p_1) \leq 0.58$ calculate $(W_f/a_{th}K) = 1080\sqrt{(p_1/v_1)}$

$$\frac{W_f}{a_{th}K} = \_\_\_\_ \text{ lb/hr-in}^2$$

7. Plot $(W_f/a_{th}K)$ vs. T_e

This procedure is repeated to cover the range of values of T_e of interest. The plot is shown in Figure IX-10, and used in Part 2 given below.

Part 2: Evaluation of Equipment Temperature Rise

Given Data:

Vaporization has just started, so that $M_f = 5$ lb at the beginning of the interval, and $T_{e1} = 610^oR$

Steps 1 through 10 are identical to those of Procedure A. Calculation for the interval from $\tau = .308$ hr to $\tau = .333$ hr gives the external heat load as $q_o' = 91$ Btu/hr (assuming $\Delta T_e = 8^o$)

11. Get $(W_f/a_{th}K)$ for T_{em} and calculate W_f

at 614^oR, $(W_f/a_{th}K) = 164$ lb/hr-in^2

$$W_f = 164x.003 = .492 \text{ lb/hr}$$

12. Get H_g from steam tables at T_{em} and calculate $q_v' = W_f H_g$

$$H_g = 1128 \text{ Btu/lb}$$
$$q_v' = .492x1128 = 555 \text{ Btu/hr}$$

13. Calculate $(M_{f2})_n = (M_{f2})_{n-1} - \left[W_f \Delta\tau\right]_n$ where n denotes current interval, n-1 denotes previous interval.

$$(M_{f2})_n = 5-.492x.025 = 4.988 \text{ lb}$$

14. Get v_f and v_{fg} at T_{e2} and calculate

$$x = \frac{V - M_{f2}\, v_f}{M_{f2}\, v_{fg}}$$

$$v_f = .01638 \text{ ft}^3\text{/lb}$$
$$v_{fg} = 79.2 \text{ ft}^3\text{/lb}$$
$$x = \frac{.0817-4.988x.01638}{4.988x79.2} = 4x10^{-7}$$

15. Get H_f and H_{fg} at T_{e2} from steam tables, and calculate

$$M_{f2}H_c = M_{f2}(H_f + x\, H_{fg})$$

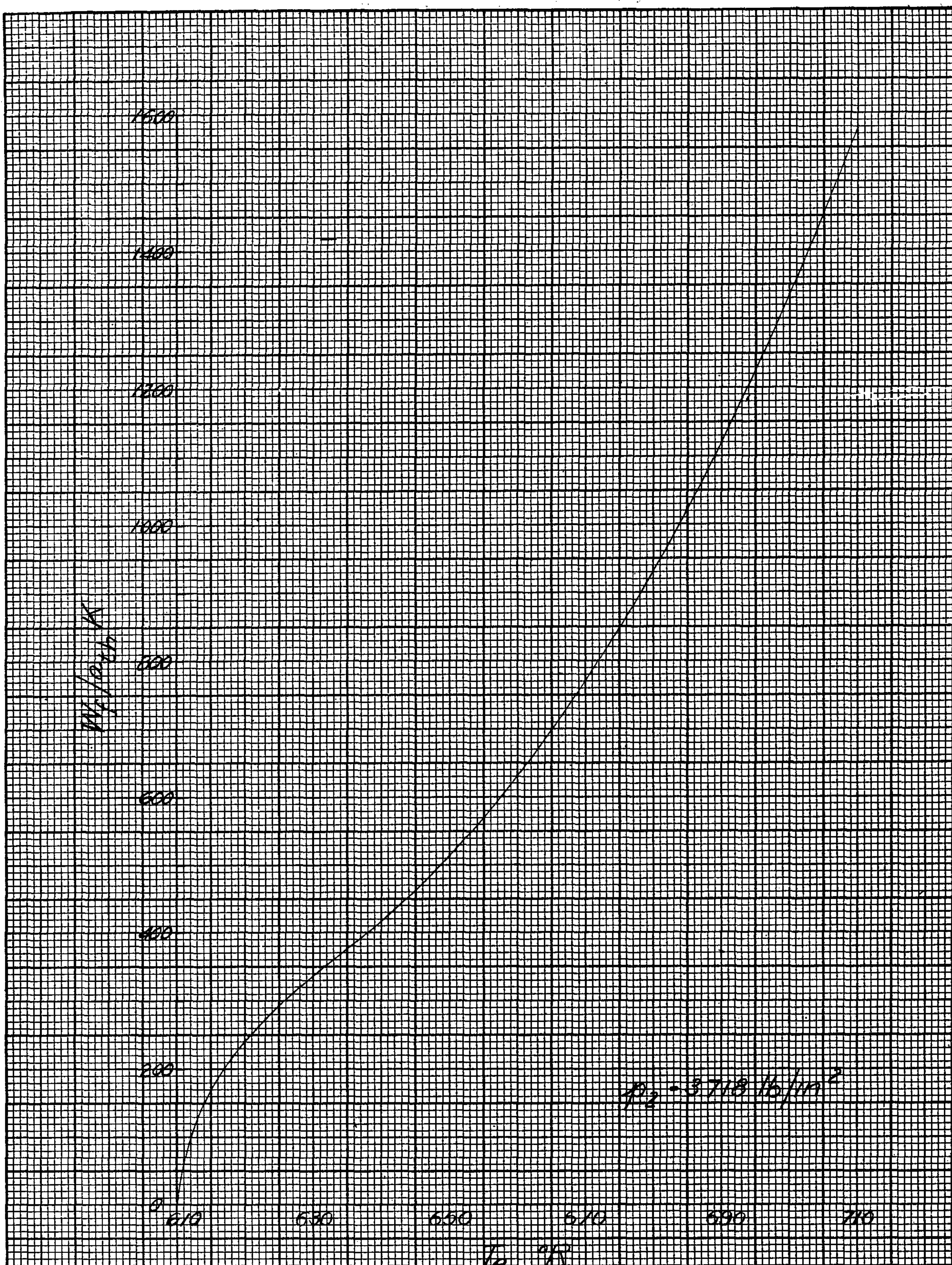

Figure IX-10

Typical Nozzle Performance Plot

$$H_f = 126.6 \text{ Btu/lb}$$
$$H_{fg} = 1003 \text{ Btu/lb}$$

$$(M_{f2}H_c) = 4.988 \text{x} 126.7 = 631 \text{ Btu}$$

16. Calculate $\Delta(M_{f2}H_c) = \left[(M_{f2}H_c)_n - (M_{f2}H_c)_{n-1}\right]$

$$\Delta(M_{f2}H_c) = 631 - (5\text{x}118.6) = 38 \text{ Btu}$$

17. Calculate

$$\Delta T_e = \frac{[q_o' + q_g' - W_f H_g]\,\Delta\tau - \Delta(M_{f2}H_c)}{M_e c_e}$$

$$T_e = \frac{.025\,[91+3413-555] - 38}{4.6} = 7.84^{\circ}R$$

18. Calculate $T_{e2} = T_{e1} + \Delta T_e$

$$T_{e2} = 617.8^{\circ}R$$

This must agree with the value assumed in step 1, otherwise repeat the procedure to convergence of the assumed and calculated values. The value of T_{e2} thus determined is the value of T_{e1} for the next interval.

2. References

(IX-1) Barnard, W. H., Ellenwood, F. O. and Hirschfeld, L. F. Elements of Heat Power Engineering Part II. Third Edition. John Wiley and Sons, Inc., New York, 1933, p. 16.

(IX-2) Keenan, J. H. and Keyes, F. G. Thermodynamic Properties of Steam. First Edition. John Wiley and Sons, Inc., New York, 1946.

(IX-3) Robinson, W. and Zimmerman, R. H. Methods for the Ultimate Dissipation of Heat Originating with Airborne Electronic Equipment. United States Air Force Technical Report No. 6493, United States Air Force, Air Materiel Command, March 1951, pp. 73-90.

SECTION X

TEMPERATURE RISE OF EQUIPMENT COMPONENTS WITH INSULATION AND WITH OR WITHOUT EVAPORATIVE COOLANT

By T. C. Taylor and Y. H. Sun

One method which can sometimes be used to limit the temperature rise of individual equipment components is to cover them with insulation. In this way the individual component is partially protected from external heating effects. Insulation used for this purpose is to be distinguished from that used on the aircraft skin to protect all of the equipment in the compartment. This more general use of insulation is discussed in Section V. The individual application of insulation provides no cooling effect, and therefore has limited value in cases where the individual component considered generates heat. In such cases the insulation may hinder the normal cooling effects of free convection somewhat. Since insulation and evaporative cooling are both applicable to individual components, they can be studied in some applications using both to determine whether it is better to use one or the other. Methods are developed in this Section to evaluate the temperature rise of individual equipments, using insulation both with and without evaporative cooling. The analysis is in both cases confined to the operation of such individual components in compartments which are not cooled. The methods are general and applicable to the use of any insulation effect for which the physical and thermal properties are known. Any evaporative coolant may also be used, provided its thermal and physical properties are known and provided it boils at a constant temperature when held at constant pressure during boiling. Because of the many independent variables present in the use of both individual insulation and evaporative coolant, no attempt is made to determine exact limits of applicability of these methods or to explore all of their independent and combined possibilities. Rather, stress is laid on the development of a suitable analytical method which the reader may apply to the smaller range of possible applications of interest to him.

SUMMARY

The use of insulation is considered, as applied to individual components for a means of protection against excessive temperature rise. Cases are studied in which the insulation is the only protective means as well as cases in which the component is also cooled by an evaporative coolant. It is assumed that the components thus protected are located in compartments containing other unprotected equipment components. These other equipments are assumed to dominate the heat transfer processes of the compartment, and thus determine the environmental temperatures to which the specially protected components are subjected. Where an evaporative coolant is used, it is controlled so as to evaporate at constant temperature. The external heat loads to the equipment are assumed to consist entirely of free convection and radiation heat transfer. The thermal capacity of both the skin insula-

tion and the compartment air is neglected, but the thermal capacity of the component insulation is included in the analysis. It is assumed that a reflective outer face is used on the component insulation to reduce the radiant heat load.

Equations are given to describe the external heat load by radiation and free convection. Equations are then presented to describe heat conduction through the component insulation, allowing for the thermal capacity of that insulation and its resulting heat absorption with rising temperature. An equation is also given based on the methods of Section IX to describe the evaporation rate when an evaporative coolant is used. Calculation procedures are developed which employ these equations in a step-wise application to evaluate the temperature rise of an individually insulated component, either with or without the added protection of an evaporative coolant.

A number of calculation results are given to show the temperature rise of individual components which are insulated. Other results are shown for cases in which evaporative coolant is used together with insulation. In these cases the insulation is used to replace a portion of the coolant equal in volume to that of the insulation. The salient conclusions based on the results of these calculations are summarized as follows:

1. The application of insulation to a non-heat generating component reduces the temperature rise of the component by an amount which is approximately proportional to the thickness of the insulation. In one particular case, the use of 1/2 in. of 36-lb/ft^3 asbestos-felt insulation reduces the temperature rise of the component so that it is approximately 70°F below the temperature of a similar component without special insulation during most of a flight of 220 minutes duration. Since both components are initially at the same temperature, some time is required to establish the temperature difference. A significant portion of this reduction of temperature rise is due to the insulation thermal capacity as distinguished from its insulating effect. The use of insulation on heat generating components may be inadvisable, since the insulation hampers the free convection cooling effect when the component is at a higher temperature than the compartment air.

2. Asbestos insulation should not be used to replace water as an evaporative coolant on an equal volume basis. The reduction in external heat load due to the insulation is not sufficient to replace the loss in cooling capacity. Therefore the remaining coolant is used up in a shorter flight time than if all of the available volume of insulation and coolant were used for coolant alone. This conclusion holds for both heat generating and non-heat generating components. In the case of the former, the reduction in flight time resulting from replacing some of the coolant with insulation is more severe. From the standpoint of space requirements, use of evaporative coolant is, therefore, a more effective means of protecting components against excessive temperature rise than insulation. It is emphasized that this conclusion is based on the study of asbestos insulation and water as evaporative coolant. Some

operating conditions, such as an extremely low initial temperature or need for good dielectric properties may prevent the use of water as an evaporative coolant. In such cases it may be necessary to use a coolant having a much lower ratio of latent heat to volume than that of water, giving a smaller value of cooling effect per unit volume of coolant. It is therefore possible that in that case the use of individual insulation would be more effective than the use of coolant on a unit volume basis.

3. The use of individual insulation instead of evaporative coolant where the former can provide satisfactory protection has three significant advantages. First, the insulation requires no control apparatus or piping, and thus does not require the use of compartment space for these items. Second, the simple nature of the insulation insures absolute operational reliability. Third, the insulation can usually be applied externally without substantial alterations to the design of the protected component. A proper application of evaporative coolant, on the other hand, requires that the component and coolant container be integrally designed so as to insure good cooling effect by means of adequate thermal conductance between all parts of the component and the coolant. If the component is to be cooled by immersion, the container must be properly designed to give adequate coolant sealing effects without interfering with component operation. This is a method not as easily applied to existing equipments, or problems of modification, as is insulation.

ANALYSIS

1. Assumptions for Analysis

As in the analysis of components protected by evaporative coolant of Section IX, it is assumed here that the components considered for special analysis are a small portion of all the equipment in a compartment. The environment temperatures of the compartment are therefore assumed to be established by all of the other equipments, and these temperatures are used in determining the external heat loads to the special equipments considered here. These external heat loads are assumed to consist of radiation heat exchange with the skin insulation and free convection heat exchange with the compartment air. It is assumed that the individual component does not exchange heat by radiation with nearby components. In addition to the external heat loads, heat generation by the specially protected component is considered.

As in the earlier analyses, the thermal capacity of the compartment air and the skin insulation is neglected. The thermal capacity of insulation on an individual equipment is included in the analysis, however. This is particularly necessary when considering small insulated items, where an insulation of any worthwhile thickness is likely to have a thermal capacity which is appreciable in comparison to that of the equipment which it protects. It is assumed that insulation placed on the equipment has an outer

facing of some reflective material, such as aluminum foil, in order to reduce the radiation heat load. This precaution is necessary because of the high emissivity of some insulating materials. In analyzing radiant heat transfer from Section V onward it has been invariably assumed that the skin insulation is faced in this manner.

In writing the heat conduction equations for the component insulation, it is assumed that the two faces of the insulation are of equal area, so that the simple equations for a plane wall may be used. Thus, if the insulation covers a body such as a cube, it is assumed that the insulation thickness is small compared to the dimensions of the cube.

Whenever insulation and evaporative coolant are used together, the constant temperature method of evaporation control is used for the coolant. This method assumes that the coolant vapor is discharged through a pressure regulator, which maintains the pressure in the coolant container constant.

The equations are developed in a general form suited to the use of any insulating material and any coolant, provided the coolant is a pure substance and evaporates at constant temperature when under constant pressure. For simplicity, in the calculations which follow the equations are all based on the use of water as evaporative coolant and asbestos felt insulation.

2. Nomenclature

Symbol	Definition	Units
A	Area	ft^2
a'	Convection group, used in equation (X-2)	
c	Specific Heat	Btu/lb-°R
H	Enthalpy	Btu/lb
h	Heat transfer coefficient	Btu/hr-ft^2-°R
k	Thermal conductivity	Btu/hr-ft-°R
L	Characteristic length for free convection	ft
M	Weight	lb
m	Weight based on unit area	lb/ft^2
q'	Heat transfer rate	Btu/hr
q"	Heat absorption rate	Btu/hr-ft^3
T	Absolute temperature	°R

Symbol	Definition	Units
U	Conductance	Btu/hr-ft^2-$^\circ$R
x	Thickness	ft
x'	Thickness	in.
γ	Weight density	lb/ft^3
δ	Pressure	atmospheres (dimensionless)
ϵ	Emissivity	dimensionless
τ	Time	hr
τ'	Time	min

Subscripts

a	Denotes compartment air
c	Denotes convection value
e	Denotes equipment or equipment component
evap	Denotes evaporation temperature
f	Denotes coolant in general
fg	Denotes change of state from liquid to vapor
g	Denotes generated value
i	Denotes insulation
L	Denotes component face of insulation on component
m	Denotes average value for a time interval
n	Denotes the n th time interval
o	Denotes external value or initial value when used as a second subscript
r	Denotes radiation value
s	Denotes outside face of component insulation
si	Denotes storage value for component insulation

Subscripts, continued

w	Denotes skin
1,2	Denotes initial and final values, respectively, for a time interval

3. Derivation of Equations

a. External Heat Load

The external heat load due to radiation and free convection to a box covered with insulation is calculated in the same way as in Section IX except for a slight change in nomenclature. When insulation is used on the equipment, the temperature of the surface exposed to the environment is T_s, so that the equation for radiation heat transfer becomes

$$q_r' = h_r A_r (T_i - T_s) \qquad \text{(X-1)}$$

where

$$h_r = 17.4\times10^{-4}\left(\frac{1}{\frac{1}{\epsilon_i}+\frac{1}{\epsilon_s}-1}\right)\left[\frac{\left(\frac{T_i}{100}\right)^4-\left(\frac{T_s}{100}\right)^4}{\left(\frac{T_i}{100}\right)-\left(\frac{T_s}{100}\right)}\right]$$

and where the function of temperatures is given in Figure AIV-1.

Similarly, the free convection heat transfer between the equipment and the compartment air is given by

$$q_c' = h_c A_c (T_a - T_s) \qquad \text{(X-2)}$$

where

$$h_c = \left(\frac{a' L^{1/4}}{\delta^{1/2}}\right)\left(\frac{\delta^{1/2}}{L^{1/4}}\right)(T_a - T_s)^{1/4}$$

for the quantity $(a' L^{1/4}/\delta^{1/2})$ evaluated at $(T_a+T_s)/2$.

In keeping with the practice of Section IX, equations (X-1 and -2) are used together with a plot of T_i and T_a vs. τ found as in Section V, to calculate the external heat loads.

b. Heat Transfer Through the Component Insulation

Heat transfers from the outer surface of the component insulation at T_s to the inner surface at T_e by solid conduction. This heat conduction cannot be treated by the simple conduction equation in a case where

these temperatures are changing, however, because of the thermal capacity and resulting heat absorption by the insulation. It can be shown that for the case of heat absorption in a solid, the rate of heat conduction into the high temperature face is given by

$$q_o' = U_i A_e (T_s - T_e) + q_{si}''' \left(\frac{A_e x_i}{2}\right) \qquad (X-3)$$

where q_{si}''' is the time rate of heat absorption per unit volume in the solid. Similarly, the rate of heat conduction out of the low-temperature face is given by

$$q_L' = U_i A_e (T_s - T_e) - q_{si}''' \left(\frac{A_e x_i}{2}\right) \qquad (X-4)$$

For a basic derivation of these physical laws the reader is referred to Reference (X-1).

Heat is absorbed in the insulation due to a temperature rise. Although equations (X-3 and -4) are for the case of a uniformly distributed heat absorption rate, an approximation can be used based on the average temperature rise in the form

$$q_{si}''' = \gamma_i c_i \left(\frac{\Delta T_e + \Delta T_s}{2\,\Delta\tau}\right) \qquad (X-5)$$

This can then be used in equations (X-3 and -4), where T_e and T_s are changed to average the values T_{em} and T_{sm} for the time interval $\Delta\tau$. The value of q_L' given by equation (X-4) is the heat transfer rate to the insulated equipment. It is this heat load which is received by the equipment and its coolant, if any.

c. Heat Balance for the Equipment

During periods when no coolant is being evaporated, the heat balance equation for the equipment is

$$(q_g' + q_L') = (M_e c_e + M_f c_f) \left(\frac{\Delta T_e}{\Delta\tau}\right) \qquad (X-6)$$

In applying this equation, M_f is zero if there is no coolant.

The heat balance for periods of coolant evaporation at constant temperature is

$$(q_g' + q_L')\,\Delta\tau = (\Delta M_f\, H_{fg}) \qquad (X-7)$$

where ΔM_f is the weight of coolant evaporated during a time interval $\Delta\tau$ in length.

4. Calculation Procedure

a. General Method

The form of the equations developed above requires the use of a stepwise calculation procedure to evaluate the temperature rise of equipment protected by insulation and with or without evaporative coolant. It is possible to calculate all of the heat transfer and heat storage rates based on temperature conditions at the beginning of a time interval. These can then be used to predict the temperatures prevailing at the end of the time interval. When using this method, the size of the time interval must be small to obtain accurate results. A more accurate method is to calculate the heat transfer and heat storage rates based on the average temperature conditions for a time interval. Since the average temperatures are not known when starting the interval calculation, they must be assumed and checked later. This method therefore involves trial and error calculations. Because of its greater accuracy, this method is described here.

b. Determination of the Compartment Environment Temperatures

Before the temperature rise of specially protected components can be calculated, it is necessary to determine the face temperature of the skin insulation and the compartment air temperature. The variation of these temperatures with time is determined as described in Sections IX and V. When the calculation is completed, a plot of T_i and T_a versus τ is prepared and used in the subsequent procedures.

c. Temperature Rise of Components Without Coolant Evaporation

The procedure described here applies to periods of operation in which there is no evaporation of coolant. To begin calculation for a time interval, it is necessary to assume values for the final temperatures of the equipment and the final face temperature on the component insulation. These are then used with the initial values for the interval to calculate average temperatures, such as $T_{sm} = (T_{s1}+T_{s2})/2$. The values of T_{i2} and T_{a2} are then found from the plot of the previous calculation for the end of the time interval, and used to calculate T_{im} and T_{am}. When all of these average temperatures are found, the radiation and free convection heat loads are calculated using equations (X-1 and -2). The surface areas A_r and A_c required for this purpose are defined in Section IX.

Equation (X-5) is used next to calculate q''_{si}, and q_L is determined by the relationship

$$q'_L = q'_o - q''_{si}(A_e x_i)$$

which is obtained by combining equations (X-3 and -4).

Equation (X-6) is next solved for ΔT_e, and T_{e2} is calculated from

$T_{e2} = T_{e1} + \Delta T_e$. This value should be in substantial agreement with the value assumed at the start of the interval calculation.

The average insulation temperature $(T_{sm}+T_{em})/2$ is found next, and the component insulation conductance is evaluated at this temperature from

$$U_i = (k_i/x_i)$$

Equation (X-3) can then be used to calculate q_o', which should agree with the value of external heat load due to radiation and convection as found earlier. If T_{e2} is found to be substantially correct, but q_o' is in error, the value of T_{sm} must be revised in the next trial. In doing this, it should be observed that reducing T_{sm} gives a greater value of q_o' as determined for radiation and free convection, and conversely. Also, reducing T_{sm} reduces the value of q_o' determined by equation (X-3), and conversely, provided that $T_{sm} > T_{em}$. Agreement on both q_o' and T_{e2} must be achieved before the interval calculation is finished.

The calculation described above is rather difficult, and it is recommended that a plot of T_{e2} and T_{s2} be kept by the computor and used to extrapolate for assumed values. The external heat loads are quite accurate for time intervals representing changes of T_i of as much as 40°F. The accuracy of the temperature rise of equipment is therefore dependent on the degree of accuracy insisted, upon in obtaining agreement for q_o' by the two calculations used. The special methods required to determine the initial temperatures for the first interval are given in the Appendix to this Section, together with a detailed procedure and example of the above interval calculation. If this calculation is used for a case using evaporative coolant, the last interval of the initial period of temperature rise must be just the right length so that $T_{e2} = T_{evap}$. This interval will therefore in general require more trials for its successful calculation than the others.

d. Calculation for the Period of Constant Temperature Evaporation

The procedure described here applies to periods of operation when a coolant is evaporating at constant temperature, and therefore holding the equipment temperature constant. The external heat load is calculated as before, based on T_{am}, T_{im} and T_{sm}. Since T_{am} and T_{im} are available from a plot by previous calculation, and since T_e is constant and equal to T_{evap}, it is only necessary to assume values for T_{s2}. With q_o' determined, q_{si}'' is calculated with equation (X-5), and equation (X-3) is solved for T_{sm}(using the equation as based on the average values T_{em} and T_{sm} instead of the instantaneous values of T_e and T_s). The value of U_i must be based on $(T_{sm}+T_e)/2$ for this. If the calculated value of T_{sm} agrees with that assumed earlier q_i' is then calculated, after which ΔM_f is found from equation (X-7). When $\Sigma(M_f)_h = M_{fo}$, all of the coolant is evaporated, and the previous procedure is resumed using $M_f = 0$. If the value of T_{sm} calculated does not agree with that corresponding to the assumed value of T_{s2}, the interval calculation must be repeated for agreement before ΔM_f may be deter-

mined. It is well to experiment in any case to determine what agreement must be had between the assumed and calculated T_{s2} to achieve desired accuracy in ΔM_f. This can be done with one interval by repeating it to perfect agreement and comparing the final result with those of earlier trials. The last interval of this calculation must be selected of such length that the coolant is just used up at the end of the interval. Time intervals can be selected in length so as to hold $(T_{i2}-T_{i1})$ to about 40°F or less, although the calculations are quite accurate for larger intervals. A detailed procedure and example of this interval calculation are given in the Appendix to this Section.

EFFECTS OF EQUIPMENT INSULATION AND EVAPORATIVE COOLANT ON THE TEMPERATURE RISE OF INDIVIDUAL COMPONENTS

1. Effect of Insulation Alone on Component Temperature Rise

The effect of using individual insulation on a component is shown in Figure X-1. The component is represented as a cube of one cubic foot volume, including the insulation on it. The characteristics of the compartment, the uninsulated equipment, and the environment temperatures are given in Figure IX-8. The characteristics of the insulated component are given in Figure X-1. The cases shown are for no heat generation by the insulated component, and no cooling effect. The insulation used is asbestos felt, having a density of 36 lb/ft^3 and a specific heat of 0.2 Btu/lb-°R.

It is apparent that the application of insulation of increasing thickness reduces the component temperature by an amount which is approximately proportional to the insulation thickness. In the case of the thickest insulation the component is held about 70°F below the temperature it would assume without insulation. It is interesting to note that a significant portion of this temperature reducing effect is due to the thermal capacity of the insulation, as distinguished from its insulating effect. To illustrate this, a case is shown for a component with no insulation, but having an added thermal capacity equal to that of a 1/2 in. covering of the asbestos insulation. This shows the temperature reduction due to the thermal capacity alone to be about 36 percent of the total temperature reduction obtained with the insulation. In many cases insulating effect is affected adversely by an increase in insulation density. In an application of this type, however, there is a compensating effect due to the increased thermal capacity of more dense insulation. This is important here because the more dense insulations are less fragile and better suited to application on the outside of a component.

In the cases of Figure X-1 it is assumed that the external size of the insulated cube is constant. Therefore an increase of insulation thickness results in a decrease of internal volume for the insulated component. The use of 1/2 in. of insulation in such manner for a one cubic foot external size reduces the internal volume by approximately 25 percent. The relative worth of insulation as compared to evaporative coolant on a volume basis is considered later in this Section. It can be inferred from the example just quoted, however, that the space requirements of insulation are rather large

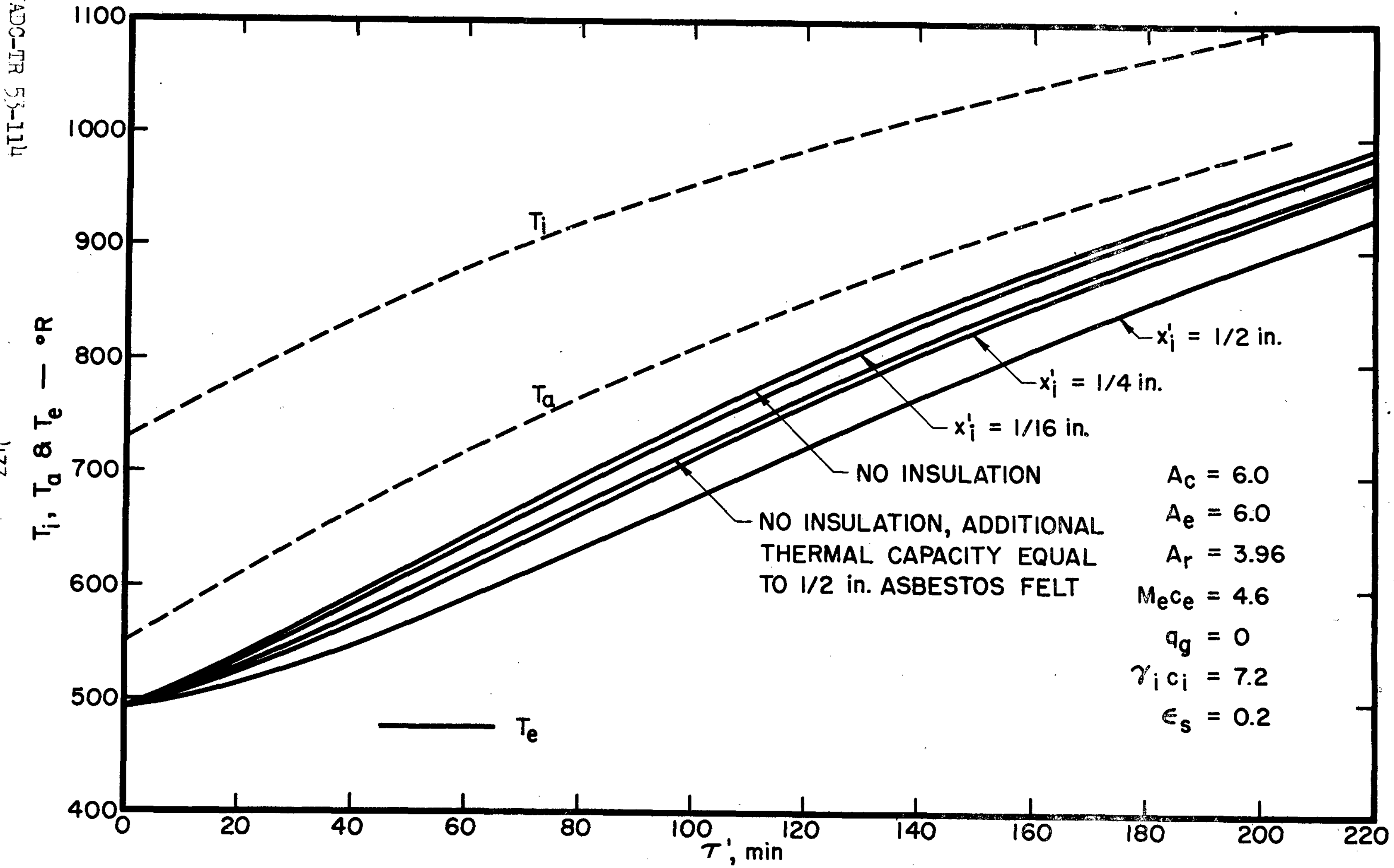

Figure X-1

Effect of Insulation on Component Temperature
Rise for Non-Heat-Generating Components

for the temperature effects produced.

It must be emphasized that the temperature rise behavior exhibited by the cases of Figure X-1 is for components which do not generate heat. With components which generate heat, it is possible that insulation would produce an undesirable effect. If the heat generation rate is great enough to bring the component to a higher temperature than the compartment air, insulation would act as an unwanted barrier to the free convection cooling effect that would result. Whether or not this condition would exist in any case can be determined from the environment temperatures and the temperature rise for a perfectly insulated component. The equation for heat balance of a perfectly insulated component is

$$q_g' = M_e c_e \left(\frac{\Delta T_e}{\Delta \tau}\right)$$

This can be used to construct a plot of T_e vs. τ, which can then be compared with the environmental temperature plot of T_i and T_a vs. τ. If T_e for the perfectly insulated equipment is at any time greater than T_a, then during such periods the insulation would be undesirable from the standpoint that it prevents some cooling effect by the compartment air. It may still be of some value in reducing the radiant heat load, however. In the actual case, the periods in which T_e is above or below T_a would not coincide exactly with those as determined by the above method, since the equipment can not be perfectly insulated. The method is nevertheless of value in a qualitative sense.

Although insulation has been shown to be of some value in reducing component temperature rise when properly applied, a definite evaluation of its worth must be based on a comparison with other methods of accomplishing the same end. In this connection it is interesting to compare the benefits of insulation with those resulting from an equivalent volume of water used as an evaporative coolant. This is done in the following paragraphs.

2. Effect of Replacing Evaporative Coolant with Insulation on Component Temperature Rise

Figure X-2 shows the effect of replacing evaporative coolant with insulation on the temperature rise of a non-heat-generating component. The characteristics of the cooled and insulated equipment are given in the figure, while the environment characteristics are taken from Figure IX-8, as before. The component is again represented as a cubic box, one cubic foot in volume as based on its external dimensions. The insulation is 36 lb/ft^3 asbestos felt, and the coolant is water, controlled to evaporate at a constant temperature of 610°R.

In the case shown for no insulation five pounds of water are provided as coolant. In the other cases a reduced amount of coolant is provided so that the total volume of the insulation plus the coolant is equal to the volume of five pounds of water. Since the external volume of the cube is constant, this provides a means of comparing the worth of the coolant with

CONFIDENTIAL

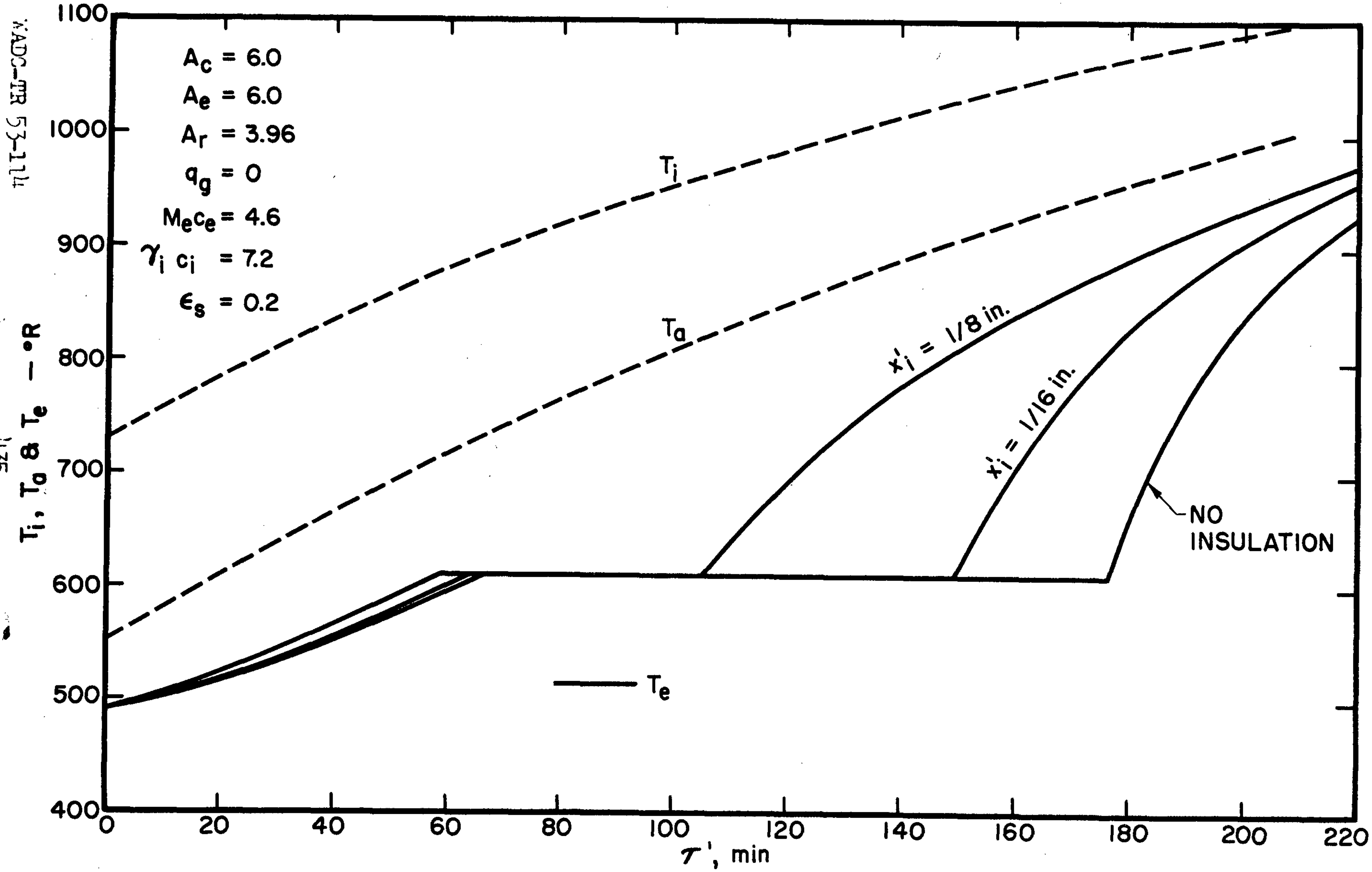

Figure X-2
Effect of Replacing Evaporative Coolant with Insulation on Component Temperature Rise

CONFIDENTIAL

that of the insulation in three cases which provide the same free installation volume inside of the insulation. It is readily seen that it is poor practice to replace some of the coolant with an equal volume of insulation, since the external heat load to the component is not reduced sufficiently that the remaining coolant can provide the same flight duration before it is used up. This proves that from the standpoint of space requirements evaporative cooling with water is a much more effective way of reducing component temperature rise than is the use of asbestos insulation. This is even more true in the case of heat generating components, since evaporative cooling does not hamper the convection cooling effect when the component temperature is above the compartment air temperature.

It is emphasized that the conclusion concerning the greater worth of evaporative coolant as compared to insulation is based on the comparison of water and asbestos insulation. It is not always possible to use water as the evaporative coolant, since properties of the coolant such as freezing point, dielectric strength, or chemical inertness may be critical. Consideration of these factors may dictate the use of a coolant which has a much lower value of latent heat per unit volume. Since this is actually the cooling effect per unit volume, the use of such a coolant could be less profitable than the use of an equivalent volume of insulation under some circumstances. Unfortunately, it is not practical to set definite limits on this possibility because of the many independent variables involved. It is therefore recommended that the reader apply the analytical methods of this Section to investigate the relative merits of coolant and insulation for whatever combination of physical properties is of interest to him.

Figure X-3 is for the same conditions as Figure X-2, except that the component generates heat at the rate $q_g' = 3413$ Btu/hr. For the single insulation thickness considered, the effects are qualitatively the same as observed from Figure X-2. In the case of the heat generating equipment, however, the reduction in flight duration is a much greater percentage of the total when some of the water volume is replaced with insulation. For an insulation thickness of 1/16 in., the flight duration is reduced about 15 percent for non-heat generating equipment, while it is reduced over 29 percent for the component with $q_g' = 3413$ Btu/hr.

DESIGN CONSIDERATIONS FOR USING INSULATION TO PROTECT INDIVIDUAL COMPONENTS

As indicated in the discussion of the calculated cases, the use of insulation as a means of protecting individual components is probably most applicable for non-heat generating components. Wherever it can be used, insulation has three important advantages over other means of protection such as the use of an evaporative coolant. First, the insulation requires no control apparatus or piping of any kind, and therefore conserves the compartment space that would otherwise be required for installing these items. Second, the physical simplicity and simple function of the insulation insures absolute operational reliability. So long as the insulation is in place and undamaged, it must perform the task for which it is properly intended. Third, the insulation is applied externally and would not ordinarily require any alteration in design of the component which it protects.

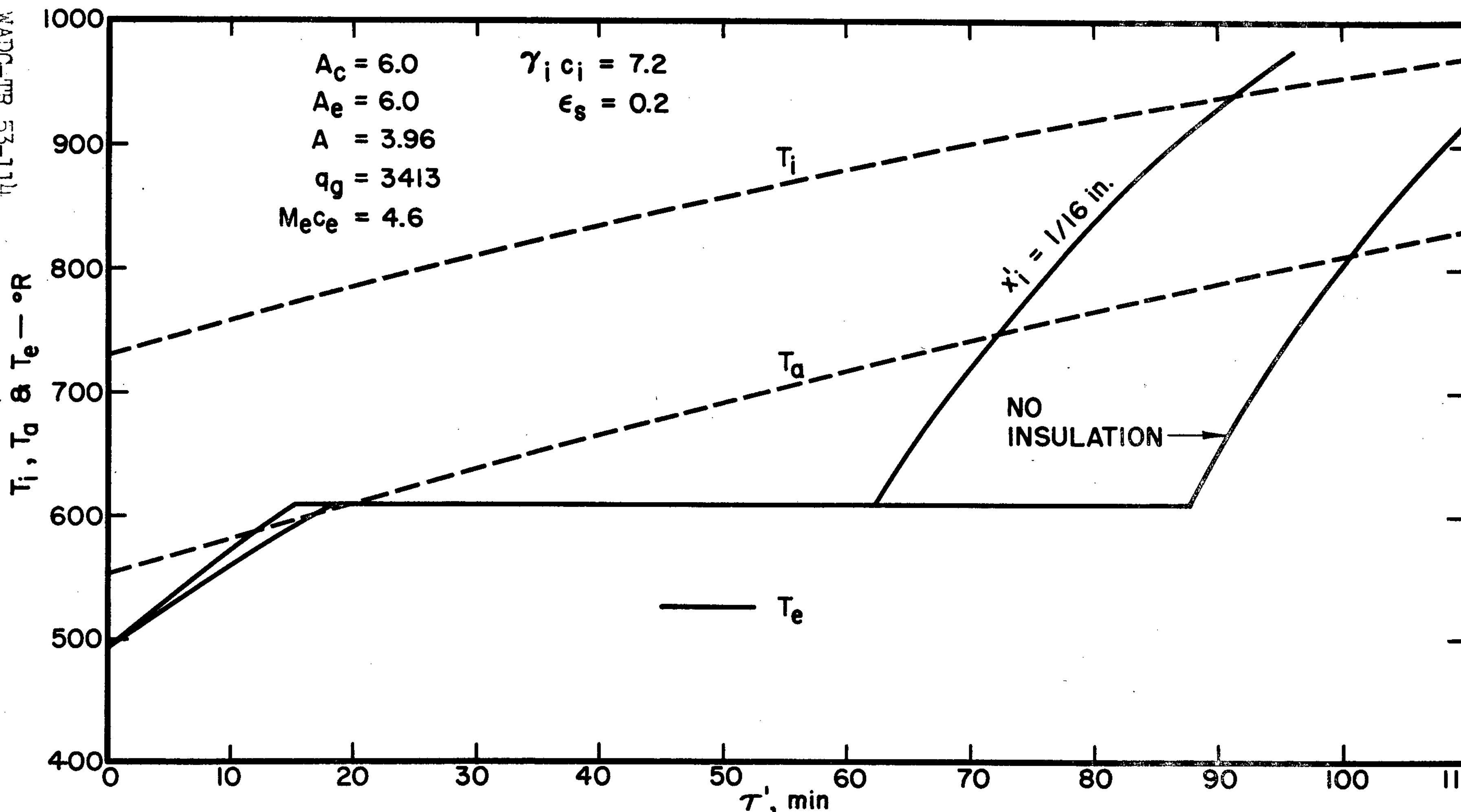

Figure X-3
Effect of Replacing Evaporative Coolant with Insulation on Component Temperature Rise

A proper application of evaporative cooling, on the other hand, requires that the coolant container and component be integrally designed so as to give adequate cooling effect by means of good thermal conductance between the coolant and all parts of the protected component. If the component is immersed in coolant, both the component and the external case must be designed for proper sealing of the coolant. Either method of applying evaporative coolant is not so likely to be suited to presently existing equipments as is insulation.

Where insulation is to be applied as the sole means of protection for a non-heat-generating component, the calculation method given as Procedure A in the Appendix to this Section may be used for design purposes. Assuming that the component temperature rise without any insulation has already been determined ($q^*_{3i} = 0$, $T_s = T_e$) an insulation thickness should next be assumed. The procedure is then used to determine the temperature rise with the assumed thickness and type of insulation. If the result is not as desired, the thickness is altered with due regard to the approximately linear relationship between the reduction of temperature rise and the insulation thickness.

When both insulation and evaporative coolant are to be considered, a logical design procedure begins with determining the amount of coolant required to give the component temperature rise desired. The design method of Section IX can be followed for this purpose. Next the insulation required to give the same temperature rise in the same time is found as indicated in the previous paragraph. The volume requirements are then determined, and considered together with any other pertinent criteria to select either the insulation or the evaporative coolant. This double design procedure will indicate the superiority of one system or the other, or possibly that they are equivalent in their advantages.

It is also possible that a combination of insulation and evaporative coolant exists which is superior in terms of volume requirements to the use of either alone. This possibility exists because of the change of environmental temperatures in the compartment with time. In other words, under some environmental temperature conditions, a given volume devoted to insulation may reduce the heat gain to the component by an amount greater than the total latent heat of the same volume of coolant. At other times, when the environmental temperatures are not so great with respect to the component, the reverse could be true. It would therefore seem that if the volume requirement of using coolant alone is substantially less than that of insulation alone, the use of some insulation together with the coolant should be considered (Procedures A and B of the Appendix to this Section), since a smaller total volume of insulation and coolant may be found. If the volume requirement of insulation alone were substantially less than that of coolant alone, the same procedure could be followed. It is less likely to be profitable, however, because of the desirability of avoiding coolant altogether where the much simpler insulation will suffice. Carrying the design procedure to the point of considering using both protective measures together is justified only where installation space in the compartment is extremely critical and where the volume of insulation and/or coolant is quite large, as might be the case where long flights at high speed are contemplated.

APPENDIX TO SECTION X

1. Calculation Procedures

Calculation procedures and example calculations are given here for the interval calculations required to evaluate the temperature rise of equipment protected by insulation. The procedures apply to individually insulated items, and it is assumed that these items are located in an uncooled compartment with or without skin insulation. In addition, the individually insulated items may also have an evaporative coolant provided for their protection. It is assumed that the individual components having these special characteristics are only a small portion of all the equipment in the compartment.

The determination of the compartment air temperature and the face temperature of the skin insulation is done by the general calculation method in the Appendix to Section V, and is not repeated here. Figure IX-8 (previous Section) shows a plot of these environment temperatures determined by such a calculation. This plot is used for calculating the external heat loads to the special equipments studied in the subsequent examples.

Procedure A: Calculation of Temperature Rise of Insulated Components Without Coolant Evaporation

Given Data:

compartment and average uninsulated equipment characteristics as shown in Figure IX-8

thermal capacity of insulated equipment $M_e c_e = 4.6$ Btu/°R

heat generation of insulated equipment $q_g' = 853$ Btu/hr

weight of coolant (water) $M_f = 3.05$ lb

total surface area of insulated component $A_e = 6.0$ ft^2

total surface area available to free convection $A_c = 6.0$ ft^2

total surface area available to radiation $A_r = 3.96$ ft^2

surface emissivities $\epsilon_i = 0.10$, $\epsilon_s = 0.20$

characteristic dimension of insulated box $L = 1$ ft

compartment pressure $\delta = 2.5$

component insulation of asbestos felt $x_i = 0.00521$ ft

thermal capacity of component insulation per unit volume $\gamma_i c_i = 7.2$ Btu/ft^3-°R

$T_{e1} = 492^\circ R$ at $\tau = 0$ hr; $T_{s1} = 497^\circ R$ at $\tau = 0$ hr

1. Select $\Delta\tau$ and assume T_{s2} and T_{e2}.

$$\Delta\tau = 0.0833 \text{ hr}$$
$$T_{e2} = 506.6^\circ R$$
$$T_{s2} = 511.4^\circ R$$

2. Calculate $T_{sm} = (T_{s1}+T_{s2})/2$ and $T_{em} = (T_{e1}+T_{e2})/2$.

$$T_{sm} = 504.2^\circ R$$
$$T_{em} = 499.3^\circ R$$

3. Get T_{i1}, T_{a1}, T_{i2} and T_{a2} from Figure IX-8.

$$T_{i1} = 728^\circ R$$
$$T_{a1} = 552^\circ R$$
$$T_{i2} = 744^\circ R$$
$$T_{a2} = 566^\circ R$$

4. Calculate $T_{im} = (T_{i1}+T_{i2})/2$ and $T_{am} = (T_{a1}+T_{a2})/2$.

$$T_{im} = 736^\circ R$$
$$T_{am} = 559^\circ R$$

5. Calculate

$$h_r = 17.4 \times 10^{-4} \left(\frac{1}{\frac{1}{\epsilon_i} + \frac{1}{\epsilon_s} - 1} \right) B$$

taking B from Figure AIV-1 for T_{im} and T_{sm}.

$$h_r = 1.24 \times 10^{-4} \times 990 = 0.1225 \text{ Btu/hr-ft}^2\text{-}^\circ R$$

6. Calculate $q_r' = h_r A_r (T_{im} - T_{sm})$

$$q_r' = 0.1225 \times 3.96 \times 231.8 = 112.5 \text{ Btu/hr}$$

7. Calculate $(T_{am}+T_{sm})/2$ and get $(a' L^{1/4} / \delta^{1/2})$ at this mean temperature from Figure AIV-3.

$$\frac{a' L^{1/4}}{\delta^{1/2}} = 0.2838$$

8. Calculate $h_c = (a' L^{1/4} / \delta^{1/2})(\delta^{1/2} / L^{1/4})(T_{am} - T_{sm})^{1/4}$

$$h_c = 0.2838 \times 1.58 \times 2.720 = 1.22 \text{ Btu/hr-ft}^2\text{-}^\circ R$$

9. Calculate $q_c' = h_c A_c (T_{am} - T_{sm})$

$$q_c' = 1.22 x 6 x 54.8 = 401 \text{ Btu/hr}$$

10. Calculate $q_o' = q_c' + q_r'$

$$q_o' = 513.5 \text{ Btu/hr}$$

11. Calculate $\Delta T_e = (T_{e2} - T_{e1})$ and $\Delta T_s = (T_{s2} - T_{s1})$ and

$$q_{si}'' = \gamma_i c_i \frac{\Delta T_e + \Delta T_s}{2 \Delta \tau}$$

$$\Delta T_e = 14.6^oR$$
$$\Delta T_s = 14.4^oR$$

$$q_{si}'' = 7.2 \left(\frac{14.5}{0.0833}\right) = 1252 \text{ Btu/ft}^3\text{-hr}$$

12. Calculate $q_L' = q_o' - q_{si}''(A_e x_i)$

$$q_L' = 513.5 - 1252 x 0.0313 = 474.3 \text{ Btu/hr}$$

13. Calculate

$$\Delta T_e = \frac{(q_g' + q_L') \Delta \tau}{(M_e c_e + M_f c_f)}$$

$$\Delta T_e = \frac{(853 + 474.3) 0.0833}{4.6 + 3.05} = 14.4^oR$$

14. Calculate $T_{e2} = T_{e1} + \Delta T_e$

$$T_{e2} = 506.4^oR$$

This result should agree with the value assumed in step 1.

15. Calculate $(T_{sm} + T_{em})/2$ and get k_i at this temperature.

$$k_i = 0.0884 \text{ Btu/hr-ft-}^oR$$

16. Calculate $U_i = (k_i / x_i)$

$$U_i = 16.97 \text{ Btu/hr-ft}^2\text{-}^oR$$

17. Calculate $q_o' = U_i A_e (T_{sm} - T_{em}) + q_{si}'' \left(\frac{A_e x_i}{2}\right)$

$$q_o' = 16.97 x 6 x 4.9 + 1252 x 0.0156 = 517.5 \text{ Btu/hr}$$

This value should agree with that calculated in step 10. If not, T_s is incorrect and new values of T_{s2} and T_{e2} should be used in a

repeated trial calculation. When satisfactory agreement within the desired limits of accuracy is achieved, continue to the next interval using the final values of T_{e2} and T_{s2} for this interval as T_{e1} and T_{s1} in the next. It is emphasized that agreement of the values of both q_o' and T_{e2} are to be achieved before the above interval calculation can be considered complete.

When working with the first time interval in a calculation such as the above, it is necessary to know the initial values of T_i, T_a, T_s and T_e. All of these are known except T_s, which is found as follows. For the time $\tau = 0$, assume T_s between T_a and T_e, and calculate

$$q_o' = U_i A_e (T_s - T_e)$$

where U_i is evaluated at $(T_s+T_e)/2$. Then calculate $(T_a+T_s)/2$ and calculate q_c' by equation (X-2) basing h_c on this average temperature. Next use equation (X-1) to calculate q_r'. The sum $(q_c'+q_r')$ should equal q_o' found above. If $(q_c'+q_r') > q_o'$, increase the value of T_s for the next trial, and conversely. Repeat this until the correct value of T_s is found.

Procedure B: Calculation for the Period of Constant Temperature Evaporation

Given Data:

All data are the same as in Procedure A. In addition, the coolant (water) is vented such that its boiling temperature is 610°R.

enthalpy of vaporization at 710°R $H_{fg} = 1008.2$ Btu/lb

Steps 1 through 10 are identical to Procedure A, except that T_e is constant and $\Delta T_e = 0$. Making the calculation for q_o as based on the time interval from $\tau = 0.671$ hr to $\tau = 0.833$ hr gives $q_o' = 640$ Btu/hr as the result of step 10. ΔT_s is assumed as 2.8°R.

11. Calculate $q_{si}'' = \gamma_i c_i \left(\frac{\Delta T_s}{2\,\Delta\tau}\right)$

$$q_{si}'' = 62.2 \text{ Btu/hr-ft}^3$$

12. Calculate $(T_{sm}+T_e)/2$ and get k_i at this average temperature.

$$k_i = 0.1049 \text{ Btu/hr-ft-}^{\circ}\text{R}$$

13. Calculate $U_i = (k_i/x_i)$

$$U_i = 20.1 \text{ Btu/hr-ft}^2\text{-}^{\circ}\text{R}$$

14. Calculate

$$T_{sm} = T_e + \left[\frac{q_o' - q_{si}''\left(\frac{A_e x_i}{2}\right)}{U_i A_e}\right]$$

$$T_{sm} = 610 + \frac{640-62.2x3x0.00521}{20.1x6} = 615.3^{o}R$$

This value should agree with T_{sm} as calculated from the assumed value of T_{s2} (for this interval, this value was $T_{sm} = 615.4^{o}R$). If not, repeat, using a new assumed value of T_{s2} until agreement is achieved.

15. Calculate $q_L' = q_o' - q_{si}''(A_e x_i)$

$$q_L' = 640-62.2x6x0.00521 = 638 \text{ Btu/hr}$$

16. Calculate

$$\Delta M_f = \frac{(q_g' + q_L')\Delta\tau}{H_{fg}}$$

$$M_f = \frac{(853+638)x0.162}{1008.2} = 0.239 \text{ lb}$$

17. Calculate $\Sigma(\Delta M_f)_n$ for the n intervals calculated during evaporation, ending with the current one. When the sum equals M_f of the given data the evaporation process is completed.

2. References

(X-1) Jakob, M. Heat Transfer Vol. I, John Wiley and Sons, Inc., New York, 1949, pp. 167-169.

SECTION XI

CRITERIA FOR SELECTION OF MEANS TO LIMIT TEMPERATURE RISE

By T. C. Taylor

In Sections V through X a number of methods of limiting the temperature rise of equipments in compartments of high speed aircraft are considered. In most of these Sections design procedures are presented, showing how to design the given system for a specified temperature rise. However, in dealing with a specific problem to limit the temperature rise of equipment, it is not always apparent which of the methods to use. It is therefore necessary to follow a logical procedure whereby those methods which are not suited to the specific problem may be eliminated. Designs for the remaining methods can then be considered in greater detail to find the one which is most appropriate.

Figure XI-1 is a summary chart showing all of the systems considered in Sections V through X. The method shown at the top of the chart consists of the uncooled compartment, using only skin insulation and thermal capacity to protect the equipment against excessive temperature rise. This is the simplest method of protection, involving the least physical complication in the compartment. The methods shown below and to the right represent systems which protect the equipment more effectively against temperature rise, but which involve special apparatus over and above that used in the simple uncooled compartment. In general, the farther down a system is on the summary chart, the more effective a means it is of limiting equipment temperature rise. Below and to the left of the uncooled compartment are shown methods of protecting individual equipment components against excessive temperature rise. As with the methods for protecting all of the equipments in a compartment, those for individual components are also shown in order of ascending effectiveness. The means for protecting individual components are considered in cases where the uncooled compartment is sufficient for most of the equipment, but where a few critical components must have special protection.

Among the systems used to protect an entire compartment and among those used for critical components there is considerable overlap in performance. In many cases it could be very difficult to select one system in preference to another on the basis of performance alone. In addition, however, there are usually other factors of a structural or functional nature which may preclude the use of one system or indicate the desirability of another. The importance of such factors is dependent on the circumstances of the particular design, and so cannot be ascertained quantitatively here. The remainder of this Section is devoted to the problem of selecting a protective system on the basis of its thermal performance. The structural and functional factors likely to be involved are also considered briefly, although their final evaluation is largely a matter of individual judgement. Systems for protecting all of the equipment in a compartment are considered first, and those for individual component protection later. Within each category the systems are considered in the order shown in Figure XI-1.

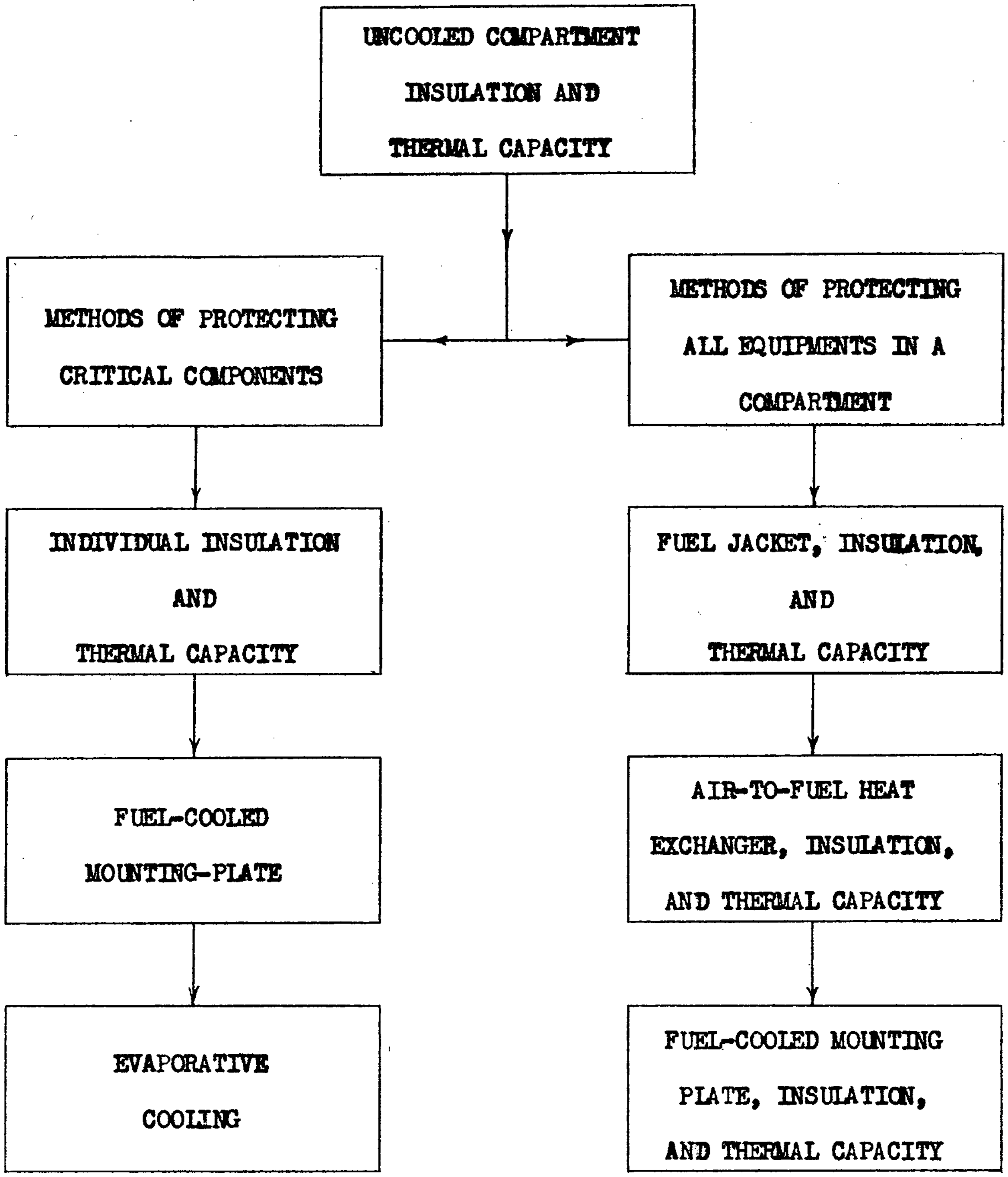

Figure XI-1

Summary Chart for the Methods of Protecting Equipment from Excessive Temperature Rise

NOMENCLATURE

Symbol	Definition	Units
c	Specific heat	Btu/lb-°R
m	Weight, based on unit skin area	lb/ft^2
q	Heat flux, based on unit skin area	Btu/hr-ft^2
T	Absolute temperature	°R
τ	Time	hr

Subscripts

a,b,c	Denote example cases, Figure XI-2
d	Denotes design value
e	Denotes equipment temperature
ed	Denotes design value of equipment temperature - maximum allowable value
eo	Denotes initial value of equipment temperature
g	Denotes generated value
o	Denotes external value
w	Denotes skin value

GENERAL INFORMATION PREREQUISITE TO SYSTEM SELECTION AND DESIGN

In order to make final selection and design of a system for limiting the temperature rise of equipment, it is necessary to know all of the characteristics of the compartment and equipment that influence the heat transfer processes. If some of these characteristics are unknown and cannot be estimated, it is not possible to evaluate the heat transfer processes and hence the amount of cooling or other protection required. The significant information prerequisite to the selection and design of a protection system is summarized as follows:

1. The skin temperature of the aircraft.

2. The total amount of skin surface in direct thermal communication with the equipment compartment.

3. The total surface area of the equipment available for free convection heat transfer.

4. The total surface area of the equipment available for radiation heat transfer with the skin or skin insulation.

5. The emissivities of all surfaces involved in radiant heat transfer.

6. The equipment temperature at the beginning of flight.

7. The allowable equipment temperature rise.

8. The desired flight duration.

9. The total weight of equipment and its average specific heat.

10. The total heat generation rate of the equipment.

11. The required compartment air pressure.

12. If an ultimate coolant, such as fuel, is to be used, the quantity and temperature-time history of the coolant available, and the physical and thermodynamic properties of the coolant.

13. If insulation is used, the physical and thermal properties of the insulation.

For analyzing the heat transfer processes of a compartment as a whole, it is convenient to express the equipment convection area, weight, and heat generation on the basis of unit compartment skin area (referring to the skin of item 2). The method of doing this is given in detail in Section V. For analyzing the heat transfer processes for a specific component, these items are expressed as total values for the component involved. Examples of this practice are found in Sections IX and X.

SELECTION OF SYSTEMS FOR PROTECTION OF ALL EQUIPMENTS IN A COMPARTMENT

1. General

As a first step in selecting a means for protecting all of the equipments in a compartment from excessive temperature rise, it is well to employ a graphical representation of certain salient factors involved. Figure XI-2 is a schematic example of this. The initial equipment temperature and maximum allowable equipment temperature are plotted versus a time axis representing the duration of flight, as shown at points T_{eo} and T_{ed}, respectively. Since the problem here is confined to that of equipment temperature rise in high speed flight, the skin temperature would be somewhere above the maximum allowable equipment temperature, as indicated by T_w. Next a line is constructed to represent the equipment temperature assuming that the equipment is perfectly insulated, and therefore exchanges no heat with its surroundings. The equation for this line is

$$T_e = T_{eo} + \left(\frac{q_g}{m_e c_e}\right)\tau$$

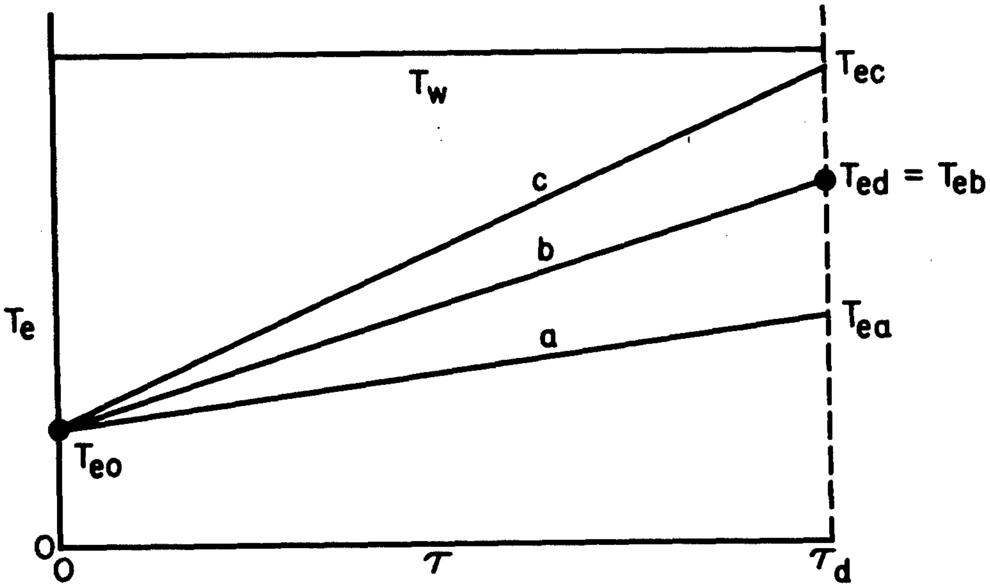

Figure XI-2. Schematic of First Step in Selection Procedure

from which it is seen that the equipment temperature rise is assumed to be due to the heat generation alone. Three examples of such a line are shown as (a), (b) and (c) in the figure, and correspond to the three general possibilities. In the case shown as (a), the temperature of perfectly insulated equipment at the end of the flight is less than T_{ed}. This indicates that the temperature of an actual equipment could be prevented from exceeding T_{ed} if sufficient insulation of the skin is provided such that

$$q_o \leq \frac{(m_e c_e)(T_{ed}-T_{eb})}{\tau_d}$$

So many factors are involved that it is impossible to state at once whether the use of insulation alone would be practical. A case such as (a) indicates that it is theoretically possible, however, so that the uncooled compartment, using only skin insulation, should be given first consideration. When the equipment does not generate heat, the case is represented as a horizontal line beginning at T_{eo}. This is obviously in the same category as case (a) of Figure XI-2, and requires that the uncooled compartment be considered first. In the case shown as (b) the temperature plot for perfectly insulated equipment intersects the point T_{ed}. It is therefore apparent that absolutely perfect insulation would have to be provided in this case if nothing but insulation were used as a protection for the equipment. Achieving this performance with insulation alone is therefore a practical impossibility, since an infinite thickness of insulation is required. In practice the effect of perfect insulation or a slight cooling effect can sometimes be achieved with a fuel jacket for the compartment. Cases such as (b) therefore require that first consideration be given to the use of a fuel

jacket. If this possibility is excluded, some cooling method must be employed in addition to skin insulation. In the case shown as (c) the temperature of the perfectly insulated equipment is greater than T_{ed}. Since external heat loads to the equipment would cause the actual temperature to exceed T_{eo} at τ_d, it follows that a case of this type absolutely requires some cooling effect in the compartment. The designer should therefore eliminate consideration of an uncooled compartment, unless he is at liberty to increase the thermal capacity $m_e c_e$ to such an extent that the case can be made to fall in the class of case (a).

The principal value of this preliminary graphical analysis lies in the possibility that it may eliminate unwarranted detailed consideration of the uncooled compartment. Otherwise a detailed consideration of all possibilities beginning with the uncooled compartment and following the order of the following paragraphs is required.

2. The Uncooled Compartment

As long as the temperature of perfectly insulated equipment can be represented by a plot such as that labeled (a) in Figure XI-2, where T_{eo} T_{ed}, the uncooled compartment is a possible means of preventing excessive equipment temperature rise. As the cases considered approach closer to case (b), the use of the uncooled compartment becomes less practical because of the great insulation thicknesses required.

A detailed consideration of the uncooled compartment involves determination of the insulation thickness required. This is done by the method given in the design portion of Section V, using either the calculation procedures or the given charts, if applicable. When this is completed, it must be determined from judgement of the particular case whether the required insulation thickness can be accommodated in the compartment or not. If the insulation thickness required is excessive, the use of a smaller amount of insulation together with some added thermal capacity in the compartment should be considered. As shown in Section V, the flight time required to produce a given temperature rise under given conditions of heat load is directly proportional to the thermal capacity. Therefore the use of deliberately added thermal capacity with the equipment is a powerful means of preventing excessive equipment temperature rise in an uncooled compartment.

It is worthwhile to devote considerable attention to the design method of Section V, and to use the facilities of the compartment to accommodate thick skin insulation and added thermal capacity as completely as possible. The performance of these two elements in preventing temperature rise is very reliable when they are properly installed, and free of the possible performance failures which attend the use of more elaborate protection measures. In general the relative value of space within the compartment and space near the skin in a given installation must be the criterion of whether to emphasize the use of insulation or of thermal capacity. Although the use of either or both in proper amounts may be possible to achieve a specified limit to the temperature rise, in cases where weight is a critical factor it may be desirable to seek an optimum combination of the two which repre-

sents a minimum cost in terms of added weight. From this viewpoint any added thermal capacity should be achieved by using a substance of high specific heat, such as water, and the insulation should consist of lightweight, effective materials.

In general the process of designing for an optimum combination of insulation and thermal capacity, from the standpoint of minimum weight or minimum volume, involves considerable computing labor. It is necessary to select a range of thermal capacities (representing the total of equipment and deliberately added thermal capacity) and then determine the corresponding insulation thicknesses. This requires a repeated application of the methods of Section V. On completing these calculations, the weight and/or volume requirements of the insulation and added thermal capacity are determined, and their sum in each case is plotted against a parameter describing either the amount of insulation or the added thermal capacity. Such a plot is then inspected to find the optimum design, or minimum point. It is possible that no optimum combination may exist, and that such a procedure would simply indicate that the result should be achieved either entirely with insulation or entirely with added thermal capacity. In general, it is not possible to predict whether an optimum design exists, because of the wide variation in materials and their physical properties which might be used in many combinations to achieve the insulation and added thermal capacity effects. If at the end of such a design effort it is found that no use of insulation, thermal capacity, or combination of the two is satisfactory, it is necessary to go on to the consideration of more elaborate protection methods.

3. The Fuel-Jacketed Compartment

In order of increasing effectiveness in protecting equipment from excessive temperature rise, the fuel-jacketed compartment follows the uncooled compartment. The fuel jacket consists of flat ducts or other appropriate means for forming a shield of fuel between the equipment and the skin of the compartment. In the interests of conserving installation space within the compartment, this jacket should obviously be located as near the skin as possible. Usual practice also requires insulation between the skin and the jacket, both to prevent exposing the fuel to the high skin temperatures and to limit the heat transfer from the skin to the fuel. It is emphasized that this fuel jacket need not surround the entire compartment unless the skin does. The fuel jacket is only provided to cover the area of the inner face of the aircraft skin which is in direct thermal communication with the compartment.

The fuel-jacketed compartment is effective in dealing with cases similar to that plotted as (b) in Figure XI-2. Since the fuel temperature is usually considerably below the temperature of the skin and of the same order as the temperature of the equipment, the fuel jacket tends to function as a nearly perfect insulator. The equipment receives some heat, however, if the fuel temperature is greater than the equipment temperature. Conversely, the equipment is cooled somewhat if the equipment temperature is above the fuel temperature. It is shown in Section VI that the true plot of equipment tem-

perature versus time must be between the plot of fuel temperature versus time and the plot for the temperature of perfectly insulated equipment. Therefore it is possible to establish a range of temperatures within which the equipment temperature must be before making a detailed design. (The range is approximate if the temperatures on entrance to the fuel jacket are used, since heat gains or losses of the fuel should actually be included in establishing its average temperature, as pointed out in Section VI.) If this range of temperatures is entirely below T_{ed}, and temperatures in the range are not detrimental to proper equipment operation, the fuel jacket is satisfactory from the standpoint of temperature rise performance. When T_{ed} is somewhere within the range of temperatures as described above, the entire design procedure of Section VI should be used to determine the significant details and predicted temperature rise performance of the equipment. If T_{ed} is below the range of temperatures between the fuel temperature and the temperature of perfectly insulated equipment, it is impossible to limit the equipment temperature to the value of T_{ed} with a fuel jacket alone. If this is the case, it may be worthwhile to consider adding thermal capacity to lower the temperature rise of perfectly insulated equipment.

The factors mentioned thus far have dealt only with the temperature rise performance of equipment in a fuel-jacketed compartment. With this type of compartment there are a number of functional and structural considerations of importance. The fuel jacket cannot be used if the resulting heat addition to the fuel would cause enough temperature rise to interfere with proper distribution and performance of the fuel in the power plant. In addition, the presence of a fuel jacket virtually precludes accessibility to the compartment through the jacketed surfaces, and the duct system involves more leakage hazard than where the fuel is not used for auxiliary purposes. Finally, in cases where the skin temperature is quite high, the insulation thickness required to protect the fuel from exposure to high temperature and objectionable heat gain may be excessive. In cases where these considerations or unsatisfactory equipment temperature rise indicates that a fuel-jacketed compartment cannot be used, it is necessary to consider one or both of the cooling methods which follow.

4. The Compartment With an Air-to-Liquid Heat Exchanger

Where the equipment generates enough heat to be of the type shown as case (c) in Figure XI-2, a cooling method must always be used, since removal of some of the generated heat is required as well as protection from external heating effects. In a compartment with an air-to-liquid heat exchanger the cooling effect is achieved by using circulated air to transfer heat from the equipment to a heat exchanger using fuel or some other suitable primary coolant. In addition, skin insulation is used to reduce the external heat loads to the equipment and thus reduce the over-all heat load to the heat exchanger. Where two principal elements of design such as insulation and the heat exchanger are present, it is necessary to consider various combinations of the two in order to achieve the best design. A procedure and example of designing for a minimum total requirement in either weight or volume is given in Section VII.

It is obvious that the use of a system of this kind assumes the availability of a coolant which is at a lower temperature than T_{ed}. Just how far below T_{ed} the fuel or coolant temperature must be is dependent on a number of factors, including the amount of cooling effect required, the air circulation rate, and the effectiveness of both the equipment and the heat exchanger as heat transfer devices. It is not possible to generalize these factors sufficiently to determine whether or not a given temperature difference is feasible in advance of preparing a detailed design. It should be observed, however, that the use of air as the secondary coolant must necessarily impose a rather large temperature potential between the equipment and the fuel as a prerequisite to a large cooling capacity. Any attempt to decrease this temperature potential must involve increased weight and size in the heat exchanger and/or increased power requirements for circulating the air. If fuel is unsatisfactory as a coolant in this application, but other coolants are available, the design procedure of Section VII can still be used, provided information is available to describe the variation of coolant temperature with flight time. If such a coolant is provided expressly for this application, its storage space and weight requirements are chargeable to the design when comparing it with other possible methods of achieving the same result. In cases where fuel is used as the coolant, and where the heat generation rate of the equipment is small, the compartment with a heat exchanger may compare unfavorably with one which uses a fuel jacket. In the former the equipment receives heat from the skin, which them requires an appropriate temperature potential for its transfer to the coolant. In the fuel jacketed compartment the equipment is protected from skin heat transfer and free convection and radiation may be sufficient to take care of a low heat generation rate.

In addition to considerations of performance and space or weight requirements, there are a number of functional and structural considerations involved in the use of an air-to-liquid heat exchanger. One significant advantage of this system is that the use of air as a secondary coolant does not require special component design, since most components are suited to operation in an atmosphere of air. Furthermore, the use of a duct distribution system with a secondary coolant permits wide freedom in the location of the cooled components. Finally, the interposition of the equipment between the skin and the coolant greatly reduces the over-all heat load to the coolant as compared to that involved when a fuel jacket is used. Therefore, the heat exchanger system can generally be used where smaller amounts of coolant are available. There are also disadvantages to the use of a heat exchanger and forced-air system. One obvious disadvantage is the apparatus required to circulate the air properly, including ducts, blower and motor. Since the air must be properly directed around the cooled components, the baffles or casings required for this are likely to present a problem where different components must be connected through moving mechanical linkages. The designer should carefully weigh the importance of these advantages and disadvantages in comparison with those of other cooling methods, such as fuel-cooled plates, before making a final system selection.

5. The Compartment With a Fuel-Cooled Mounting Plate

Another method for cooling equipments in cases of the type (c) of Figure XI-2 is to use a fuel-cooled mounting plate. This naturally assumes that the fuel to be used as a coolant is available at temperatures below the maximum allowable equipment temperature. The fuel-cooled surface is a metal plate or structure, through which there are passages for the circulation of fuel coolant. The cooled equipment components are attached to the plate in a manner which provides a good path for the direct conduction of heat from the components to the plate. As with the heat exchanger discussed previously, skin insulation may also be used in the compartment. A detailed procedure and examples of the design of fuel-cooled mounting plates are given in Section VIII.

An outstanding characteristic of this method of cooling equipment is that it can be used to maintain the equipment at a temperature quite close to the coolant temperature. In order to take full advantage of this, however, it is necessary to design the equipment components specially so that they effectively conduct heat to whichever of their surfaces or parts are attached to the fuel-cooled plate. With metallic mechanical equipment this need present no problem. With components which are assemblies of a number of small heat generating bodies, such as electronic equipment, special designs which differ somewhat from current practice would probably be required.

As with other cooling or protection methods, there are structural and functional considerations involved in the use of fuel-cooled mounting plates. A disadvantage of their use is that there is some restriction to the location of the cooled components if they are all to be placed on the same mounting plate. If certain components had to be held in a particular spatial position with respect to others, and could not be mounted to base areas in the same plane, more than one cooling plate would be required. Another disadvantage in common with the use of an air-to-fuel heat exchanger is the pressure drop introduced in the fuel circulating system due to use of the fuel as a coolant. However, cooling plates of high cooling capacity can usually be designed to operate with rather small pressure drop, so that this factor is unimportant except where fuel systems which operate at very low pressures are used. A pronounced advantage of the method using a fuel-cooled plate is that it does not employ a secondary coolant. The ductwork and other circulating apparatus used for a secondary coolant are therefore not present. This not only saves space and weight, but results in good accessibility for the cooled components. The importance of these advantages and disadvantages must be carefully weighed in the light of a specific cooling problem before making final selection of a cooling system.

SELECTION OF SYSTEMS FOR PROTECTION OF INDIVIDUAL COMPONENTS

1. General

There are situations in which the problem of preventing excessive temperature rise of equipment does not present any difficulty except for a few critical components in a group. It might be found, for instance, that

all of the components of a compartment save one or two are adequately protected by using a reasonable amount of skin insulation and/or added thermal capacity. In cases such as this it is in the interests of space and weight economy as well as performance reliability to concentrate on providing special protection only for those critical components which actually need it. There are a number of factors which may result in critical temperature rise of an individual component. As pointed out in Section IX, a component with a low thermal capacity as compared to the average for all of the equipment in the compartment rises in temperature more rapidly than does all other equipment on the average. A component with a higher than average value of surface emissivity behaves in similar manner if its surface is exposed so that it receives heat by radiation. Another critical situation is that where a component is a concentrated source of generated heat. In this connection, it should be noted that the use of an average heat generation rate for all of the components of a compartment in calculating their temperature rise is based on the assumption that the heat generation is distributed quite evenly among the components. Where this is not the case the heat generating components may require special cooling if they are to be restricted to a reasonable temperature rise. Whether or not a specific component which departs appreciably from average conditions requires special protection can be determined approximately by the calculation methods of Section IX. The environment temperatures are determined first as based on the heat transfer processes for the average equipments. The temperature rise of the individual component without special protection is then calculated as in Section IX, assuming no radiation heat transfer with the other components. If this temperature rise is too great, the special protection methods described below must be considered.

2. The Individual Component with Insulation and/or Added Thermal Capacity

The simplest method of protecting an individual component is to cover it with insulation and/or add to its thermal capacity. The first of these reduces the external heat load to the component if the environment temperatures are above the component temperature. The addition of thermal capacity does not reduce heat loads, but tends to offset their effect of raising the component temperature, whether the heat load be external or generated by the component. The temperature rise of a component provided with either of these special means of protection is easily calculated using the methods of Section IX or X. The designer should use these methods, first assuming the addition of as much thermal capacity as is feasible in terms of added weight and space, thereby determining if the protection problem is within the scope of those which can be solved with added thermal capacity. If so, the amount added may then be reduced arbitrarily until by successive trials the proper amount for the application is found. Similarly, for insulation alone, the greatest feasible thickness should be selected first, and the temperature rise evaluated as in Section X. If the temperature rise is less than the maximum allowable, the insulation thickness may then be reduced by successive trials until the minimum amount for the application is found. In specific instances it may be desired to use both added thermal capacity and insulation. The optimum combination of the two is likely to

depend on an efficient utilization of space for the two protection means. For instance, a component may consist of an assemblage of parts enclosing certain voids, which could be used to enclose added thermal capacity (e.g., sealed cans of water) without penalty to the over-all size of the component. If this were not sufficient, insulation might be added to make up the difference in performance required.

It is emphasized that the use of insulation as a means of protection for heat generating components may be of no value, since it hinders cooling effects if the component is above the compartment air temperature. This subject is discussed at length in Section X. Added thermal capacity can be used with benefit in any case.

It is recommended that thorough consideration be given to the use of thermal capacity and insulation before discarding the method in favor of more elaborate ones. The method offers a performance reliability which in general cannot be achieved by more complicated means. If the method is unsuited, and some cooling must be provided, either of the two cooling schemes which follow should be studied.

3. The Individual Component Mounted on a Fuel-Cooled Mounting Plate

A simple method for cooling a component to prevent excessive temperature rise is to use a fuel-cooled mounting plate. The same considerations apply to this application as when cooling all of the equipment in the compartment in this manner. As pointed out in Section VIII, however, the method of determining the external heat load to the cooled equipment is different when only one or a few components are cooled. In this case the environmental temperatures of the compartment are assumed to be established by the uncooled contents of the compartment. The external heat load to the cooled component is therefore calculated just as it is for special components of the type considered in Sections IX and X. Section VIII should be consulted for the details of designing a fuel-cooled mounting plate. When a detailed design is completed, it should be compared on the basis of the performance it offers and all of the constructional and functional considerations involved with another applicable cooling method, such as that described next. The general advantages and disadvantages of cooling plates as a cooling device are discussed earlier in this Section, on page XI-10.

4. The Individual Component with Evaporative Coolant

Evaporative cooling is the most effective means of cooling an individual component when measured in terms of its performance. Since the evaporation temperature of any substance is controlled by its pressure, a wide variety of coolant evaporation temperatures is available through use of a pressure-regulated coolant discharge. The designer, therefore, enjoys some freedom in the design of equipment components, since comparatively low operating temperatures can be provided, if necessary. A design procedure for finding the amount of evaporative coolant required to provide a desired cooling effect at a given temperature for a given flight duration and known

environmental conditions for the component is given in Section IX. The use of insulation on the component together with evaporative coolant is considered in Section X.

Notwithstanding the wide range of cooling performance available with an evaporative coolant, there are other considerations which may preclude its use. The most obvious of these is the need for providing the coolant itself. Whereas the use of fuel as a coolant is only making auxiliary use of a medium which is already present on the aircraft, the use of an evaporative coolant requires storage facilities for the coolant, with inevitable space and weight penalties. Whether or not this presents a significant problem depends on the size of the cooling job to be performed. Another disadvantage is the requirement of some adequate means of coolant control. Although constant-temperature evaporation of an expendable coolant can be obtained with a simple pressure regulator in the discharge line, this is nevertheless a complication not required in the simpler protection methods. As such it introduces a possibility of failure in performance. Other possible disadvantages are related to the manner in which the coolant protection is applied to the component. If the most complete protection is desired, the component should be immersed in the liquid coolant, possibly requiring special component design. For less complete but still very effective protection, the component is entirely enclosed so that it and its enclosure are in very good thermal contact with a container of the coolant. This results in limited access to the component or its parts. In the method least desirable from a performance standpoint, the coolant is contained in a mounting surface to which the component is attached in the same manner as to a fuel-cooled plate. As with the latter, the component must then be designed to give high thermal conductance from all of its parts to the plate. The accessibility of the component is highest in this last method of application. All of these factors must be compared with those for the other systems before selecting a method for the protection of individual components. A preliminary survey of these factors may eliminate one method from consideration. Otherwise it is necessary to complete detailed designs of two or more protection methods in order to make a proper selection from among them.

APPENDIX I

PHYSICAL PROPERTIES

A table and charts are given here for physical properties which are frequently required for the calculations described in this Report. The values of temperature and pressure for the NACA Standard Atmosphere are given in Table AI-1. Physical properties of Air and JP-3 fuel are given in Figures AI-1 and AI-2, respectively.

Table AI-1. Variation of Atmospheric Pressure and Temperature with Altitude (N.A.C.A. Standard Atmosphere)

Altitude, 1000-ft	θ_0*	δ_0**	Altitude, 1000-ft	θ_0*	δ_0**
0	1.0000	1.0000	30	0.7940	0.2970
2	0.9863	0.9298	32	0.7803	0.2709
4	0.9724	0.8637	34	0.7665	0.2467
6	0.9588	0.8014	36	0.7561	0.2244
8	0.9451	0.7428	38	0.7561	0.2038
10	0.9314	0.6877	40	0.7561	0.1851
12	0.9175	0.6360	42	0.7561	0.1681
14	0.9038	0.5875	44	0.7561	0.1527
16	0.8902	0.5420	46	0.7561	0.1387
18	0.8763	0.4994	48	0.7561	0.1260
20	0.8626	0.4596	50	0.7561	0.1145
22	0.8489	0.4223	60	0.7561	0.0713
24	0.8353	0.3876	70	0.7561	0.0442
26	0.8214	0.3552	80	0.7561	0.0274
28	0.8077	0.3251	90	0.7561	0.0170
			100	0.7561	0.0106

*θ_0 = (Temperature, °R)/519

**δ_0 = (Pressure, lb/ft^2)/2118

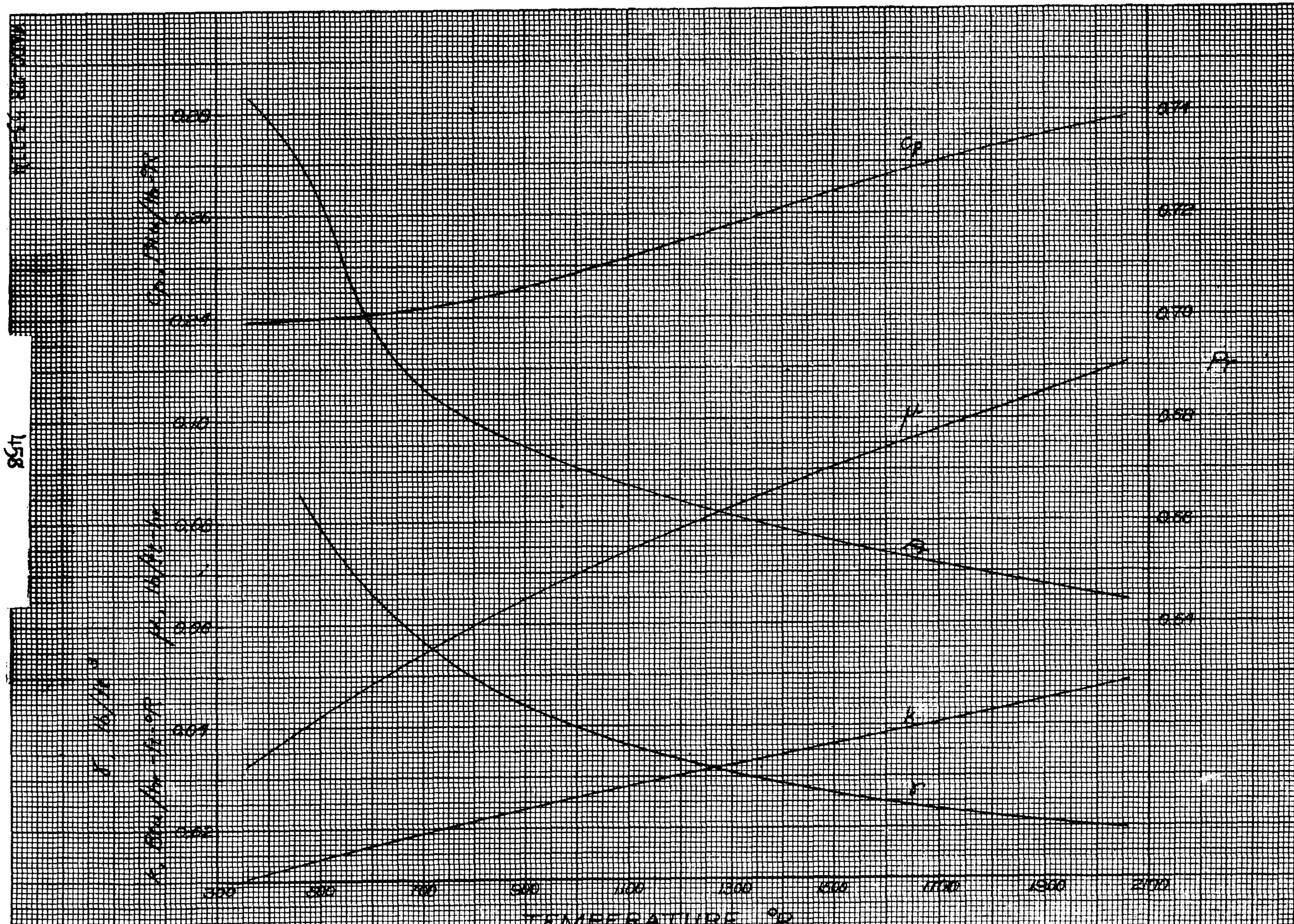

Figure AI-1
Physical Properties of Air

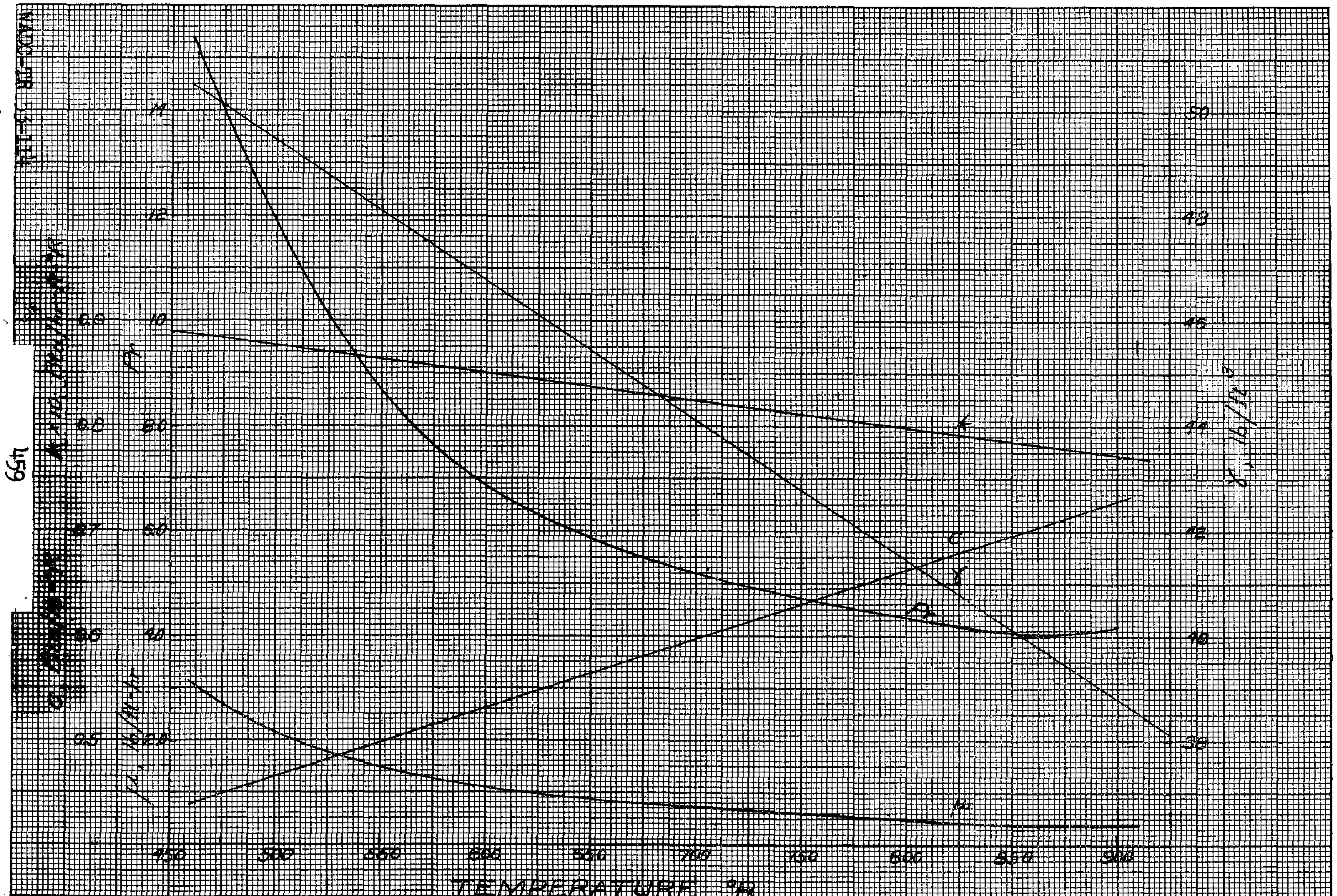

Figure AT-2
Physical Properties of JP-3 Fuel

APPENDIX II

INSULATION CHARACTERISTICS

The use of insulation is considered as a means of protecting equipments against excessive temperature rise in several Sections of this Report. It is pointed out, particularly in Sections V and X, that the thermal conductivity of insulating materials varies with temperature. Data are presented in this Appendix to show this variation for a number of insulating materials. A method is also given for expressing such data in a form which is convenient for calculations of transient heat transfer processes.

Figure AII-1 shows the thermal conductivity of a number of insulating materials as a function of the mean insulation temperature. For practical purposes this temperature can be considered as the average of the two insulation face temperatures. For all of the materials shown the thermal conductivity increases with increasing temperatures. Furthermore, in most cases (asbestos being a notable exception) the variation of k with T is almost linear, further justifying the use of the arithmetic mean temperature as the true mean for describing thermal conductivity. The asbestos, rock wool, glass wool, and Refrasil insulations are loose materials that are most conveniently used in batt form. The values shown for aluminum foil are commercial values, while those shown as 0.2-in. reflective gaps are determined analytically. The calculation is based on the use of three 0.2-in. gaps in series, and accounts for both heat transfer by radiation and by gaseous conduction. The emissivities used are $\epsilon_1 = 0.18$ and $\epsilon_2 = 0.18$ for each gap. The result of such a calculation is a conductance for the over-all thickness of 0.6 in. which is converted to an equivalent conductivity for Figure AII-1. An actual conductivity for reflective gaps would probably be higher than that shown because of heat conduction through structural members required to maintain the proper gap spacing. The properties of reflective gaps as an insulating material are of particular interest, since this type of insulation is well suited to high-temperature service, especially where the application is short-lived as with an expendable missile.

In order to account for the variation of thermal conductivity of insulating materials in a transient calculation, it is convenient to use a plot of special form. An example of this is given in Figure AII-2. One face temperature of the insulation is assumed to be constant at 1355°R, and the other face temperature, which is variable, is given by the abscissa scale. All values of thermal conductivity are then divided by the value when the variable face temperature is 460°R, and these ratios are plotted against their corresponding values of the variable face temperature. The actual value of the ratio plotted for any face temperature is the value which corresponds to the temperature $(1355+T_i)/2$, where T_i is the variable face temperature. Since for a given insulation thickness the conductance is directly proportional to the thermal conductivity, the ordinate may be labeled as a ratio of insulation conductances.

To use such a chart in transient calculation, it is necessary to know the value of T_i at the beginning of the calculation, and to define the value

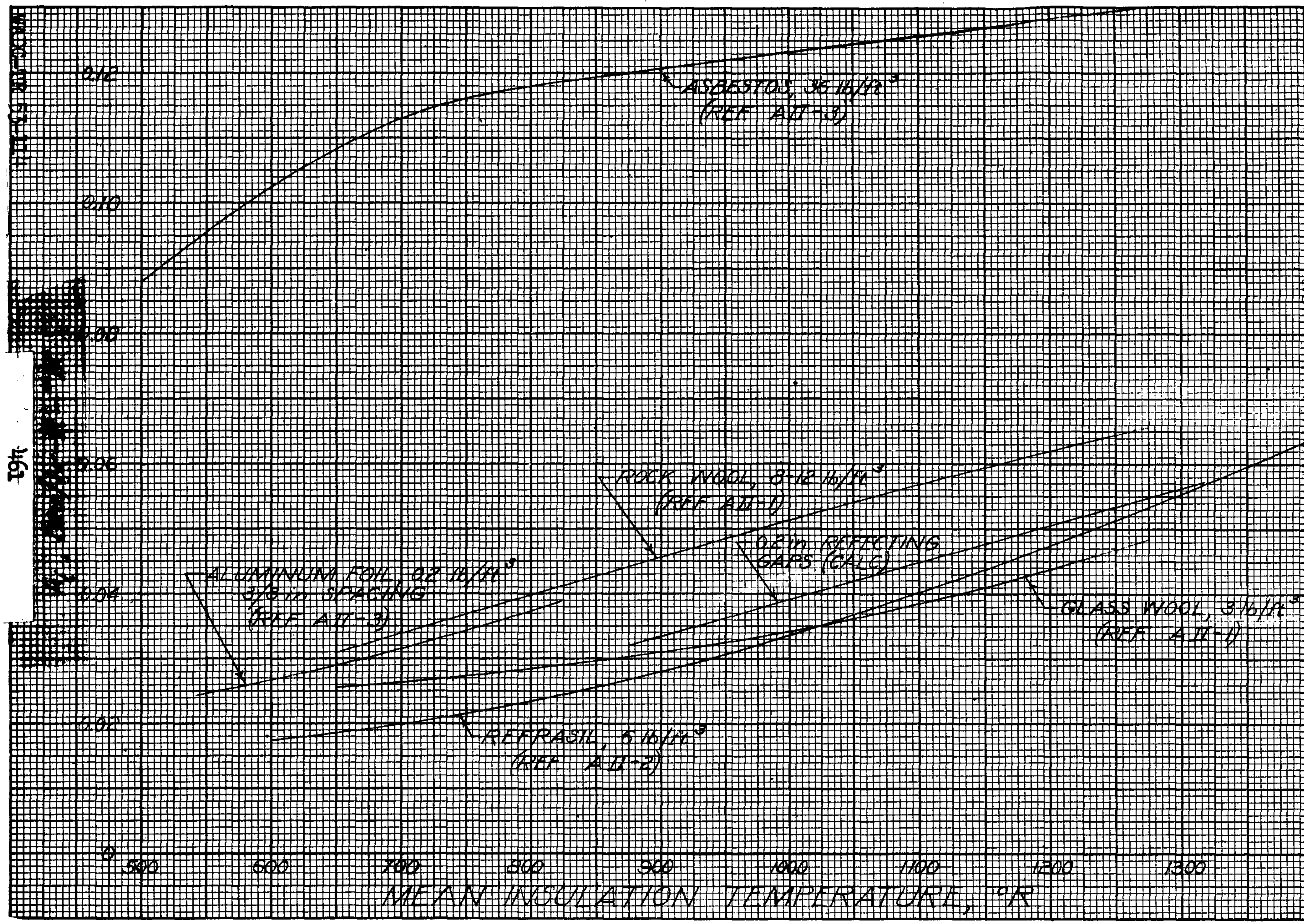

Figure AII-1
Effect of Temperature on the Thermal Conductivity of Some Insulating Materials

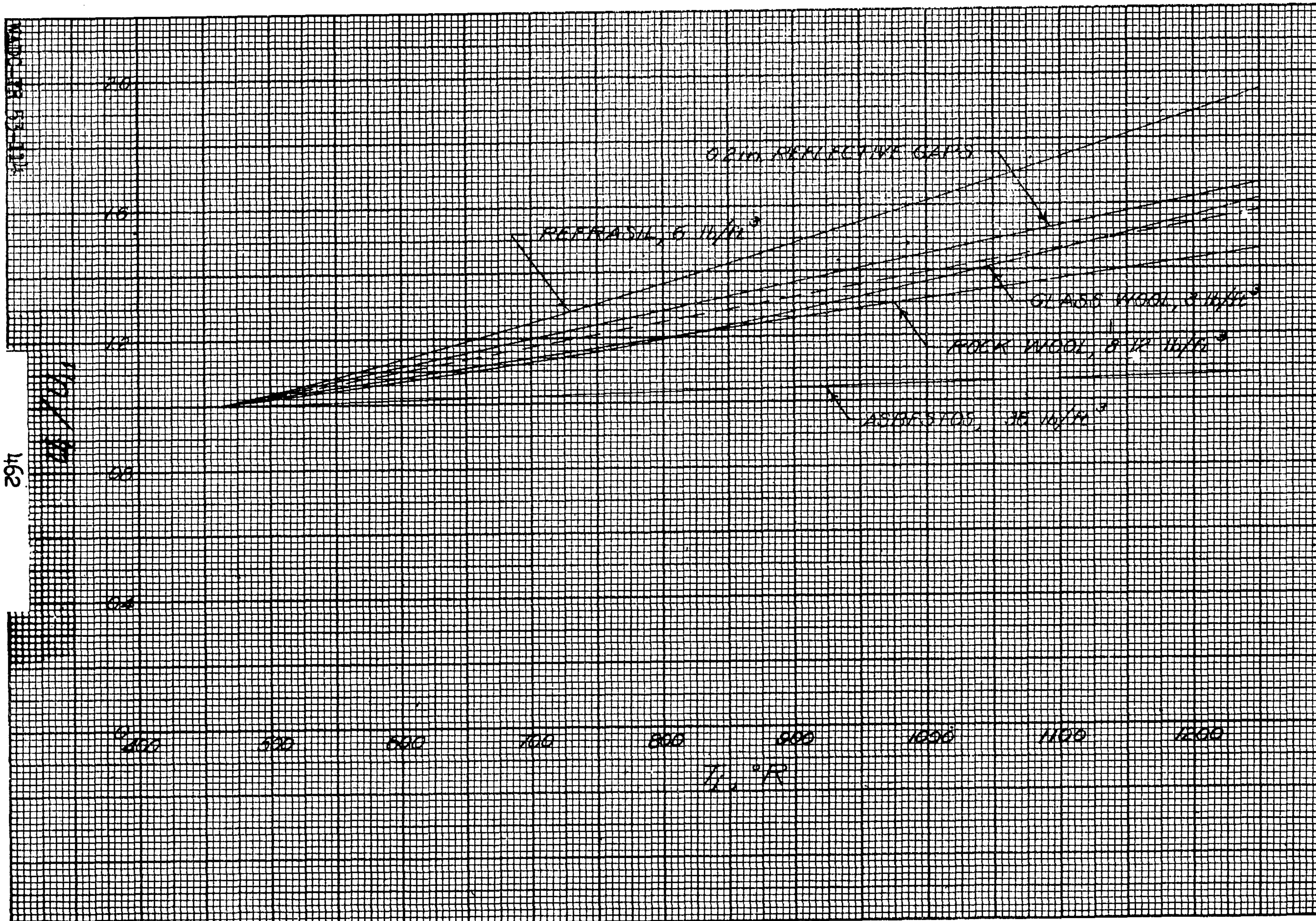

Figure AII-2
Method of Representing the Variation of Insulating Effect with Temperature for Calculations

of U_i as applying for this temperature condition. Then the chart is used as in the following example.

1. Assume that at the beginning of a flight $T_i = 700^oR$, and that sufficient insulation is provided such that $U_i = 0.6$ when $T_i = 700^oR$.

2. From Figure AII-2, if rock wool is used, $(U_i/U_{i1}) = 1.145$. Then clearly $U_{i1} = (0.6/1.145) = 0.524$

3. The value of U_i at any subsequent value of $T_i = a$ is therefore given by

$$(U_i)_a = \left(\frac{U_i}{U_{i1}}\right)_a \times 0.524$$

The use of such a chart together with the proper definition of U_i is a worthwhile aid to transient calculations when the outside face temperature is constant. Although the chart was prepared for an outside face temperature of 1355^oR, it is readily shown that it may be used for other face temperatures as well, provided that (U_i/U_{i1}) is a linear function of the mean insulation temperature.

Assuming a linear relationship, U_i may be represented by

$$U_i = A + B\,T_m = A + B\left(\frac{T_w + T_i}{2}\right)$$

where A and B are constants, and where T_i is the temperature of one face of the insulation while T_w is the temperature of the other. From this, if T_w is constant, it is clear that

$$\frac{dU_i}{dT_i} = \frac{B}{2} = \text{constant}$$

Therefore, whatever the constant value of T_w, if U_i be displayed as a function of T_i, and defined at some initial T_i the same values of U_i are obtained for all other values of T_i as though a different T_w were used.

The dashed-line of Figure AII-2 represents the variation of thermal conductivity with temperature which is used to represent rock wool in all of the calculations of this report. From the standpoint of heat transfer rate, it is obviously conservative compared to actual data. In addition, however, it has the advantage of representing glass wool and reflective gap insulation quite accurately. Since the insulation data can be represented with good accuracy by the straight dashed line, the variation of thermal conductivity with temperature is substantially linear. This same plot is therefore used for skin temperatures T_w other than 1355^oR.

REFERENCES

(AII-1) Wilkes, G. B. Heat Insulation. John Wiley and Sons, Inc., New York, 1950.

(AII-2) Crisman, R. B. Methods for Determining Refrigeration and Insulation Characteristics of Supersonic Aircraft. Cornell Aeronautical Laboratory. Report B.C.-531-S-13, December, 1949. (Confidential)

(AII-3) McAdams, W. H. Heat Transmission. Second Edition. McGraw-Hill Book Company, Inc., New York, 1942.

APPENDIX III

FUEL TEMPERATURE RISE IN HIGH SPEED FLIGHT

The use of fuel as a coolant for protecting equipment against excessive temperature rise in high speed flight considered in Sections I, II, and VI through VIII. When fuel is to be used as a coolant, it is necessary to have information available describing its variation of temperature with flight time. In this Appendix equations are developed which can be used to calculate the temperature rise of fuel in storage tanks which are cylindrical in shape.

ANALYSIS

1. Assumptions

The fundamental assumptions on which this analysis is based, are:

1. The fuel tank is cylindrical in shape, with the axis horizontal.

2. Heat transfer occurs through the cylindrical surface of the tank, but the ends are perfectly insulated.

3. The tank is pressurized to prevent flashing of the fuel into vapor. The tank contains a nitrogen bag which expands as the fuel is used, thereby eliminating sloshing.

4. Heat transfer coefficients on the fuel-side and air-side of the tank wall are independent of position.

5. The recovery factor is neglected, and the air temperature for purposes of heat transfer is taken as the stagnation temperature corresponding to flight speed and altitude.

6. The tank wall and any insulation used on it have no thermal capacity.

7. The weight-rate of fuel consumption is constant during flight.

8. The temperature drop due to heat transfer through the tank wall and the skin is neglected.

9. Heat transfer to the fuel occurs only through that portion of the cylindrical tank surface actually wetted by the fuel at any time.

Figure AIII-1 is a schematic drawing of a fuel tank described by these assumptions. The case shown is that of a tank provided with insulation. The cylindrical surface area of the tank subtended by the angle α is denoted by A_f and is called the tank wall area wetted by the fuel. Differences be-

tween A_f on the inside of the tank and the corresponding area subtended by the angle α on the skin are neglected.

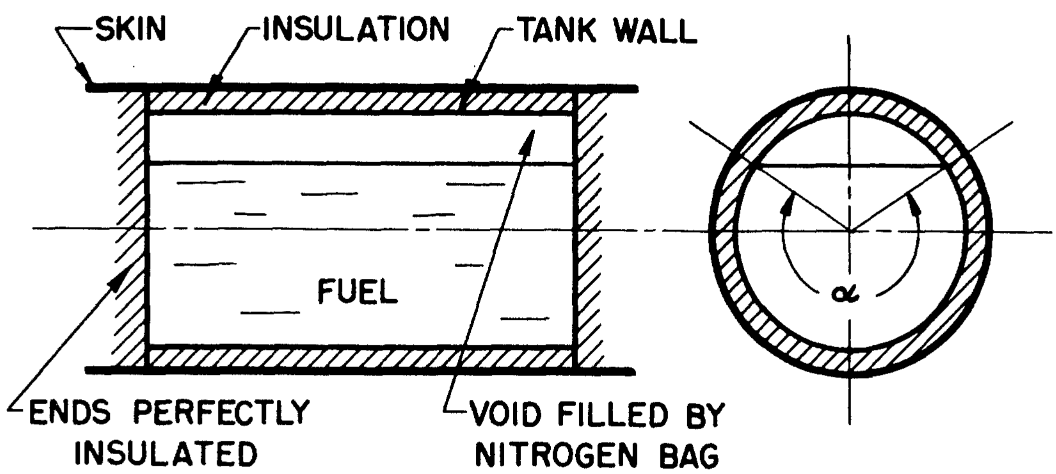

Figure AIII-1. Schematic of Cylindrical Fuel Tank

2. Nomenclature

Symbol	Definition	Units
A	Area	ft^2
a	A convection group defined where used	
C	Heat capacity	Btu/°R
c	Specific heat	Btu/lb-°R
c_p	Specific heat at constant pressure	Btu/lb-°R
c_v	Specific heat at constant volume	Btu/lb-°R
D	Fuel tank diameter	ft
g	Gravitational constant = 4.17×10^8	ft/hr^2
h	Heat transfer coefficient	Btu/hr-ft^2-°R
K	Conductance	Btu/hr-°R
k	Thermal conductivity	Btu/hr-ft-°R

Symbol	Definition	Units
M	Mach number	dimensionless
T	Absolute temperature	^{o}R
U	Unit insulation conductance	Btu/hr-ft^{2}-^{o}R
u	Velocity	ft/hr
V	Volume	ft^{3}
v	Specific volume	ft^{3}/lb
W	Weight	lb
W'	Weight rate	lb/hr
x	Length or thickness	ft
α	Angle	any
β	Volume coefficient of thermal expansion	$^{o}R^{-1}$
γ	Weight density	lb/ft^{3}
μ	Viscosity	lb/ft-hr
τ	Time	hr

Subscripts

a	Denotes air
aw	Denotes air-to-skin
d	Denotes time at end of flight or time fuel tank is empty
f	Denotes fuel
i	Denotes insulation or inside when used with heat transfer coefficient
if	Denotes insulation-to-fuel
it	Denotes fuel tank insulation
o	Denotes original value or outside when used with heat transfer coefficient
os	Denotes atmospheric static temperature

Subscripts, continued

sf	Denotes heat storage rate of fuel
w	Denotes skin
wi	Denotes skin-to-inner-face of insulation
1,2	Denotes initial and final values for a time interval

3. Derivation of Equations

Under the assumptions, a general heat balance for the case of a tank with insulation is

$$q_{aw} = q_{wi} = q_{if} = q_{sf} \qquad \text{(AIII-1)}$$

where it is assumed that the insulation is located inside of the aircraft skin, on the outside of the fuel tank wall. Expressed in terms of conductances and temperature potentials this becomes

$$K_{aw}(T_a-T_w) = K_{wi}(T_w-T_i) = K_{if}(T_i-T_f) = \frac{C}{\Delta\tau}(T_{f2}-T_{f1}) \qquad \text{(AIII-2)}$$

Equation (AIII-2) is strictly true when based on mean temperature values and mean conductance values for the time interval $\Delta\tau$ corresponding to a fuel temperature rise $(T_{f2}-T_{f1})$. As an approximation, the conductances are based on temperatures prevailing at the beginning of a time interval. Then for short time intervals, where the heat transfer rate does not change greatly during the interval, the following relationship is derived from equation (AIII-2)

$$(T_{f2}-T_{f1}) = \left(\frac{\Delta\tau}{C}\right) K_{aw}(T_{a1}-T_{w1}) \qquad \text{(AIII-3)}$$

The following equations also follow from equation (AIII-2).

$$\frac{T_{a2} - T_{w2}}{T_{a2} - T_{f2}} = \frac{\frac{1}{K_{aw}}}{\frac{1}{K_{aw}} + \frac{1}{K_{wi}} + \frac{1}{K_{if}}} \qquad \text{(AIII-4)}$$

$$\frac{T_{i2} - T_{f2}}{T_{a2} - T_{f2}} = \frac{\frac{1}{K_{if}}}{\frac{1}{K_{aw}} + \frac{1}{K_{wi}} + \frac{1}{K_{if}}} \qquad \text{(AIII-5)}$$

For a constant flight speed and altitude, T_a is constant so that $T_{a2} = T_{a1}$. Equations (AIII-3, -4, and -5) can therefore be used in a stepwise calculation to determine the fuel temperature rise.

Before a calculation procedure can be established, it is necessary to define the conductances appearing in the above equations. The conductance K_{aw} is defined as

$$K_{aw} = h_o A_f \qquad \text{(AIII-6)}$$

where the external heat transfer coefficient h_o is defined by (Ref. AIII-2)

$$h_o = 0.028 \frac{k}{x} \left(\frac{\gamma u x}{\mu}\right)^{0.8} \left(\frac{c_p \mu}{k}\right)^{1/3} \qquad \text{(AIII-7)}$$

The value of x to be used depends on the application, since it is a characteristic length depending on the external configuration of a body and on the position on the surface of the body. The value used for this study of fuel temperatures is $x = 10$ ft. To facilitate calculation, it is convenient to prepare a plot of h_o versus $(T_a+T_w)/2$, thereby eliminating repeated evaluation of the physical properties of air at this average film temperature. An example of such a plot is given in Figure AIII-2 for flight Mach numbers of 2.5, 3.0, and 3.5 at an altitude of 40,000 ft.

The value of A_f varies with time depending on the rate of fuel consumption and the fuel temperature. It is assumed that the fuel tank is full at the beginning of flight and contains W_{fo} pounds of fuel. The weight of fuel at any subsequent time is therefore given by

$$W_f = W_{fo} - W_f' \tau \qquad \text{(AIII-8)}$$

where τ is the time elapsed since the beginning of the flight. The fractional weight of fuel remaining in the tank at any time is therefore (W_f/W_{fo}). The specific volume of the fuel at any time is given by

$$v = v_o(1 + \beta \Delta T_f) \qquad \text{(AIII-9)}$$

where ΔT_f represents the temperature rise of the fuel above the temperature on which v_o is based. The actual volume of the fuel in the tank at any time is therefore given by

$$V = W_f v$$

but since $V_o = W_{fo} v_o$

$$\frac{V}{V_o} = \frac{W_f}{W_{fo}} (1+\beta \Delta T_f) \qquad \text{(AIII-10)}$$

A representative value of β for JP-3 fuel is $\beta = 0.000565/^\circ F$. For the case of a cylindrical tank in the horizontal position, as assumed here, a simple relationship between the ratio (V/V_o) and (A_f/A_{fo}) can be used. Figure AIII-3 displays this relationship for the range from a completely filled to an empty tank. The value of A_f is determined from this for use in the conductance relationship.

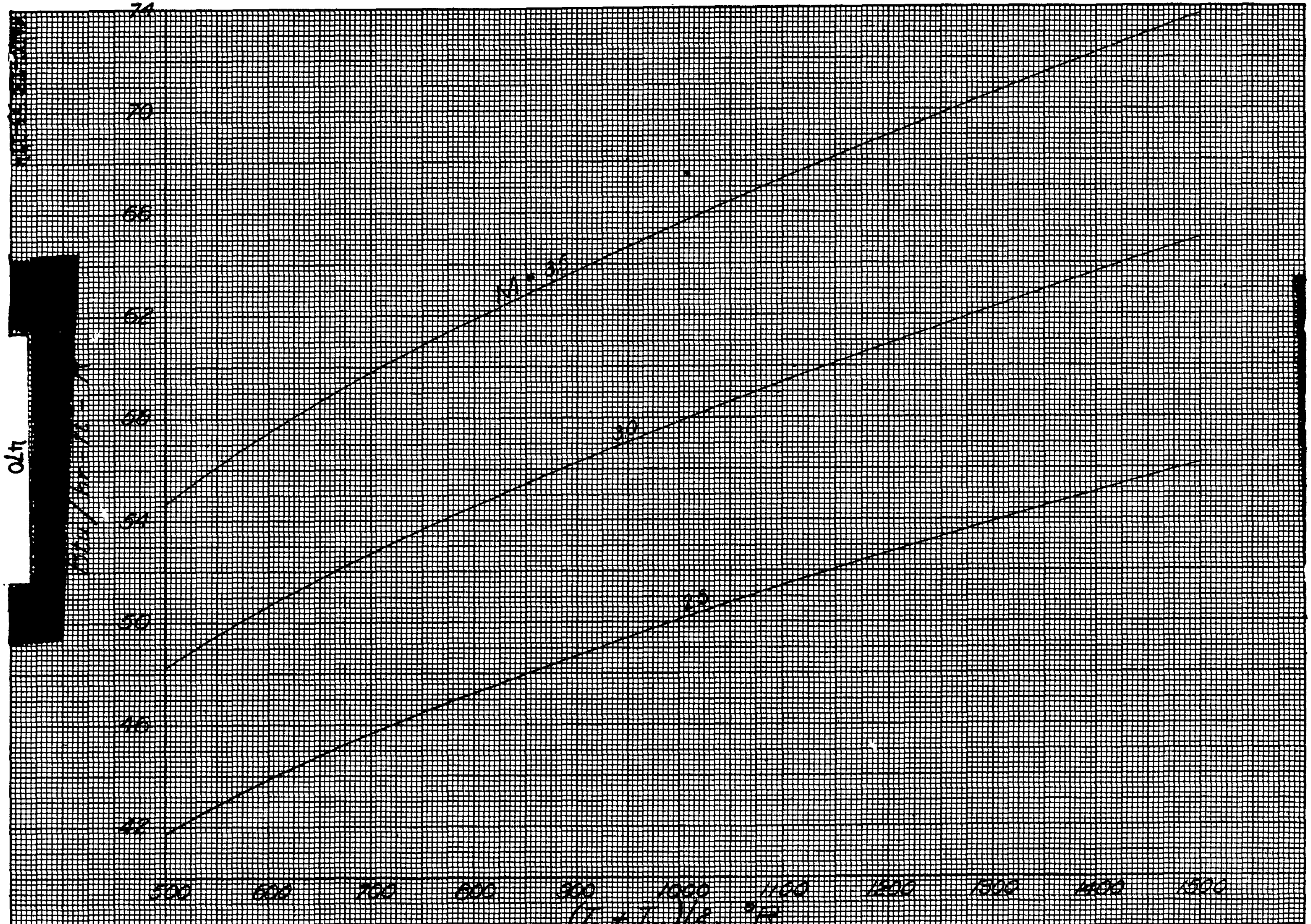

[redacted]

Figure AIII-2
Forced Convection Heat Transfer Coefficient on Outside of Aircraft Skin

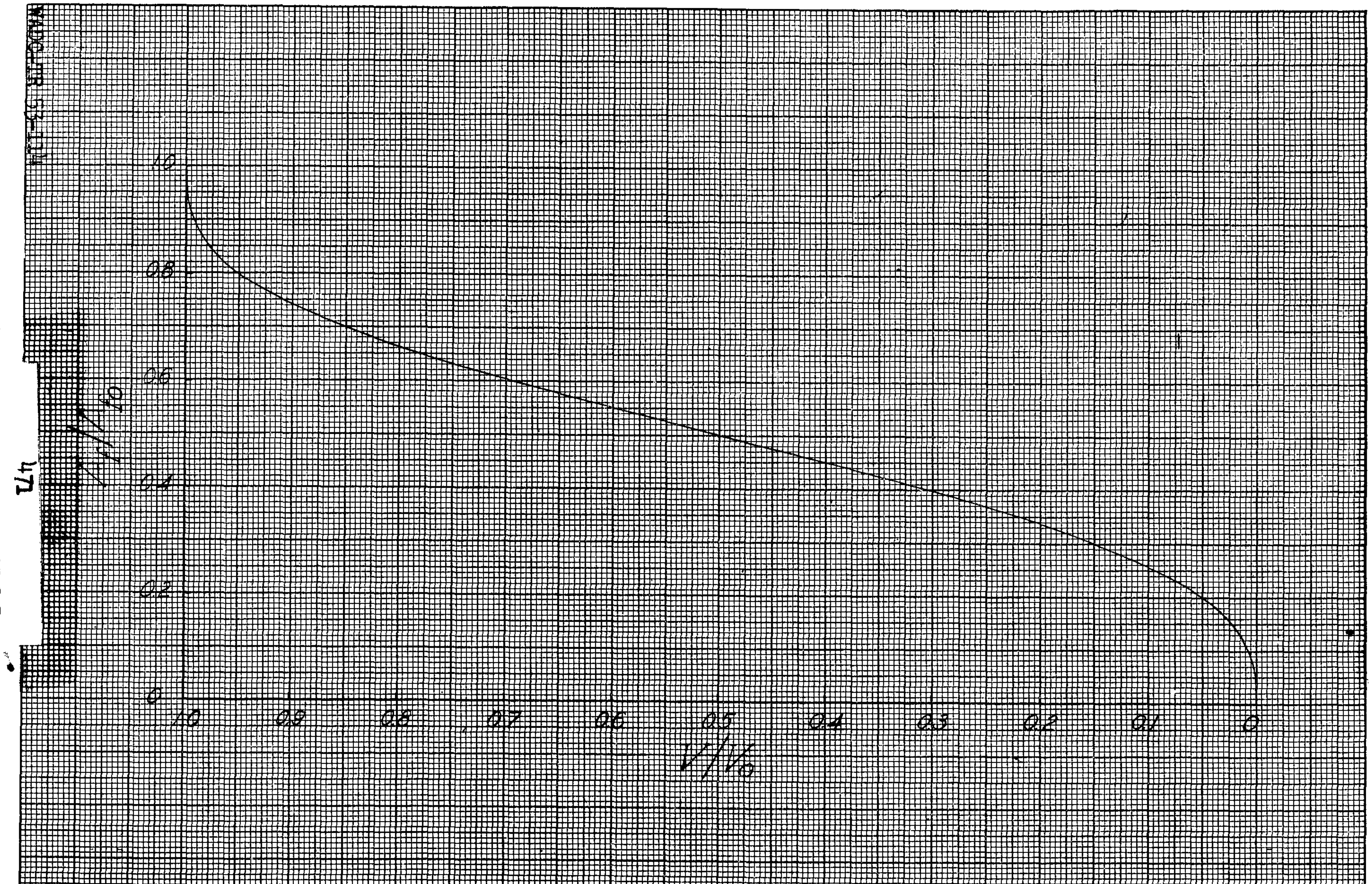

Figure AIII-3
Variation of Wetted Surface in Tank With Fuel Volume

The conductance K_{if} is defined as

$$K_{if} = h_i A_f \qquad \text{(AIII-11)}$$

where h_i is the heat transfer coefficient for free convection of the fuel in the tank. A good representation of this is (Ref. AIII-1),

$$h_i = 0.1k \left[a(T_i - T_f)\right]^{1/3} \qquad \text{(AIII-12)}$$

where

$$a = \frac{g\beta \gamma^2 c}{\mu k}$$

For convenience in calculation, the value of h_i has been prepared in graphical form for an appropriate range of temperatures T_w and T_f or T_i and T_f. T_i is involved in the equation for h_i only if an insulating effect is used between the skin and the tank wall. Otherwise T_i is replaced with T_w in the equation for h_i. The plot is given in Figure AIII-4. Physical properties of the fuel involved in h_i are determined at the average convection film temperature of $(T_w+T_f)/2$ or $(T_i+T_f)/2$.

The conductance K_{wi} is simply that for heat conduction through insulation, and is given by

$$K_{wi} = (k_i/x_i) \qquad \text{(AIII-13)}$$

The heat capacitance C is simply the thermal capacity of the fuel in the storage tank at any instant, and is given by

$$C = W_f c \qquad \text{(AIII-14)}$$

These equations and conductance definitions can now be combined into a calculation procedure for the evaluation of temperature rise. The procedure given below is for the case where insulation is used. The case where insulation is not used is a simpler one for which the reader can easily construct a similar procedure. Conductances are based on the temperatures prevailing at the beginning of an interval. Fuel weight and wetted areas are taken at their average values for a time interval.

4. Calculation Procedure for Fuel Temperature Rise

1. Calculate T_a for the flight Mach number and altitude from

$$T_a = T_{os}\left[1 + \left(\frac{c_p - c_v}{2c_v}\right) M^2\right]$$

T_a = ______ °R

(This calculation need not be repeated if flight is at constant speed and altitude.)

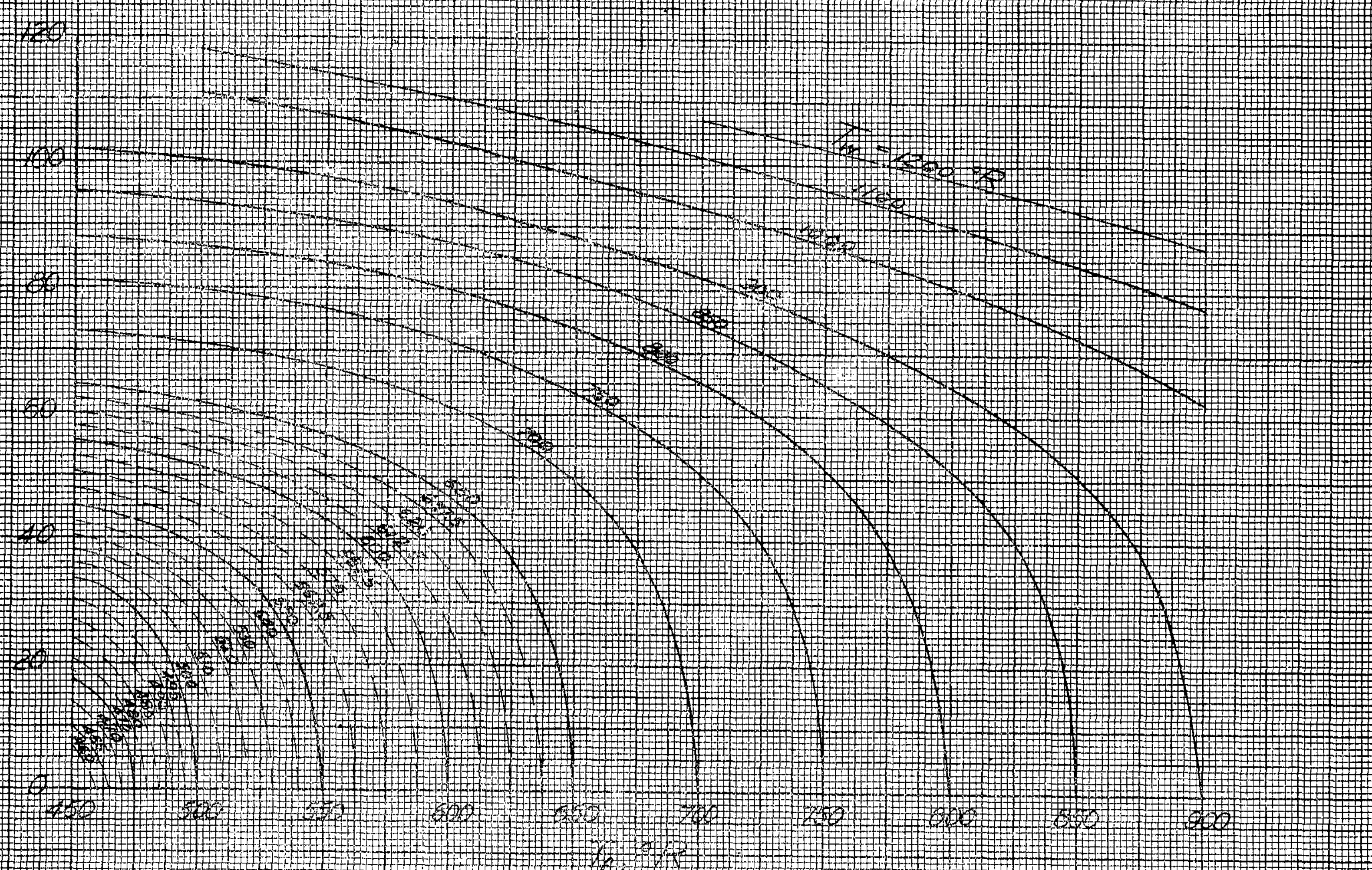

Figure AIII-4

Free Convection Heat Transfer Coefficient on Inside of Tank Wall

2. Choose the length of the time interval $\Delta\tau$.

$\Delta\tau$ = _____ hr

3. Calculate the weight of fuel remaining in the tank

$$W_f = W_{fo} - W_f'\tau$$

for τ at the middle of $\Delta\tau$.

W_f = _____ lb

4. Calculate

$$\frac{V}{V_o} = \frac{W_f}{W_{fo}} (1+\beta\,\Delta T_f)$$

where ΔT_f is based on T_{f1} for the interval.
(for JP-3 fuel, B = 0.000565)

(V/V_o) = _____

5. Find (A_f/A_{fo}) from the plot, Figure AIII-3, and calculate A_f.

A_f = _____ ft^2

6. Get h_o for flight speed and altitude (for example, from Figure AIII-2).

h_o = _____ Btu/hr-ft^2-^{o}R

7. Calculate $K_{aw} = h_o A_f$

K_{aw} = _____ Btu/hr-^{o}R

8. Calculate $C = W_f c$ (for JP-3 fuel, get c at T_{f1} from Figure AI-2).

C = _____ Btu/^{o}R

9. Calculate $(T_a - T_{w1})$

$(T_a - T_{w1})$ = _____ ^{o}F

10. Calculate $(T_{f2} - T_{f1}) = (\Delta\tau/C)K_{aw}(T_a - T_{w1})$, then $T_{f2} = (T_{f2} - T_{f1}) + T_{f1}$

T_{f2} = _____ ^{o}R

11. Calculate $K_{wi} = k_i/x_i$ evaluating k_i at $(T_{w1}+T_{i1})/2$ if it is desired to account for the variation of insulation thermal conductivity with temperature.

K_{wi} = _____ Btu/hr-^{o}R

12. Get h_i for T_{i1} and T_{f1} (for JP-3 fuel, use Figure AIII-4)

h_i = _____ Btu/hr-ft^2-^{o}R

13. Calculate $K_{if} = h_i A_f$

$K_{if} =$ _____ $Btu/hr-{}^{o}R$

14. Calculate

$$(T_a - T_{w2}) = \frac{\frac{1}{K_{aw}} (T_a - T_{f2})}{\frac{1}{K_{aw}} + \frac{1}{K_{wi}} + \frac{1}{K_{if}}}$$

$(T_a - T_{w2}) =$ _____ ${}^{o}F$

15. Calculate $T_{w2} = T_a - (T_a - T_{w2})$

$T_{w2} =$ _____ ${}^{o}R$

16. Calculate

$$(T_{i2} - T_{f2}) = \frac{\frac{1}{K_{if}} (T_a - T_{f2})}{\frac{1}{K_{aw}} + \frac{1}{K_{wi}} + \frac{1}{K_{if}}}$$

$(T_{i2} - T_{f2}) =$ _____ ${}^{o}F$

17. Calculate $T_{i2} = T_{f2} + (T_{i2} - T_{f2})$

$T_{i2} =$ _____ ${}^{o}R$

When this interval calculation is completed, the values of T_{f2}, T_{i2}, and T_{w2} are used as T_{f1}, T_{i1}, and T_{w1} in the next interval, and the entire procedure is repeated.

RESULTS

To explore the possibilities of using fuel as a coolant, a large number of calculations were made for both insulated and uninsulated fuel tanks. The significant results are given here.

Figure AIII-5 shows the effect of tank diameter and flight speed on the temperature rise of JP-3 fuel. It is assumed that the fuel is consumed at a uniform rate, and that the tanks are emptied in 0.25 hr. The solid lines indicate temperature rise of the fuel, and show clearly that the fuel is heated more rapidly in a tank of smaller diameter. This results from the greater ratio of tank surface area to weight of fuel in the smaller tank. Since the heat is transferred through the wetted surface area of the tank, the smaller tank gives a higher ratio of heat transferred to fuel thermal capacity, and hence a more rapid temperature rise. The upper dashed lines show the corresponding tank wall temperatures (also the skin temperature, since no insulation is used). The lower dashed lines show fuel temperatures for the fuel in a 2 ft and 6 ft diameter tank at $M = 2.5$. The lower stagna-

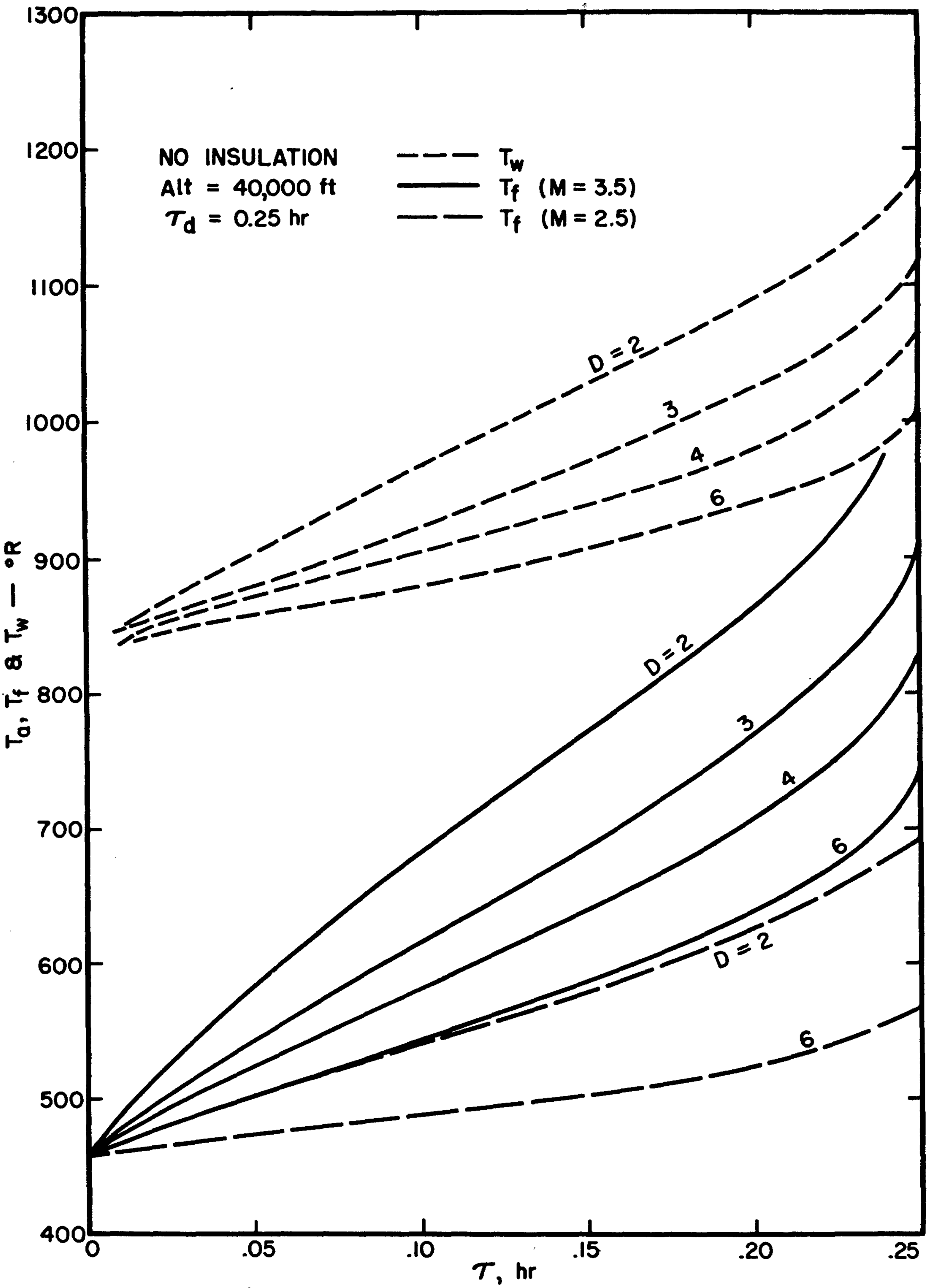

Figure AIII-5
Effect of Flight Speed and Tank Diameter on Fuel Temperature Rise

tion temperature at lower flight speed results in slower heating of the fuel. In all of the cases of Figure AIII-5 the rapid temperature rise at the end of the flight is due to the great increase in ratio of wetted surface to fuel weight as the cylindrical tank approachs the empty point.

Figure AIII-6 shows the effect of tank diameter on temperature rise of JP-3 fuel when the fuel is consumed at a rate such that the tank would be empty at the end of a two-hour flight. The flight Mach number is 3.5, and the altitude is 40,000 ft. It is readily seen that very high fuel temperatures are reached in less than two hours, indicating that some insulation effect would be required if the fuel were to remain serviceable to the end of the two-hour flight. It should be noted that the temperature rise here for the first 0.25 hr is less than that for the 0.25-hr flight in Figure AIII-5, because of the lower fuel consumption rate.

Figure AIII-7 is a summary plot for calculation data based on JP-3 fuel, M = 3.5, Alt = 40,000 ft, no insulation, and a fuel consumption rate corresponding to a two-hr flight. For any tank diameter, the chart can be used to determine the fuel temperature that is reached at a particular flight time. It is readily seen that insulation is required to achieve the longer flight time, even where the tank is quite large. The high temperatures that are reached in a short time without insulation not only make the fuel useless as a coolant, but would probably interfere with its use in the power plant as well.

Figure AIII-8 shows the effect of fuel consumption rate on the temperature rise of JP-3 fuel at three flight speeds and an altitude of 40,000 ft. An uninsulated, 3 ft diameter tank is assumed. The fuel consumption rates are such as to give an empty tank in 0.25 hr, 0.50 hr, 1.0 hr, and 2.0 hr. The effect whereby the fuel temperature in a tank of high consumption rate is at first below and later above that for a lower consumption rate is readily explained. It is simply due to the change of wetted surface to volume ratio as a cylindrical tank in the horizontal position is drained from the full to the empty condition. In the lower portion of the figure fuel temperatures are shown for the same range of Mach numbers, but using insulation on the tank. The insulation conductance is $U_{it} = (k_i/x_i) = 0.25$ Btu/hr-ft^2-^{o}R. It is seen that the insulation has a powerful effect on limiting the fuel temperature rise, retaining it at low temperatures which would make it very useful as a coolant. The initial temperature of 460^{o}R (0^{o}F) could be achieved by precooling, or might be approximated in an air-launched craft. An insulation conductance of 0.25 represents approximately a two-inch thickness of a material such as rock wool.

Figure AIII-9 shows the effect of various amounts of insulation on the temperature rise of JP-3 fuel. The flight conditions and tank size are given in the figure. As compared to the case of no insulation, it is seen that relatively small thicknesses of rigid insulation would have significant effect in limiting the fuel temperature rise. For example U = 10, would probably represent no more than a one-quarter inch thickness of most rigid cellular materials. Data taken from this figure are used in describing fuel temperatures in various Sections of this report. In the calculations on which the curves in Figures AIII-8 and -9 are based, the insulation thermal

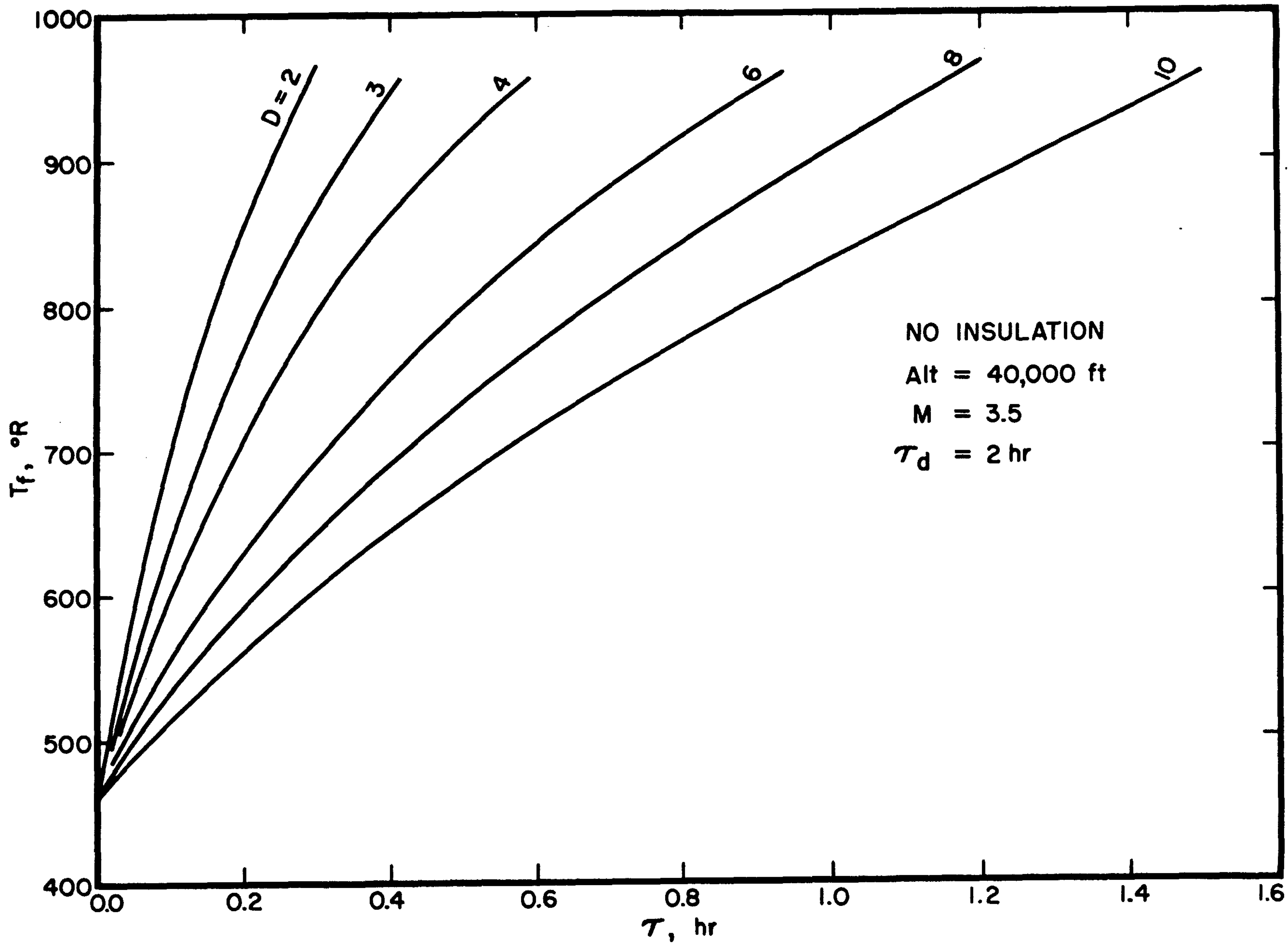

Figure AIII-6

Effect of Tank Diameter on Fuel Temperature Rise

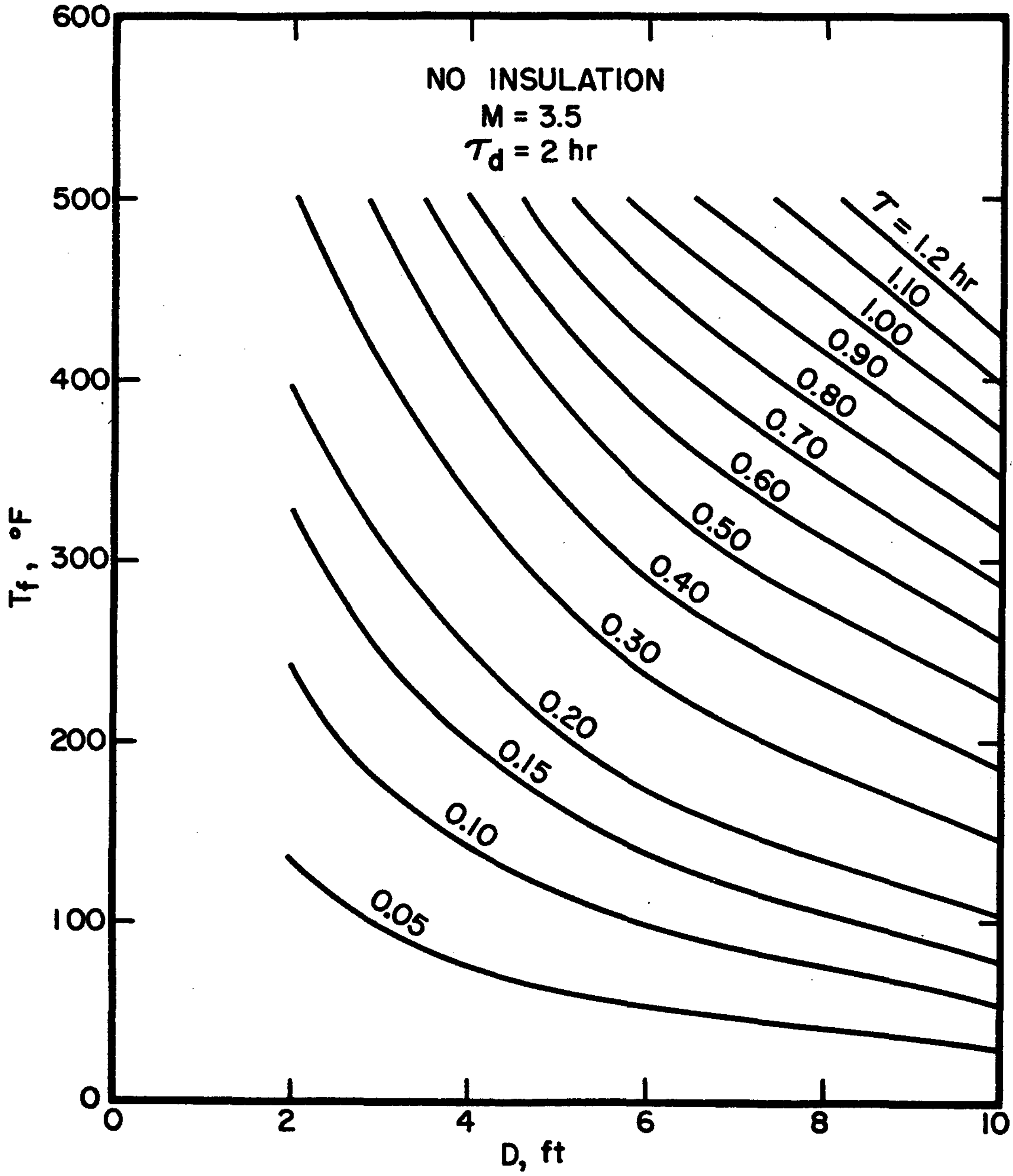

Figure AIII-7

Summary Chart Relating Tank Diameter and Fuel Temperature at Various Times Within a Projected Flight of Two Hours

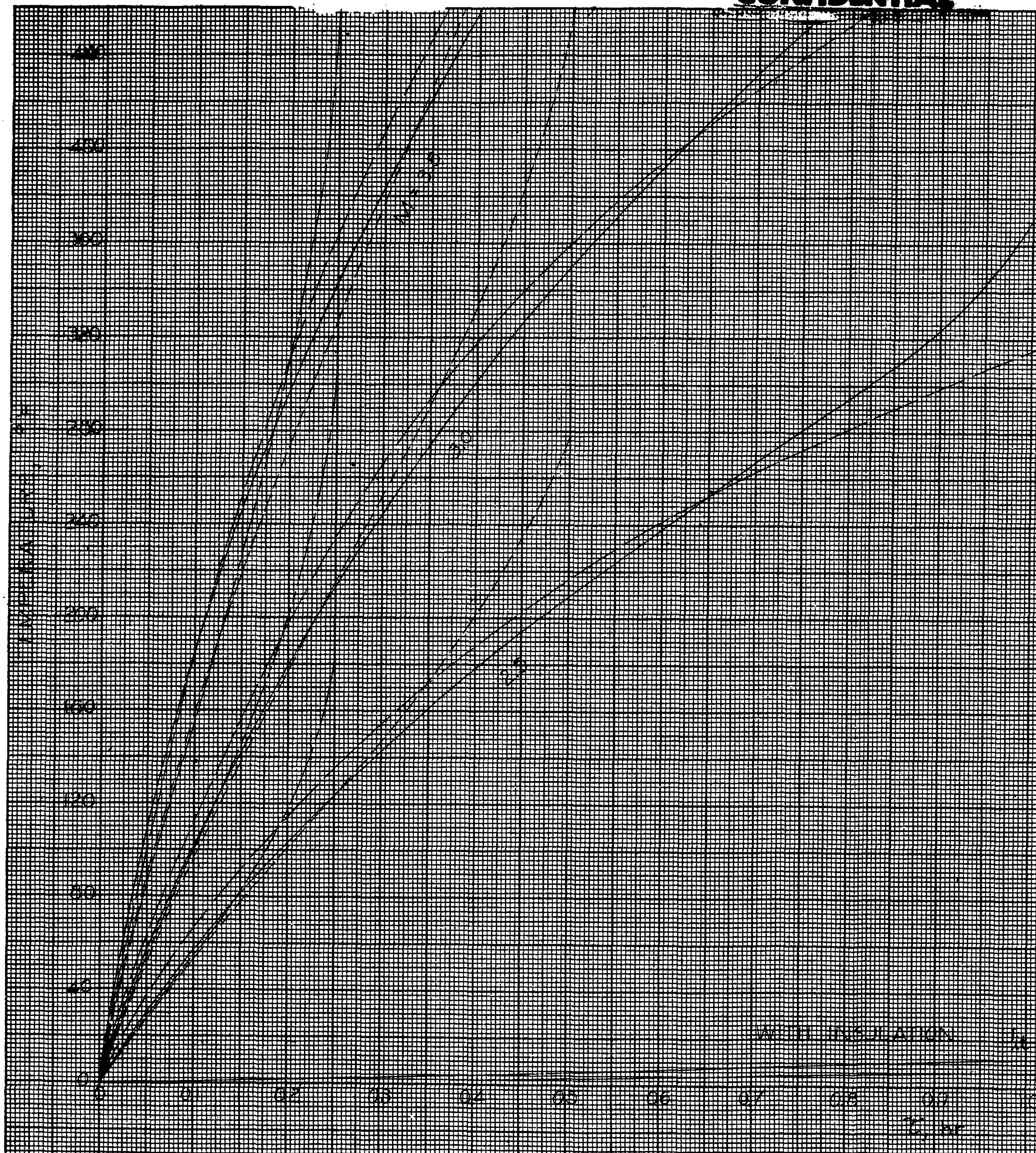

WADC-TR 53-318

Figure AIII-8

Effect of Flight Duration (Rate of Fuel Consumption) and Flight Speed on the Fuel Temperature R

(1)

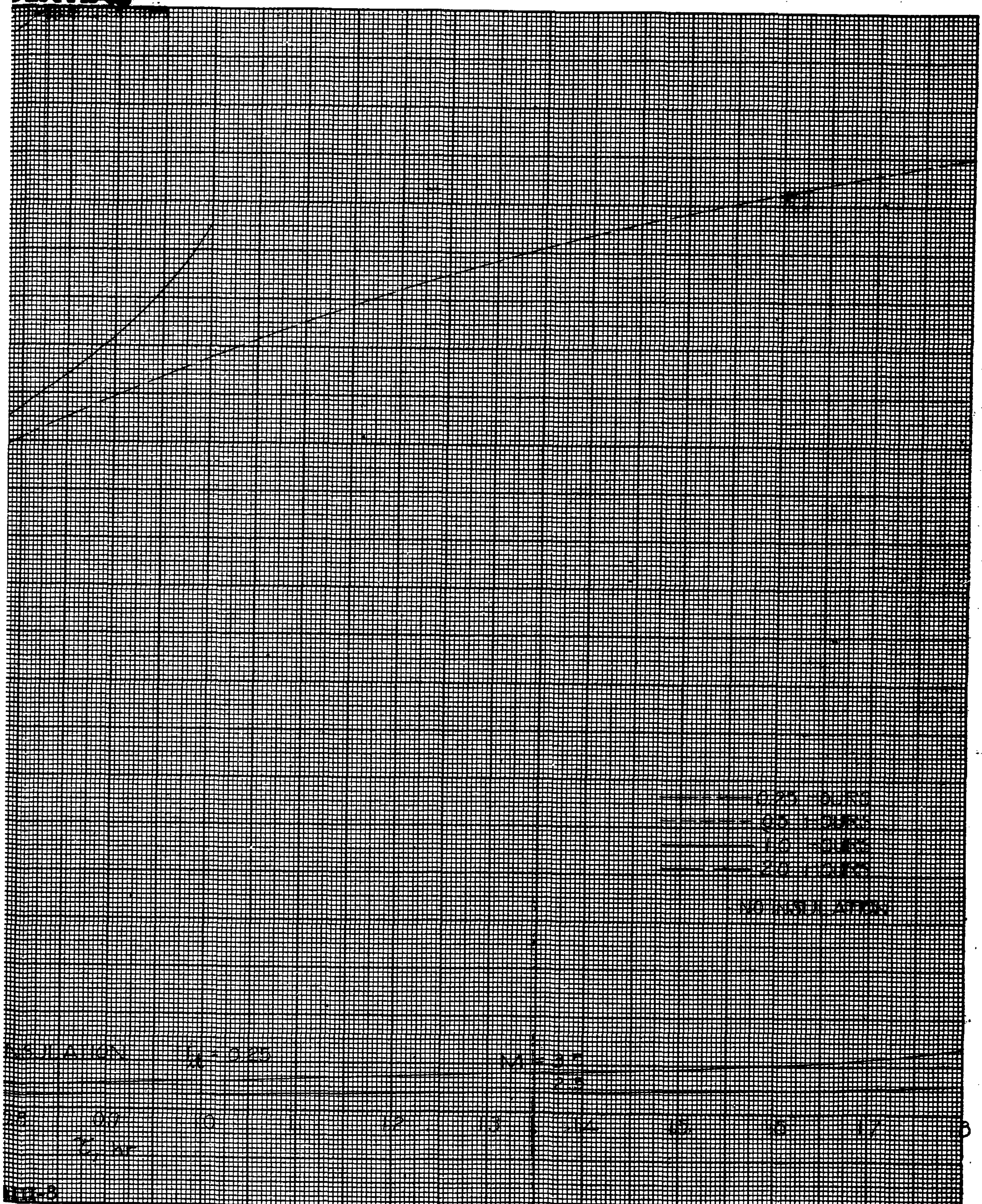

III-8

of Fuel Consumption) Insulation,
he Fuel Temperature Rise
)

2

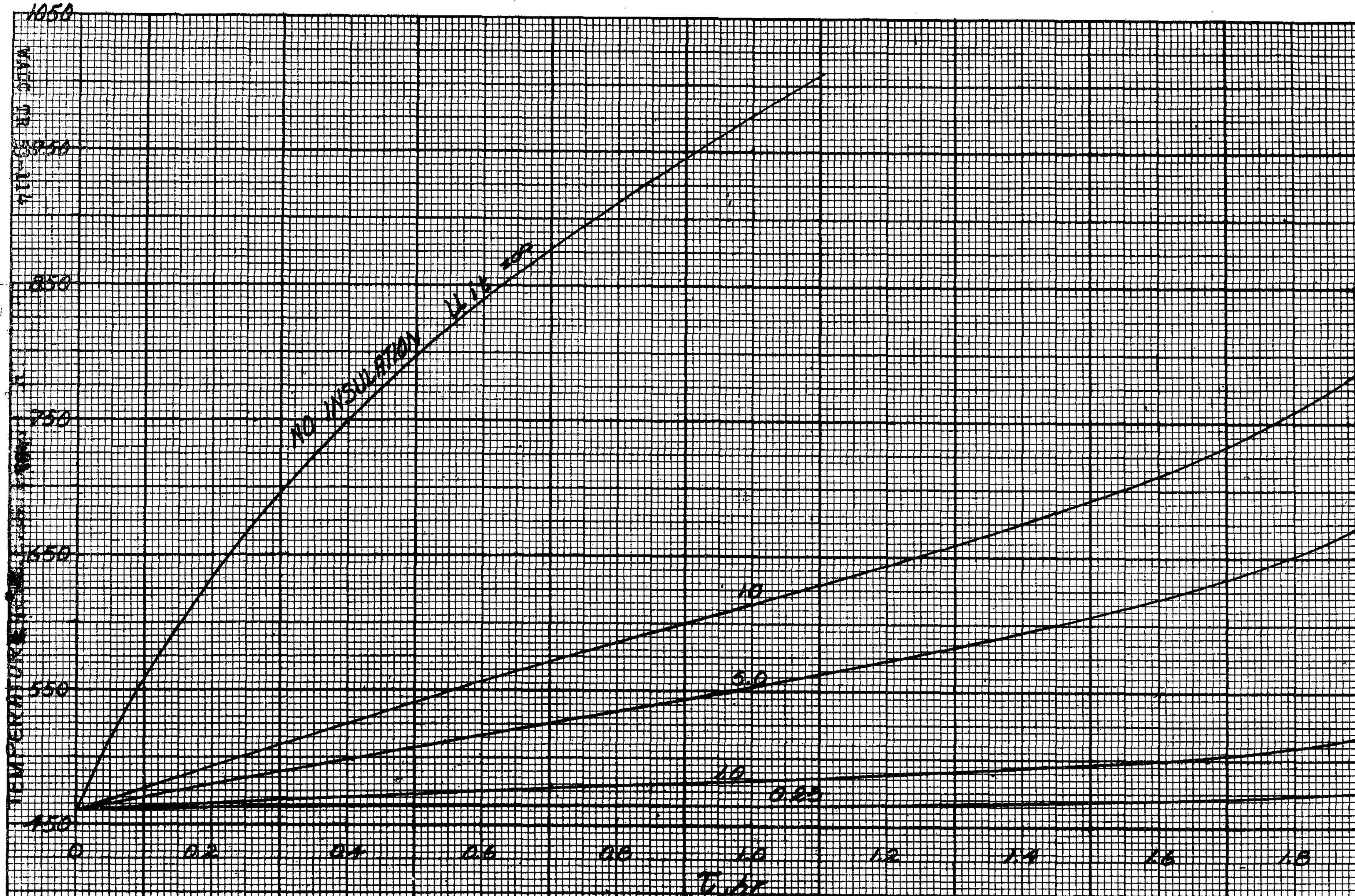

Figure III-9
Effect of Insulation on the Fuel Temperature Rise

conductivity is assumed constant with changing temperature.

REFERENCES

(AIII-1) Brown, A. I. and Marco, S. M. Introduction to Heat Transfer. Second Edition. McGraw-Hill Book Company, Inc., New York, 1951, p. 135.

(AIII-2) Fischer, W. W. and Norris, R. H. "Supersonic Convective Heat-Transfer Correlation From Skin-Temperature Measurements on a V-2 Rocket in Flight." Transactions of the American Society of Mechanical Engineers. Volume 71, 1949, p. 458.

APPENDIX IV

COMPILATION OF GENERAL CALCULATION AIDS

The group of charts given in this Appendix is a compilation of graphical aids to calculation. Most of the charts are used in several Sections of this Report, and are intended to lessen the calculation labor or eliminate physical property evaluations required for some heat transfer calculations.

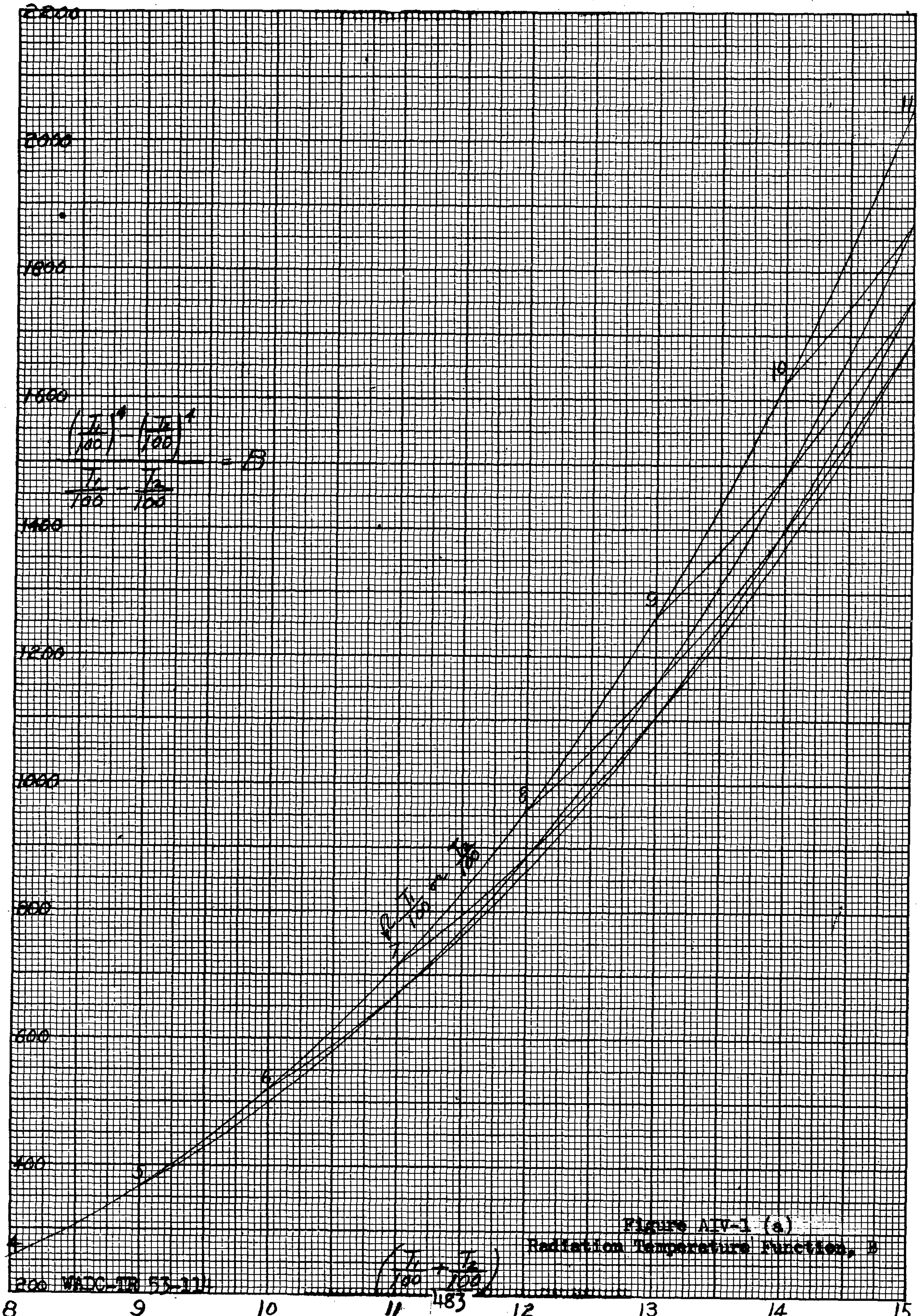

Figure AIV-1 (a)
Radiation Temperature Function, B

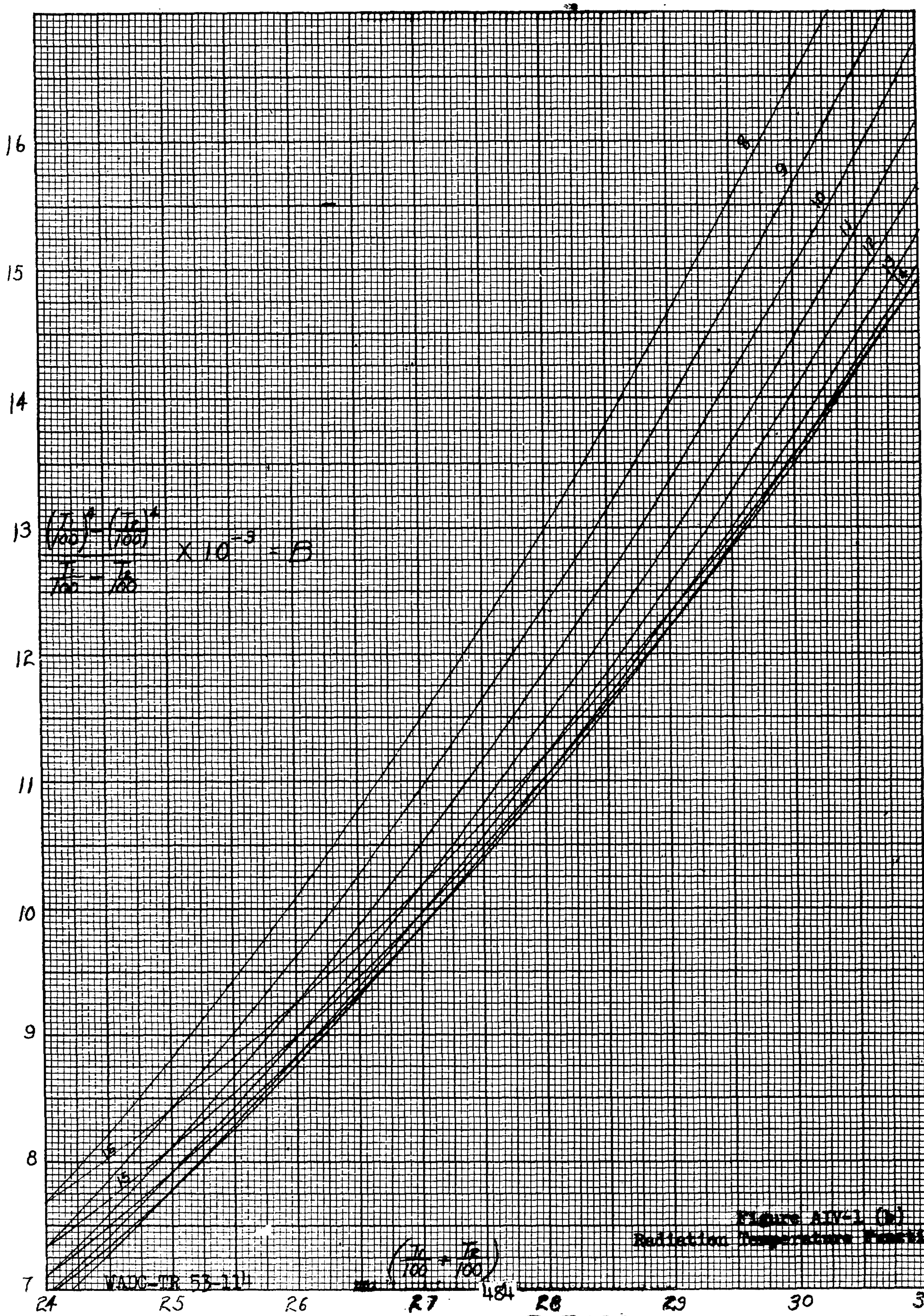

Figure AIV-1 (b)
Radiation Temperature Function, B

CONFIDENTIAL

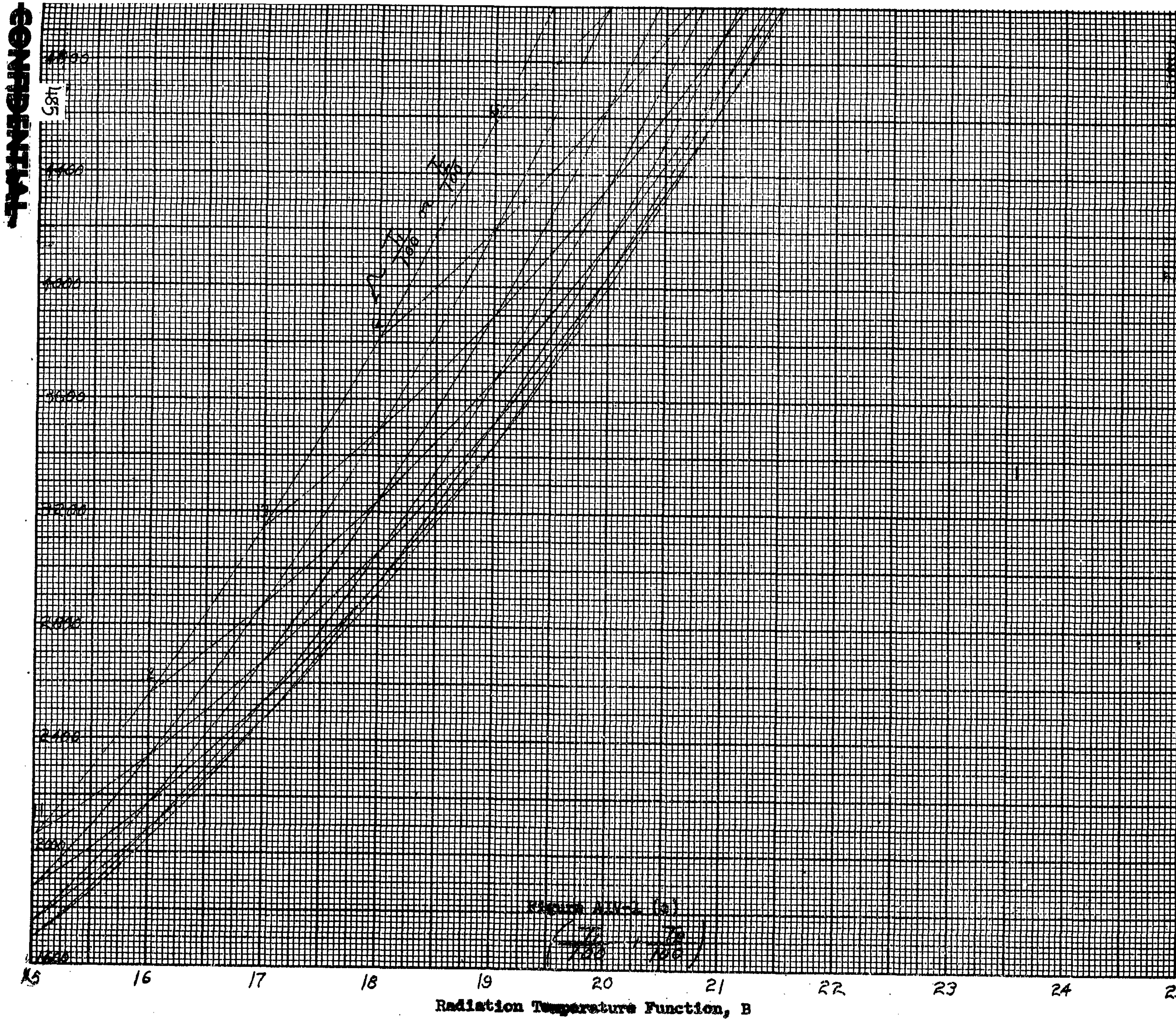

Figure AIV-1 (b)

485

CONFIDENTIAL

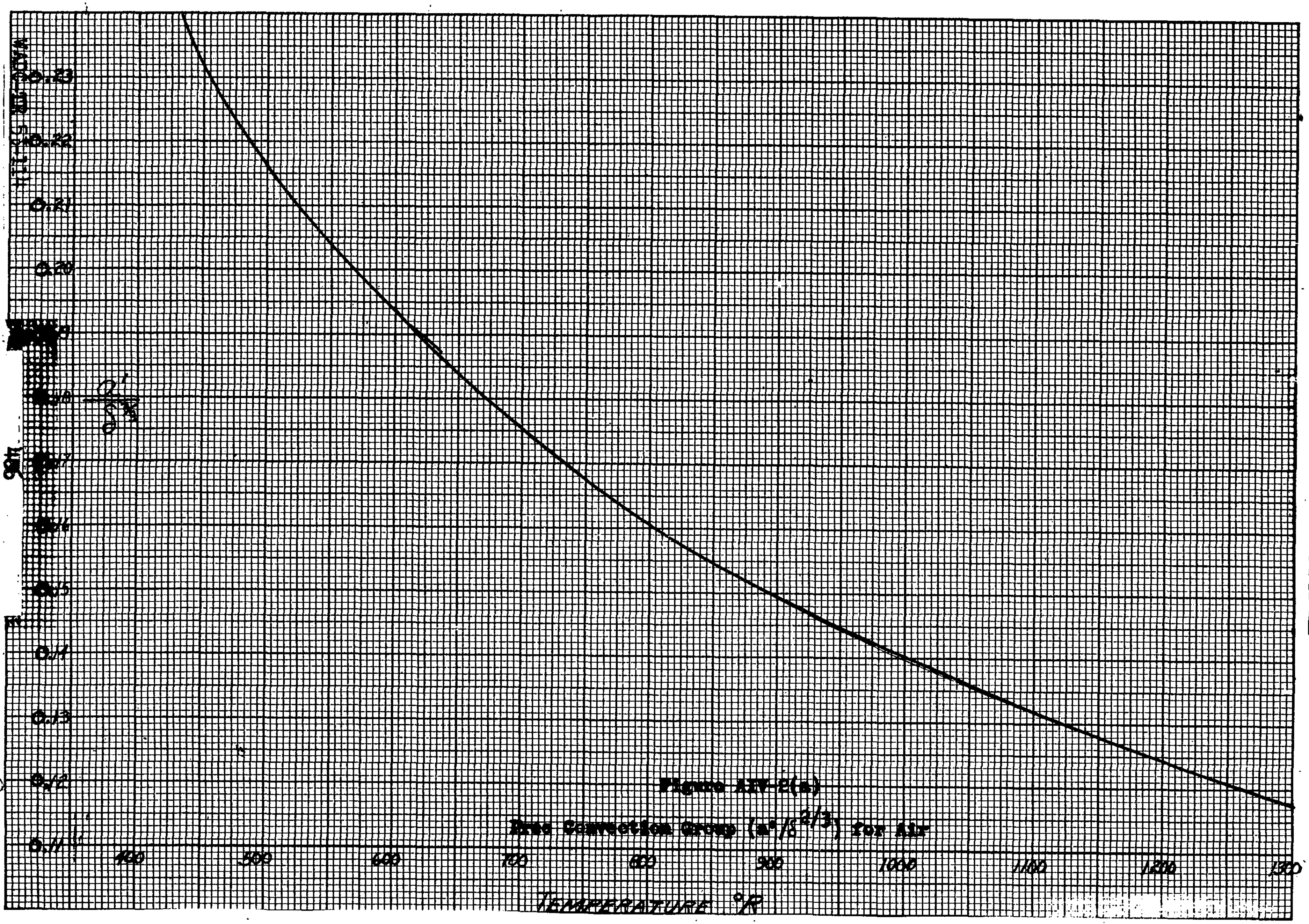

Figure AIV-2(a)

Free Convection Group $(a'/\delta^{2/3})$ for Air

(1)

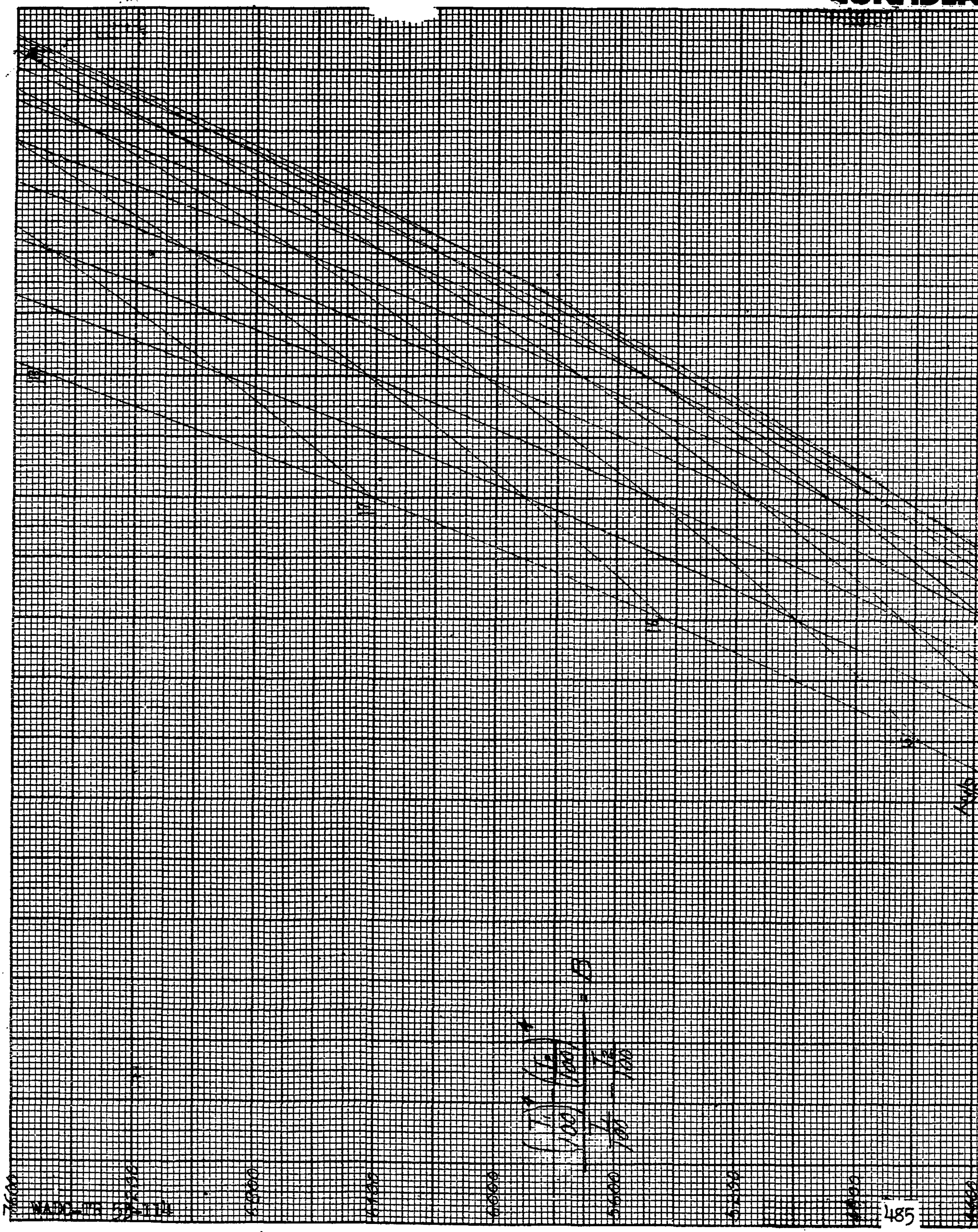

2

CONFIDENTIAL

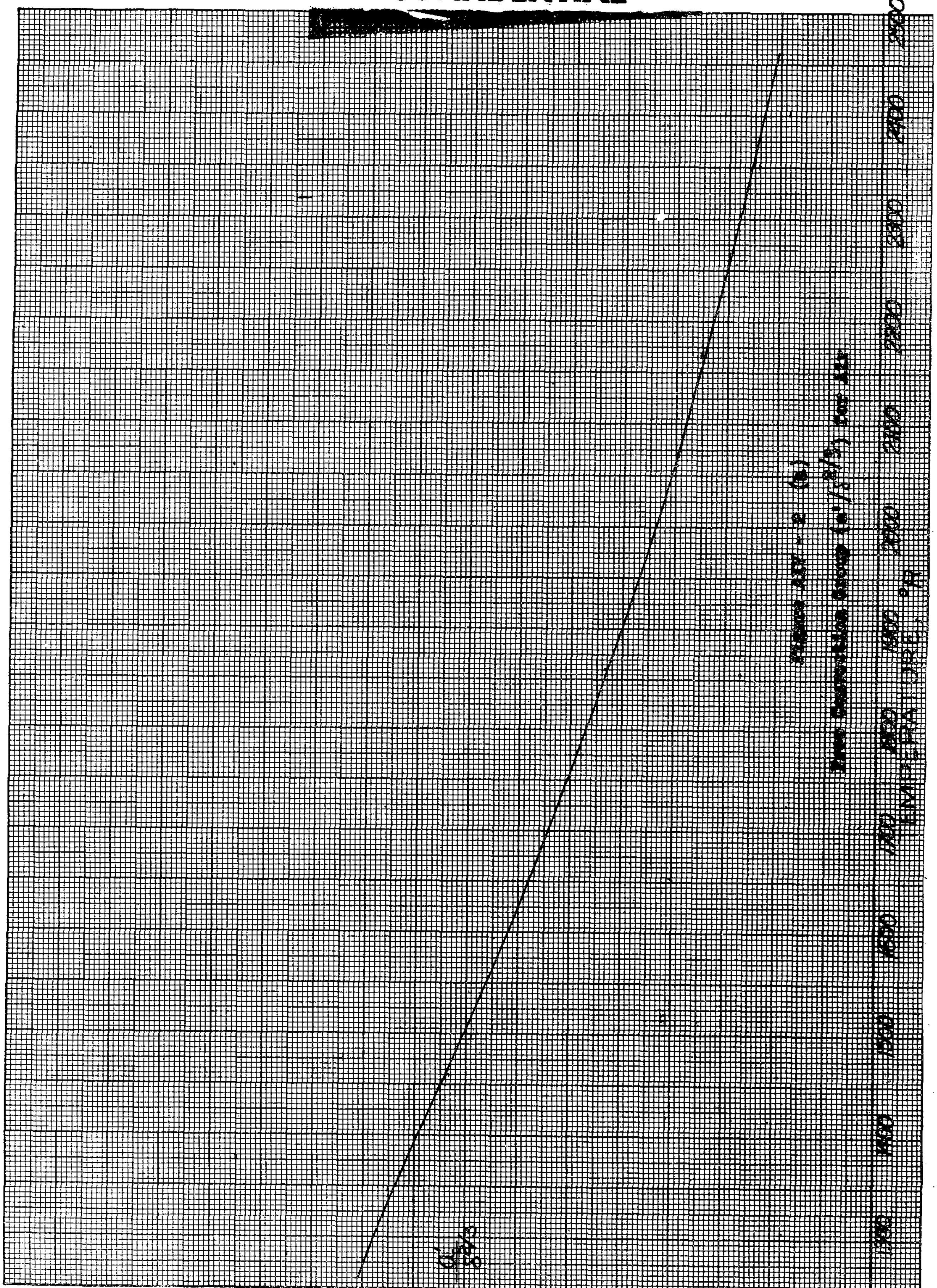

CONFIDENTIAL

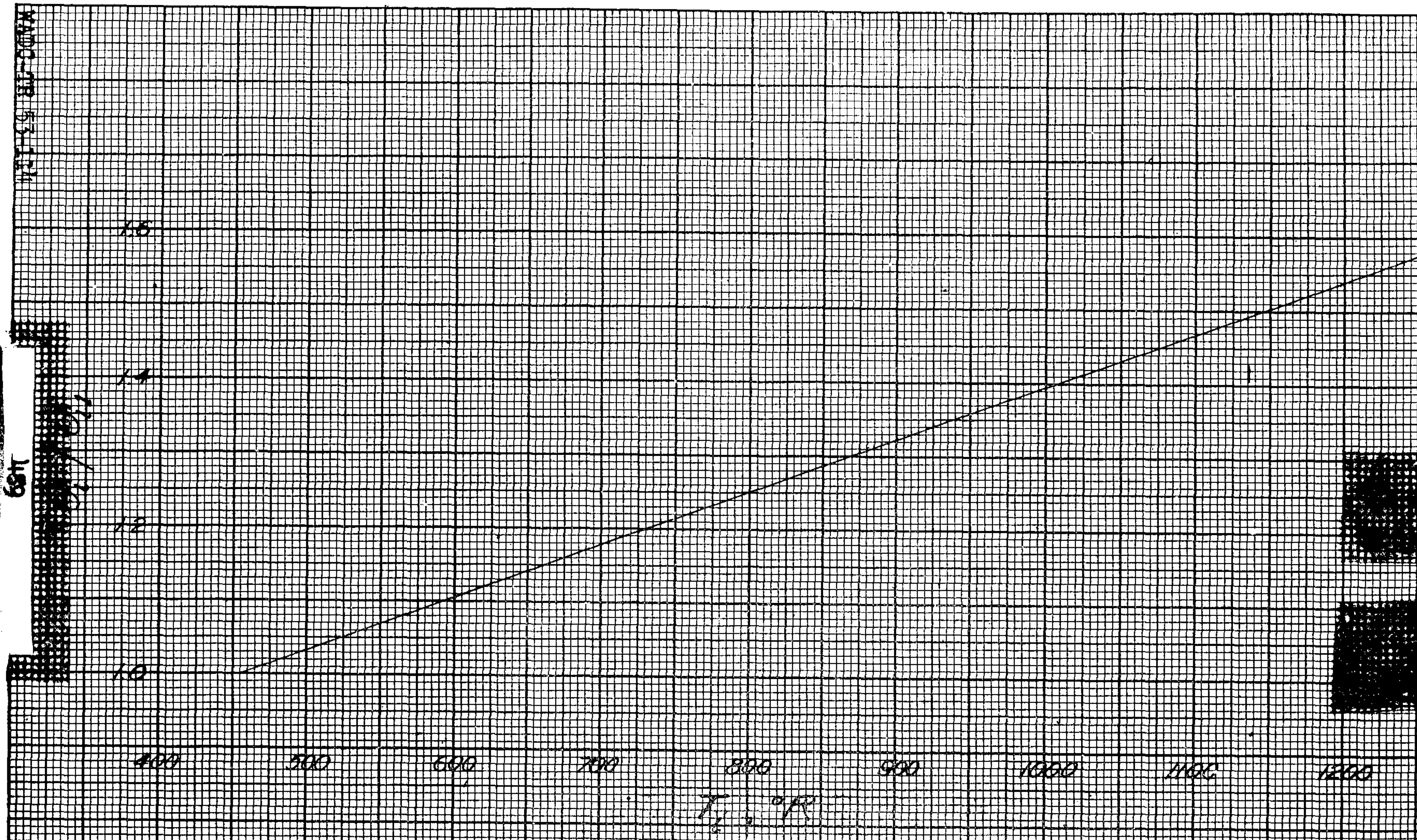

Figure 4.IV-4

Variation of Insulating Effect with Insulation Face Temperature
For Rock Wool, Glass Wool, Reflective Gaps